

RPL-TDR-64-68

*498-P \$6.00*

**ROCKET ENGINE VALVE POPPET  
AND SEAT DESIGN DATA**

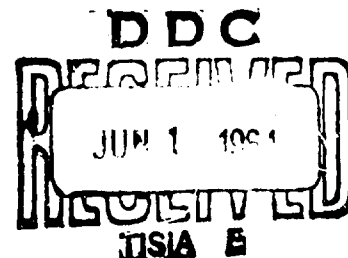
**TECHNICAL DOCUMENTARY REPORT  
NO. RPL-TDR-64-68**

**MAY 1964**

**AIR FORCE ROCKET PROPULSION LABORATORY  
RESEARCH AND TECHNOLOGY DIVISION  
AIR FORCE SYSTEMS COMMAND  
EDWARDS, CALIFORNIA**

**PROJECT NO. 6753  
TASK NO. 675304**

**(PREPARED UNDER CONTRACT NO. AF04(611)-8392 BY  
ROCKETDYNE, A DIVISION OF NORTH AMERICAN AVIATION INC.,  
CANOGA PARK, CALIFORNIA; EDITED BY G.F. TELLIER)**



RPL-TDR-64-68

ROCKET ENGINE VALVE POPPET  
AND SEAT DESIGN DATA

TECHNICAL DOCUMENTARY REPORT  
NO. RPL-TDR-64-68  
May 1964

Air Force Rocket Propulsion Laboratory  
Research and Technology Division  
Air Force Systems Command  
Edwards, California

Project No. 6753, Task No. 675304

(Prepared under Contract No. AF04(611)-8392 by  
Rocketdyne, a Division of North American Aviation,  
Inc., Canoga Park, California; Edited by G. F.  
Tellier)

## **NOTICES**

**Qualified requestors  
may obtain copies of  
this report from D.D.C.**

**D.D.C. release to  
O.T.S. is authorized.**

## FOREWORD

This report was prepared under G.O. 8369 in compliance with Part I, Paragraph B.7 of Contract AF04(611)-8392, covering a period of performance from July 1962 through October 1963.

Rocketdyne contributors to the reported effort were D. A. Bianco, T. Caywood, M. D. Ferguson, J. W. Lewellen, P. Mannes and T. W. Rose with G. F. Tellier as Project Engineer; the Program Manager was R. A. Byron. The report was compiled by Messrs. Tellier and Caywood.

Air Force Administration of the program was by the Air Force Rocket Propulsion Laboratory, Edwards Air Force Base with Lt. P. Olekszyk and J. Lawrence as Project Engineers for Phases I and II, respectively.

Specialized fabrication and preparation of test models was contracted with L. A. Gauge Co., Inc., Sun Valley, California, whose cooperation and interest is gratefully acknowledged.

This report was given Rocketdyne Report No. R-5494.



## ABSTRACT

Presented is a description of the work accomplished in summarizing current valve design technology and providing fundamental metal-to-metal seating characteristic design data.

The program was conducted in two phases.

Phase I <sup>is</sup> ~~was~~ a survey of pertinent patents, technical literature, and industry data to determine current technology levels and indicate specific areas where information was lacking or obsolete. The accumulated material produced little worthwhile information on either the mechanics of sealing or the correlation between theoretical and actual characteristics.

Phase II effort involved analytical and empirical studies of the detail aspects of valve sealing. Test models were fabricated with particular emphasis placed on describing the resultant sealing surfaces. Leakage flow data were obtained for the near-seated condition resulting in good correlation with theoretical predictions. The stress-leakage relationship in the on-seated condition was empirically investigated as a function of surface and material variations, pressure, and fluid. The resulting information, together with inspection evidence supporting deduced test surface finish conditions, is presented. A mathematical seat model and analytical technique was formulated which permits order-of-magnitude prediction of the stress-leakage characteristic and is presented in the form of derivation and graphs of parametric stress vs leakage data. ( )

## CONTENTS

Foroword . . . . .	iii
Abstract . . . . .	v
Introduction . . . . .	1
Survey . . . . .	3
Patent Search . . . . .	3
Literature Survey . . . . .	9
Industry Survey . . . . .	15
Definition of the Development Effort (Phase II) . . . . .	19
Surface Studies . . . . .	27
Surface Terminology and Representation . . . . .	27
Measuring Methods and Devices . . . . .	33
Real Surface . . . . .	40
Contact Area and Loading Effects . . . . .	44
Surface Study Results . . . . .	50
Leakage Flow Analysis . . . . .	53
Defining Parameters . . . . .	53
Simplified Flow Equations for Smooth Parallel Plates . . . . .	53
Static Pressure Distributions . . . . .	59
Sample Computation . . . . .	62
Nomenclature . . . . .	70
Surface Analysis . . . . .	73
Equivalent Spacing Heights for Surface Deviations . . . . .	74
Model Surface Deformations . . . . .	76
Stress-Leakage Equations . . . . .	88
Parametric Stress-Leakage Data . . . . .	91
Nomenclature . . . . .	100
Design, Fabrication, and Development of	
Test Fixture and Models . . . . .	103
Design . . . . .	105
Fabrication and Dimensional Check . . . . .	121
Development . . . . .	125
Surface Finishing of Models . . . . .	137
Preliminary Procedures . . . . .	137

Loose Abrasive (Wet) Lapping . . . . .	138
Dry Lapping . . . . .	140
Polishing . . . . .	142
Cleaning . . . . .	143
Model Inspection Equipment, Procedures, and Data . . . . .	145
Model Inspection Equipment . . . . .	145
Inspection and Data Interpretation Procedures . . . . .	181
Experimental Test Program . . . . .	185
Experimental Test Setup . . . . .	185
Assembly and General Test Procedures . . . . .	196
Near-Seated Tests . . . . .	200
On-Seat Tests . . . . .	214
Conclusions . . . . .	253
Recommendations for Future Effort . . . . .	257
References . . . . .	261
<u>Appendix A</u> . . . . .	A-1
Literature Survey . . . . .	A-1
Scope of Search . . . . .	A-1
Sources Searched . . . . .	A-3
Organization and Appraisal of the Literature . . . . .	A-5
1.0 Valve Selection and Evaluation . . . . .	A-7
2.0 Steady Flow Characteristics . . . . .	A-35
3.0 Steady-State Forces . . . . .	A-59
4.0 Transient Factors . . . . .	A-71
5.0 Valve Sealing . . . . .	A-85
6.0 Valve Design Data . . . . .	A-113
7.0 Books . . . . .	A-121
Author Index . . . . .	A-125
Late Entries . . . . .	A-129
Bibliography Subjects Index . . . . .	A-131
<u>Appendix B</u> . . . . .	B-1
Industry Survey . . . . .	B-1
Factors in Valve Design . . . . .	B-2
Classification of Valves . . . . .	B-4

Conical Poppet Seat Designs	.	.	.	.	.	.	.	.	.	B-7
Spherical Poppet Seat Designs	.	.	.	.	.	.	.	.	.	B-23
Flat Poppet Seat Designs	.	.	.	.	.	.	.	.	.	B-43
Special Poppet Seat Designs	.	.	.	.	.	.	.	.	.	B-69
Rotating Ball Designs	.	.	.	.	.	.	.	.	.	B-79

## ILLUSTRATIONS

1. Standard Surface Symbol With Representative Surface Characteristics . . . . .	30
2. Incremental Division of Theoretical Surface Profile . . . . .	31
3. Surface Symbol for Optical Measurement . . . . .	32
4. Stylus Interpretation of a Rectangular Shape . . . . .	34
5. Stylus Interpretation of a Combination Shape . . . . .	35
6. Light Interference With an Optical Flat . . . . .	37
7. Principle of the Light Section Microscope . . . . .	40
8. Pressure Profiles . . . . .	60
9. Typical 1.0-Inch Poppet and Seat Model . . . . .	63
10. Theoretical Nitrogen Flow Through The Valve Model Shown in Fig. 9 . . . . .	65
11. Model Surface Geometry With Defining Equations . . . . .	77
12. Average Height Values for Various Wave Forms . . . . .	78
13. Sinusoidal Model Surfaces . . . . .	82
14. Model of Hemispherical Nodule . . . . .	87
15. Typical 1/2-Inch Poppet and Seat Model . . . . .	92
16. Theoretical Parametric Stress vs Leakage Curves for Steel . . . . .	95
17. Theoretical Parametric Stress vs Leakage Curves for Aluminum . . . . .	96
18. Theoretical Parametric Stress vs Leakage Curves for Tungsten Carbide . . . . .	97
19. Division of Total Flow in Fig. 16 through 18 . . . . .	99
20. Valve Poppet and Seat Model Tester Assembly . . . . .	107
21. 1.0-Inch Model Seat . . . . .	109
22. Model Poppet . . . . .	110
23. 0.5-Inch Model Seat . . . . .	111
24. Piston Centering Force Diagram . . . . .	114

25.	Test Part Being Lapped . . . . .	139
26.	Test Model A, Seat, 0.0065 x 0.0065-Inch Interference Photo . . . . .	147
27.	Test Model A, Seat, 0.035 x 0.033-Inch Interference Photo Showing Dub-Off and Pressure Tap . . . . .	147
28.	Test Model A, Poppet, 0.0065 x 0.0065-Inch Interference Photo, Cross Lay . . . . .	147
29.	Test Model B, Poppet, 0.0065 x 0.0065-Inch Interference Photo Showing 0.0005-Inch Radius Profilometer Stylus Scratches . . . . .	147
30.	Test Model B, Seat, 0.033 x 0.033-Inch Interference Photo Showing Dub-Off . . . . .	149
31.	Test Model D, Poppet, 0.0065 x 0.0065-Inch Plain Photo Showing 0.0001-Inch Radius Proficorder Stylus Scratches . . . . .	149
32.	Test Model E, Poppet, 0.0065 x 0.0065-Inch Interference Photo, Cross Lay . . . . .	149
33.	Test Model E, Seat, 0.0065 x 0.0065-Inch Interference Photo, Cross Lay, Polished . . . . .	149
34.	Test Model E, Seat, 0.033 x 0.035-Inch Interference Photo Showing Polish-Caused Dub-Off . . . . .	151
35.	Test Model F, Seat, 0.0065 x 0.0065-Inch Interference Photo, Cross Lay, Narrow Bandwidth . . . . .	151
36.	Test Model F, Seat, 0.0065 x 0.0065-Inch Interference Photo, Cross Lay, Same Location as Fig. 35 Except Wide Bandwidth . . . . .	151
37.	Test Model F, Seat, 0.0065 x 0.0065-Inch Interference Photo With Lay Showing 0.0005-Inch- Radius Profilometer Stylus Scratches . . . . .	151
38.	Test Model F, Seat, 0.033 x 0.033-Inch Interference Photo . . . . .	153
39.	Test Model F, Poppet, 0.0065 x 0.0065-Inch Interference Photo, Cross Lay . . . . .	153

40.	Test Model G, Poppet, 0.0065 x 0.0065-Inch	
	Interference Photo, Wide Bandwidth . . . . .	153
41.	Test Model G, Poppet, 0.0065 x 0.0065-Inch	
	Interference Photo, Narrow Bandwidth Showing	
	Test Scratch . . . . .	153
42.	Test Model H, Poppet, 0.0065 x 0.0065-Inch	
	Interference Photo . . . . .	155
43.	Test Model H, Seat, 0.033 x 0.033-Inch	
	Interference Photo . . . . .	155
44.	Test Model I, Poppet, 0.0065 x 0.0065-Inch	
	Interference Photo . . . . .	155
45.	Test Model J, Poppet 0.0065 x 0.0065-Inch	
	Radius Proficorder Stylus Scratch . . . . .	155
46.	Test Model J, Poppet, 0.0065 x 0.0065-Inch	
	Interference Photo Showing 0.0005-Inch-Radius	
	Profilometer Stylus Scratches . . . . .	157
47.	Test Model J, Seat, 0.033 x 0.033-Inch	
	Interference Photo Showing Dub-Off . . . . .	157
48.	Test Model K, Seat, 0.0065 x 0.0065-Inch	
	Interference Photo Showing 0.0005-Inch-Radius	
	Profilometer Stylus Scratches . . . . .	157
49.	Test Model K, Poppet, 0.0065 x 0.0065-Inch	
	Interference Photo Showing 0.0005-Inch-Radius	
	Profilometer Stylus Scratches . . . . .	157
50.	Test Model K, Seat, 0.0065 x 0.0065-Inch Interference	
	Photo Across Circumferentially Polished Lay . . . . .	159
51.	Test Model K, Seat, 0.033 x 0.033-Inch	
	Interference Photo . . . . .	159
52.	Test Model K, Seat, 0.033 x 0.033-Inch	
	Interference Photo Showing Dub-Off . . . . .	159
53.	Optical Flat, 0.0065 x 0.0065-Inch	
	Interference Photo . . . . .	159

54.	Profilometer Stylus, 0.0005-Inch Radius, 0.016 x 0.016-Inch Plain Photo . . . . .	161
55.	Proficorder Stylus, 0.0005-Inch Radius, 0.016 x 0.016-Inch Plain Photo . . . . .	161
56.	Proficorder Stylus, 0.0001-Inch Radius, 0.016 x 0.016-Inch Plain Photo . . . . .	161
57.	Test Model A, Poppet Profile Record, Cross Lay . . . . .	163
58.	Test Model B, Poppet Profile Record . . . . .	163
59.	Test Model B, Seat Profile Record . . . . .	163
60.	Test Model C, Poppet Profile Record . . . . .	163
61.	Test Model D, Poppet Profile Record . . . . .	164
62.	Test Model H, Seat Profile Record . . . . .	164
63.	Test Model I, Poppet Profile Record . . . . .	164
64.	Test Model J, Poppet Profile Record . . . . .	164
65.	Cleveland and Johansson Indicating Comparitors and Test Poppet . . . . .	166
66.	Profilometer and Test Poppet . . . . .	168
67.	Proficorder Indicating Tester Piston . . . . .	169
68.	Proficorder Indicating Test Poppet . . . . .	170
69.	Optical Flat and Test Poppet Showing Helium Light Interference Bands . . . . .	177
70.	Leitz Interference Microscope and Test Seat . . . . .	178
71.	Leitz Microhardness Tester and Test Poppet . . . . .	180
72.	Experimental Setup Showing Tester With Pressure and Flow Instrumentation . . . . .	186
73.	Tester With Merns Electronic Indicator . . . . .	187
74.	Interior of Tester . . . . .	188
75.	Load Cell Electronics and Recorder . . . . .	189
76.	Test Setup Schematic . . . . .	190
77.	Nitrogen Flow Data, Part 1 . . . . .	202
78.	Nitrogen Flow Data, Part 2 . . . . .	203
79.	Helium Flow Data, Part 1 . . . . .	204
80.	Helium Flow Data, Part 2 . . . . .	205



81.	Argon Flow Data, Part 1 . . . . .	206
82.	Argon Flow Data, Part 2 . . . . .	207
83.	Laminar Pressure Distribution at Various Pressure Levels . . . . .	210
84.	Pressure Distribution vs Poppet Seat Height . . . . .	211
85.	Stress vs Leakage Data for Test Model A, Tests 1 and 2 . . . . .	216
86.	Stress vs Leakage Data for Test Model B, Test 3 . . . . .	219
87.	Stress vs Leakage Data for Test Model B, Tests 3 through 5 . . . . .	220
88.	Stress vs Leakage Data for Test Model C, Tests 6 and 7 . . . . .	222
89.	Stress vs Leakage Data for Test Model D, Tests 8 and 9 . . . . .	223
90.	Data Correlation for Test Models B, C, D, and K . . . . .	224
91.	Stress vs Leakage Data for Test Model E, Tests 10 and 11 . . . . .	227
92.	Stress vs Leakage Data for Test Model E, Test 12 . . . . .	229
93.	Stress vs Leakage Data for Test Model F, Tests 13 and 14 . . . . .	230
94.	Data Correlation for Test Models E, F, and G . . . . .	232
95.	Stress vs Leakage Data for Test Model G, Tests 15 and 16 . . . . .	236
96.	Stress vs Leakage Data for Test Models H and I, Tests 17 through 19 . . . . .	238
97.	Schematic of Poppet and Seat Model Gross Curvature . . . . .	240
98.	Stress vs Leakage Data for Test Model B, Tests 20 and 21 . . . . .	243
99.	Stress vs Leakage Data for Test Model J, Tests 22 and 23 . . . . .	247
100.	Stress vs Leakage Data for Test Model K, Tests 24 and 25 . . . . .	249

B-1.	Space Engine Regulator	B-8
B-2.	Hydraulic Relief Valve	B-10
B-3.	Ignition Monitor Valve	B-12
B-4.	Propellant Control Solenoid Valve I	B-14
B-5.	Propellant Control Solenoid Valve II	B-16
B-6.	Pneumatic Relief Valve	B-18
B-7.	Tank Vent Valve	B-20
B-8.	Piloted Solenoid Valve	B-24
B-9.	Snap Action Relief Valve	B-26
B-10.	Propellant Control Solenoid Valve III	B-28
B-11.	Propellant Control Solenoid Valve IV	B-30
B-12.	All-Metal Check Valve	B-32
B-13.	Inverted Relief Valve	B-34
B-14.	Absolute Pressure Regulator	B-36
B-15.	Hydraulic Control Solenoid Valve	B-38
B-16.	Precision Loader	B-40
B-17.	High-Pressure Relief Valve	B-42
B-18.	High-Pressure Relief Valve	B-44
B-19.	Fluorine Tank Relief Valve	B-46
B-20.	High-Capacity Relief Valve	B-50
B-21.	Electro-Pneumatic Thrust Controller	B-52
B-22.	Tank Pressurization Valve	B-54
B-23.	Regulator Inlet Valve	B-56
B-24.	Pilot Control Solenoid Valve	B-58
B-25.	Gas Generator Control Valves	B-60
B-26.	Low Temperature Relief Valve	B-64
B-27.	Vent Port Check Valve	B-66
B-28.	Fuel Igniter Shutoff Valve	B-70
B-29.	Two-Way Solenoid Valve	B-72
B-30.	Balanced Pressure Regulator	B-74
B-31.	Cylindrical Valve	B-76
B-32.	Propellant Ball Valve	B-80
B-33.	Cryogenic Ball Valve	B-82
B-34.	Propellant Control Ball Valve	B-84
B-35.	Propellant Butterfly Valve	B-88
B-36.	Modified Butterfly Valve	B-92
B-37.	Metal Seal Butterfly Valve	B-94

## TABLES

1. Summary of Patent Search Categories . . . . .	4
2. Noteworthy Patents . . . . .	8
3. Summary of Literature Survey . . . . .	11
4. Valve Seating Factors . . . . .	21
5. Comparison of Arithmetical Averaging Instruments . . . . .	35
6. Poppet and Seat Experimental Test Parameters . . . . .	104
7. Finishing of Poppets and Seats . . . . .	141
8. Poppet and Seat Model Inspection Data . . . . .	146
9. Comparison of Computed Equivalent Height Parameters ( $2h_e$ ) with Inspection Data . . . . .	251

## INTRODUCTION

Poppet and seat design is largely an individual effort in which the designer draws upon past experience, ingenuity, and a repertory of design data. The data, to a degree, is a measure of the designer's capability because there is seldom ample time or finances to undertake lengthy analyses or experimental evaluations. Because of the limited access of test-correlated design information, rocket engine valves are continuously being redeveloped throughout the missile and spacecraft industry. Attendant advances in the state-of-the-art have been slow with new developments obscured and often not pursued.

To reduce this waste, a program to create a component designers handbook has been instituted. Inputs from various contractors will cover the major aspects of component design endeavor.

This report describes the work accomplished by Rocketdyne in gathering the present technology in valve design and providing fundamental information in the area of least information, valve seating and leakage.

The program was conducted in two phases from July 1962 through October 1963. Phase I was a survey of patents, literature, and industry. The purpose of the survey was to compile existing data and direct the main effort of the program by defining the needs of valve designers. While information was found to be required in many facets of valve poppet and seat design, a concentration of the effort on the most specific problem area, valve seating, would result in more worthwhile data and avoid generalizations of little design value. Consequently, Phase II was devoted to a detailed analytical and experimental investigation of metal surfaces, their measurement, and a definition of some of the governing leakage equations. The experimental effort was confined to simple flat poppet and seat models fabricated and tested so that individual variables could be controlled, measured, and if possible, analytically correlated with

with seating equations describing leakage, seat-land pressure distribution, and surface deformations with load. Where correlation was not possible, the detail definition of the material and geometric surface properties provide a qualitative frame of reference for design purposes. Combined with an understanding of the configuration and deformation characteristics of surfaces, design decisions can be based on more than guess work.

## SURVEY

An extensive survey of patents, literature, and industry has been completed. The purpose of the survey phase was to compile existing useful design data and define the needs of valve designers based on an analysis of the survey results.

### PATENT SEARCH

#### Purpose

The purpose of the patent search was to uncover worthwhile designs not in common use.

#### Approach

The Manual of Classification for the U.S. Patent Office was analyzed for the classes most likely to contain pertinent material. Classes 137, (Fluid Handling) and 251 (Valves and Valve Actuation) were studied for applicable subclasses. Although class 137 contained all line condition change responsive valves, i.e., check valves, regulators, relief valves, dealing in valves per se, class 251 was considered more directly applicable to poppets and seats. Class 251 definitions were obtained, and further study resulted in ordering original and cross-reference patent lists for the 26 subclasses (Table 1).

An analysis of the patent lists and a short computer program to sort duplicate numbers from cross references led to ordering 273 original and 248 cross-reference patents. The original patents covered all those filed in the 26 subclasses from patent number 2,500,000 (approximately

TABLE 1

## SUMMARY OF PATENT SEARCH CATEGORIES

Subclass No.	Name	Original Patents (No Duplicates)					Cross Reference Patents Including Duplicates			Cross Reference Patents Without Duplicates 1955	Duplicates 1955
		1955	1950	1945	1940	Total	1955	1950	Total		
12	Fluid Actuated or Retarded	--	--	--	--	--	--	--	--		
61	Diaphragm or Bellows Type	33	57	64	79	138	169	343	974		
62	Piston Type	13	24	28	31	74	128	211	735		
75	With Snap Actuation	8	15	18	26	86	108	274	417		
281	Balanced Valves	0	0	1	1	11	5	10	29		
282	Reciprocating	10	15	15	18	43	132	155	343		
304	Rotary Valves	0	0	0	0	10	17	21	104		
305	Butterfly	4	6	7	8	18	34	49	149		
306	Head and/or Seat Packing	19	21	22	22	34	36	37	47	31	5
309	Plug	7	10	11	14	43	23	34	130		
314	Seate and/or Interface Seals	3	5	6	7	18	13	18	51	10	3
315	Spherical Head	8	10	11	13	17	52	59	87	47	5
318	Reciprocating Valve	--	--	--	--	--	--	--	--		
324	Piston	5	10	13	14	33	59	79	212		
326	Gate	4	4	5	7	22	24	39	198		
327	Bifaced	9	13	16	19	49	38	47	167		
328	Seate	9	15	15	18	59	57	64	137		
331	Diaphragm	19	26	28	33	44	55	91	198		
356	Valve	1	2	3	5	24	28	41	154		
357	Removable Seat Engaging Element	7	13	16	22	82	78	145	626	18	11
358	Reinforced Flexible Material	4	6	7	9	39	29	37	110	16	1
359	Seats	1	3	10	13	50	17	41	164		

TABLE 1  
(Continued)

Subclass No.	Name	Original Patents (No Duplicates)					Cross Reference Patents Including Duplicates			Cross Reference Patents Without Duplicates 1955	Duplicates 1955
		1955	1950	1945	1940	Total	1955	1950	Total		
360	Removable	2	3	4	9	33	48	76	364	32	16
361	Mounted Between Casing	1	3	4	6	19	42	62	247	32	10
362	Compression or Tension Retained	3	3	3	4	23	28	44	88	22	6
363	With Seal	2	4	6	8	21	47	73	172	27	20
364	Head Engaging Gasket	0	3	3	5	13	25	30	59	12	13
365	Retained by Seat Deformation	0	0	3	1	19	3	3	16	1	2
	TOTALS	174	273	321	397	1022	1295	2085	5978		
	TOTALS						340			248	92
						THESE PATENTS ORDERED					

NOTE: Patents From Approximate Date Noted to 7/26/62

Exact Patent Numbers Represented by Dates

1940 2,150,000  
1945 2,350,000  
1950 2,500,000  
1955 2,700,000



1950) up to 26 July 1962. The cross references were sorted from 2358 patent numbers comprising the original and cross-reference patents in the 26 subclasses spanning the same period. Because of the quantities involved, only cross-referenced patents from 11 of the 26 subclasses were ordered from patent number 2,700,000 (approximately 1955) up to 26 July 1962.

The patents were given three separate appraisals. The first appraisal categorized the patents as "not applicable" and "possibly applicable." The potentially useful patents were then more carefully screened for potential application and/or useful ideas. A close examination of the remaining patents was made by the responsible program personnel.

A meeting held with Space Technology Laboratories (STL) to compare the Rocketdyne program with their advanced valve program (NASA) resulted in obtaining 80 valve patents from their search. These patents were assessed, bringing the total number of patents covered to 601.

### Results

Table 1 summarizes the numerical results of the search. Of particular note is the number of cross-reference duplicates (92 out of 340 or 27 percent).

A study of the 273 original patents revealed no useful designs. Furthermore, the general application of the vast majority of the original patent valves would be industrial with little relation to the commonly recognized aircraft configurations. The cross-reference patents contained 11 designs of interest viz., six ball valves, two butterfly valves, and one expansible sleeve valve. A review of STL patents indicated seven designs of interest comprising four poppet designs of known aircraft application, two ball valves, and one self-aligning poppet arrangement.

These noteworthy designs are listed in Table 2 with pertinent data and a brief description of key features. Except for the valves of known aircraft application, further consideration of these designs might show some to be worthwhile approaches.

### Conclusions

Appraisal of the search approach and the results obtained has led to the following conclusions:

1. The key features claimed in patents are, in most cases, unproved and buried under wording which necessitates careful study by experts to ascertain net worth. Even then the results of the study are of questionable value.
2. A small cross section of the patent literature has been reviewed. A rough estimate of the time required to search the 512 most pertinent subclasses of classes 137 and 251 through 1950 can be obtained by extrapolating the data of Table 1 (26 subclasses partially reviewed). Such an estimate indicates that the patent files contain approximately 5400 original and 14,000 cross-reference patents. Considering the manhours expended by Rocketdyne to study 600 patents, the 19,400 patents could require up to 5 man-years to digest. A complete search would probably exceed 10-man-years. In view of this appraisal, it is concluded that the attempt to uncover worthwhile approaches to poppet and seat design through a patent literature search is not economically productive or even feasible in the manner described herein.

TABLE 2

## NOTECORTHY PATENTS

Issue Date	Patent No.	Classification	Source	Assignee	Valve Name	Remarks
4/57	2,788,016	137-246.19	XR*	Rockwell Mfg. Co.	Ball Valve	Plastic lubricant ported to sealing surface for seal and ease of actuation
5/56	2,747,608	137-325		Grove Valve and Regulator Co.	Expandible Sleeve	Reinforced resilient sleeve controls flow through a fluted barrier
5/62	3,036,600	137,625.12		Fisher Governor Co.	Ball Valve	Tested at 1000 psig with liquid oxygen; protected lip seal design with throttling holes
2/56	2,734,715	251-171		Hydril Co.	Ball Valve	Plastic seal mechanically pressurized for seal; removed before actuation
12/60	2,963,262	251-172	XR	H. J. Shafer, Ohio	Ball Valve	Vented O-ring to prevent blowout
3/62	3,026,083	251-173		United Kingdom Atomic Energy Authority, London	Butterfly Valve	Pressurized metal sleeves effect seal with O-ring on gate
4/57	2,789,785	251-174		Standard-Thomson Corp.	Butterfly Valve	Oval-shaped gate seals against flexible metal sleeve
6/59	2,890,856	251-174		ACF Industries, Inc.	Ball Valve	Metal lip seal pressure deformed in operation
3/60	2,930,576	251-175	STL**	Worcester Valve Co.	Ball Valve	Floating seals allow seal on downstream side only for free rotation
11/60	2,959,188	137-540		H. G. Kepner, Illinois	Poppet Check Valve	Incorporates O-ring seal in proven design (Kepner Products)
12/58	2,863,473	137-599.2		V. W. Eckel, Calif.	Balanced Solenoid Valve	Unique flow passage design for inline balanced solenoid valve
6/61	2,989,990	137-625.42		General Dynamics Corp.	Ball Valve	Special seal design for sea water (submarine) service
4/60	2,934,090	137,625.5	STL	Marotta Valve	Three-Way Solenoid Valve	Valve used extensively in aerospace industry (plastic seats)
6/58	2,840,336	251-85		Hydro-Aire, Inc.	Poppet Valve	Self-aligning poppet and seat incorporating a soft seal
10/58	2,768,806	251-174		Koehler Aircraft Products	Ball Valve	Spring-loaded seal mechanism incorporating a thin resilient sheet
2/62	3,022,972	251-362		Marotta Valve	Poppet Valve	High-pressure valve seat of plastic construction

\* Cross reference patents obtained by Rocketdyne

\*\* Space Technology Laboratories, Inc.

## LITERATURE SURVEY

### Purpose

The purpose of the literature survey was to (1) assess the available literature on the pertinent aspects of valve design and thus facilitate direction of the development phase of this program, and (2) present the literature in a bibliographic form expressly suitable for use in valve design.

### Approach

An attempt was made to obtain all of the pertinent literature, and much of what was considered potentially applicable, through an exhaustive literature search. The methods and scope of the search are in Appendix A with the bibliography.

Briefly, the search consisted of a thorough review of all pertinent index-type references and available card catalogues considered useful in the Los Angeles area. Fourteen technical indexes and five card catalogues were searched under 47 categories. These sources covered domestic and foreign translations of reports, articles, bibliographies, texts, and graduate theses. The time spanned by these sources was approximately 1951 to 1962. Material through the classification of secret was reviewed. The total number of references extracted was approximately 600; however, only the most applicable 286 references were retained for inclusion in the bibliography.

### Organization and Appraisal of the Literature

The literature has been organized under 7 major headings and 24 sub-headings to facilitate retrieval and over-all appraisal.

All but 49 of the 286 documents referenced were examined for subject content under the various subheadings. In addition to the primary topic, subject matter which was considered to be useful to valve designers is noted following the abstract and also referenced within the applicable subsections.

The references and cross references within a specific heading combine to make up the total literature available on that subject. If it is assumed that the references cited represent all available literature, at least on the most pertinent subjects, an appraisal of the extent of literature published would be useful for ascertaining areas requiring additional research. While no claims for such completeness can be made, a review of the citations within each reference has shown that virtually all pertinent literature has been referenced; therefore, the indication of exhaustiveness is evident.

Table 3 summarizes the numerical results of the survey. The first chart shows the number of references and cross references contained within each subsection along with the percent of total references. With these data, the gross quantity of published information on a given subject can be ascertained.

The second bar chart uses the subject appraisal of each document to show the total subject material within a given subsection. Each bar represents the sum of the original references plus the total of the individual subjects contained within each reference. (The 15 percent of the literature not obtained for appraisal is not included.) The subsections spanned by the subject matter are indicated by the number at the end of each bar. With the aid of this chart, the scope of subject material covered by each subsection can be determined. Therefore subsections such as 1.3 and 7.0 covering numerous subjects, are readily recognized.

TABLE 3  
SUMMARY OF LITERATURE SURVEY

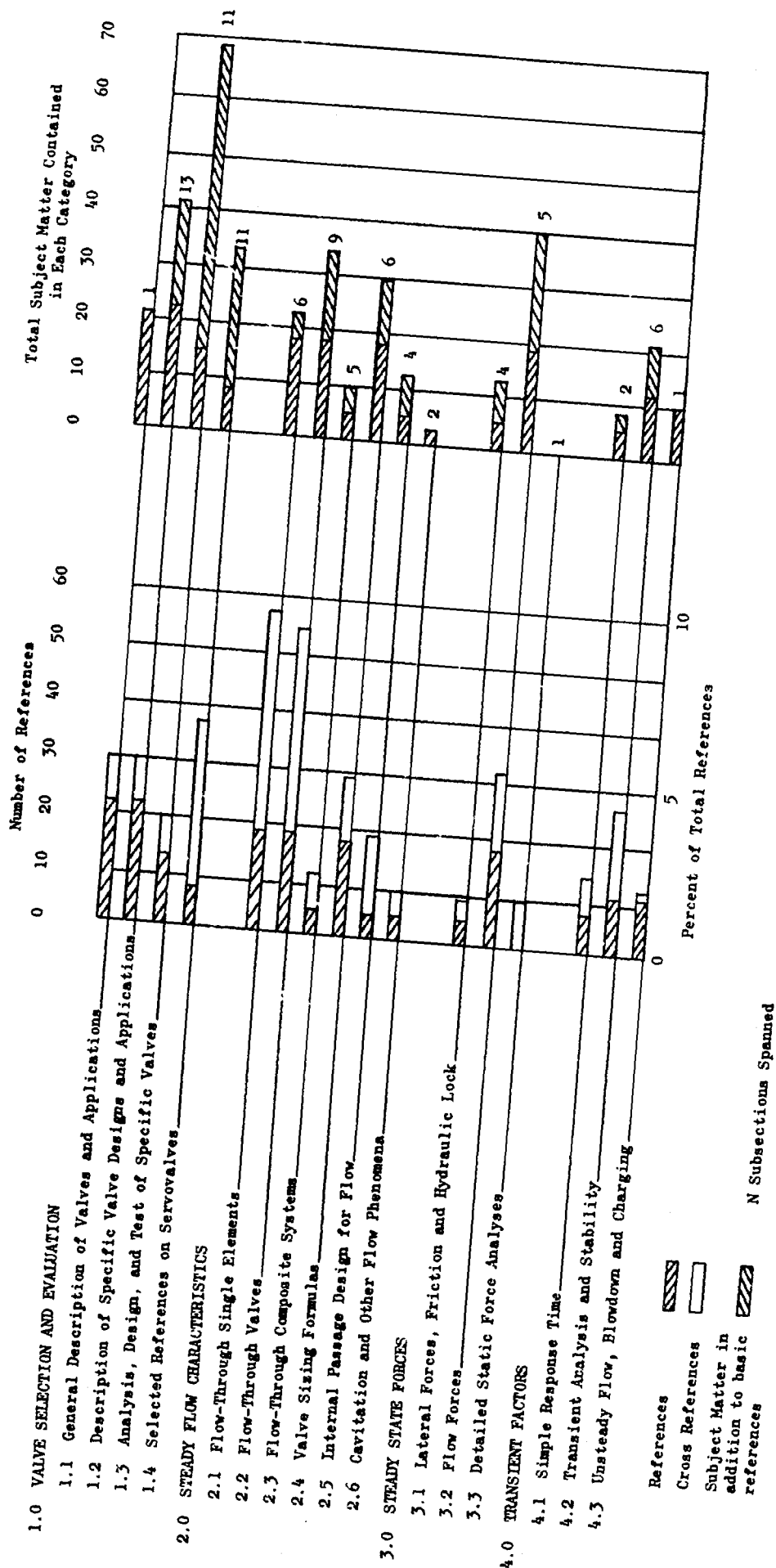
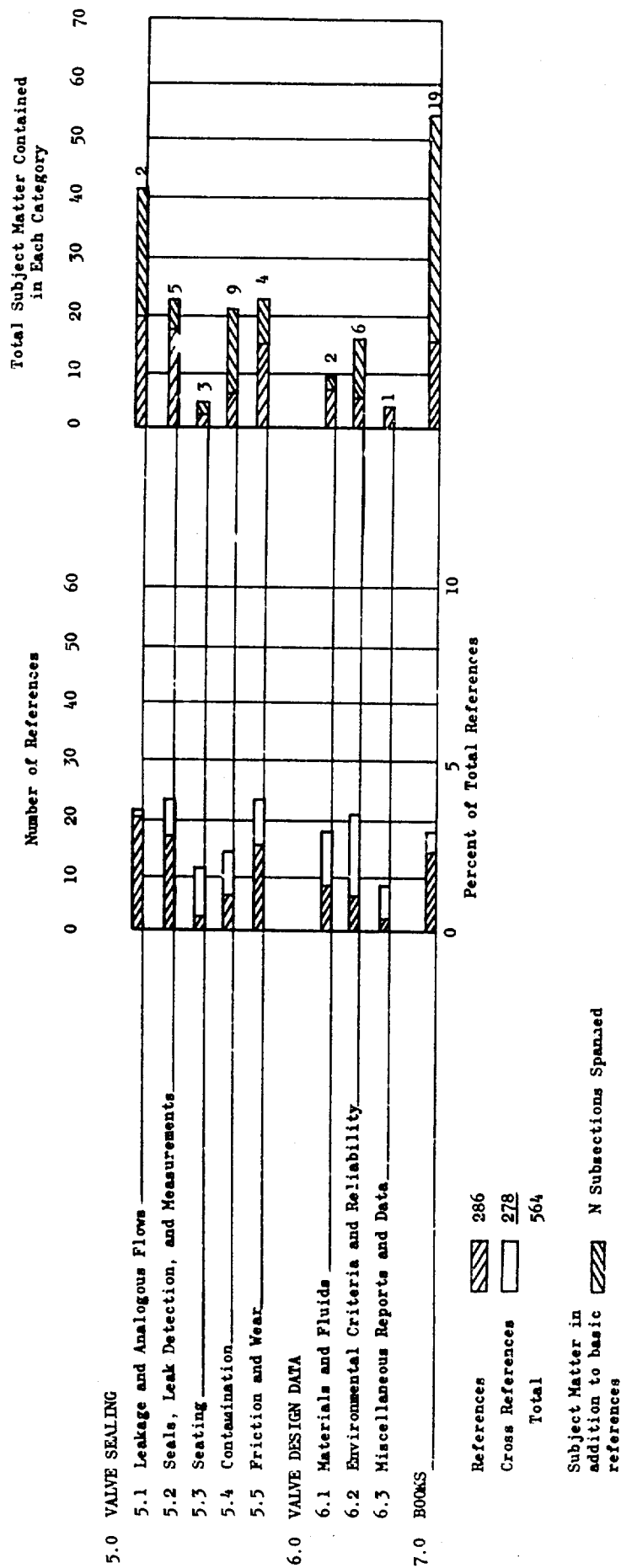


TABLE 3

(Continued)



A count of the references and their industry orientation shows that 175 of the 286 references are on valves per se (61 percent). Of these, 59 percent are aircraft oriented. The over-all orientation of the bibliography is aircraft with 197 of the references so cited.

### Conclusions

Analysis of the bibliography and Table 3 has led to the following conclusions:

1. Excluding material on servovalves, there are no definitive articles, books, or reports dealing broadly with the general subject of rocket and spacecraft valve design. Furthermore, only one article was found (7.0-12, "Handbook of Astronautical Engineering") describing a group or class of such aerospace valves for the purpose of selection or evaluation (such as in subsection 1.1, "General Description of Valves and Applications," which is entirely on industrial valves).
2. Except for the literature on servovalves, the state-of-the-art development programs of subsection 1.3, "Analysis, Design, and Test of Specific Valves," are the most comprehensive documents published on aerospace valves. However, because these programs were hardware oriented, very little attempt was made to correlate analyses with results (or draw pertinent conclusions). Their value to valve designers and this program is depreciated accordingly.
3. Analytically correlated design information pertaining to flow is restricted almost entirely to subsection 2.1, (orifice, venturi, fitting, labyrinth, pipe, etc.).
4. There is almost no information on passage design for flow. What is available requires tedious study of the detail designs and flow data. Because techniques of gaseous flow measurement used by most valve manufacturers are accurate to at best 10 percent, the results of such a study would be equally uncertain.



However, there is a preponderance of flow-formula data to the point of confusion. These data can result in serious errors in sizing aerospace valves.

5. Other than butterfly and servospool valves, there is little information on the subject of flow forces. A recent ASME paper (3.2-7, "Discharge Coefficients and Steady State Flow Forces for Hydraulic Poppet Valves" by J. A. Stone) discusses the results of analysis and test on hydraulic poppet valves but does not cover effects in the near-seated condition. There is no literature in the bibliography on the effect of flow forces on ball valves.
6. What little practical data is available on transients requires boiling down (rules-of-thumb and handbook data) for the average designer. A study of the servovalve literature would probably be rewarding in this area.
7. The literature on valve sealing, covering aspects of leakage, seals, seating, contamination, and wear, contains a minimum of analytical design information. The numerous references cited in subsection 5.1 are predominantly analogous flows (this information has been included to facilitate leakage studies).
8. Although appraisal of the literature could only be done on a surface basis because of the quantity involved, it was the consensus that in original work, the correlation of analysis with test is seldom done except in journals similar to those of ASME, MIT efforts, etc. Apparently, unless the "why" is being financed, no efforts are made to validate calculations other than a successful end product (usually hardware). The result is (1) the loss of much valuable design information, and (2) a preponderance of questionable derivations that are frequently misleading.
9. Reliability in valves was the subject of only one reference (6.2-2, "A Theoretical Technique for Predicting the Reliability of Solenoid Valves" by G. M. Eisendohr) in which an attempt was made to mathematically correlate the reliability of an aircraft solenoid valve with certain key design parameters.

The literature expounds upon reliability as of paramount importance in design. However, to be predictably reliable, the performance must first be either analytically or statistically predictable. Very little analytical correlation is evidenced in the literature, and proving reliability statistically is impossible with the normally few components available.

It is concluded that to obtain state-of-the-art advancements in reliability, the performance predictability of valves must be enhanced through correlation of analyses with actual tests and thus obtain an understanding of the "why" of the performance. This effort will lead to advances in performance.

## INDUSTRY SURVEY

### Purpose

The purpose of the industry survey was to (1) establish poppet and seat design approaches, fabrication, and analysis as is presently represented within industry, and (2) assist in defining the Phase II development effort.

### Approach

Form letters were sent to 210 aerospace valve manufacturers in an attempt to contact a realistic cross section of industry within the limited survey time. The letter presented the object of the program and invited the manufacturers' cooperation in compiling information for a component designer's handbook. Specific information requested by the letter is reproduced below.

A. Please furnish cutaway drawings, with lists of material, of typical valve closure mechanism designs that reflect your organization's most current design efforts. Selection of these designs shall be based on the following requirements:

1. Designs must have satisfactorily completed a period of development and/or intended use.

2. Configurations of valve closure mechanisms may include (1) conical, spherical, and flat poppet and seat, (2) rotating ball, (3) butterfly, or (4) other proven configurations. Any type of valve may be utilized that exemplifies typical designs manufactured by your company, such as check, solenoid, relief, regulators, pressure actuated, etc.
3. Cylindrical slide and sleeve (spool) configurations normally used for hydraulic system selector, sequence and/or servo control, are categorically excluded from the program due to other previous extensive work in this area.

B. To allow a useful classification and parametrization of the designs, it is necessary that the following information be included with each design submitted:

1. A brief description, including applications and outstanding features.
2. Key parameters, with a minimum of those listed below:
  - a. Fluids tested with and/or designed for (indicate if tests were with fluid other than the design fluid).
  - b. Operating pressure range (primarily applicable to specific poppet and seat).
  - c. Operating temperature range (including ambient and line fluid).
  - d. Flow capacity (this value may be in the forms of equivalent orifice diameter and  $C_d$ , flow coefficient, or flow curves).
  - e. Endurance, cycles (list the test temperature and pressures).
  - f. Leakage (list test pressure, temperature and fluid).
  - g. Vibration characteristics.
  - h. Port sizes (inlet and outlet).
3. Describe advantages and disadvantages of valve closure mechanism. This list should be completed with reference to the intended application as well as potential extended service.
4. Outline any useful analytical approaches to the poppet and seat design that have been correlated with test results.

C. General valve design data, either analytical or empirical, internally published in the form of charts, tables and graphs which would advance the capabilities of valve designers would be appreciated.

Personal interviews were conducted with the engineering management of 22 valve firms within the Los Angeles metropolitan area to support and implement the letter request. The interviews were to accomplish the following:

1. Enlist the cooperation of the manufacturer by presenting advantages of the program to the valve industry.

2. Discuss the manufacturer's designs to determine program applicability and obtain the specific information requested in the letter.
3. Determine the manufacturer's general approach to valve design and analysis.
4. Coevaluate the needs of industry for poppet and seat research.

To use Rocketdyne aerospace valve experience, Rocketdyne furnished information in accordance with the letter to industry.

### Results

Analysis of the returns indicated that 67 of the 210 contacts responded; of those, 37 contributed information in varying amounts with the remainder declining to submit data for several reasons, i.e., insufficient time, proprietorship, inapplicability, etc. Because of limited time and late arrival of considerable material, data from only 10 sources could be assimilated. Those manufacturers providing comprehensive information as requested in the letter have been rated excellent, regardless of the time element.

Within the scope of the survey program, more material was received than could be processed. Inclusion of the data received late or which required additional processing time, could not be included in the final report because of financial limitations.

Handbook Data. Reliable valve designs and state-of-the-art advancements stem from a systematic evaluation of the over-all design problem, unconfined by archaic rules, particularly in the configurational stage. Generalizations often convey confusing contradictions and tend to become rules which limit new concepts. The handbook information resulting from the survey has been prepared to avoid these pitfalls while still providing data on numerous valve designs. Appendix B shows 37 proven

valve designs representing the state-of-the-art in which the salient features of performance and construction have been noted in addition to information on application, fabrication, advantages, and disadvantages. Limitations of the data are covered in the report.

The report outlines factors in valve design as information useful for valve evaluation and design and a classification of valves to assist in standardization. It also provides a common ground for aerospace terminology.

### Conclusions

Consideration of the survey results has led to the following conclusions:

1. Insufficient data were received from industry to allow parameterization of the key features and functional parameters of aerospace valves. Had sufficient information been received, considerably more time would have been required to prepare it for publication.
2. The manufacturing information essential to a complete understanding of the valve design and why it performs is extremely limited. Such information is considered proprietary by practically all manufacturers and is predominantly maintained as shop and assembly know-how.
3. The personal interviews have shown that the pressures of maintaining a competitive position in the industry generally curtail the analytical effort expended in designing new valves. It is usually found more economical to combine a minimum analysis (static force and flow capacity) with designer-company experience in producing a prototype, which can be modified through test, to meet design requirements. What correlated design data industry has is for the most part directly related to a specific line of

valves and considered proprietary. The application of this type of information to the program is questionable because it generally takes the form of raw test data and would require considerable evaluation and editing for handbook publication.

4. The expressions of nearly all manufacturers have shown that the know-how most needed to advance the state-of-the-art is in the field of valve seating, with emphasis being placed first on leakage and second on near-seated flow forces (depending on the manufacturer's product). Flow capacity and transient analysis are also recognized as areas requiring effort but more for optimization as evidenced by the relative ease with which flow areas and actuator forces can be changed.

#### DEFINITION OF THE DEVELOPMENT EFFORT (PHASE II)

The survey phase resulted in an organized classification and bibliography of the published literature in addition to an extensive representation of state-of-the-art valve designs. A detailed analysis of the survey data clearly indicated the almost total lack of basic information on valve seating and leakage.

Valve seating, which is the very heart of valve design, is probably the most tested, most questioned, and still the least understood part of poppet and seat design. Typical questions asked by experienced component designers are:

1. How does fluid leakage vary with load, contact area, land width, surface finish, and various material properties?
2. If fluid conditions are changed through a variation in pressure, temperature, or by exchanging fluids, what is the resultant leakage?
3. What are the motions of poppets and seats during transitional seating, and how do these motions affect leakage and other poppet functions?

4. What are the characteristics of the wear processes beneficial and detrimental to sealing?
5. What are the characteristic sealing properties of metal seats in the first 50 millionths of an inch of metal structure?
6. What is the pressure distribution across the seating land open and closed (i.e. effective area), and how does the distribution vary with opening?

This situation is odd because the valve closure receives most consideration in flyable hardware because of power and weight limitations. However, the great number of interrelated variables and inaccessability of adequate measurement equipment combine to impose a severe economic retardant upon the development of even a general understanding, let alone quantitative definition of the seating characteristics. Furthermore, when outstanding performance is achieved by some novel configuration or fabrication process the information is considered proprietary information. Even in these cases, the reasons behind a specific performance is seldom understood, and explanations range far and wide.

The process of economically bringing two pieces of material together to close off a flow of fluid is not a simple one. An examination of the known variables reveals an intermingling of many specialities, e.g., metrology for precision measurements, fluid mechanics for leakage analysis, physical chemistry for surface compositions and interactions between seating materials and fluids, stress analysis for seating stresses, and deformations and basic research in surface contacts, friction, and wear to provide a background of experimental evidence supported by learned theory.

Table 4 is an outline of the valve seating factors considered in defining the scope and depth of the Phase II effort. Because of the extremely complex nature of valve seating, only a few of the almost unlimited variables and combinations could be examined either empirically or analytically. An attempt has been made to reduce the variables to a recognized few which can be successfully approached and used in solving future valve seating problems.

TABLE 4

VALVE SEATING FACTORS

1. SYSTEM AND ENVIRONMENTAL PARAMETERS
  - A. Fluid properties
    1. Density
    2. Viscosity
    3. Thermal conductivity
    4. Specific heat
    5. Vapor pressure
    6. Lubricity and corrosivity
    7. Surface tension
  - B. Pressure
    1. Static, internal, external,  $\Delta P$
    2. Fluid inertia, dynamic shocks, and cavitation
  - C. Fluid contaminants
    1. Metallic and hydrocarbon solids, oxides, etc.
    2. Water and ice
  - D. Environment
    1. Temperature
    2. Vibration, acceleration, and shock
    3. Vacuum
    4. Radiation
2. DESIGN PARAMETERS
  - A. Poppet and seat interface and closure geometry
    1. Concentricity
    2. Normality
    3. Sphericity
    4. Roundness
    5. Flatness



TABLE 4

(Continued)

6. Angularity
  7. Clearances
  8. Length-to-diameter ratio
  9. Self-alignment capability
  10. Average surface finish (AA)
  11. Topography, texture, and general surface lay
  12. Scratches, nodules, and pits
  13. Radii
  14. Contact land width
  15. Contact area
- B. Forces
1. Near seated pressure forces
    - a. Total acting on poppet
    - b. Across seat land
  2. Seated Forces
    - a. Theoretically perfect geometry
      - (1) Actuation force
      - (2) Pressure force over flow area
      - (3) Pressure force over seat land
      - (4) Coordinate seating forces
    - b. Eccentric and abnormal loading
    - c. Friction
    - d. Cyclic impact
- C. Material properties of closure interfaces (surfaces)
1. Moduli
  2. Yield strength
  3. Shear strength
  4. Tensile strength

TABLE 4

(Continued)

5. Hardness
6. Wear properties
7. Density
8. Specific heat
9. Thermal conductivity
10. Coefficient of expansion
11. Impact properties
12. Fatigue properties
13. Frictional properties
14. Corrosive properties
- D. Stress distribution and deformations of closure interfaces (surfaces)
  1. Theoretically perfect geometry
  2. Imperfect geometry
    - a. Angular conic
    - b. Out of round conic
    - c. Ellipsoidal sphere
    - d. Convex, concave, or wavy flat
  3. Surface microstructure (texture)

The general approach taken to encompass the study of seating is to design a tester capable of functioning like a valve while allowing accurate and precise measurements of position, loads, pressures, leakage, deformations, etc. Because a valve must operate for a large number of cycles (100 to more than 1,000,000), the cyclic effects are paramount. Many valves have been designed that function perfectly as a static seal, these are termed failures. Consequently, the tester must be additionally capable of cycling the poppet and seat in a controlled manner so that quantitative data on load, leakage, and the wear phenomena can be observed, recorded, and measured.

Before dynamic effects can be studied, however, the static characteristics of the seating variables must be ascertained for comparison purposes. The stages of operation in poppet-type valves are full open, partially open, just contacting, and fully closed or loaded. To provide a complete range of flow data and correlation between raw fabricated surfaces contacted but unloaded, study of the near-seated position must precede the on-seat and loaded condition. The near-seated region is defined as that separation from the seat which encompasses a complete transition through the various regimes of flow. Variation in effective seating area resulting from changes in pressure distribution can be evaluated in this region because there is evidence that dynamic instability of pressure-sensitive valves might be triggered by or a function of such nonlinear forces.

Concurrent with the tester design, an analytical study is required to (1) define metal surfaces normally associated with valve seats, (2) develop suitable leakage flow equations, and (3) combine the findings of (1) and (2) into a mathematical description of model seating surfaces so that the effects of variation in the many parameters could be evaluated and correlated with the experimental results.

A major decision is the size and configuration of the poppet and seat models. In consideration of the difficulties in suitably describing large, and thus easily defined and fabricated models of hypothetical

surfaces, a more practical approach would be to fabricate actual valve seating surfaces to span the known range of leakage performance. The resulting test data, backed by complete inspection records, would thus be of direct design value in comparison with actual valve performance characteristics.

A summary of the Phase II effort is outlined below. The scope of the effort was narrowed during Phase II excluding investigation of spherical and conical seats (as originally planned) in favor of more extensive testing on flat seats. The configurational aspects of valve seating, along with a study of various seat coatings, is to be the subject of a future program.

1. Investigation of variables

- A. Fabrication methods for fine metal surfaces
- B. Microgeometry of metal seating surfaces
- C. Physiochemical properties of metal surfaces
- D. Leakage flows
- E. Seating forces, stress and deformations considering land width, contact area, surface finish and material properties
- F. Variation of leakage with seat load

2. Design and fabrication

- A. Test fixture capable of performing static tests, on and off-seat, and dynamic cycle tests with flat, conical and spherical poppets and seats
- B. Poppet and seat models covering a range of material properties

3. Test program parameters with leakage as the dependent variable and load the independent variable

- A. Off seat height
- B. Pressure distribution across seat land

- C. Seat land width
  - D. Fluid properties
  - E. Surface texture
  - F. Flatness
  - G. Scratches
  - H. Parallelism
4. Test fluids
- A. Nitrogen
  - B. Helium
  - C. Argon

## SURFACE STUDIES

Considerable work has been done in recent years to explain and define the phenomena of friction and wear. Optical and mechanical instruments have been developed to observe and measure the minute structure of surfaces. Surface contact theories have evolved from data from numerous experimental research programs which have synthesized models of surface asperities amenable to an analytical treatment. Evaluation of the accumulated results of these many researchers, combined with a knowledge of the detail surface finishing methods, will support analysis of the mechanism of valve seat leakage.

### SURFACE TERMINOLOGY AND REPRESENTATION

Definitions of terms relating to the subject are given as well as parameters which generally describe the average surface. The following definitions have been extracted from Ref. 2.

#### Surface Texture

Surface texture is concerned with the geometric irregularities of solid surfaces produced by the various machining and finishing processes. It is the repetitive or random deviations from the nominal surface which form the pattern of the surface.

Nominal Surface. Nominal surface is the intended surface contour, the shape and extent of which is usually shown and dimensioned on a drawing or descriptive specification.

Profile. The profile is the contour of a surface in a plane perpendicular to the surface, unless some other angle is specified.

Centerline (Median Line). The centerline is the line about which roughness is measured, and is the line parallel to the general direction of the profile within the limits of the roughness-width cutoff, such that the sums of the areas contained between it and those parts of the profile which lie on either side of it are equal.

Roughness. Roughness consists of the finer irregularities in the surface texture usually including those irregularities which result from the inherent action of the production process. These are considered to include traverse feed marks and other irregularities within the limits of the roughness-width cutoff.

Roughness Height. Roughness height is rated as the arithmetical average deviation expressed in microinches measured normal to the centerline.

Roughness Width. Roughness width is the distance parallel to the nominal surface between successive peaks or ridges which constitute the predominant pattern of the roughness. Roughness width is rated in inches.

Roughness-Width Cutoff (Sampling Length). The roughness-width cutoff is the greatest spacing of repetitive surface irregularities to be included in the measurement of average roughness height. Roughness-width cutoff must always be greater than the roughness width to obtain the total roughness height rating. In most electrical averaging instruments, the roughness-width cutoff can be selected. It is a characteristic of the instrument rather than that of the surface being measured. In selecting the roughness-width cutoff, care must be taken to choose a value which will include all of the surface irregularities which it is desired to assess. Roughness-width cutoff is rated in inches, and standard values include 0.003, 0.010, 0.030 and 0.100.

Waviness. Waviness is the usually widely spaced component of surface texture and is generally of wider spacing than the roughness-width cut-off. Waviness may result from such factors as deflections, vibration, chatter, heat treatment, or warping strains. Roughness may be considered as superimposed on a wavy surface.

Waviness Height. Waviness height is rated in inches as the peak-to-valley distance.

Waviness Width. Waviness width is rated in inches as the spacing of successive wave peaks or successive wave valleys.

Lay. The lay is the direction of the predominant surface pattern ordinarily determined by the production method used.

Flaws. Flaws are irregularities which occur at one place, or at relatively infrequent or widely varying intervals in a surface. Flaws include such defects as cracks, blow holes, checks, ridges, and scratches. Unless otherwise specified, the effect of flaws is not included in the roughness height measurements.

### Surface Symbols

The symbol used to designate surface irregularities is the check mark with the horizontal extension (Fig. 1).



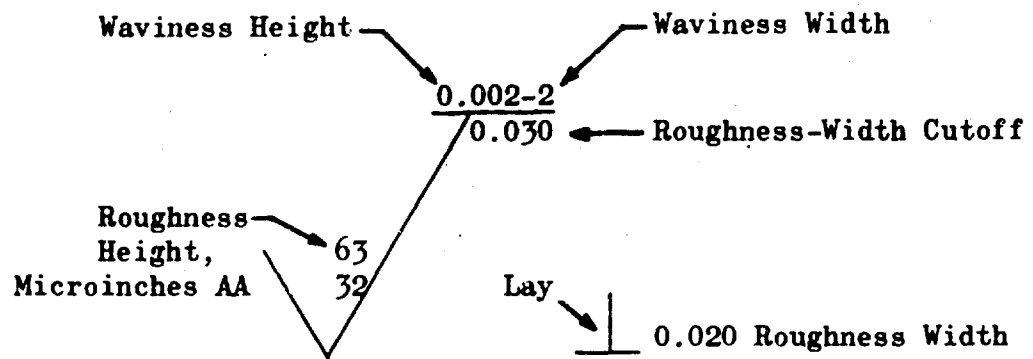


Figure 1. Standard Surface Symbol With Representative Surface Characteristics

### Arithmetical Average

The arithmetical average deviation from the centerline may be described in the following form.

$$AA = \frac{1}{l} \int_{x=0}^{x=l} |Y| dx$$

where

$Y$  = ordinate of the curve of the measured profile

$l$  = length over which the average is taken

An approximation of the average roughness may be found by adding the absolute value of the  $Y$ -increments and dividing the sum by the number of increments taken (Fig. 2).

$$AA = \frac{Y_a + Y_b + Y_c \dots \dots + Y_n}{n}$$

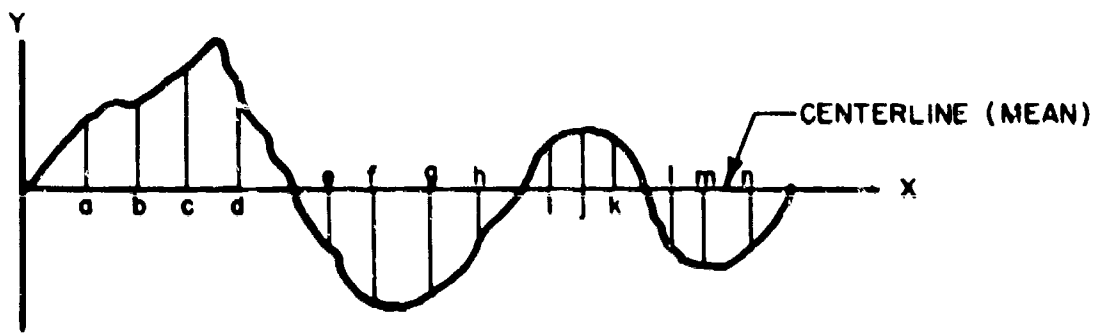


Figure 2. Incremental Division of Theoretical Surface Profile

Another method of measuring the average deviation is the root-mean-square (rms) technique which has had much usage in the past. This average is defined by

$$\text{rms} = \left[ \frac{1}{l} \int_{x=0}^{x=l} Y^2 dx \right]^{1/2}$$

and, as with the approximate method for AA above, may be found by squaring each value of the Y-increment, summing and dividing by the number of increments, and then taking the square root. The effect is to weight the larger heights. Instruments designed for rms roughness values read somewhat higher (Fig. 2) than those calibrated for arithmetical average when compared on a given surface. The arithmetical average method has replaced the rms technique as an index of surface quality.

#### Peak-to-Valley Measurement Proposal

Interest has been increasing in the desirability of specifying surface quality by peak-to-valley measurements rather than arithmetical average roughness. This would be most applicable in situations requiring extremely smooth finishes and where specifications of scratches were

important. Reliable measurement can best be made with the interference microscope (microinterferometer), noting that very smooth surfaces, as those produced by lapping, usually have more or less uniform irregularities with few deeper scratches.

Specifications. The following specifications for peak-to-valley parameters are being considered by the ASA (Ref. 3) for inclusion in a future standard:

1. Peak-to-valley height of general (average) surface texture shall not exceed XX microinches in XX inch.
2. Peak-to-valley height of individual irregularities shall not exceed XX microinches, and there shall be no more than X irregularities per X inch.
3. Pitting or voids contained in XX sq in. are acceptable.

The tentative standard is being prepared which will involve measuring the surface texture by optical methods.

Symbols for Optical Measurement. A proposal has been made to the ASA standards committee (Ref. 3) suggesting the surface finish symbol shown in Fig. 3 for surfaces requiring optical measurement.

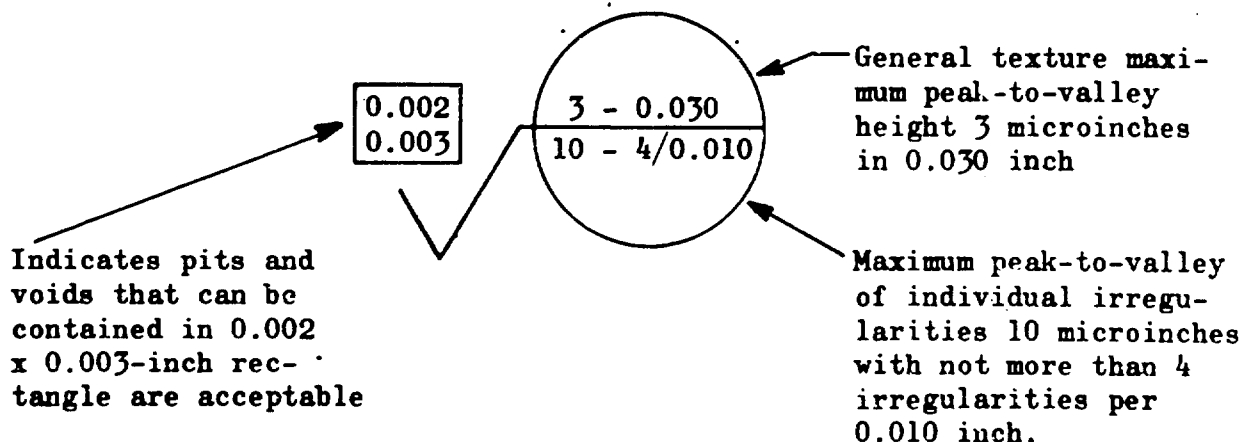


Figure 3. Surface Symbol for Optical Measurement

## MEASURING METHODS AND DEVICES

A brief review of surface roughness measuring devices will include only instruments capable of measuring finishes at the level significant to this study.

### Stylus Instruments

The most common method of measuring surface roughness is by moving a cone-shaped diamond stylus over the surface and translating its vertical motion to a value of average deviation from the mean. Factors which affect the resulting reading include the radius of the stylus, its force upon the surface, and the reference surface or skid upon which the tracer is supported. Error may be introduced because of mechanical vibration and electrical limitations. The almost universally used devices use stylus tracers with electrical amplification and may be grouped as follows:

Continuously Averaging Instantaneous Readout. This is a tracer type instrument using either the standard 0.0005-inch radius stylus or the 0.0001-inch stylus for fine finishes. Vertical movements of the stylus are converted into voltage and amplified to actuate a direct reading dial. These readings are in rms or arithmetical average with the lower limit of surface discrimination down to about 1 microinch. This device shows variations in average roughness height but does not indicate asperity configuration or wavelength greater than the set cutoff value.

Permanent Record. This is an electromechanical stylus instrument for measuring and recording roundness, flatness, roughness, scratches, flaws, and total profiles. The magnified readings or traces are recorded on a chart with vertical magnification of up to 50,000 times, enabling discriminate study of minute surface variations including waviness and asperity angle.

Probably the most important factor contributing to misinterpretation of surface roughness is the stylus tip radius size. It is obvious that some valleys and cracks cannot be reached by stylus tips of 0.0005- and 0.0001-inch radius found in most instruments. Also, these instruments evaluate the roughness along a thin line which undermines accuracy because the three-dimensional aspect is not taken into account. This situation might be minimized by traversing in various directions and also by having knowledge of the distribution of the irregularities.

Interesting comparisons have been made of various tip radii effects on similar surfaces (Ref. 18). Results showed that for a turned surface, the 0.001-inch stylus read 53-microinch AA finish while the 0.0001-inch stylus gave a reading of 52-microinch AA, hardly a significant difference. But in three ground surfaces, the blunter instrument could not bottom consistently, therefore, giving smaller measurements. For these surfaces, the 0.001-inch radius tip measured 1.6-microinch AA for the first, 5.5 for the second, and 22 for the third. The 0.0001-inch tip measured 1.8, 7, and 31-microinch AA, respectively. The difference in stylus effect is more pronounced in the rougher finishes for those ground surfaces.

The precision of stylus instruments was tested by comparison with standards which were constructed and measured optically by Bickel (Ref. 4). One observation was the effect of the tracer radius in interpreting sharp corners as being rounded (Fig. 4).

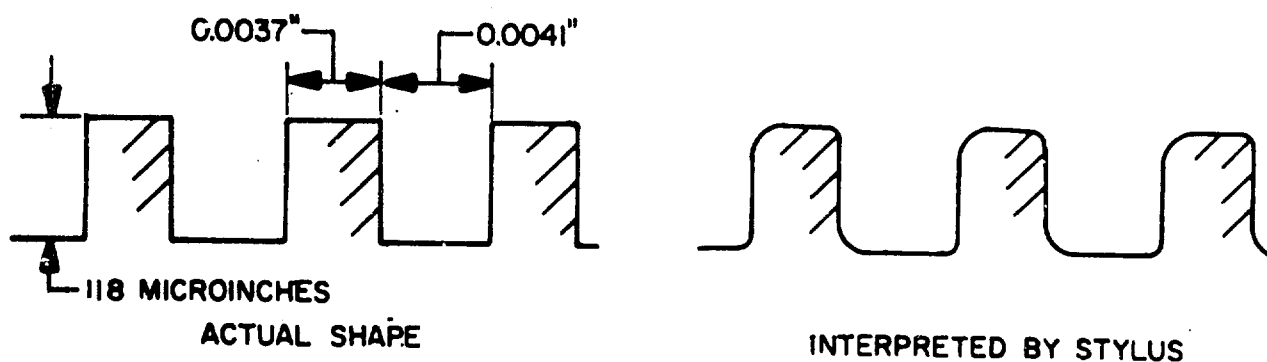


Figure 4. Stylus Interpretation of a Rectangular Shape

While profiles of simple sine wave shapes could be accurately followed by the stylus, the combined form of rectangular shapes upon a sine wave (Fig. 5) could not be contoured satisfactorily.

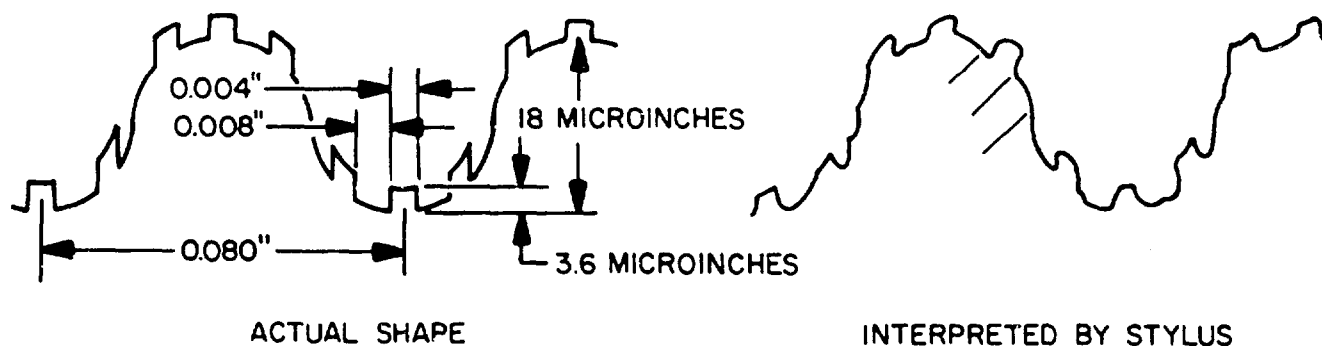


Figure 5. Stylus Interpretation of a Combination Shape

Table 5 indicates the results obtained by Bickel in a comparison of three stylus instruments (set at the cutoff values noted) while measuring rectangular profiles similar to those shown in Fig. 4.

TABLE 5  
COMPARISON OF ARITHMETICAL AVERAGING  
INSTRUMENTS (MICROINCHES AA)

Calculated	Instrument A 0.030 inch	Instrument B 0.060 inch	Instrument C 0.030 inch
2.7	2.6	2.36	3.2
25.0	25.6	26.4	30.0
58.0	57.0	53.3	68.0
120.0	124.0	128.0	136.0

A calculated curve which relates the stylus radius error with the average roughness height of precision reference specimens used to calibrate these instruments is found in Appendix C of Ref. 2. The reference specimen profile is made up of a series of known sizes of peaks and valleys having included angles of 150 degrees. For example, use of stylus tips having 0.0005- and 0.0001-inch radii for a reference specimen of a 4-microinch AA result in errors of 77 and 12 percent, respectively, indicating the relative capability of each tip radius to bottom the 150-degree included angle.

### Taper Sectioning

Taper sectioning is a method whereby the surface roughness is magnified by slicing (grinding and lapping) the surface at an oblique angle. The magnification of the surface asperities of a taper section is a function of the taper angle; for example, if the section is cut at 2.3 degrees, the vertical dimension would be 25 times the horizontal. Most materials require hard surface electroplating to prevent damage when cutting. This method of surface study is most accurate when the irregularities are wedge shaped or produced by unidirectional processes. When ground surfaces of this type are viewed they appear as jagged, sharp peaks with an irregular pattern. Lapped multidirectional surfaces are very difficult to evaluate because they include pits, gouges and material that appears to be floating on the surface. Evidently, what is seen considering various sized cones as the surface makeup will depend on the sectioning angle and at what point it cuts each cone.

Excellent taper sectioning can be seen in Plate I of Ref. 6 and pages 191 and 192 of Ref. 20. These microphotographs show the irregular contour of various finishes on metal surfaces. One particular photo (Ref. 20) shows a 1.6 microinch rms surface whose vertical dimensions are optically magnified to 10,000 X. The surface appears to be less jagged than other photos of higher rms values. A taper section microphotograph (Ref. 20 )

shows a surface finished by loose-abrasive lapping. It is unique in that no definite trace can be observed, rather what is seen are outlines of cones or "mountains" of various sizes superimposed and scattered throughout. Analysis of such surfaces would be difficult even though the surface can be microscopically resolved to 1 microinch.

### Optical Interference

The use of the principle of light wave interference makes it possible to measure surface finishes to a high degree of precision. Monochromatic light is directed through a transparent material with an accurate flat side which lies on the surface being inspected (Fig. 6). The two surfaces are separated by a thin wedge of air. Light waves are reflected from the work piece and the optical flat surfaces so that waves in phase produce bands of light and conversely when they are out of phase the waves interfere, producing dark bands. Alternate bands of light and dark approximately the same width appear at right angles to the direction of the air wedge. The bands give the effect of a contour map, decreasing in width and increasing in number as the wedge separation distance increases. Conversely, on a flat surface the bands will appear straight and parallel. The distance from a point on one band to the next band is equal to  $1/2$  of the wave length of the light used. The waviness and jaggedness of the interference bands are an indication of the surface irregularity and can be measured.

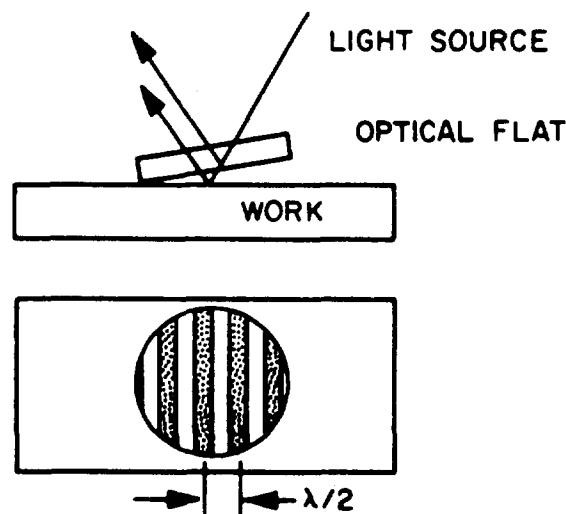


Figure 6. Light Interference With an Optical Flat



Optical Flats. Optical flats are precision glass or quartz plates that are flat to less than 0.000001 inch and generally used to check flatness (Fig. 6). Interference is the phenomenon upon which this method is based. Normally a source of monochromatic light is used.

Some of the light sources available are white light with a wave length ( $\lambda$ ) of approximately 20 microinches, yellow-orange light at 23.2 microinches, and green light whose wave length is 21.5 microinches.

Microinterferometry. Microinterferometry is the use of the optical flat and monochromatic light source with a microscope to give a very sensitive method of surface investigation. Instruments of this type, which are used to measure surface roughness, are known as interference microscopes or microinterferometers. The Zeiss instrument (Ref. 15) has magnification lenses of 80, 200 and 480 X, and uses a reference mirror on one side of the optical axis in place of the optical flat and two light beams. Various reflecting powers are available so the brightness of the test piece can be matched, giving sharp fringes.

This type of equipment is best applied to highly finished or glossy surfaces where the deviation of surface heights is within a few light wave lengths. Coarse surfaces cause the contour lines to become very close together and interpretation very difficult.

Multiple Beam Interferometry. Most of the advances towards the high degree of sensitivity of the multiple beam interferometry method of measuring surface contour have been made recently. Surfaces of the optical flat and the specimen surface are coated with silver having a high reflecting coefficient and also a high transmission coefficient so that incident light will be reflected back and forth resulting in an interference pattern of all these beams (Ref. 19 and 22). The dark bands usually observed in other optical methods are reduced to thin lines which are able to reveal fine detail down to 0.02 microinch.

## Electron Microscope

The high resolving power of the electron microscope makes it useful for the determination of fine finishes. Its main difficulty is that the electrons must pass through the specimen before striking a photographic plate, thereby limiting its use to thin sections. Another drawback is the necessity of using high vacuum and strong electron beams which can cause physical changes in certain specimens (Ref. 5).

The surface roughness is estimated by light and dark areas on the photographic plate. Electrons hitting high spots have a longer path to travel so that a smaller portion of them will pass through. The relative density on the photo plate is an indication of the variation of surface height.

In certain instances (thick sections), it is impractical to use the actual specimen so plastic replicas of the surface are used. The surface is coated with a film which is then stripped off and examined. In practice, resolution down to 0.2 microinch or magnification of 10,000 diameters (Ref. 9) is usual, although linear magnification of 50,000 is possible with this type of instrument under optimum conditions. Excellent microphotographs of polished surfaces obtained by this technique can be seen on pages 188 and 189 of Ref. 5.

The disadvantages of the replica technique can be avoided by the electron reflection method where the surface is viewed obliquely and the surface protuberances are seen in profile. This method was studied by Halliday (Ref. 10) and is shown to be particularly suitable for the examination of surfaces on which the irregularities are small, therefore, ground, lapped, finely abraded and polished surfaces can be studied.

## Profile or Light Section Microscope

This simple optical method gives a detail picture of the surface but only of a very thin plane. The light source provided through a narrow

slit falls on the specimen at an angle of 45 degrees to the surface of the specimen. Seen in the optical system is a cross section of local irregularities made by a line of light following the surface contour (Fig. 7).

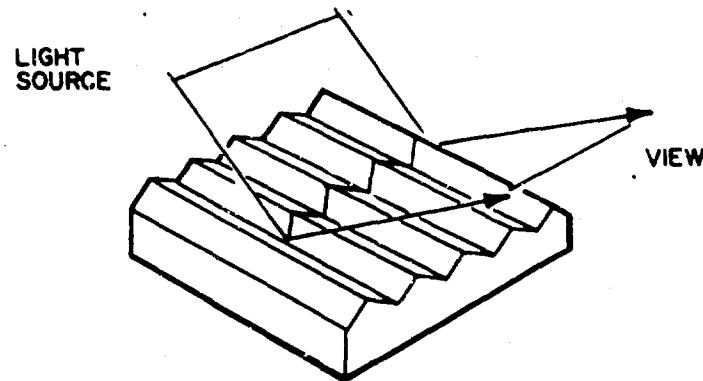


Figure 7. Principle of the Light Section Microscope

The smallest irregularity visible is on the order of the wave length of light or microinches (Ref. 5). Sensitivity of this method is between 20 and 1600 microinches in deviation from the plane surface. It is considerably less sensitive than interferometry, being based on simple magnification rather than interference.

#### REAL SURFACE

To properly visualize real surfaces requires the ability to think small coupled with first hand experience. There are many variations possible in ground and lapped surfaces because of the complexity of even the most regular fine finishes. Some idea of the scope of the topography can be obtained with the analogy of a plowed field or a mountainous terrain. Metal surface asperities undergo transformations similar to erosion as the surface is made smooth. Peaks are removed, and the remaining slopes become less steep.

## Dimensions

Real surface dimensions are measured normally in microinches or millionths of an inch with 40 microinches to the micron ( $10^{-6}$  meters) and 250 Angstrom units to the microinch. Metal valve seats are normally finished to less than 16 microinches AA by grinding and lapping, which places the upper peak-to-valley measurement at less than 100 microinches (0.0001 inch). At the other end of the spectrum, the lower limit of interest is in the vicinity of 1 microinch based on current day achievements.

To more completely describe the surface geometry, an angle is often associated with surface asperities. This angle is the slope of individual undulations relative to the nominal profile. Except for machine-induced regularities, the asperity slope has wide variation from minute fractions of a degree to approaching the vertical, depending upon the scale of roughness viewed. As with the mountains, large-scale undulations have shallow angles and range from a gross flat characteristic of one gradual curve to periodic waviness. Superimposed upon the larger undulations are smaller and smaller facets, and the smaller the facet viewed the larger the slope angle may be.

A detailed examination of ground, lapped, and abraded surfaces was undertaken by Halliday (Ref. 10) using reflection electron microscopy. Micrographs of aluminum, copper, mild steel and hardened tool steel show asperity slope angles and heights from 0.1 degree and 0.4 microinch for electropolished aluminum to 30 degrees and 70 microinches for ground, hardened steel. Finer surfaces of approximately a 10-microinch height had corresponding asperity angles of about 1 to 2 degrees. This places the base dimensions of these asperities between 100 and 1000 microinches.

## Configuration

It has often been assumed that the irregularities or asperities of finishes that have been ground or lapped multidirectionally are generally cone shaped. They begin in the shape of wedges, scratches, etc., but are

slowly rounded as cuts are taken radially. Examining any one irregularity microscopically would show smaller irregularities pointing to a situation of flatness not being possible in an absolute sense.

Bowden and Taber (Ref. 6) describe investigations of yield pressure as a function of the included angle of a single cone-shaped asperity in an analysis of the plasticity characteristics of the cone.

Other surface investigators in various experiments concluded that meaningful results are possible when assuming conical asperity shapes (Ref. 1, 12, 13, and 16). Archard (Ref. 11) discussed some interesting data of an experiment by Halliday who, by reflection electron microscopy, measured the slopes of surface irregularities of various steel and copper cylinders that were rough etched and rolled against each other with contact force high enough to cause plastic flow. The resultant maximum slope angle measured 1.2 degrees and the minimum was 0.8 degree.

Archard's conclusions suggested that asperities of angles less than some calculable amount will plastically yield until they reach the shallow, low, wide base shapes measured above. These asperities of wide included angles will elastically deform into the surface until the surface is flat and the load supported.

Many of the approximations of the conical shape and size can be applied to the pyramidal shape. This shape can be assumed to result if a surface is finished by a process involving abrasion or cutting in two directions normal to each other. In unidirection processes such as turning or super-finishing, the wedge shape irregularity results. Scratches fall into this category. As the wedge shapes become shorter in length as in grinding, they approach more closely the pyramidal shapes.

The geometry of spherical shaped asperities has been assumed by Archard (Ref. 1), Kragelsky (Ref. 11), and Bowden and Tabor (Ref. 6) in contact analyses where this idealized configuration lessened the mathematical

difficulties involved. It is probable that among the various shapes suggested, the spherical one is most unlikely to occur except in unique cases. However, with a situation of worn, broken, or deformed peak points, almost any shape asperity may approximate the sphere if only at its tip.

There is little information on the statistical distribution of asperities of fine surfaces. The surface of the most finely finished material can be described as irregular if very sensitive instruments are used to examine it. Indications are that all surfaces contain random irregularities of various sizes with scratches, cracks, and intermittent flaws. Application of distribution laws can only be done theoretically with approximation as the result.

A paper by Reason (Ref. 17) shows profile charts of two actual surfaces whose profiles do not appear congruent but having similar AA values. These inconsistencies have been recognized by researchers in the field (Ref. 4, 7, and 20) in considering the multitudinous variables affecting surface geometry and it has been suggested by Reason (Ref. 17) that for some surfaces, the process of manufacturing may need to be specified with the AA used as a simple controlling measure. This approach is obviously applicable to many critical valve sealing surfaces.

### Visual Appearance

In describing real surfaces, a great deal of importance is often placed on visual effects and what is assumed from them. At best, the resolving power of optical microscopes is 6.7 microinches<sup>1</sup>, and no configurations smaller than this dimension can be clearly seen. Matte surfaces contain irregularities smaller than 40 microinches set at random angles so as to scatter the majority of light. The darker the surface the more scattered

---

<sup>1</sup>1/3 wave length of maximum intensity

the light and thus rougher the surface. Conversely, polished surfaces have broad areas which reflect a great deal of light similar to a mirror; however, in normal terms of peak-to-valley roughness, both surfaces can have the same average value.

Attempting to judge surface texture on a purely visual basis is generally misleading. Matte surfaces will tend to hide defects and scratches. However, a smooth appearing, mirror-like surface may contain relatively large undulations.

### Composition

The surface layer is composed of a mixture of absorbed gases, oxides, and various other contaminants in amounts depending upon past history. It is these contaminants which maintain sufficient separation between mating surfaces to preclude welding. Bowden and Tabor (Ref. 6) indicate that freshly lapped or ground metals (iron, nickel, chromium, and aluminum) will acquire a layer of oxide between 10 and 100 Angstroms thick in about 5 minutes or less. It is the breakdown of these oxides and other films which lead to wear and galling or seizure.

Because of the work-hardening nature of the finishing process, the hardness of the surface layer will be greater than the basis metal. Soft, work-hardenable materials will have a larger increase than hardened steels. In addition, hardness within the crystalline grain structure of metals may vary considerably. This can induce roughness between contacting surfaces under loaded conditions.

### CONTACT AREA AND LOADING EFFECTS

If two relatively smooth surfaces are brought together, contact will take place only in isolated spots. The irregular nature of the surfaces will permit stable touching at three points of contact until increased load causes a combination of plastic flow of the initially contacted asperities and elastic deformation of the supporting base material.

Gross areas of contact may be completely defined when the contact is curvilinear as in bearings and curved rollers, etc. The Hertz theory of elastic contacts (Ref. 21) describes a contact stress distribution which allows computation of gross bearing area, maximum stress, and deformation. Nominally flat surfaces which are not perfectly flat, do not have well defined regions of gross contact until loads are such as to bring the geometric total of the bearing surfaces in intimate contact. Even then the real contact area is only a relatively small percentage of the gross or apparent bearing area because of surface roughness.

In their study of friction and lubrication, Bowden and Tabor (Ref. 6) have evolved contact theories to describe the real contact area between metal surfaces. These are based on observed evidence that (1) real contact area increases in direct proportion to applied load, and (2) friction force, while independent of apparent area is a function of the real area of contact. If the contacting asperities are assumed in a state full plasticity and welded at contact, the force required to shear the welds would be the friction force. The real area of contact is defined by the plastic flow pressure ( $P_m$ ), or stress, of the surface asperities and load ( $W$ ), so that

$$A_r = \frac{W}{P_m}$$

The plastic flow pressure has been evaluated for pyramidal and spherical shapes, and for the shallow slope angles normal for asperities, is related to the elastic limit ( $Y$ ) by a constant. It is, therefore, independent of the applied load; for fully work-hardened metal

$$P_m \cong 2.8Y.$$

The real area of contact is also defined by the material shear strength ( $S$ ) and friction force ( $f$ ) as

$$A_r = \frac{f}{S}$$



and it follows that the friction coefficient

$$\mu = \frac{f}{W} = \frac{A_r S}{A_r P_m} = \frac{S}{P_m}$$

This relationship has been experimentally correlated for a number of different materials. Considering that valve seats normally work well below the yield strength it is apparent that the real areas of contact computed from the above equation would result in a very small percentage of the apparent area in real contact. If it can be assumed that the apparent contact area ( $A_a$ ) is defined, the ratio of real to apparent area is equal to the ratio of apparent stress ( $S_a$ ) to plastic flow pressure ( $P_m$ )

or,

$$\frac{A_r}{A_a} = \frac{W/P_m}{W/S_a} = \frac{S_a}{P_m} = \frac{S_a}{2.8Y}$$

A typical hardened valve seat ( $Y = 250,000$  psi) operating at 10,000 psi apparent stress would then have a real contact area equal to 1.4 percent of the apparent contact seating area.

In flat surface experiments (Ref. 6), two steel surfaces, lapped flat within a few fringes, of 0.124 and 3.25 sq in. were brought together under various loads, and the electrical resistance between them was measured to determine the real contact area. Results for the 3.25 sq in. pair are duplicated on the following page.

Load, pounds	Apparent Stress, psi	n Contacts	Diameter of Each Contact, inches	Fraction Of Area In Contact	R, 10 <sup>-5</sup> Ohms
4.4	1.35	3	0.004	1/100,000	50.0
11.0	3.38	5	0.005	1/40,000	25.0
44.0	11.4	9	0.007	1/10,000	9.0
220.0	68.0	22	0.009	1/2,000	2.5
1100.0	338.0	35	0.017	1/400	0.9

The results indicate real area proportional to load. However, the range of apparent stress is far below valve seat stresses.

Through analysis of wear experiments, Archard (Ref. 1) has concluded that real surfaces support their loads predominantly in an elastic manner with only a small percentage of the contacts undergoing plastic flow. Friction between real surfaces has been experimentally proven to be proportional to the real area of contact. Archard has examined mathematical models of spherical surface protuberances pressing on a flat plate and has shown that real contact area is a power function of the load or

$$A \propto W^n$$

where  $n = 2/3$  for a single protuberance (Hertz) and approaches unity for numerous protuberances. This conclusion was also reached by Kragelsky (Ref. 11). Consequently, it was concluded (Ref. 1) that surface welding was a consequence of singular encounters occurring infrequently, and the more typical event is an elastic contact in which protuberances separate without damage. The elastic event thus determines friction and not welding as concluded by Bowden and Tabor.

In substantiation of his views, Archard describes the results of reflection electron microscopic examination (Ref. 10) of some metal surfaces (aluminum, copper, iron, nickel, steel, etc.) pressed flat (base metal plastically flowed) by a carefully polished hardened steel anvil. It was shown that

the resulting slopes of the asperities were in all cases less than 1.2 degrees, and following compression, were entirely elastic in that the asperities could be pressed just flat without plastic flow. Moreover, in experiments involving phase contrast microscopy observation of nominally flat, ground, polished, and lapped specimens against a metallized glass surface, Dyson and Hirst (Ref. 8) concluded that the bearing area may be comprised of considerably more points of contact than noted by Bowden and Tabor. Instead of 9 contacts at a 0.007-inch diameter and 44 pounds, they measured many contacts of only a "few microns" (0.0001 to 0.0002 inch) under similar conditions. This evidence supports Archard's hypothesis of bearing area increasing directly with load through an increase in number of contacts.

The elastic theory would suggest that low slopes of irregularities of the fine finishes being considered applicable to valve seats would preclude the occurrence of plastic flow. The significance here is important when considering the effect of removing the load which allows, in this reversible process, a return to the original state of the surface.

Further substantiation of Archard's views of elastic behavior of surface asperities are provided by O'Connor (Ref. 14) in examining the role of asperities in transmitting tangential forces. An idealized surface with a sinusoidal profile is assumed in contact with a flat surface of the same material under an average pressure. For purely elastic deformation, the Hertz theory indicates real to apparent area of contact

$$\frac{A_r}{A_a} = 0.684 \left( \frac{P}{E} \frac{\lambda}{h} \right)^{1/2}$$

with

$$\frac{\lambda}{h} > 1.27 \frac{EP}{Y^2}$$

as required microgeometry for elastic behavior

where

P = average Hertz contact pressure

E = elastic modulus

A<sub>a</sub> = apparent area

Y = yield strength

A<sub>r</sub> = real area

For full plasticity, the required load is approximately 75 times that required for initial yield; therefore, the criterion for fully plastic behavior is

$$\frac{\lambda}{h} < 0.017 \frac{EP}{Y^2}$$

Microscopic examination of several surfaces varying from rough-and-soft ( $\lambda/h$  of 5 and DPH \* 145) to smooth-and-hard ( $\lambda/h$  of 30 and DPH 700) indicated a general correlation with the above analysis; i.e., the asperities of the soft material yielded plastically while the hard surface indicated no signs of yielding, either directly or with profile records. These experiments were performed using a normal load of 13,440 pounds between two surfaces, one of which was flat and the finish varied and the other curved to a 30-inch radius with the surface hard and polished. The high normal load resulted in elastic contact circles of approximately a 1/2-inch diameter and maximum contact pressures for the hard and soft materials of 83,000 psi and 53,000 psi, respectively. Although the asperities of the soft material yielded, its real area of contact was only slightly larger than the harder specimen. The  $A_r/A_a$  values for the soft metal that were calculated and microscopically measured was 0.28 at the center or maximum pressure area, whereas the calculated value for the harder material was 0.20.

---

\*DPH = Vickers diamond pyramid hardness number

The paper concludes that the majority of surface irregularities of typical engineering surfaces are deformed elastically, or at least do not reach the condition of full plasticity. Under these conditions, the area of real contact is determined by the surface topograph ( $\lambda/h$ ) as well as hardness of the material, and is appreciably greater than a purely plastic analysis would suggest.

## SURFACE STUDY RESULTS

The understanding provided by the study of surface finishing methods, measurements, and the efforts of researchers in related fields has also provided an understanding of the vast scope of real material contacts. It is apparent from the small amount of available data and conflicting theories just how complex the contact problem really is and it is not hard to imagine why design data on the valve seating are nonexistent in the current literature. One of the basic problems is the complex interaction of plastic-elastic phenomena taking place in many surfaces because of extremes in dimension and material properties. All real material contacts have degrees of elastic and plastic deformation taking place during loading. The question is, which is characteristic and how much? Because the poppet and seat program is restricted to the relatively hard and smooth materials normally associated with valve seating elements, the number of variables is restricted accordingly, and the following conclusions have been formulated on that basis:

1. Archard's elastic theory of multiple contacts (Ref. 1) best describes the growth of real contact area (area is directly proportional to load and increases because of increasing the number of contacts).
2. Because of the extreme uniformity of seating surfaces a simplified elastic analysis based upon a uniformly smooth surface may be developed to describe the controlling parameters for the deformation of real surface profiles. This analysis will provide background and direction for the experimental effort, and

in addition, will result in a mathematical tool for extrapolating valve seat design, tempered by the inspection and test data from actual valve seats.

## LEAKAGE FLOW ANALYSIS

### DEFINING PARAMETERS

In considering the leakage and flow across a valve seat, a number of equations must be taken into account. These range from the nozzle equation which generally applies to the wide open valve to the viscous and molecular flow equations applicable under seated conditions. The equations derived in this section are presented for compressible and noncompressible fluids for flow through parallel plates. The equations are equally applicable to flat, conical, and spherical valve configurations because the near and on-seated passage configurations approximate the parallel plate model. A specific example of nitrogen valve flow through a model valve seat is presented in subsequent paragraphs. This practical example will illustrate how each flow regime blends into the next to build the over-all flow-leakage characteristic curve.

### SIMPLIFIED FLOW EQUATIONS FOR SMOOTH PARALLEL PLATES

#### Nozzle Flow

The compressible and incompressible flow equations derive from the basic Euler momentum relationship. The Euler equation gives the following relationship between velocity, pressure, and density

$$\frac{1}{2} V^2 + \int \frac{dP}{\rho} = \text{Constant} \quad (\text{see page 70 for nomenclature})$$

For the incompressible consideration, density ( $\rho$ ) is constant, and the resultant relationship is known as the Bernoulli equation. If the inlet velocity is neglected, the following equation evolves for flow of an

incompressible fluid through a nozzle

$$\omega = CA \sqrt{2 g \rho (P_1 - P_2)}$$

This equation requires a discharge coefficient (C) to correct the ideal frictionless flow to the actual case. The discharge coefficient is a function of the specific configuration being considered, therefore, it is derived from empirical data.

For the specific application of this equation to a valve configuration, area (A) is usually expressed as a function of the stroke height ( $h_p$ ) and the seat perimeter (W). This substitution can be made in the nozzle and the turbulent channel equations.

For the compressible flow analysis, the density is not constant and therefore the integral of  $dP/\rho$  must be evaluated for specific assumptions. For an adiabatic, frictionless process considering a perfect gas, the following equation is derived

$$\omega = \frac{CAP_1}{\sqrt{RT_1}} \sqrt{gk \left( \frac{2}{k+1} \right)^{\frac{k+1}{k-1}}}$$

As in the case of the incompressible flow, a discharge coefficient is required to account for the irreversibility of flow. The above equation further assumes that a choked or sonic flow exists across the nozzle.

In practice, leakage is most often expressed in terms of a volumetric flow. For compressible fluids, where density is a variable function of pressure and temperature, standard conditions ( $P_s, T_s, \rho_s$ ) must be defined. The conversion relationship for all fluids is

$$Q = \frac{\omega}{\rho_s} = \omega \frac{RT_s}{P_s}$$

Therefore, for both incompressible and compressible flow; at standard conditions, the weight and volumetric flows differ by a constant.



The nozzle equations can be applied to a poppet valve configuration (similar to an orifice) from the wide open condition to the near-seated position. When the valve closure height has decreased to the position where wall friction at the seating surface (and thus land length) is significant, the nozzle regime terminates and turbulent channel flow commences. There is no precise point at which nozzle flow terminates, the transition being a complex function of the particular channel geometry and Reynolds number. However, in general, if the length to height ratio is 10 or greater, channel flow is imminent.

### Turbulent Channel Flow

In this flow regime, the same basic continuity and momentum considerations hold with the addition of a term for the effects of friction. In the case of an incompressible fluid, the basic Bernoulli equation is modified to the form

$$\Delta P = \frac{fL}{D} \frac{\rho V^2}{2g}$$

where flow is defined by continuity as

$$\omega = \rho A V.$$

The first equation expresses differential pressure as a function of friction factor ( $f$ ) and velocity ( $V$ ). The friction factor is related to velocity through empirical parametric curves of friction vs Reynolds number and wall roughness (Moody diagram Ref. 23). The solution to these equations is by trial and error.

The equations for flow in the turbulent channel regime were developed for flow-through circular tubes. To apply the equations to other channel configurations, the tube diameter in these equations must be expressed in terms of hydraulic diameter ( $D$ ). Hydraulic diameter is

defined as four times the ratio of the cross-sectional area to the wetted perimeter. For parallel plates, the hydraulic diameter is equal to twice the plate spacing ( $2h_p$ ).

The equations used to compute compressible fluid flow in this regime are obtained from Shapiro (Ref. 24). They assume an adiabatic constant-area flow and include the effects of internal fluid and wall friction and fluid momentum. To compute the weight flowrate, two equations are required. The first is a relationship between entrance mach number ( $M$ ) and friction factor ( $f$ ) for the condition of choked flow at the exit of the valve seat channel ( $M=1$ )

$$\frac{fL}{D} = \frac{1-M^2}{kM^2} + \frac{k+1}{2k} \ln \frac{(k+1) M^2}{2(1 + \frac{k-1}{2} M^2)}$$

As in the incompressible case, the solution of this equation is by trial and error. Shapiro's text gives considerable assistance in the solution of this equation by tabulating  $fL/D$  vs Mach number, thus permitting interpolation of desired information. For the subsonic solution, reference is made to Shapiro's text.

Once the entrance Mach number and density are determined, they are used in the continuity equation to compute the weight flowrate based on the inlet conditions

$$\omega = \rho A M \sqrt{k g R T_1}$$

The equations in this section are confined to the turbulent flow regime, i.e., Reynold numbers greater than 2000. However, these equations can be extended into the initial portion of the laminar flow regime where fluid momentum is still an important consideration. In this case, the friction factor is a linear function of Reynolds number and is given for the parallel plate consideration as

$$f = 96/R_e$$

## Laminar Flow

The analysis of fluid flow in this regime assumes that the temperature is constant (isothermal), that the fluid momentum effects are negligible, and that viscous shear forces govern the flow. These assumptions result in the Poiseuille equation for flow through stationary flat plates (Ref. 25)

$$-\frac{dP}{dx} = \frac{12 \mu V_{\text{average}}}{h^2}$$

By using the continuity equation, the relationship is reduced to express the viscous flow through flat plates

$$\omega = \frac{\rho w h_p^3 (P_1 - P_2)}{12 \mu L}$$

For a compressible gas, thermal effects are present; however, the assumption of isothermal condition can be made because of the small channel thickness and low velocity. The compressible version of the Poiseuille equation is obtained by assuming an average density across the seat land and a perfect gas; therefore,

$$\omega = \frac{w h_p^3 (P_1^2 - P_2^2)}{24 \mu L R T}$$

This same basic relationship can be derived for flow between circular flat plates. This equation contains the natural log of the radius ratio which accounts for radial divergence of the flow and is as follows:

$$\omega = \frac{\pi h_p^3}{12 \mu \ln \frac{r_2}{r_1}} \left( \frac{P_1^2 - P_2^2}{R T} \right)$$

Normally, this divergence can be neglected as the  $r_2/r_1$  ratio is close to unity. When this ratio is greater than 1.4, divergence should be considered.

## Transition and Molecular Flow

The determination of molecular flow involves the application of the kinetic theory of gases. A flow equation derived (Ref. 26) for the molecular regime is as follows

$$Q = \frac{4}{3} \frac{V_a}{\int_0^L \frac{H}{A^2} dL} (P_1 - P_2)$$

This equation relates the flow (Q) to the mean molecular speed ( $V_a$ ), differential pressure ( $P_1 - P_2$ ), and geometry where (H) is the channel perimeter. When this basic relationship is applied to parallel planes, the equation has the form

$$\omega = \frac{4}{3} \sqrt{\frac{2}{\pi}} \frac{W h_p^2}{L} \frac{(P_1 - P_2)}{\sqrt{\frac{RT}{g}}}$$

There exists a transition region where both molecular and laminar (viscous) flow effects are operating. The limits of these regions are approximately defined by the ratio of mean free path of the molecule ( $\lambda'$ ) to the characteristic dimension of the channel ( $h_p$ ) when:

$\lambda'/h_p < 0.01$ , flow is viscous

$\lambda'/h_p$  is 0.01 to 1.0, transitional flow exists

$\lambda'/h_p > 1.0$ , flow is molecular

A modified equation proposed for flow in the transition region is

$$\omega_{\text{total}} = \omega_{\text{viscous}} + \epsilon \omega_{\text{molecular}}$$

The molecular flow factor ( $\epsilon$ ) is generally close to unity. It takes into consideration such items as the difference in gases and physical properties of the passage walls. For simplicity,  $\epsilon$  has been assumed as unity;

therefore, the transitional equation reduces to the direct addition of the viscous and molecular flow quantities. The predicted flows in the transition region will be slightly higher as a result.

## STATIC PRESSURE DISTRIBUTIONS

Static pressure distribution across a valve seat is of interest to the valve designer in determining the forces associated with a particular configuration. These forces determine such external performance parameters as cracking and reseal in relief valves or influence stability in the case of regulators. The theoretical aspects of pressure distribution for the various flow regimes are discussed in the subsequent paragraphs.

### Nozzle Flow Regime

There has been a considerable amount of analytical work conducted on converging nozzles, particularly for compressible flow. However, the particular model under investigation has essentially constant cross section along the flow path; therefore the model is analogous to a short-tube orifice. The pressure profile along this orifice configuration is similar to the converging nozzle because the flow separates from the walls after entering the seating separation and exits with the stream contracted (vena contracta). Unfortunately, this analysis is basically qualitative, and the determination of the pressure profile in this configuration must be determined experimentally.

### Turbulent Channel Flow Regime

For the incompressible fluid, the pressure drop is a direct function of the length of the path; therefore, the pressure profile is a straight line across the seat land. This results in an effective seat diameter location at the land midpoint.

The pressure distribution for the compressible gas consideration is somewhat more complex. Shapiro's equation discussed previously assumes that the exit velocity is sonic and that the corresponding length computed is for a specific inlet velocity. By assuming various channel lengths and computing the inlet conditions, the pressure profile can be determined for the complete channel. In general, the pressure profile along the channel approximates a straight line for the higher Reynolds numbers. However, as the valve model closes (corresponding to a decrease in  $h$  and Reynolds number), the pressure profile progressively approaches the parabolic shape found in the laminar flow regime.

### Laminar Flow Regime

Unlike the analysis of pressure distribution in the nozzle and turbulent channel regimes, the laminar consideration is straightforward. Because the density is essentially constant for the incompressible fluid, the pressure profile will be a straight line with the effective area located at the midpoint (Fig. 8).

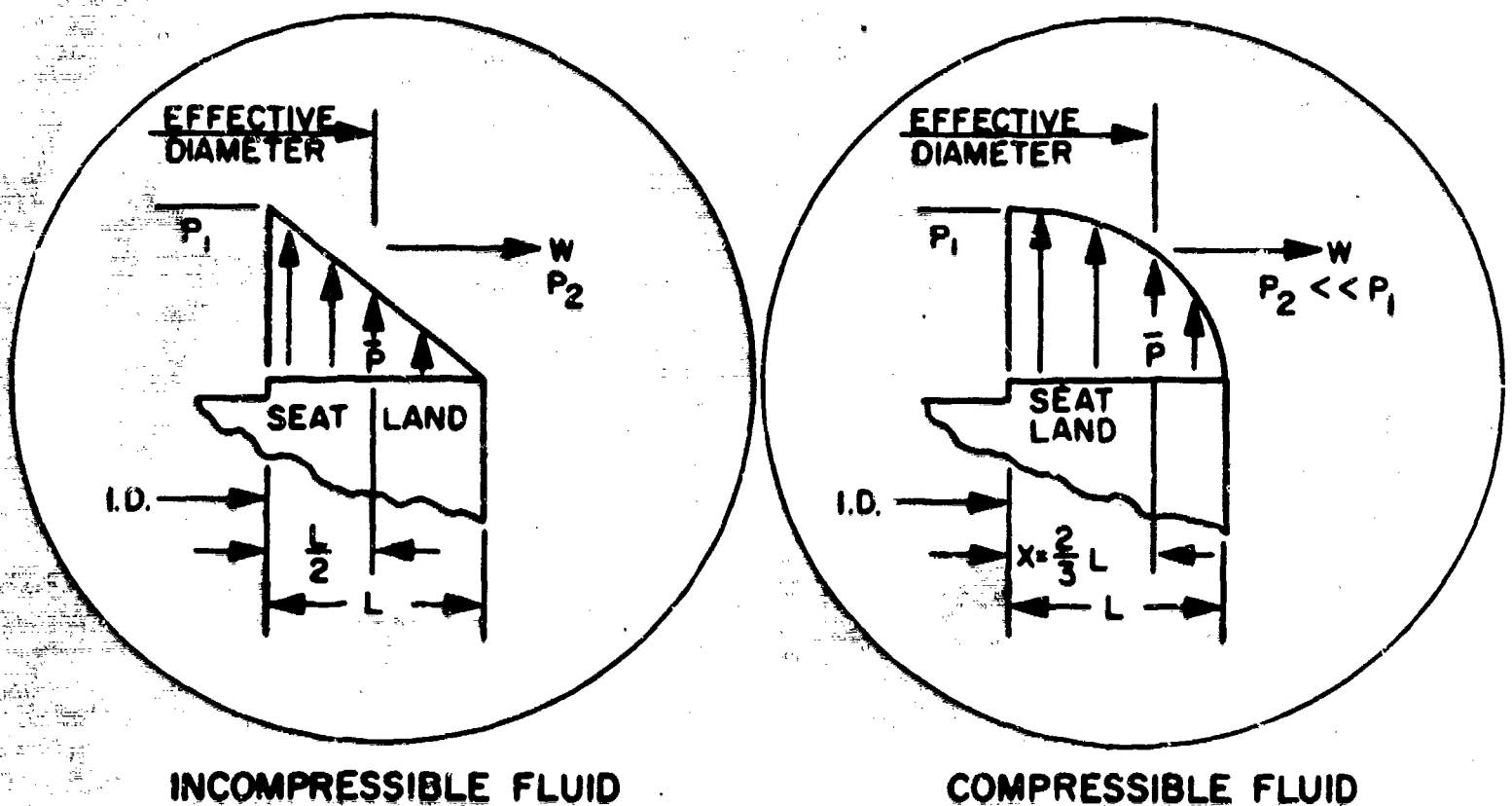


Figure 8. Pressure Profiles

Based on the laminar flow equation for compressible media, the following formula can be derived which expresses the variable pressure (P) as a function of the distance along the seat land (X)

$$P = P_1 \left\{ 1 - \frac{X}{L} \left[ 1 - \left( \frac{P_2}{P_1} \right)^2 \right] \right\}^{1/2}$$

The resulting curve is parabolic in shape (Fig. 8). To find the average pressure ( $\bar{P}$ ) over the entire land, the previous equation is integrated to give the following relationship

$$\bar{P} = \frac{2}{3} \frac{P_1^3 - P_2^3}{P_1^2 - P_2^2}$$

If  $P_2$  can be neglected, the average pressure for the seat land reduces to

$$\bar{P} \approx \frac{2}{3} P_1$$

It follows that for L small relative to the ID and  $P_2 \ll P_1$ , the effective seat diameter for compressible media is located at  $2/3$  of the distance across the seat land.

For the special case where the radial divergence must be taken into account, i.e., when L is large relative to the ID, the first equation must be modified. It can be seen in the following equation that  $X/L$  has been replaced by a radius function in the original equation, and the variable pressure (P) is now a function of the radial distance (r) along the seat land.

$$P = P_1 \left\{ 1 - \frac{\ln \frac{r}{r_1}}{\ln \frac{r_2}{r_1}} \left[ 1 - \left( \frac{P_2}{P_1} \right)^2 \right] \right\}^{1/2}$$

Because  $r_1$  and  $r_2$  are both variables in the general solution of the equation, a single pressure profile curve cannot be determined. However, the general effect of radial divergence is to straighten out the parabolic curve, and for the extreme case, actually reverse the curve so that the effective diameter is less than the land midpoint.

Detail consideration was not given to the transition and molecular pressure distributions because these flow regimes almost always occur under highly stressed seating conditions, and therefore, the force resulting from small differences in the effective seat area is negligible relative to the total seat force.

#### SAMPLE COMPUTATION

To illustrate how the previously developed flow equations are used, the following sample computation is presented. The seat model selected is the 1-inch configuration used in the off-seat leakage tests. A cross-section of this seat configuration is shown in Fig. 9. Flow is from the inside (ID) to the outside (OD) of the 0.060-inch flat seat land. Leakage has been computed for nitrogen gas at a 100-psig inlet pressure, a 70 F inlet gas temperature, and a 14.7-psia outlet pressure.

Figure 10 presents the leakage spectrum for the sample computation. The various flow regimes, i.e., nozzle, turbulent channel, laminar, transitional, and molecular are identified on the curve. Also, the limits of each regime are shown. A range of theoretical parametric data has been computed for various pressures and gases and is presented with the test data in the experimental test program section.

The following parameters are known values for this seat configuration and are used in the flow equations to compute the noted leakage characteristics.

Discharge coefficient,  $C = 0.95$

Gravitational acceleration,  $g = 1.39 \times 10^6 \text{ in./min}^2$



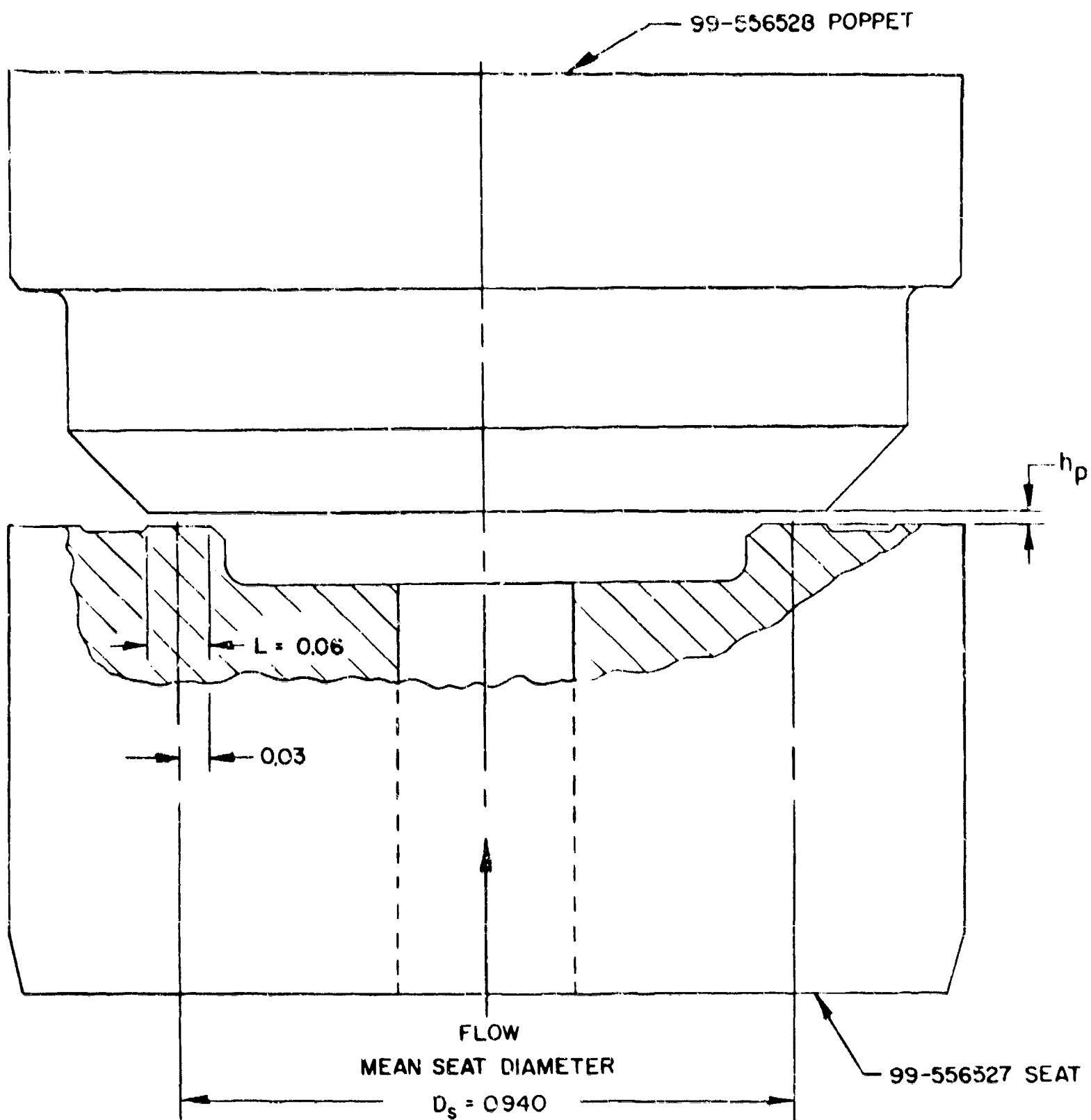


Figure 9. Typical 1.0-Inch Poppet and Seat Model

Specific heat ratio,  $k = 1.4$

Channel length,  $L = 0.060$  inch

Inlet pressure,  $P_1 = 114.7$  psia

Discharge pressure,  $P_2 = P_s = 14.7$  psia

Gas constant,  $R = 663$  in./R

Absolute temperature,  $T_1 = T_s = 530$  R

Channel perimeter ( $\pi D_s$ ),  $W = 2.95$  inches

Absolute viscosity,  $\mu = 4.40 \times 10^{-11}$  lb-min/in.<sup>2</sup>

### Nozzle Flow

For a compressible fluid flowing sonically the following equation is used

$$Q = \frac{RT_s}{P_s} \left[ \frac{C W h_p P_1}{\sqrt{RT_1}} \sqrt{gK \left( \frac{2}{k+1} \right)^{\frac{k+1}{k-1}}} \right]$$

Using the assumptions and data outlined previously

$$Q = 1.045 \times 10^7 h_p$$

The orifice flow ceases, and turbulent channel flow commences at a height ( $h_p$ ) of approximately  $6 \times 10^3$  microinches (Fig. 10). The land width is 0.060 inch giving an  $L/h_p$  ratio of 10 for the break point.

### Turbulent Channel Flow

Flow in this regime is defined by a curve on log-log paper; therefore, a sample calculation of one point will illustrate the method used. Leakage is computed for a stroke height ( $h_p$ ) of 0.001 inch in the following steps:

1. Hydraulic diameter,  $D = 2h_p = 0.002$  inch

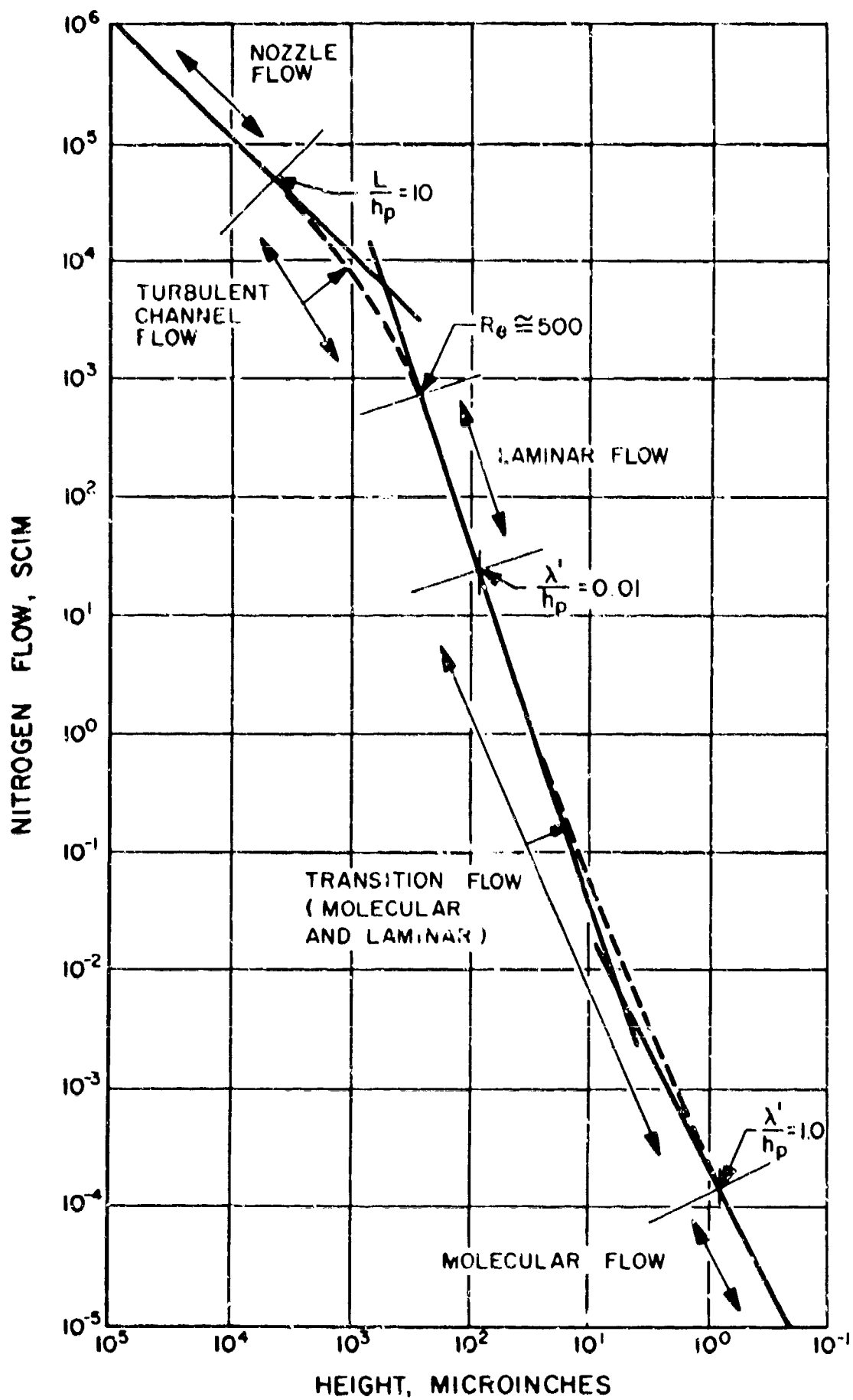


Figure 10. Theoretical Nitrogen Flow Through The Valve Model Shown in Fig. 9

2. A friction coefficient ( $f$ ) is estimated at 0.040. This is the starting point for the trial and error solution; ( $f$ ) will be verified at the conclusion of this computation.
3. Compute  $fL/D = 1.20$
4. Compute the entrance Mach number ( $M$ ) from following equation (Table B.4, Ref. 24)

$$\frac{fL}{D} = \frac{1 - M^2}{kM} + \frac{k+1}{2k} \ln \frac{(k+1) M^2}{2(1 + \frac{k-1}{2} M^2)}$$

for

$fL/D = 1.20$ , entrance Mach number

$M = 0.49$

5. Assuming an isentropic entrance condition, entrance static pressure ( $P_1$ ) can be computed from the following equation where  $P_o$  is the stagnation (total) pressure of 114.7 psia, and  $M$  is the entrance Mach number

$$\frac{P_o}{P_1} = \left(1 + \frac{k-1}{2} M^2\right)^{\frac{k}{k-1}}$$

therefore, static pressure,  $P = 97.3$  psia.

6. Again, assuming isentropic conditions, the entrance static temperature ( $T_1$ ) is computed from the following equation for a total temperature ( $T_o$ ) of 530 R.

$$\frac{T_o}{T_1} = 1 + \frac{k-1}{2} M^2$$

therefore, static temperature ( $T_1$ ) = 506 R

7. The following series of equations are used to compute the flow (Q) in the channel

$$V_1 = M \sqrt{kg RT_1}$$

$$\rho_1 = \frac{P_1}{RT_1}$$

$$A = Wh_p$$

$$\omega = \rho_1 AV_1$$

$$Q = \omega \frac{RT_s}{P_s}$$

from which the flow,  $Q = 7960$  scim

8. To prove the flow computation, the originally estimated friction coefficient (f) is checked. Reynolds number is first computed:

$$R_e = \frac{DV_1 \rho_1}{\mu} = 3.95 \times 10^3$$

Using the computed value for Reynolds number, a friction coefficient is determined from the Moody diagram. The friction coefficient determined from this curve is 0.0395, and is close enough to the original estimate of 0.040 so that a recomputation is not necessary.

The curve plotted from this and other data points is shown as a dashed line in Fig. 10. This flow regime extends into the initial portion of laminar flow, i.e.,  $R_e$  below 2000 where fluid momentum is still an important consideration.

### Laminar Flow

Laminar flow for nitrogen gas is computed from the Poiseuille equation in the following form

$$Q = \frac{RT_s}{P_s} \left[ \frac{Wh_p^3 (P_1^2 - P_2^2)}{24 \mu L RT} \right]$$

Using the assumptions and data outlined,

$$Q = 4.08 \times 10^{13} h_p^3$$

This flow regime continues until molecular flow can be detected and the transition flow (laminar + molecular) begins.

### Transition and Molecular Flow

The equation used to compute leakage in the molecular regime is as follows:

$$Q = \frac{RT_s}{P_s} \left[ \frac{4}{3} \sqrt{\frac{2}{\pi}} \frac{Wh_p^2 (P_1 - P_2)}{L \sqrt{RT/g}} \right]$$

Using the assumptions and data outlined,

$$Q = 2.49 \times 10^8 h_p^2$$

This flow regime is plotted on the lower right of Fig. 10. The dashed line connecting the laminar and molecular flow regimes is simply the sum of the two leakage values. Therefore, the transition equation is

$$Q_{\text{Transition}} = Q_{\text{Laminar}} + Q_{\text{Molecular}}$$

The boundaries of this transition regime are defined by the following limits

$$\bar{\lambda}/h_p = 0.01 \text{ to } 1.0$$

The molecular mean free path ( $\lambda'$ ) is 3.61 microinches for nitrogen at standard conditions (70 F and 14.7 psia). For a mean pressure of 50 psig,  $\bar{\lambda}' = 0.82$  microinch.

The corresponding height limitation of the transition regime is between 0.82 and 82 microinches (Fig. 10).

## NOMENCLATURE

A	= area, sq in.
C	= discharge coefficient
D	= hydraulic diameter, inches
f	= friction coefficient
g	= gravitational acceleration, in./min <sup>2</sup>
$h_p$	= parallel plate channel height, inches
k	= ratio of specific heats
L or X	= channel length, inches
M	= entrance mach number
P	= static pressure, psia
Q	= volumetric flow at standard conditions of temperature ( $T_s$ ) and pressure ( $P_s$ ), in. <sup>3</sup> /min or for compressible flow, scim
$r_1$	= inside radius, inches
$r_2$	= outside radius, inches
R	= gas constant, in./R
$R_e$	= Reynolds number
T	= static temperature, R
V	= velocity, in./min
W	= channel width or perimeter, inches

## Greek Symbols

$\omega$	= weight flowrate, lb/min
$\mu$	= viscosity, lb-min/in. <sup>2</sup>
$\rho$	= density, lb/in. <sup>3</sup>
$\lambda'$	= mean molecular free path, inches



## Subscripts

- 1 = inlet or entrance conditions
- 2 = outlet or discharge conditions
- 0 = stagnation conditions
- s = standard conditions

## SURFACE ANALYSIS

Study has shown that real surfaces are exceedingly complex, and that an attempt to describe their deformation characteristics on an individual asperity basis is impossible. Similar to one-dimensional pipe flow, simplifications must be made so that a minimum analysis will point the way and hopefully provide quantitative data within one order of magnitude.

A fundamental problem in the analysis of surface geometry is the definition of the controlling surface characteristics for the specific application. In one case, waviness is undesirable, while in others, scratches, pits, lay, roughness, nodules, or even an approximation of these defects through appearance and feel may dictate requirements for the finished surface. If valve seat leakage is to be considered from initial contact to the molecular diffusion level, all defects must be measured to a relative degree. Nodular protuberances and/or contaminants hold the poppet off seat at light loads often out of parallel and influence the general compliance capability into the higher load region where waviness and gross curvature differentials must be pressed out before compressing the stiffer roughness. Finally, scratches must be raised from below by the internal compressive stresses created in the material by the seating force. Not considered within the scope of this program, but possibly a source of molecular diffusion leakage, are surface films of a porous nature. Each of the recognized surface characteristics must be analytically described so that their proportional influence on valve seat leakage may be quantitatively evaluated.

The purpose of this analysis is to first provide a means for numerically describing the various constituents of seating surfaces commensurate with measuring ability, and second to derive relationships relating seat load to leakage. Because these relationships will be based upon simple, imperfect models, it is to be expected that experimental correlation will be necessary to show the real situation. However, the understanding provided by these relationships will result in the properly directed pursuit of advanced designs and performance.

## EQUIVALENT SPACING HEIGHTS FOR SURFACE DEVIATIONS

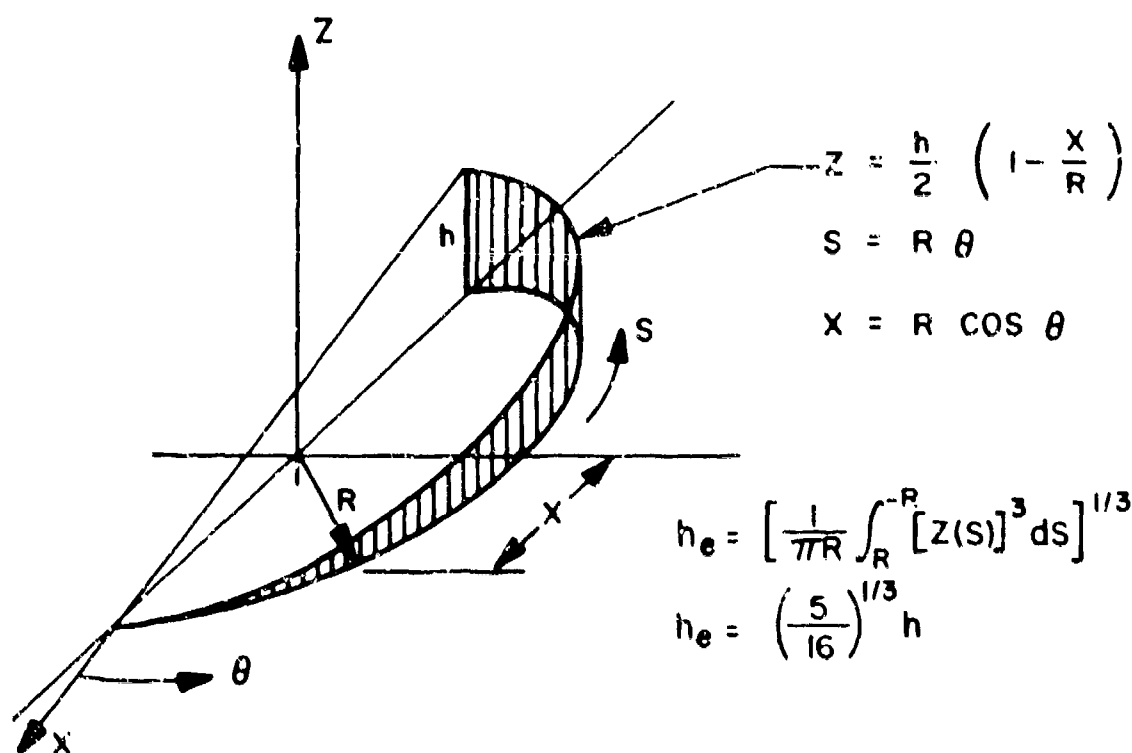
The deviations of seating geometry may be broadly divided into the following:

1. Gross abnormalities of geometry such as out-of-parallel plates, broad curvatures measured as a deviation from a flat plain, or spherically mating surfaces
2. Parameters of surface texture previously noted, i.e., roughness, waviness, local peaks, pits, and scratches

The leakage flow through, and as a result of, these various surface deviations may be indirectly determined by computing the equivalent parallel plate spacing of each deviation for that portion of the seating surface it occupies. As previously shown, valve seat leakage takes place mainly in the laminar and molecular flow regimes. In laminar flow between parallel plates the defining geometry is length, width, and separation height cubed ( $h^3$ ). The same conditions hold for molecular flow except the separation height is squared ( $h^2$ ). Thus, the cubical and square weighted height averages of the various surface geometries used to obtain the equivalent parallel plate spacing  $h_e$ , are of interest. These averages differ from the surface roughness averages (AA and rms) in that they are for the peak-to-valley spacing and are not taken about a mean line.

### Gross Geometry Deviations

Valve seat leakage caused by gross separations in the interface is mainly laminar but may be turbulent channel or nozzle flow. For the laminar case, cubically weighted averages ( $h_{eL}$ ) have been computed for typical deviations of gross geometry. An example of the approach is shown below for the out-of-parallel situation of a flat poppet and seat. It has been assumed that the seat land is sufficiently narrow with respect to the mean diameter that radial divergence and nonradial flow at the point of contact contribute negligible error.



Curve  $Z$  is one-half of a sine wave when unwrapped; and therefore, the same result is obtained by integrating over the length  $(\pi R)$ . Cylindrically out-of-flat defects (concave and convex) also result in sine wave when unwrapped; therefore, their cubical average is identical to the above.

It can be shown for these models that the assumption of perfect radial flow results in small error because more than 90 percent of the total flow discharges from the wide 180 degrees of the periphery. Therefore, only 10 percent of the flow is involved in the contact regions where the flow is partially circumferential.

### Surface Texture Deviations

Except for rare instances, loaded on-seat leakage is a combination of laminar and molecular flow (for gases). The leak path is through the

interstices formed by the contacting asperities. As with gross surface deviations, weighted averages of the spacing ( $h$ ) can be computed for various regular geometric wave forms. For the laminar regime, the cubical average ( $h_{eL}$ ) is applicable; for molecular flow ( $h_{eM}$ ).

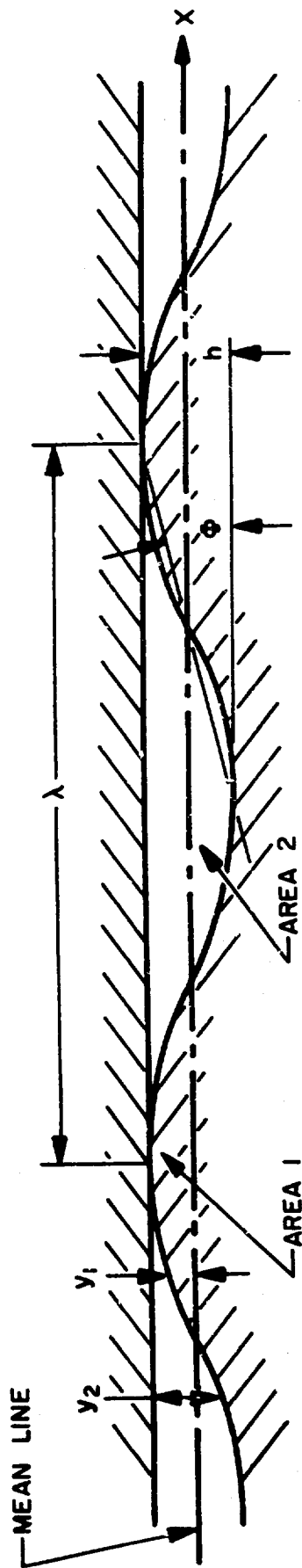
The geometrical terms and equations used to describe model surfaces are summarized in the sinusoidal representation shown in Fig. 11. The height ( $h$ ) and wave length ( $\lambda$ ), can be assumed to represent various other wave forms and exist as waviness or roughness or a combination of both. For example, a sinusoidal curve of smaller  $h$  and  $\lambda$  can be superimposed upon the sine wave shown. In addition, these waves can be imagined to be either linear into the paper or undulating in a similar fashion as that indicated resulting in a three-dimensional series of hills and valleys which contain a smaller version of the same. For the fine surfaces under consideration ( $h = 0.5$  to  $20$  microinches), the average asperity angle ( $\Phi$ ) will seldom exceed  $4$  degrees, and sharp lapping scratches do not have slope angles much greater than  $10$  degrees.

Various averages have been computed from the equations shown in Fig. 11 for a number of regular geometric wave forms (Fig. 12). These factors may be used to estimate the variations between surfaces and the possible effects on leakage performance.

The remaining surface defects important to valve seating are nodules and scratches. (Localized pits, do not increase leakage and are not considered.) Geometric interpretations of these defects may be obtained by the same parameters defining roughness ( $h$  and  $\Phi$ ) in addition to a density factor which relates the percentage area of these defects to the total area.

#### MODEL SURFACE DEFORMATIONS

The deformation of simplified model surfaces is based on the assumption of total elasticity of the interfacial contacts and substrata with uniform unit loading over the seating land. The nominal plastic deformations









$$AA = \frac{1}{\lambda} \int_0^{\lambda} |y_1| dx ; \text{ rms } = \left[ \frac{1}{\lambda} \int_0^{\lambda} y_1^2 dx \right]^{1/2}$$

$$h_{eL} = \left[ \frac{1}{\lambda} \int_0^{\lambda} y_2^3 dx \right]^{1/3} ; h_{eM} = \left[ \frac{1}{\lambda} \int_0^{\lambda} y_2^2 dx \right]^{1/2}$$

$$\text{Average Asperity Angle } \Phi \approx \frac{2h}{\lambda}$$

Location of Mean Line Defined by Area 1 = Area 2

Figure 11. Model Surface Geometry With Defining Equations

WAVE FORM: $h = 1$	$M_L^*$	$M_M^*$	AA	rms	$\frac{h}{AA}$	$\frac{h}{rms}$	$\frac{G}{h}$	$\frac{G}{AA}$	$\frac{rms}{AA}$
UNIFORMLY RANDOM 	---	---	0.2	0.25	5.0	4.0	0.5	2.5	1.25
ROUND CRESTED PARABOLIC 	0.523	---	0.256	0.298	3.91	3.36	0.333	1.29	1.16
SHARP CRESTED PARABOLIC 	0.770	---	0.256	0.298	3.91	3.36	0.667	2.60	1.16
SINUSOIDAL 	0.678	0.612	0.318	0.353	3.14	2.83	0.5	1.57	1.11
SAW TOOTH 	0.630	0.578	0.25	0.289	4.0	3.46	0.5	2.0	1.16
SQUARE 	1.0	1.0	0.5	0.5	2.0	2.0	0.5	1.0	1.0

\* $h_{eL} = M_L^* h$ ;  $h_{eM} = M_M^* h$

Figure 12. Average Height Values for Various Wave Forms

that take place in real contacts will be neglected as contributing little to the load required to effect a shutoff. Each model defect will be treated separately, and it is assumed that loads may be superimposed to arrive at a final solution. Therefore, the load to depress nodules into the waviness will be added to the load required to flatten waviness which in turn will be added to the load necessary for compressing the roughness component. No simple analysis exists which describes the characteristics of scratches or shallow vee grooves in a compressed surface; therefore, the results of model tests must be reviewed to arrive at some quantitative evaluation. It is additionally assumed that the deformations of one defect do not affect another. This is not actually the case because all defects are an integral part of the surface. However, the incurred error is assumed negligible because the relative stiffness of nodule tips or wave crests is generally small compared with the substrata. This assumption becomes increasingly invalid as the protuberance spreads out and approaches the general plane comprised of the average roughness.

Analysis of the deformations is based upon Hertz equations for curvilinear contacts. These equations have been reduced to a relatively simple form in Roark (Ref. 27) for a variety of singular contacts. Included are sphere on plate, sphere on sphere, cylinder on plate, cylinder on cylinder, cylinders crossed at right angles, etc. From these geometrical shapes and the previous data on model surfaces, a variety of models may be set up for analysis. The primary difference between each of these configurations is the spring rate, or the load to achieve a given deflection, and the load that the contact can support before plastic flow results. For example, the sphere on sphere is considerably more deformable than the cylinder on cylinder.

#### Deformation of Waviness and Roughness

Consideration of the various types of surfaces fabricated in the test program resulting from grinding, lapping, and polishing has indicated that the most likely model configuration is one which is multidirectional.



Real surface contacts consist of combinations of crossed ridges and contacting spherical protuberances or nodules, interlaced with scratches. A loose abrasive lapped surface of general matte appearance has an extremely nodular structure, generally termed homogenous or multidirectional, which is interspersed with numerous nicks and scratches laying below the general terrain. The diamond lapped surface generally has a definite lay either unidirectional or criss-crossed. The lay characteristic is caused by the scratches which have raised ridges along their lips or edges. Even in unidirectional diamond lapping these scratches criss-cross each other in angles of a few degrees, thus breaking ridge continuity.

From these observations and those noted in the literature (see Surface Studies), the model selected for analysis and data correlation is the sinusoidal surface in one direction mating with a similar surface rotated 90 degrees. The result is a multiplicity of crossed-rods contacts. This model has the advantage that the wave lengths and heights of each surface may be varied independently without destroying the model concept; also, resultant deflections are very near that obtained for spherical contacts.

Of primary concern is what happens to the displaced metal as the surfaces are loaded. Under an elastic condition, a change in volume of the stressed members will occur, and one assumption might be that the depressed metal simply disappears. It is more likely that for the extremely shallow hills and valleys of most seating surfaces, the valleys rise as the hills are depressed.

A second consideration is that as the surface asperities are compressed, a point is eventually reached when the assumed model is not the controlling characteristic, and deformation has rendered the model invalid. This transition is gradual and will tend to cause a general stiffening of the surface so that more load will be required to decrease leakage than the analysis predicts. However, the primary objective of the analysis is to place the controlling variables in proper perspective with test data used to establish a reference datum. After a better understanding of the real situation is achieved, a more sophisticated analysis will undoubtedly provide improved correlation.

4

The variation of the average leakage path ( $h_c$ ) with load (or gross seat stress) can be established from Fig. 13.

The approach of the two sinusoidal surfaces shown (Fig. 13) is approximated by the Hertz equation for the deformation of two cylinders modified by a factor  $\epsilon$  which may be assumed to vary from 1 to 2. If  $\epsilon = 1$ , the displaced material is assumed to disappear into the surface. If  $\epsilon = 2$ , the valleys are assumed to rise in proportion to the deformation of the peaks. The deformation in terms of the periodic surfaces shown is

$$\delta = 2C \left[ \frac{S^2}{a^2} (h_1 \lambda_2^2 + h_2 \lambda_1^2) \right]^{1/3}$$

where

$$S = \frac{F}{\pi D_s L}$$

and

$a$  = elastic constant for two contacting surfaces, psi

$$a = \frac{E_1}{1 - \nu_1^2} + \frac{E_2}{1 - \nu_2^2}$$

$C$  = function of  $\lambda$  and  $h$

$D_s$  = mean seat diameter, inches

$E$  = elastic modulus, psi

$F$  = total seat load, pounds

$h$  = peak-to-valley height, inches

$L$  = seat land width, inches

$S$  = apparent contact stress (also equal to individual contact load divided by  $\lambda_1 \times \lambda_2$ ), psi

$\delta$  = contact deformation defined by the approach of points remote from the contact, inches

$\nu$  = Poisson ratio

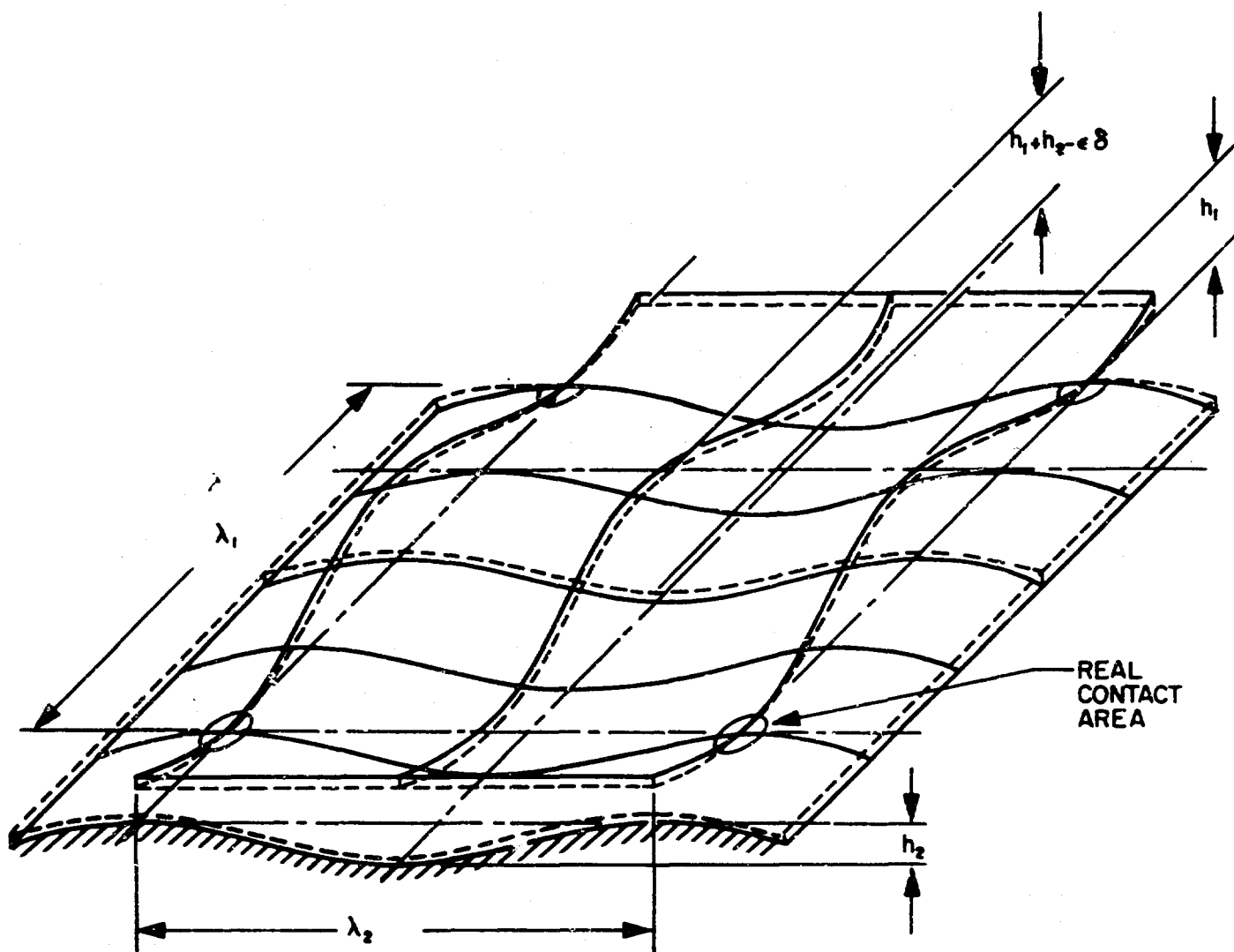


Figure 13. Sinusoidal Model Surfaces

The maximum seat load, or apparent stress, is based upon metal failure from subsurface shear which is assumed equal to one-half the yield strength of the material in normal tension. The maximum shear stress is equal to one-third the maximum contact stress. Relating these terms results in an expression for maximum apparent stress based on geometry and yield strength

$$S_m = \left( \frac{\pi}{4} A^{1/2} B Y \right)^3 \frac{\alpha^2 \lambda_1^3 \lambda_2^3}{(\lambda_1^2 h_2 + \lambda_2^2 h_1)^2}$$

where

$$S_m = \frac{F_m}{\pi D_s L}$$

and

A and B = functions of  $\lambda$  and h

$F_m$  = maximum seat load, pounds

$S_m$  = maximum apparent contact stress, psi

Y = yield strength, psi

$\alpha$  = elastic constant for two contacting surfaces, 1/psi

$$\alpha = \frac{1 - \nu_1^2}{E_1} + \frac{1 - \nu_2^2}{E_2}$$

Values of Variables A, B, and C

$\frac{\lambda_1^2/h_1}{\lambda_2^2/h_2}$	1	2	3	4	6	10
A	0.91	1.2	1.4	1.5	1.8	2.2
B	1	0.63	0.48	0.40	0.31	0.22
C	2.08	2.0	2.0	1.9	1.8	1.6

Combining the deformation equation with the relation for the averaged heights ( $h_{eL}$  and  $h_{eM}$ ) results in an expression relating the apparent seat stress to the equivalent leakage path in terms of the surface microgeometry and material properties. The general expression is

$$H_e = M (H - \epsilon \delta)$$

where

$$H = h_1 + h_2$$

$$M = \text{either the laminar or molecular factors of Fig. 12}$$

Simplification for Identical Surfaces. The previous equations have been derived so that surfaces of different roughness and wave lengths may be evaluated. Where the two seating surfaces differ appreciably, the deflections must be computed from these equations. In general, however, the techniques used to finish a poppet are also used on the seat, and the resulting surfaces are quite similar, if not identical. Considerable mathematical simplification of the previous equations is afforded if the two surfaces are treated as identical. In most cases, nominal differences can be simply averaged. Assuming  $\epsilon = 3/2$  (valleys rise 1/2 the peak deformation) the equations are reduced as follows:

$$\delta = \left( \frac{36 \alpha^2 S^2 h^3}{\Phi^2} \right)^{1/3} = \left( \frac{4.5 \alpha^2 S^2 H^3}{\Phi^2} \right)^{1/3}$$

$$\Phi \approx \frac{2h}{\lambda} = \frac{H}{\lambda}$$

$$S_m = \frac{0.42 \alpha^2 Y^3}{\Phi^2}$$

$$H_{eL} = 0.68 (H - \frac{3}{2} \delta) = 1.36 (h - \frac{3}{4} \delta)$$

$$H_{eM} = 0.61 (H - \frac{3}{2} \delta) = 1.22 (h - \frac{3}{4} \delta)$$

The flattening stress ( $S_f$ ) may be obtained by letting  $\delta = 4/3 h$ ;  $H_e$  is zero, and theoretically, leakage is zero. Although flattening stress is only hypothetical (because of other surface defects), it results in a valuable criterion of surface deformability. The flattening stress for the assumed model is

$$S_f = \frac{0.257 \Phi}{\alpha}$$

which indicates that for any elastic material, the apparent stress to achieve a given deformation is dependent upon only the average asperity angle. The analogy of the corrugated tin roof helps visualize this relation. It is apparent that increasing the number of corrugations per foot will increase the stiffness of the structure and vice versa.

The relative importance between waviness and roughness can be obtained by computing the ratio of the waviness to roughness flattening loads; therefore,

$$\frac{S_{f_w}}{S_{f_r}} = \frac{\Phi_w}{\Phi_r}$$

In most cases, the roughness will not be flattened; therefore, the above criterion should be determined using the actual apparent stress applied.

### Deformation of Nodules

The treatment of nodular deformations is the same as for roughness except for the introduction of a density function ( $\beta$ ) and a slightly different model assumption. Because most nodular contacts are more

round than elongated and quite larger than the opposing roughness, the assumed model is a sphere on flat plate. Referring to Fig. 14, the derived equations are

$$\beta = \frac{d}{\lambda_n}$$

$$\delta_n = \left( \frac{18 \alpha^2 S_n^2 h_n^3}{\beta^4 \Phi_n^2} \right)^{1/3}$$

$$S_{m_n} = \frac{1.1 \beta^2 \alpha^2 Y^3}{\Phi_n^2}$$

$$S_{f_n} = \frac{0.236 \beta^2 \Phi_n}{\alpha}$$

If  $\beta = 1$ , these equations represent a flat surface contacting a surface comprised entirely of spherical caps. Ratios of these equations with those of the previous models for surfaces of equal height and wavelength give the following results:

$$\frac{\delta_n}{\delta} = \left( \frac{18}{4.5} \right)^{1/3} = 1.6$$

$$\frac{S_{m_n}}{S_m} = \frac{1.1}{0.42} = 2.6$$

$$\frac{S_{f_n}}{S_f} = \frac{0.236}{0.257} = 0.92$$

These ratios indicate that the nodular surface is not only more compliant than the crossed rods model but is also more capable of supporting a given load elastically. The load to flatten is nearly the same for both

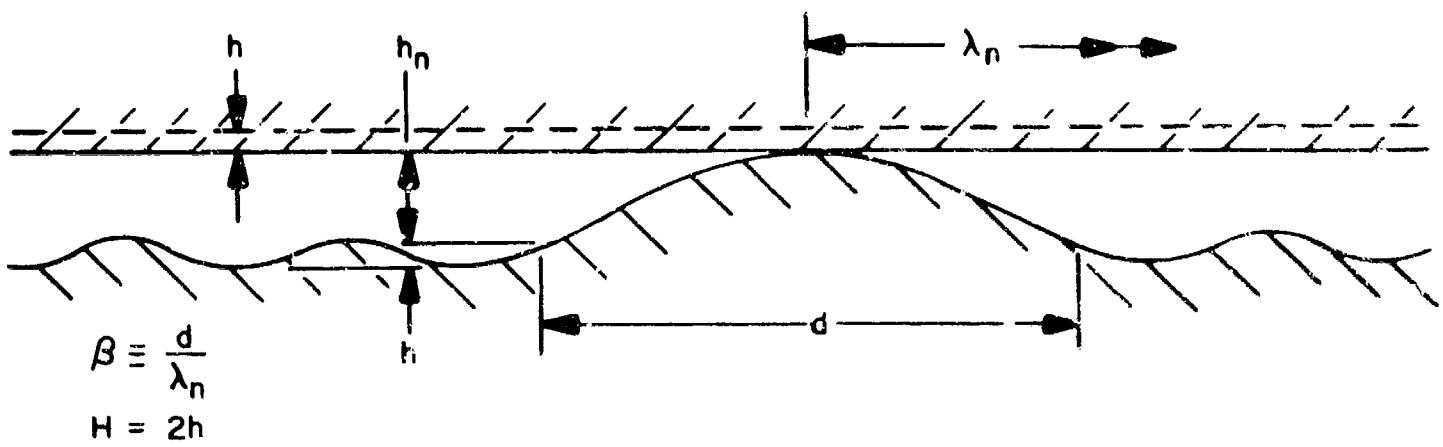


Figure 14. Model of Hemispherical Nodule



models. The reason for the greater compliance and strength of the entirely nodular surface is because it is not sinusoidal; therefore, it has more effective contact area per wavelength ( $\lambda$ ).

Of primary concern in this analysis is the flattening stress because, in most cases, fully separated seat leakage would be quite high. As with waviness, the ratio of nodule-to-roughness flattening stresses will allow an estimation of the relative importance of nodules

$$\frac{S_{f_n}}{S_{f_r}} = \frac{\beta^2 \Phi_n}{\Phi_r}$$

If the seat load is insufficient to flatten nodules, the equivalent height may be approximated by adding the nodular space to the equivalent heights for the asperities of both surfaces; therefore, the general expression is

$$H_{en} = h_n - \delta_n + M H$$

The load to flatten nodules or waviness subtracts from the total load so the roughness deformation expression is modified accordingly

$$\delta_r = \left[ \frac{36 \alpha^2 h^3 (S - S_n - S_w)^2}{\Phi^2} \right]^{1/3}$$

## STRESS-LEAKAGE EQUATIONS

The deformation and leakage flow equations previously developed may be combined to obtain a composite equation relating all of the known variables. While such an expression is exceedingly cumbersome and is better handled in parts, it does allow at one viewing a consideration of all variables.

### Assumptions

The assumptions leading to the final equations are as follows:

1. Leakage flow is described by the laminar and molecular flow equations for parallel plates. Total flow is the sum of molecular and laminar flow.
2. Appropriately weighted averaging factors may be used to obtain equivalent parallel plate heights for calculating leakage.
3. Seat load is uniformly applied and is uniformly distributed across the seat land (L).
4. Mating surfaces are sinusoidal in one direction, cross-layed at 90 degrees, and have the same peak-to-valley height and wave length (there are no superimposed nodules or waviness).
5. Surface deformation equations are valid up to  $3/2$  of the yield strength based on Vicker's hardness tests.
6. Hertz theory is valid for peak deformation to define the decrease in h up to some value to be determined by test.

### Stress-Leakage Equations

$$S_m = \frac{0.42 \alpha^2 Y^3}{\Phi^2}$$

$$S_f = \frac{0.257 \Phi}{\alpha}$$

$$\delta = \left( \frac{4.5 \alpha^2 S^2 H^3}{\Phi^2} \right)^{1/3}$$

$$H_{eL} = 0.68 (H - 3/2 \delta)$$

$$H_{eM} = 0.61 (H - 3/2 \delta)$$

$$H = h_1 + h_2$$

$$\omega_L = \frac{\pi D_s H_{eL}^3 (P_1^2 - P_2^2)}{24 \mu L RT}$$

$$\text{NOTE: } RT = \frac{P}{\rho}$$

$$\omega_M = \frac{4}{3} \sqrt{2\pi} \frac{D_s H_{eM}^2 (P_1 - P_2)}{L \sqrt{RT/g}}$$

$$Q = \frac{\omega}{\rho} = \omega \frac{RT_s}{P_s}$$

For

$$P_s = 14.7 \text{ psia}$$

$$T_s = 70 \text{ F} = 530 \text{ R}$$

$$g = 32.2 \text{ ft/sec}^2 = 1.39 \times 10^6 \text{ in./min}^2$$

$$Q_L = \frac{4.71 D_s H_{eL}^3 (P_1^2 - P_2^2)}{\mu LT}$$

$$Q_M = \frac{1.42 \times 10^5 D_s H_{eM}^2 (P_1 - P_2)}{L} \sqrt{\frac{R}{T}}$$

$$Q = Q_L + Q_M$$

### Composite Equation

$$Q = \frac{4.71 D_s (P_1^2 - P_2^2)}{\mu L T} \left[ M_L (H - \epsilon \delta) \right]^3 + \frac{1.42 \times 10^5 D_s (P_1 - P_2)}{L} \sqrt{\frac{R}{T}} \left[ M_M (H - \epsilon \delta) \right]^2$$

### PARAMETRIC STRESS-LEAKAGE DATA

Parametric data have been computed from the previous equations in support of the experimental test program. The poppet and seat model design is shown in Fig. 15 with appropriate dimensions. Test and configuration constants and parameterized variables are summarized below with the reduced equations.

### Test and Configuration Constants

The test and configuration constants are as follows:

Inlet pressure,  $P_1 = 1015$  psia

Outlet Pressure,  $P_2 = 14.7$  psia

Gas temperature,  $T = 70$  F = 530 R

Gas constant,  $R = 663$  in./R (nitrogen)

Gas viscosity,  $\mu = 4.4 \times 10^{-11}$  lb-min/in.<sup>2</sup> (nitrogen)

Mean seat diameter,  $D_s = 0.470$  inch

Seat land width,  $L = 0.03$  inch

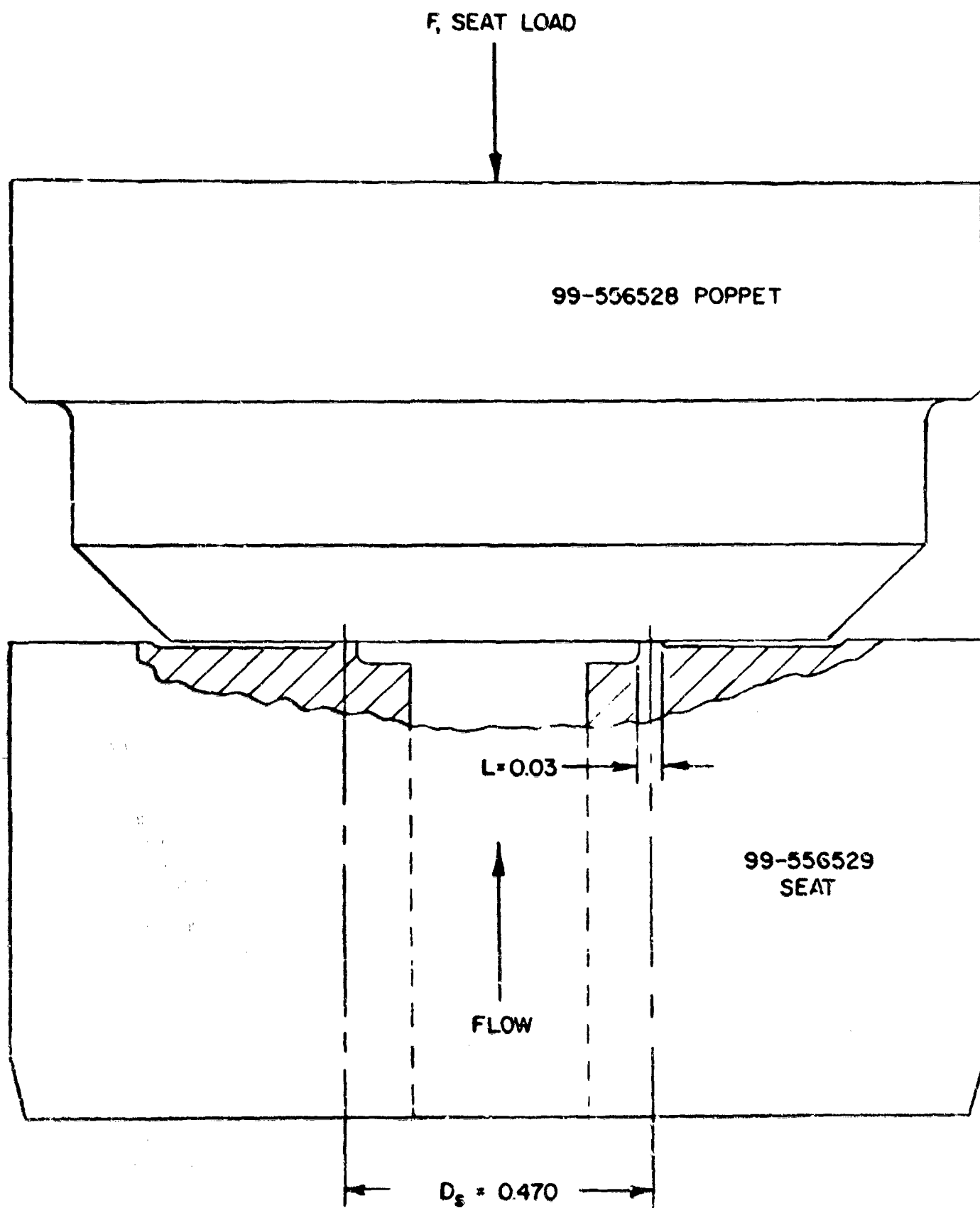


Figure 15. Typical 1/2-Inch Poppet and Seat Model

### Reduced Equations for 1/2-Inch Model Seat

The reduced equations are as follows:

$$Q_L = 3.26 \times 10^{15} H_{eL}^3$$

$$Q_M = 2.49 \times 10^9 H_{eM}^2$$

$$Q_L = 3.26 \times 10^{15} \left\{ 1.36 \left[ h - \frac{3}{4} \left( \frac{36 \alpha^2 s^2 h^3}{\Phi^2} \right)^{1/3} \right] \right\}^3$$

$$Q_M = 2.49 \times 10^9 \left\{ 1.22 \left[ h - \frac{3}{4} \left( \frac{36 \alpha^2 s^2 h^3}{\Phi^2} \right)^{1/3} \right] \right\}^2$$

$$Q = Q_L + Q_M$$

### Material Parameters

The following lists the material parameters.

Material	Vickers Hardness Number kg./mm <sup>2</sup>	Yield Strength Criterion, psi	Elastic Constant,* 1/psi	Elastic Modulus, psi
440C Stainless Steel	800	610,000	$0.0607 \times 10^{-6}$	$30 \times 10^6$
6061-T651 Aluminum	123	93,800	$0.182 \times 10^{-6}$	$10 \times 10^6$
Tungsten Carbide	1330	1,000,000	$0.0202 \times 10^{-6}$	$90 \times 10^6$

\*Poisson's ratio,  $\nu \cong 0.3$

## Surface Profile Parameters

The surface profile parameters are:

1. Peak-to-valley height for one surface (second surface identical),  
 $h = 1, 1.5, 2, 3, 4.5, 6, 9, 12$  and  $18 \times 10^{-6}$  inches

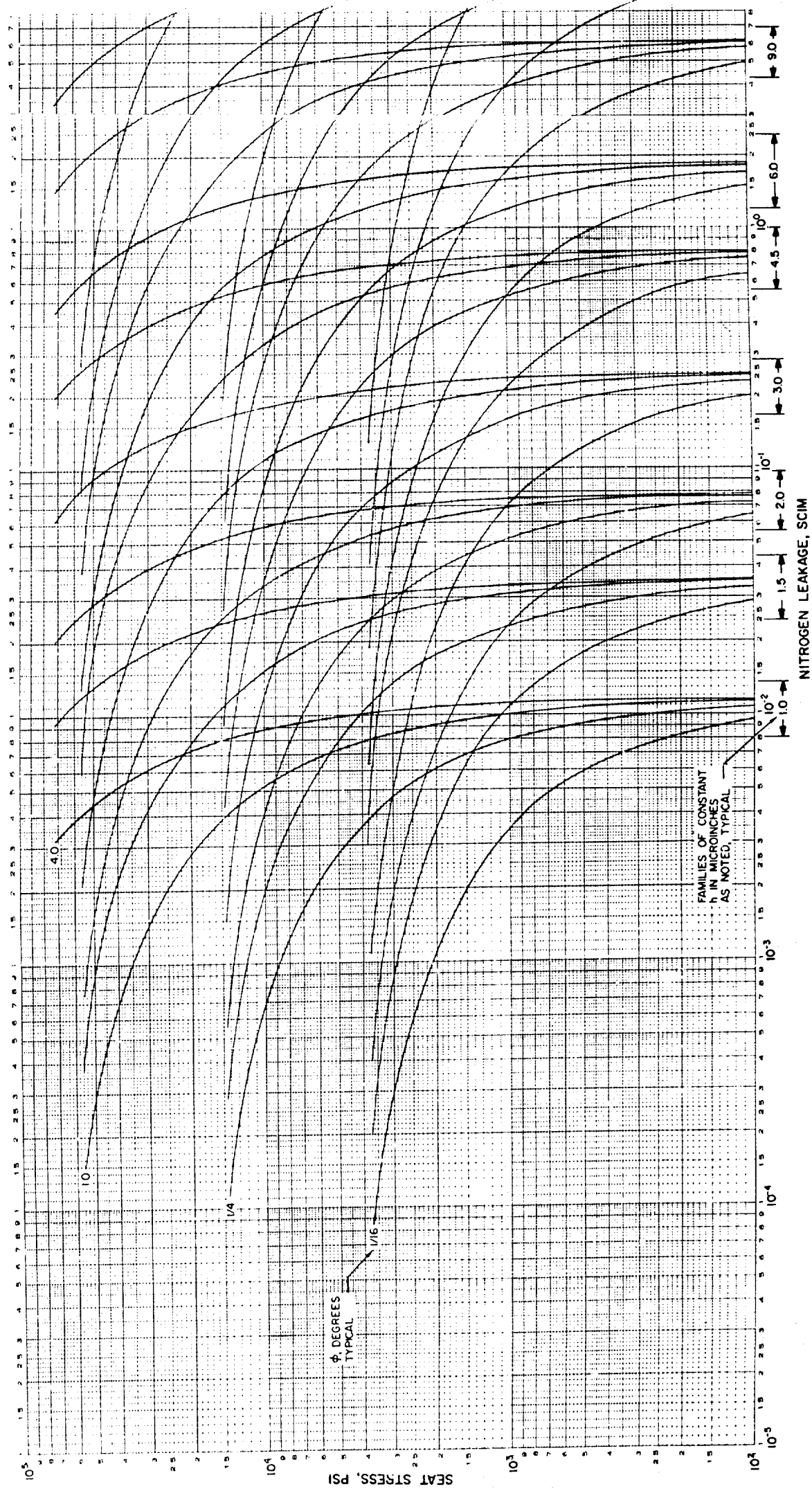
NOTE: These  $h$  values correspond to approximate AA values of  $1/3, 1/2, 2/3, 1.0, 1.5, 2.0, 3.0, 4.0$ , and  $6.0$  microinches.

2. Average asperity angle,  $\Phi = 1/16, 1/4, 1$  and  $4$  degrees (must be in radians for use in equations).

The parametric curves of leakage vs apparent seat stress are shown in Fig. 16 through 18 for the constants and variables noted above. The curves cover a span of  $10^7$  acin for seat stress from 100 to 100,000 psi. The basic parameter for each family of curves is  $h$  (e.g.,  $h = 1.0$  microinch) with variations of  $\Phi$  showing the span from typical waviness to roughness. An evaluation of these curves shows the effect of  $h$ ,  $\Phi$ , and  $\alpha$  on leakage.

Interpreting the curves requires certain precautions and observations. Multicycle log-log paper can be very misleading because of the great span of data. For example, consider the scope of data in the first cycle (100 to 1000 psi) in relationship with the second, then the third. Also, the curves represent deformation of a uniform surface and not the more complex model of knobs on knobs on knobs proposed by Archard (see Surface Studies). The effect of waviness superimposed on roughness (a beginning of Archard's model) can be evaluated by subtracting the apparent stress to flatten waviness from the total available apparent stress to arrive at a final leakage value. To find the leakage of both waviness and roughness when waviness is not eliminated, the waviness leakage is added to the roughness leakage obtained at the 100-psi (essentially zero) stress level.

A





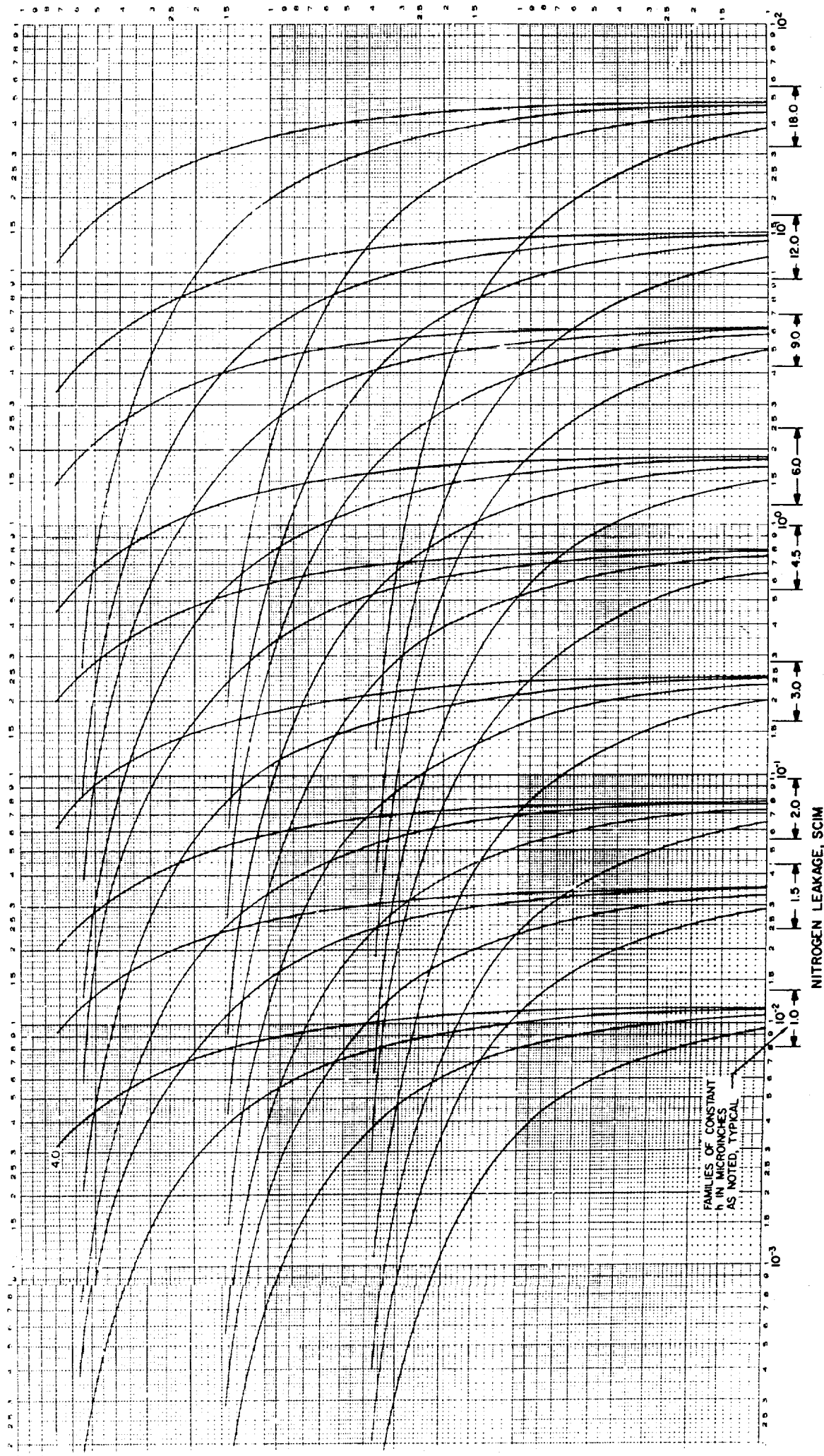
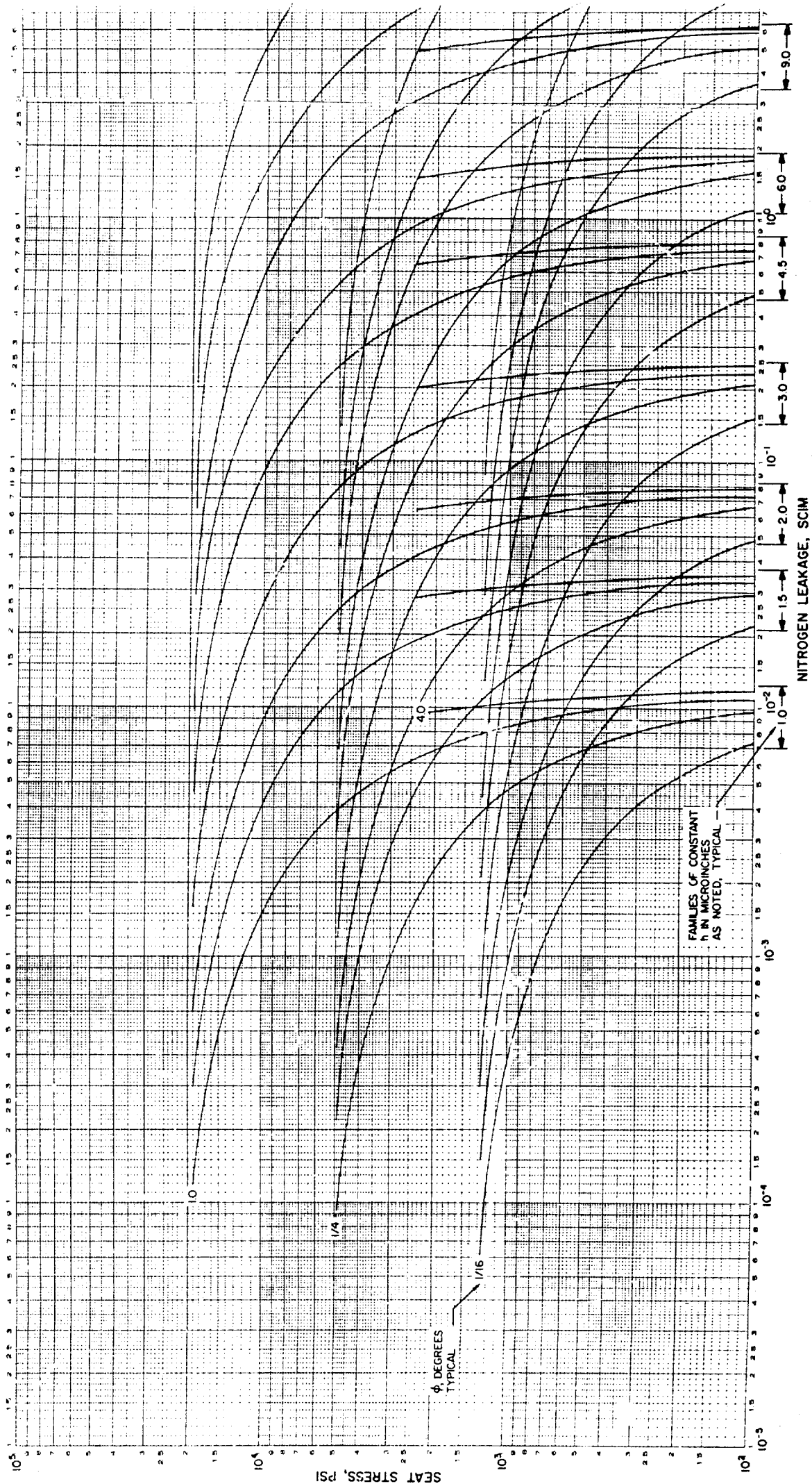


Figure 16. Theoretical Parametric Stress vs Leakage Curves for Steel

A



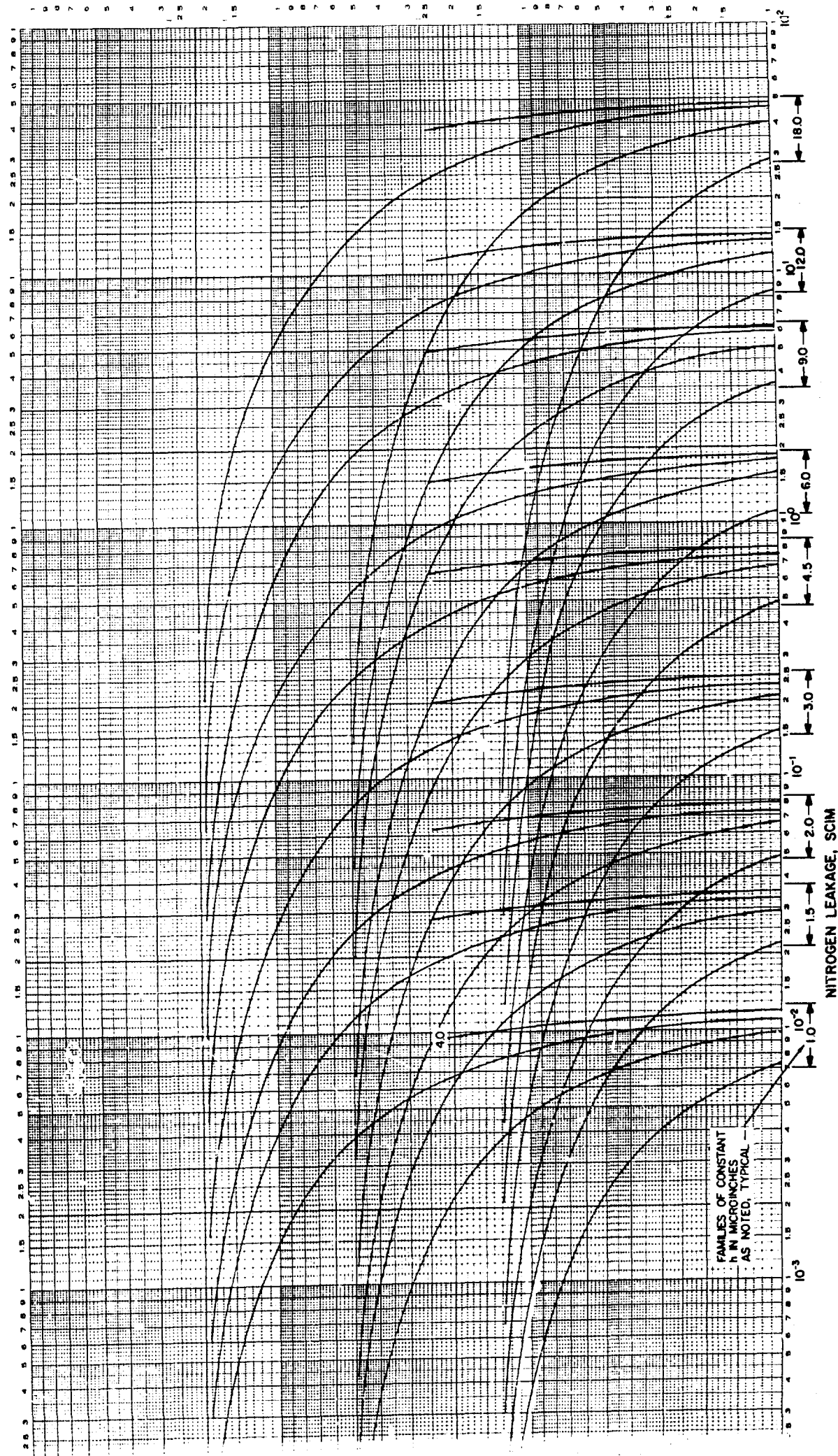


Figure 17. Theoretical Parametric Stress vs Leakage Curves for Aluminum





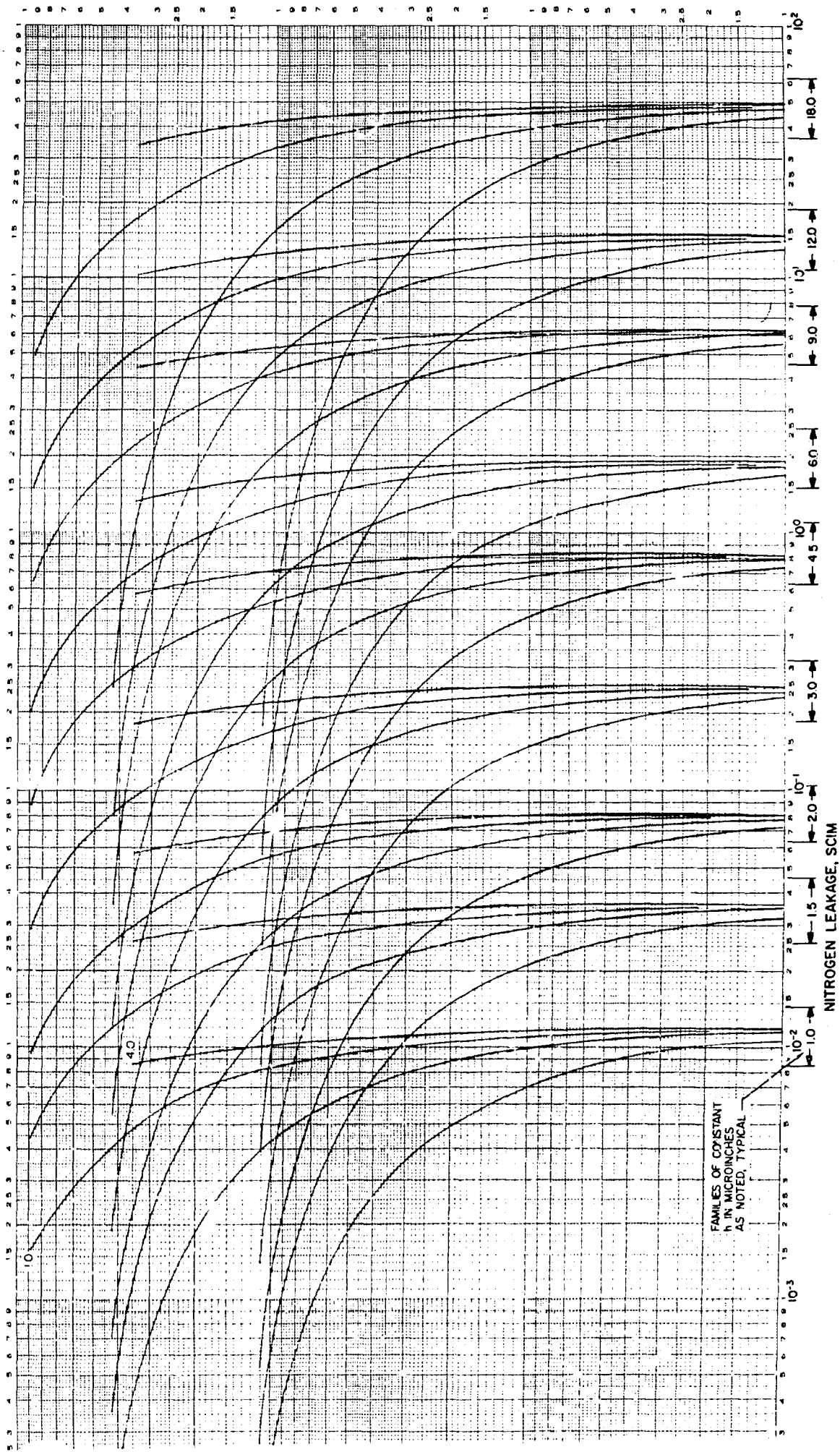


Figure 18. Theoretical Parametric Stress vs Leakage Curves for Tungsten Carbide

Stress-leakage data for other test conditions and valve seat configurations may be obtained by applying appropriate ratios of the variable parameters to the governing equations. Because the total leakage described by these curves is a combination of laminar and molecular flow, the division of this flow must first be determined so that the ratios may be applied separately to each term of the total flow equation ( $Q = Q_L + Q_M$ ). Figure 19 plots the ratios of  $Q_M/Q$  and  $Q_L/Q$  in percent for the parametric data curves of Fig. 16 through 18; i.e., for the specific model at a 1000-psig inlet pressure.

Stress-leakage data for other test conditions and valve seat configurations may be obtained by applying appropriate ratios of the variable parameters to the governing equations. Because the total leakage described by these curves is a combination of laminar and molecular flow, the division of this flow must first be determined so that the ratios may be applied separately to each term of the total flow equation ( $Q = Q_L + Q_M$ ). Figure 19 plots the ratios of  $Q_M/Q$  and  $Q_L/Q$  in percent for the parametric data curves of Fig. 16 through 18; i.e., for the specific model at a 1000-psig inlet pressure.

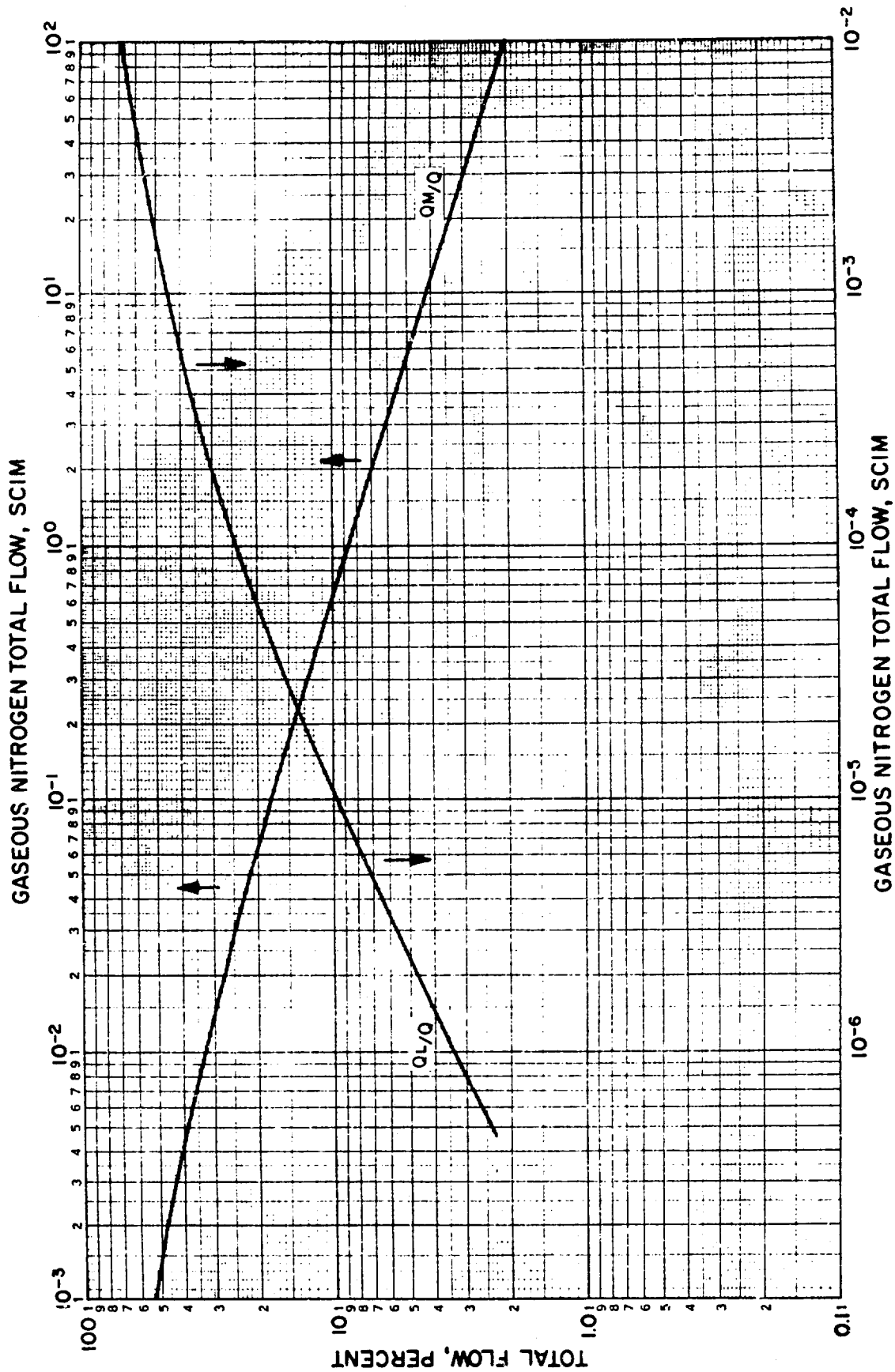


Figure 19. Division of Total Flow in Figs. 16 through 18



## NOMENCLATURE

$a$	=	elastic constant for two contacting surfaces, psi
AA	=	arithmetic average, microinches
A and B	=	functions of $h$ and $\lambda$ in $S_m$ equation
C	=	function of $h$ and $\lambda$ in $\delta$ equation
$d$	=	nodule base diameter, inches
$D_s$	=	mean seat diameter, inches
E	=	elastic modulus, psi
F	=	total seat load, pounds
$g$	=	gravitational acceleration, in./min <sup>2</sup>
$h$	=	average peak-to-valley height for one surface, inches
$h_e$	=	equivalent parallel plate height for one surface (i.e., weighted peak-to-valley height), inches
H	=	average peak-to-valley height for two contacting surfaces, inches
$H_e$	=	weighted peak-to-valley height for two contacting surfaces, inches
L	=	seat land width, inches
M	=	laminar or molecular weighting factor
P	=	pressure, psia
Q	=	flow, scim
R	=	gas constant, in./R
S	=	total apparent seat stress, psi
$S_f$	=	apparent seat stress to flatten, psi
$S_m$	=	apparent seat stress to surface yield, psi
T	=	temperature, R
Y	=	surface yield strength, psi

#### Greek Symbols:

$\alpha$  = elastic constant for two contacting surfaces, 1/psi

$\beta$  = nodule density function

$\delta$  = surface deformation, inches

$\epsilon$  = surface deformation factor

$\lambda$  = average asperity wave length, inches

$\mu$  = viscosity, lb-min/in.<sup>2</sup>

$\nu$  = Poisson's ratio

$\rho$  = density, lb/in.<sup>3</sup>

$\Phi$  = average asperity slope, radians

$\omega$  = weight flowrate, lb/min

#### Subscripts:

1 = inlet conditions or surface (1)

2 = outlet conditions or surface (2)

L = laminar factor or flow

M = molecular factor or flow

n = nodule

r = roughness

s = standard conditions of temperature and pressure, i.e., 70 F and 14.7 psia

w = waviness

## DESIGN, FABRICATION, AND DEVELOPMENT OF TEST FIXTURE AND MODELS

The definition of the development effort following the Survey Phase outlined the general requirements for a test fixture and facility to provide test data on valve seating. The design of a test fixture for experimental model evaluation posed some formidable problems because in addition to the capability for precise measurement of various test parameters, the tester should not influence the data. Primarily, the tester was to provide information on poppet and seat forces in the near-seated and seated positions, leakage flow as a function of inlet pressure, and seat position and load for flat, metal-to-metal poppets and seats. However, testing of conical and spherical-shaped metal models was considered in the design as well as a capability for cycle testing to evaluate the effects of dynamic loading.

An analysis of test capabilities led to the model hardware definition outlined in Table 6 and the test fixture requirements.

### TEST FIXTURE REQUIREMENTS

Test fluid	Helium, nitrogen, and argon at 70 F
Seat inlet pressure	0 to 1500 psig; measurement accuracy $\pm 2\frac{1}{2}$ percent
Seat loading	0 to 3000 pounds based on 0.500-inch diameter seat, 0.030-inch land width, and 60,000-psi seat stress with 5 percent measurement accuracy
Model position control	20-microinch parallelism total over a 1.0-inch diameter between poppet and seat mating faces; linear poppet-to-seat gap control from contact to 0.001 inch and detection of 5-microinch change
Leakage measurement	$10^{-3}$ scim to 10 scim

TABLE 6

## POPPET AND SEAT EXPERIMENTAL TEST PARAMETERS

99-556528	99-556527 Seat 1.000-inch Diameter			99-556529 Seat 0.500-inch Diameter (3)									
	(1) 0.0001 to 0.002 Gap (-31)	(2) Land Width 0.010 0.050 0.060 (-7) (-5) (-3)		440 C CRES (-3)									
(4) Parallelism, $\mu$ in.	7	7	7	4	4	4	4	4	4	4	4	4	4
	3	3	3	3	3	3	3	3	3	3	3	3	3
	2	2	2	1/2	3-5	7-9	9-15	19-27	41-51	40-60	90-110	4	4
	2	2	2	1/2	3-5	7-9	9-15	19-27	41-51	40-60	90-110	4	4
Tungsten Carbide (-5)	Pressure Distribution vs Load	Leakage vs Load		Finish	Finish	Finish	Flatness	Flatness	Flatness	Parallel		Finish	Flatness
440 C CRES (-3)	4			Finish Cycle	Finish Cycle	Finish Cycle	Flatness Cycle	Flatness Cycle	Flatness	Parallel Cycle	Parallel	Finish Cycle	Flatness
17-4 CRES (-7)	1/2			Finish Cycle	Finish Cycle	Finish Cycle	Flatness Cycle	Flatness Cycle	Flatness	Parallel Cycle	Parallel	Finish Cycle	Flatness
6061-T651 Aluminum (-9)	4			Finish Cycle	Finish Cycle	Finish Cycle	Flatness Cycle	Flatness Cycle	Flatness	Parallel Cycle	Parallel	Finish Cycle	Flatness

NOTES:

1. 1.000 OD x 0.060 land (includes nine 0.005-inch diameter holes in land for pressure distribution measurement)
2. 1.000 OD x 0.030, 1.000 OD x 0.010 and 1.000 OD x 0.060-inch land
3. 0.500 OD x 0.030-inch land
4. Parallelism figures shown refer to the accuracy maintained on the sealing surfaces of the test model with respect to the locating surfaces in the fixture. Maximum deviation of poppet and seat sealing surfaces is the sum of the poppet and seat plus 20 microinches of the tester locating surfaces.

Cycling	Approximately 1000 cycles per seat; impact levels to be established by test
Test models	Poppet and seats to be readily changed without impairing positional accuracy

## DESIGN

Figures 20 through 23 are detail drawings of the test fixture and models used during the program.

### Seat-Loading

The first design feature to be established was that the poppet be loaded by a pneumatically pressurized piston. The primary advantages of such a method are simplicity and cleanliness of the system, availability of high-pressure gases and necessary control components, and ease of control for static and dynamic testing.

Selection of the piston size represented a compromise influenced by such considerations as reasonable pressurization levels required to produce sufficient stress in the model seat land and a high length-to-diameter (L/D) ratio to minimize poppet-to-seat parallelism deviation. A nominal piston diameter of 1.5 inches (loading area of 1.767 sq in.) was selected in conjunction with a 0.0001 to 0.0002-inch piston-bore diametral clearance and an L/D ratio of approximately 5. Assuming 2000 psig as a minimum bottle supply pressure, the resultant maximum seat load is 3530 pounds corresponding to a seat stress for the 0.500-inch OD, 0.03-inch land width seat of 80,000 psi.

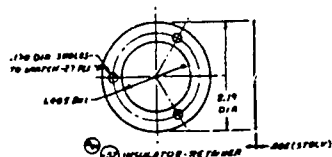
The piston size basically dictated the dimensions of the balance of the tester resulting in a unit weighing approximately 50 pounds permitting reasonable handling ease.

## Seat Load Measurement

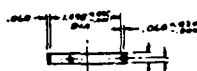
An accurate measurement of model seat loading was one of the prime test parameters and of sufficient importance to warrant dual verification methods. The precisely controlled piston diameter in conjunction with precision (0.1 percent of full scale) Heise pressure gages provided the first and most simple means of load measurement. In the low, sensitive load region using a precision 100-psi gage, load accuracy of less than 0.2 pound may be realized. Therefore, the lowest load which could be controlled within the desired 5-percent accuracy was 0.177/0.05 or 3.5 pounds.

The second method used for load measurement was a system of strain gages arranged to form load cells. A three-cell system mounted directly on the model test piston was used to (1) eliminate errors resulting from friction and side loads from intermediate members, (2) provide a three-point mounting which would eliminate errors from locating points deviating from a true plane, and (3) allow an analysis of eccentric loads created by nonuniform seat loading. Item 3 originates predominately from the loading of nonparallel seating surfaces but also from possible nonuniform distribution of the seat inlet pressure. To provide allowance for nonparallel seating and cycling impacts, each cell had to be capable of taking a 3000-pound load.

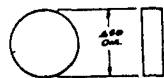
Several systems were studied ranging from commercial units mounted externally with interchangeable elements for different ranges to a custom design which would cover the entire range. The latter used either piezoresistive or conventional resistive strain gages to be mounted directly on cells machined as part of the piston, each cell being capable of covering the entire range. All systems required an electrical amplifier and readout method of high gain and stability. The piezoresistive method had the advantage of high sensitivity and output directly from the sensing element which eliminated much electronic equipment. Its



1. MAT'L: ALUMINUM, 6061-T6, 1/2" THICK  
NOTES: -22 INSULATOR

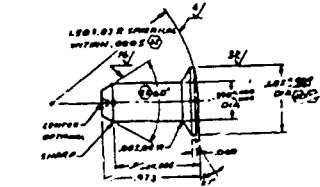


2. INSIDE WITH SECT 1/4" DIA DOUBLE PAIR  
TYPED (HOLE LOCUS: 1.00 DIA, 1.00 DIA, 1.00 DIA)  
1. MAT'L: 6061 ALUMINUM, 1/2" THICK, CLASS 100,  
COND A, 1/2" DIA 1.19 BAR  
NOTES: -23 PLUG



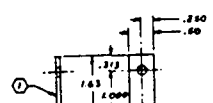
3. SPACER  
SCALE: 2 TIMES

1. MAT'L: TUNGSTEN CARBIDE, ROCKWELL A 90 MIN  
NOTES: -24 SPACER



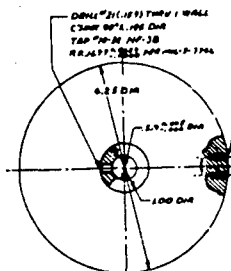
4. PIN-CENTERING  
SCALE: 2 TIMES

1. MAT'L: 6061 ALUMINUM, 1/2" THICK, CLASS 100,  
COND A, 1/2" DIA 1.19 BAR  
NOTES: -25 PIN



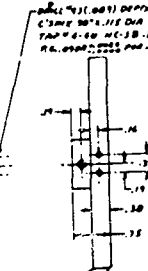
5. PLATE - SPRING RETAINER

2. PASSIVATE PER RADIO-DIB  
1. MAT'L: 303 CRS, MIL-S-8839, COMP 303,  
COND A, 1/2" DIA 1.19 BAR  
NOTES: -26 PLATE



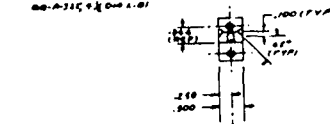
6. INDOOR WHEEL

1. MAT'L: 6061 ALUMINUM, 1/2" THICK  
COND A, 1/2" DIA 1.19 BAR



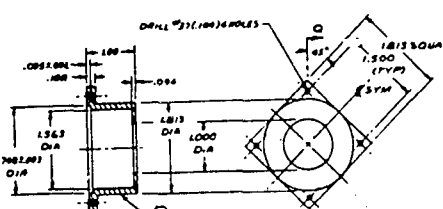
7. POINTER

1. MAT'L: 6061 ALUMINUM, 1/2" THICK  
COND A, 1/2" DIA 1.19 BAR



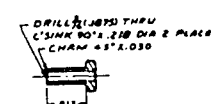
8. BRACKET - SPRING

1. 0.03 FILLET RADI  
2. PASSIVATE PER RADIO-DIB  
1. MAT'L: 303 CRS, MIL-S-7120, COMP 303,  
COND A, 1/2" DIA 1.19 BAR  
NOTES: -27 BRACKET



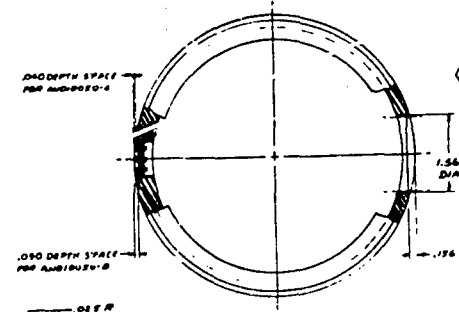
9. ADAPTOR-ELEC CONNECTOR

1. ANDISS PER MIL-A-2631 TYPE I (RAD-009-003)  
2. 0.03 FILLET RADI  
1. MAT'L: 2024-T351 AL ALLOY, 60-A-248, COND 117, 1/2" DIA 1.19 BAR  
NOTES: -28 ADAPTOR



10. BOLT-SEAT RETAINING

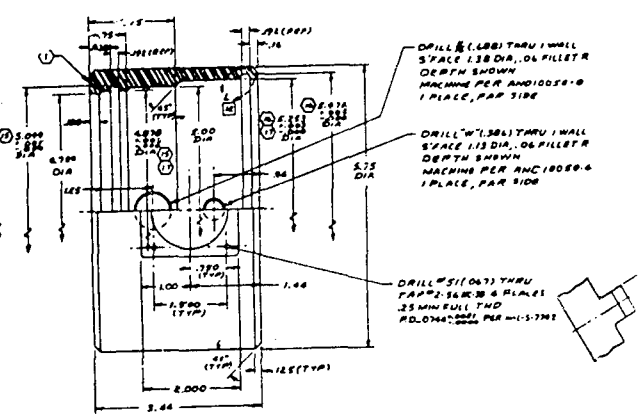
1. PASSIVATE PER RADIO-DIB  
2. MAKE FROM NATION'S-6A BOLT  
(4-10LBS OR DISCALUT, 15,000 PSI MIN)  
NOTES: -29 BOLT



11. RING - COVER



DETAIL 1  
TYPE 2 PLACES  
SCALE: 2 TIMES

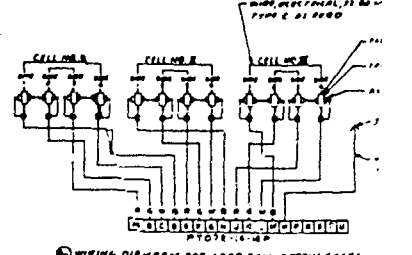
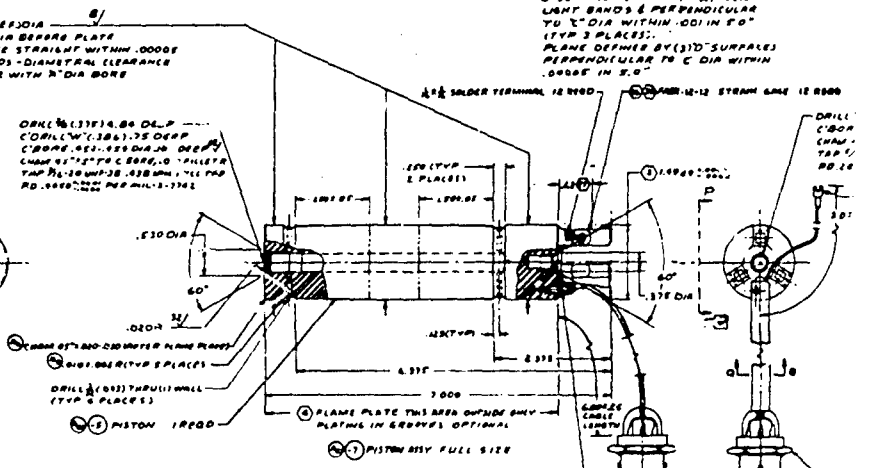
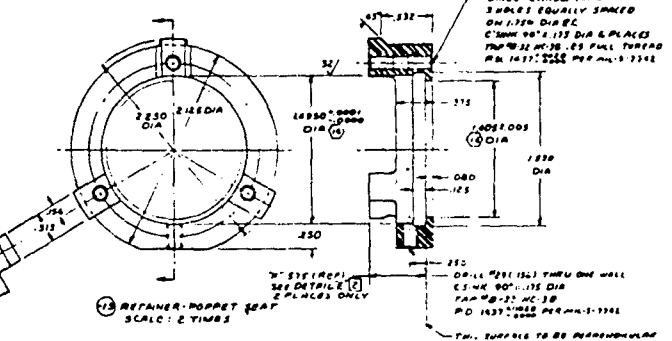
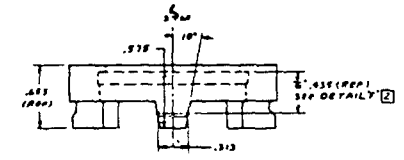
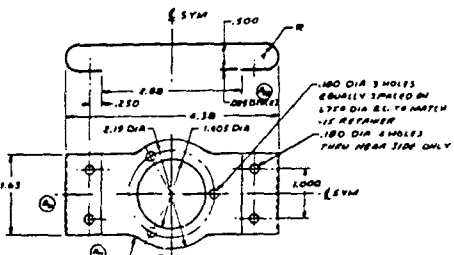
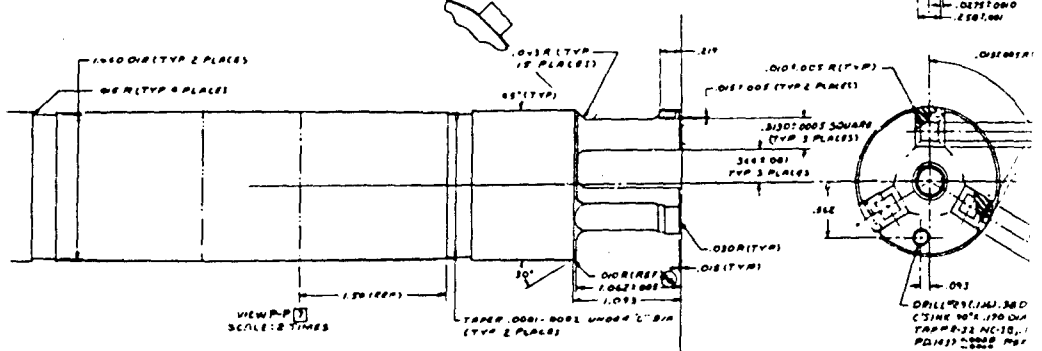
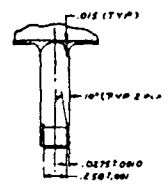
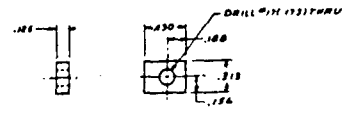
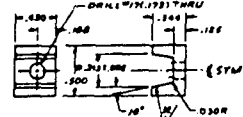
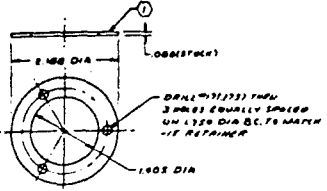


1. 0.03 FILLET RADI  
2. PASSIVATE PER RADIO-DIB  
1. MAT'L: 2024-T351 AL ALLOY, 60-A-248, COND 117, 1/2" DIA 1.19 BAR  
NOTES: -30 RING

68  
97  
19  
335  
100

US NAVY

250



6. 63/ ALL SURFALDS  
(a) 1 CONCENTRIC WITHIN .008 IN  
2 .030 FILLET RADIUS  
3 PASSIVATE PER METHOD-08  
4 HEAT TREAT 80-60 BOTH WAYS 1' PER MIL. IN LIFTING PLATE  
5 WELD 1/8" C (REF. 00-7-76) CLASS 90C, CONDA, 2 1/2 DIA. 75  
NOTES: 15 RETAINED

[illegible][illegible]

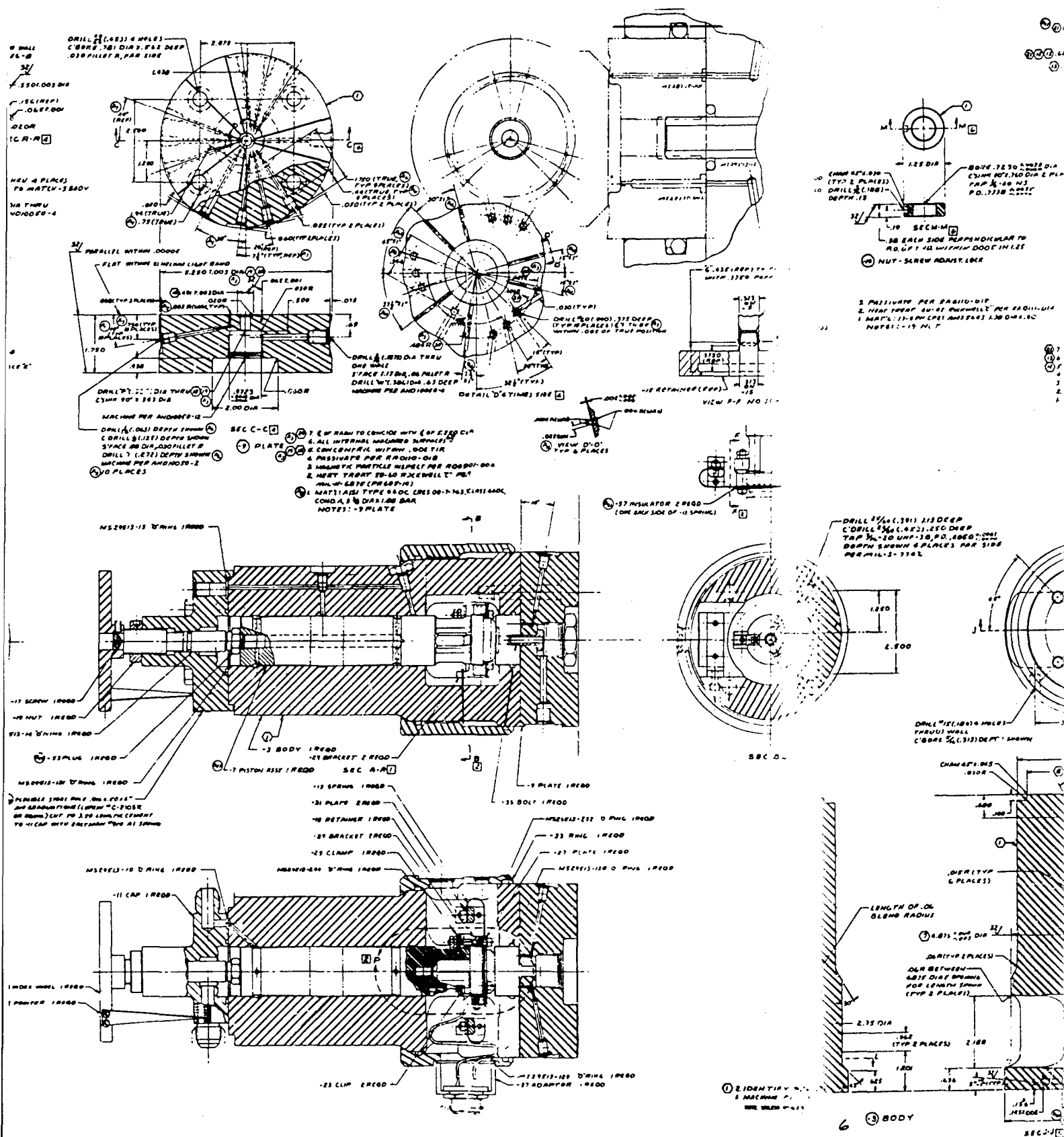
1-12 SCREW IN RD  
 MAKE AROW #8. 12% HONEST SET  
 CONF. REMOVE FOR THIS AS SHOWN

④ WIRING DIAGRAM FOR LOAD CELL STRAIN GAUGE  
& ELECTRICAL CONTACT LEAD ④



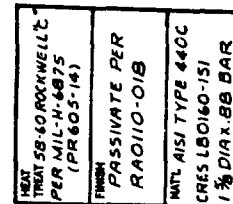


- ② 1. CONCENTRIC WITHIN .0005 TIR =  
 ⑦ 2. CONCENTRIC WITHIN .001 TIR =  
 ③ ④ ⑤ ⑥ 3. ALL INTERNAL UNFINISHED SURFACES  
 4. CONCENTRIC WITHIN .002 TIR  
 5. PASSIVE AND RADIUS .015  
 6. AEROSTATIC PRINCIPLE CORRECT FOR .00001-.0005  
 7. MACH TYPICAL 18-20 FOR 100000 L PER  
 MIL-IN. BEST (PRACTICE)  
 8. MACH .1, AIR FLOW 100-200 PSIG, 1-263, CLASS 4000,  
 CONOA, 1 1/2 DIA 2000 BAR  
 NOTES - 3 BODY



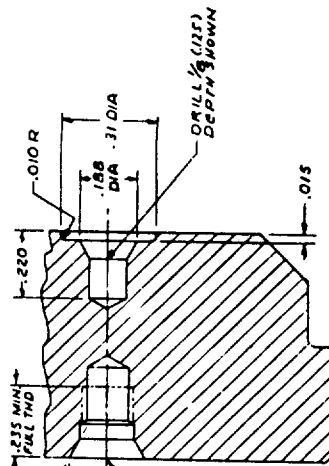
[illegible]





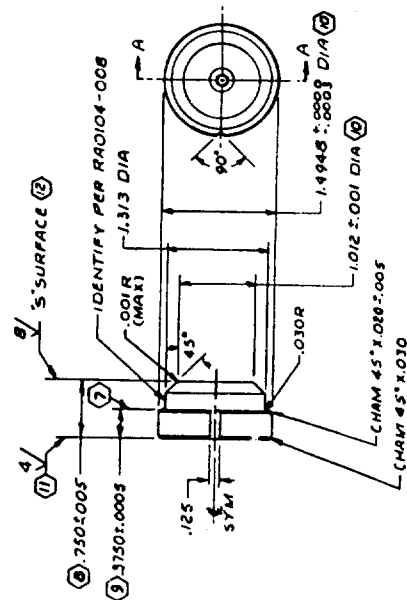
NOTE: UNLESS OTHERWISE SPECIFIED

109



SECTION A-A  
4 TIMES SIZE  
-3, -7, 6, -9 ONLY

DRILL #29 (.130) .300 DEEP  
(DRILL #17 (.173) .100 DEEP  
CHAMFER AS SHOWN  
CHAMFER .010 DIA .010 DEEP  
PO. 1.012 ± .005 PER MIL. S. 1761

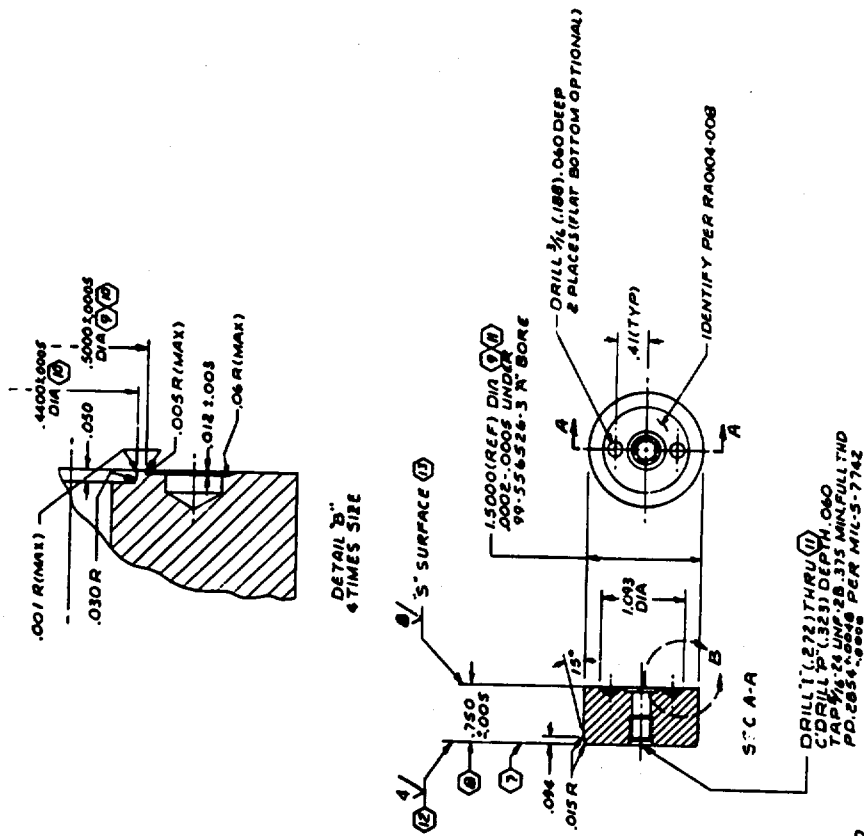


13. S' SURFACE LEFT "AS GROUND"
12. FLAT WITHIN ONE HELIUM LIGHT BAND
11. CONCENTRIC WITHIN .002 TIR
10. PARALLEL WITHIN .003
9. PARALLEL WITHIN .003
8. PERPENDICULAR TO 1.4948 DIA WITHIN .0003 IN 1.5"
7. HEAT TREAT 40-45 ROCKWELL "C" PER RADIO-014
6. 3 HEAT TREAT 58-60 ROCKWELL "C" PER MIL-N-8875 (PR605-14)
5. 9 6061-T651 AL ALLOY, 90-A-325, TEMP T651 1 1/2 X .88 BAR
4. 7 17-4 PH CRES AMS 5643 1 1/2 DIA X .88 BAR
3. 5 TUNGSTEN CARBIDE ROCKWELL "H" 90-93 1 1/2 DIA X .88 BAR
2. 3 AISI TYPE 140C L8060-151 1 1/2 DIA X .88 BAR
1. 3/4" ALL SURFACES EXCEPT HOLE #4

NOTE: UNLESS OTHERWISE SPECIFIED

HEAT TREAT	-56-9 NONE -3 NOTED ⑤ -7 NO: 20 ⑥
FINISH	-5 6-9 NONE -3 6-7 PASSIVATE PER RADIO-018
MTL	NOTED ① ② ③ ④

Figure 22. Model Poppet  
(Drawing No. 99-556528)



11. 5" SURFACE LEFT "AS GROUND"
12. FLAT WITHIN ONE HELIUM LIGHT BAND
13. CONCENTRIC WITHIN .001 TIR
14. CONCENTRIC WITHIN .001 TIR
15. PARALLEL WITHIN .00050
16. PERPENDICULAR TO 15000 DIA WITHIN .0003 IN 1.5"
17. HEAT TREAT 40-45 ROCKWELL "C"
18. HEAT TREAT 58-60 ROCKWELL "C"
19. PER MIL-N-6875 (PACOF-14)
20. 17-4 PH CRES AMS5643 1/8" DIA X .88 BAR
21. 17-4 PH CRES AMS5643 1/8" DIA X .88 BAR
22. 17-4 PH CRES AMS5643 1/8" DIA X .88 BAR
23. 17-4 PH CRES AMS5643 1/8" DIA X .88 BAR
24. 17-4 PH CRES AMS5643 1/8" DIA X .88 BAR
25. 17-4 PH CRES AMS5643 1/8" DIA X .88 BAR
26. 17-4 PH CRES AMS5643 1/8" DIA X .88 BAR
27. 17-4 PH CRES AMS5643 1/8" DIA X .88 BAR
28. 17-4 PH CRES AMS5643 1/8" DIA X .88 BAR
29. 17-4 PH CRES AMS5643 1/8" DIA X .88 BAR
30. 17-4 PH CRES AMS5643 1/8" DIA X .88 BAR
31. 17-4 PH CRES AMS5643 1/8" DIA X .88 BAR
32. 17-4 PH CRES AMS5643 1/8" DIA X .88 BAR
33. 17-4 PH CRES AMS5643 1/8" DIA X .88 BAR
34. 17-4 PH CRES AMS5643 1/8" DIA X .88 BAR
35. 17-4 PH CRES AMS5643 1/8" DIA X .88 BAR
36. 17-4 PH CRES AMS5643 1/8" DIA X .88 BAR
37. 17-4 PH CRES AMS5643 1/8" DIA X .88 BAR
38. 17-4 PH CRES AMS5643 1/8" DIA X .88 BAR
39. 17-4 PH CRES AMS5643 1/8" DIA X .88 BAR
40. 17-4 PH CRES AMS5643 1/8" DIA X .88 BAR
41. 17-4 PH CRES AMS5643 1/8" DIA X .88 BAR
42. 17-4 PH CRES AMS5643 1/8" DIA X .88 BAR
43. 17-4 PH CRES AMS5643 1/8" DIA X .88 BAR
44. 17-4 PH CRES AMS5643 1/8" DIA X .88 BAR
45. 17-4 PH CRES AMS5643 1/8" DIA X .88 BAR
46. 17-4 PH CRES AMS5643 1/8" DIA X .88 BAR
47. 17-4 PH CRES AMS5643 1/8" DIA X .88 BAR
48. 17-4 PH CRES AMS5643 1/8" DIA X .88 BAR
49. 17-4 PH CRES AMS5643 1/8" DIA X .88 BAR
50. 17-4 PH CRES AMS5643 1/8" DIA X .88 BAR
51. 17-4 PH CRES AMS5643 1/8" DIA X .88 BAR
52. 17-4 PH CRES AMS5643 1/8" DIA X .88 BAR
53. 17-4 PH CRES AMS5643 1/8" DIA X .88 BAR
54. 17-4 PH CRES AMS5643 1/8" DIA X .88 BAR
55. 17-4 PH CRES AMS5643 1/8" DIA X .88 BAR
56. 17-4 PH CRES AMS5643 1/8" DIA X .88 BAR
57. 17-4 PH CRES AMS5643 1/8" DIA X .88 BAR
58. 17-4 PH CRES AMS5643 1/8" DIA X .88 BAR
59. 17-4 PH CRES AMS5643 1/8" DIA X .88 BAR
60. 17-4 PH CRES AMS5643 1/8" DIA X .88 BAR
61. 17-4 PH CRES AMS5643 1/8" DIA X .88 BAR
62. 17-4 PH CRES AMS5643 1/8" DIA X .88 BAR
63. 17-4 PH CRES AMS5643 1/8" DIA X .88 BAR
64. 17-4 PH CRES AMS5643 1/8" DIA X .88 BAR
65. 17-4 PH CRES AMS5643 1/8" DIA X .88 BAR
66. 17-4 PH CRES AMS5643 1/8" DIA X .88 BAR
67. 17-4 PH CRES AMS5643 1/8" DIA X .88 BAR
68. 17-4 PH CRES AMS5643 1/8" DIA X .88 BAR
69. 17-4 PH CRES AMS5643 1/8" DIA X .88 BAR
70. 17-4 PH CRES AMS5643 1/8" DIA X .88 BAR
71. 17-4 PH CRES AMS5643 1/8" DIA X .88 BAR
72. 17-4 PH CRES AMS5643 1/8" DIA X .88 BAR
73. 17-4 PH CRES AMS5643 1/8" DIA X .88 BAR
74. 17-4 PH CRES AMS5643 1/8" DIA X .88 BAR
75. 17-4 PH CRES AMS5643 1/8" DIA X .88 BAR
76. 17-4 PH CRES AMS5643 1/8" DIA X .88 BAR
77. 17-4 PH CRES AMS5643 1/8" DIA X .88 BAR
78. 17-4 PH CRES AMS5643 1/8" DIA X .88 BAR
79. 17-4 PH CRES AMS5643 1/8" DIA X .88 BAR
80. 17-4 PH CRES AMS5643 1/8" DIA X .88 BAR
81. 17-4 PH CRES AMS5643 1/8" DIA X .88 BAR
82. 17-4 PH CRES AMS5643 1/8" DIA X .88 BAR
83. 17-4 PH CRES AMS5643 1/8" DIA X .88 BAR
84. 17-4 PH CRES AMS5643 1/8" DIA X .88 BAR
85. 17-4 PH CRES AMS5643 1/8" DIA X .88 BAR
86. 17-4 PH CRES AMS5643 1/8" DIA X .88 BAR
87. 17-4 PH CRES AMS5643 1/8" DIA X .88 BAR
88. 17-4 PH CRES AMS5643 1/8" DIA X .88 BAR
89. 17-4 PH CRES AMS5643 1/8" DIA X .88 BAR
90. 17-4 PH CRES AMS5643 1/8" DIA X .88 BAR
91. 17-4 PH CRES AMS5643 1/8" DIA X .88 BAR
92. 17-4 PH CRES AMS5643 1/8" DIA X .88 BAR
93. 17-4 PH CRES AMS5643 1/8" DIA X .88 BAR
94. 17-4 PH CRES AMS5643 1/8" DIA X .88 BAR
95. 17-4 PH CRES AMS5643 1/8" DIA X .88 BAR
96. 17-4 PH CRES AMS5643 1/8" DIA X .88 BAR
97. 17-4 PH CRES AMS5643 1/8" DIA X .88 BAR
98. 17-4 PH CRES AMS5643 1/8" DIA X .88 BAR
99. 17-4 PH CRES AMS5643 1/8" DIA X .88 BAR
100. 17-4 PH CRES AMS5643 1/8" DIA X .88 BAR

Figure 23. 0.5-Inch Model Seat  
(Drawing No. 99-556529)



disadvantage, however, was extreme sensitivity to temperature changes at low strain levels where temperature variations may be caused either by external sources or self-heating. The result is an apparent change in load and unstable output.

The conventional strain gage system is less sensitive to temperature variations and has a well established history of application and use. Its low output, however, requires a high-gain amplifier with associated problems in stability and reliability. As both systems possessed desirable features, a parallel effort was undertaken with the results of development testing to dictate final choice.

The conventional or resistive system used a Baldwin-Lima-Hamilton type SR-4 etched constantan foil strain gage (P/N FABX-12-12). This unit consisted of two identical gages with strain axes 90 degrees opposed, one mounted directly on the other with a bakelite backing. Each piston leg (load cell) would use four of these gages mounted with one element of each parallel and the other perpendicular to the piston centerline. This provided four active elements wired in series to amplify input strain with four dummy elements providing temperature compensation. Each load cell comprised the active leg of a bridge circuit, used a separate amplifier, and through suitable switching, the output would be individually displayed on a direct-inking chart recorder.

The piezoresistive system to be evaluated was manufactured by Microsystems, Inc., and used a matched set of temperature-compensated gages (P/N DC6A7-16-350) for each load cell. The gages, also wired in a bridge circuit, were high-output units requiring no intermediate amplification, and therefore, could be fed directly into the recorder.

#### Position Control

The precise control of test model displacement (gap) and relationship of poppet and seat alignment and parallelism was considered paramount if

accurate, repeatable data were to be obtained. Consequently, this aspect of the test fixture received considerable design and development effort.

Piston Centering. A hydraulic system for centering the piston in the body during testing was designed to eliminate friction and rigidly support the piston. The design was based on the phenomenon of the radial force acting on a piston with axial hydraulic flow through the clearance between piston and cylinder. It can be shown that with flow through a diverging or converging clearance of an eccentric piston, an asymmetrical pressure distribution is set up which will develop a radial force acting to either force the piston against the cylinder or center it in the cylinder. The former often produces, in piston-type control valves, a condition called "hydraulic lock," while the latter case is used in this design to float the piston in the body.

The relationship (Fig. 24) among radial force, hydraulic pressure, and piston-cylinder dimensions are defined in Ref. 28 as follows:

$$\frac{\pi}{4} \tau \left( \frac{2 + \tau}{\sqrt{4\tau + \tau^2}} - 1 \right) = \frac{F_c}{L D \Delta P}$$

$$F_c = \frac{\pi L D \Delta P \tau}{4} \left( \frac{2 + \tau}{\sqrt{4\tau + \tau^2}} - 1 \right)$$

where

D = cylinder diameter

F<sub>c</sub> = radial force on piston distributed over length of taper as large end of taper just contacts wall of cylinder

L = length of taper

ΔP = pressure difference between ends of taper

τ =  $\frac{\text{diametral taper of piston}}{\text{diametral clearance at large end of taper}}$

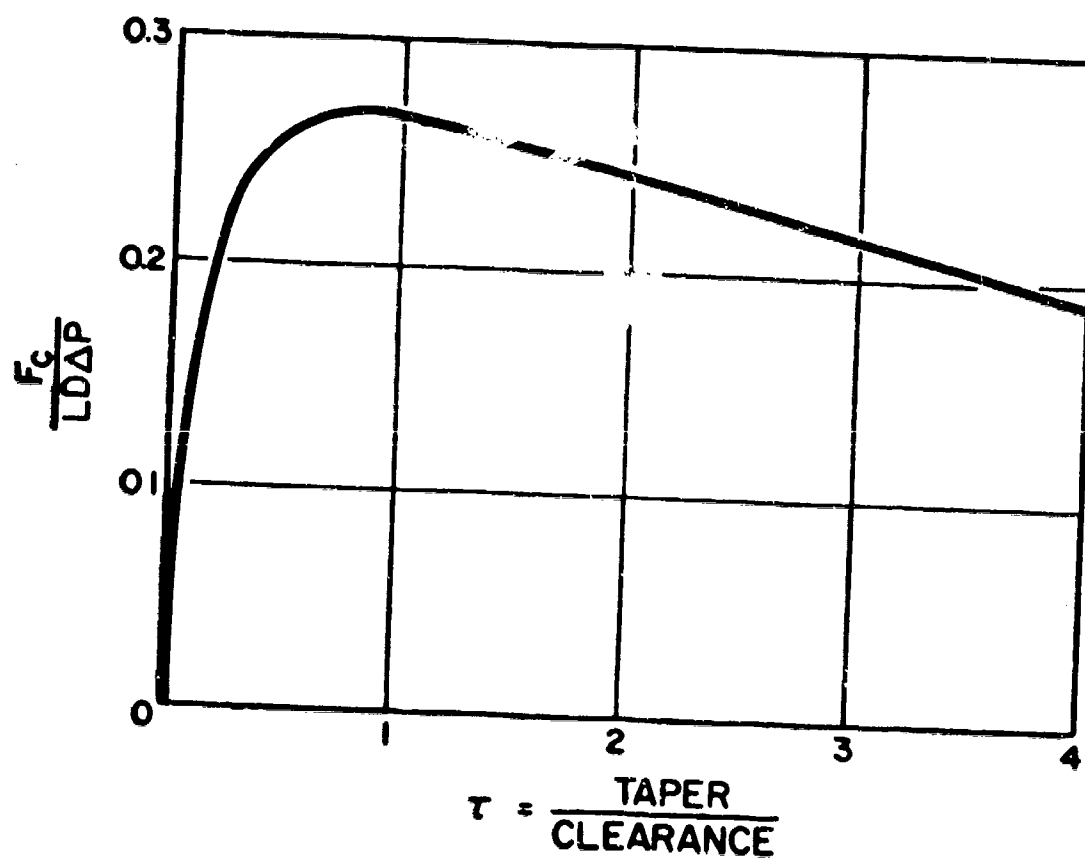
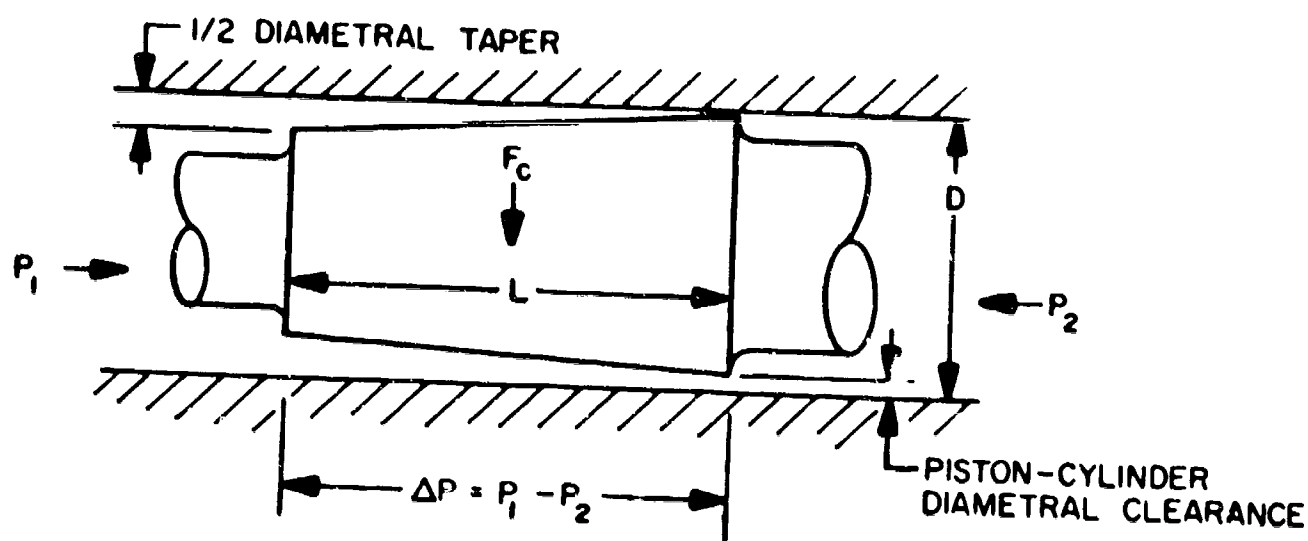


Figure 24. Piston Centering Force Diagram (Blackburn)

For a given pressure differential acting on a particular piston, the centering force increases with larger tapers to a maximum at  $\tau$  equals to approximately 0.9 and then slowly drops off (Fig. 24). It was hypothesized that with this design, the location of  $F_c$  occurs at approximately  $1/2 L$  when  $\tau$  is such as to give maximum  $F_c$ .

This principal was applied to the tester assembly by incorporating two identical tapers on the piston to produce a pair of centering forces which would provide a restoring moment to any eccentricity developed in poppet to seat loading. The taper to clearance ratio ( $\tau$ ) was kept near 1.0 by using the following approach:

1. Clearance between piston and cylinder was established at a minimum consistent with current lapping practices for this size piston (1.500-inch diameter x 6.0 inch length).
2. As the small degree of tapering necessary could only be accomplished by a more or less "cut-and-try" hand lapping process, tolerances were established to provide a minimum taper. This provided allowances for subsequent modification without a great sacrifice in centering capability.

The final design resulted in a piston-to-cylinder clearance of 0.0001 to 0.0002 inch and a diametral taper of 0.0001 to 0.0002 inch. The resultant lateral forces are computed as follows:

$$\tau_{\min} = \frac{0.0001}{0.0002} = 0.5$$

$$\tau_{\max} = \frac{0.0002}{0.0001} = 2.0$$

$$F_c = \frac{\pi \times 1.5 \times \Delta P}{4} \left( \frac{2 + \tau}{\sqrt{4\tau + \tau^2}} - 1 \right)$$

$$F_c = 1.178 \Delta P \tau \left( \frac{2 + \tau}{\sqrt{4\tau + \tau^2}} - 1 \right)$$

$$F_{c_{\max}} (\tau = 0.9) = 1.178 \times 0.9 \left( \frac{2 + 0.9}{\sqrt{4 \times 0.9 + 0.9^2}} - 1 \right) \Delta P$$

$$= 0.41 \times \Delta P$$

$$F_c (\text{for } \tau = 0.5) = 0.39 \times \Delta P$$

$$F_{c_{\min}} (\text{for } \tau = 2.0) = 0.36 \times \Delta P$$

Distance between the tapers was fixed at 2.50 inches so that for minimum  $F_c$  the available centering moment is

$$M = 2.5 \times F_c = 2.50 \times 0.36 \Delta P$$

The maximum decentering force loading the piston against the cylinder bore is developed when the maximum available load (3000 pounds) is concentrated on one edge of the (0.500-inch diameter) test seat. Therefore, the required moment is

$$M = 3000 \left( \frac{0.500}{2} \right) = 750 \text{ in.-lb}$$

The hydraulic film pressure ( $\Delta P$ ) required to provide piston centering is then:

$$\Delta P = \frac{750}{2.50 \times 0.36} = 830 \text{ psi}$$

This could easily be provided from a pneumatically pressurized hydraulic supply.

The hydraulic fluid chosen was SAE 70 lubricating oil, which has relatively high viscosity (2000 centipoise) for low leakage, maximum viscosity permitting fine filtration, and good lubricating qualities.

Leakage would be controlled by the piston-to-cylinder clearance as the "no-friction" requirement did not allow conventional seals. The double taper scheme includes four lands across which leakage is produced because of the film pressure. From Blackburn, hydraulic leakage is

$$Q = \frac{\pi D b^3 \left[ 1 + 1.5 \left( \frac{\epsilon}{b} \right)^3 \right] \Delta P}{12 \mu L}$$

where

$b$  = radial clearance, 0.0001 inch

$D$  = piston diameter, 1.5 inches

$L$  = length of seal land, 0.25 inch

$\Delta P$  = pressure drop across the seal land, 1200 psi

$Q$  = leakage, in.<sup>3</sup>/sec

$\epsilon$  = eccentricity of piston to cylinder, 0.0001 inch

$\mu$  = fluid viscosity (2000 centipoise =  $2000 \times 1.45 \times 10^{-7}$  lb-sec/sq in.)

Therefore, for four lands all at maximum eccentricity pressurized to 1200 psi and using SAE 70 oil, the leakage ( $Q$ ) is 0.38 cc/hr. The pressurized supply tank was designed to provide approximately 100 cc of oil over ullage requirements which would allow 50 or more hours of operation at maximum pressure.

It was recognized that the SAE 70 oil would probably not allow impact or cycling frequencies high enough to provide a good range of test data. The hydraulic fluid would be changed at the time of test to a lower viscosity oil or air to provide faster piston travel.

Position Measurement. Establishing and measuring the poppet-to-seat gap and related factors such as parallelism and flatness that have a direct bearing on its affect upon flow was expected to be one of the most difficult tasks in the test program. The required measurement accuracy was largely determined by the type of test involved. However, the tester was designed to provide measurements of the vertical movements of the poppet and seat seating surfaces relative to a reference plane that were accurate to  $\pm 5$  microinches. This was accomplished by the use of a Merz electronic height indicator mounted on the same surface as the tester which takes readings directly from reference surfaces precision lapped on the test poppets and seats. For the test poppet, the reference surface is the back face which bears on the load cells, and for the test seat, it is a land outside the seating area which is lapped to become a continuation of the seating surface. Access to these reference surfaces on the poppets and seats is made through openings on opposite sides of the tester. Height readings may be taken with pressure and load either on or off, permitting maximum accuracy through the continual monitoring of dimensional change. The parallel relationship of the test poppet and seat in the tester was accomplished by mounting the poppet directly on the load cells and the seat directly on the base plate which is maintained in intimate contact with the base of the body. Parallelism deviations of the seating surfaces then are a function of parallelism of the model test poppet and seat seating surface to locating surface planes and the tester body base to load cell locating surface. Tolerances established for critical details hold parallelism to 34 microinches maximum over a 1.0-inch seat diameter.

Clearance between piston and bore (0.0001 to 0.0002-inch diametral), under zero film pressure conditions, permits a maximum theoretical cocking of 36 microinches across the 1.0-inch diameter seat which results (at zero load) in a maximum deviation from parallel of 70 microinches.

A further aid to the establishment of an accurate reference of actual seat position was provided through an electrical contact. An aluminum oxide coating on the piston and insulating spacers between the flexure

and poppet provided electrical insulation between the test poppet and test seat. A small wire was attached to the test poppet and was contained as part of the load cell cable. A circuit composed of a flashlight battery, high resistance, and microammeter was used to give an indication of electrical contact.

Vertical deflections of the body under load are of no concern because seat-to-poppet location is referenced to the base plate and symmetry of cross section is maintained to eliminate bending. Deflection of the base plate occurs as bending with the application of poppet loads. Rigid bolting to the body and the 1.72-inch thickness limit the bending at the 3000-pound load level to approximately 15 microinches. This is an insignificant amount when considered as a distortion of the base tending to raise the edges by this amount but not changing the basic reference dimension between the bottom of the plate and the test seat.

The four base plate to body bolts were torqued to 150 in.-lb which produced approximately 2000 pounds preload per bolt. This represented over 2-1/2 times the 3000-pound potential load to prevent plate-to-body separation.

Concentricity and Antirotation. When replacing the test poppet or seat after inspection or for cleaning, the angular and radial relationship of the parts must be unchanged so that duplicate test conditions may be observed. To achieve this control, the test poppets were provided with a V-groove which was located to the piston through a retaining ring with a set screw. The piston, in turn, was oriented to the tester body through the retaining ring with a flexure device which prevented rotary motion while offering insignificant axial force. The test seats and tester body base were witness marked permitting orientation within 0.003 inch at the 1.5-inch OD. Concentricity and clearances of the fixture details were controlled to maintain less than a 0.003-inch total eccentricity between the seating diameters.



## Cycling

Dynamic loading and cycling of test poppets and seats may be accomplished by the pneumatic piston pressurizing system. Control pressure applied to the piston provides the closing force with impact levels dependent on the viscosity of the hydraulic film centering fluid and the rate of application of control pressure. Opening is provided by venting the control pressure while maintaining a positive pressure in the poppet cavity. Test fixture provisions for dynamic testing were: (1) provision for a 0.250-inch stroke in the piston and flexure, (2) rigid clamping of the load cells to the test poppet to prevent fretting, (3) a rigid base plate and heavy bolts to the body to prevent flange separation upon impact, (4) lightweight clamps between test poppet, flexure, and load cell to minimize inertia loads into the load cells, (5) strain gage wiring and cable construction to withstand impact and abrasion, and (6) cavity closure to withstand a 50-psig pressure.

## Contamination Control

Potential problems arising from contamination are primarily a result of the introduction of foreign particles into close-fitting clearances or mating surfaces. This causes misalignment of critical surfaces, friction and possibly galling between the piston and body, and scratches, pits, and deformation in test seating surfaces. The main sources of contamination are the assembly area, test fluid, pressurizing containers, and plumbing. Clean room practice and rigid assembly disciplines were the only control for the first problem area while 2-micron filters were planned for fluid control. (Subsequent test problems necessitated the use of 1/2-micron absolute filtration for test seat gas and film pressurant systems.) A further aid to cleanliness was the use of easily cleaned metal-to-metal seal and tubing between filter and tester.

## FABRICATION AND DIMENSIONAL CHECK

The critical details of the tester which control test data accuracy are the body, piston load cell assembly, and model test poppets and seats. The full potential of the tester can be used only if the critical dimensions and characteristics of these details are considered in the assembly and test procedure. Following is a summary of the fabrication and checking of those items which determine the capabilities of the tester.

### Body

Critical body bore and base dimensions affect the precision with which the test poppets and seats are held in alignment. Final sizing of the bore was accomplished with a cylindrical lap which was longer than the body to develop straightness. Its diameter was checked with a Sheffield air gauge by comparing the body with a standard test piece having a bore size known within 5 microinches. The completed bore diameter was 1.500120 inches throughout the center section with the end opposite the load cells (top) 40 microinches greater, tapering for a 0.7-inch length to the first relief groove. The load cell end of the body was 20 microinches larger than the center.

Checking for roundness was conducted with the Sheffield air gauge and supplemented later with a Merz electronic indicator when checking normality of the bore with respect to the base. No deviation from roundness could be found so it is assumed that any deviation from a true cylinder was less than 10 microinches, the estimated accuracy of measurement.

Straightness of the bore was checked with a mandrel and later by air bearing performance using the tester piston. The mandrel was chrome plated, ground, and cylindrically roll and ring lapped to provide less than 20 microinches of clearance with the bore. Lubricated with lanolin,

the body would drop over this mandrel under its own weight with no observed tendency to drag or interfere as the end of the mandrel passed over the shoulders along the bore. This performance was checked with the mandrel rotated to five or more different positions relative to the body.

Surface finish of the bore was not checked accurately, but may be assumed to be on the order of 4 microinches AA.

The base of the body was checked for flatness and normality to the bore by the use of an optical flat and the Proficorder, a recording stylus instrument, in conjunction with the Merz height indicator.

Flatness checks of the base showed a concave condition with the center approximately 6 microinches lower than the edge, and over-all flatness within this. Normality of the base was checked by rotating the body on the Proficorder, base up, and simultaneously indicating base and a 5-inch length of the bore. Multiple setups to verify repeatable accuracy of readings showed an average normality deviation of 10 microinches in 5 inches (Fig. 20 requirement was 50 microinches in 5 inches).

### Piston

Finishing of the piston to the required tolerances presented problems originating with the extremely hard aluminum oxide coating on the OD and the relatively small surfaces on the cell locating pads which required the minimum dimensional error. Sizing of the OD was the first step and was accomplished by cylindrical grinding and then roll lapping. After grinding the OD for approximately one-half of the length, the part was reversed for the remainder of the operation to provide maximum rigidity and allow grinding the end faces of the load cells. Roll lapping with rolls longer than the part improved surface finish, straightness, and over-all taper characteristics. The 0.0002- x 1.5-inch-long film

centering tapers were hand lapped using diamond compound with a stick lap. Control of the runout of the taper at the OD was maintained by masking the OD. Checking this runout after completion to within 0.010 inch along the length was no problem because the difference in surface appearance between roll and stick lapping provided a distinct line.

Measurement of all diameters and tapers for size and uniformity was conducted with a Johansson Mikrokator, and inspection of roundness and over-all straightness was accomplished with the Proficorder. The three load cell end faces were simultaneously finished by hand lapping to produce flatness of the individual faces and approximately a 4-microinch AA surface finish. An optical flat showed individual flatness (to within approximately 0.001 inch of the edges) to be within 4 microinches and all points to be within 20 microinches of a common plane.

Checking the normality of the common plane established by the load cell end faces with respect to the OD was done with the Proficorder. The piston was set load cells down on an optical flat which was placed on the Proficorder turntable for measurement. Inspection traces were then made at various points along the piston OD and tapers. These records indicated surface profile (deviation from roundness), straightness (centerline deviation from a straight line), normality (centerline deviation from perpendicular with respect to the common plane established by the load cell end faces), and orientation of the centerline deviation angle with respect to the individual cells (which cell was long or short to produce the deviation from perpendicular). Several measurements were made to verify the results and indicated the following:

Roundness. Maximum deviation from a true circle was 20 microinches with a profile of a wavy nature having hills and valleys running parallel to the axis. Average distance between hills (measured around the circumference) was approximately 0.13 inch at each end with the center section of more random nature but predominately about 0.25 inch between hills.

Straightness. Maximum deviation of the centers of the top, center, and bottom diameters from a straight line was 3 microinches.

Normality. Maximum deviation of the common centerline of the top, center, and bottom diameters from perpendicular with respect to the load cell end face plane was 10 microinches in 5 inches (Fig. 20 requirement was 50 microinches in 5 inches).

Orientation. Cell No. 3 was shorter than the others by approximately 2 microinches, which is small in proportion to the surface profile deviations in the faces.

Additional traces taken at different points along the film-centering tapers indicated that stick lapping had increased the waviness characteristic but had not developed any significant eccentricity. The uneven profile did, however, while in test using a pressurized fluid film, create an effective eccentricity in the tapered areas. Partial correction of this was made by relapping lands and tapers with ring-type laps to improve roundness and increase the amount of the taper. The final profile resulted in lands round within 5 microinches and taper round to within 10 microinches. The top taper was 0.0006 to 0.0007 in 1.5 inches and the bottom taper 0.0010 in 1.38 inches with an additional 0.0005-inch reduction in the last 0.12 inch next to the relief groove. No evidence of eccentricity between lands, or tapers and lands greater than 10 microinches T.I.R. was noted. Final Mikrokator readings on the land diameters indicated:

Bottom land (at load cells)	= 1.499885 inches
Center land	= 1.499935 inches
Top land	= 1.499920 inches

## Poppet and Seat Test Models

Test model poppet and seat details are shown in Fig. 21 through 23. Figure 21 details the near-sealed test seat as used. Figures 22 and 23 represent blanks on which finished seating surfaces (Table 6) were prepared.

Part No. 99-556527-31 with a seating land 0.060-inch wide and 1.000-inch OD incorporated nine 0.005-inch-diameter holes for recording pressure distribution throughout the seat area. Hardness of the material (440 C) posed a drilling problem which was solved by the use of electrical discharge (Elox) machining. The 0.005-inch diameter holes were done before heat treat or other drilling with only the OD semifinished and the drilled face ground flat. Drills were 0.004-inch-diameter brass wire rotated in operation. Hole location was established by using a plastic sheet which had been previously accurately drilled on a jig borer type setup using conventional drills. The holes were drilled deeper than required on the finished part to provide finish stock on the seat face and allow drilling from the opposite side to establish the final 0.005-inch-diameter hole length. After heat treat, the OD, ends, and seat profile were ground to provide hole locations accurate to within 0.001 inch of true position. Hole diameters check  $0.0051 \pm 0.0003$  inch (8 of 9 holes), and rounding of the corners intersecting the seat does not exceed 0.0005 inch as observed under the Lietz interference microscope.

## DEVELOPMENT

### Load Cells

A major development program was conducted to establish the load measurement system best suited for the application. Model load cells were fabricated using material identical to the poppet, ground to maintain the same active cross section, and tested using various arrangements of semiconductor and conventional strain gages.

Semiconductor Strain Gage. The semiconductor strain gages evaluated were supplied by Microsystems, Inc., and installed with the assistance of their engineering personnel. The installation considered most effective used a matched set of temperature-compensated gages (P/N DC6A7-16-350). This provided four active elements (2 each on 2 opposite faces) which were wired to give, at no load, a nearly balanced Wheatstone bridge. Temperature compensation of this gage through a 100 F range is provided by using active elements which have positive and negative gage factors. Changes in length of the active section caused by temperature create no resistive imbalance, while changes in length as a result of load essentially double the change in individual element resistance as it is observed across the bridge. Mounting pairs on opposite faces, and in the same plane as the primary bending modes, tended to minimize the effects of bending loads.

The arrangement provided approximately a 10-millivolt output for a 30-pound load when using a 6-volt battery for energizing and a potentiometer for exact balancing and zero adjustment. When applied directly to the input of the recorder, this signal gave full-scale deflection corresponding to a sensitivity of 0.3 pound per division (line) on the recorder chart. High load capacity also was ensured because the 3000-pound design load for the cell strained the elements to approximately one-third of specified capacity.

Problems were noted in this system when it appeared that the effective change in resistance of an element, produced by a small (0 to 5 pound) load, was of the same magnitude as that created by the changes in temperature resulting from self-heating at these low power levels. Small changes, induced by load (application of 1 pound) or temperature changes (a finger touching the loading face of the cell momentarily), created a cyclic-type variation in output which took 20 or 30 minutes to stabilize. Instability under zero load conditions appeared to be worse than while under load. An attempt was made to improve this condition by installing a permanent resistor in series with one element, which would provide a

more nearly perfect balance under zero load. (Installing a compensating shunt in the external circuit was also attempted, but with no significant improvement.) Opening the bridge circuit and adding 8.8 ohms to the initial 350 ohms of one element was performed at Microsystems, Inc., which produced a resistance balance within 1.0 ohm. Some improvement in performance resulted, but was of a small order.

Some further improvement was gained by using an a-c energizing voltage of 5 to 10 volts at 10 kilocycles. Cyclic instability was still present. A typical test showed that after application of a 1-pound load, output would drift to as much as 50 percent above and below the applied load, eventually stabilizing after 15 or 20 minutes. Some cursory testing at loads up to 30 pounds showed similar characteristics, but to a lesser degree. The need for a stable zero load reference in tester calibration kept development of the semiconductor-type load cell concentrated in this area. It appeared that further improvement in stability and drift characteristics could only be made by more sophisticated electronic circuitry or an improved semiconductor sensing element. It was theorized that an electrical system could be devised to maintain a constant current in individual elements and eliminate variations in self-heating. The use of an improved semiconductor was also suggested by Microsystems, Inc. Either design, however, required more development time than was available for this program, so the semiconductor method was dropped in favor of conventional strain gaging and appropriate additional equipment.

#### Conventional Strain Gage.

Preliminary. Details of the conventional strain gage arrangement and wiring diagram are shown in Fig. 20. The units are attached to the tester piston legs with a heat curing epoxy bond after initial lapping of the piston OD, tapers, and end faces. (Final piston lapping was accomplished after installation checkout and calibration of the strain gages.) During preliminary testing, hysteresis appeared to be a problem but was virtually eliminated by curing the load cell epoxy bond for 2-1/2 days at 300 F.



Conversion of load induced strains to an electrical signal involved incorporation of the active strain gages as one leg of Wheatstone bridge circuit and recording the change in resistance produced by a change in load. Temperature changes anticipated in normal operation, however, produced apparent strains on the same order of magnitude as the 1- to 2-pound load accuracy required in the low load range. This phenomenon was moderated by the application of a regulated a-c voltage (10 volts, 3 kilocycles) as the reference voltage across the Wheatstone bridge, which produced a stabilizing power level around which the load cell operated. Mechanical loads applied to the cell then produced a modulated output which was amplified, demodulated, and the d-c signal fed into the L&N Recorder to produce a load reading.

To maintain stability a Consolidated Electrodynamics Corp. (CEC) high-frequency power supply was used for the 10-volt, 3-kilocycle reference voltage, and a CEC 113-B system for amplification and demodulation of the load cell output signal. The entire system, including the L&N Recorder was powered through a Sola 115-volt regulating transformer.

Load Calibration. Weights (up to 100 pounds) were applied by means of a sling, which applied the load through a steel pointer rounded to approximately a 0.030-inch radius. A loading plate was made from 0.020-inch-thick CRES sheet, using punch marks for loading points, which located the sling pointer consistently within 0.010 inch of the center of any cell loading face and distributed the load over approximately a 0.060-inch diameter to prevent damage to the loading face. Test weights were checked on an Ohaus 5-pound-capacity balance having an accuracy of 0.001 pound, and 0.005 pound at 10 pounds. Maximum error in weight combinations amounted to 0.060 pound in 100 pounds, or 0.06 percent of the applied load.

Loading to 3000 pounds was performed on an Instron testing machine. Assurance of load application was somewhat in question at loads below 2000 pounds because the center of load application of the Instron device was

not known better than approximately 0.15 inch. This problem was eliminated between 2000- and 3000-pound loads by using a 0.005-inch-thick brass shim on the cell loading face. Visual observation of the clearance between the Instron loading ram and the two free cells at loads over 2000 pounds provided an accurate reference of load centering. Yielding of the brass shim was reflected as tipping of the poppet under load and the resulting change in clearance at the two free cells easily detected. Accuracy of the Instron machine was within 13 pounds at this level, and so calibrating loads between 2000 and 3000 pounds were accurate within 1 percent of applied load. Calibrating resistors for the load cell system established in this manner introduce errors by not being exactly matched to calibrating loads and by the necessity for changing range on the amplifier system. However, accuracy of the system in use was continually monitored in the tester by reference to known pressure loads, and may be taken as well within 5 percent of applied load.

Final Load Cell Checkout. Checkout of the load cell system was performed with the piston removed from the tester to measure and define the following characteristics:

Zero Output Stability. With no load on the cells, recorder output was observed to determine drift characteristics. Stability was good for the high load ranges (100-, 300-, 1000- and 3000-pound ranges) where variations less than 0.5 percent of full scale were observed over 1/2- to 1-hour periods. Zero drift, when on the 30-pound range, was as much as 0.2 pound over 1- to 2-hour periods.

Zero Repeatability. With the application and removal of load, recorder output was observed to determine repeatability of zero load indication. Repeatability for the high load ranges was better than 0.5 percent of full scale. Variations in zero load, when on the 30-pound scale up to 0.2 pound were noted.

Sensitivity. With the application and removal of small loads, the ability of the system to accurately resolve the change was checked, indicating that load changes of 0.3 percent of full scale (0.1 pound on the 30-pound range) may be detected.

Accuracy (Linearity). Ability to accurately record load changes upon application or removal of known loads was observed. Maximum individual cell deviation at the most sensitive (30-pound) range is shown below with the noted accuracy applied to all ranges.

<u>Applied Load, pounds</u>	<u>Load Reading, pounds</u>	<u>Full Scale Error, percent</u>	<u>Applied Load Error, percent</u>
5	4.85	0.5	3.0
10	9.92	0.3	0.8
20	19.76	0.8	1.2
30	29.85	0.5	0.5

Extraneous Signal Sensitivity. With no load on the cells at the 30-pound range, changes in recorder output were observed as a result of grasping or moving connecting cables and components or bringing metallic objects near the equipment. No effects could be observed from the above. Likewise, during the course of calibration and subsequent tester operation, there were no noticeable changes observed when operating near electric motors or appliances.

Temperature. With no load on the cells at the 30-pound range, changes in recorder output were observed when the temperature of the cell was changed by grasping with the fingers or laying metallic objects on the cell load bearing surfaces. The time required for return to a

stable output was the characteristic checked as well as any shift in zero point. The application of body heat changed the zero point as much as 3 pounds with as long as 10 minutes required for stabilization at the original set point. Applying the weight loading plate or the test poppet and locking ring assembly changed the zero point approximately 1 to 2 pounds with 5 to 10 minutes required for stabilization.

Calibration. The initial calibration involved establishing fixed electrical resistors which could be installed in the electronic circuit to simulate known mechanical loads. These resistors, since they are not subject to significant changes with time, were used for day-to-day calibration of the load cell system. Resistances were varied until they simulated load cell output noted under actual calibration load conditions. The resultant calibrating resistors were accurate to within 0.5 percent of their equivalent load. A check for stability of these resistors was made after the first 4 weeks of operation. At this time, the maximum change in output observed, which includes readout accuracy, was 0.7 pound at 30 pounds or 2.3 percent.

Switch and Contact Resistance Variations. Several switches and frequently installed connectors were designed into the system which created the possibility of erroneous output because of changes in circuit resistance. These included recorder cell and calibration resistor selection switches and the pin and socket type connector used with each calibrating resistor. Switching from cell to cell, selecting calibrating resistors, and removing and installing calibrating resistors was repeatedly done under load and no-load conditions resulting in repeatable readings within 0.5 percent of full-scale reading on any range.

### Piston Centering

Pneumatic Test. Extensive testing of the hydraulic piston centering principle was conducted to verify the capability of maintaining a radial load on the piston without contact between piston and body. Preliminary

results showed that performance was not as predicted; therefore, special tests were performed to support further analysis and possible improvement. Rework of the piston taper profile was indicated as the answer to improved performance.

The major part of the development and testing was conducted with a second piston (S/N 2) while the first piston (S/N 1) was having strain gages installed and tested. Tests were performed while pressurizing each taper independently as well as with a common pressure using nitrogen gas as the pressurizing fluid. Use of the 1/2-micron filter eliminated contamination problems. Testing with the test fixture in a horizontal position provided a highly sensitive means of detecting piston-to-body contact. Special components fabricated for test purposes included a pressurizing tube installed in the top of the piston extending through the tester cap and a set of plugs for the top cross holes in the piston. This allowed independent taper pressurization and, by taking height readings at the pressurizing rod and load cells, an indication of radial piston motion as a function of pressure.

An indication of the magnitude of the friction present when testing as an "air bearing" was found by tilting the tester slightly from the horizontal and noting when the weight of the piston would provide free axial movement. Tilting to less than 0.03 inch from the horizontal was sufficient to promote axial movement with film pressure "floating" the piston. This represents a coefficient of friction of less than 0.006. The friction force then, using 3.0 pounds as the piston weight providing the radial load, is less than 0.02 pound. (During preliminary testing, a cursory test was made to check the decentering effect, or hydraulic lock, with flow through the tapers reversed. As predicted, friction was present with the application of less than 1 psig and increased as pressure was increased.)

The first tests (piston S/N 2) showed that with both tapers pressurized and the tester horizontal (1) the piston was being forced against one side of the bore at all pressures, (2) the direction of axial movement,

when checked with the Merz, changed as the piston was rotated but did not change when the body was rotated to different positions, and (3) filling and pressurizing with SAE 10 lubricating oil gave essentially the same results. (Verification here of identical performance with either gas or oil as the film pressurant justified the use of gas for the remainder of the tester evaluation program.) The following test, with independent taper pressurization, showed that the top taper (at the end opposite the load cells) floated the piston at pressures from 75 to 220 psi depending upon piston rotation, while the bottom taper (next to the load cells) forced the piston in the direction of cell No. 2 with the application of pressure.

Conclusions drawn from this test were that pressure applied to the top taper created a centering force proportional to the pressure which was balanced at a point very near the center of the bore. Furthermore, the couple created by the pressure acting on the sealing land adjacent to the taper produced a floating piston at all pressures. Pressure on the bottom taper, however, caused a force, when coupled with the adjacent sealing land, which produced cocking of the piston at all pressures.

Profilometer inspection of the piston taper and sealing land profiles showed deviations from true roundness believed to be the source of the trouble. Waviness deviations from true roundness as great as 25 micro-inches were present in both the seal lands and tapers. The seal land adjacent to the bottom taper in particular had an outstanding low area. (These deviations originated in cylindrical grinding and in some cases may have been exaggerated by finish roll lapping and hand stick lapping of the tapers.)

The corrective action taken to improve performance was to rework the tapers and sealing lands to improve roundness and at the same time produce more clearance and taper. A cut-and-try procedure was used in an attempt to evaluate the significance of improved roundness vs additional clearance and taper. Ring lapping both sealing lands and tapers is

credited with the most significant improvement, producing a finished profile to within 7 microinches of true roundness. Increasing both tapers and the clearance of the sealing lands at the ends also improved performance. Incorporating a series of 0.0005- to 0.0008-inch wide relief grooves in the center land did not help while increasing the clearance at the center land (reducing piston diameter) appeared to actually increase the decentering forces.

Film centering performance and radial load capacity after this series of rework operations on piston No. 2 were greatly improved but did not meet the desired performance requirements. Although the piston would float with both tapers pressurized at intermediate stroke positions, contact was made between the piston OD and body bore as the piston was moved to within approximately 0.06 inch of the seated position. With only the top taper pressurized, the piston would float at all positions but had very little radial load capacity. It was assumed that the minor deviation in roundness still remaining with some probable eccentricity was magnified by the effective shortening of the distance between radial forces as the tapers were increased.

At this point, it was believed that enough test data had been accumulated on piston No. 2 to make it feasible to proceed with piston No. 1 which had strain gages installed and tested. The performance of piston No. 1 was only slightly better than No. 2, therefore, the tapers and end lands were ring lapped. The following final dimensions resulted in a compromise between very nearly full-floating capabilities with both tapers pressurized and the maximum radial load capacity with the top taper only pressurized. (Pressurization of the bottom taper still created friction when the piston was within 0.030 inch of the sealed position.)

Bottom land clearance	=	0.00024 to 0.00029 inch
Bottom taper	=	0.0010 inch in 1.38 inches
Center land clearance	=	0.00018 inch
Top taper	=	0.0007 inch in 1.5 inches
Top land clearance	=	0.00012 inch

Load Capacity. The decision to use the piston "as is" with only top-taper pressurization at a sacrifice in side load carrying ability was based on the urgency of proceeding with the test program and the low load requirements for the first phase of the test program. Actual load carrying capacity was not accurately checked but would support the weight of the piston with the tester horizontal and pressurized at 100 psig. Load carrying capacity increased with pressure and was estimated to be in excess of 20 pounds applied at the load cells when pressurized to 1000 psig. This was considered satisfactory for the first phase of the test program in which very near-parallel seating surfaces with no significant side loads, were anticipated.

At this point, it was concluded that the resultant radial loads developed by the tapers were approaching a location near the large ends of the tapers, or the center of the piston. Assuming that the decentering forces are caused by an effective eccentricity between the two tapers and the OD of the piston the fact that they were close coupled as compared with the length of the piston meant that an eccentricity on the order of a few microinches was sufficient to cause metal-to-metal contact at the ends of the piston. It is theorized that the accommodation of high side loads could be provided by reversing the tapers (the present piston could be replated to do this) which would locate the resultant centering loads near the ends of the piston. An additional improvement which could be incorporated in rework would include ring lapping the OD before final sizing to provide better roundness and effective concentricity between tapers and ends.

Hydraulic Oil Assembly. Assembly of the tester with SAE 70 lubricating oil for hydraulic film pressurization was a procedure requiring considerable attention to the elimination of contamination and entrapped air. All detail parts were cleaned with benzine and blown dry with nitrogen gas filtered with the 1/2-micron (Millipore) filter. Before assembly, a quantity of SAE 70 oil sufficient to provide several refillings of the supply tank was also filtered through the Millipore filter. This was accomplished to minimize the clogging of the filter during future testing.



Filling of the tester piston to body clearance spaces and manifolds was conducted with the top cap and piston plug removed and the fixture vertical. As oil was poured into the center hole in the piston air was removed by using a small diameter wire as a probe into the center hole in the piston and the angular-drilled supply hole in the top of the body.

Bleeding of the supply system after installation of the piston plug and the top cap of the tester was accomplished by cracking the tube connections between the tester and the supply sump. Verification of complete air and contamination removal was not positively proven but subsequent operation of the tester did not show evidence of either condition. Continuous monitoring of friction between piston and bore during the test program indicated a continuous pressurized oil film and no indication of binding caused by contamination.

## SURFACE FINISHING OF MODELS

All of the test models evaluated in the program had either lapped or lapped and polished finishes which typify the metal-to-metal valve seat surfaces currently found on aircraft and missile components. Lapping is a method of producing extremely uniform and smooth surfaces by means of a charged lap (dry lapping) or a lap in conjunction with loose abrasive compound (wet lapping).

The actual lapping process includes a number of variables which are controlled by the individual operator and must be evaluated in a subjective manner. For example, lapping pressure, motion of the workpiece on the lap and the amount of compound used are subject to variation in individual technique. As a general rule, light lapping pressure and stroking are conducted in a random fashion so that the movement of the part describes an ever-changing path. Frequent rotation of the part also helps to even out the surface texture.

The object of this portion of the program was to investigate these variables and techniques to better understand what is required to achieve a given desired surface. It was intended that the surface roughness parameter would be varied on test models while other parameters such as surface lay, waviness, material, hardness, etc., were maintained constant.

### PRELIMINARY PROCEDURES

The subject test specimens were first prepared with a fine uniform grind finish of about 8 AA and were maintained flat within approximately 2 light bands to minimize the amount of stock to be removed during lapping. Similarly, the seating and rear faces were ground parallel within 50 microinches.

The condition of the actual lapping plates to be used was considered next. To achieve the desired test surfaces, the lapping plates were held between flat and one helium light band (12 microinches) convex. Plates deviating from this were refinished or relegated to rough lapping operations. Accordingly, verification of an acceptable plate condition was made before its use for test model preparation.

#### LOOSE ABRASIVE (WET) LAPPING

The theory of loose abrasive lapping is that rolling abrasive particles wear the workpiece by occasional cutting. The abrasives are held in suspension by a special lapping compound which is generally diluted with kerosene or similar hydrocarbons. A feature of many abrasives is that they wear or break down into smaller crystals so that a progressively finer finish is obtained with continued use.

The texture produced from wet lapping is a multidirectional surface consisting of uniformly random hills and valleys over the entire surface. The surface may contain scratches although they are not the predominate surface characteristic. Figure 25 shows a test part being lapped with the loose abrasive technique. A measure of the quantity of compound used in this technique can be seen in this figure.

The initial goal of this effort was to vary the surface roughness from 1/2 to 8 AA in incremental steps while keeping the other surface parameters constant. The action of a variety of compounds on 440C steel test parts was investigated before defining a final finishing method; these included aluminum oxide, silicon carbide, and corundum. The normal surface roughness on a production lapped part was 2 to 3 microinches AA (0.03-inch cutoff) as lapped with a 900-grit aluminum oxide compound. Unfortunately, semiuniform surfaces above this roughness level were very difficult to achieve. The major problem with the rougher surfaces was



5AJ81-9/17/63-C1A

Figure 25. Test Part Being Lapped

139

the presence of scratches and edge rounding (or dub-off). Eventually, uniform surfaces of 4 and 6 microinches AA were achieved using the 280-grit corundum compound. Both surfaces were obtained with the same compound but at different stages of compound breakdown. For surface roughness below the 2- to 3-microinch AA level, a diamond lapping technique was used. This operation produces a different surface lay than that of the loose abrasive operation and will be covered in the discussion of dry lapping techniques.

The test parts which were to be used for the evaluation of material properties and gross geometry were prepared with the 900-grit aluminum oxide compound. The various compounds used on the final poppet and seat models including the polishing technique used are shown in Table 7.

#### DRY LAPPING

Dry lapping uses very little compound on the lapping plate. Diamond compounds are generally used for this process although other compounds could be used in this manner. The cutting action is caused by compound embedded in the lapping plate with minute cutting edges protruding above the lap surface. The cutting action will be the function of the particle size and the degree of embedment.

The characteristic surface texture of a dry-lapped material is that of multiple scratches on a smooth undulating surface. If the final strokes are made in a straight line, without turning the part, a unidirectional surface will result. All of the test poppets and seats lapped with diamond compound had this type of surface texture. These parts included test models E, F, and G which were fabricated to evaluate the stress vs leakage relationship for ultrafine surface finishes. Diamond compounds are necessary to satisfactorily cut extremely hard materials such as tungsten carbide; therefore, the poppet of test model A was also diamond lapped.

TABLE 7

## FINISHING OF POPPETS AND SEATS

Test Model	Nominal Finish, microinches	Material	Compound	Polish
A*, B, H and I	2AA	440C	900-Grit Aluminum Oxide	1200-Grit Aluminum Oxide on Paper
C	4AA	440C	280-Grit Corundum	Not Polished
D	6AA	440C	280-Grit Corundum	Not Polished
E, F, and G	1/2 and 1/4 AA	440C	4- to 8-micron Diamond	0 to 2 Diamond on Paper
A**	1AA	Tungsten Carbide	4- to 8-micron Diamond	4 to 8 Diamond on Paper
J	2AA	17-4	900-Grit Aluminum Oxide	1200-Grit Aluminum Oxide on Paper
K	2AA	Aluminum	900-Grit Aluminum Oxide	1200-Grit Aluminum Oxide on Paper

\* Seat only

\*\* Poppet only

## POLISHING

The surface finish on most materials after lapping has a dull matte texture. To improve the finish and brighten the surface for inspection, lapped parts are generally lightly polished. This polishing is accomplished by embedding a fine compound in a resilient lap. The polishing operation realigns the surface texture, leaving shallow smooth-sided troughs made up of facets inclined at small angles. Realignment of these facets at nearly the same angle produces a highly reflective configuration which is the visual characteristic of a polished metal surface.

The compounds used for polishing are generally very fine. For the test poppets and seats, 1200-grit aluminum oxide and 0- to 2-micron diamond compounds were used most frequently. The resilient lap used was bond writing paper which was taped to a flat granite surface plate.

Inspection of the surface texture under the interference microscope requires a reasonable degree of reflectivity; therefore, most of the test poppets and seats were lightly polished. The exceptions were the 4 and 6 AA surfaces where a rough texture was of interest. Polishing of these surfaces to a reasonable degree of reflectivity would have reduced the roughness by as much as 50 percent.

One of the problems in lapping, and especially polishing, is the tendency to radius (dub-off) the workpiece edges. The resilient lap tends to apply greater pressure and collect more compound at the edges of the part. This dub-off only becomes critical in narrow seat lands where the dub-off is a large portion of the total land width. Control of dub-off during polishing is accomplished by using light even strokes and keeping the polishing to a minimum.

## CLEANING

After lapping and polishing, all models were ultrasonically cleaned for one minute in hot trichloroethylene. Final treatment consisted of wiping with lint-free paper and benzene. None of the models were passivated or otherwise treated before testing.



## MODEL INSPECTION EQUIPMENT, PROCEDURES, AND DATA

The poppet and seat model inspection data provide the measurements necessary to correlate configuration with test and analytical results. Because of the extremely small dimensions of surface profiles normally associated with metal-to-metal valve seating, no one piece of inspection equipment can provide a comprehensive definition of the surface in question. For example, only a small indication of the actual three-dimensional profile is obtained from a stylus instrument while optical devices give a three-dimensional view, but for measurement purposes, cover a very limited field. This results, to a degree, in a subjective interpretation of raw data from several instruments to arrive at a practical estimation of the parameters of interest.

Aside from normal inspection checks to indicate primary conformance with drawing requirements, four additional parameters were considered to best define the seating surfaces and preclude erroneous test information input. These parameters were parallelism, flatness, surface texture (peak-to-valley parameter,  $h$ ; average asperity angle,  $\Phi$ ; nodules; and scratches), and surface hardness. To obtain this information, several types of optical, mechanical, and electromechanical measuring instruments were used. The following paragraphs describe the specific equipment and procedures employed to arrive at the final interpreted dimensional results for both gross dimensions and surface profile as shown in Table 8. Figures 26 through 64 illustrate specific and typical plain and interference microphotographs and stylus traces used in compiling Table 8.

### MODEL INSPECTION EQUIPMENT

The inspection equipment used may roughly be categorized into three types; comparitor, stylus, and optical. Each has certain advantages and limitations, and the proper evaluation of these characteristics is necessary to place the measurements obtained in proper perspective.

TABLE 8

## POPPET AND SEAT MODEL INSPECTION DATA

Test Model	Part No.	Test Model Description (1)	Seat Land Data					Profilometer Surface Finish Arithmetic Average, microinch				Surface Texture Parameters (Reduced from Profilometer and Microinterferometry Data)												Test Number From Test Section																																																																																																																																																																																																																																																																																																																																																																																																																																																																																																																																																																																																																																																																																																																																																																																																																																																																																																																																																																																																																																																																																																																																																																																																																																																																																																																																																																																																																																																									
			Serial No.	OD, inches	Total Width, inches	(2) Flat Width, (L), inches	Mean Diameter (D <sub>m</sub> ), inches	Seat Land Area (A <sub>s</sub> ), sq in.	Lay	Cutoff, inches				Roughness			Waviness			Nodes			Scratches																																																																																																																																																																																																																																																																																																																																																																																																																																																																																																																																																																																																																																																																																																																																																																																																																																																																																																																																																																																																																																																																																																																																																																																																																																																																																																																																																																																																																																																										
										in. R. Tip				h, micro-inch	Φ, degrees	h, micro-inch	Φ, degrees	h, micro-inch	β, degrees	h, micro-inch	β, degrees	h, micro-inch	β, degrees																																																																																																																																																																																																																																																																																																																																																																																																																																																																																																																																																																																																																																																																																																																																																																																																																																																																																																																																																																																																																																																																																																																																																																																																																																																																																																																																																																																																																																																										
										0.0005	0.010	0.005	0.030												0.010	in. R. Tip																																																																																																																																																																																																																																																																																																																																																																																																																																																																																																																																																																																																																																																																																																																																																																																																																																																																																																																																																																																																																																																																																																																																																																																																																																																																																																																																																																																																																																																							
A	28-5	1AA Tungsten Carbide Poppet	02						With	1.5	0.6	0.4	1.5	1.1	1.0		1.5	0.066																																																																																																																																																																																																																																																																																																																																																																																																																																																																																																																																																																																																																																																																																																																																																																																																																																																																																																																																																																																																																																																																																																																																																																																																																																																																																																																																																																																																																																																															

(1) Nominal finish noted. Except for test model A (1.0-inch diameter), all seats were 0.5-inch diameter.

(2) Excludes corner duress

\* Multidirectional

\*\* RM indicates rework from previous configuration

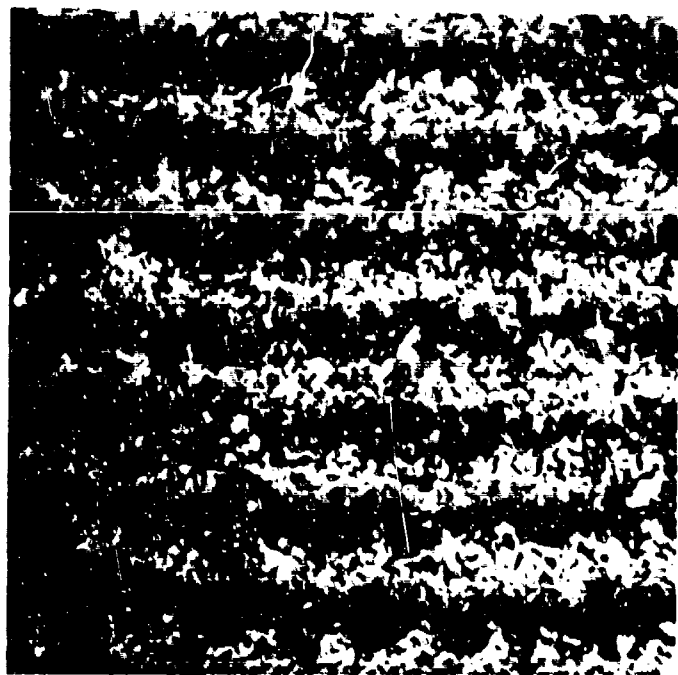


Figure 26. Test Model A, Seat,  
0.0065 x 0.0065-Inch Interference  
Photo

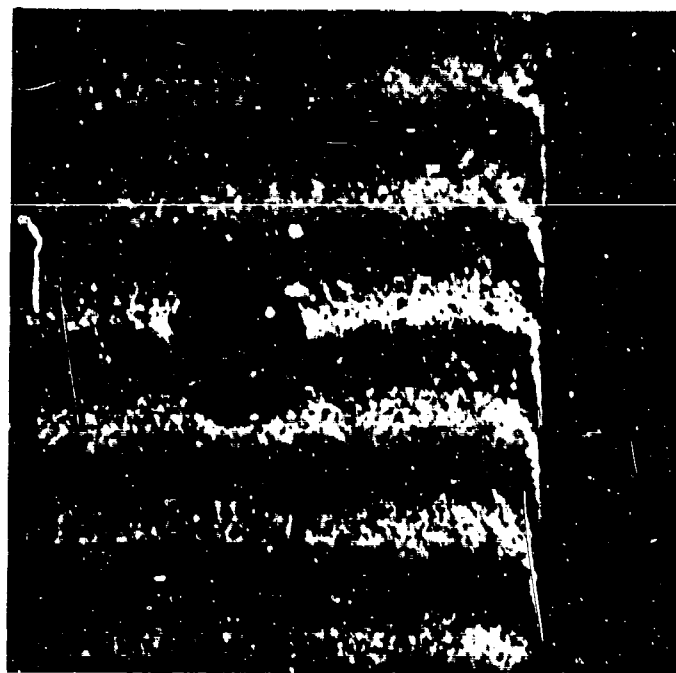


Figure 27. Test Model A, Seat,  
0.033 x 0.033-Inch Interference  
Photo Showing Dub-Off and  
Pressure Tap

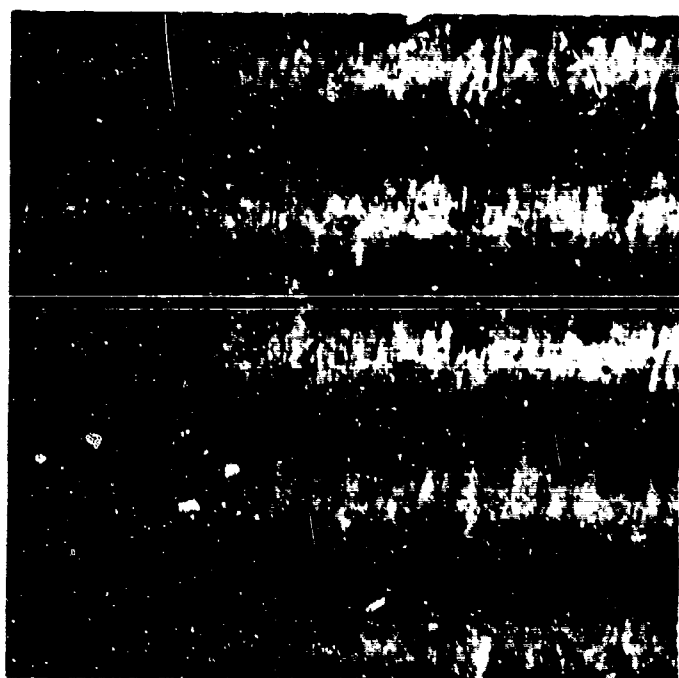


Figure 28. Test Model A, Poppet,  
0.0065 x 0.0065-Inch Interference  
Photo, Cross Lay

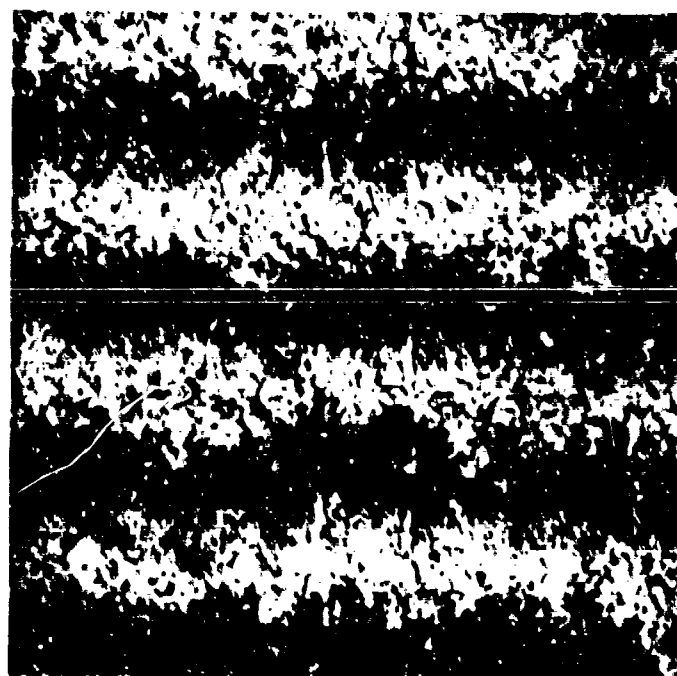


Figure 29. Test Model B, Poppet,  
0.0065 x 0.0065-Inch Interference  
Photo Showing 0.0005-Inch Radius  
Profilometer Stylus Scratches

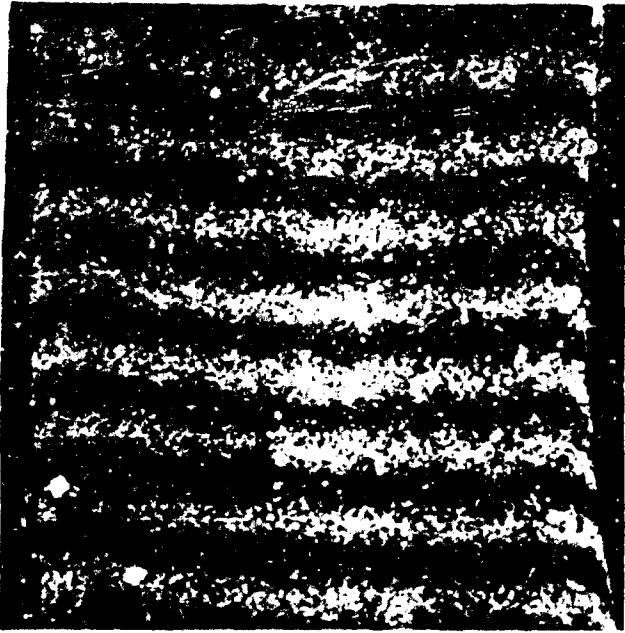


Figure 30. Test Model B, Seat,  
0.055 x 0.055-Inch Interference  
Photo Showing Dub-Off

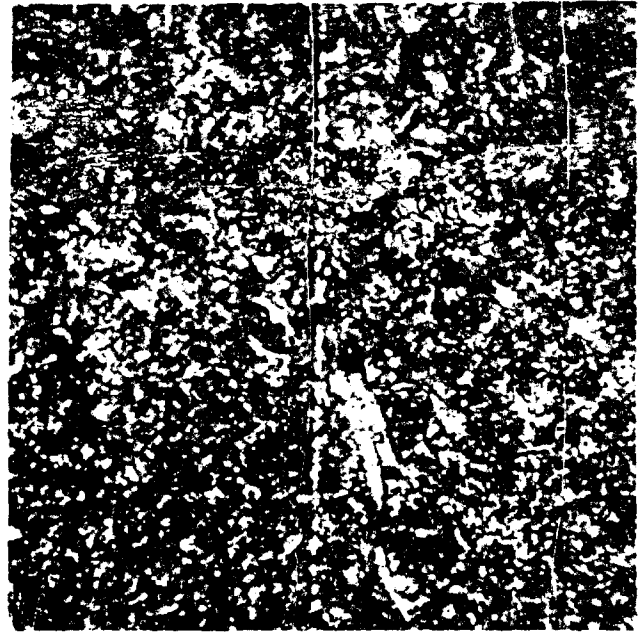


Figure 31. Test Model D, Poppet,  
0.0065 x 0.0065-Inch Plain Photo  
Showing 0.0001-Inch Radius Pro-  
ficorder Stylus Scratches

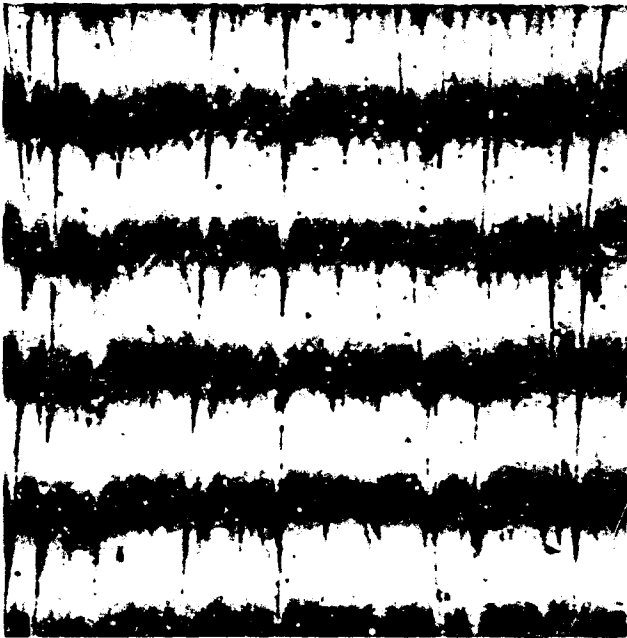


Figure 32. Test Model E, Poppet,  
0.0065 x 0.0065-Inch Interference  
Photo, Cross Lay

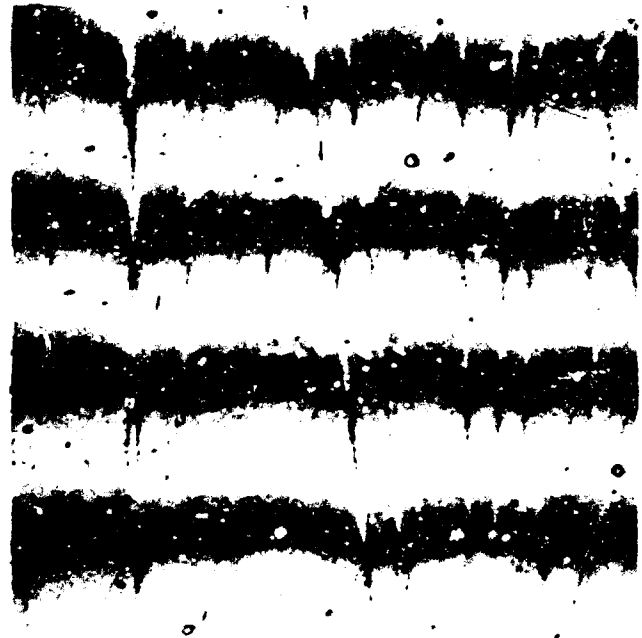


Figure 33. Test Model E, Seat,  
0.0065 x 0.0065-Inch Interference  
Photo, Cross Lay, Polished



Figure 34. Test Model E, Seat,  
0.033 x 0.033-Inch Interference  
Photo Showing Polish-Caused  
Dub-Off

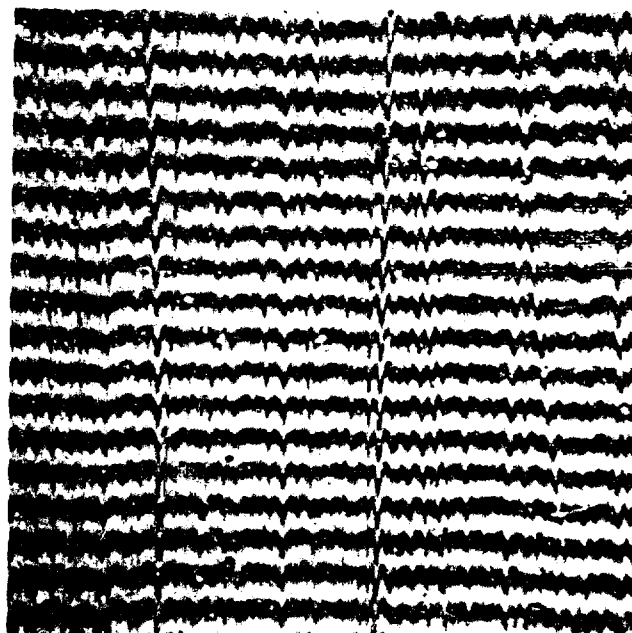


Figure 35. Test Model F, Seat,  
0.0065 x 0.0065-Inch Interference  
Photo, Cross Lay, Narrow Bandwidth

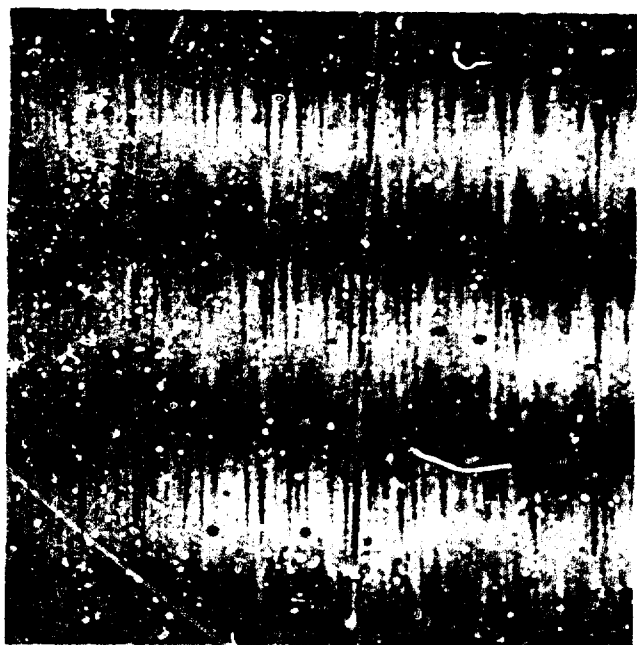


Figure 36. Test Model F, Seat,  
0.0065 x 0.0065-Inch Interference  
Photo, Cross Lay, Same Location  
as Fig. 35 Except Wide Bandwidth

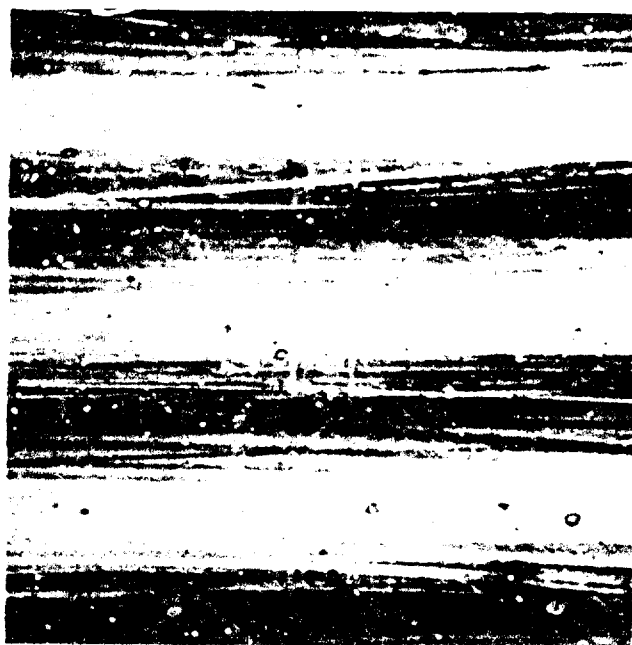


Figure 37. Test Model F, Seat,  
0.0065 x 0.0065-Inch Interference  
Photo With Lay Showing 0.0005-  
Inch-Radius Profilometer Stylus  
Scratches

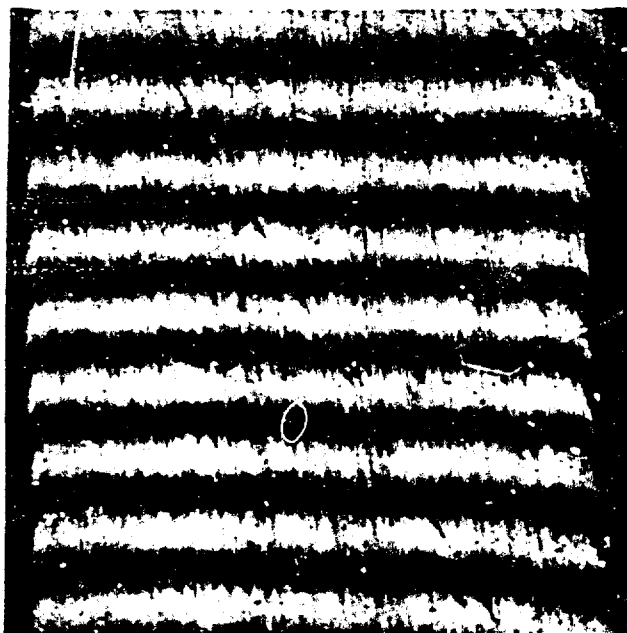


Figure 38. Test Model F, Seat,  
0.033 x 0.033-Inch Interference  
Photo

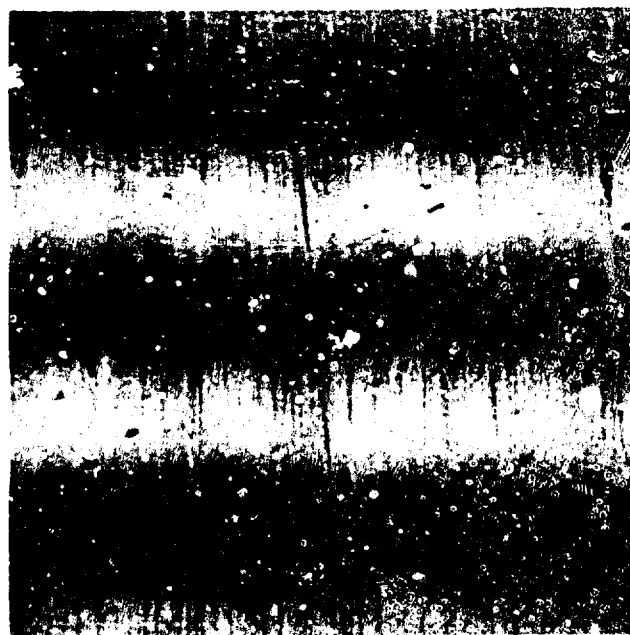


Figure 39. Test Model F, Poppet,  
0.0065 x 0.0065-Inch Interference  
Photo, Cross Lay



Figure 40. Test Model G, Poppet,  
0.0065 x 0.0065-Inch Interference  
Photo, Wide Bandwidth

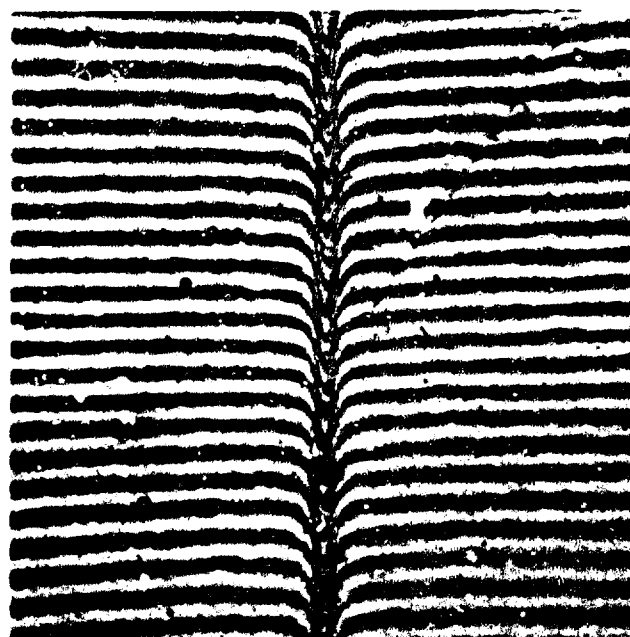


Figure 41. Test Model G, Poppet,  
0.0065 x 0.0065-Inch Interference  
Photo, Narrow Bandwidth Showing  
Test Scratch

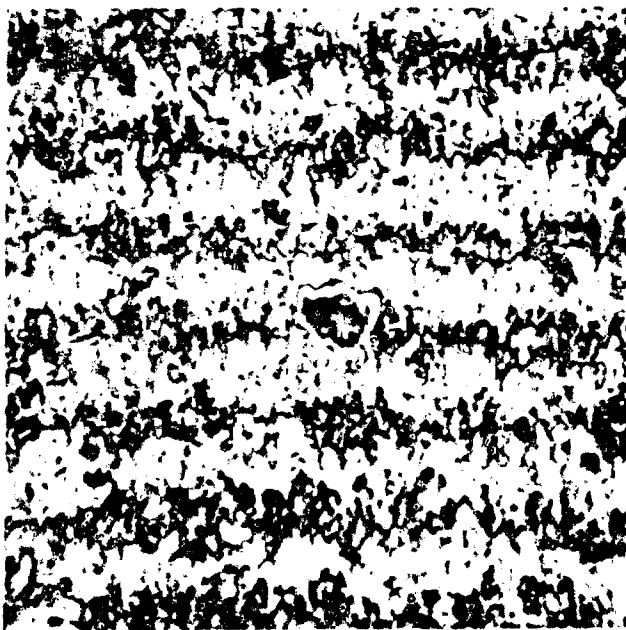


Figure 42. Test Model H, Poppet,  
0.0065 x 0.0065-Inch Interference  
Photo

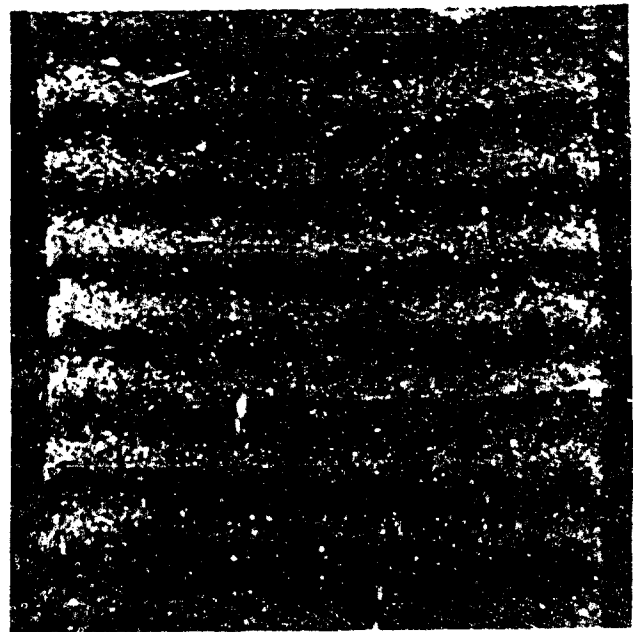


Figure 43. Test Model H, Seat,  
0.033 x 0.033-Inch Interference  
Photo



Figure 44. Test Model I, Poppet,  
0.0065 x 0.0065-Inch Interference  
Photo

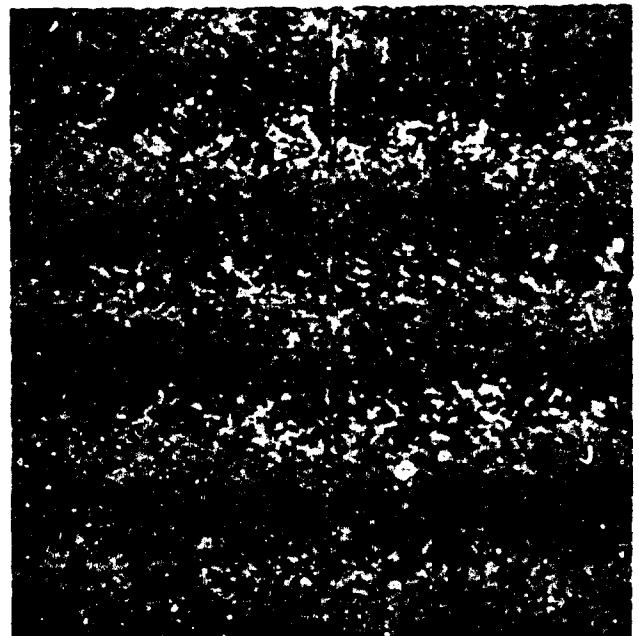


Figure 45. Test Model J, Poppet  
0.0065 x 0.0065-Inch Interference  
Photo Showing 0.0001-Inch Radius  
Proficorder Stylus Scratch



Figure 46. Test Model J, Poppet,  
0.0065 x 0.0065-Inch Interference  
Photo Showing 0.0005-Inch-Radius  
Profilometer Stylus Scratches

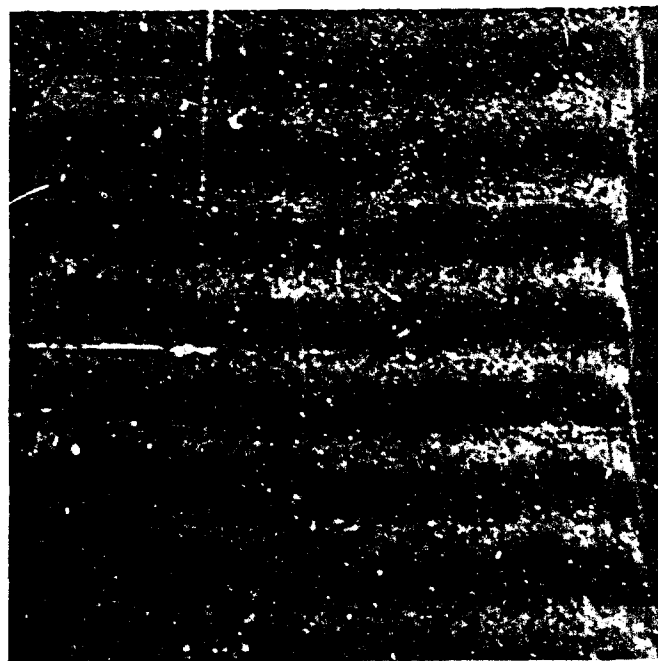


Figure 47. Test Model J, Seat,  
0.055 x 0.055-Inch Interference  
Photo Showing Dub-Off

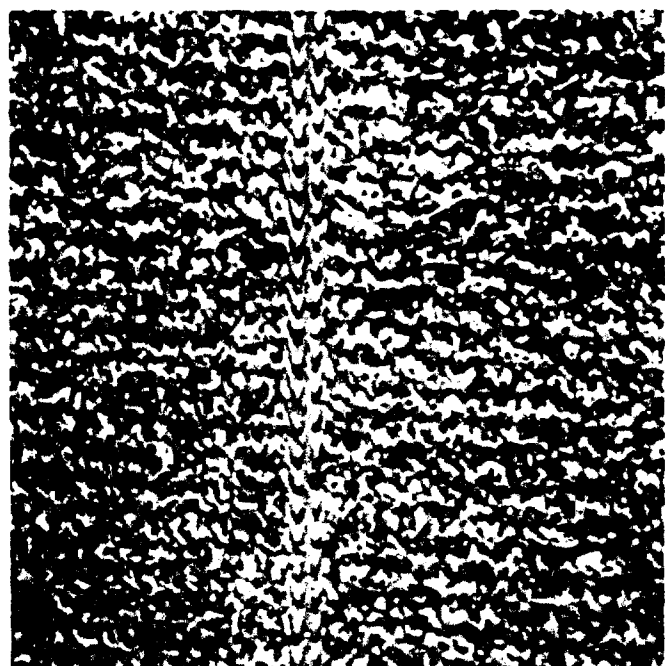


Figure 48. Test Model K, Seat,  
0.0065 x 0.0065-Inch Interference  
Photo Showing 0.0005-Inch-Radius  
Profilometer Stylus Scratches

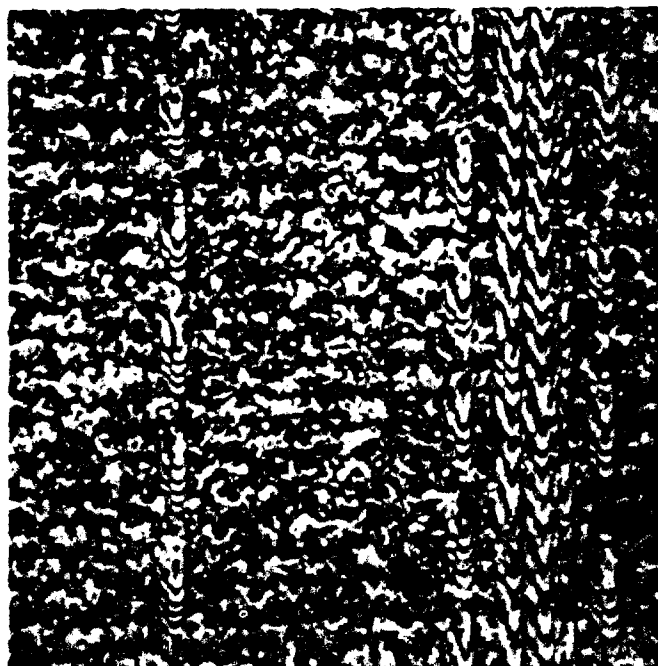


Figure 49. Test Model K, Poppet,  
0.0065 x 0.0065-Inch Interference  
Photo Showing 0.0005-Inch-Radius  
Profilometer Stylus Scratches

Preceding Page Blank



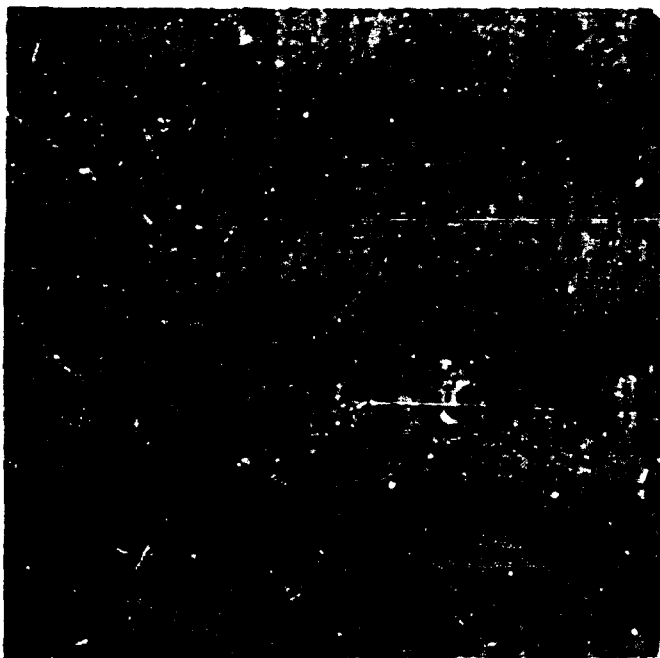


Figure 50. Test Model K, Seat,  
0.0065 x 0.0065-Inch Interference  
Photo Across Circumferentially  
Polished Lay

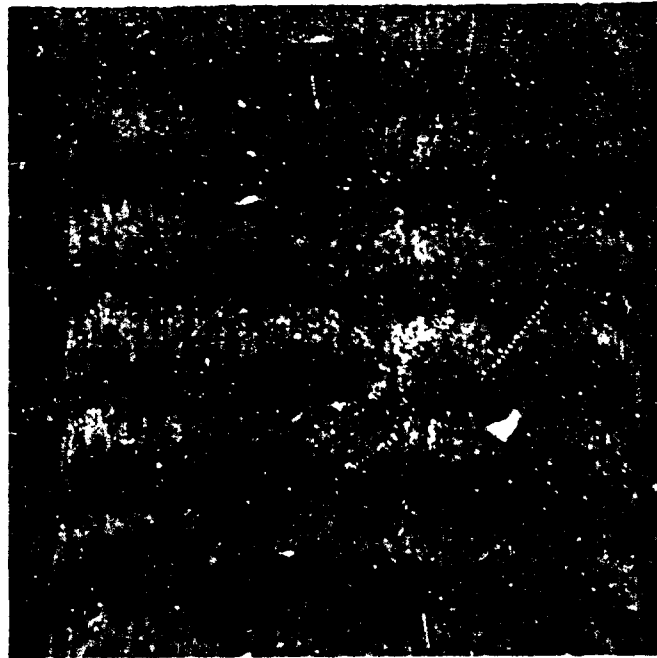


Figure 51. Test Model K, Seat,  
0.033 x 0.033-Inch Interference  
Photo

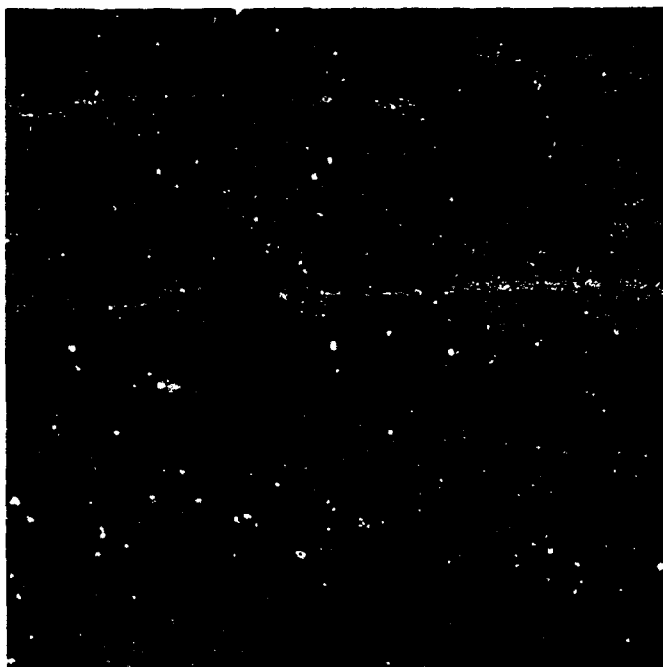


Figure 52. Test Model K, Seat,  
0.033 x 0.033-Inch Interference  
Photo Showing Dub-Off

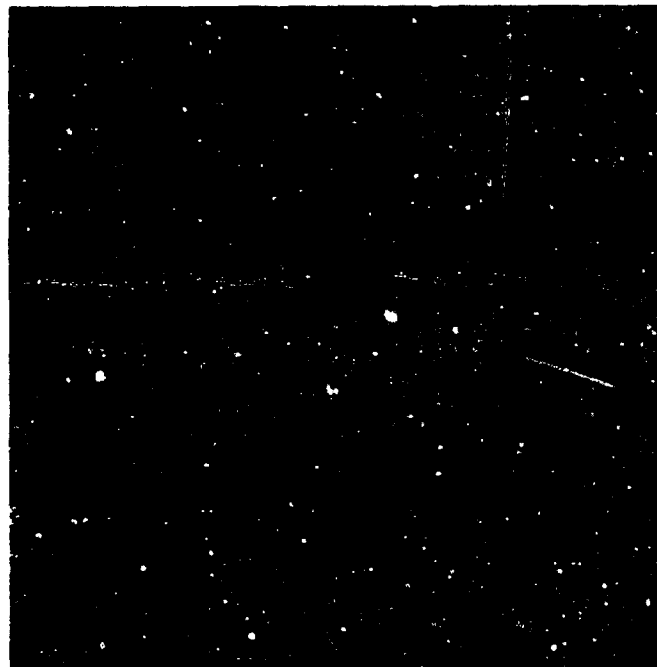


Figure 53. Optical Flat, 0.0065 x  
0.0065-Inch Interference Photo  
(lines and dots are from optics  
flaws)

Preceding Page Blank



Figure 54. Profilometer Stylus,  
0.0005-Inch Radius, 0.016 x 0.016-  
Inch Plain Photo



Figure 55. Proficorder Stylus,  
0.0005-Inch Radius, 0.016 x 0.016-  
Inch Plain Photo

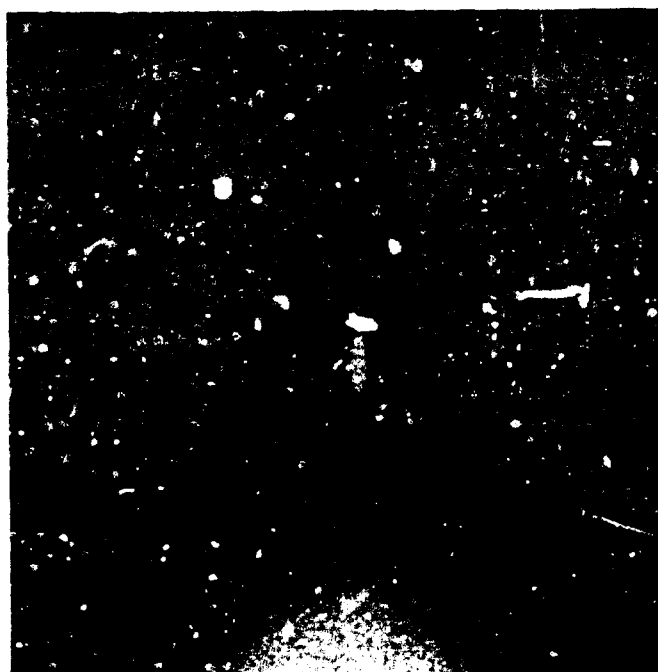


Figure 56. Proficorder Stylus,  
0.0001-Inch Radius, 0.016 x 0.016-  
Inch Plain Photo

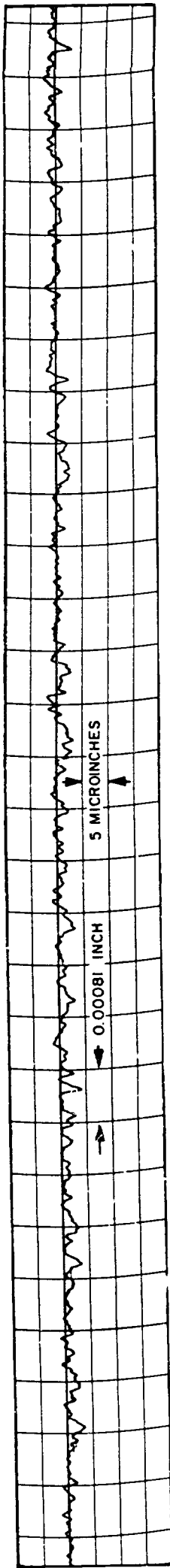


Figure 57. Test Model A, Poppet Profile Record, Gross Lay

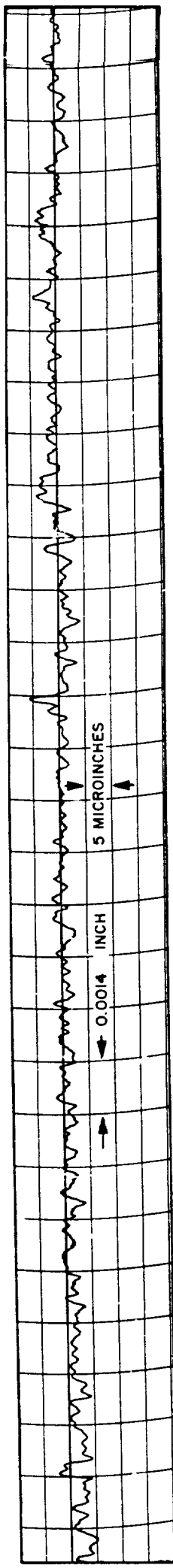


Figure 58. Test Model B, Poppet Profile Record

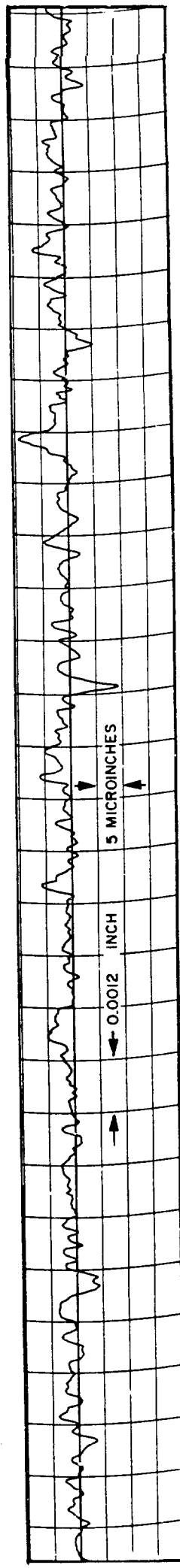


Figure 59. Test Model B, Seat Profile Record

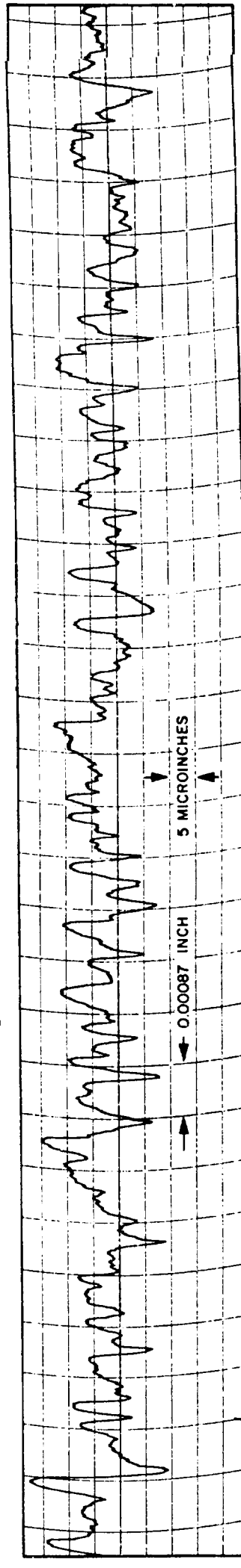


Figure 60. Test Model C, Poppet Profile Record

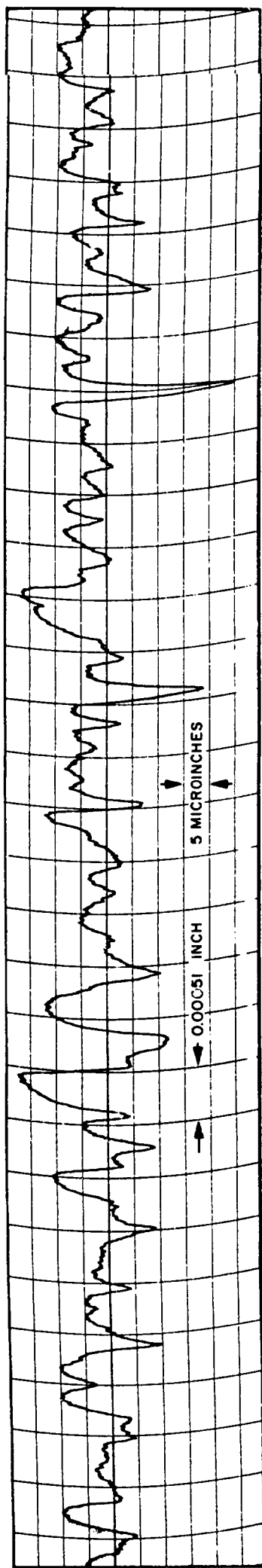


Figure 61. Test Model D, Poppet Profile Record

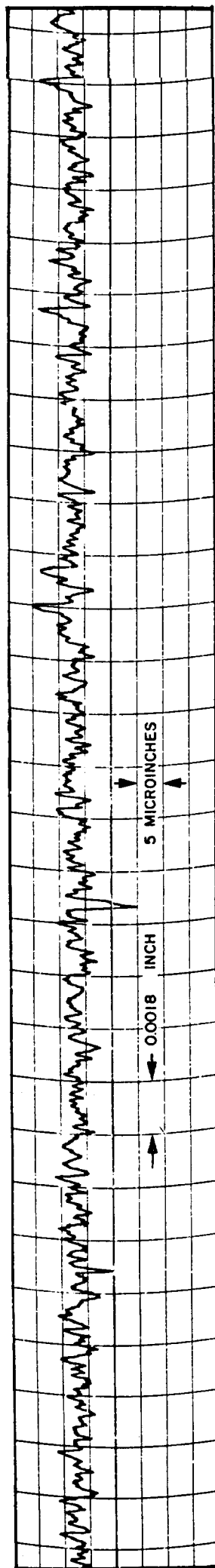


Figure 62. Test Model H, Seat Profile Record

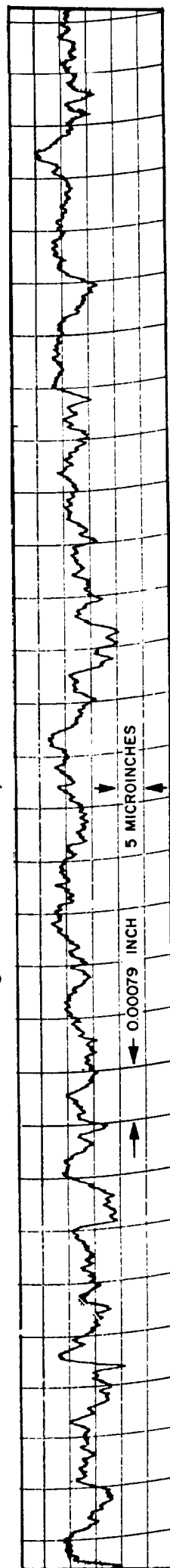


Figure 63. Test Model I, Poppet Profile Record

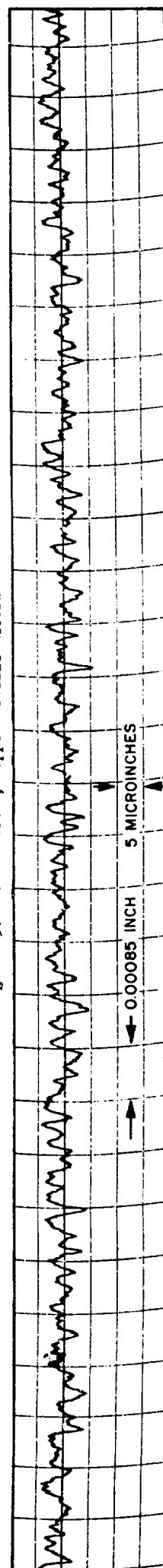


Figure 64. Test Model J, Poppet Profile Record

## Indicating Comparitors

This type of instrument uses a fixed anvil and vertically movable head to spot check height variations of a workpiece with reference to a precisely known dimension. In practice, one or a multiple stack of gauge blocks is wrung to the anvil to provide the reference height for zero-setting the indicator. The reference stack is then replaced by the workpiece which is wrung to the anvil at discrete intervals under the indicator head and height differences noted. Such a device is particularly suitable for absolute height and parallel measurements within its accuracy capabilities. However, because the work piece must be wrung to the anvil each time a new point is to be measured, a continuous indication of surface variation is not possible.

The two types of comparitor, one mechanical and the other electronic, used in fabrication and inspection of the test models are shown in Fig. 65. The mechanical unit on the left is the Mikrokator made by the C. E. Johansson Gage Co. and is capable of difference measurements of about 5 microinches. Because the parallelism requirement for both the off-seat (1-inch seating diameter) and on-seat (1/2-inch diameter) test specimens was 5 microinches, the Mikrokator was used only during fabrication and for initial gross inspection tests.

For final inspection, the electronic comparitor shown on the right in Fig. 65 was used. This unit, the Micro-Ac, is made by the Cleveland Instrument Co. and can measure surface deviations down to 0.5 microinch. Basically a reluctance-type position indicator coupled with a high-gain amplifier, the unit has the disadvantage of being quite temperature sensitive at the higher gain (0.5-microinch) setting. For optimum results, this type indicator must be located in a temperature-controlled room and further isolated from drafts and operator body heat. Even the act of wringing small parts to the anvil adds sufficient heat to the workpiece



5AJ81-9/17/63-CIG

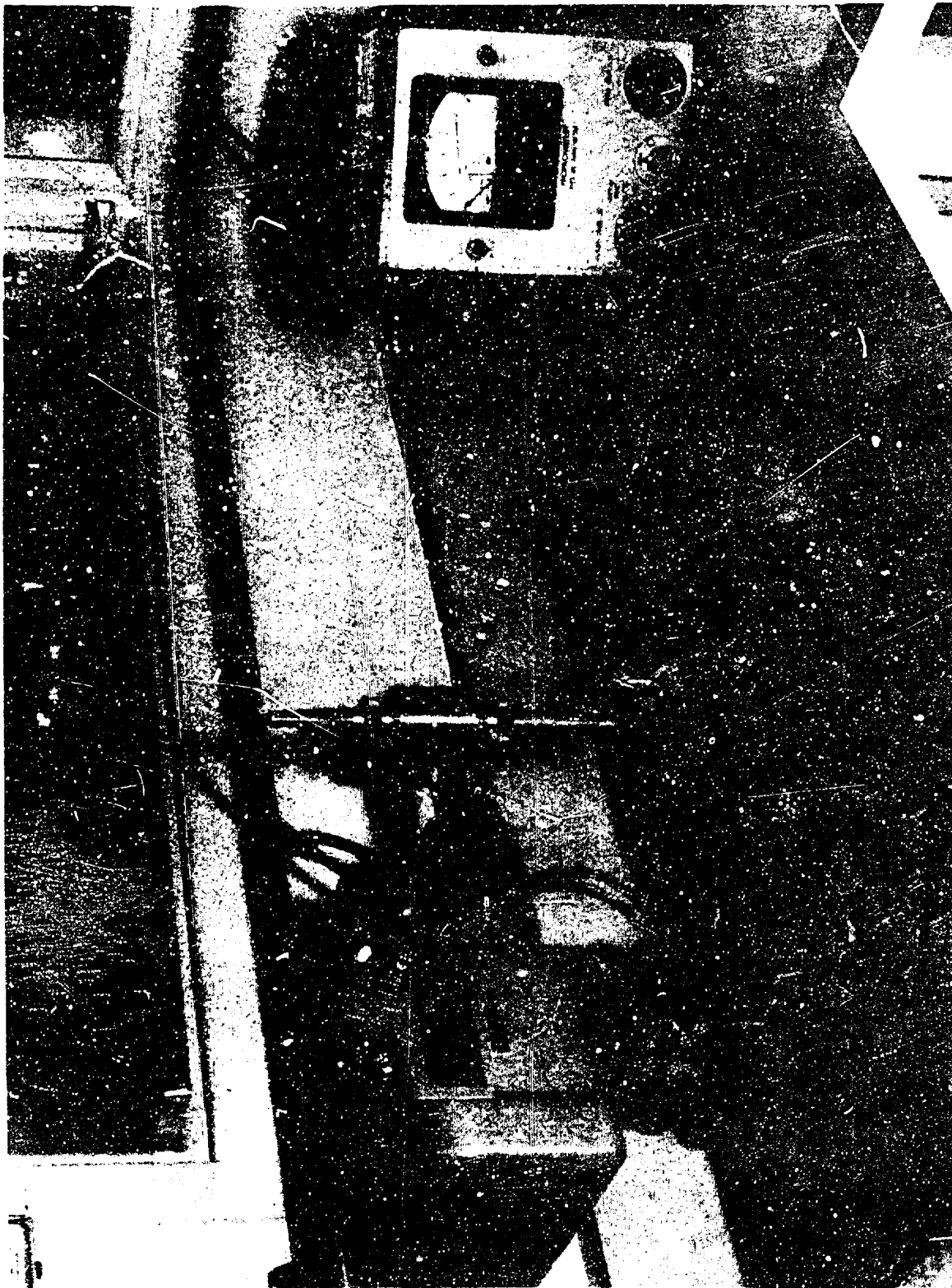
Figure 65. Cleveland and Johansson Indicating Comparitors and Test Poppet

to preclude instantaneous accurate measurement. During inspection of the test models, it was found that a 1.5- to 30-minute waiting period was required after an initial workpiece setup to obtain consistent measurements to the nearest microinch.

### Stylus Instruments

Two types of stylus instrument were used in fabrication and inspection of the test models, the Profilometer and Proficorder both manufactured by the Micrometrical Mfg. Co. The Profilometer (Fig. 66) is an electro-mechanical device incorporating a piloter or tracer arm, displacement head, and amplifier with meter output display. This unit, as well as the Proficorder uses a standard 0.0005-inch-radius stylus tip (supplied with a calibration plate) and a special 0.0001-inch-radius tip. The Profilometer output is readily switched between AA and rms and can be set for 0.003-, 0.010-, and 0.030-inch cutoff values. As the displacement head traverses the workpiece, the motion of the stylus generates a voltage proportional to the height of the measured surface irregularities, which is continuously averaged by the electronic system and displayed on the output meter. Therefore, the Profilometer shows the variations in average roughness height but does not indicate asperity configuration or wavelength variation greater than the set cutoff value.

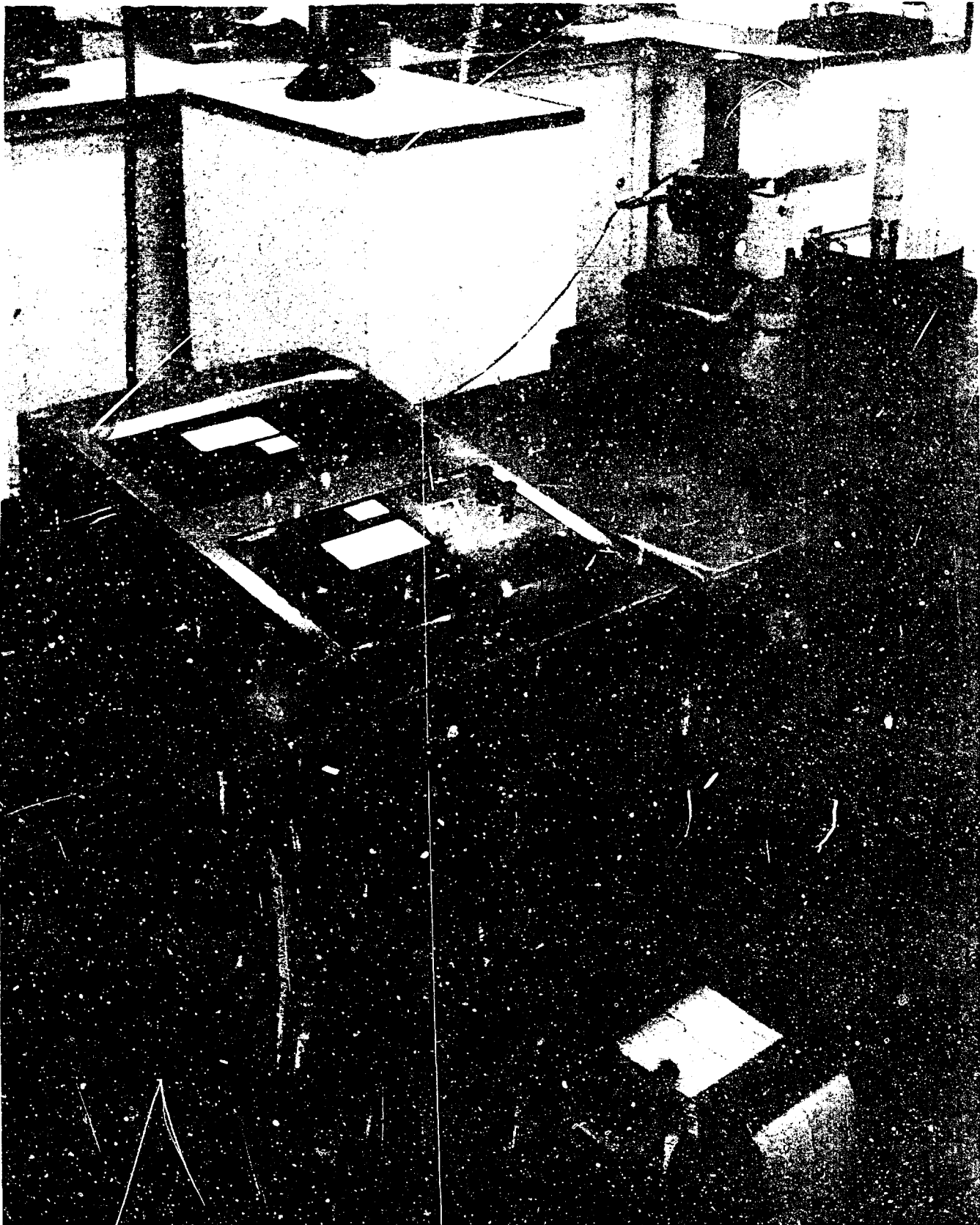
For direct continuous surface irregularity measurement, including roughness, waviness, and asperity angle variations with permanent information display, the Proficorder was used. Figures 67 and 68 show this instrument setup for typical measurements. The indicating head is similar to that of the Profilometer but the output is presented on a continuous strip chart permitting more discriminate evaluation of surface conditions. Unlike the Profilometer, the workpiece mounted on a rotating table moves relative to the indicating head, permitting the use of this instrument for flatness and parallelism measurements. Calibration of the Proficorder indicated a repeatable response to a 50-microinch step input accurate within 2 percent or 1 microinch.



5AJ81-9/17/63-CIB

Figure 66. Profilometer and Test Poppet





5AJ81-9/17/63-C1J

Figure 67. Proficorder Indicating Tester Piston



5AJ81-9/17/63-CH

Figure 68. Proficorder Indicating Test Poppet

In using the Profilometer and the Proficorder, several sources of error or extraneous inputs were encountered and evaluated. The first of these is vibration noise inherent in the instruments used and from external sources. The latter problem is a function of shock mounting and isolation from ambient disturbances. Proficorder calibration checks indicated the total noise level resulting from internal and external vibration sources was less than 1 microinch.

For the particular Profilometer used during periods when nearby machinery was in use, an ambient-induced noise level of 0.7 to 0.8 microinch was noted. Accordingly, data were taken when ambient vibration was minimal, and continuous monitoring of this influence was practiced to apply proper corrections. In addition, this Profilometer exhibited a peculiar vibration phenomenon apparently associated with the tracer system, which showed up particularly at the 0.030-inch cutoff level. The first indication of this problem was an observed difference between roughness values obtained on the extend and retract portions of the tracer cycle. To evaluate this condition, an optical flat was used as a test specimen and checked with the 0.0005-inch-radius tip stylus. The results, as tabulated below, were essentially verified by the 0.0001-inch tip stylus.

AVERAGE PROFILE VALUES IN MICROINCHES AT CUTOFF NOTED				
Cutoff, inches		0.030	0.010	0.003
rms	Extend	1.7	0.40	0.25
	Retract	0.9	0.35	0.25
AA	Extend	1.7	0.35	0.25
	Retract	0.8	0.30	0.25
Residual Vibration (AA)		0.25	0.25	0.20

Not only is there a marked difference in the extend and retract readings at a 0.030-inch cutoff, but the readings are much higher than at the other cutoff levels. The test optical flat surface profile has been checked on the Proficorder and the interference microscope (Fig. 53).

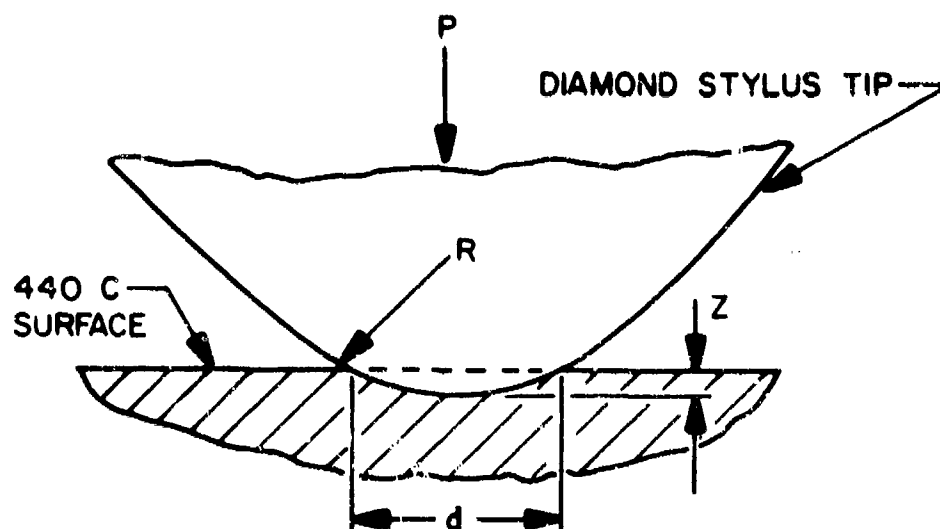
Both instruments indicated total surface deviation less than 1-microinch; therefore, the corresponding AA reading should be about 0.3 microinch or below. Based on this information and the previous limitations imposed by residual vibrations, it was concluded that readings below 1.0 microinch for the 0.030-inch cutoff and 0.3 microinch for the 0.010- and 0.003-inch cutoff are essentially meaningless for this particular Profilometer. Only the retract values were recorded for the inspection data.

Profirecorder data on surfaces of 1 microinch AA (3 microinches peak-to-valley) and greater are considered sufficiently accurate. Below these specified limitations, the interference microscope information was used to define the test surfaces.

The remaining stylus instrument errors considered apply to the stylus and include contact stress and influences of tip radius and wear on asperity depth measurements.

An elastic stress analysis assuming Hertz contact was undertaken for the 0.0005-inch radius tip with a 2.5-gram load on hardened 440C stainless steel ( $R_c 64$ ). The stress condition was well into the plastic region. Next, assuming that the plastic stress level is 2.8 times the yield of the metal, a simple plastic analysis was performed. The results of the analysis are shown on the following page. The diameter (d), or track width, is a function of the load only and not the tip radius.

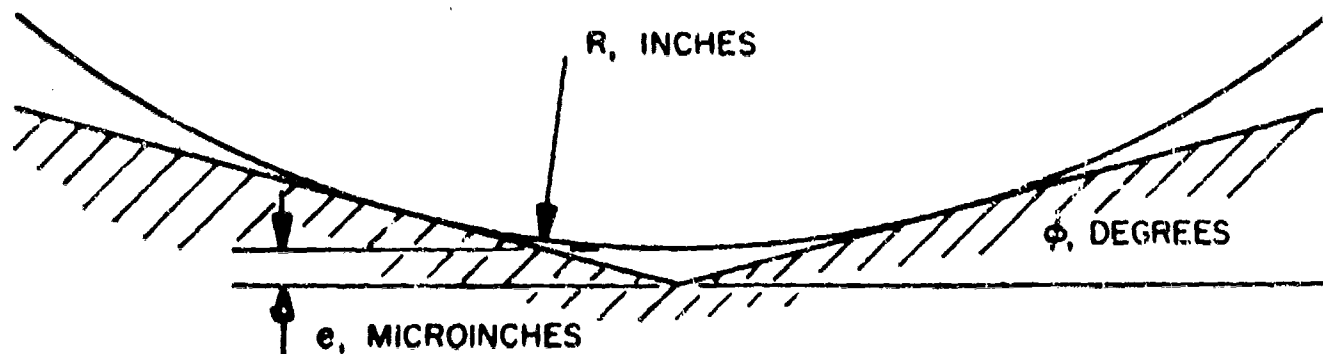
This analysis indicates that a 1.76-microinch track depth and a 84-microinch width would be made for the 0.0005-inch radius tip at the Profilometer specification loading of 2.5 grams. An example of stylus-caused surface damage can be seen in Fig. 45. Although visible, the track depth (in this instance from a 0.0001-inch radius tip) was not as deep as the calculations would indicate. However, this could be attributed to a worn stylus tip. This assumption is substantiated by the fact that there is very little evidence of plastic flow by the 0.0001-inch-radius tip on the very smooth surfaces examined with the interference



Pressure, grams	0.0005-Inch Radius		0.0001-Inch Radius	
	Z, Microinches	d, Microinches	Z, Microinches	d, Microinches
0.1	0.0704	16.8	0.352	16.8
1.0	0.704	53.0	3.52	53.0
2.5	1.76	84.0	8.80	84.0

microscope. While this analysis has shown that stylus tips can and do mark the surface a limited amount, it is concluded that the basic surface contour is followed by the stylus (except for deep pits) because of the constant plastic flow depth noted in these instances.

Further analyses were performed to determine the bottoming errors resulting from stylus tip radius and wear. The bottoming error is caused by the tip radius not being able to follow the asperity completely into the valley. The following sketch illustrates this condition.



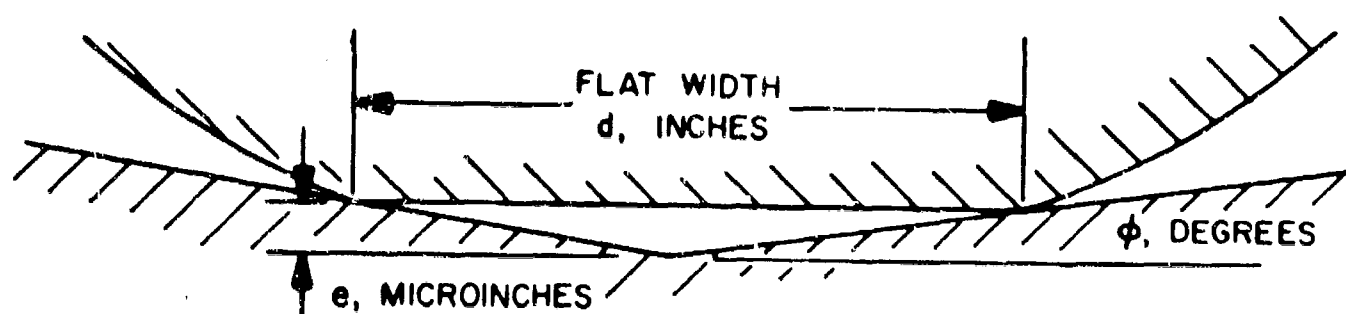
The bottoming errors (e) tabulated below have been computed using the equation

$$e = R \left( \frac{1}{\cos \Phi} - 1 \right) \approx \frac{R \Phi^2}{6560}$$

Angle, $\Phi$ degrees	Values of e, Microinches	
	0.0005-Inch Radius	0.0001-Inch Radius
1	0.076	0.0152
2	0.306	0.0612
4	1.25	0.245
8	5.00	1.00
10	7.75	1.55

For the test models inspected (Table 8), the relationship of  $\Phi$  and the roughness height (h) are such that the errors tabulated above, though significant, are minimal. Obviously, the 0.0001-inch-radius stylus results in greater accuracy and should be used when measuring fine or very sharp surfaces.

A worn stylus limits the depth to which the tip can enter a valley. This can be seen from the sketch and calculated errors shown below. From the equation  $e = d/2 \tan \Phi$ , this error is independent of tip radius ( $d > 2 R \sin \Phi$ ).



Angle $\phi$ , degrees	Values of $e$ , Microinches	
	$d = 50 \times 10^{-6}$ , inches	$d = 100 \times 10^{-6}$ , inches
1	0.436	0.872
4	1.75	3.50
8	3.50	7.00
12	5.30	10.00

Errors resulting from worn tips are appreciable, particularly at the greater angles. During the inspection of the scratch configuration (test model G), a discrepancy was noted between the interference microphotograph and the Proficorder data. Based on the microphotograph, the scratch depth was 31 microinches while the Proficorder, with a 0.0001-inch-radius tip, indicated 20 microinches. Because the 0.0001-inch-radius stylus was used, this discrepancy was not caused by a bottoming error. However, it could have resulted from a worn tip because the scratch angle was 11 degrees. Microphotographs of tip stylii are shown in Fig. 54 through 56. While the large flat on the worn 0.0005-inch-radius tip is quite apparent, a 100-microinch flat with worn and faired edges would not be readily discernible and could account for the 10-microinch discrepancy noted above.

## Optical Instruments

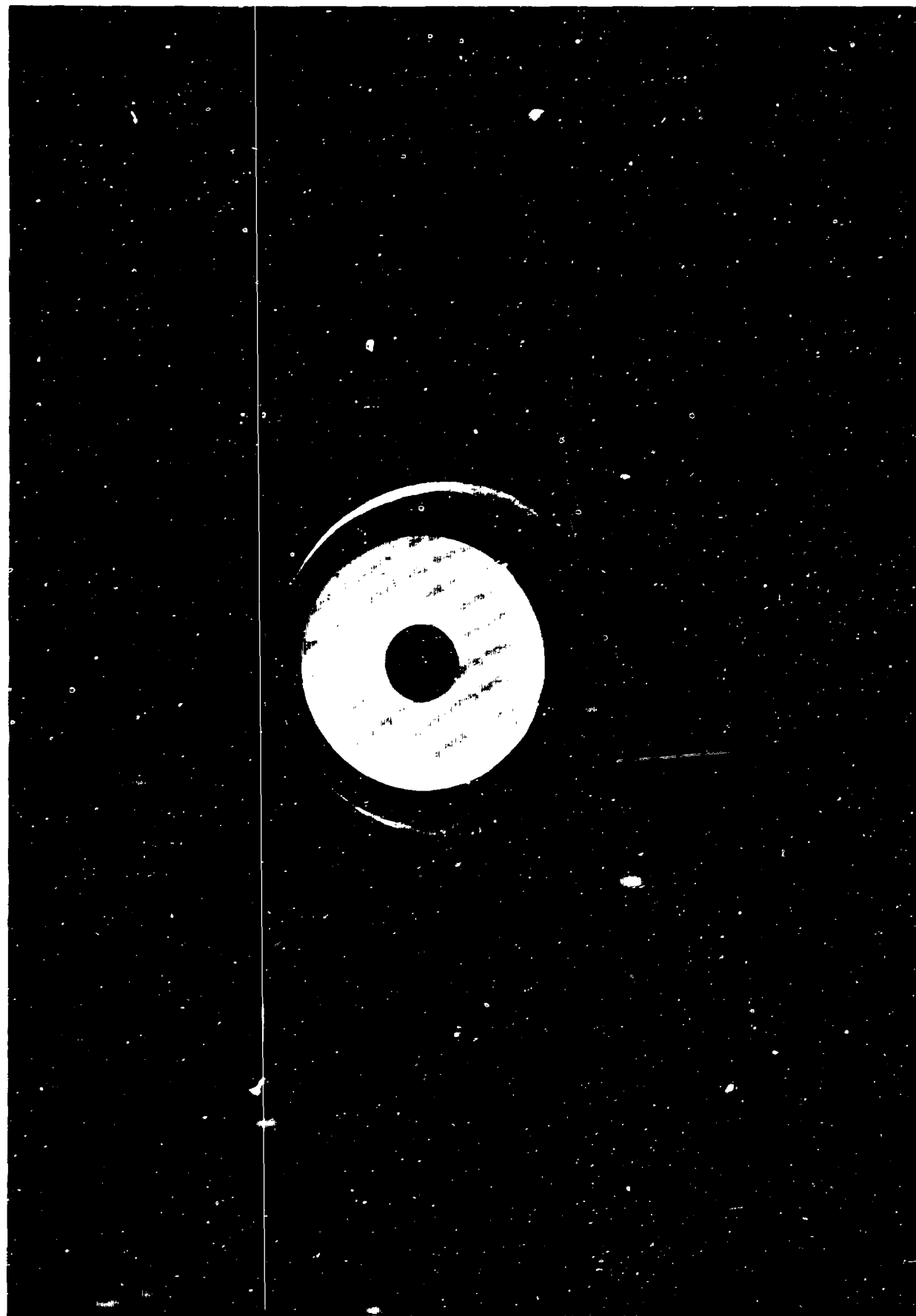
Several optical devices were used in the program for test model inspection and supplementary data. Included were the optical flat, interference and plain microscopes, and the microhardness tester which is not purely optical.

The optical flat is used extensively for production operations where gross flatness measurements are required. It was used to verify over-all flatness of all poppets and seats to within 6 microinches and was particularly useful for rapidly measuring the cylindrical-shaped poppets of test models H and I used in the out-of-flat stress leakage tests. Figure 69 shows a typical use of the optical flat in measuring gross flatness.

A Leitz interference microscope was used for more discrete flatness measurements of seating lands and areas and fine finish evaluation. Figure 70 shows the unit with a Polaroid camera attachment for photographing test specimens. This device may be used for plain or interference viewing and provides 100, 200, and 500 power magnifications. Surface texture characteristics of all test surfaces were determined in full or in part through 500 power viewing. For evaluation of seat land dub-off and large surface deviations, 200 and 100 power magnifications were used. The interference microscope was extensively used throughout the test program and was invaluable in the definition of such items as scratch extent where an area rather than line view is absolutely required.

Aside from multiple power magnification, the Leitz interference microscope permits two-band pattern adjustments. First, the band density across the part can be varied. Figures 35 and 36 illustrate different band densities on identically magnified part locations. From the example, it can be seen that the large scratches which are difficult to measure with a few bands are quite plain when the number of bands is increased. Secondly, there is the capability of rotating the bands 360 degrees. This enables the observer to view the various lay directions without moving the part.





5AJ81-9/17/63-CIC

Figure 69. Optical Flat and Test Poppet Showing Helium Light Interference Bands



5AJ81-9/17/63-CLK

Figure 70. Leitz Interference Microscope and Test Seat

For gross surface defect assessment and general low-power viewing, a 40 power Bausch and Lomb microscope was used. This unit provided excellent naked eye assistance without complicating the viewed surface with minuscule defects and variations.

Test specimen hardness was determined by the Vickers test, using a Leitz microhardness tester (Fig. 71). This instrument is capable of taking hardness measurements with loads from 15 to 1000 grams. A pyramidal-shaped diamond indenter having a depth-to-diagonal ratio of 1:7 was used, and the diagonal indentation width was directly measured through a self-contained optical-recticule system.

Vickers diamond pyramid hardness number (DPH) is defined as the pressure distributed over the contact area of the indentation. The mathematical expression is:

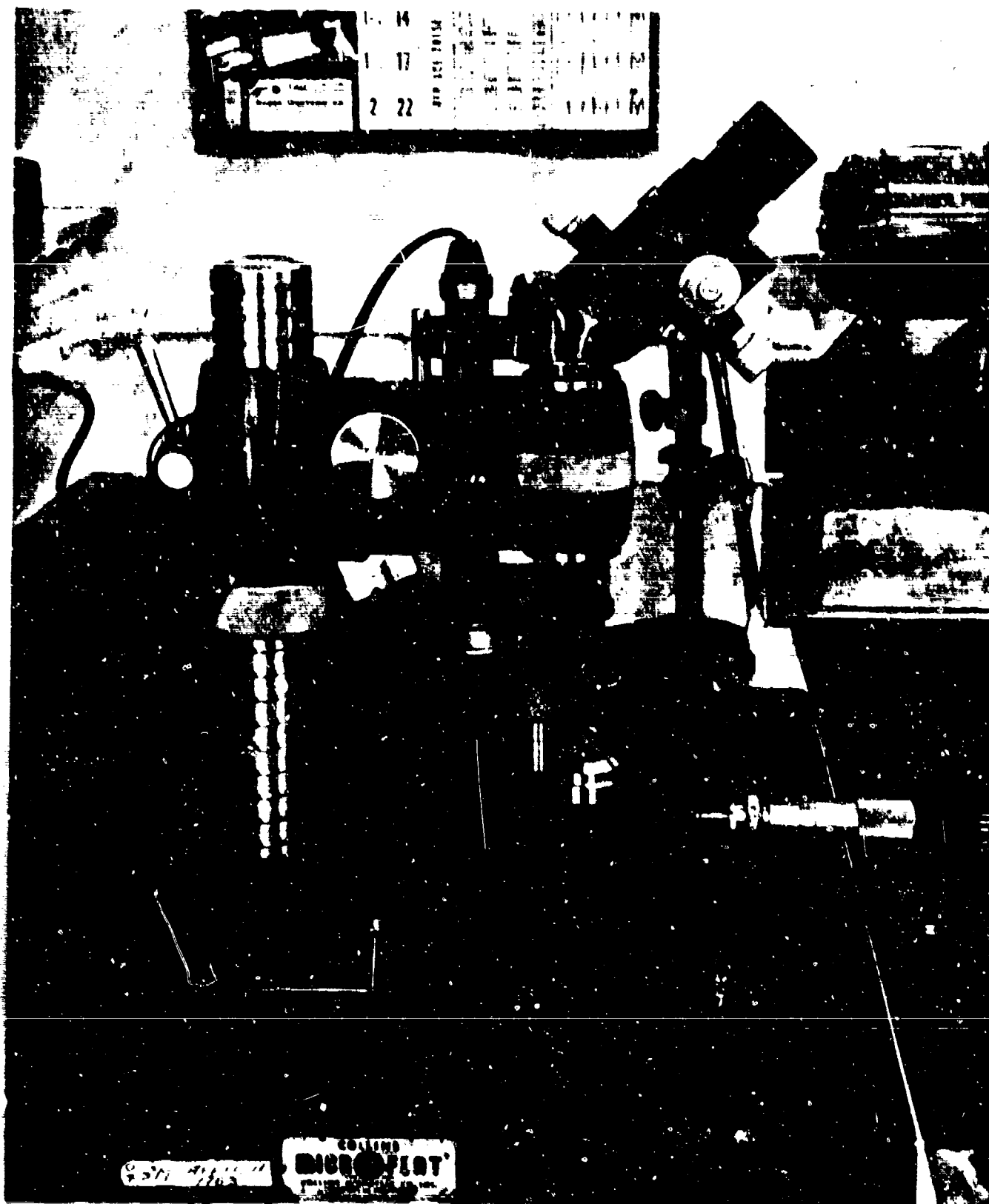
$$DPH = \frac{P}{0.5393 d^2}$$

where

P = load, kilograms

d = diagonal distance, millimeters

Because only the surface hardness was of interest, the indentation loads used were 15 to 100 grams. The procedure used was to make two indentations and average the diagonal dimensions from each. Accurate measurements on the test surface profiles limit the minimum diagonal to approximately 10 microns (0.0004 inch); therefore, only the 100-gram data were measured on the steel and carbide parts. Figures 26 and 28 show interference microphotographs of indentations at both loads. Note roughness interference and also that the depth may be determined by counting interference bands but not as accurately as direct measurement because the exact edge cannot be exactly discerned.



5AJ81-9/17/63-C1L

Figure 71. Leitz Microhardness Tester and Test Poppet

The hardness pressure may be used for an estimate of yield strengths. The plastic flow pressure for fully work-hardened metal is approximately 2.8 times the yield strength (Y). Hardness values and approximate yield strengths for each of the test model materials are tabulated below.

Material	15-Gram Average Diagonal, Microns	100-Gram Average Diagonal, Microns	Vickers Hardness Number, Kg/mm <sup>2</sup>	Yield Strength Criterion, psi x 10 <sup>3</sup>
440C Stainless Steel	--	15.2	800	406
6061-T651 Aluminum	15.5	40.0	123*	62.5*
Tungsten Carbide	--	11.8	1330	676

\*Based on 15-gram load

#### INSPECTION AND DATA INTERPRETATION PROCEDURES

In obtaining the inspection data presented in Table 8, certain procedures and ground rules were used to obtain the best and most representative values. These techniques apply to the physical measurement of various properties and the information deduced from those measurements.

Parallelism of the test parts was of particular importance during the off-seat tests where poppets and seats were brought together within a few microinches without touching. Here, seat displacement was measured from the rear poppet face; therefore, deviations between the rear and seating faces could introduce error. For the out-of-parallel tests, the poppet faces were deliberately lapped out of parallel. In the latter case particularly, parallelism was measured on the Proficorder in addition to comparator checks. By wringing the test poppets to an optical flat preleveled on the Proficorder table, continuous indication of the parallelism characteristics was obtained with a 1/16-inch ball stylus and the instrument set for waviness.

Although gross test model flatness was measured with the optical flat, the flatness of seat lands required special attention because one of the problems with lapped and polished surfaces was the tendency to radius the edges of the part. This action, commonly called dub-off, becomes critical in narrow seat lands where the dub-off may represent a large portion of the land width. The interference microscope was used to assess this condition in the seat models. Figure 34 is an interference microphotograph of test seat E which exhibits considerable dub-off. As a result, the effective seat area was decreased, and the seat stress was proportionally increased. Each of the seat models tested was examined for dub-off and the stress area adjusted accordingly. The criterion used was that the permissible dub-off would be no greater than the maximum surface roughness. The inspection data (Table 8) shows that the "flat land width" column, which is used in computing effective seat land area deviates in some instances from the values listed in the "total land width" column.

The Profilometer data presented in Table 8 are based on the arithmetic average (AA) reading which has supplanted the rms average. Though not illustrated, rms readings were taken and found to be 1.1 to 1.15 times higher than the AA readings. Information is tabulated for the 0.0005- and 0.0001-inch-radius tip stylus. In general the 0.0001-inch-radius tip indicates somewhat higher readings at all cutoff values because of the deeper penetration of the small tip.

The diamond lapped surfaces (test models E, F, and G) had roughness readings very close to the previously noted optical flat value of less than 1 microinch, indicating an extremely smooth surface. However, interference microscope data taken on these same surfaces show that, even though the surfaces are very smooth, there is a definite difference in each of the detail surface textures.

Of all the test model parameters to be measured, surface texture was the most complex. To simplify the process, the surface was first catalogued by the type of lay (multidirectional, unidirectional, circumferential,

or radial). This was followed by further reduction into roughness, waviness, nodules, and scratches. There are other characteristics such as pits and ridges, but those categories mentioned are considered to have major influence on the stress vs leakage relationship.

The surface texture parameters of Table 8 represent a composite reduction and interpretation of Proficorder and interference microscope data. The previously noted errors and limitations of the Proficorder were considered, and appropriate corrections were applied during evaluation of this particular information. All Proficorder traces (Fig. 57 through 64), were taken with a 0.0001-inch-radius stylus tip and across the prevailing lay where possible. For best resolution and to minimize point-to-point stylus skip, the slowest possible table speed was used. However, as workpiece motion is rotary, the surface speed varies proportionally with the measurement diameter, thus accounting for the different linear displacement calibrations. In general, the Proficorder information was most helpful in the evaluation of the multidirectional textured surfaces and supported the more qualitative interference microphotographs. However, for assessment of unidirectional surfaces, the interference microscope provided the most direct approach. The multidirectional finish of Fig. 26 results in poor definition as compared with the cross lay view of Fig. 36. There exists, therefore, a fringe area (very smooth, multidirectional surfaces) where the accuracy limits of the Proficorder and indefinite resolution of the interference microscope particularly necessitated subjective interpretation.

Figures 26 through 56 illustrate surfaces as viewed through this instrument. These microphotographs have been cut to the definite calibrated size described in each figure so that the photos may be scaled to obtain specific dimensions. Approximate magnifications are:

1.  $0.0065 \times 0.0065 = 462X$  (50 x objective lens)
2.  $0.016 \times 0.016 = 187X$  (20 x objective lens)
3.  $0.033 \times 0.033 = 91X$  (10 x objective lens)

In addition, the microphotographs have generally all been oriented such that the top side of the interference bands represent the surface profile, and therefore, scratches appear as V-grooves that point downward (Fig. 36 and 41).

To consistently evaluate the surface profile input data, the following distinct parameters with resolution limits were established:

1. Roughness

$h = 0.5$  microinch and above

$\Phi = 0.1$  degree and above

2. Waviness

$h = 0.5$  microinch and above

$\Phi = 1.0$  and below

3. Nodules

$h = 25$  percent above the maximum peak-to-valley roughness ( $h$ )

$\Phi =$  no confines

$\beta = 1$  percent and above

4. Scratches

$h = 1$  microinch and greater which occur below level of surface roughness (or waviness)

$\Phi =$  no confines

$\beta = 1$  percent and above

These ground rules were established for both Proficorder and interference microscope inspection data and, in general, reflect the practical limits for obtaining these data. (For example,  $h$  values cannot be resolved any lower than 0.5 microinch on either instrument.) An overlap is provided for roughness and waviness angles ( $\Phi$ ) because these two categories merge into each other, and a finite division cannot be made.



## EXPERIMENTAL TEST PROGRAM

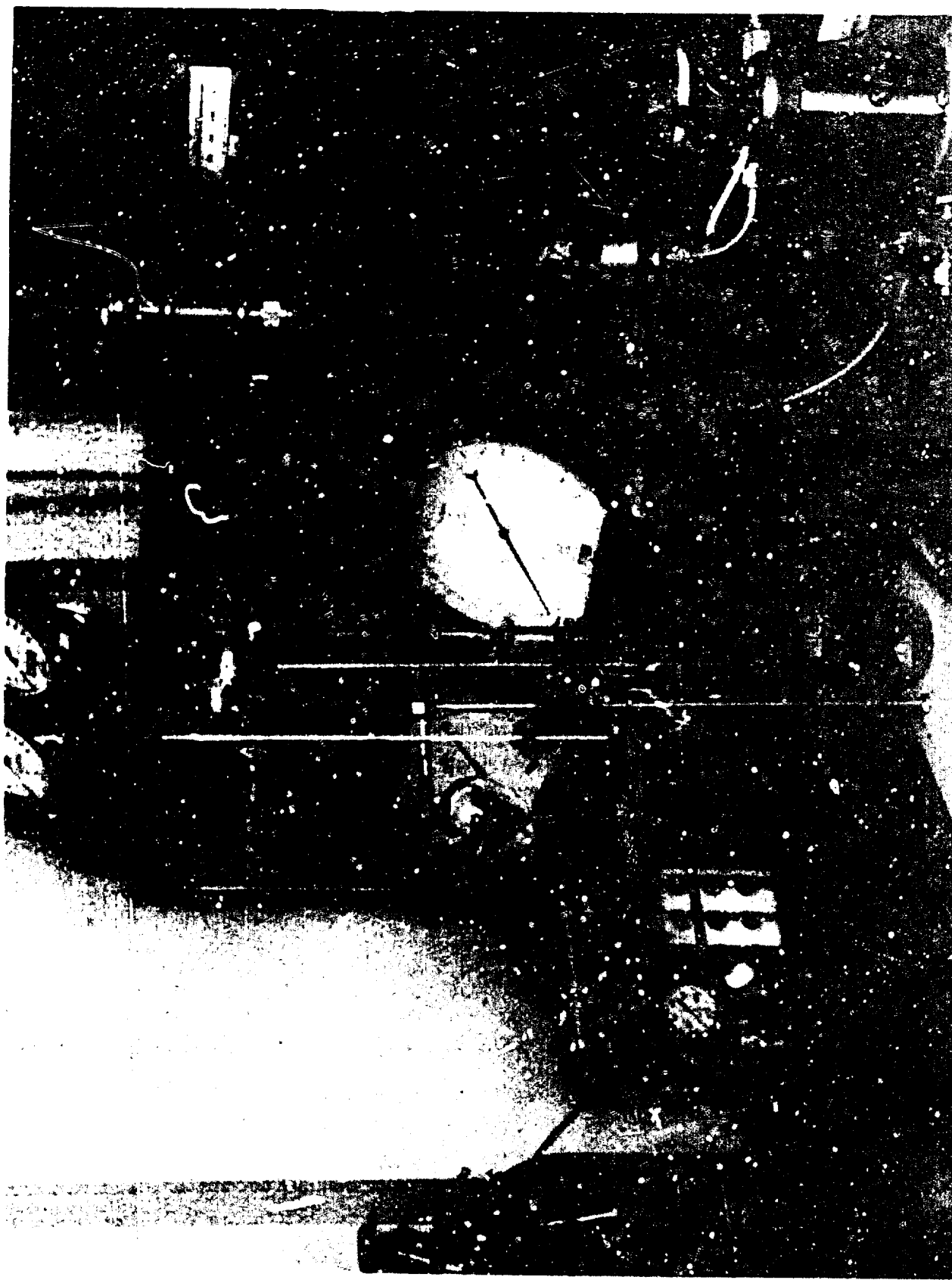
The experimental program was designed to support the leakage and seating analyses, and to provide design data where an analytical approach was not possible.

A basic objective was to identify the various surface parameters controlling leakage for the specific model pair tested. This was not possible in all cases; however, the detail dimensions obtained in Table 8 will provide insight into the mechanism of leakage indicated by the test results.

The experimental approach taken was to initially study near-seated valve-seating parameters so that the leakage and pressure distribution analyses could be verified. The near-seated region was thus defined as that separation from the seat which encompassed a complete transition through the various flow regimes (Leakage Flow Analysis). The capabilities and problems associated with the tester would be uncovered and corrected at this time. It was only through a thorough understanding of the tester that its influence on the seating characteristics could be determined. In addition, the precise linear measurements required for near-seated testing were intimately related to the tester and its instrumentation. Following the near-seated tests, the on-seat tests of the various models were conducted.

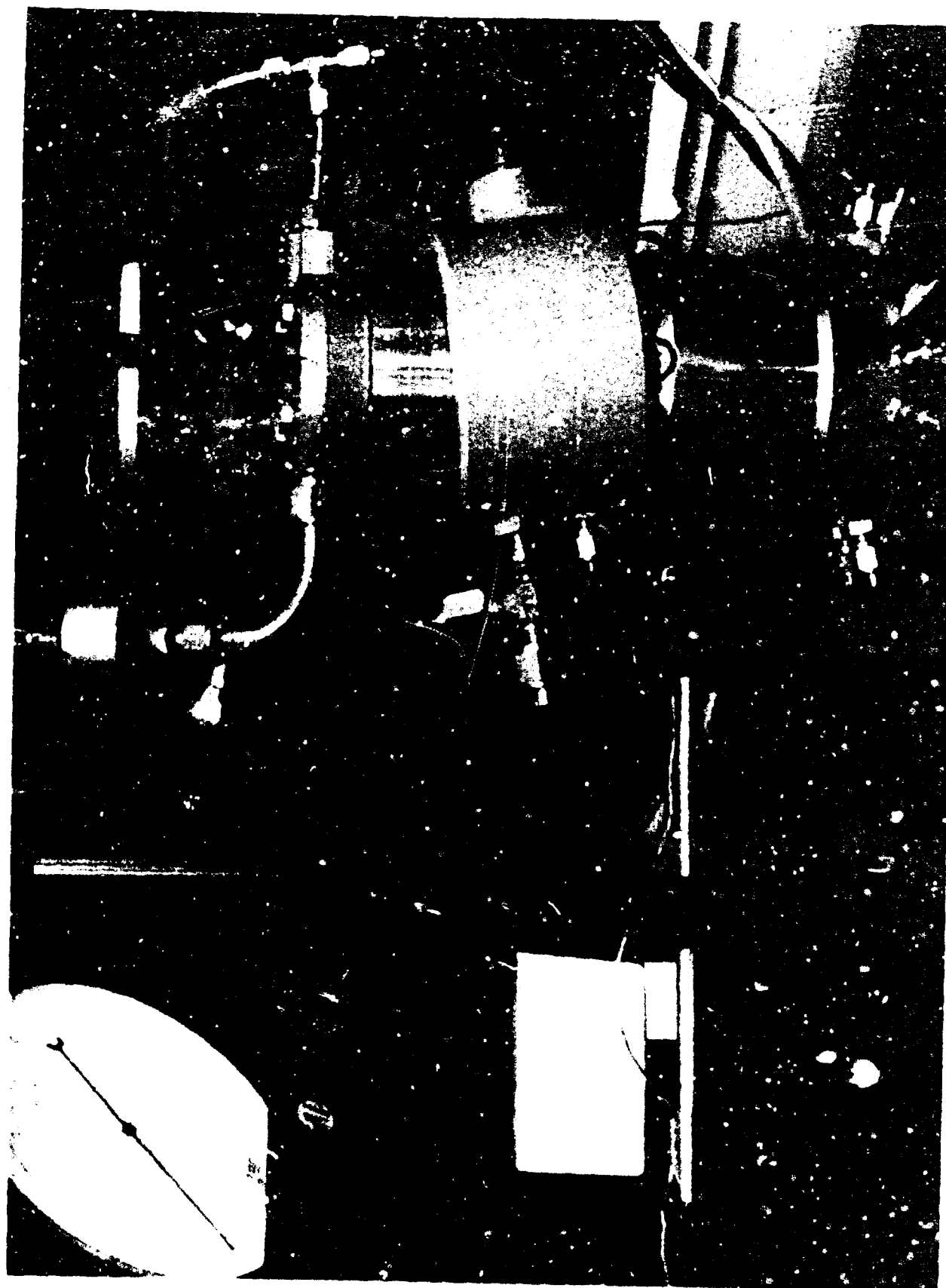
## EXPERIMENTAL TEST SETUP

The poppet and seat tester was set up in an enclosed temperature-controlled room that contained all of the necessary pressure-, flow-, and linear-measurement devices to conduct seating tests, and microscopes for visual surface inspection. Other surface inspection equipment was located nearby so that measurements could be made when necessary. Figures 72 through 75 show the tester and associated instrumentation. A schematic of the test setup is shown in Fig. 76.



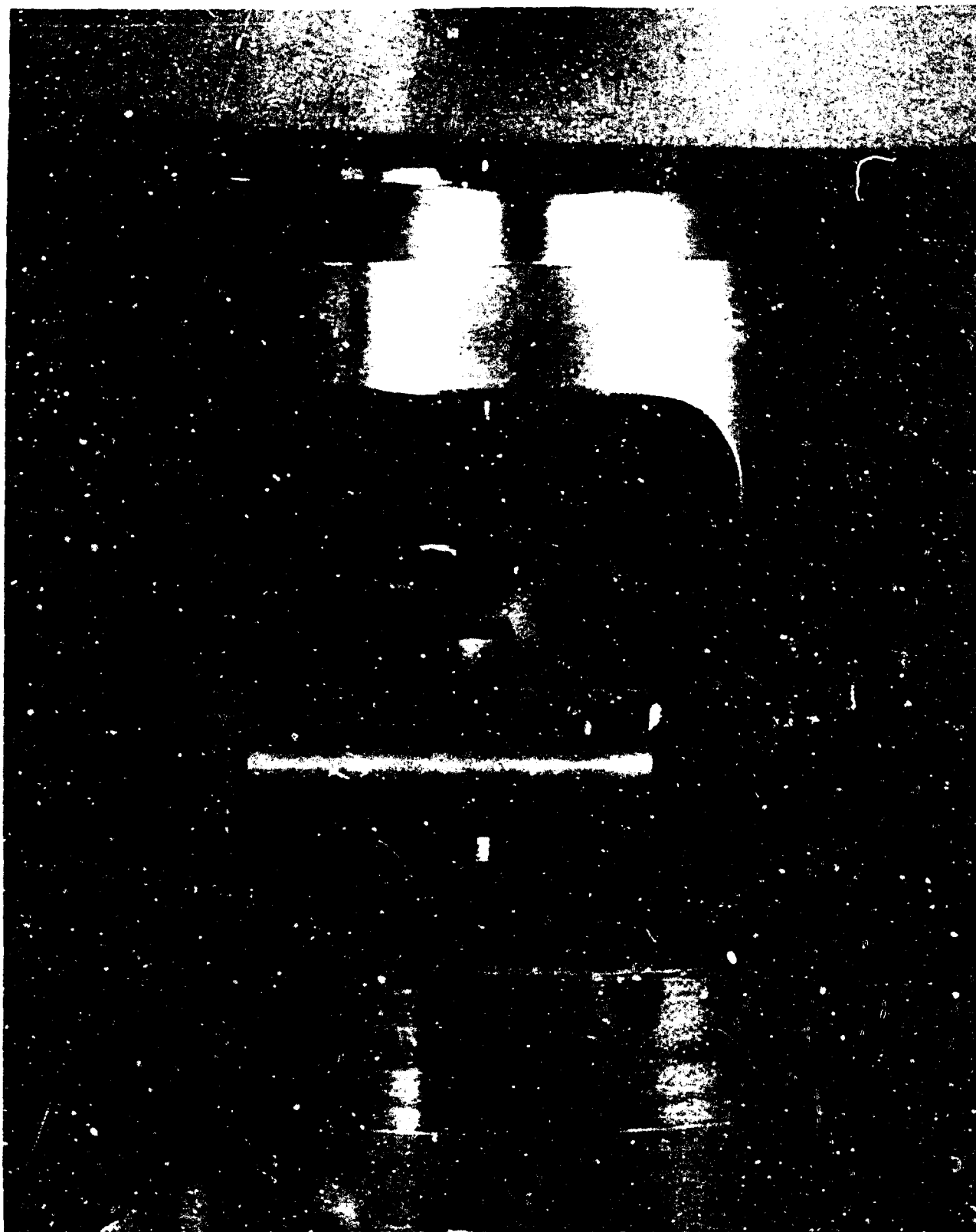
5AJ81-9/17/63-CIF

Figure 72. Experimental Setup Showing Tester With  
Pressure and Flow Instrumentation



5AJ81-9/17/63-C1D

Figure 77. Tester With Merz Electronic Indicator



5AJ81-9/17/63-C1I

Figure 74. Interior of Tester



5Af81-9 17 65-C1E

Figure 75. Load Cell Electronic and Recorder

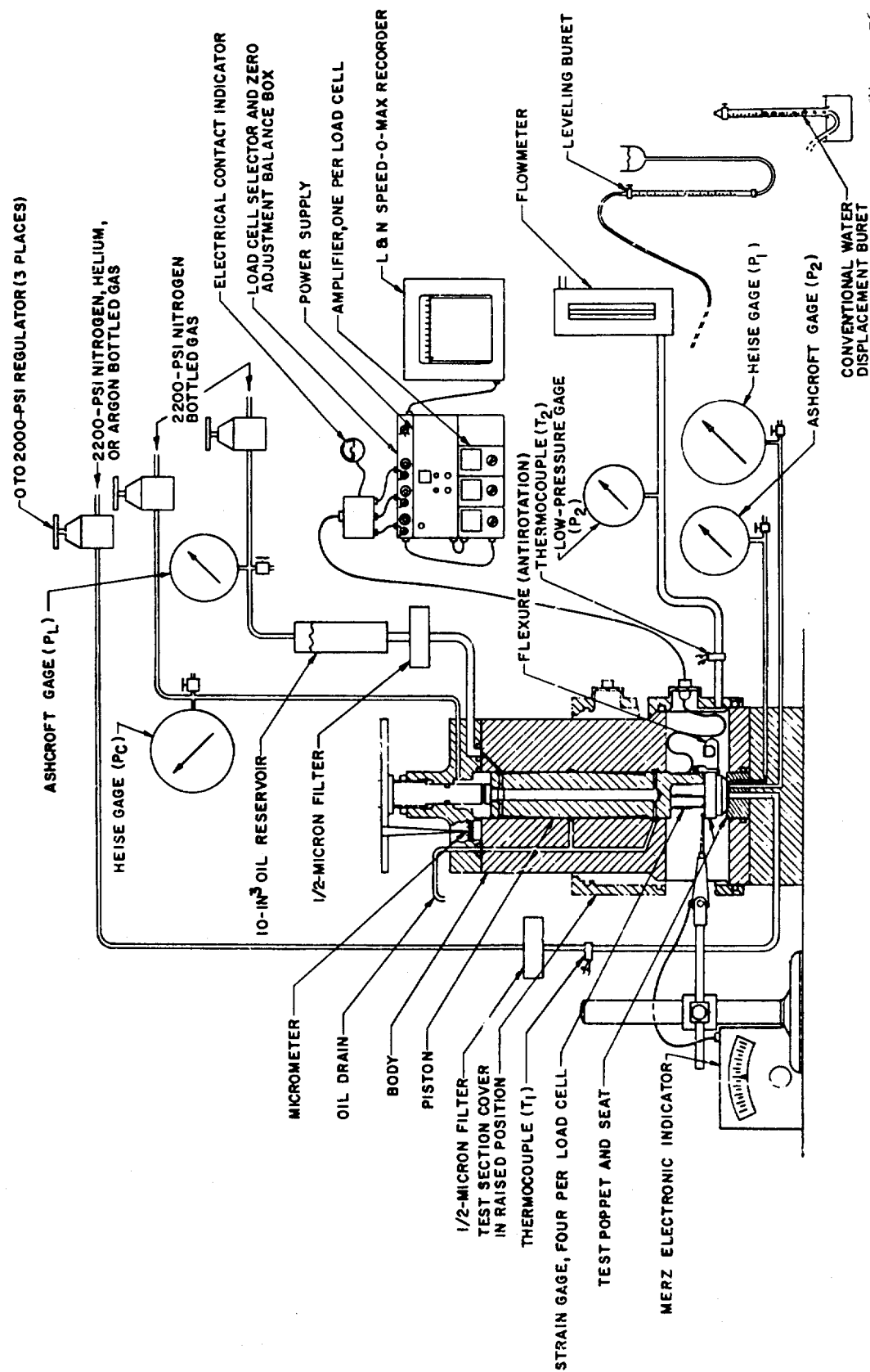


Figure 76. Test Setup Schematic

## Linear Measurements

The tester was located on a granite surface that was smooth and flat within 25 microinches. This surface was used as a reference datum for all height measurements. The height readout instruments used were the Merz electronic indicator gage (Fig. 73) and the precision micrometer screw and scale, which was a part of the tester (Fig. 20). The scale reading was used to indicate poppet position, and the Merz was used for backup and calibration and to determine poppet and seat parallelism and deflection.

Zero position, or contact indication, was by an electrical signal supplied by a microammeter. The tester piston and poppet was electrically insulated from the seat. A 1-1/2-volt battery in series with a 1.2-megohm resistor provided a source of electrical energy which did not visibly (500X) pit or burn the surfaces.

## Pressure Measurement

The tester was connected to a complex of pressure gages to provide a range of inlet and load-control pressures. Heise gages (600 to 1000 psig), 0.1-percent accurate, allowed for an extended range with a negligible loss in measurement accuracy. To provide accurate differential measurements, all gages were parallel connected and calibrated against one Heise gage.

## Hydraulic Film System

This was an auxiliary system used only to provide centering film pressure to the hydraulic piston. A source of gas pressure was connected to a small reservoir (10 cu in.) which contained SAE 70-weight oil. The oil was filtered through a 1/2-micron absolute membrane element before entering the piston (Fig. 76).

## Load Measurement

Load measurements were obtained from the Leeds and Northrup recorder and load cell system or the piston area controll pressure relationship. In both cases, compensation for the weight of the piston and inlet pressure was necessary when determining net seat loads. For the load cells, compensation was accomplished by proper zero-setting. The following expressions were used to compute apparent seat stress.

$$S = \frac{F_1 + F_2 + F_3 - P_1 A_e}{A_s} = \frac{P_c A_p + W - P_1 A_e}{A_s}$$

where

S = apparent seat stress

F = load cell force readout for cells 1, 2 and 3

P<sub>1</sub> = inlet pressure, psig

A<sub>e</sub> = poppet effective area, sq in.

A<sub>s</sub> = seat land area, sq in.

P<sub>c</sub> = piston control pressure, psig

W = piston assembly weight, 3.65 pounds

A<sub>p</sub> = piston area = 1.767 sq in.

For the on-seat tests, it was easy to establish the balance piston control pressure for each seat at a given inlet pressure. This pressure was determined by balancing piston control pressure force against inlet pressure force at zero load contact. The piston weight and inlet force are thus cancelled and apparent seat stress is

$$S = \frac{\Delta P_c A_p}{A_s},$$

where  $\Delta P_c$  is the increase in piston control pressure above the balance pressure.



## Gas Pressure Feed

Bottled gas was the source for the high pressure that was required to perform the various tests. Because remote control was not required, bottle regulators were used to control the 2300-psig gas from 0 to 1500 psig. Pressures within 0.5 psi could be maintained manually using the Heise gages for readout. All of the gas was filtered before using it in the setup (Fig. 76).

## Leakage Flow Measurement

Because of the importance of the leakage flow measurements, several devices were investigated for low-rate leaks before selecting the buret systems indicated in Fig. 76. Of the two systems evaluated in detail, the first was the conventional method of introducing the leak through water at the base of an inverted buret to displace a column of water. This is satisfactory and accurate for larger flows; however, leakage measurements under 0.1 scim require small bore tubes to obtain readings in a reasonable time, and when used in the above manner, large gas bubbles tend to stick at the base of the tube. Reducing the diameter of the gas bubbles by a small-exit orifice helps to attain the measurement, but this causes back pressure on the leak which must be overcome before a stable reading can be taken. In measuring small leaks, positive or negative pressure differentials cause extraneous leakage resulting in large errors.

The second method, which overcomes these difficulties was successfully employed for low-rate leakage testing. The gas leak was introduced through a modified buret stop cock valve at the top of the buret rather than bubbling it through the water. A leveling bottle connected to the base of the buret provides a control of both the level and internal pressure after introducing the leak. By dropping the height of the bottle to match the level in the buret as the leak volume increase, the pressure

differential in the system can be maintained negligibly small. Capillary effects may be cancelled by determining the differential heights of the two water levels at atmospheric pressure and maintaining this difference throughout the timed run.

Examination of the equations that correct for water head, vapor pressure, and ambient conditions for the conventional system and leveling bottle show the advantage of the second method. These expressions assume a constant temperature.

#### Conventional.

$$Q_s = \frac{3.66 T_s}{T t P_s} \left[ \rho_L V_1 (h_1 - h_2) + \Delta V (P_a - \rho_L h_2 - P_v) \right]$$

#### Leveling.

$$Q_s = \frac{3.66 \Delta V (P_a - P_v) T_s}{T t P_s}$$

where

$P_s$  = standard atmospheric pressure, psia

$P_a$  = atmospheric pressure, psia

$P_v$  = vapor pressure of water at temperature, psia

$h$  = water level head, inches

$V_1$  = initial volume in buret, cc

$\Delta V$  = change in volume as a result of leakage, cc

$T$  = gas temperature (assumed equal to water temperature), R

$T_s$  = standard atmospheric temperature, R

$t$  = time, seconds

$Q_s$  = leakage, scim

$\rho_L$  = liquid density (with water used) lb/in.<sup>3</sup>

The leveling system requires fewer corrections. Investigation of errors in leveling indicates that they can be made negligibly small. This is accomplished by taking continuous readings to cancel out surface tension effects, and by maintaining the total leakage volume at not more than 1000 times the amount of the leak. The second consideration stems from the precision with which the two levels can be observed and maintained during test. The leveling error as a result of the volume consideration is

$$\text{Error} = \frac{\rho_L \Delta h (V_L + \Delta V + V_1)}{(P_a - P_v + \rho_L \Delta h) \Delta V},$$

where  $\Delta h$  is the leveling head error and  $V_L$  is the total leakage volume external from the buret. This relation indicates that within visual leveling capabilities there is a minimum leak volume,  $\Delta V$ , which can be measured for a given error and total volume ( $V_L + V_1$ ). For the 23 cu in. volume enclosed by the tester cover, the minimum leak volume,  $\Delta V$ , for a 5-percent error (0.02-inch  $\Delta h$  reading error assumed) is 0.023 cu in. or 0.38 cc. Thus, for a 1-minute test, the minimum rate is 0.023 scim which is 1/1000 of the total volume. To allow lower rates to be measured without increased time, the external leak volume was reduced by placing an O-ring seal between the poppet and seat. A 0.04-inch-diameter brass tube was inserted through the seal which, in turn, was connected to the buret via 52 inches of small-diameter (0.038-inch ID) plastic tubing. The volume of this system, external to the buret, is less than 0.1 cu in., thus for a 5-percent error only  $1 \times 10^{-4}$  cu in. or 0.00164 cc leakage need be captured. This volume was increased to 0.005 cc during tests to compensate for surface tension errors induced by film contaminate inside of the burets and initial buret volume,  $V_1$ .

Four precision burets were used to cover the low range of leakage; these were 100 milliliter for the conventional method (bubble under) and 10, 5 and 1 milliliters for leveling. The 5 and 1 milliliter tubes, having fine graduations of 0.01 and 0.002 milliliter, respectively, were predominately used. The larger tubes were primarily used to calibrate the low-range, ball-float Brooks rotameters which covered leakage from about 0.1 to 110 scim. Standard laboratory calibrations from positive displacement meters were used for the high-range rotameters which covered flows to 14 scfm nitrogen.

### Temperature Measurement

Room temperatures were constantly monitored with two ordinary thermometers. Inlet and outlet gas temperatures were indicated with thermocouples and an Alnor millivoltmeter pyrometer. Except for a minor drop in inlet gas temperature during high off-seat flow, all temperatures remained within 65 to 75 F. Temperature control was more than adequate to neglect correction for flow; however, the precision of the linear measurements was decidedly affected and, while the temperature was not critical, its variable affect during off-seat flow on spacing had to be considered.

### ASSEMBLY AND GENERAL TEST PROCEDURES

Operating the tester and associated equipment required observance of a number of procedural steps to avoid damage to the seating surfaces and also to ensure the validity of the parameter being tested. Very often tests were performed and theories evolved to explain the results only to later find that other variables in addition to the one under evaluation had influenced the experimental results. Consequently, almost all tests were performed more than once to ensure repeatability and allow a thorough definition of the test parameters.

## Poppet and Seat Assembly

The primary consideration in assembly of the test poppets and seats into the tester was contamination. The seat being placed into a recess containing a lubricated O-ring posed the most difficulty. The part was first thoroughly cleaned with either trichloroethylene or benzene and then lightly lubricated on the OD which allowed easy insertion into the body cavity. To ensure positive bottoming, the seat was hand forced into the base plate, which contains a number of fine radial grooves, and simultaneously rotated through at least 90 degrees before indexing to a set of scribe marks. Contaminants were thus wiped off the mating faces. With the seat held in position, the locking bolt was installed at 20 to 25 in.-lb torque. To check for proper installation, the parallelism of the seat to base plate was measured with the Merz indicator. All seats were parallel to the base within 10 microinches over the seating diameter. Just before installing the poppet, the inlet system was blown clean for 5 seconds, and the seat surface was cleaned with benzene under a low volume gas purge. The final check on the seating surface was to wipe off lint particles with a fine brush while purging. Under bright light such particles were easily discernible on the reflective seating surfaces.

Two methods of poppet assembly were used. The first is shown on the tester assembly drawing (Fig. 20) and incorporates a retainer, flexure spring, and clips for positively positioning the poppet relative to the seat. This arrangement was used for the near-seated tests and some of the on-seat tests before realizing the influence of slight out-of-parallel conditions upon the on-seat stress leakage characteristics. The second arrangement (Fig. 20, Detail P) loads the poppet through a ball joint. In this case, the poppet is not closely positioned, but is free to conform with the seat. With this test method, all loads must be obtained from piston control pressure readings because the three load cell legs do not contact the seat.

During poppet installation, extreme care was required so as not to damage the seating surfaces by edge contacts. A continuous internal gas purge was used so that no dust particles could enter the seating area. In some cases, a thin sheet of polyethylene was inserted between the poppet and seat to preclude metal-to-metal contact before complete assembly. This technique achieved its objective but often introduced contaminants which, once mated, had to be vigorously scrubbed from the seating surfaces. When using the poppet-to-seat O-ring seal for leakage tap-off, the ball joint was used and in this case the poppet could be easily hand positioned on the O-ring which held the surfaces apart before loading.

### Near-Seated Tests

These tests all used Model A (Table 8). The basic problem in this test series was to establish a datum or zero height point. The leakage at electrical contact provided this datum. Once correlated with the roughness and other geometrical parameters of the tests, it allowed a repeatable starting point for all tests to be established. The value of this datum is apparent when it is considered that electrical contact is a no-load condition. If an electrical contact can be obtained at a level commensurate with the surface roughness profile being tested, it is reasonably assured that what is being tested is the profile and not some other variable such as a ridge, nodule or other protuberance, out-of-parallel face, or contaminant.

After a reasonable datum or electric contact leakage had been established, off-seat flow tests were performed. For these tests, the inlet pressure was measured directly between the seat interfaces from a 1/32-inch drill hole pressure tap provided in the seat (Fig. 21) ensuring a true reading. Position control was maintained by the micrometer screw which also provided the necessary position reference.

Two critical problems encountered in the flow tests were the dependence of positional accuracy at low gaps on inlet pressure and at large gaps on temperature. Because the micrometer screw required a precision ball joint for loading the variable deformation of the joint contact affected the flow gap as a function of inlet pressure changes. Calibration of the screw between 30- and 1000-psig inlet pressures showed it to be precise and repeatable; however, at gaps below 0.0001 inch, the inlet pressure had to be maintained within 1.0 psi to keep system loads essentially constant, and thus position constant.

The second problem was caused by shrinkage of the poppet and seat interfaces because of temperature drops at high flowrates (nozzle regime). This required establishing a reference micrometer zero at electrical contact (with proper leakage) and rapidly obtaining a stabilized high flow reading.

In all cases, the correlation of leakage with the electrical contact provided a ready reference from which to collect the off-seat flow data, and the precision of the flow curves presented later is attributed to this reliable reference.

The pressure profile across the seat was measured by nine pressure taps located in the seat (Fig. 21). After determining that the profile did not vary around the seating diameter, only three radial taps were used. Initially, there was a problem with slow pressure rise time in the gage system. Readings below a 100-microinch seat spacing required more than 15 minutes to stabilize. This problem was partially alleviated by filling the gage and line with water which allowed readings to be obtained at 50 microinches off-seat within a 5-minute stabilization period.

### On-Seated Tests

These tests were performed with test models A through K. Initial tests were performed with the poppet loaded through the three load cells because

preliminary tests with the ball joint method of poppet loading did not appear to make significant difference; however, at light loads and fine finishes, a slight out-of-parallel condition was found to radically affect the stress-leakage curve.

With the poppet clamped to the piston, it was possible to ensure contaminant free parallel surfaces by the electrical contact test. With the ball joint, however, the leakage correlation at light loads (apparent stress of 100 psi or approximately 4 pounds) had to be used as a criterion of a clean surface. The problem with this method was that if the gap contained a foreign particle, the light load would generally imbed it into the surface. The net result was to cause an initial high-leakage low-rate characteristic curve which is not representative of the metal surface.

In most cases, cleaning contaminants from the hardened steel seating surfaces necessitated removal of the poppet from the tester and a thorough scrubbing of both surfaces with lint-free wiping paper. While hard rubbing in one area would tend to brighten the surface, and sometimes even produce apparent scratches, the depth of marks was always much less than 1 microinch. These observations do not apply to aluminum which was found to damage quite easily.

## NEAR-SEATED TESTS

Test data were obtained for comparison with theoretically predicted flow characteristics of near-seated models. Included were investigations of leakage and pressure profile for the nozzle, turbulent channel, and laminar flow regimes.

### Near-Seated Flow Tests

Parametric off-seat flow tests were performed to substantiate the leakage flow analysis using the poppet and seat combination of test model A (1-inch seat diameter and 0.060-inch land width). Leakage flow from  $10^{-1}$



to  $10^4$  scim was measured for poppet stroke (h) ranging from 20 micro-inches to 0.006 inch. Data were obtained at 30-, 100-, 300-, and 1000-psig inlet pressure levels with nitrogen and, for comparison, tests were also performed at 100 psig with helium and argon. All test results were corrected to standard conditions of 14.7 psia and 70 F.

Because the measured flow varies over several orders of magnitude, the complete data for each test series are presented on two separate graphs which are grouped as follows:

Nitrogen: Figures 77 and 78

Helium: Figures 79 and 80

Argon: Figures 81 and 82

To minimize confusion, the theoretical curves, computed from the equations outlined in the Leakage Flow Analysis section, are continuously plotted while the actual test data points are represented by symbols. Because the theoretical trend of the nozzle to the laminar transition (turbulent channel regime) is sufficiently shown by the 30 and 100-psig data of Fig. 77, these curves were not computed for the 300- and 1000-psig nitrogen tests nor for the other gases.

The reference used in all of the flow data is the point where electrical contact occurs. This position represents approximately 20 microinches height when equated to flow between two flat plates. The physical determination of this point in the test setup involves some error. Based on comparative measurement with the Merz (and other instruments), it was determined that the micrometer adjustment for position is accurate to approximately  $\pm 2$  microinches. In addition to this, there is a possible error because of an out of parallel condition between the poppet and seat; however, experiments have shown that this error can be controlled to less than 5 microinches. Contamination can also introduce error into the evaluation of electrical contact. Contamination is an elusive variable

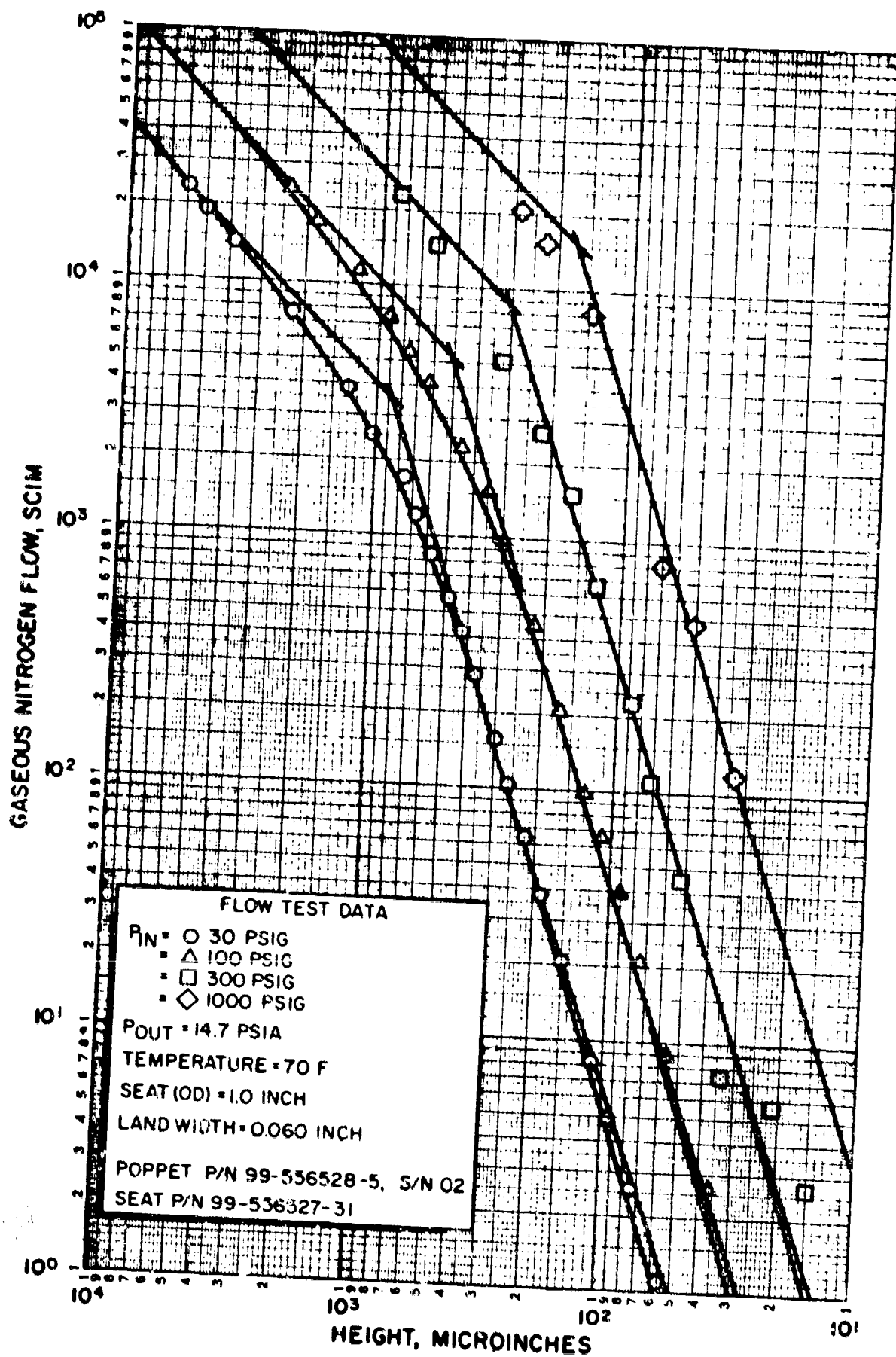


Figure 77. Nitrogen Flow Data, Part 1

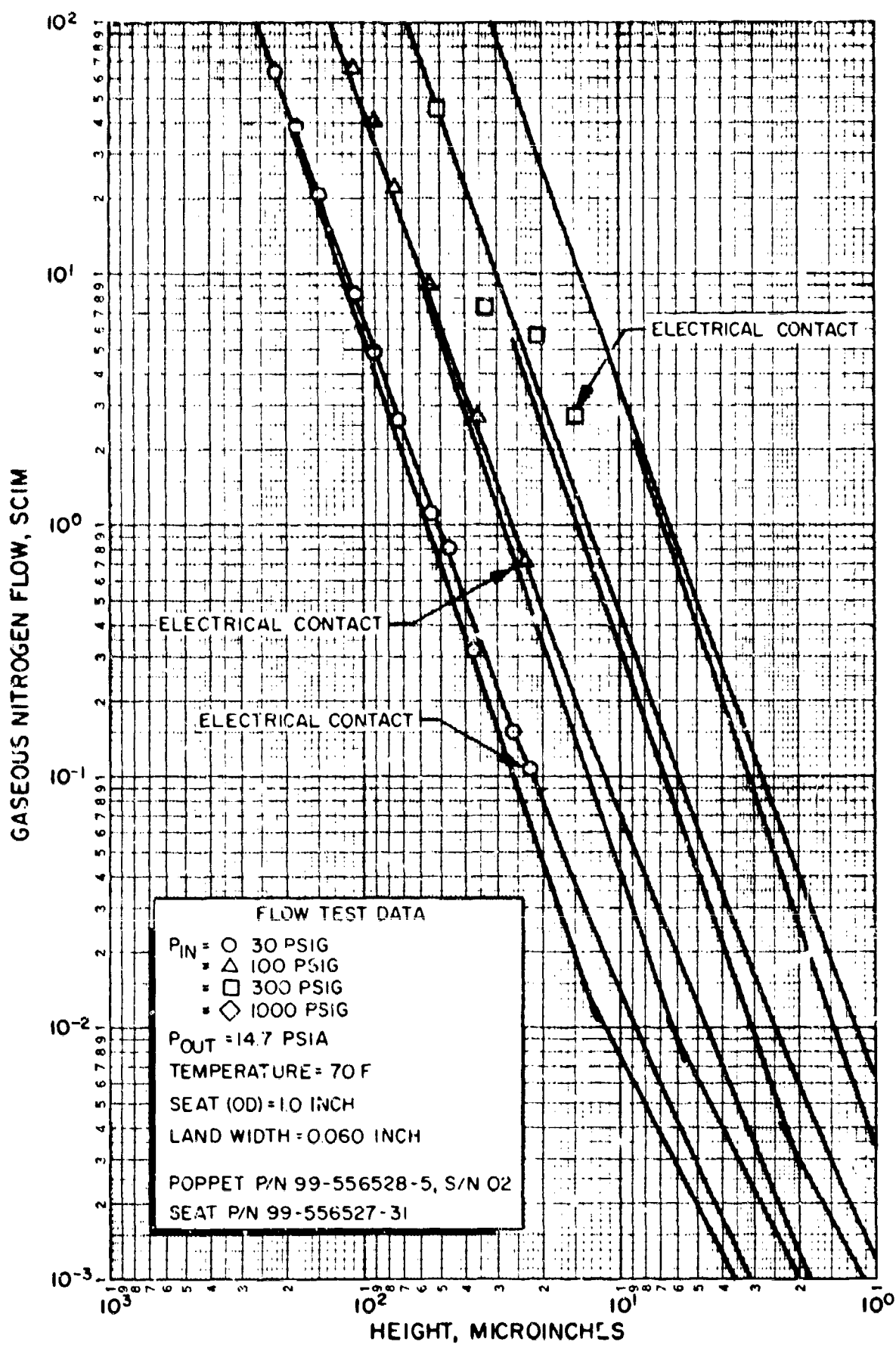


Figure 78. Nitrogen Flow Data, Part 2

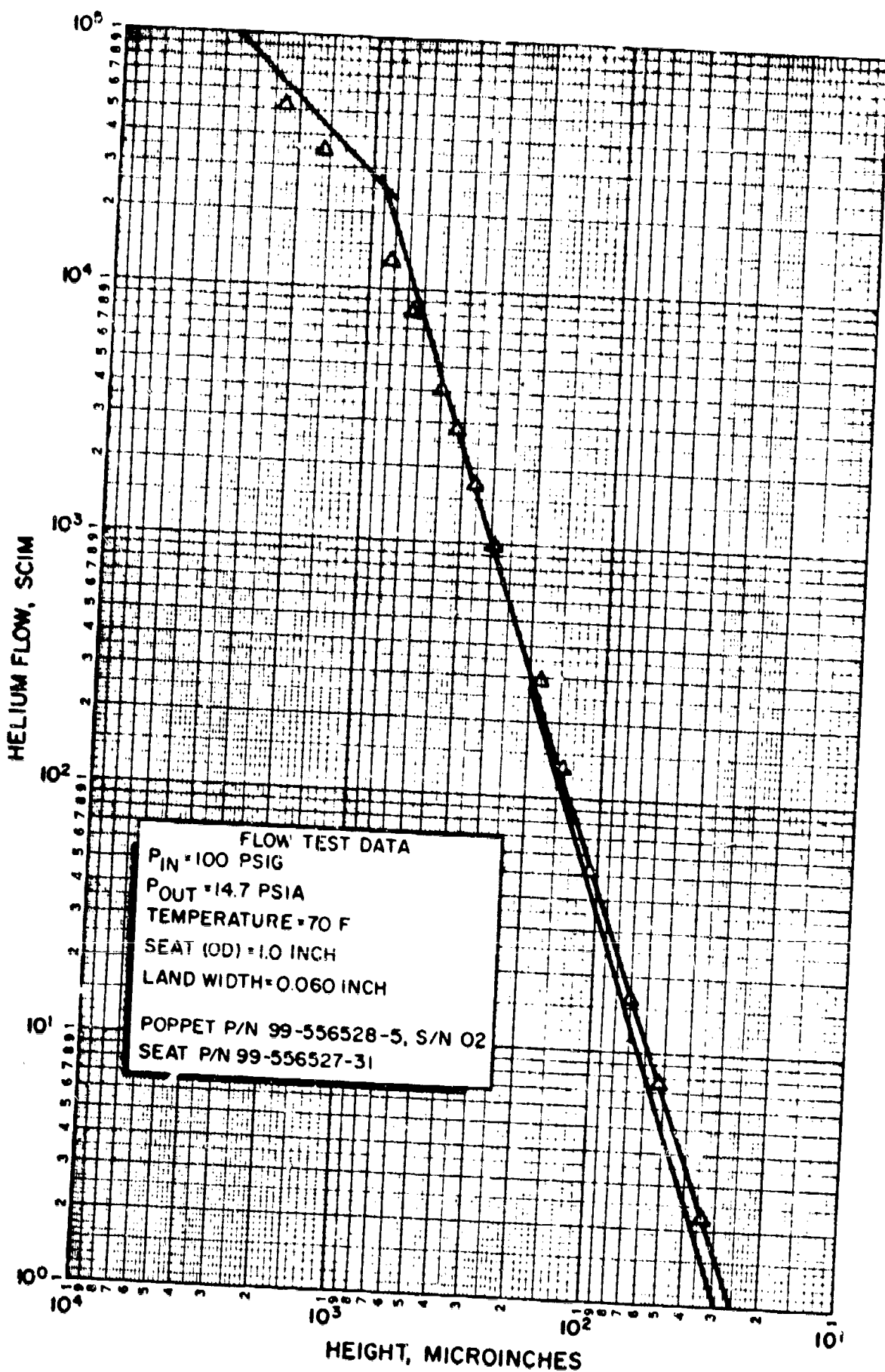


Figure 79. Helium Flow Data, Part 1

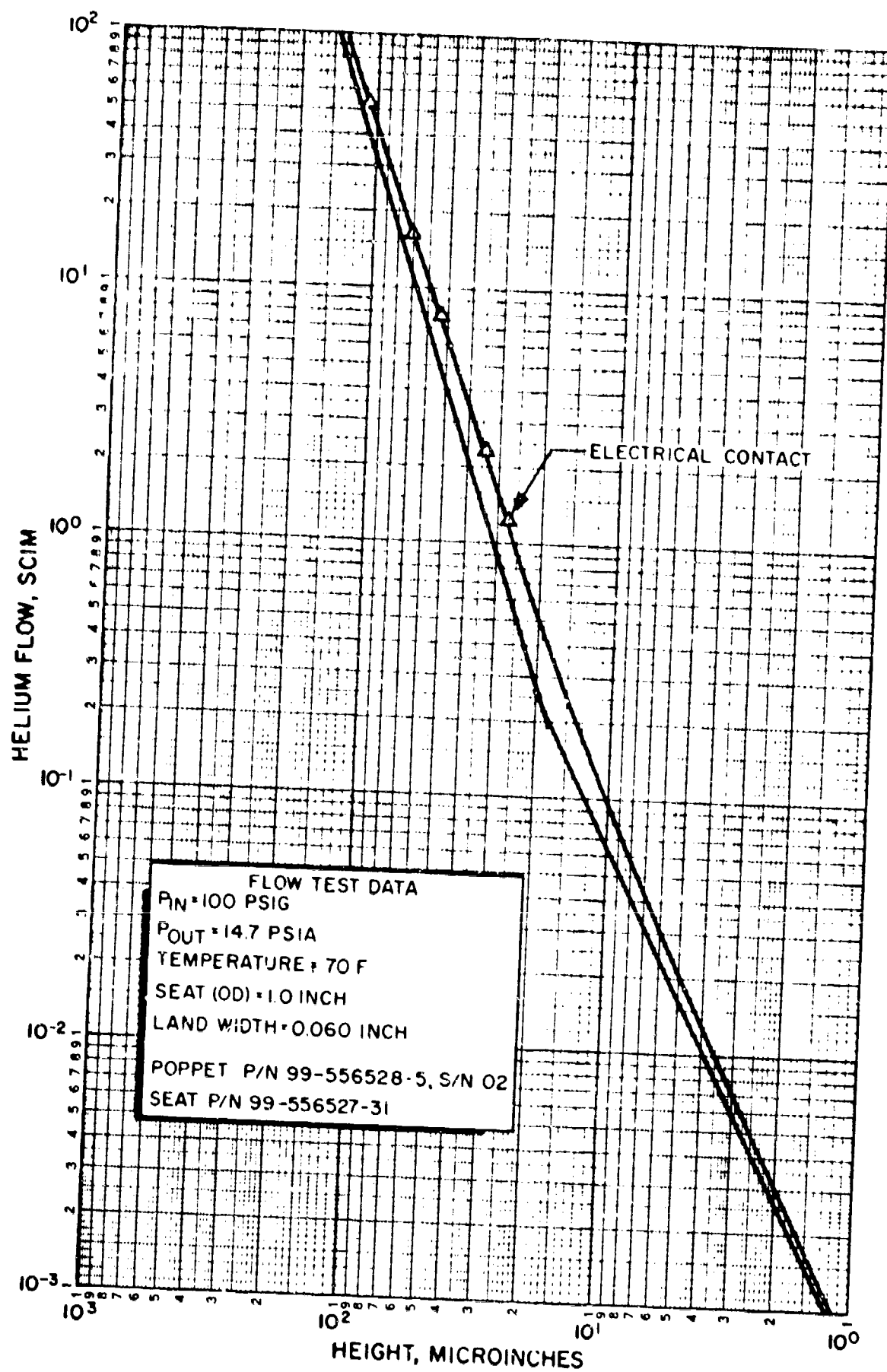


Figure 80. Helium Flow Data, Part 2

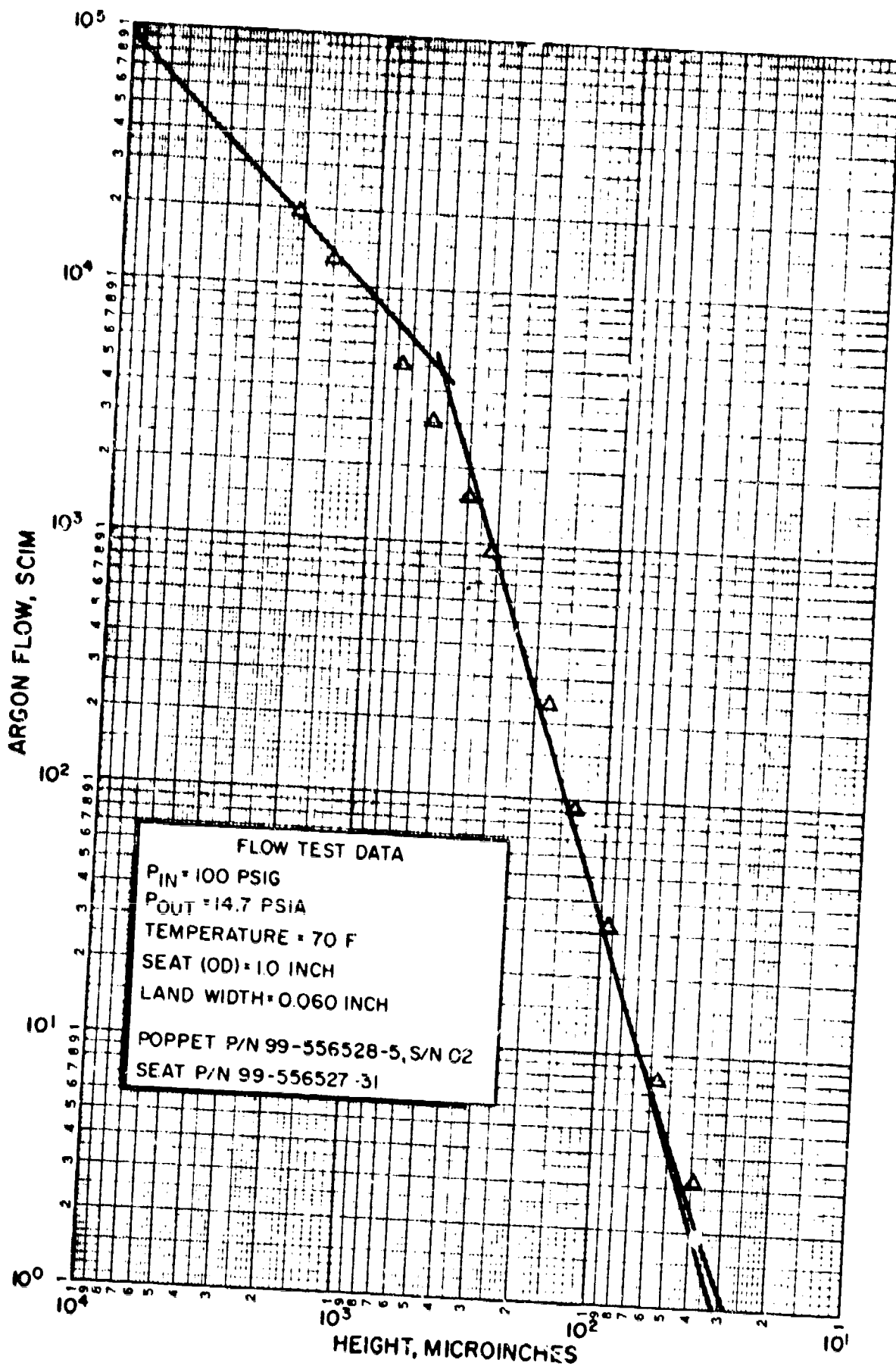


Figure 81. Argon Flow Data, Part 1

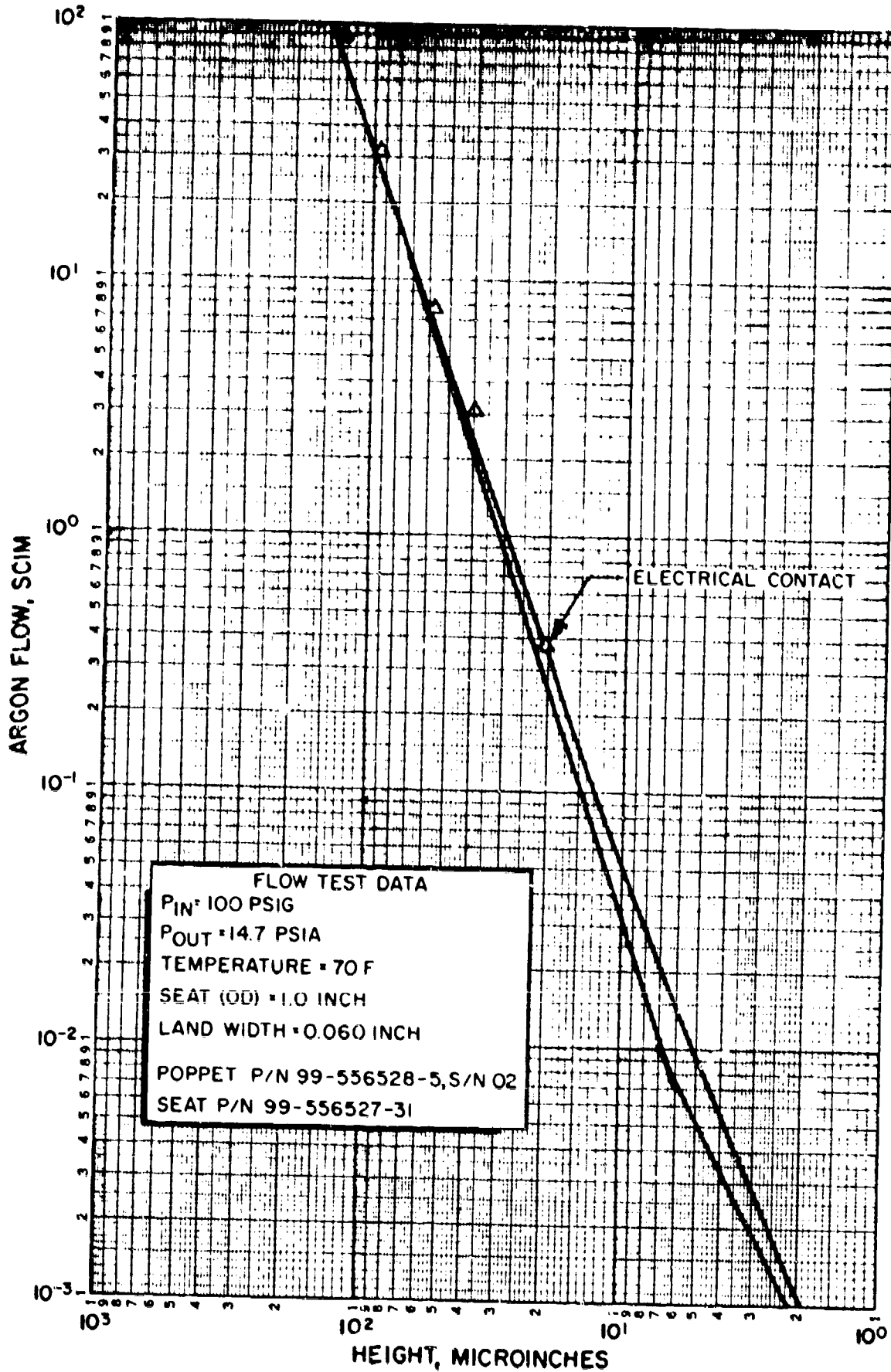


Figure 82. Argon Flow Data, Part 2

which is relatively easy to detect but extremely difficult to accurately evaluate. Generally, the test setup was torn down and the poppet and seat cleaned (or refinished) when contamination was detected. In summary, it appears that the point of electrical contact could vary by as much as 10 microinches. An examination of the test data showed a range from 20 to 27 microinches. These data points were determined by placing the flow at electrical contact on the theoretical flow curve to establish the equivalent parallel plate height ( $h_p$ ).

Except for the reference point of electrical contact, the empirical and theoretical flow data are plotted independent of each other. There is a high degree of correlation between experimental and theoretical data through several orders of magnitude of flow. The correlation was found throughout the pressure range and gas media investigated. The flow regimes covered include nozzle, turbulent channel, laminar, and approaching the region of molecular flow. (A detail examination of these flow regimes appears in the Leakage Flow Analysis section where a specific example, illustrating how each flow regime blends into the next to build the over-all flow-leakage characteristic curve, is presented.) Some data scatter resulted at the high-pressure conditions (300 and 1000 psig) because of the difficulty in controlling poppet position with the micrometer head at these higher pressures and resultant loads. In the 1000-psig condition, control pressure was necessary to enable the adjustment of the micrometer. Consequently, no electrical contact point was established because of the difficulty in maintaining a sufficiently precise load balance.

If the near-seated test data are examined for the significant flow characteristic, laminar flow is selected as being the most representative regime. When the laminar flow curves are compared for each of the three gases the flow does not vary by more than 30 percent for any given height ( $h$ ). This can be verified by the laminar equation for volumetric flow which shows that flow for various gases is a function of viscosity only. (Viscosity for the common gases varies by, at most, 2:1 for any given



pressure and temperature.) The significance of this observation is that if leakage data are known for one particular gas, it will serve as an estimate for most any other gas of interest. Also, if it can be assumed that the predominate characteristic for a system leakages is laminar flow, the rate of change of bottle storage pressure will be a function of gas viscosity and thus essentially the same for most gases.

### Seat Land Pressure Distribution

Verification of the pressure distribution, or pressure profile, analysis was performed using the 1-inch poppet and seat of test model A. The seat was designed with several series of three pressure taps located across the land face. Data were obtained for nitrogen supply pressures of 30, 100, 300, and 1000 psig with the stroke (h), varied so that laminar turbulent channel and nozzle flow regimes were covered. In addition, laminar regime data at 100 psig were taken with helium and argon.

Figure 83 shows pressure distribution across the test seat land in the laminar regime for various inlet pressure conditions. The pressure parameter is presented in nondimensional form so that the various levels can be compared on a common basis. Actual data points are represented by symbols, and the theoretical curves are continuously plotted, terminating at various pressure levels as a function of the back pressure - inlet pressure relationship. In general, the test data closely correlate with the theoretical. Within the accuracy of measurements, helium and argon test data at 100 psig were identical to the nitrogen, indicating that the pressure distribution characteristic is not a function of the particular gas involved for the laminar regime.

Figure 84 shows pressure distribution across the seat land for various poppet-seat heights. The range of heights was selected to cover the nozzle, turbulent channel, and well into the laminar flow regime. It can be seen from the curves that height has a definite effect on the

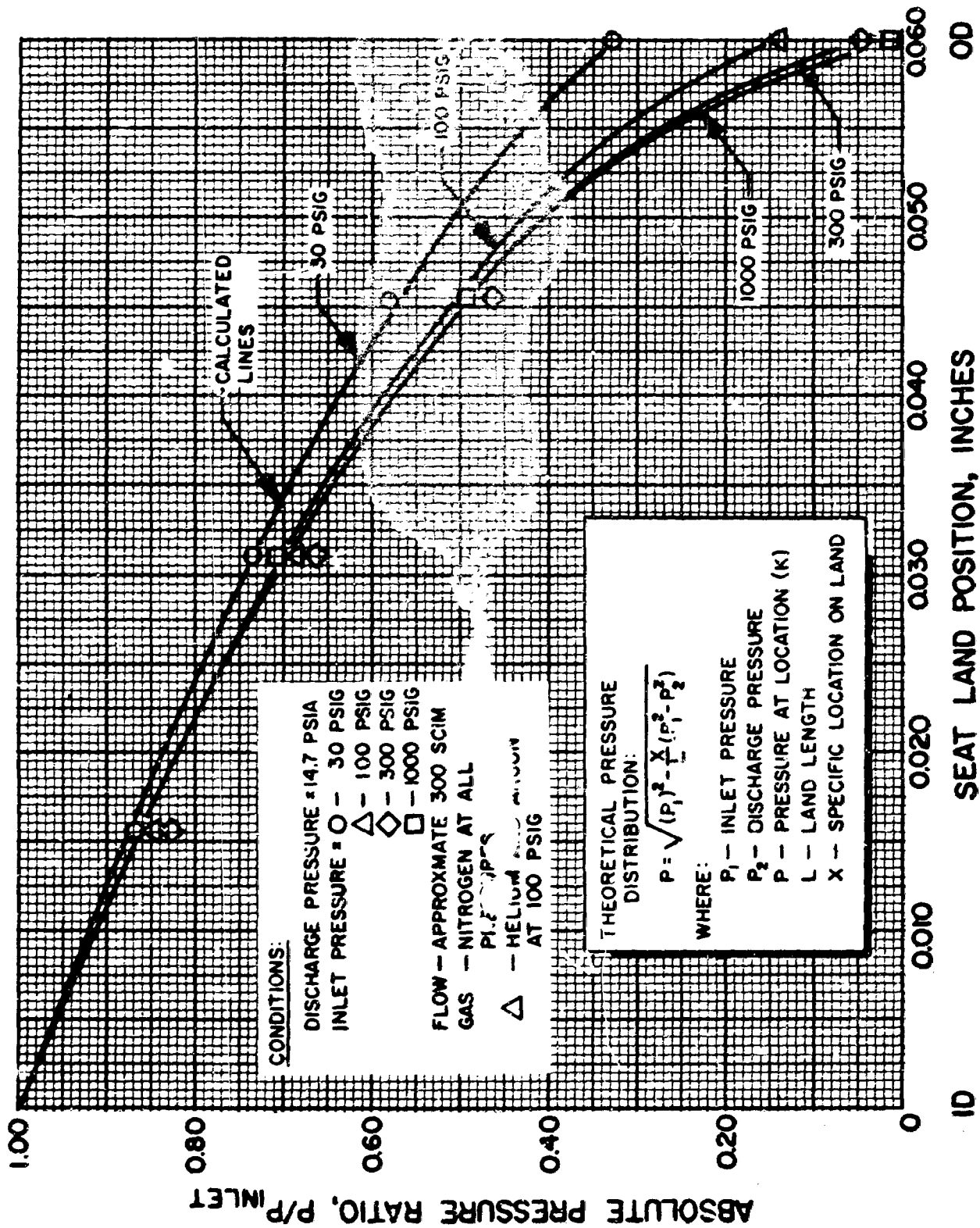


Figure 83. Laminar Pressure Distribution at Various Pressure Levels

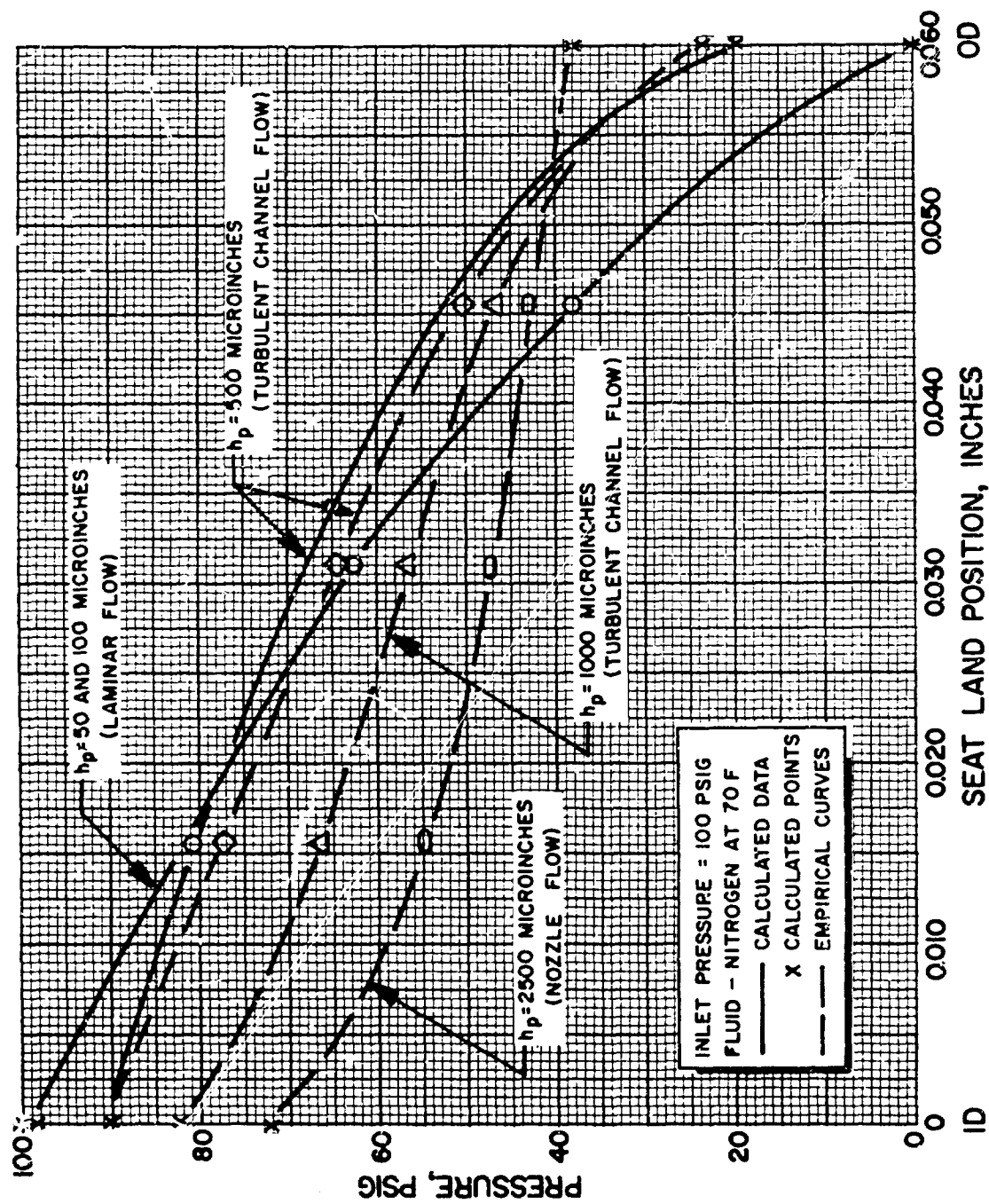


Figure 84. Pressure Distribution vs Poppet Seat Height

shape of the pressure distribution profile. The 50- and 100-microinch data, being in the laminar flow regime, are identical and follow the parabolic laminar curve very closely. However, at heights above this point, the profile gradually changes with increasing height until it approaches that of a nozzle at  $h_p = 2500$  microinches. Because there were no pressure taps located at the entrance and exit of the land, these points were computed. Entrance conditions are computed on the basis of isentropic gas flow. The dashed lines on the graph represent an extrapolation of the test data points indicated.

The theory and test data correlation in the turbulent channel regime is shown in Fig. 84 for the 500-microinch height. Reasonable agreement was obtained. As the height is increased from 500 microinches, inlet conditions increasingly influence the pressure profile. Because of this and attendant analytical complexities, correlation analysis of the 1000- and 500-microinch height was not attempted.

Because the pressure profile varies as a function of stroke, it will cause the effective seating diameter to vary also. For example, the effective diameter for the laminar regime is located at  $2/3$  of the land length. However, as stroke increases such that flow is in the turbulent channel regime, the effective diameter decreases. When stroke becomes even greater so that flow is in the nozzle regime, the effective diameter is very near the land midpoint. This variation in effective diameter could be a contributory cause of valve instability in the near-seated position, particularly for valves having a relatively wide seat land.

To verify the effective seating area as determined by the pressure distribution profile analysis, this parameter was checked by load cells and pressure force-balance methods. The data were taken with the identical 1-inch poppet and seat used in the pressure distribution tests. The force-balance tests were performed by lifting the piston with inlet

pressure ( $P_1$ ) while controlling the piston position at electrical contact with control pressure ( $P_c$ ). Knowing the control piston area and weight of the piston assembly, the effective seat area ( $A_e$ ) is compared using the following equation.

$$A_e = \frac{1.767 P_c + 3.65}{P_1}$$

For the load cells, the following simple relationship was used for effective area and total load cell force ( $F$ ). The additive term in the equation is the weight of the test poppet and ring clamp assembly.

$$A_e = \frac{F + 0.86}{P_1}$$

Based on the theoretical pressure profile, the effective area is computed from the following equation

$$A_e = \pi \left( \frac{OD}{2} - \frac{1}{3} L \right)^2$$

The following table shows the computed effective area for the three test methods. All information was taken in the laminar flow regime ( $h < 0.0002$  inch).

COMPUTED EFFECTIVE AREA, IN. <sup>2</sup>		
Force-Balance	Load Cells	Pressure Profile
0.720	0.705	0.724

The various methods correlate within 2.8 percent which is reasonable in view of load cell resolution and the various gage and reading errors. However, considering the measurement variables involved, the pressure force-balance method is more accurate and agrees very closely with the pressure profile analysis.

## ON-SEAT TESTS

The concluding portion of the test program involved investigation of the stress-leakage characteristic exhibited by test models A through K. The objective was to evaluate the parametric influences of surface roughness variations (achieved by wet and dry lapping) and gross geometry (scratches, out-of-flat and parallel) on this characteristic. In addition, the use of several model materials would permit some evaluation of bulk modulus and yield strength effects on leakage. The assimilation of these data serves a twofold purpose: (1) the explicit information provides an index to the sealing capabilities of various configurations, and (2) it affords the comparison of theoretical and empirical results. The extent to which the mathematical model describes the surfaces and the validity of test model inspection data may thus be correlated with actual functional capabilities.

The test data are presented as stress vs leakage characteristic curves. All data plotted on the graphs represent individual data points reduced and corrected by previously noted methods. Curves interconnecting the data points are interpreted as a singular best fit and, therefore, do not represent the result of data averaging. In general, all data are well within 5-percent accuracy. Certain exceptions are extreme low leakage ( $< 10^{-4}$  scim) and seat stress between 400 and 100 psi where errors of up to 25 percent may occur.

The arrows shown on the test curves indicate the direction of the recorded data similar to hysteresis loops.

### Preliminary Tests (Model A)

After the off-seat flow-leakage tests were completed, a series of preliminary tests were performed on the 1-inch (Model A) poppet and seat configuration. The tungsten carbide poppet was diamond lapped to a surface

finish of approximately 1-microinch AA. The surface texture information (Table 8) was obtained from the Proficorder trace (Fig. 57) and the interference microphotograph (Fig. 28). Both of these figures represent cross lay on the poppet and show a surface roughness of 3.0 microinches peak to valley and an angle of 2 degrees. Also, approximately 20 percent of the surface is covered with 4-microinch scratches. In evaluating the surface texture with lay, an interference microphotograph was used. This specific photograph is not shown; however, a representative with-lay configuration is illustrated on the diamond lapped part shown in Fig. 37.

The 440C seat surface of test model A was multidirectional with a peak-to-valley roughness (h) of 6 microinches, a 1-degree angle, and approximately 6 percent of the surface having 4.3-microinch nodules (Fig. 26). (The diamond-shaped patterns are the indentations made from the 100- and 15-gram Vickers microhardness tests.) The Proficorder trace for this surface is not shown; however, the surface texture of test model B seat (Fig. 59) is representative of the subject test part configuration.

Test 1 (Fig. 85) is a preliminary run to a 5600-psi seat stress, at a 100-psig inlet pressure with the poppet clamped to the tester piston legs. Test 2 was conducted under identical conditions except that the stress was increased to 15,000 psi. The two stress vs leakage curves are not identical at the low stress levels which is attributed to the presence of contamination in test 2. The test models were disassembled for inspection, and evidence of contamination was found. At this point in the test program, the 0.5-micron absolute porous membrane filter element was installed in the inlet line.

Because the poppet and seat are of different materials (elastic modulus) and roughness, it is difficult to correlate the analytical and empirical results. However, in examining the curve shape of test 1, the similarity to the theoretical curves (Fig. 16 through 18) is quite evident. A more detailed correlation of test and theory is made on the subsequent test models.

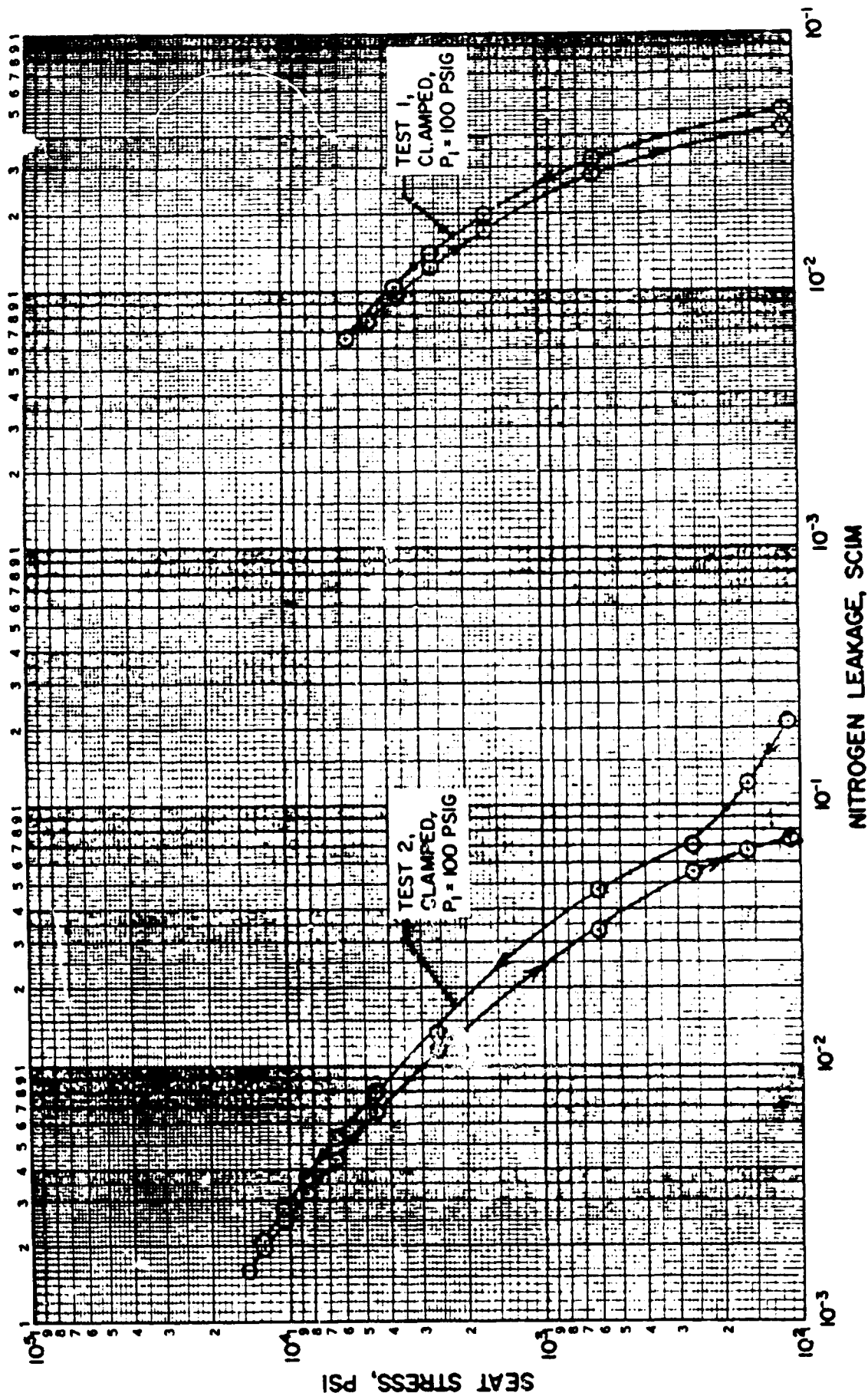


Figure 85. Stress vs Leakage Data for Test Model A, Tests 1 and 2



One observation which can be made, however, is the low stress level peak-to-valley correlation between the inspection data and test curve 1. At a 100-psi stress, the calculated peak-to-valley height (from flow data) for both surfaces is 13 microinches, and at a 1000-psi stress, the peak to valley height is 10 microinches. From Table 8, the combined peak-to-valley height is 9 microinches with 4.3-microinch superimposed nodules for a total of 13.3 microinches. These figures indicate that at roughly a 1000-psi seat stress, the nodules have been compressed, and essentially the entire surface is in contact. This observation was true for all of the test models at the 1000-psi stress level. At seat stresses below 1000 psi, nodules and contaminants play a major role in the stress vs leakage data.

#### 2-, 4-, and 6- Microinch AA Finish Tests (Models B, C, and D)

These tests were performed to evaluate the surface roughness parameter and are grouped together because they are all of the multidirectional surface texture configuration. Comparison of the three surfaces tested can be seen on the inspection chart of Table 8. A rough evaluation of the peak-to-valley height parameter (h) in terms of the arithmetic average (AA) can be made by dividing the h value by 3. For example, the seat of test model B has a peak-to-valley roughness of 6.6 microinches which, if divided by 3, would result in an approximate AA of 2.2 microinches. This value corresponds to the AA reading of the Profilometer with the 0.0001-inch-radius tip at 0.010-inch cutoff. The surface texture parameters for these models (Table 8) were defined, primarily by the Proficorder traces and secondarily the interference microphotographs plus additional verification from the Profilometer data.

The poppet and seat of test model B are of slightly different surface roughness. Examination of the Proficorder trace (Fig. 58) and the interference microphotograph (Fig. 29) show the poppet surface h to be 4.5 microinches with an angle of 0.75 degree. The seat is slightly rougher

at 6.6 microinches  $h$  and an angle of 1.2 degrees, as determined by the trace in Fig. 59. Both surfaces contain widely scattered nodules from 3 to 4 microinches in height.

The poppet and seat of test model C have similar surface roughness (approximately 4 microinch AA); therefore, only one Proficorder trace has been included (Fig. 60) which is representative of both. Surface roughness ( $h$ ) is 14 microinches at an angle of 2.8 degrees. In addition, this surface has a waviness of 5 microinches with 3.3-microinch nodules superimposed on the waviness.

Test model D is very similar to model C except that the roughness has increased to 19 microinches with an angle of 3.5 degrees, and the nodules are slightly higher at 5 microinches. Nodule density of model D remains low at approximately 4 percent. The Proficorder trace (Fig. 61) was used to define test model D. The matte, nonreflective nature of this pitted surface is shown in Fig. 31.

The first stress vs leakage information obtained on test model B was run at 300 psig with the poppet in a clamped position. Test data for this configuration are shown as test 3 (Fig. 86) and represent the first and second test loops on the "fresh" surface for stresses up to 60,000 psi. Arrows on the curve indicate the loop direction and show that some plastic flow has taken place in the first cycle.

Test 4 (Fig. 87) represents the sixth cycle on this test surface and was conducted at 1000 psig with the ball loading device. To check the data of test 3, test 5 was conducted at a 300-psig inlet pressure with the ball loading device. The results of test 5 are plotted along with an overlay of test 3 which indicates that the stress vs leakage characteristics have not changed with cycles. The difference between the two curves at low stress levels is attributed to the clamped vs unclamped (ball) loading methods. Clamping the poppet to the piston results in a potential out-of-parallel condition which may be as much as 10 microinches over a 1/2-inch seat diameter.

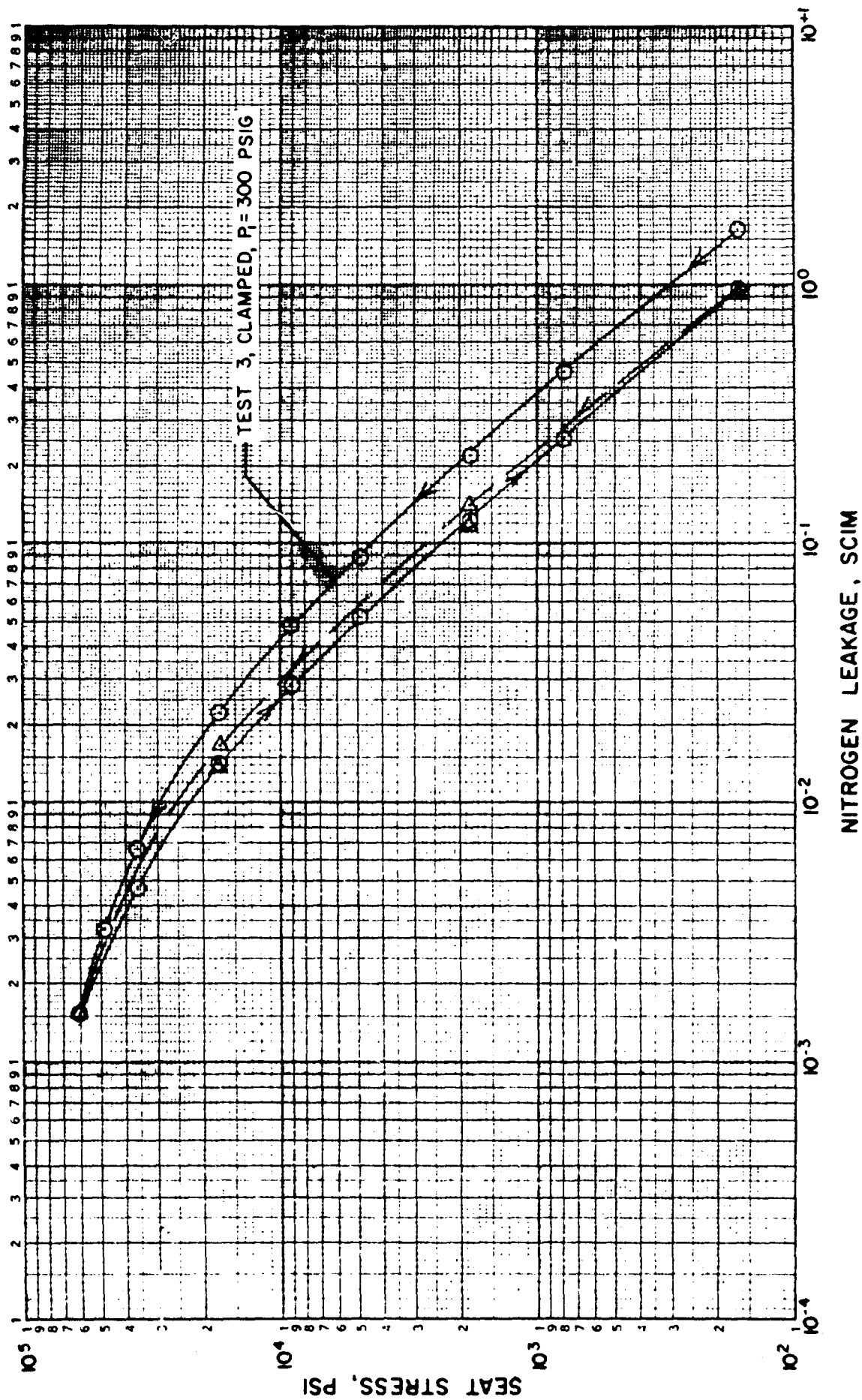


Figure 86 . Stress vs Leakage Data for Test Model B, Test 3

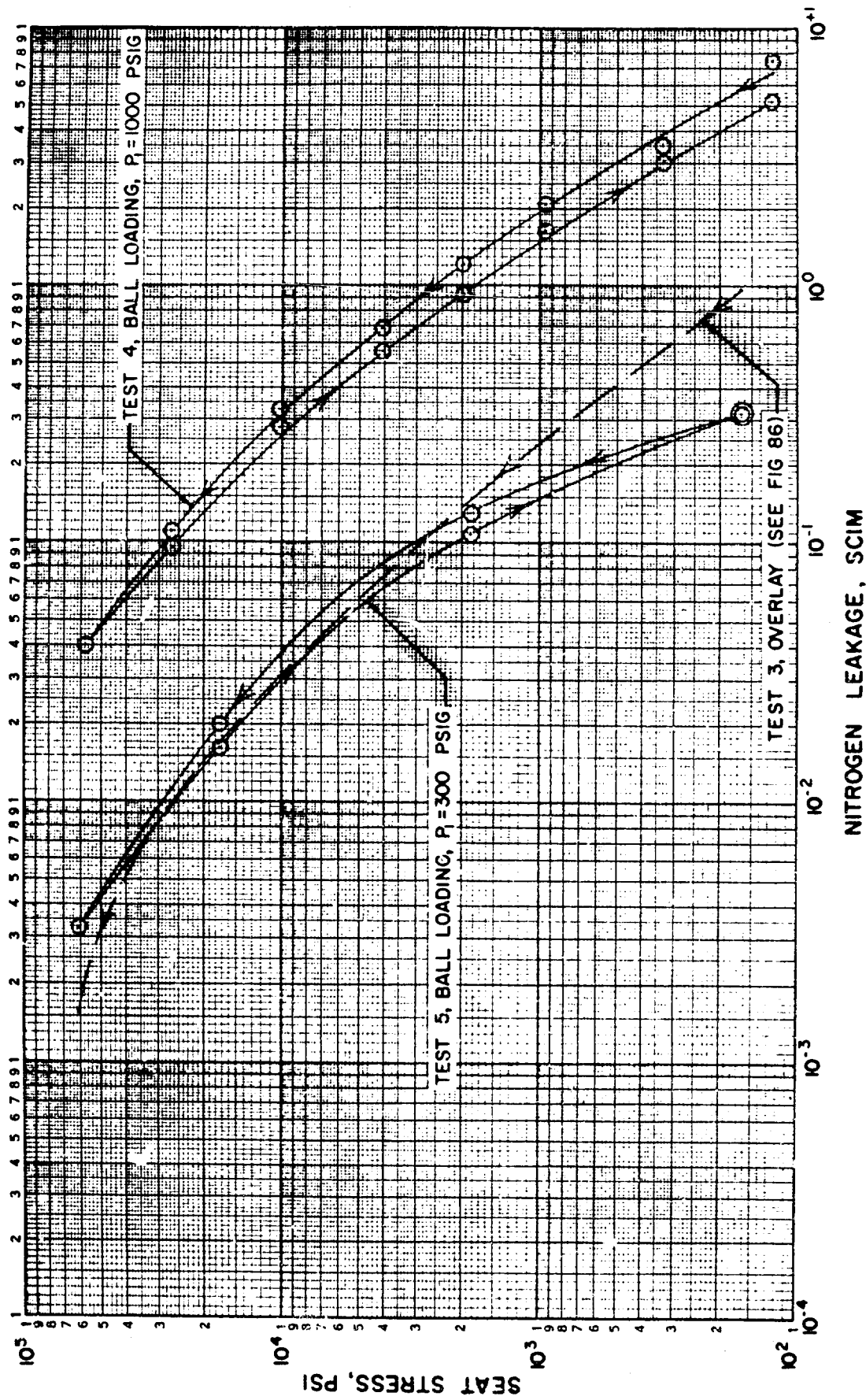


Figure 87. Stress vs Leakage Data for Test Model B, Tests 3 through 5

All of the data for test model C are shown in Fig. 88. Test 6 illustrates the first two cycles on the fresh surface conducted at 300 psig, and shows considerably more plastic deformation hysteresis than exhibited by test model B. Tests 6 and 7 were run with the poppet clamped, and show the typical low stress leakage characteristics found with test model B when clamped. Test 7 was conducted at 1000 psig, and represents the third and fourth cycles on this test model. The test surfaces were not separated between tests 6 and 7.

The first test on test model D (test 8) was run in a manner similar to model C (clamped) at 300 psig. After the first two cycles were achieved, contact was broken between the poppet and seat, and two more cycles were run (test 9). Both tests showed the plastic deformation characteristic on the first cycle (Fig. 89).

To compare the test results with the theoretical stress vs leakage curves, the final (elastic) stress cycle for an increasing load from tests 4 (2 microinches AA), 7 (4 microinches AA), and 9 (6 microinches AA) have been reproduced in Fig. 90 with the bounding and best-fit theoretical data superimposed. While actual and theoretical data fall in the same region, the over-all curve shapes do not closely match. The reason for the theoretical curve shape stems directly from the model assumptions and needs no further explanation. The test curves are another matter because the deviation at both low and high stress levels is marked.

The inspection data have shown that all surfaces are composed of a varying distribution of defects and roughness rather than a uniform roughness. It follows, therefore, that the real surface will not match the assumed model in stress vs leakage characteristics except over short spans. The primary reason for this is that the real bearing area is increasing with applied load in two ways. The first is caused by increasing the number of individual contacts with load and is not considered in the analysis; the second is as assumed in the analysis, that is, increasing the total bearing area as a result of increasing individual contact areas.

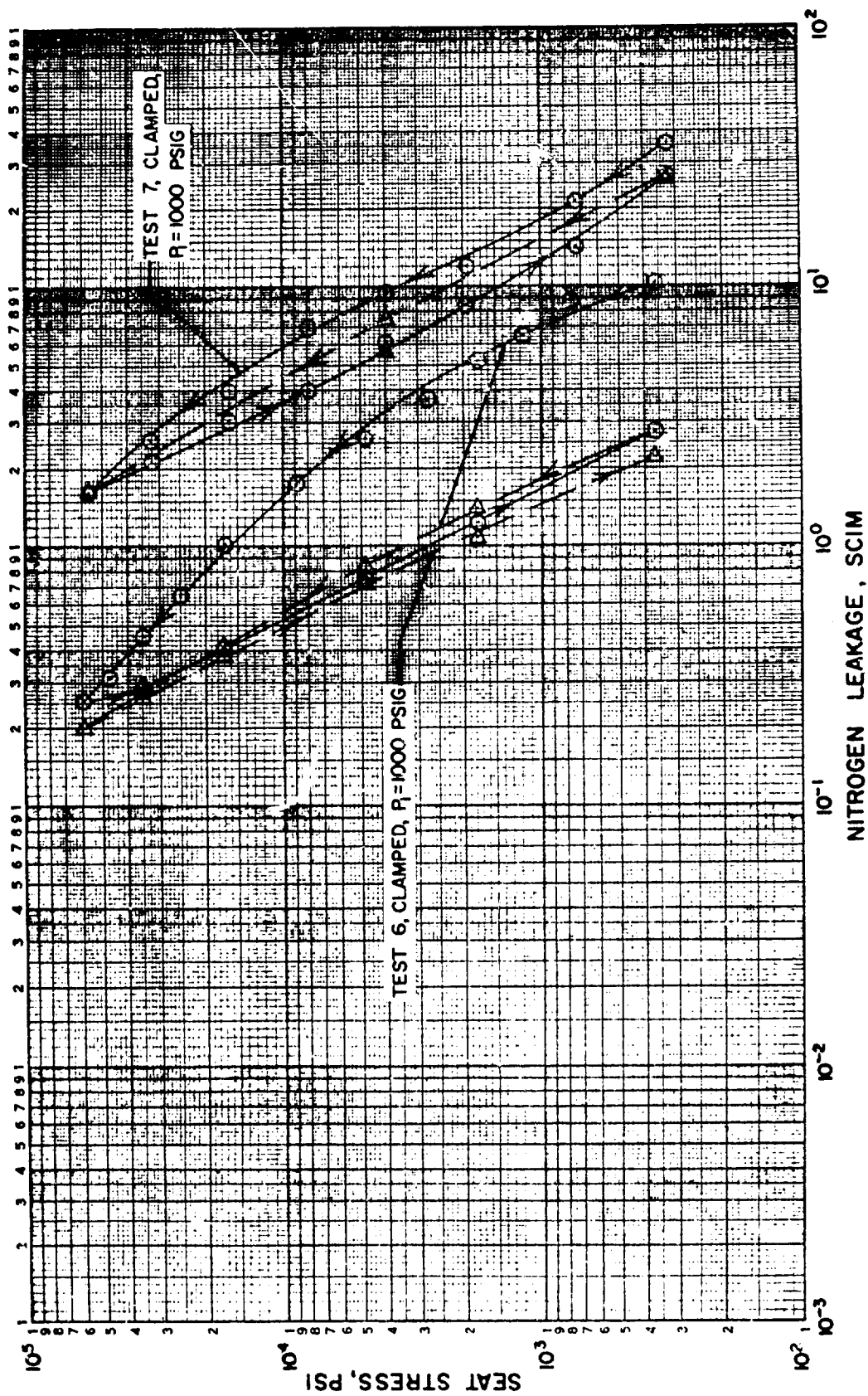


Figure 88. Stress vs Leakage Data for Test Model C, Tests 6 and 7

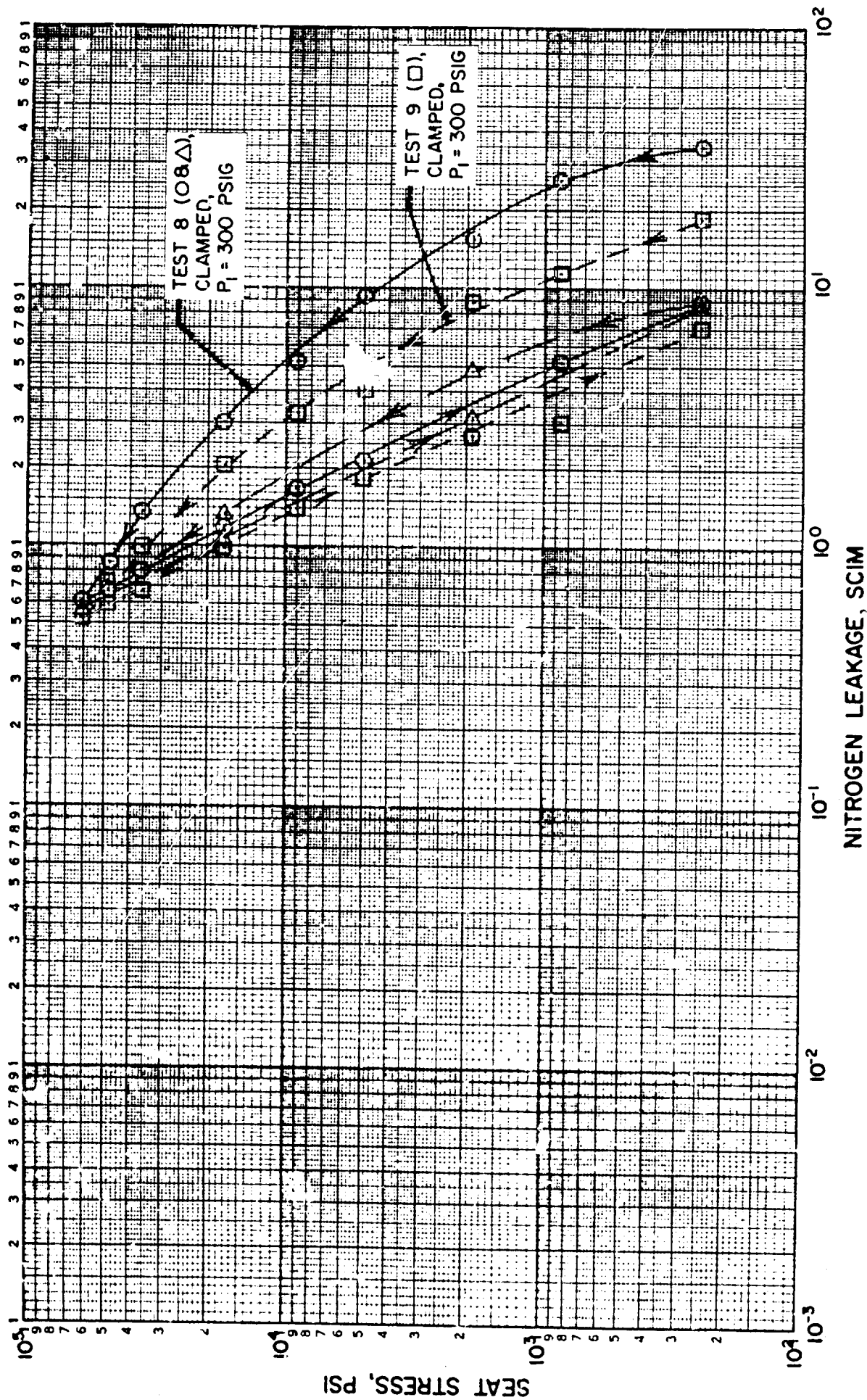


Figure 89. Stress vs Leakage Data for Test Model D, Tests 8 and 9



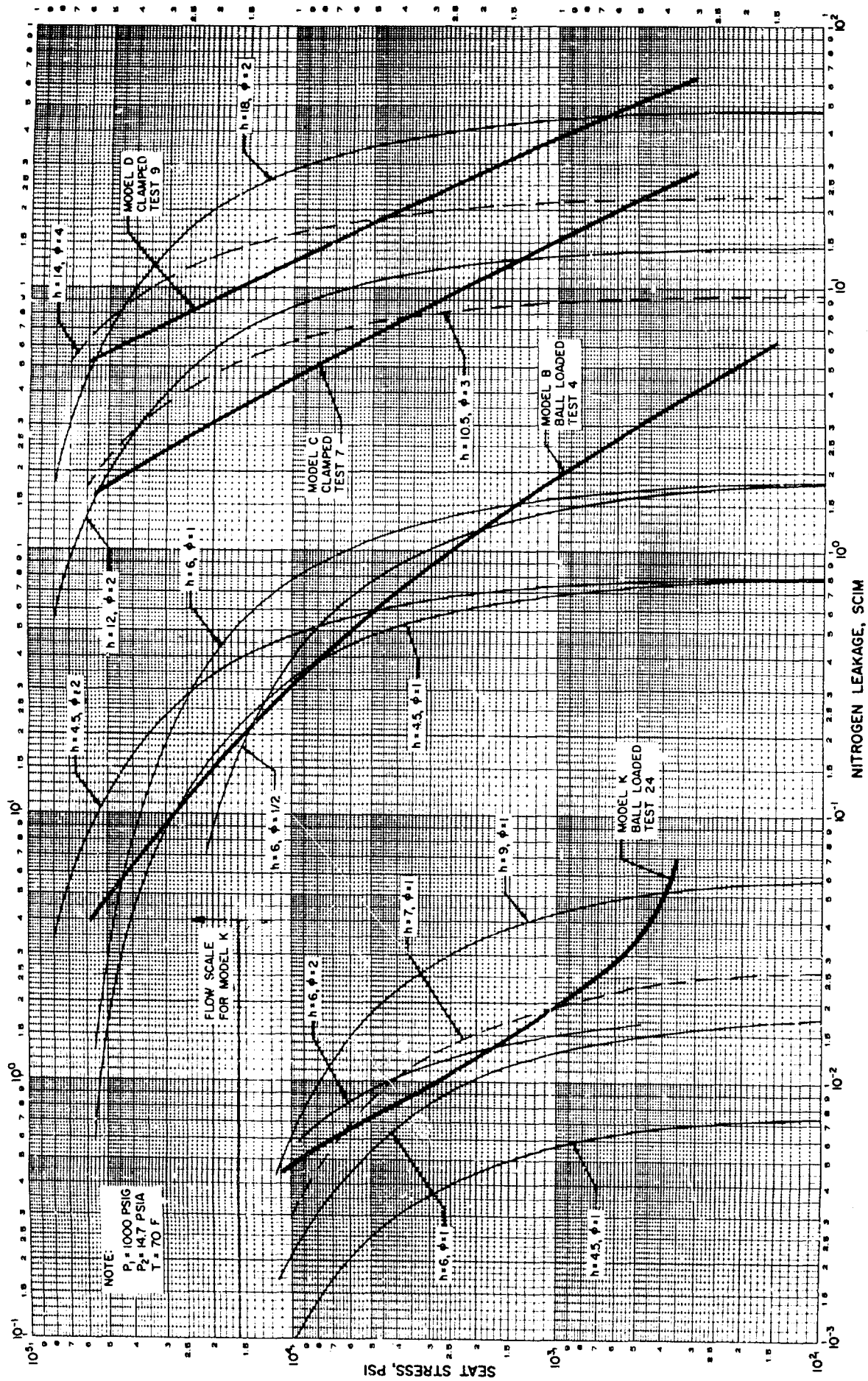


Figure 90. Data Correlation for Test Models B, C, D, and K



Because of the fewer number of higher asperities, the stress vs leakage characteristic has an initial high-leakage value at low loads and, depending upon the height distribution of the asperities, the rate at which the leakage decreases (with load) may be very high as is evident in some cases or quite low as in test 1 (Fig. 85). As the asperities are compressed into the surface, it is impossible to completely flatten most valve seating surfaces because of the asperity distribution characteristic. Moreover, most real surfaces have scratches, and while these may contribute little to the total leakage at lower loads, their influence becomes increasingly evident as the asperities are decreased in height. These are the reasons why the seat stress vs leakage test curves do not fall off to a zero leak condition as the theoretical analysis predicts.

The stress vs leakage characteristic below a 1000-psi apparent stress is generally atypical of the normal working stress condition because of an out-of-parallel situation, contaminants and/or nodules can greatly influence the curve shape. Above 1000 psi, these defects may influence the remaining curve but only slightly. This is more adequately illustrated in a subsequent portion of this section where the inspection peak-to-valley height data are directly compared with the equivalent peak-to-valley height calculated from the test curves.

The nominal 4- and 6-microinch AA surfaces did not conform to the desired configuration (similar to the 2-microinch AA surface) but instead were more complex, being composed of waviness, roughness, and some nodules. Also, the average asperity angle was greater, which made these surfaces both stiffer and yet less capable of elastically supporting a load. Consequently, the initial load cycles resulted in considerable plastic deformation (Fig. 89). The data correlation for these surfaces (4- and 6-microinch AA) are limited, and it can only be concluded that leakage agreement within a factor of 5 was obtained. These models are not typical of lapped valve seating surfaces because of their extreme roughness.

However, the nominal 2 AA model had a sufficiently uniform structure to exhibit the typical model characteristic curve with increasing load (test 3, Fig. 86). Data correlation for this model are within a factor of 3 over a 1000- to 60,000-psi stress span.

#### 1/4 to 3/4 Microinch AA Finish Tests

##### (Diamond Lapped Models E and F)

This test series was a continuation of the surface roughness evaluation started on the 2-, 4- and 6-microinch AA test models (B, C, and D). Because of the nature of diamond lapped surfaces, two aspects of the surface texture were changed relative to models B, C, and D. First, the lay is unidirectional rather than multidirectional, and second, the surface contains a large number of scratches. In this instance, the scratches are significant only because the surface roughness is quite small.

The first tests on the diamond lapped models were conducted on test model E. Microphotographs describing the test surface are found in Fig. 32 through 34. The surface (Fig. 32 and 33) is composed of a relatively smooth surface roughness and a number of deep scratches (pointing down). The inspection data (Table 8) show the poppet surface roughness to be 1.8 microinches peak to valley at an average angle of 0.32 degree with 24 percent of the surface area covered with 5.0-microinch scratches. The roughness and scratch values are slightly lower for the seat with the scratch density being only 9 percent. The seat has considerable roundness (dub-off) which reduces the effective stress area by an estimated 44 percent (Fig. 34). As a result, stress vs leakage data were obtained up to approximately 100,000 psi.

Test 10 (Fig. 91) was conducted at 1000 psig with the poppet clamped and represents the second stress cycle on this configuration. A third cycle was run which duplicated the results of test 10. Without breaking seat contact, the inlet pressure was lowered to 300 psig, and stress vs leakage

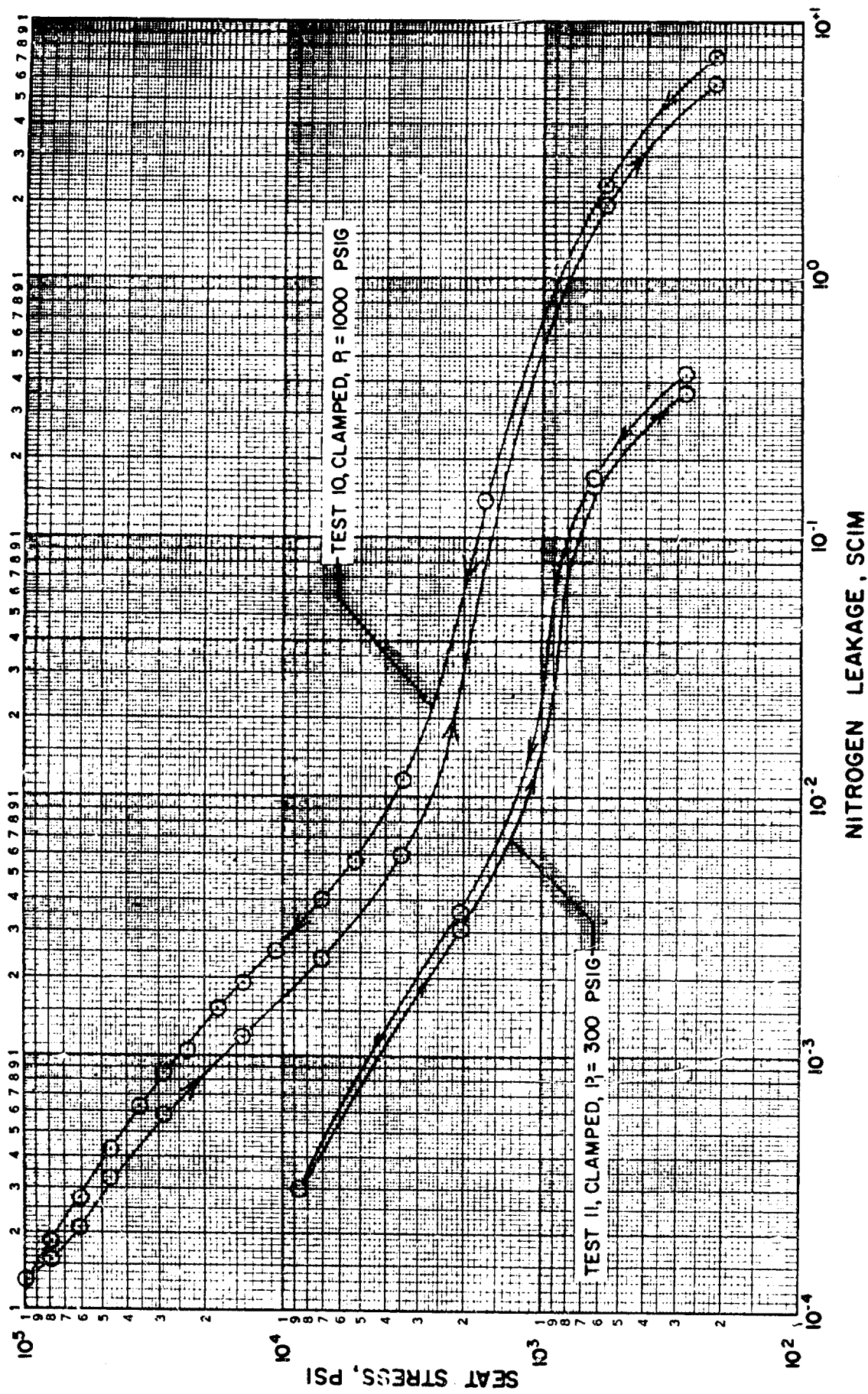


Figure 91. Stress vs Leakage Data for Test Model E, Tests 10 and 11

data were taken (test 11) for comparison purposes. This test was terminated at an 8600-psi stress because obtaining the lower leakage values with the buret system involves considerable time.

Test 12 (Fig. 92) was run at 1000 psi with test model E using the ball loading device; this curve represents the eighth cycle to a 100,000-psi seat stress. The curve shows a wide hysteresis loop which was repeatable indicating elastic deformation. Because these surfaces are very close to being optically smooth and unpassivated, the hysteresis loop might be attributed to atomic attraction, although this is not proved. A comparison of tests 10 and 12 (Fig. 92) shows the decreased leakage obtained with the ball joint and the relatively large effect the out-of-parallel situation of test 10 had on the sealing ability of these ultra-smooth surfaces.

A second series of tests on the diamond lap surfaces was run with test model F for the purpose of testing a nonrounded (no dub-off) seat configuration. In addition, the poppet and seat were oriented at different positions to determine the effect of lay on the stress vs leakage relationship. The microphotographs shown in Fig. 35 through 39 describe the poppet and seat surfaces tested. Figure 38 shows that the roundness has essentially been eliminated on the seat land. To keep the land edges square, very little surface polishing was done; therefore, the surface is slightly rougher than model seat E. Inspection data for model seat F (Table 8) shows the surface roughness to be 2.2 microinches with an angle of 0.39 degree. The scratches are only 3.8 microinches deep on the average. However, the scratch density of 38 percent is significant. The poppet of test model F has been reworked from model E so that the surface is composed of only scratches and a waviness of less than 1 microinch.

Test 13 (Fig. 93) is the fourth cycle to a 60,000-psi stress with the poppet and seat oriented in a cross lay position. The results of this and the previous 3 cycles conducted at 1000-psig pressure on this configuration repeated within 5 percent. Test 14 is identical to test 13

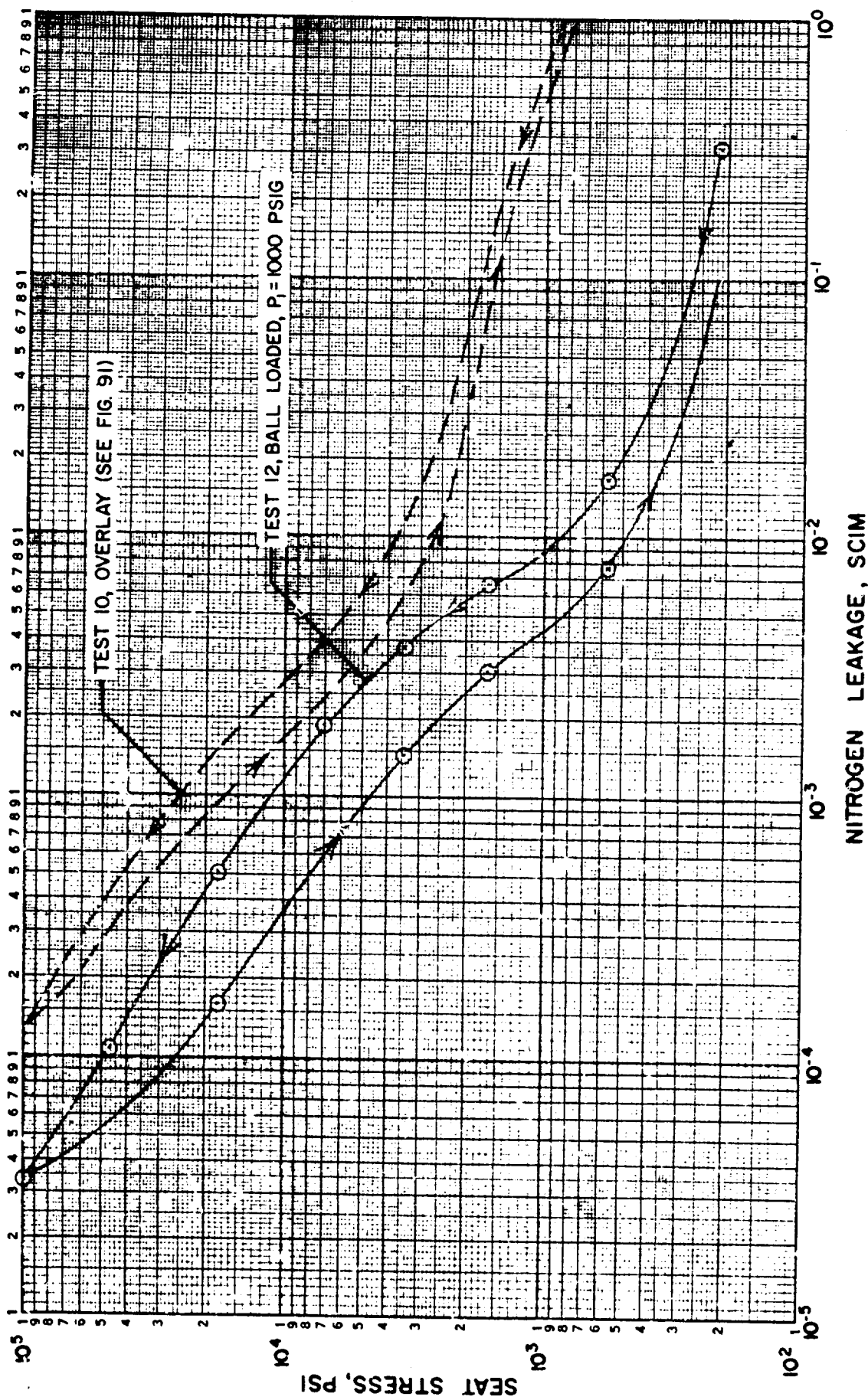


Figure 92. Stress vs Leakage Data for Test Model E, Test 12

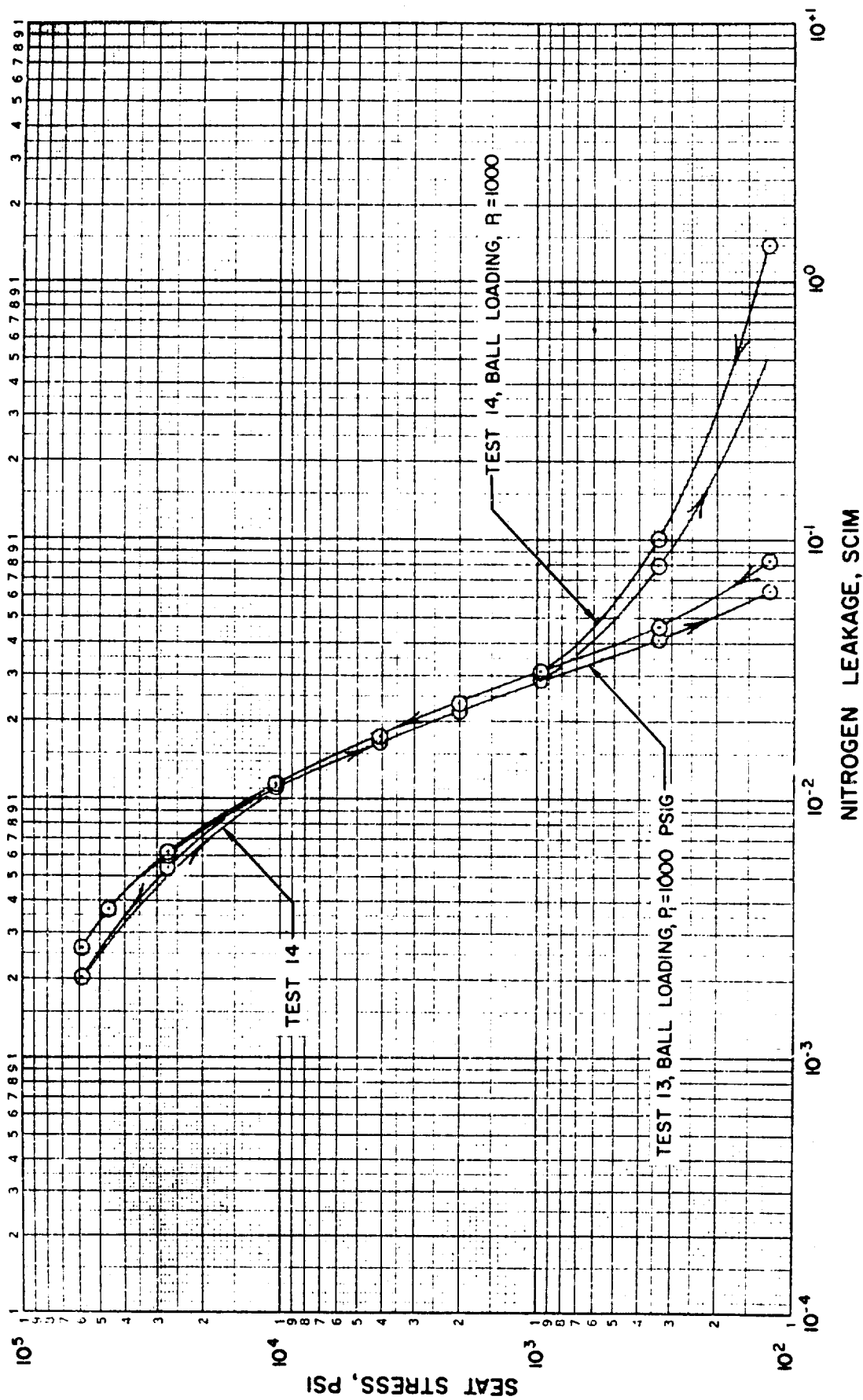


Figure 93. Stress vs Leakage Data for Test Model F, Tests 13 and 14

except that the poppet was rotated 0.90 degree to evaluate the parallel lay configuration (the ball loading device was used in both tests). From the results, the lay orientation does not affect the stress leakage relationship. The high leakage of test 14 at stresses below 1000 psi is attributed to contamination rather than an out-of-parallel condition because the ball loading device was used.

Data correlation with the theoretical stress leakage relationships are shown in Fig. 94. Tests 12 and 13 are plotted as representative of the data obtained with test models E and F. For the stress range between 1000 and 10,000 psi, test 13 is closely matched with the theoretical curve where peak-to-valley height is 1.5 microinches and an angle of 1/2 degree. An average roughness value for the poppet and seat is close to the theoretically selected values (Table 8).

In examining the theoretical correlation for test 12, it appears that the best fit is a height of 1.0 and an angle of 1/4 degree. These values do not precisely match the inspection information obtained; however, the height and angle are of the right order of magnitude.

Because the scratches in these test models are an appreciable percentage of the surface area, it is worth evaluating their effect in terms of leakage. The equation used is an approximate solution based on the analytical model developed in the Surface Analysis section. This model evaluates flow through a sine wave surface, whereas scratches would be better described as saw tooth. The equivalent flat plate height factor for laminar flow ( $M_L$ ) is 0.68 for the sine wave as compared to 0.63 for the saw tooth. The corresponding molecular flow factor ( $M_M$ ) is 0.58 for the saw tooth surface. By substituting these factors in the leakage equation, eliminating the deflection term, evaluating for a single surface only, and using the density factor ( $\beta$ ) found in the inspection data, the following equation evolves for scratches.



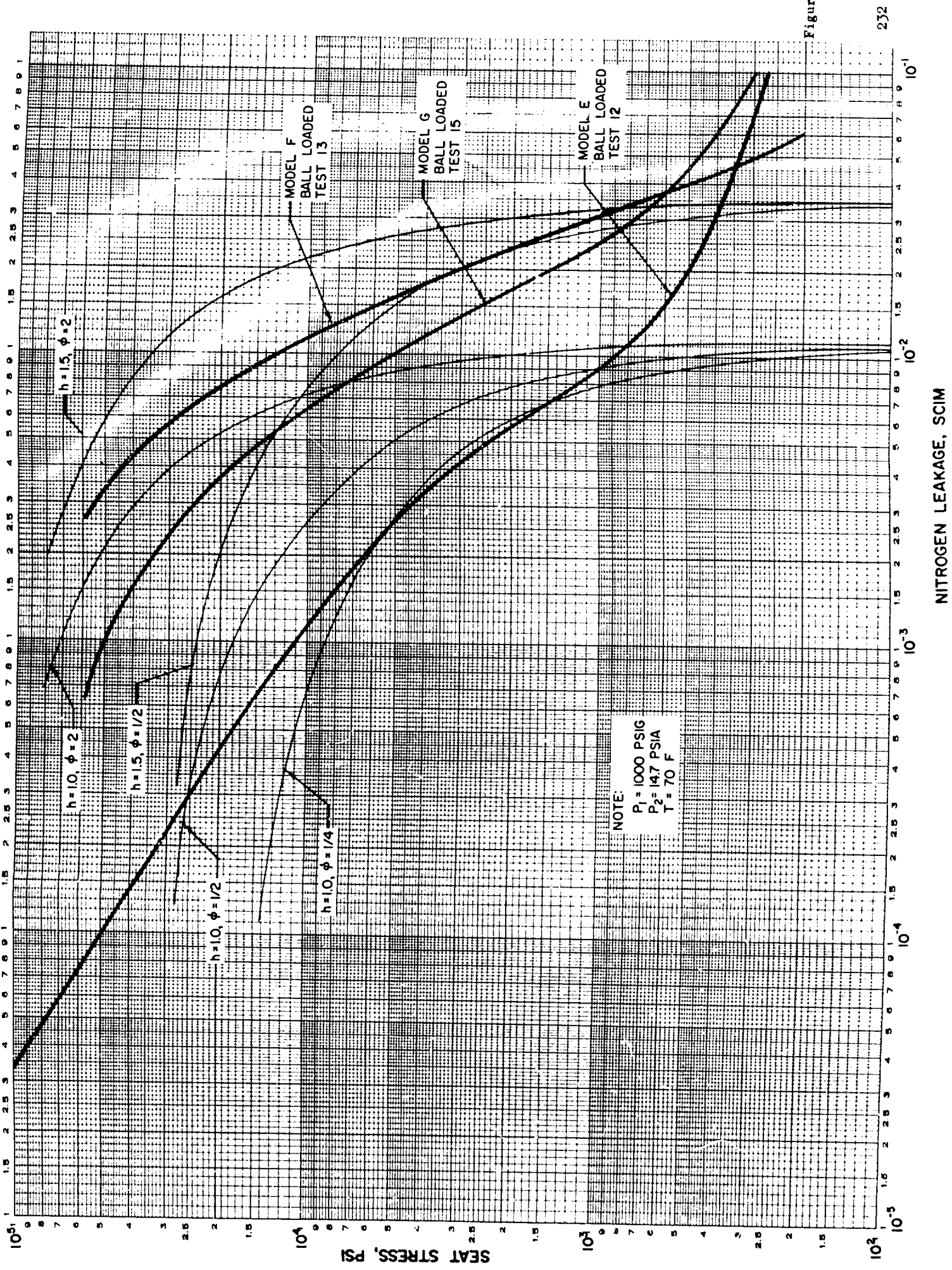


Figure 94. Data Correlation for Test Models E, F, and G



$$Q = \beta \left\{ \frac{4.7 D_s (P_1^2 - P_2^2)}{\mu LT} [M_L h]^3 + \frac{1.4 \times 10^5 D_s (P_1 - P_2)}{L} \sqrt{\frac{R}{T}} [M_M h]^2 \right\}$$

By computing the scratch leakage and comparing it with low-stress (1000 psi) test leakage, an estimate may be made of the controlling surface characteristics. For example, the scratches of test model F (Fig. 93) occupy a large percentage of the seating surfaces and hence will result in significant leakage. For the seat which has a scratch depth of 3.8 microinches and a density of 38 percent, the computed scratch flow is  $2.2 \times 10^{-2}$  scim. The corresponding poppet flow is  $0.8 \times 10^{-2}$  scim for a scratch depth of 4.0 microinches and a density of 12 percent. The total scratch flow of  $3.0 \times 10^{-2}$ , compared to  $3.0 \times 10^{-2}$  scim at a 1000-psi seat stress, indicates that a predominant portion of the over-all leakage is a result of the scratches. This analysis cannot be carried further at this time because a stress vs leakage relationship has not been developed for the scratch configuration.

#### Scratch Test (Test Model G)

This test was performed on a controlled scratch configuration to obtain general correlative information on the flow and stress vs leakage relationships for scratches. The test poppet and seat are the same as used in test model F except that the poppet was reworked to a fine polished finish. Examination of the inspection data of Table 8 shows that the reworked model G poppet has no measurable roughness or waviness and contains only widely scattered nodules with an average height of 2.3 microinches. Figure 40 shows an interference microphotograph of this surface.

For the scratch evaluation, the polished poppet was scratched radially using the diamond indenter from the Leitz microhardness tester. This indenter is the Vickers pyramid configuration which has a depth-to-diagonal ratio of 1/7. After four scratches located at 90 degree intervals

were scribed on the surface, the poppet was polished to remove the feather edges along the scratch. Figure 41 shows a typical scratch (No. 2 in the following table) after the polishing operation. Each of the scratches were slightly different, and the following table describes the average depth (h), width ( $\lambda$ ), and angle ( $\Phi$ ) for all four.

Scratch No.	Depth, microinches	Width, microinches	Angle, degrees
1	31.8	522	7.0
2	31.8	391	9.3
3	42.4	391	12.4
4	37.1	435	9.4

Test 15 (Fig. 95) was performed on test model G at 1000 psig, which establishes the stress vs leakage characteristics of the model before the application of the four scratches. The curve represents the fourth cycle to a 60,000-psi stress conducted with the ball loading device. The high leakage rate below the 1000-psi stress was attributed to contamination. Test 16 illustrates test model G leakage information after the scratches were scribed on the poppet. This curve represents the sum of the surface texture leakage and the leakage through the four scratches. To find the net scratch leakage, the curve of test 15 is subtracted from curve of test 16. This scratch leakage is shown as a dashed line in Fig. 95.

To correlate net scratch leakage with analytical data, the following equation was used:

$$Q = \frac{1.5 (\lambda) (P_1^2 - P_2^2)}{\mu L T} \left[ M_L h \right]^3 + \frac{4.5 \times 10^4 (\lambda) (P_1 - P_2)}{L} \sqrt{\frac{R}{T}} \left[ M_M h \right]^2$$

This basic equation was presented in the Surface Analysis section and has been modified by substituting scratch width ( $\lambda$ ) for  $(\pi D_g)$  and eliminating the deflection term.  $M_L$  and  $M_M$  are the flat plate averaging factors for a saw tooth surface and are 0.63 for laminar flow ( $M_L$ ) and 0.58 for molecular flow ( $M_M$ ).

Because the four scratches are not identical, data were computed independently for each as follows:

Scratch No. 1	$Q = 0.8 \times 10^{-2} \text{ scim}$
Scratch No. 2	$Q = 0.6 \times 10^{-2} \text{ scim}$
Scratch No. 3	$Q = 1.5 \times 10^{-2} \text{ scim}$
Scratch No. 4	$Q = 1.1 \times 10^{-2} \text{ scim}$
<hr/>	
$\Sigma$	$Q = 4.0 \times 10^{-2} \text{ scim}$

The flow correlates very well (10 percent at a 1000-psi stress) with the net scratch leakage of Fig. 95). A mathematical stress vs leakage model has not been developed for scratch flow, but it can be seen from the experimental results that the scratch leakage has been reduced by one-half at a 60,000-psi stress. Several more tests with scratches of varying depth should be performed before any conclusion can be reached as to the stress vs leakage relationship for scratches.

#### Out-of-Flat Tests (Models H and I)

These tests were performed to determine the effect of the gross geometry deviation of poppet (and seat) flatness. The models constructed had a gentle curvature in one plane, i.e., a small arc length of a cylindrical surface. Two models were fabricated, one having a height curvature of 8 microinches (model H), the other 24 microinches (model I). Both out-of-flat surfaces were made on the poppet because it has a continuous flat

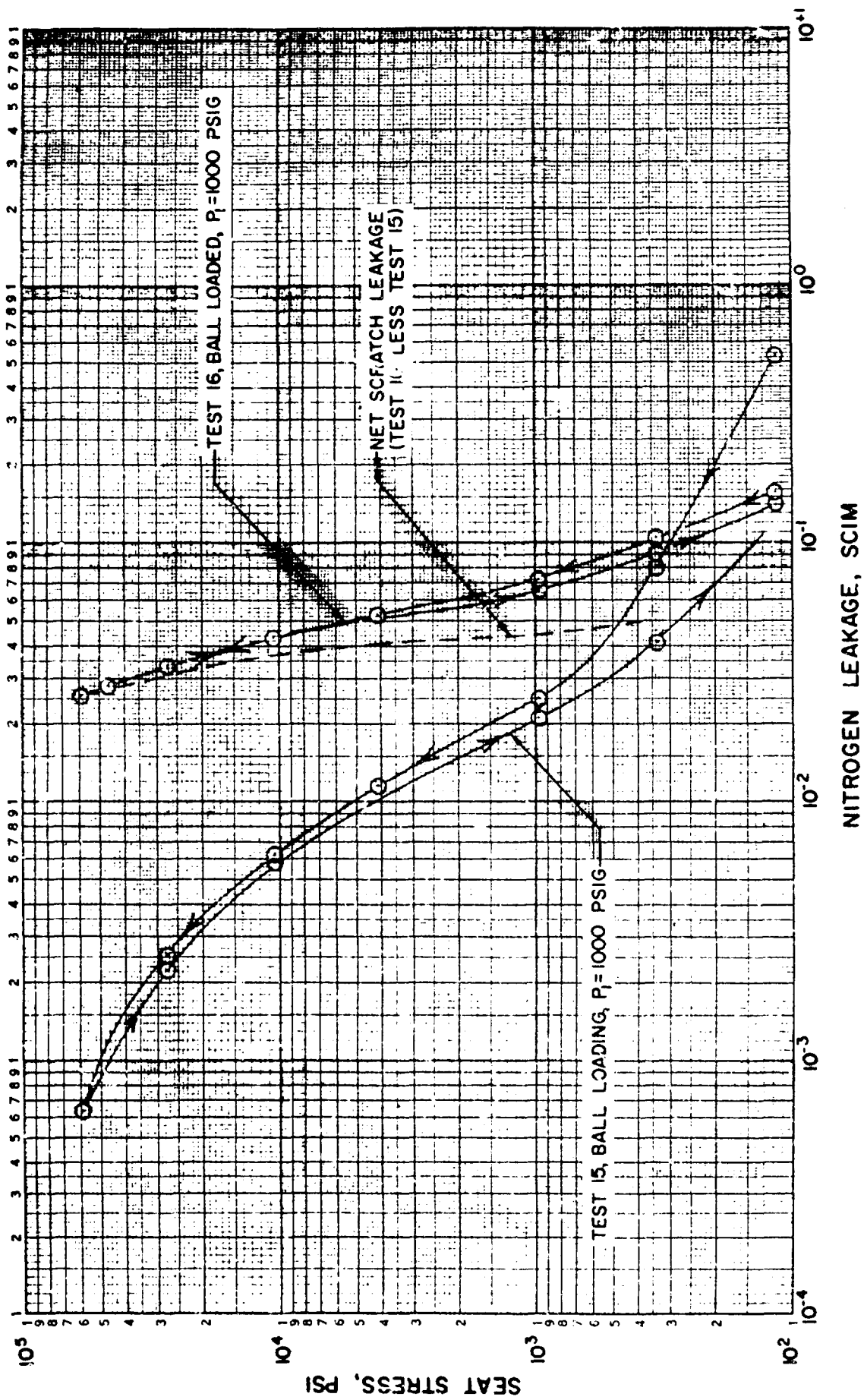


Figure 95. Stress vs Leakage Data for Test Model G, Tests 15 and 16

surface which is easily measured. The common seat was flat within 3 microinches. Surface measurements were taken on the Proficorder, Cleveland Height Comparitor, and an optical flat to ensure correct definition of the surface contour.

The intention was to keep the surface roughness of these test models the same as the 2-microinch AA multidirectional surface of model B. This surface texture was used as a datum to examine other variables such as gross geometry and material properties. Because of the variables in the lapping process, however, models H and I turned out to be slightly rougher than the 2-microinch AA standard surface.

The surface texture of the test model H poppet was the same as the seat which had a surface roughness of 7.4 microinches and an angle of 1.2 degrees. The surface had no waviness, but 5 percent of the surface was composed of nodules with an average height of 4.4 microinches. These parameters were determined from the Proficorder trace of Fig. 62 and the interference microphotographs of Fig. 42 and 43.

The seat was common to models H and I; however, the model H poppet was reworked after test to the model I configuration. The model I poppet had a roughness of 7.9 microinches, an angle of 1.3 degrees, and widely scattered nodules 4.7 microinches in height. These parameters were determined from the Proficorder trace of Fig. 63 and interference microphotograph of Fig. 44. Even though the surface roughness of these models was close to 2.5 microinches AA, it was assumed that they approximated the datum roughness value (2-microinch AA); therefore, gross geometry flatness change could be viewed as an independent variable.

The test results of models H and I are shown in Fig. 96. Tests 17 and 18 were conducted on the 8-microinch cylinder (model H) at an inlet pressure of 1000 psig and stresses up to 60,000 psi. Test 17 was conducted with the poppet clamped whereas test 18 was with the ball loading device

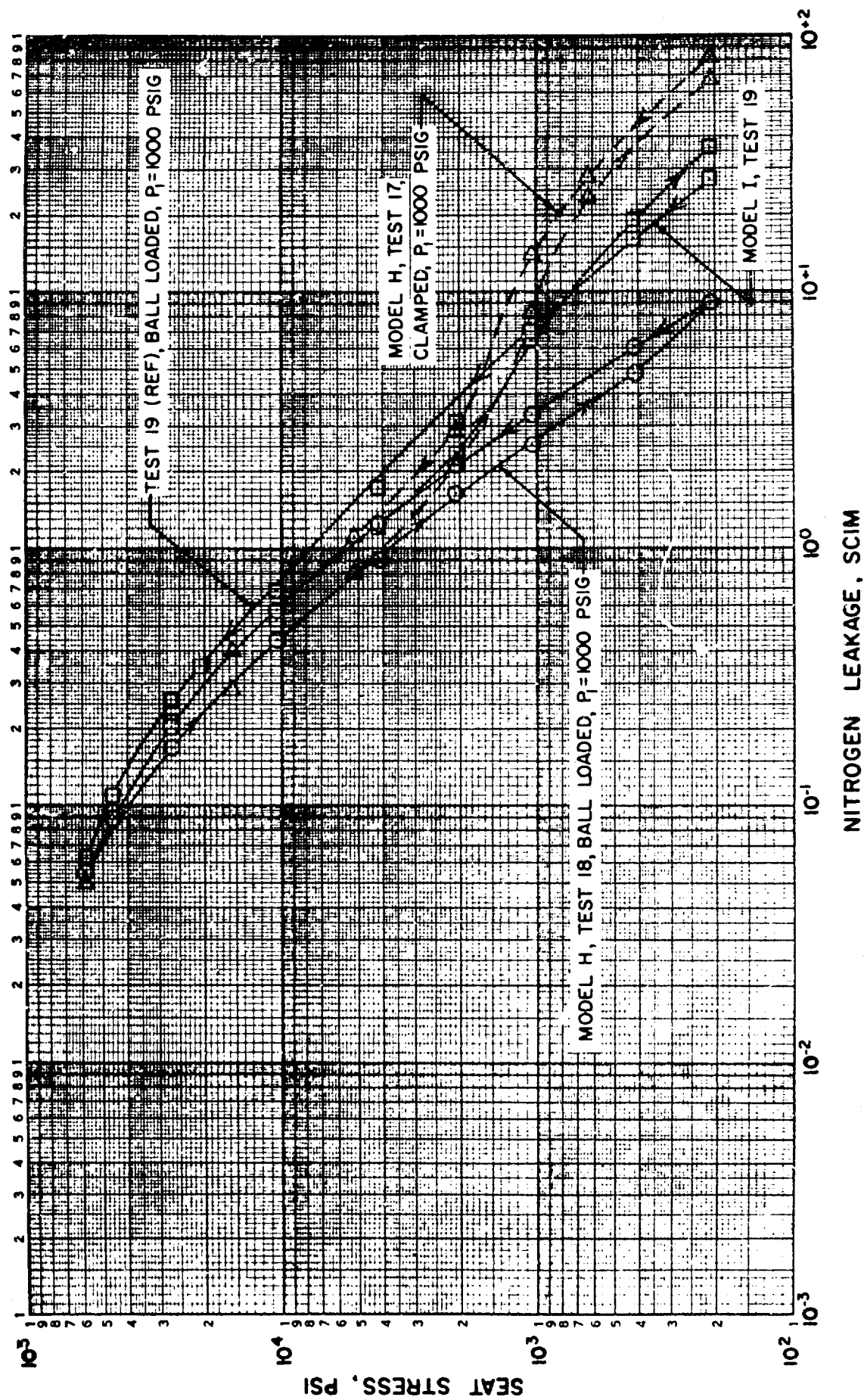


Figure 96. Stress vs Leakage Data for Test Models H and I, Tests 17 through 19

installed. Here again, the out-of-flat condition caused by clamping the poppet to the piston is attributed to the difference in leakage at the low stress levels.

Test 19 is the stress vs leakage curve for the 24-microinch cylinder (model I) conducted with the ball loading device.

In examining the curves of Fig. 96 and comparing the curve shape with the test data obtained from test model B, the conclusion reached was that the out-of-flat condition did not appreciably alter the stress vs leakage characteristics. This conclusion is further supported by the similarity of the 8-microinch (test 18) and the 24-microinch (test 19) curves. These two curves were very close at high stresses and differed only by a factor of 2 to 3 at the low stress levels.

A simplified deformation analysis based on Hertz contact of a cylinder on a flat plate can be made for these out-of-flat surfaces to support the above conclusions. The unwrapped, out-of-flat curve describes two cycles of a sine wave. An approximation to the load required to flatten each peak may be obtained by assuming the peaks are represented by two cylindrical segments having chordal distances of  $1/2$  the mean seat circumference. This results in a minimum deformation for a given load. A schematic of the assumed model is shown in Fig. 97. It is assumed that the  $L/D_s$  and  $h/L$  ratios are small.

The assumed cylinder diameter may be expressed as:

$$d = \frac{\pi^2 D_s^2}{16h}$$

Describing the total seat load in terms of apparent seat stress the expression for deformation is:

$$\delta = \ln \left( \frac{4.4 h}{D_s^3 S \alpha} \right)^{1.57 D_s S \alpha}$$

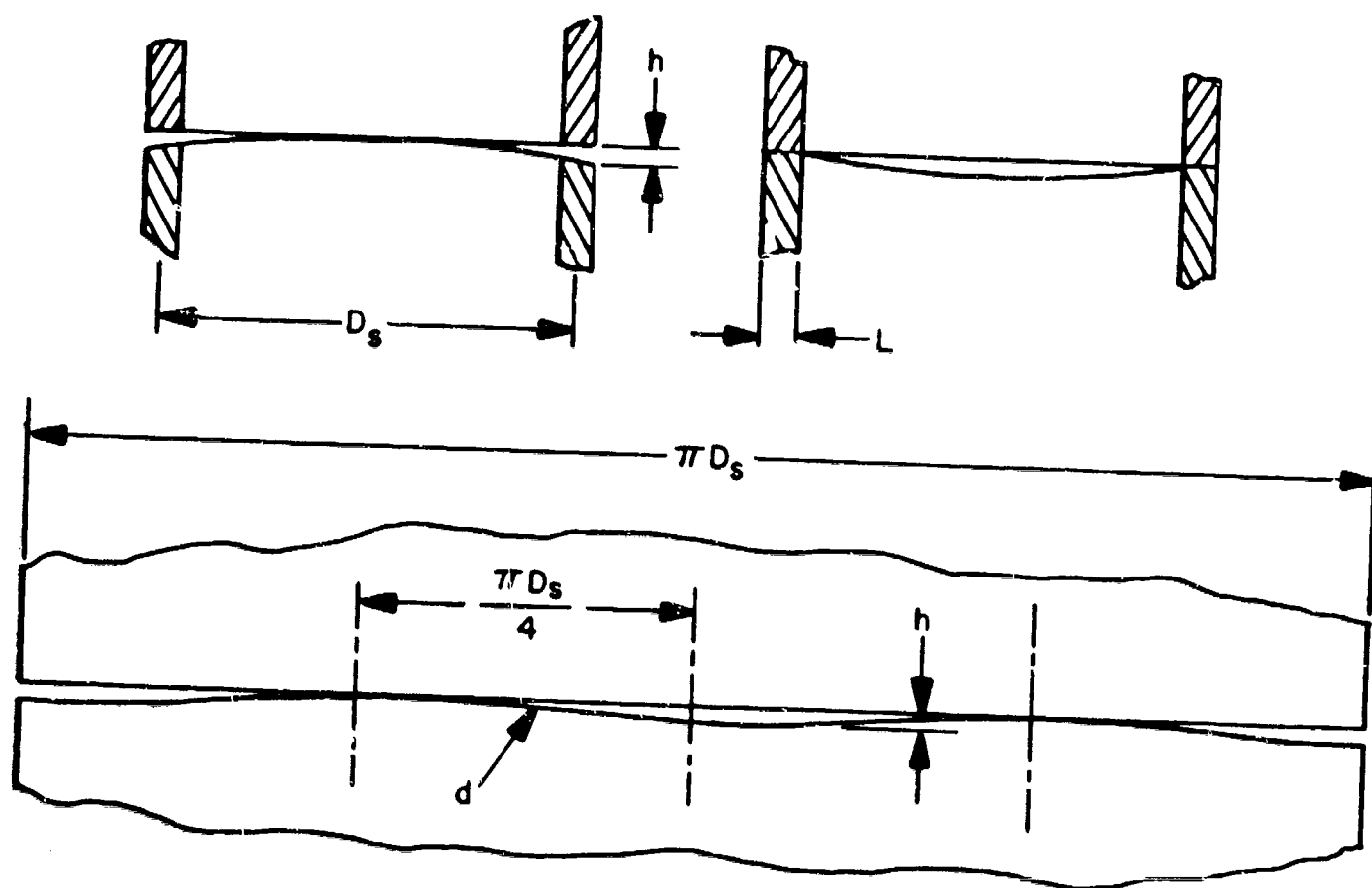


Figure 97. Schematic of Poppet and Seat Model Gross Curvature



or in terms of total seat load, F,

$$\delta = \left( \frac{13.8 h L}{D_s^2 F \alpha} \right)^{\frac{F \alpha}{2L}}$$

where

$D_s$  = mean seat diameter, inches

F = total seat loads, pounds

h = peak-to-valley height, inches

L = land width, inches

S = apparent seat stress, psi

$\alpha$  = elastic constant for both materials, 1/psi as previously defined

$\delta$  = peak deformation, inches

Introducing the test parameters into the stress vs deflection equation above for the 24-microinch curve and solving (by trial and error) for stress required to flatten the curvature ( $\delta = 24$  microinches) results in an indicated stress of 100 psi. While this approach is very approximate, the order of magnitude is significant and supports the hypothesis that gross flatness is not a significant factor in these tests. This must not be taken as a general rule, however, because of the general independence of gross (substrata) deformation and surface deformation. For example, a very narrow seat land of typical corner construction (as in a conically seated valve) could have very high unit surface loads (stresses) for a relatively small seat load. Deformation of the substrata would therefore be small, and gross curvatures could be the significant parameter of the over-all stress vs leakage characteristic.

### Cut-of-Parallel Tests (Test Model B)

The configuration used for the out-of-parallel tests was test model B with the poppet canted relative to the seat by 125 microinches at the 0.5-inch diameter. This was accomplished by lapping the back face of the poppet out of parallel relative to the front face, thus leaving the original 2-microinch AA surface texture perfectly intact. The Proficorder and the Cleveland height indicator were used to verify the parallelism measurements.

Test results for the out-of-parallel configuration are shown in Fig. 98. Test 20 is a comparison rerun of model B at a 1000-psig inlet pressure and the poppet clamped to the piston. The poppet was then lapped out of parallel 125 microinches and retested; the data shown for test 21 represent the first six cycles (virtually no hysteresis was observed). It can be seen from a comparison of the two test curves that as stress is increased, the out-of-parallel structure suddenly collapses, and the stress vs leakage curve is nearly identical from then on to the original parallel configuration.

The following analysis is presented to show where the various deflections, which ultimately bring the two surfaces into a parallel and mating condition, occur. The data recorded for the three most significant seat stresses are tabulated below from the piston pressure and load cells.

Net Piston Force, pounds	Apparent Seat Stress, psi	Load Cells, pounds			$\Sigma F = F_T$ , pounds	Error, percent
		F <sub>1</sub>	F <sub>2</sub>	F <sub>3</sub>		
224	1,040	79	72	60	211	6.2
669	11,430	258	187	193	638	4.9
2650	58,200	897	830	842	2570	3.1

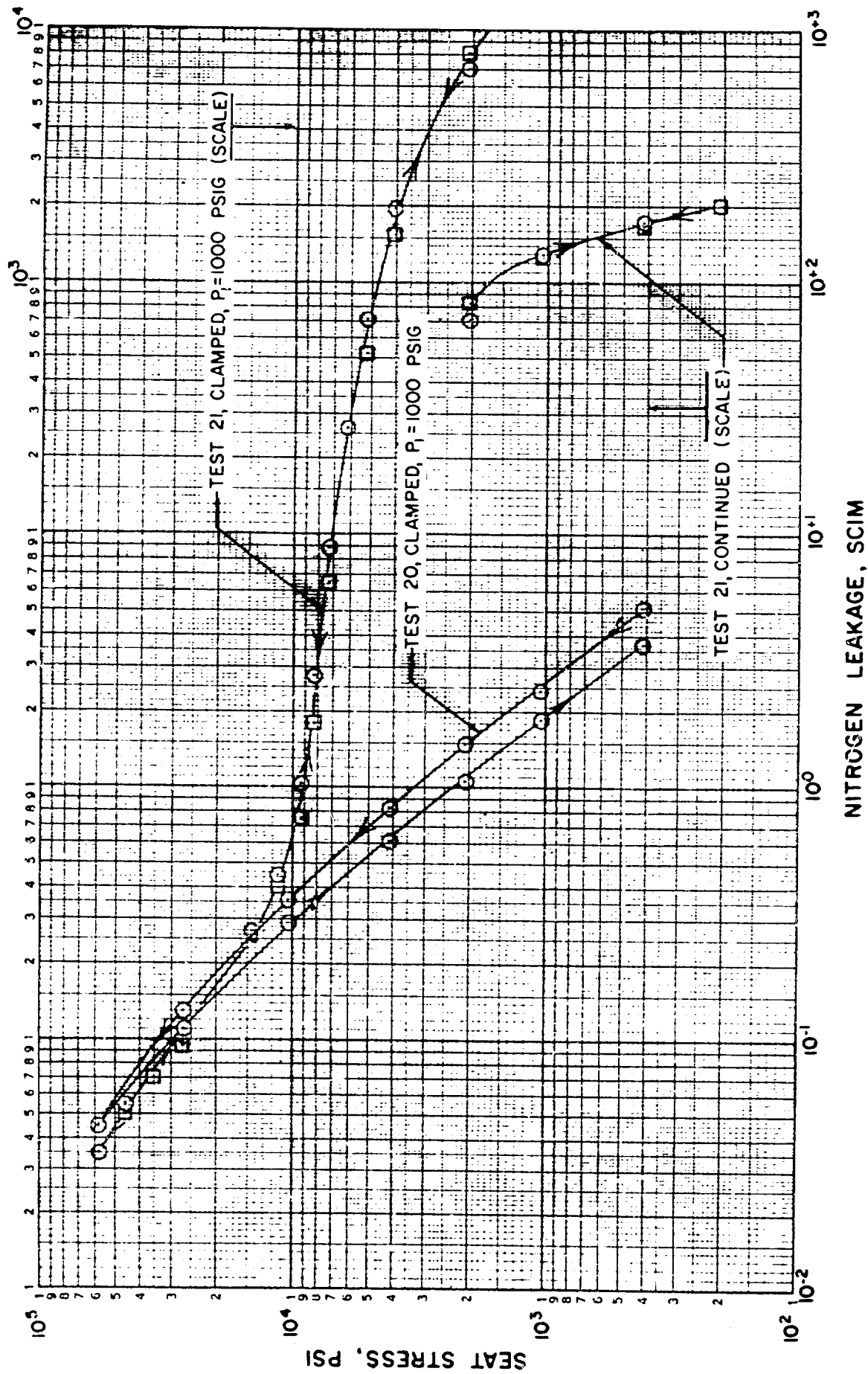


Figure 98. Stress vs Leakage Data for Test Model B, Tests 20 and 21

The 125-microinch high point was located directly under cell No. 1. The variation in load between the three cells is not very large.

From the dimensions of the load cells, poppet, and seat, an estimate of the deformation attributable to each of these parts may be made. The remainder, allowing for piston cocking, must be from interfacial deformation.

#### Load Cell Deformation ( $e_1, e_2, e_3$ ).

$$e \approx \frac{FL}{EA} \approx \frac{1.0 F}{30 \times 10^6 \times 0.313^2} \approx 0.34 \times 10^{-6} F$$

where

E = elastic modulus, psi

A = area, sq in.

L = length, inches

F = individual load cell force, pounds

e = deformation, inches

#### Poppet Deflection ( $e_p$ ).

$$e_p = 0.0173 \times 10^{-6} F_T$$

#### Seat Deflection ( $e_s$ ).

$$e_s = 0.014 \times 10^{-6} F_T$$

The deflections computed from the above expressions are summarized below for each of the previously noted seat stress levels; all deflection are in microinches.

Apparent Seat Stress S, psi	$e_1$	Average $e_2$ and $e_3$	$e_p$	$e_s$	$\Delta e$
1,040	26.8	22.4	3.9	3.1	2.4
11,430	87.7	64.6	11.6	9.4	23.3
58,200	305.0	284.0	45.8	37.1	21.0

In the table,  $\Delta e = e_1 - (\text{average } e_2 \text{ and } e_3)$ . The righting allowed by piston clearance is approximately 20 microinches. The differential load cell deformation is approximately 22 microinches or 28 microinches across a 1-inch diameter, which reduces to 14 microinches across the 1/2-inch seat diameter. Considering the relative stiffness of both the poppet and seat, probably very little differential deformation occurs within these parts. The difference between the 125-microinch out-of-parallel dimension and the 34 microinch ( $20 + 14$ ) differential leaves 91 microinches for net interfacial deformation. From these figures, it is concluded that the deflection indicated by the large change in leakage at the 10,000-psi level is a result primarily of interfacial deformation.

#### Material Parameter Tests (Models J and K)

The two additional material parameters studied were 17-4 PH steel and 6061-T651 aluminum. The 17-4 PH steel has the same elastic modulus as the 440 C steel tested previously; however, the yield strength is approximately 3/4 that of 440 C. Tests were performed with the 17-4 PH steel to ascertain if decreased strength would have any effect on stress vs leakage characteristics. The aluminum poppets and seats were included to determine any changes resulting from a different modulus of elasticity. The surface texture of both materials was approximately 2-microinch AA for comparison with the tests run on the 440C material (model B).

Test model J was the 17-4 PH material test configuration, and the surface texture (Table 8) was very similar to test model B except that there were no nodules on model J. The poppet and seat of this test model had essentially the same surface texture. The average asperity height was 6 micro-inches with an angle of 1.6 degrees as measured by the Proficorder chart (Fig. 64) and the interference microphotographs (Fig. 45 through 47). Figure 45 shows the scratch caused by the 0.0009-inch-radius Proficorder stylus. Figure 46 is included to show Profilometer scratches on this relatively hard surface. The interference bands on this photo are not well defined because of poor focus.

Tests 22 and 23 were performed on the model J configuration (Fig. 99). Both tests were conducted at 300-psig inlet pressure with the ball loading device installed. Test 22 was the first cycle down and back and test 23 was a repeat cycle after poppet-to-seat contact was broken to check for contamination. The seat was carefully examined, and the system was purged with nitrogen; however, noting the high leakage at low stress for both tests, it must be concluded that the contamination was not removed. A comparison of the high stress leakage portion of the data of test model J with those of test model B (Fig. 87) shows very close correlation. It is concluded from this comparison that the two materials, 440C and 17-4 PH have essentially the same stress vs leakage characteristics, and that variations of yield strength do not influence these characteristics. However, it is further presumed that if the two materials had been tested into regions of gross plastic surface stress, significant differences would have been found.

Test model K is the 6061-T651 aluminum test model configuration. The inspection data were rather difficult to obtain on the aluminum parts because the stylus-type instruments would plastically deform the surface as the data were obtained. The interference microphotographs (Fig. 48 and 49) show stylus-caused surface damage. As a result, Fig. 50 was used to determine the surface texture parameters of Table 8 for this model. The texture is very similar to the 2-microinch AA, 440C test model B with a peak-to-valley height of 6 microinches and an angle of

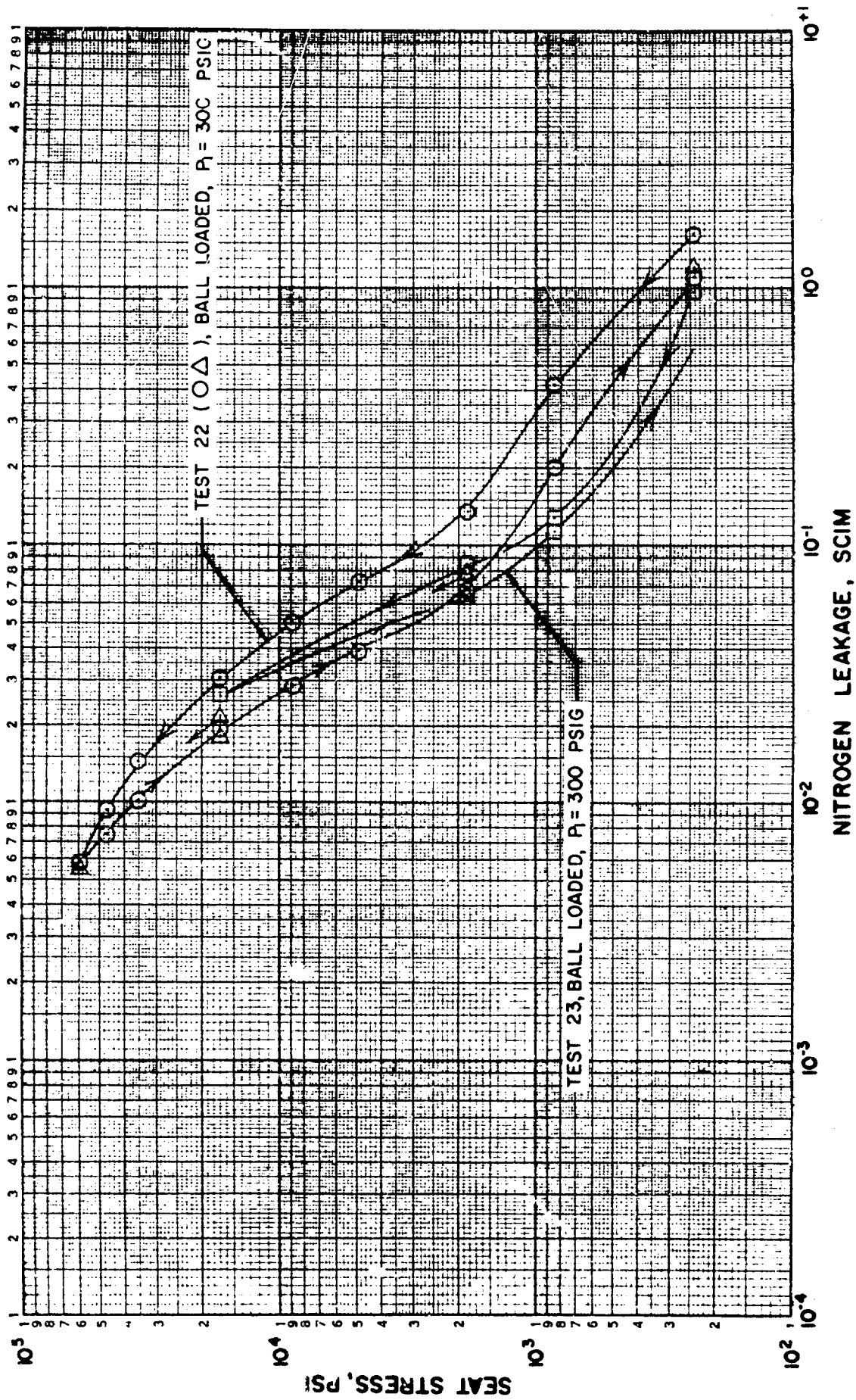


Figure 99. Stress vs Leakage Data for Test Model J, Tests 22 and 23

1.3 degrees. Unlike model B, however, the aluminum model contains 5-microinch scratches over about 6 percent of the surface. (Several unsuccessful attempts were made during the lapping operation to eliminate these scratches.) Because of the low number of scratches, it was concluded that this model surface texture approximated the 2-microinch AA surface of model B so that the elastic modulus factor could be viewed independently.

Figure 100 shows the test performed on the model K configuration. Test 24 represents a series of three separate tests where the stress was progressively increased with each test group. The first test (initial contact) was conducted from 350 to 2080 psi, the second from 350 to 5330 psi, and the third from 350 to 10,750 psi; the surfaces were not separated between tests. All tests were run at a 1000-psig inlet pressure using the ball loading device. Before the data were recorded for each test group, the model was cycled 5 times (350 to 2080 psi; 350 to 5330 psi, and 350 to 10,750 psi) to ensure that the elastic characteristics were being measured. The test results (Fig. 100) indicate that plastic deformation has taken place with each successive increase in the level of operating stress. The dashed line indicates the estimated initial loading characteristic indicating progressive plasticity. It should be emphasized, however, that the three cycles were elastic and thus repeatable. The bulk yield of the aluminum material (approximately 31,000 psi) was not reached in these tests, and it is concluded that the plastic deformation was taking place only at the asperity level. This is further illustrated by Fig. 51 which shows no edge yielding, only slight lapping dub-off.

Test 25 was conducted at a 1000-psig inlet pressure with the poppet clamped. The stress was increased to 60,000 psi, which is approximately twice the bulk yield strength of the aluminum material; therefore, considerable plastic deformation took place. Figure 52 shows how the seat land has been permanently deformed because of the over-stressed condition.



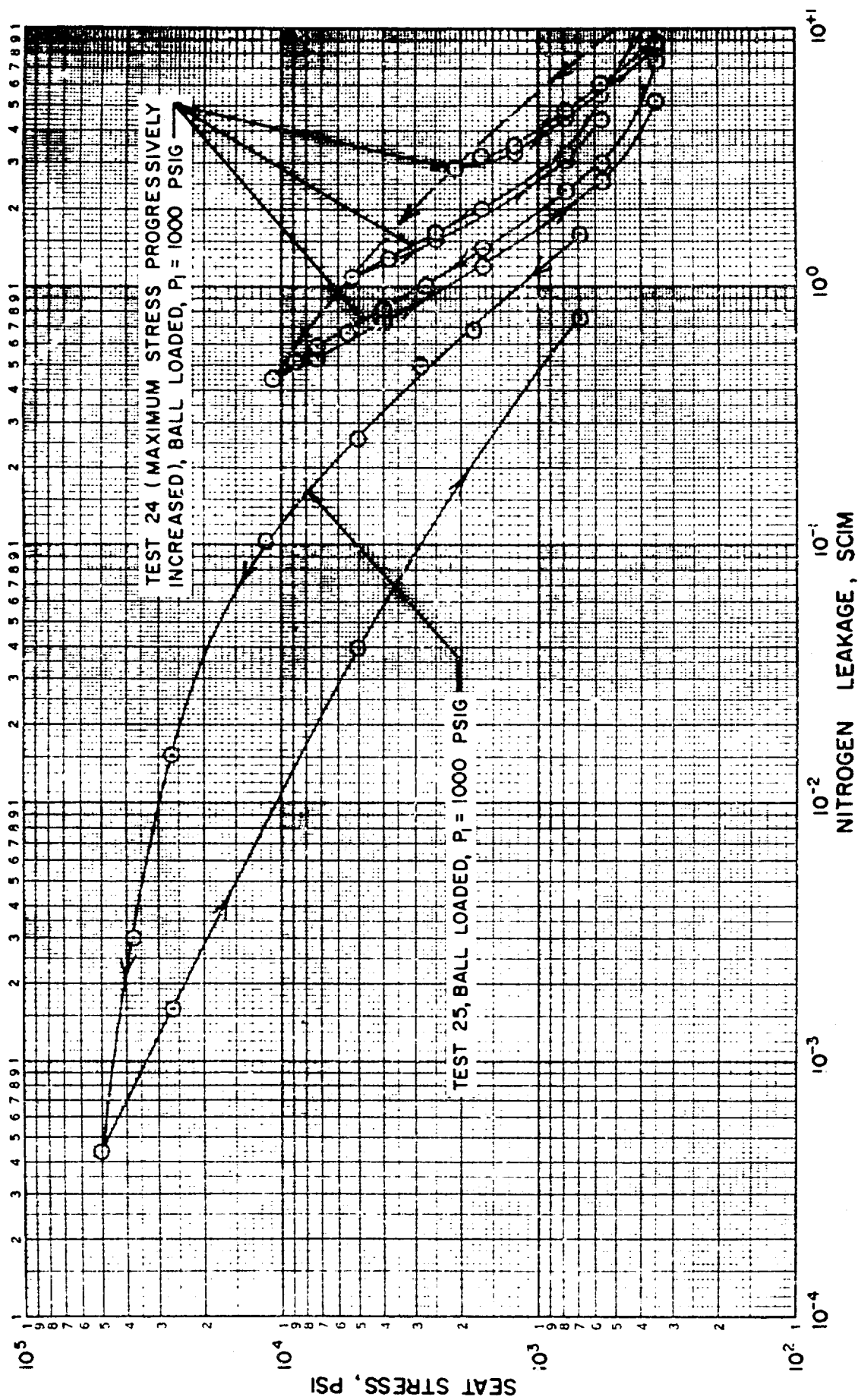


Figure 100. Stress vs Leakage Data for Test Model K, Tests 24 and 25

This figure shows the permanent seat deformation to be nine light bands or approximately 95 microinches. Practically all of this deformation has occurred on the OD half of the seat land as shown in the right side of Fig. 52. The unequal deformation is attributed to the fact that the seat ID is more confined, causing an unsymmetrical stress distribution across the seat.

Figure 90 shows the fit of theoretical stress vs leakage data compared with test 24. The best fit is represented by the  $h = 7$ ,  $\Phi = 1$ -degree curve which agrees favorably with inspection data of  $h = 6$ ,  $\Phi = 1.3$  degrees. The high leakage at low stress is attributed to the waviness and probable slight out-of-parallel condition caused by the clamped poppet.

#### Inspection Data Correlation

To compare the over-all correlation of the physical dimensions taken from the inspection records with the equivalent height parameter ( $h_e$ ) computed from the leakage equations, these data are summarized in Table 9. The leakage values at the three stress levels are taken directly from the test curves. The corresponding equivalent peak-to-valley height for both surfaces ( $2h_e = H_e$ ) is computed based upon the assumption of sinusoidally wavy surfaces. The next-to-last column reproduces the inspection data of Table 8 in which the peak-to-valley parameter for both surfaces is added; this was added to the waviness and nodule parameters to arrive at the last column.

At the 1000-psi stress level, a fair correlation exists between the computed and measured peak-to-valley dimension. From this it might be concluded that this stress level is such as to bring the roughness into full contact but with little deformation. Comparison of the 100-psi stress level computed peak-to-valley dimension with the last column shows the

TABLE 9

COMPARISON OF COMPUTED EQUIVALENT HEIGHT PARAMETERS  
( $2h_e$ ) WITH INSPECTION DATA

Test Model and Number	Test Pressure, psig	Seat Stress = 100 psi		Seat Stress = 1000 psi		Seat Stress = 10,000 psi		(h) of Roughness For Both Surfaces (3)	(h) of Roughness + Waviness + Nodules For Both (3)
		Estimated Q, scim	$2h_e$ , inches	Q, scim	$2h_e$ , microinches	Q, scim	$2h_e$ , microinches		
A-1	100	$5.0 \times 10^{-2}$	13.4	$2.5 \times 10^{-2}$	10.3	$3.0 \times 10^{-3}$	4.4	9.0	14.7
B-5	300	$3.7 \times 10^{-1}$	14.8	$1.7 \times 10^{-1}$	11.2	$3.7 \times 10^{-2}$	6.4	11.1	18.7
C-6(1)	300	$1.5 \times 10^1$	53.0	$7.0 \times 10^0$	40.0	$1.6 \times 10^0$	24.0	--	--
C-6(2)	300	$5.0 \times 10^0$	35.0	$1.8 \times 10^0$	26.0	$5.6 \times 10^{-1}$	8.6	28.0	44.6
D-8(1)	300	$4.0 \times 10^1$	79.0	$2.4 \times 10^1$	63.0	$5.3 \times 10^0$	37.0	--	--
D-8(2)	300	$1.0 \times 10^1$	46.0	$6.2 \times 10^0$	39.0	$1.9 \times 10^0$	26.0	38.0	58.4
E-12	1000	$2.0 \times 10^{-2}$	2.4	$8.8 \times 10^{-3}$	1.8	$1.2 \times 10^{-3}$	0.82	3.2	--
F-13	1000	$9.0 \times 10^{-2}$	4.1	$3.1 \times 10^{-2}$	2.8	$1.2 \times 10^{-2}$	2.0	3.0	--
G-15	1000	$6.0 \times 10^{-2}$	3.6	$2.5 \times 10^{-2}$	2.6	$6.5 \times 10^{-3}$	1.6	2.2	4.5
H-18	1000	$1.2 \times 10^1$	23.0	$3.4 \times 10^0$	15.0	$6.1 \times 10^{-1}$	8.0	14.8	23.6
I-19	1000	$4.0 \times 10^1$	34.0	$7.5 \times 10^0$	19.0	$7.5 \times 10^{-1}$	8.8	15.5	24.6
J-23	300	$3.0 \times 10^{-1}$	14.0	$1.1 \times 10^{-1}$	9.6	$3.5 \times 10^{-2}$	6.3	12.0	12.0
K-24	1000	$1.0 \times 10^1$	21.0	$2.0 \times 10^0$	12.0	$4.7 \times 10^{-1}$	7.4	12.0	18.0

(1) First Cycle

(2) Last Cycle

(3) After Test

influence of nodules, waviness, slight out-of-parallel, and contamination at low loads. A fair correlation exists although a better model might simply be parallel plates as a result of the relatively large separation between the two surfaces.

Referring back to the 1000-psi stress column, the degree of success in establishing the 2-microinch AA datum surface is evident. Test models B, H, I, and J were nominally 2-microinch AA surfaces (K excluded because it was aluminum). The variation in surface preparation, test method, and contamination level have served to cause the corresponding variation in leakage at the 1000-psi stress level. This variation is reduced as stress is increased (Q at 10,000 psi).

From these and previous data, it might be broadly concluded that the surface complexity and the basic inaccuracy of measuring equipment precludes outright analytical prediction to any better than a factor of 10. Based on test data, an extrapolation within a factor of 2 should be entirely possible.

## CONCLUSIONS

The program has resulted in the following conclusions:

1. Established flow equations can be applied to valve seat leakage throughout the entire flow spectrum, i.e., for a given fluid and closure configuration the established regimes are:
  - a. Nozzle:  $Q \sim P_1 h$
  - b. Turbulent channel:  $Q \sim f(P_1, h, L, f, R_e, \text{etc.})$
  - c. Laminar:  $Q \sim P_1^2 h^3 / L$
  - d. Transition:  $Q \sim (P_1^2 h^3 + P_1 h^2) / L$
  - e. Molecular:  $Q \sim P_1 h^2 / L$
  - f. Diffusion laws
2. Almost all valve seat leakage takes place in the laminar and molecular flow regimes, but primarily in the laminar regime.
3. The effective seat diameter for compressible fluids within the turbulent channel and laminar flow regimes varies from the mid-land position to  $2/3$  of the seat land width (ID to OD) as the valve seat closes. This can represent a large change in effective seat area through a very short stroke if the land area is comparable to the seat ID area.
4. Because most valve seat leakage is described by the laminar flow equation, the volumetric leakage (scim) is essentially independent of the specific gas. This is because the controlling parameter is viscosity which does not vary appreciably from gas to gas.
5. Valve seat leakage takes place through the minute interstices provided by the surface profiles of mating seats and is controlled primarily by the roughness peak-to-valley parameter. Approximation to parallel plate flow for real surface profiles may be

obtained by applying appropriately weighted factors to the average peak-to-valley measurement to arrive at an equivalent parallel plate separation. It follows that, given a perfectly smooth surface, no seat load is required to seal.

6. Valve seating is essentially a totally elastic process of forcing two relatively smooth surfaces into intimate contact. Plasticity may play an important role on the initial few contacts for soft materials; however, after the seat is set, very little plastic flow takes place on subsequent cycles. Proof of this is shown in the repeated-cycle, stress vs leakage curves on the typical aluminum valve seat.
7. The deformability of a given valve seat is a function of the relative "sharpness" of the surface profile. The sharpness characteristic is broadly described by a peak-to-valley average slope angle. Similar to a corrugated tin roof, the sharper the angle, the more rigid the structure. The deformability is also controlled by the elastic characteristics of the respective materials; i.e., modulus and Poisson's ratio. It follows that under equal loading and test conditions, a rough surface could leak less than a fine surface. Naturally, the rougher surface will leak more at initial contact. For example, the curves of Fig. 16 for  $h = 6$ ,  $\Phi = 1/4$  degree and  $h = 4.5$ ,  $\Phi = 1$  degree cross at  $S = 4000$  psi; therefore at higher stresses, the initially rougher surface will leak less than the smoother surface.
8. Other than the gross geometry parameters such as land width, seat diameter, and general seating arrangement, valve closures are not designed in the full sense of the word. Engineering drawings do not, for the most part, specify the real controlling parameters but only point the way toward a fabrication process. Few valve seat drawings specify  $1/4$ -,  $1/2$ -, 1-, or even 2-microinch AA finish requirements for seats actually requiring these fine surface finishes for sealing. Consequently, metal valve seats are being "developed" to meet leakage requirements.

The limitations of present inspection tools combined with the prodigious amount of detail inspection required, among other problems, preclude specifying exact surface profiles on engineering drawings. As a result, valve seats will continue to be developed rather than specified. This is economically sound only if the basic ground work of design is sufficiently thorough to allow the necessary degree of development latitude. In many cases of valve development, the trial and error process is unsuccessful and necessitates complete redesign. In other instances, lengthy development efforts result in a compromise of the design requirements and functional objectives to meet schedule. The knowledge provided by this program of the controlling parameters of seating surfaces and leakage equations will result in a greater development latitude through more accurate design and provide the development engineer with the necessary tools to point the direction for varying the configuration within the design latitude to meet specific functional requirements.

## RECOMMENDATIONS FOR FUTURE EFFORT

A review of the material covered in this report indicates that significant advances in understanding of the mechanism of metal-to-metal sealing have been made. However, the virtually boundless scope of the field of endeavor has necessitated that with the time and manpower allotted only an extremely small facet be examined. Furthermore, the complexities of real surface structure have precluded all but the most fundamental approach to understanding and definition of the pertinent problem areas. The correlation of test and theoretical data noted herein has been encouraging but it is recognized that the mathematical seat model represents an extremely simplified or "ideal" condition.

The analysis or interpretation of actual test model surface characteristics has been quite subjective, and explicit conclusions drawn from this study are minimal. This is partly because of the limitations of current inspection equipment and/or methods but also to the physical limitations of time, manpower, and quantity of test surfaces available.

Only the basic mechanics of the manufacturing processes involved in producing valve seat quality finishes have been investigated. The effects of such variables as grit degradation with use, extent of slurry wetting, and lap material on the surface structure of lapped parts, are to a great extent unknown. Moreover, the effort to date has been directed toward studies of lapped surfaces only while other processes exist which could produce finishes of similar sealing capabilities.

The effort just completed and reported herein has established the basic groundwork and potential approaches to further understanding of the subject. From this basic information, a logical extension of the effort may be defined. The subsequent paragraphs describe the recommended areas of future effort.



First, a continuation of development of basic seating data for existing, flat-seated models to fully define the bound of elastic and elastoplastic metal seating is recommended. Similar information, perhaps not to the same extent, should be gathered for conical and spherical configurations. Therefore, the influence of geometry on sealing capabilities may be evaluated. Furthermore, the effect of common manufacturing discrepancies, such as out-of-roundness, asphericity and misalignment on valve poppet and seats may best be investigated on conical and spherical models.

In conjunction with the above, the formulation of additional theoretical stress vs leakage relationships will be required. Additionally, the development of an improved mathematical model is necessary to better approximate real surfaces being tested. An analysis approach considering roughness superimposed on waviness is recommended. Analyses of flow forces and pressure profile characteristics on the conical and spherical configurations to complement the work already accomplished on flat-seated geometry is also necessary.

Certainly one of the most important criteria of the functional capability of a valve seat is the influence of cycling on sealing surfaces. Aside from certain design rules, the effects of cycling are generally not fully considered until the actual hardware and test stages are reached. Therefore, dynamic cycle tests of selected configurations are recommended to obtain a relative comparison of endurance life for various materials, surface textures, etc. Because the stress vs leakage relationship, as a function of impact level and number of cycles, is the major test parameter, adequate and perhaps somewhat sophisticated instrumentation will be required.

Continued emphasis on the defining surface finishing processes is necessary. Specific effort should be directed toward methods of minimizing personal technique influences on finished surfaces to permit some index for consistency of quality. Detailed examination of all known constituents

of a given process may well lead to a better understanding of the resultant finish. This emphasis should not be limited to the lapping process but should also include turning, grinding, honing, polishing, burnishing and wet blasting, or shot-peening and is recommended as part of future effort.

In conjunction with the machining process described is the possibility that plating of poppets or seats will extend sealing life and capabilities. Already in use to improve static sealing, some evidence exists which indicates that dynamic sealing surface(s) may also be improved through the use of suitable plating. It is recommended that two approaches be investigated: (1) the use of a soft nonwork-hardenable material such as gold or silver which can plastically flow into valleys and scratches of sealing surfaces with subsequent leakage reduction, and (2) thin coatings of tungsten or molybdenum which can be chemically converted to a lubricant state. The latter process will not only tend to fill leakage interstices but could provide, through lubrication, increased wear resistance.

A correlation of liquid and gas leakage characteristics for given surface structures is needed. The accumulation of theoretical and empirical data supporting suitable conversion factors would be the most informative design data, and the inclusion of this effort is recommended.

## REFERENCES

1. Archard, J. F.: "Single Contacts and Multiple Encounters," Journal of Applied Physics, Vol. 32, No. 8, August 1961.
2. ASA B46.1-1962, Surface Texture, American Standards Association, American Society of Mechanical Engineers, New York.
3. ASA Sectional Committee B46, Minutes of Meeting of Subcommittee 5 at National Bureau of Standards, 15 May 1962.
4. Bickel, Dr. Ing. E.: "Testing the Precision of Electric Instruments for the Measurement of Surface Roughness," Microtecnic, Vol. 14, No. 4, August 1960.
5. Bikerman, J. J.: Surface Chemistry, Academic Press Inc., New York, 1958.
6. Bowden, F. P. and D. Tabor: The Friction and Lubrication of Solids, Oxford University Press, London, 1954.
7. Broadston, James A.: Control of Surface Quality, Surface Checking Gage Co., Hollywood, California, Report No. NA-8150, 1960.
8. Dyson, J. and W. Hirst: "The True Contact Area Between Solids," Proc. Phys. Soc., London, B67, 1954, 309.
9. Gregg, S. J.: Surface Chemistry of Solids, Whitefriars Press Ltd., London, 1951.
10. Halliday, J. S.: "Surface Examination by Reflection Electron Microscopy," Proc. Inst. Mech. Engrs. London, Vol. 169, 1955.
11. Kragelsky, I. V. and N. B. Demkin: "Contact Area of Rough Surfaces," Wear, Vol. 3, May 1960
12. Ling, F. F.: "On Asperity Distributions of Metallic Surfaces," Journal of Applied Physics, Vol. 29, No. 8, August 1958.

Preceding Page Blank

13. Ling, F. F.: "Some Factors Influencing the Area-Load Characteristics for Semismooth Contiguous Surfaces Under Static Loading," Trans. ASME, Vol. 80, Paper No. 57 A-246, September 1957.
14. O'Conner, J. J. and K. Johnson: "The Role of Surface Asperities in Transmitting Tangential Forces Between Metals," ASME, Paper No. 62-Lubs-14 for meeting of June 1962.
15. Handbook 77, Precision Measurement and Calibration, Vol. 3, National Bureau of Standards, February 1961.
16. Rabinowicz, E.: "Influence of Surface Energy on Friction and Wear Phenomena," Journal of Applied Physics, Vol. 32, No. 8, August 1961.
17. Reason, R. E.: "Orderly Progress in Surface Measurement," Engineering, Vol. 189, February 1960.
18. Reason, R. E.: "Significance and Measurement of Surface Finish," Grinding and Finishing, Vol. 2, September, October, November 1956.
19. Sugg, Ronald E.: "An Interferometer for Examining Polished Surfaces," Mechanical Engineering, Vol. 75, No. 8, August 1953.
20. Tarasov, L. P.: "Relation of Surface-Roughness Readings to Actual Surface Profile," Trans. ASME, Vol. 67, April 1945.
21. Timoshenko, S. and J. N. Goodier: Theory of Elasticity, McGraw-Hill Book Co., New York, N. Y., 1951.
22. Tolansky, S.: "Surface Microtopography," International Science and Technology, Vol. 9, September 1962.
23. Moody, L. F.: "Friction Factors for Pipe Flow," Trans. ASME, Vol 66, 1948, 671.
24. Shapiro, A.H.: The Dynamics and Thermodynamics of Compressible Fluid Flow, Vol. 1, Ronald Press, New York, 1953.
25. Knudsen, J. G., et al: Fluid Dynamics and Heat Transfer, McGraw-Hill Book Co., Inc., New York, 1958.
26. Dushman, S., et al: Scientific Foundations of Vacuum Technique, John Wiley and Sons, New York, 1962.

27. Roark, R. J.: Formulas for Stress and Strain, McGraw Hill Book Co. Inc., New York, 1954.
28. Blackburn, J. F., G. Reethof, and J. L. Shearer, Editors: Fluid Power Control, The Technology Press of M.I.T. and John Wiley and Sons, Inc., New York and London, 1960.

## APPENDIX A

### LITERATURE SURVEY

#### SCOPE OF SEARCH

The search consisted of a thorough review of all pertinent index-type references and available card catalogues thought to be useful in the Los Angeles area. Rocketdyne contains a most complete set of indexes of both periodical and aperiodical literature, and because of their extensive facilities and capable staff, the search was centered there.

Fourteen technical indexes and five card catalogues were searched under 47 categories. These sources covered both domestic and foreign translations of reports, articles, bibliographies, texts and graduate theses. The time spanned by these sources was approximately 1951 to 31 August 1962. Material through the classification of secret was reviewed. The total number of references extracted was approximately 600. This number was later reduced to 286 of the most applicable references.

In conducting the search a list of descriptors (descriptive words) and subject headings was decided upon, modified periodically and systematically searched in each index or card catalogue. Unfortunately, the information desired fell into no clear categories and the resulting descriptors are as diverse and generalized as "fluid flow" and as specific as "reed valve." On occasion, complete indexes were scanned for apropos headings, and if any were found they were added to the descriptor list.

Fluid meters and servo control valves were purposefully omitted from this search. Fluid meters was considered too far removed from the "valve closure mechanism" type of information. Servo control valves were not included because this field has already a wealth of information available and is, in addition, beyond the scope of the survey. The reader will, however, note several references to servo valve material

and fluid flowmeters in the bibliography. This apparent contradiction came about since some articles, although dealing in servo system components, were not so titled, or if so titled, contained information deemed useful to other than servo valve designers. This area is certainly quite "grey," but generally, references dealing predominantly with servo control systems or methods of flow measurement were excluded while references such as flapper valve mechanisms, bibliographies, comprehensive reports, although servo oriented, were referenced.

Soon after the inception of the search, it became apparent each source had its own methods of indexing material. The same reference would be indexed under several very different descriptors, the specific descriptor being dependent upon which index was being consulted. For this reason, this report contains lists of those descriptors under which information was found for each of the more fruitful sources.

Card catalogues were searched under all headings referenced and any others peculiar to that specific catalogue.

ASTIA (Armed Services Technical Information Agency) was searched since they index most projects sponsored by the Government. This search was of two parts. The initial search was by ASTIA personnel at Arlington, Virginia, the second by Rocketdyne personnel at both the Rocketdyne Library and at the ASTIA office in Pasadena.

The ASTIA card index was searched for the period of 1953 through 1959 (in 1959 the Cumulative Indexes were started). The categories under which information was sought were the same as the list of ASTIA descriptors found in the source lists. The ASTIA material covered by the period of 1959 through 31 August 1962 was reviewed at the Rocketdyne Library in the Cumulative Indexes and individual biweekly Technical Abstract Bulletins. Since the ASTIA Cumulative Indexes have no abstracts, only lists of reference numbers, and because of the preponderance of material listed under Fluid Flow, Fluid Mechanics and Compressible Flow, all biweekly Technical Abstract Bulletins were 100 percent scanned under Division 9, Fluid Mechanics.

All reports with IDEP (Inter Service Data Exchange Program) classifications were categorically excluded from the search. These are, by definition, test reports which were not deemed applicable to this program because they are not accompanied by detailed design information. Those 1962 ASTIA Technical Abstract Bulletins too recent to be indexed, numbers 62-1-1 through 62-1-6 (1 January 1962 through 15 March 1962), were scanned only through Divisions 9, 26 and 27, Fluid Mechanics, Production Management and Propulsion Systems, respectively. Experience had shown these Divisions to be the most fruitful.

#### SOURCES SEARCHED

The following is a listing of the sources investigated with period spanned and applicable descriptors for the more fruitful sources.

<u>SOURCE</u>	<u>PERIOD</u>
Air Force Scientific Research Bibliography	1950-1956
Applied Mechanics Reviews	1954-1962
compressible flow	machine design
fluid machinery	machine elements
hydraulic components	pneumatic components
hydraulic controls	pneumatic controls
hydraulics	valves
incompressible flow	
Applied Sciences and Technology Index	1951-1962
fluids	liquids
gas flow	metals wear
gas leakage	pneumatic components
hydraulic analogies	pneumatic controls
hydraulic components	sealing
hydraulic controls	seals
hydrodynamics	valves
Armed Service Technical Information Agency Tabular Bulletins, Cumulative Indexes and Card Catalog	1953-1962
butterfly valve	orifices
check valves	plug valves
control valve	pneumatic valves
gas leaks	pressure regulators
gas seals	reed valves
gas valves	rotary seals



gate valves	rotary valves	
globe valves	safety valves	
high pressure valves	seals	
hydraulic valves	sleeve valves	
metal seals	valves	
California Institute of Technology Card Catalogue and Thesis Index		1951-1962
Catalogue of United States Government Publications		1951-1962
Chemical Abstracts		1951-1961
flow control of gases	valves	
flow control of liquids		
Engineering Index		1951-1961
flow of fluids	pneumatic controls	
hydraulic components	metals wear	
hydraulic controls	sealing	
hydrodynamics	seals	
leakage	valves	
pneumatic components	wear	
Journal National Bureau of Standards		1951-1959
Jet Propulsion Laboratory Card Catalogue & Literature Search List		1951-1962
National Aeronautics and Space Administration Index of Technical Publications		1951-1962
Pacific Aeronautical Library Uniterm Index		1955-1962
Rocketdyne Card Catalogue		1951-1962
Science Abstracts Section A		1951-1962
flow	pneumatic components	
gases	pneumatic controls	
hydraulic components	liquids	
hydraulic controls		
Subject Guide to Books in Print		1961
University of California at Los Angeles Card Catalogue		1951-1962
United States Government Research Reports		1955-1962

## ORGANIZATION AND APPRAISAL OF THE LITERATURE

The literature has been organized under 7 major headings and 24 sub-headings to ease retrieval and facilitate over-all appraisal. A description of the content of each of the major headings listed below is contained within the bibliography

- 1.0 Valve Selection and Evaluation
- 2 0 Steady Flow Characteristics
- 3.0 Steady State Forces
- 4.0 Transient Factors
- 5 0 Valve Sealing
- 6.0 Valve Design Data
- 7 0 Books

The references within each group are listed alphabetically first by source and then by author.

All but 49 of the 286 documents referenced were examined for subject content under the various subheadings. In addition to the primary topic, subject matter which was considered to be useful to valve designers is noted following the abstract and also referenced within the applicable subsections. The subjects foldout after the author index will allow a ready perusal of the reference subject matter. An appraisal of each document has been added noting industry orientation,<sup>(1)</sup> primary fluid category and hardware description (if any). Where a specific valve is involved the valve closure and seat detail are also noted.

Articles and reports considered to be especially timely, comprehensive or useful have been asterisked.

---

(1) "Aircraft" or "industrial" orientation was decided on the basis of the industry at which the references were directed. If the direction was uncertain or none indicated, the reference was noted "aircraft."

## 1.0 VALVE SELECTION AND EVALUATION

This section contains those data considered most pertinent to configuration analysis. It is comprised of both generalized descriptive matter in addition to highly detailed analyses on specific valve designs. Broadly speaking, design information about valves which is either generalized or extremely comprehensive is located under the subheadings listed below. Because of the extensiveness of this section, material contained therein has been considerably cross-referenced within other sections. The subdivisions of the section are as follows:

- 1.1 General Description of Valves and Applications
- 1.2 Description of Specific Valve Designs and Applications
- 1.3 Analysis, Design and Test of Specific Valves
- 1.4 Selected References on Servo Valves

Data within 1.1 is almost entirely descriptive. Here is information relative to the advantages and disadvantages of various designs and how to best utilize them. Subsection 1.2 is on a par with 1.1 except that specific designs are discussed. The material in 1.2 was considered to contain insufficient data to be placed in subsection 1.3 which contains the most comprehensive reports on specific valve designs.

References on servo valves, subsection 1.4, are of a broad and general nature. Although this survey was not directed toward servos, these comprehensive reports have been included because of their applicability, in general, to other valve closure mechanisms. Where servo valves have been specifically analyzed (in the references) for characteristics falling under other headings, they are so categorized and will be found under the 1.4 cross references.

## General Description of Valves and Applications

### 1.1-1 CONTROL VALVES: A GUIDE TO THEIR SELECTION AND USE

Beard, C. S.

AUTOMATIC CONTROL

p. 18+, August 1957

This article shows how system variables influence the final choice of a valve and where to use it.

Industrial

### 1.1-2 HOW CONTROL VALVES BEHAVE

Holzbock, W. G.

CHEMICAL ENGINEERING

66:137-40, #5, 1959

For satisfactory valve operation, consider process and valve characteristics when selecting control valves.

Industrial

### 1.1-3 SELECT SPECIAL CONTROL VALVES

Holzbock, W. G.

CHEMICAL ENGINEERING

66:139-44, #9, 1959

**Bellows Seal:** Where toxic or valuable fluids need leakproof valves.

**Venturi Throat:** Handle high fluid velocities.

**Three-Way:** For variable-flow mixing.

**Diaphragm Control:** Easily handle slurries or corrosive fluids.

**Butterfly:** Large flow at low pressures.

**Piston Operated Pneumatic:** For high fluid pressures.

**Spline Plug:** For small flows.

Industrial

### 1.1-4 FACTORS IN SELECTING VALVES FOR COMPRESSIBLE FLOW

Roth, G. L.

CONTROL ENGINEERING

pp. 46-53, December 1955

1 - Usually, these factors are important in selecting a valve:  
**VALVE SERVICE** - ability to withstand extremes of temperature, pressure, vibration, corrosion, etc., and still maintain desired operation.

**VALVE WEIGHT**, which should be at a minimum.

**VALVE MAINTENANCE** costs; they are mainly functions of individual valve design and production methods.

2 - But application engineers should also stress these points:  
VALVE PERFORMANCE CHARACTERISTICS. Are they properly correlated with the system's operational characteristics? System components upstream and downstream of the valve must be considered.

3 - Particularly in choosing one of the following valves:

- A. Butterfly Valve
- B. Slide (or Gate) Valve
- C. Barrel Valve
- D. Poppet Valve

Industrial, Pneumatic, Flow Control Valves.

1.1-5 ALTERNATE VALVE STUDIES, VALVES

McLean, H. J. et al.

GENERAL ELECTRIC COMPANY, GENERAL ENGINEERING LABORATORY,  
ELECTROMECHANICAL DIVISION

CEL 53. April 15, 1952

Industrial

1.1-6 BASIC VALVE TYPES AND FLOW CHARACTERISTICS

Beard, C. S.

INSTRUMENTS AND AUTOMATION.

29:490-502, March 1956

The flow characteristic of a valve establishes its control action in service. Here is a thorough analysis of the characteristics of available valves, and a discussion of available valve types - quick opening, piston, plug cocks, streamlined, rubber pinch, Saunders Patent, rubber sleeve, butterfly, angle, rotary piston, rotary disc, slide, remote manual loading, ball and seat, and low-flow control valves.

Industrial, Flow Control Valves

1.1-7 FLOW CONTROL VALVES

HYDRAULICS AND PNEUMATICS

14:73-8, July 1961

This article covers basic flow control valve design, performance, and function in a circuit. It will help circuit designers select the right valves for cylinder and fluid motor speed control. Previous articles in this series on directional and pressure control valves appeared in February and April issues of HYDRAULICS AND PNEUMATICS.

Industrial, Hydraulic, Flow Control Valves

**1.1-8 PRESSURE CONTROL VALVES**  
**HYDRAULICS AND PNEUMATICS**  
14-69-77, April 1961

This is the second in a series of three articles of hydraulic valves. The first article appeared in the February 1961 issue of HYDRAULICS & PNEUMATICS and covered directional control valves. The third article will be published in the June issue and will describe flow control valves. The series explains basic design and performance characteristics. It presents important factors in selecting the proper valve for a particular application.

Industrial, Hydraulic, Pressure Control Valves

**1.1-9 DIRECTIONAL CONTROL VALVES**  
**HYDRAULICS AND PNEUMATICS**  
pp. 55-63, February 1961

Hydraulic valves can be divided, according to their function, into directional controls, pressure control, and flow controls. This series of three articles will give you an understanding of basic designs and performance characteristics. It will present the important factors which you must be familiar with to select the best valve for a particular application, and to develop a circuit to suit the job.

Industrial, Hydraulic, Direction Control Valves

**1.1-10 MOBILE EQUIPMENT HYDRAULICS, A DESIGN PRIMER -- PART 4. VALVES**  
**Henke, R. W.**  
**HYDRAULICS AND PNEUMATICS**  
14-81-5, 98, September 1961

Mobile equipment places severe demands on hydraulic valves. They must be rugged, have good metering characteristics, be versatile, and require a minimum of service. Mobile equipment circuits seldom require the precise fixed flows or repetitive cycling of machine tools. However, they do require accurate metering to give the operator maximum control over the machine's functions.

Industrial, Hydraulic Valves

**1.1-11 WHAT TO LOOK FOR IN AIR VALVES**  
**Morris, A. E.**  
**APPLIED HYDRAULICS AND PNEUMATICS**  
pp. 67-82, April 1959

How do you find out what's the best air valve for your job? The smart designer checks more than its mounting dimensions and price. He wants to know how it works, its design and construction features, what it's made of. This comprehensive survey of air valves

shows basic designs. Understanding each type, and what its advantages are, will help you design the simplest and most effective fluid power systems.

#### Industrial, Pneumatic Valves

#### 1.1-12 BACK PRESSURE - HOW IT AFFECTS VALVE OPERATION

Pippenger, J. J.  
APPLIED HYDRAULICS  
October 1954

This article deals with the effect of back pressure on hydraulic control valve design. bib.

#### Industrial

#### 1.1-13 STANDARD CLASSIFICATION AND TERMINOLOGY FOR POWER-ACTUATED VALVES INSTRUMENTS AND AUTOMATION

29:898-900. May 1956

Terminology recommended by The Fluid Controls Institute, Inc.

#### Industrial

#### 1.1-14 SELECTION OF A CONTROL VALVE

Beard, C. S.  
INSTRUMENTS AND AUTOMATION  
29:2412-5. December 1956

Final selection of the control valve requires consideration of all the factors discussed in this series. This resume of these factors is based on the Recommended Practice RP 20.1 of the ISA.

#### Industrial

#### 1.1-15 MECHANICAL FEATURES

Beard, C. S.  
INSTRUMENTS AND AUTOMATION  
29:698-703, April 1956

Mechanical features of valve bodies must be considered by the engineer selecting a valve for his job. These features include end connections, body design, guides, seats, stem connection, packing gland, seals and radiators.

#### Industrial

**1.1-16 SELECTION OF CONTROL VALVES**

Brockett, G. F.

INSTRUMENTS

June 1953

Practical considerations in selection of a control valve include body design and construction, materials of construction, stuffing-box factors, choice of inner valve, and choice of valve operator.

Industrial, Flow Control Valves

**1.1-17 CONTROL VALVES**

Love, R. E.

INSTRUMENTS & AUTOMATION

pp. 776-7, May 1954

A resume of valve operators and bodies - including basic features, valve selection, and valve sizing.

Industrial

**1.1-18 TERMINOLOGY OF PROCESS CONTROL VALVES**

Washburn, W. D. et al.

INSTRUMENTS AND AUTOMATION

29:901-3, May 1956

see also ASME paper 55-A-91

Abstracted from ASME Paper 55-A-91, contributed by the Instruments and Regulators Division for presentation at the ASME Diamond Jubilee Annual Meeting, Chicago, Ill., Nov. 13-18, 1955.

Industrial

**1.1-19 VALVES**

Edwards, T. W.

POWER

105:69-85, June 1961

The factors in selection... recent advances in materials and fluid-loss technology ... a study of fluid-end types ... valve actuators available ... and finally, practical ideas on maintenance.

Industrial



# 1.1-20 HYDRAULIC CONTROL VALVES. I-RELIEF VALVES

Pippenger, J. J.  
PRODUCT ENGINEERING  
pp. 174-81, December 1956

This article is intended to cover the identification, function, construction, installation and maintenance of relief valves in relation to the circuit as a whole and to help in analyzing and predicting malfunction and making satisfactory correction. In some instances it may be of assistance in tailoring a valve to a specific application. bib.

Industrial, Hydraulic Relief Valves

# 1.1-21 FLOW CHARACTERISTICS IN CONTROL VALVES AND REGULATORS

Leibleich, N.  
1952 PROCEEDINGS OF SOUTHWESTERN GAS MEASUREMENT

Industrial

# 1.1-22 INDUSTRIAL HYDRAULICS MANUAL

VICKERS, INC., Detroit, Michigan  
Manual #935100, 1957

Industrial

# 1.1 CROSS REFERENCES

7.0-2  
-3  
-4  
-7  
-9  
-12  
-13

## Description of Specific Valve Designs and Applications

### 1.2-1 CHECK VALVES

Van Deerlin, D.  
APPLIED HYDRAULICS  
pp. 71+, April 1957

Check valves are used to pass flow freely in one direction and seal tightly against flow in the opposite direction. Here are several designs including the relatively new poppet type.

Aircraft, Check Valve, Swing and Poppet, Metal to Metal & Soft Seat

### 1.2-2 CONTRIBUTIONS TO HYDRAULIC CONTROL--6. NEW VALVE CONFIGURATIONS FOR HIGH PERFORMANCE HYDRAULIC AND PNEUMATIC SYSTEMS

Lee, S. Y.  
AMERICAN SOCIETY OF MECHANICAL ENGINEERS, TRANSACTIONS  
76.905-12, August 1954  
See also paper 53-A-139

In high-performance hydraulic and pneumatic systems, three-way or four-way valves of very high precision are required. Conventional spool-type valves used for this purpose have been found to be difficult and expensive to manufacture. This paper describes a new type of metering orifice and several valve designs utilizing this metering orifice. These valves have proved to be considerably easier to make and more trouble-free than the piston-type design with the same performance. Flow-force-reduction methods for this type also are described. The work to be reported here was carried out at the Dynamic Analysis and Control Laboratory and was supported by the U.S. Navy Bureau of Ordnance Contract NOrd 9661 with the Division of Industrial Cooperation of the Massachusetts Institute of Technology.

1.4, 3.1, 3.2

Aircraft, Servo Control Valve, Plate

### 1.2-3 STUDY OF VALVING IN MILITARY RESPIRATORS. 1. OUTLET VALVES

Muirhead, J. C. et al.  
CANADA, DEFENCE RESEARCH CHEMICAL LABORATORIES  
DRCL Report 165. May 1954. SECRET  
AD 40309

Aircraft, Pneumatic Valve

1.2-4 SPRING LOADED RELIEF VALVES

Bigham, J. E.  
CHEMICAL ENGINEERING  
65:133-6, #3, 1958

Here are the factors to consider for correct relief valve discharge under various conditions in process equipment. Capacity formulas show how to find valve area.

Industrial, Pneumatic Relief Valve, Direct Operated

1.2-5 HOW TO DESIGN A PRESSURE RELIEF SYSTEM

Conison, J.  
CHEMICAL ENGINEERING  
67:109-14, #15, 1960

Adequate relief devices but undersized headers can be disastrous - proper design can help ensure the safety of your plant. Here is a new approach.

2.1, 2.3

Industrial, Pneumatic Relief Valve, Direct Operated

1.2-6 VALVE: PNEUMATIC CHECK 3000 PSI

Martin, M. W.  
CONSOLIDATED VULTEE AIRCRAFT CORPORATION  
Report FZC-4-139(A). 3 June 1954  
AD 60779

Aircraft, Pneumatic, Check Valve

1.2-7 APPLICATION OF THE PLUG VALVE AS A PRESSURE AND FLOW CONTROLLER

Gaines, W. L.  
GAS AGE. 119:29-32+, February 4, 1957

Southern Natural's experience indicates the pneumatic plug valve controller to be a valuable tool in gas pressure and flow control work.....

Industrial, Rotary Flow Control Valve

1.2-8 CAN 4-WAY SPOOL VALVES BE IMPROVED?

Dodge, L.  
HYDRAULICS AND PNEUMATICS  
15:80-85, July 1962

As the most widely used valve, the 4-way commands the attention of many hydraulic designers. These valves perform anywhere from

adequately to excellently, yet new demands continually challenge engineers for new, improved valves. Here are new ideas and designs (some perhaps controversial) for 4-way, spool-type directional control valves.

3.1. 3.2

Aircraft Hydraulic, Flow Control Valve, Spool

- 1.2-9 SAFETY AND RELIEF VALVES  
Marion, F. D. et al.  
INSTRUMENTS AND AUTOMATION  
30:2249-54, December 1957

Proper application of the proper type of safety device requires knowledge of the types available, and ingenuity in foreseeing all possible causes for trouble. Here are the available types.

Industrial, Relief Valves, Direct Operated, Poppet, Metal to Metal Seat.

- 1.2-10 THE PRESENT STATUS OF HIGH PRESSURE MEASUREMENT AND CONTROL.  
PARTS 1 AND 2  
Howe, W. H.  
ISA JOURNAL  
2:77-9, 109-13, 1955

Valve design for high pressures. bib.

Industrial, Flow Control Valve, Poppet Metal to Metal Seat, Very High Pressure.

- 1.2-11 PUMP AND CONTROL VALVE DESIGN DETERMINED BY MINIMUM COST  
Roby, M. A. et al.  
ISA PROCEEDINGS  
Preprint 3-SF-60 for meeting of May 9-12, 1960

Based on a survey of several hundred control valve installations, a series of charts have been developed for selecting the proper valve and pump sizes to yield the lowest over-all cost for installed equipment.

Industrial Valve

- 1.2-12 PROPELLANT VALVES IN SMALL LIQUID ENGINES  
CALIFORNIA INSTITUTE OF TECHNOLOGY, JET PROPULSION LABORATORY  
Literature Search 82. CONFIDENTIAL  
July 1958

Aircraft, Propellant Valve

- 1.2-13 A HIGH PRESSURE GAS VALVE FOR USE UP TO 3000 ATMOSPHERES  
Robinson, D. W.  
JOURNAL OF SCIENTIFIC INSTRUMENTS  
30:483-4, 1953

A high-pressure gas valve for use up to 3000 atmospheres.

Industrial, Pneumatic Flow Control Valve, Manual Operated,  
Poppet, Very High Pressure

- 1.2-14 BUTTERFLY VALVES FOR HIGH PERFORMANCE APPLICATIONS  
Dahle, B.  
MACHINE DESIGN  
30:105-9, December 25, 1958

Inherent advantages have made butterfly valves ideal for modulating air flow in pneumatic systems, within limits. This article presents a close look at recent advances in design which have extended the operational limits of these valves.

2.2, 3.2

Aircraft, 2-Way Flow Control Valve, Butterfly, Metal to Metal and Soft Seat

- 1.2-15 A SOLID PROPELLANT GAS GENERATING SYSTEM FOR A SMALL TURBINE-DRIVEN POWER SUPPLY  
Downey, R. B.  
MASSACHUSETTS INSTITUTE OF TECHNOLOGY, DEPT. OF MECHANICAL ENGINEERING  
S. B. Thesis, February 1955

The solid propellant characteristics which were found to be pertinent to the operation of a gas generator system are described. The method which was used to determine the propellant requirements of a turbine-alternator auxiliary power supply is presented. The reasons for the selection of a particular propellant are given and the development of a suitable igniter for the system is described. A large portion of the report concerns the development of a simple type of pressure-regulating valve for use with propellant gases. The design of the several regulators which were built and the modifications which were necessary to overcome successfully such problems as erosion, overheating, and stability are discussed. An analysis of pressure-regulator stability is presented. The test facility, equipment, test methods and instrumentation are described.

4.2, 5.5

Aircraft, Hot Gas Pressure Regulator

## 1.2-16 SOLID FUELS AS HOT-GAS ENERGY-SOURCES

Mann, R. W.

MASSACHUSETTS INSTITUTE OF TECHNOLOGY, DYNAMIC ANALYSIS AND  
CONTROL LABORATORY

Report No. 122, April 30, 1959

The solid fuel as an energy source for isolated systems is compared with other sources on a specific weight and volume basis. Chemical, thermodynamic, and physical properties of the solid fuel, and its products of combustion are discussed and related to a design technique by which the grain configuration for specific applications can be determined. The ignition process is discussed, as is the problem associated with heat transfer prior to ignition and during burning. Finally, the design of a hot-gas pressure regulator is described and several solid fueled devices developed at D.A.C.L. are referenced.

4.2, 5.4, 6.2

Aircraft, Hot Gas Pressure Regulator, Poppet, Metal to Metal Seat

## 1.2-17 RELIEF VALVES

Kowalski, S.

MISSILE DESIGN AND DEVELOPMENT

pp. 64-6, June 1960

This article compares the characteristics of conventional and inverted type relief valves. bib.

4.2

Aircraft, Relief Valve, Direct Operated, Poppet

## 1.2-18 DESIGN AND DEVELOPMENT OF THE HIGH TEMPERATURE FUEL VAPOR VENT VALVE

NORTH AMERICAN AVIATION, INCORPORATED, DOWNEY

Report No. AL 2674, September 1957

Contract AF 33(600)28649

AD 147818

This report documents the design and development of a high-temperature vent valve capable of operating in an 800-F atmosphere, and of passing 4 lb/sec of fuel vapor at an inlet pressure of 30 psia and with a pressure drop of less than 1 psi. The leakage requirement across the seat when in a closed position is a maximum of 100 scfm with an inlet pressure of 30 psia, an outlet pressure of 0.5 psia, and a valve actuation pressure of 175 psig.

2.2, 2.5

Aircraft, Pneumatic Vent Valve, Remote Pilot Poppet, Metal to Metal Seat

1.2-19 DESIGN AND DEVELOPMENT OF ABSOLUTE PRESSURE REGULATOR AND VENT VALVE

NORTH AMERICAN AVIATION, INCORPORATED, DOWNEY  
Report AL 2729, October 1957  
Contract AF 33(600)28469

The development, operation, constituent parts and analyses of a pressure regulating valve are described. Purpose of the valve is to maintain compartment absolute pressure between 15 and 17 psia. The present design evolved from valves used in X-10 and XSM-64 missiles, but differs from them in that it acts as a pressurizing as well as a vent valve. No models of the latest design were constructed, but it is believed that all functions of the valve would meet specifications. An outline of the proposed functional and environmental tests is included.

Aircraft, Pneumatic Vent Valve & Pressure Regulator, Piloted, Poppet, Metal to Metal Soft Seat

1.2-20 THE DEVELOPMENT OF AN ELECTRO-PNEUMATIC VALVE

Madigan, M. F.  
PLESSEY COMPANY LIMITED, GREAT BRITAIN  
Interim Report. Report PL.G.W. 35. May 1954. SECRET  
AD 39226

Aircraft, Pneumatic Valve

1.2-21 VALVE FOR GAS SERVICE TO 50,000 POUNDS PER SQUARE INCH

Mills, R. L.  
REVIEW OF SCIENTIFIC INSTRUMENTS  
27:332-4, 1956

This article describes the design of a very high pressure hand valve. bib.

Industrial, Pneumatic, 2-Way Flow Control Valve, Manual Operated, Poppet, Metal to Metal Seat

1.2-22 EVALUATION OF HIGH TEMPERATURE VALVE DIAPHRAGMS AND SAUNDERS TYPE VALVES DEVELOPED UNDER CONTRACT

Lemp, J. F. Jr. et al.  
U. S. ARMY CHEMICAL CORPS, BIOLOGICAL LABORATORIES  
BWL Technical Memo 2-31. January 1959  
AD 252406L

Industrial Valve

**1.2-23 EVALUATION OF THE ECLIPSE-PIONEER MODEL 845449 PROPELLANT VALVE ASSEMBLY**

Brown, P. et al.

U. S. NAVAL AIR MISSILE TEST CENTER

Technical Report 79. May 1951

AD 140714

An evaluation of the Eclipse-Pioneer Model 845449 Propellant-Valve Assembly as a component of a LARK propulsion system has been made. The evaluation combined a theoretical analysis of valve operating characteristics with supporting data obtained from bench tests. It is concluded that the valve assembly is unsatisfactory in its present configuration, but probably could be made acceptable by incorporating several modifications.

2.2, 3.3

Aircraft, Propellant, 2-Way Flow Control Valve, Remote Pilot, Poppet, Metal to Metal Seat

**1.2 CROSS REFERENCES**

1.4-2  
-4

6.2-1  
-2

7.0-4  
-16



## Analysis, Design and Test of Specific Valves

### \*1.3-1 DESIGN, DEVELOPMENT AND TESTING OF MULTIPLE-PASSAGE PNEUMATIC SOLENOID VALVE AIRESEARCH PART 319152 VOLUMES I AND II

Horacek, H. P.

AIRESEARCH MANUFACTURING COMPANY

Report No. AE-7474-R, Volumes 1 & 2. July 1960

AFBMD TR 60-179 Volumes 1 & 2

Contract AF 04(647)163

AD 243350 and AD 243351

The multiple-passage solenoid valve configuration developed consists of a four-way valve controlled by an integrally mounted, internally vented, solenoid-operated pilot valve. Both the main valve and the solenoid valve employ double poppet and seat arrangement. The solenoid coil developed is capable of operation over a temperature range of  $-320^{\circ}\text{F}$  to  $+250^{\circ}\text{F}$  with no appreciable change in current. The valve is designed for operation with cryogenic fluids in ballistic missile pressurization systems, and is capable of operating with inlet pressures up to 5000 psig.

2.2, 2.5, 3.3, 4.1, 4.3, 5.3, 6.2

Aircraft, Pneumatic, Solenoid Operated Valve, Pilot Operated, 4-Way, Poppet, Metal to Metal Seat

### 1.3-2 DESIGN, DEVELOPMENT AND TESTING OF NON-MODULATING PRESSURE CONTROL VALVES, VOLUMES I TO II

Smith, L. K.

FREBANK COMPANY

AFBSD TR 61-71, Volumes 1 to 3. December 1961

Contract AF 04(647)429

AD 273063, AD 273064 (for Volumes 1 and 2)

The purpose of the program was to develop highly reliable gas pressure control valves using the Belleville spring snap-action concept. The developed units would be simple, rugged, highly vibration and temperature resistant, and suitable for missile or spacecraft applications.

The design and development of a regulator and relief valve are described. Results of demonstration tests for the relief valve are given. Conclusions of test results are stated, together with recommendations for further development.

The program is described in three volumes. Volume I describes in detail the design and development of a regulator and relief valve. Volume II provides detailed drawings, assembly procedures, specifications, and an earlier technical note issued

during the initial phase of the program. Volume III presents a detailed mathematical analysis of the snap action regulator prepared by the Aeronutronic Division of the Ford Motor Co.

2.2, 2.5, 4.1, 4.2, 4.3, 5.3, 6.2

Aircraft, Pneumatic, Direct Operated Relief Valve, Poppet, Metal to Metal Spherical Seat.

- 1.3-3 DEVELOPMENT OF A VERY QUICK ACTING ELECTROHYDRAULIC VALVE  
Read, F. W.  
GREAT BRITAIN, ROYAL AIRCRAFT ESTABLISHMENT  
Technical Note IAP 1030. June 1954

Aircraft, Hydraulic

- 1.3-4 ANALYTICAL AND EXPERIMENTAL STUDY OF TRANSIENT RESPONSE OF PRESSURE REGULATING RELIEF VALVE IN HYDRAULIC CIRCUIT  
Gold, H. et al.  
NATIONAL ADVISORY COMMITTEE ON AERONAUTICS  
Technical Note 3102. March 1954

Aircraft, Hydraulic, Pressure Regulator & Relief Valve

- \*1.3-5 DESIGN AND DEVELOPMENT OF THE XSM-64A BOOSTER LIQUID OXYGEN TANK VENT VALVE  
NORTH AMERICAN AVIATION, INCORPORATED, DOWNEY  
Report No. AL 2671. September 1957  
Contract AF 33(600)28469  
AD 158018

The history, description, analysis, and development of a pneumatically assisted valve for venting the liquid oxygen tank is described. Although intended to vent oxygen vapors from a guided missile, the design is adaptable to the venting of any large liquefied gas tank, either grounded or airborne.

The final valve design has a maximum venting rate of 60 lb/sec of oxygen vapor at 45 psig inlet pressure. It is designed to operate at ambient temperatures of -40°F and +165°F and fluid temperatures as low as -320°F. The valve was designed to vent tank pressures between 0 psig and 45 psig, the cracking pressure being a function of the pneumatic actuation pressure supplied to aid the spring. The design is satisfactory for all standard airborne and ground environmental conditions.

The principal conclusion reached is that valves having these requirements should use pneumatic actuation pressure in conjunction with spring forces to give the proper force balance

under all operating conditions. Another conclusion is that the Teflon dynamic seals described are superior to heated "O"-rings.

2.2, 2.5, 3.2, 3.3, 4.1, 4.2, 5.3, 6.2

Aircraft, Cryogenic, Vent & Relief Valve, Pilot Operated,  
Poppet, Soft Lip Seal

**\*1.3-6 DESIGN, DEVELOPMENT AND TESTING OF ADVANCED PNEUMATIC SOLENOID VALVE (SINGLE PASSAGE) PART NO. 4683-59302**

Bacha, C. P.

NORTH AMERICAN AVIATION, INCORPORATED, DOWNEY

Report No. MD 59-79. AFBMD TR 59-18. November 1959.

AD 232180

Contract AF 04(647)160

Design, development, operation, and analysis of a single-passage pneumatic solenoid valve are described. Results of performance demonstration, flight rating, and qualification tests are given and analyzed. Standard test equipment used is listed, and descriptions are given of procedures and arrangements for special tests such as combined environment and limit tests. Conclusions derived from test results are stated, along with recommendations for further development.

2.2, 2.5, 3.3, 4.1, 5.3, 6.2

Aircraft, Cryogenic, Pilot Operated Solenoid Valve, Poppet,  
Metal to Metal Spherical Seat

**1.3-7 DESIGN, DEVELOPMENT AND TESTING OF ADVANCED PNEUMATIC SOLENOID VALVE (SINGLE PASSAGE) PART NO. 4683-59302**

Bacha, C. P.

NORTH AMERICAN AVIATION, INCORPORATED, DOWNEY

Report MD 60-98. AFBMD TR 60-203. September 1960

Contract AF 04(647)160

AD 249079

This work supplements report AFBMD-TR-59-18 (MD 59-79) on design, development, and testing of the single-passage solenoid valve. Results of tests with RP-1, liquid nitrogen, liquid hydrogen, and helium (at liquid hydrogen temperature) are reported, and design improvements incorporated during fabrication of a second lot of valves are described. Previously published documents, including the equipment specification, test procedure, lapping and assembly processes, liquid and low-temperature test requirements, and the solenoid specifications are included.

See 1.3-6

**\*1.3-8 DESIGN, DEVELOPMENT AND TESTING OF A LIQUID HYDROGEN TANK VENT AND RELIEF VALVE**

Neal, A. E. et al.

PARKER AIRCRAFT COMPANY

Report S6OR1616. AFFTC TR 60-71. December 1960

Contract AF 33(616)6710. Project 6753

AD 259086

A summary is presented of the design and development of a liquid H propellant tank vent and relief valve for use in rocket propulsion systems, missiles, and space vehicles. A study was made of the physical properties of liquid H and the properties of materials at liquid H temperatures. Materials were chosen to ensure the reliability, minimum weight, and low leakage of this component. The validity of the valve concept as a pressure control device was well established. A valve was developed with a high degree of steady state accuracy, adequate response characteristics, and consistent crack and reseat characteristics within the specified operating temperature range. An adequate and simple means of thermal compensation of an absolute pressure reference device was developed. Satisfactory operation at -420 F of a valve seat with low seating force and of Mylar diaphragms was demonstrated.

2.2, 3.3, 4.1, 5.3, 6.2

Aircraft, Cryogenic, Vent & Relief Valves, Pilot Operated Poppet, Metal to Metal Flat Seat

**1.3-9 DESIGN, DEVELOPMENT AND TESTING OF A LIQUID HYDROGEN SHUTOFF VALVE**

Hughes, P. R. et al.

PARKER AIRCRAFT COMPANY

Report S6OR1617. AFFTC TR 60-72. December 1960

Contract AF 33(616)6710. Project 6753

AD 259087

Research concerns the development of a liquid hydrogen shutoff valve for use in a rocket propulsion system of a missile or space vehicle. A study was made of the physical properties of liquid hydrogen and the properties of materials at liquid hydrogen temperatures. The prime design objectives for this component were reliability of operation, minimum weight, and low leakage. The validity of the valve concept as a liquid hydrogen shutoff device was well established by development testing of the elements of the final unit. The program has resulted in a valve design with essentially zero leakage at the specified operating temperatures. The valve seat configuration that produced this result was a spherically lapped metal poppet and seat with relatively high unit seat loading. Satisfactory operation of a hydraulically formed bellows for use as a high pressure actuator was demonstrated. Development testing of

components was accomplished with liquid hydrogen. Relatively simple and economical test equipment was used. This was adequate for conducting small scale tests with liquid hydrogen.

2.2, 4.1, 5.3

Aircraft, Cryogenic, Shutoff Valve, Pressure Actuated, Poppet, Spherical Metal to Metal Seat

1.3-10 GAS REGULATOR DESIGN STUDY

Borchert, W. O. et al.

REACTION MOTORS INCORPORATED

Final Report. RMI-493-F. March 1953-May 1954

Contract AF 33(600)23215, AD 70704

Aircraft, Pneumatic, Pressure Regulator

1.3-11 DEVELOPMENT OF GAS REGULATOR

Chamberlain, R. E. et al.

REACTION MOTORS INCORPORATED

Final Report. Report RMI-062-F. WADC YT 57-734

March 1953 to August 1956

Contract AF 33(600)29801

AD 142700

Aircraft, Pneumatic, Pressure Regulator

\*1.3-12 ANALYSIS, DESIGN AND DEVELOPMENT OF HIGH-FLOW HELIUM PRESSURE REGULATOR

ROBERTSHAW-FULTON CONTROLS CO., AERONAUTICAL & INSTRUMENT DIV., FLUID CONTROLS ENGINEERING DEPT.

AFBMD-TR-60-72(1). June 1960

Contract AF 04(647)161

This two-volume technical report describes the work done under contract AF 04(647)161. The work performed includes analysis, design, development and test of a high-flow helium pressure regulator for ballistic missile propulsion system pressurization.

Volume One covers the major aspects of the program, and includes three basic subdivisions of effort:

1. An account of extensive dynamic control analyses performed on the developmental regulator systems, using analog computers.
2. The design and development work.
3. Testing accomplished on various regulator configurations.

Volume Two covers two analytical studies of the charging and venting of single and double volumes through nozzles. This material is presented separately for convenient reference.

4.2, 4.3, 5.2

Aircraft, Pneumatic, Pressure Regulator

- \*1.3-13 DESIGN, DEVELOPMENT, AND TESTING OF ADVANCED HELIUM PRESSURE REGULATOR, PART NO. 551302  
ROCKETDYNE ENGINEERING  
Rocketdyne Report R-2175  
AFBMD-TR-6055, July 1960  
Contract AF04(647)160

The purpose of this program was to develop a component which would advance the state of the art of gaseous helium pressure regulators.

The engineering analysis and design of the component are presented. A description of test facilities, test and development procedures, and the results of development, Performance, Demonstration, Flight Rating, and Qualification Testing are given and analyzed. Conclusions derived from test results and recommendations for future design improvements are presented. In Volume 2, complete detail and assembly drawings, certain specifications, and official test data are presented.

2.2, 2.5, 3.3, 4.2, 5.2, 5.3, 6.2

Aircraft, Pneumatic, Pressure Regulator, Poppet, Metal to Metal Seat

- \*1.3-14 DESIGN, DEVELOPMENT, AND TESTING OF ADVANCED LIQUID OXYGEN TANK VENT AND RELIEF VALVE, PART NO. 551430  
Tomlinson, L. E. et al.  
ROCKETDYNE ENGINEERING  
Rocketdyne Report R-2175  
AFBMD-TR-60-55, March 1960  
Contract AF04(647)160

The purpose of this program was to develop a component which would advance the state of the art of liquid oxygen tank relief valves. The engineering analysis and design of the component are presented. A description of test facilities, procedures, and the results of development, performance demonstration, flight rating, and qualification testing is given and analyzed. Conclusions derived from test results and recommendations for future design improvements and applications are presented.

2.2, 3.3, 4.1, 6.2

Aircraft, Cryogenic, Vent and Relief Valve, Pilot Operated, Poppet, Soft Seat

1.3-15 DESIGN DATA FOR REDESIGN OF SUBMARINE HYDRAULIC VALVES AND COMPONENTS

Hockenhull, I. et al.

U. S. NAVY, PORTSMOUTH NAVAL SHIPYARD

Technical Report P-11685. June 1955

AD 82637

Aircraft, Hydraulic Valve

1.3 CROSS REFERENCES

1.4-2

-4

-5

-6

-7

### Selected References on Servo Valves

- 1.4-1 COMPARISON OF HYDRAULIC, PNEUMATIC AND ELECTRO-MECHANICAL SERVO SYSTEMS: EVALUATION OF SERVOS  
CALIFORNIA INSTITUTE OF TECHNOLOGY, JET PROPULSION LABORATORY  
Literature Search 312. UNCLASSIFIED With CONFIDENTIAL  
supplement February 1961

- \*1.4-2 HYDRAULIC AND SERVO CONTROL VALVES, PARTS 1 THROUGH 7  
COOK ELECTRIC COMPANY, COOK RESEARCH LABORATORY  
WADC TR 55-29  
PART 1 - April 1955  
Contract No. AF 33(616)2447  
AD 70616

A summary of the present state of the art of electro-hydraulic servo valves suitable for aircraft and missile application is presented. This information was obtained from direct visits to both the valve manufacturers and the valve users; namely, the missile and aircraft manufacturers. The valve manufacturers were contacted to obtain detailed design and performance data on the valves; the valve users were contacted to determine the system and valve requirements and to determine how adequately the valves presently being used meet these requirements.

A brief description of the principle of operation of servo valves, in addition to a discussion of the various types, is also presented to provide a background for interpreting the data.

Aircraft, Hydraulic, Servo, Flapper and Spool

PART 2 - August 1956  
Contract No. AF 33(616)2447  
AD 97222

Static and Dynamic test procedures for testing electro-Hydraulic servo valves are developed. Descriptions are presented of tests on nine servo valves, including three Moog valves, two Bell valves, one Cadillac Gage flow control valve, one Cadillac Gage pressure control valve, one Midwestern valve and one MIT hole and plug type of valve. All test data are presented in graphical form. An analysis of test results and a listing of servo valves are also presented.

4.2

Aircraft, Hydraulic, Servo, Flapper and Spool



PART 3 - April 1957

Contract No. AF 33(616)3341

AD 118285

A state-of-the-art summary describing the electrohydraulic valves which have been brought out in the last two years is presented. Valves brought out prior to this are described in WADC TR 55-29 Part 1. Some of the manufacturing problems are reviewed.

A summary of information compiled from visits to aircraft and missile manufacturers is also presented. Their comments as to the performance of the valves presently used in their vehicles are reviewed. In addition, a general discussion of system design procedures plus a listing of typical system characteristics is presented.

1.2

Aircraft, Hydraulic, Servo, Flapper and Spool

PART 4 - August 1957

Contract No. AF 33(616)3341

AD 204815

This report deals with the following four investigations:

- (1) Experimental verification of linearized analysis as applied to electrohydraulic servo valves,
- (2) Investigation of the gain compensation of servo valves,
- (3) Analog study of a typical missile system, and
- (4) Test of three new electrohydraulic servo valves.

4.2

Aircraft, Hydraulic, Servo, Flapper and Spool

PART 5 - August 1958

Contract No. AF 33(616)5136

AD 208266

Analog computer simulation of an electrohydraulic servo valve, investigation of pressure control valves, and design of a high-temperature test facility are discussed. Analytical relations are developed which describe the internal nonlinear operations of the valve. These equations are mechanized on an analog computer and the results verified for static conditions.

The advisability of using a pressure control valve as opposed to a flow control valve in closed loop operation is investigated. The development of a pressure control valve transfer function and experimental verification of the analytical results is included. The requirements for a valve testing facility capable of providing and utilizing oil at 750°F, and an ambient temperature up to 1200°F, are presented.

1.3, 2.2, 2.4, 3.2, 4.2, 6.2

Aircraft, Hydraulic, Servo, Flapper and Spool

PART 6 - November 1958

Contract No. AF 33(616)5136

AD 211733

This report is divided into four sections. Design and operation of a test fixture intended for analysis of servo valve operation under various levels of oil contamination are described. Information on servo valve life and reliability, as obtained from valve manufacturers and users, is presented, and the various design features influencing reliability are discussed. Design and construction of a valve-actuator assembly for use in a nuclear radiation environment are described, and test results on this unit under gamma radiation are presented. A series of evaluation tests was run on one unit each of three new types of valves, and the test results are presented and discussed.

5.4, 5.5, 6.2

Aircraft, Hydraulic, Servo, Flapper and Spool

PART 7 - January 1959

Contract No. AF 33(616)5136

AD 231657

This report is divided into three sections. The first includes a discussion of valve failure and wear mechanisms as the result of contaminated oil, and description, plus test results on certain valves which should tend to reduce such failure. The time-modulated valve and an integral valve-actuator unit were tested. In Section 2, results of particle counts on oil from operational aircraft are presented, suggested maximum allowable counts are given, and a method for testing valves under various levels of oil contamination outlined. Results of operating a servo valve and its load under nuclear irradiation at a Convair, Fort Worth reactor are presented and discussed in the third section.

5.4, 5.5, 6.2

Aircraft, Hydraulic, Servo, Flapper and Spool

1.4-3 HOT GAS SERVOMECHANISM THEORY AND TECHNOLOGY, AN ANNOTATED BIBLIOGRAPHY

Graziano, E. E.

LOCKHEED AIRCRAFT CORPORATION

Sd 61-57. Report No. 3-80-61-34. October 1961

Contract NOrd 17017

AD 269242

A selected list (60) of annotated references on hot gas servo-mechanisms including design, analysis, components, and experience. Some references are to classified reports with unclassified titles, and these are not annotated so that this bibliography may be more widely circulated. Selected items in related areas, such as pneumatics are included.

Aircraft, Pneumatic, Spool

\*1.4-4

#### FLUID POWER CONTROL

MASSACHUSETTS INSTITUTE OF TECHNOLOGY, DYNAMIC ANALYSIS  
AND CONTROL LABORATORY

Contract AF 33 (616)2356. CONFIDENTIAL

Quarterly Progress Report No. 1, Series B. February-April 1954. AD 50931

Quarterly Progress Report No. 2, May-July 1954. AD 63791

Quarterly Progress Report No. 3, Series B. August-October 1954. AD 63792

Quarterly Progress Report No. 4. Series B. November 1954-January 1955. AD 71265

Quarterly Progress Report No. 5. Series B. February-April 1955. AD 68074

Quarterly Progress Report No. 6. May-July 1955. AD 71948

Contract AF 33(616)2356 and Contract AF 33(616)3173.

CONFIDENTIAL

Summary Report. February 1954-December 1955. AD 89064

Contract AF 33(616)3173

Progress Report. December 1955-March 1957. AD 132287

Summary Report. WADC TR 58-596. March 1957-September 1958  
AD 219895

1.2, 1.3, 2.1, 2.2, 3.2, 4.2

Aircraft, Hydraulic, Pneumatic, Servo, Spool, Flapper, Jet-Pipe

1.4-5

#### BASIC RESEARCH AND DEVELOPMENT IN FLUID POWER CONTROL FOR U.S. AIR FORCE

Shearer, L. L.

MASSACHUSETTS INSTITUTE OF TECHNOLOGY, DYNAMIC ANALYSIS  
AND CONTROL LABORATORY

WADC TR 59-275, October 1958-January 1959

Contract AF 33(616)6120

AD 215853

In connection with many of the control problems anticipated in the development of future systems for the penetration of space and effective deployment of various kinds of space vehicles, a number of investigations are being carried out on gas-operated systems. This program, coordinated with the activities of the Flight Control Laboratory, Wright Air Development Center, Ohio, is aimed at applications involving hot-gas control systems to meet advanced system requirements.

Among the most serious problems involved in the development of hot gas systems are: (1) finding simple yet effective means of controlling the flow and/or pressure of hot-gas power; (2) developing fast-response servomotors to operate on hot gas with a minimum of static or stick-slip friction; and (3) gaining a better understanding of the factors which can cause dynamic instability of components and/or complete systems. Some aspects of each of these three major problem areas are discussed in the following parts of this report which describe the work currently underway on this contract.

1.3, 2.2

Aircraft, Pneumatic, Servo, Flapper

**\*1.4-6 BASIC RESEARCH AND DEVELOPMENT IN FLUID POWER CONTROL FOR THE U.S. AIR FORCE**

Mann, J. R., et al.

MASSACHUSETTS INSTITUTE OF TECHNOLOGY, DYNAMIC ANALYSIS AND CONTROL LABORATORY

Contract AF 33(616)6120. Project 8225

Progress Report No. 2 WADD TR 59-491 February-May 1959  
AD 229465

Progress Report No. 3 WADD TR 59-7. June-September 1959  
AD 232965

Progress Report No. 7 WADD TR 61-179. August 1961  
AD 267050

This report describes continuing applied research and development work on problems vital to the design and development of high performance hydraulic and pneumatic control equipment for advanced systems. Increased emphasis on high pressure pneumatic components and systems reflects the approach to an ultimate objective of employing hot-gas power to operate such systems. Control valves, relays, servomotors, gas bearings, fluid power and signal transmission, hot-gas contamination, hot-gas gyros, and techniques of control are the major items discussed in this report.

1.3, 2.2, 3.2, 4.2

Aircraft, Pneumatic, Servo, Flapper, Jet-Pipe

**1.4-7 OPTIMUM DESIGN PARAMETERS OF A PNEUMATIC JET PIPE VALVE**

Reid, K. N. Jr.

MASSACHUSETTS INSTITUTE OF TECHNOLOGY, DEPARTMENT OF MECHANICAL ENGINEERING

Thesis. June 1960

The pneumatic systems designer must have available the pressure-flow displacement characteristics of pneumatic valves. Once these characteristics are known, the valves can be treated

analytically in the design of fluid power circuits. This paper presents experimental pressure-flow displacement relationships for a conventional jet-pipe valve operating with compressed air. The ratio of the jet-pipe nozzle diameter to the receiving hole diameter, the jet-pipe nozzle to receiving hole spacing, and the pressure level of the jet-pipe supply are discussed as to their effect on the over-all characteristics of the valve. Optimum design conditions are established on the basis of a maximum power transfer criterion. The jet-pipe valve is compared with other typical valves from the standpoint of power transfer, reliability, and load sensitivity.

1.3, 2.2, 2.5, 4.2

Aircraft, Pneumatic, Servo, Jet-Pipe

#### 1.4-8 A STUDY OF PNEUMATIC AND HYDRAULIC SERVOMECHANISMS

Chelomey, V. N.

U. S. AIR FORCE SYSTEMS COMMAND, FOREIGN TECHNICAL DIVISION,  
WRIGHT PATTERSON AIR FORCE BASE

Translation No. FTD-TT-61-107. 14 December 1961

From Avtomaticheskoye Upravlenie i Vychislitel'naya Tekhnika,  
Moscow, pp. 166-81, 1958

AD 268864

In the present article we examine question in the theory of pneumatic and hydraulic servomechanisms, with valve distribution, used as steering mechanisms.

Aircraft, Servo

#### 1.4 CROSS REFERENCES

1.2-2	2.2-3	3.1-1	3.2-1	4.2-1	5.4-1	7.0-4
	-5	-2	-2	-2	-3	-7
	-10	-3	-3	-4	-4	
		-4	-5	-6	-5	
		-5	-8	-7	-6	
			-10		-7	
			-15			

## 2.0 STEADY FLOW CHARACTERISTICS

This section contains references dealing primarily with gross fluid flow. The subdivisions are as follows:

- 2.1 Flow Through Single Elements
- 2.2 Flow Through Valves
- 2.3 Flow Through Composite Systems
- 2.4 Valve Sizing Formulas
- 2.5 Internal Passage Design for Flow
- 2.6 Cavitation and Other Flow Phenomena

Subsection 2.1 contains pertinent data on flow through orifices, nozzles, venturis, fittings, pipe lines, etc. Material containing analysis and/or test information on valve flow such as discharge coefficients or partial open flow characteristics is located within subsection 2.2. System flow and the analysis of the system effect on the valve or the converse is covered in subsection 2.3. All literature specifically describing or proposing formulas for either valve sizing or specification is contained within subsection 2.4. Cross references in this subsection apply only to those articles or reports which suggest original approaches. The criteria for classification under 2.5 is that the material must contribute significantly to the detail design considerations of the subject. Material having detail design information (i.e., detail drawings) accompanied with flow test data has been cross referenced in 2.5. Material on cavitation and other flow phenomena is contained in 2.6, however, if the material was equally divided in subject content, the higher category took precedent (e.g., "Cavitation and Flow Forces in Butterfly Valves" would be found under 3.2, Flow Forces). Cross reference should be reviewed accordingly.

## Flow Through Single Elements

### 2.1-1 FLOW THROUGH ANNULAR ORIFICES

Bell, K. J. et al.

AMERICAN SOCIETY OF MECHANICAL ENGINEERS, TRANSACTIONS

79-593-601, April 1957

Coefficients for the annular orifice formed between a circular disk and a cylindrical tube are reported for twenty-one orifices having disk diameter to tube diameter ratios in the range of 0.95 to 0.996, and orifice length-to-width ratios from 0.118 to 33.3. The orifice Reynolds-number range is from 2.0 to 20,000 for both tangent and concentric orientations of the disk. Comparison with previous data indicates that the results also apply to the annular orifice formed when a rod extends through a circular hole in a plate. Theoretical and semi-empirical equations are developed to predict coefficients for annular orifices.

Industrial

### 2.1-2 DISCHARGE COEFFICIENTS OF SMALL DIAMETER ORIFICES AND FLOW NOZZLES

Grace, H. P.

AMERICAN SOCIETY OF MECHANICAL ENGINEERS, TRANSACTIONS

73-639-47, 1951

Discharge coefficients were determined in a standard 1-in. pipe for thick-plate and knife-edge orifices of 1/32-in. to 3/4-in. dia., and for critical (sonic) flow nozzles of 1/32-in. to 1/4-in. dia. With properly constructed knife-edge orifices, the discharge coefficients were established with  $\pm 0.5$  percent for all sizes, but, with small orifices of 1/4 to 1-hole-dia. thickness, the discharge coefficients were not reproducible. Thick-plate orifices (1-hole-dia. thick) were found to be as good or better than nozzles in constancy of discharge coefficients when used under critical-flow conditions.

Industrial, Pneumatic

### \*2.1-3 CRITICAL FLOW THROUGH SHARP-EDGED ORIFICES

Perry, A. J. Jr.

AMERICAN SOCIETY OF MECHANICAL ENGINEERS

Paper 48-A-146 for Meeting November 28, 1948

An investigation was made to discover the flow rates of air through sharp-edged orifices in which the pressure drop was below the critical, the relationship of pressure, temperature, and orifice area; and a comparison between the nozzle and the orifice. Equations are derived for expressing orifice flow in both the critical and subcritical regions.

Industrial, Pneumatic

2.1-4 STUDY OF FLUID FLOW THROUGH FLEXIBLE ORIFICES

Ulrich, R. D. et al.

ASHRAE JOURNAL (American Society of Heating, Refrigerating,  
and Air Conditioning Engineers).

3:63-70, October 1961

A method is developed for predicting the flow rate-pressure drop relationship for a given geometrical situation and rubber hardness for a flexible orifice.

Industrial

2.1-5 WHERE COMPRESSIBILITY MUST BE CONSIDERED, CALCULATE FLUID FLOW BY BASIC EQUATIONS

Polentz, L. M.

CHEMICAL ENGINEERING

64:282, 284, 286, #8, 1957

Problems show how to account for thermodynamic effects for compressible fluid flow through pipelines and orifices.

Industrial, Pneumatic

2.1-6 BASIC EQUATIONS ARE FASTER AND ACCURATE

Polentz, L. M.

CHEMICAL ENGINEERING

64:270, 272, 274, 276, #7, 1957

This article presents a summary of pipe flow relationships. bib.

Industrial, Pneumatic

\*2.1-7 FLOW OF FLUIDS THROUGH VALVES, FITTINGS, AND PIPE

CRANE COMPANY

TP-409, TP-410. 1956, 1957

This is a comprehensive handbook on fluid flow covering the more practical aspects of flow through pipe, valves and fittings. Examples of solutions to flow problems are given in addition to considerable empirical data. This report represents an outstanding contribution to industry. bib.

2.2, 2.3, 2.4, 2.5, 6.1

Industrial



**2.1-8 REVIEW OF THE LITERATURE ON TWO-PHASE (GAS-LIQUID) FLUID FLOW IN PIPES**

Gresham, W. A., Jr. et al.

ENGINEERING EXPERIMENT STATION OF THE GEORGIA INSTITUTE OF TECHNOLOGY.

WADS-TR 55-422, June 1955

Contract AF 33(616)2660

AD 95752

All available literature on the subject of two-phase (gas-liquid) fluid flow was studied and the significant literature is summarized in this report.

Gas-liquid flow can be classified into at least seven different types of flow in horizontal ducts and five types in vertical ducts. For a given combination of fluids, it is possible to roughly correlate the flow types with the flow rates.

Most of the early workers utilized friction factor-type relations in their attempts to correlate the pressure drops and flow rates. The first generalized relation was presented by Martinelli and co-workers who correlated the two-phase pressure drop with that of the liquid or gas assumed to flow alone in the duct. Most subsequent investigators have used modifications of this correlation. A few investigators have attempted to solve relations based on the continuity, energy, and momentum equations.

Abstracts of one hundred and eight references are included.

Aircraft

**2.1-9 ON THE FLOW OF A COMPRESSIBLE FLUID THROUGH ORIFICES**

Jobson, D. A.

GREAT BRITAIN, AERONAUTICAL RESEARCH COUNCIL

ARC Report 16,376. CONFIDENTIAL. December 1953

AD 41023

Aircraft, Pneumatic

**2.1-10 FRICTION FACTOR PLOT: FOR SMOOTH CIRCULAR CONDUITS, CONCENTRIC ANNULI, AND PARALLEL PLATES**

Lohrenz, J. et al.

INDUSTRIAL AND ENGINEERING CHEMISTRY

52:703-6, August 1960

This new approach to the old annulus problem presents a friction factor correlation which can be used without difficulty and which yields a satisfactorily constant value of the critical Reynolds number.

A literature survey of the experimental studies of pressure drop for fluid flow through concentric annuli was completed.

Industrial

2.1-11 FLOW OF A COMPRESSIBLE FLUID THROUGH A SERIES OF IDENTICAL ORIFICES

Robinson, C. S. L.  
JOURNAL OF APPLIED MECHANICS  
15:308-10, 1948

This paper contains a method for computing the weight flow of a gas or vapor through a number of like orifices. It is based upon the general equation for a single orifice and upon certain reasonable assumptions. There are included curves showing the influence of the number of orifices. For expansions beyond the over-all critical-pressure ratio, the effect of each additional orifice is increasingly reduced. For example, increasing the number of like orifices from 6 to 7 will decrease the flow only about 5 percent. Two applications of this study are suggested; i.e., to multiple-orifice devices for heat-exchange equipment, and to labyrinth packing for shaft seals.

Industrial, Pneumatic

2.1-12 DISCHARGE COEFFICIENTS FOR FLOW THROUGH ROUND-EDGED ORIFICES

Tuffias, R. H.  
MASSACHUSETTS INSTITUTE OF TECHNOLOGY, DEPARTMENT OF  
MECHANICAL ENGINEERING  
SM Thesis, August 1957

Aircraft

2.1-13 INVESTIGATION OF FLOW COEFFICIENT OF CIRCULAR, SQUARE, AND ELLIPTICAL ORIFICES AT HIGH PRESSURE RATIOS

Callaghan, E. E. and Bowden, D. T.  
NATIONAL ADVISORY COMMITTEE ON AERONAUTICS  
Technical Note 1957, September 1949

An experimental investigation has been conducted to determine the orifice coefficient of a jet directed perpendicularly to an air stream as a function of pressure ratio and jet Reynolds number for circular, square, and elliptical orifices. The effect of air-stream velocity on the jet flow was also determined for three tunnel-air velocities. Equations for the flow coefficients in terms of jet Reynolds number and pressure ratio were obtained for the various shapes. Excellent correlation was obtained between the results for a jet discharging into still air and the results for a jet discharging into a moving air stream, provided that the correct outlet pressure was used.

Aircraft, Pneumatic

## **2.1-14 CALCULATING THE ENERGY LOSSES IN HYDRAULIC SYSTEMS**

Sverdrup, N. M.

PRODUCT ENGINEERING

pp 146-52, April 1951

Graphical methods of analyses that save time and make tedious mathematical calculations unnecessary. Charts for frictional and energy loss coefficients in AN hydraulic fittings, circular pipes, and other elements used in hydraulic circuits.

Aircraft, Hydraulic

## **2.1-15 A VERSATILE PNEUMATIC INSTRUMENT BASED ON CRITICAL FLOW**

Wildhack, W. A.

REVIEW OF SCIENTIFIC INSTRUMENTS

21:25-30, January 1950

Gas flows through two restrictions in series, the second one or both being a nozzle operating with sonic throat velocity so that discharge is independent of the downstream pressure. For fixed restrictions, the ratio of entrance pressures at the two restrictions depends on their relative sizes and the ratio of entrance temperatures. After calibration, the pressure ratio may be used to measure temperature with a sensitivity of 1°C or better over a range of 2000°C. With the same arrangement, the temperature being constant, the intermediate pressure is a direct measure of mass flow. A sensitivity of better than 0.1 percent is possible in this measurement. For given temperatures, the device can be used as a "pressure divider," with the intermediate pressure controlled by adjusting the restrictions, or as a pneumatic micrometer. Gas analysis is accomplished by removing one component of the gas flow between nozzles. A vacuum pump is used, if necessary, to ensure critical discharge through one or both nozzles; divergent cones on nozzles may be used to minimize pressure drop.

Industrial, Pneumatic

## **2.1-16 EFFECT OF ABSOLUTE AIR PRESSURE ON THE ORIFICE COEFFICIENT OF A FLAT PLATE ORIFICE AT LOW REYNOLDS NUMBERS**

Dobbins, R. A.

SYLVANIA ELECTRIC PRODUCTS INCORPORATED

Report TR-14-2-22. 9 August 1955

Contract AF 33(038)21250

AD 7-826

Aircraft

2.1-17 AN ANALYTICAL STUDY ON SF-1 METERING CONTROL VALVES

Russell, J. G. et al.  
THOMPSON RAMO WOOLDRIDGE, INCORPORATED  
WADC TR 59-332. November 1957  
Contract AF 33(616)5179  
AD 227239

A study was made of methods to measure and control the flow of hydrogen in the liquid phase, the gaseous phase, and the two phase mixture. A survey was conducted of previous and allied work. Existing designs and new designs of fluid measuring and controlling equipment were analyzed for operation with the fluid. A flow measuring device for two phase mixture was designed and partially fabricated. A test installation was designed and partially constructed.

6.1

Aircraft, Cryogenic

\*2.1-18 VERIFICATION OF A THEORETICAL METHOD OF DETERMINING DISCHARGE COEFFICIENTS FOR VENTURIS OPERATING AT CRITICAL FLOW CONDITIONS

Smith, R. E. et al.  
U. S. AIR FORCE, ARNOLD ENGINEERING DEVELOPMENT CENTER  
AEDC TR 61-8. September 1961  
Contract AF40(600)800. Project 931002  
AD 263714

When the accurate measurement of the flow rates of air or gases is required, the use of a venturi flowmeter which operates at critical flow conditions has certain advantages. A venturi contour designed specifically for use at critical flow conditions is described, and a theoretical method is presented for determining the discharge coefficient of this venturi.

An experimental investigation was conducted to determine the discharge coefficient of such a venturi, and the results are compared with the theoretical values. This investigation covered a range of Reynolds number from  $0.4 \times 10^6$  to  $5.4 \times 10^6$  based on venturi throat diameter. The venturi used had a throat diameter of 5.6436 in. and, therefore, an airflow capacity of 8.6 lb/sec at an inlet total pressure of one atmosphere and an inlet total temperature of 519°R. The values of discharge coefficient ranged from 0.992 to 0.994, and the theoretically and experimentally determined coefficients agreed within  $\pm 0.06$  percent over the range of conditions investigated.

Aircraft, Pneumatic

2.1-19 IMPROVED METHODS OF FLOW CALCULATIONS OF THE RATES OF FLOW THROUGH SHARP EDGED CONCENTRIC ORIFICES

Murdock, J. W. et al.

U. S. NAVAL BOILER AND TURBINE LABORATORY

Interim Report #1. NBTL Test Report I-83. May 1953

AD 35591

This report presents methods and physical data for accurate calculation of the rate of flow through sharp-edged concentric orifices, constructed and installed in accordance with the standards set by the Joint Committee of the American Society of Mechanical Engineers and the American Gas Association Orifice Meter Committee. Flow coefficient data are presented for all four standard tap locations and physical data for Air, Oxygen, Steam and Water. By use of standard forms, precise calculations can be made without prior knowledge of fluid flow theory. Assumptions of Reynolds number and successive approximations before reaching the final answer are eliminated.

Aircraft

2.1 CROSS REFERENCES

1.2-5	1.4-4	2.2-13	2.3-3	2.4-15	2.5-2	2.6-2
				-16	-4	
				-17		

5.1-1	5.4-1	6.2-7	7.0-1
-2			-4
-3			-6
-4			-15
-5			
-6			
-7			
-8			
-9			
-10			
-11			
-12			
-13			
-14			
-15			
-16			
-17			
-18			
-19			
-20			
-21			

## Flow Through Valves

### \*2.2-1 BUTTERFLY VALVE FLOW CHARACTERISTICS

McPherson, M. B. et al.

AMERICAN SOCIETY OF CIVIL ENGINEERS, PROCEEDINGS

83(HY-1 No. 1167): 1-28, February 1957

Flow coefficients are given for free and submerged discharge as well as two cases with enclosed flow piping. The effects of type of installation, blade shape and closure angle for control-type valves (using water) are demonstrated. Correlation of analytical relations with performance provides a basis for predicting incipient cavitation.

2.4, 2.5, 2.6

Industrial, Water, Flow Control Valve, Butterfly

### 2.2-2 DISCHARGE COEFFICIENTS FOR GATES AND VALVES

Thomas, C. W.

AMERICAN SOCIETY OF CIVIL ENGINEERS, PROCEEDINGS

81(No. 746):1-26, July 1955

Conservation of our water resources demands accurate measurement of water. Rather than construct separate devices for control and measurement, this paper suggests the use of certain control valves and gates as measuring devices when good calibrations are available. As supporting evidence that such is possible, model and prototype comparisons are made and the results confirm to a reliable degree the validity of the proposal.

Industrial, Water, Poppet Valve

### 2.2-3 CONTRIBUTIONS TO HYDRAULIC CONTROL--3. PRESSURE FLOW RELATIONSHIPS FOR FOUR-WAY VALVES

Blackburn, J. F.

AMERICAN SOCIETY OF MECHANICAL ENGINEERS, TRANSACTIONS

75:1163-70, 1953

The characteristics of several types of 4-way flow-control valves are derived without making linearizing assumptions. These characteristics are plotted as load flow versus load pressures, in a manner analogous to the plate characteristic of a vacuum tube. Several different coefficients are derived and tabulated, and the valves are compared from the standpoint of linearity, sensitivity, power output and losses.

1.4

Aircraft, Hydraulic, Servo Control Valve 4-Way, Spool

2.2-4 SOME HYDRODYNAMIC ASPECTS OF VALVES

Ehrich, F. F.

AMERICAN SOCIETY OF MECHANICAL ENGINEERS

Paper 55-A-114 for meeting of November 13, 18, 1955

Free streamline-potential flow analysis is used to analyze the flow regulation in two-dimensional configurations approximating the flapper valve, the needle valve, the orifice-plate valve, the gate valve, the butterfly valve, and the spool valve. Experimental data are reported which evaluate the accuracy of some of the derived expressions and also evaluate the possibility of applying the results to three-dimensional, axisymmetric configurations. Results are presented in tabular and graphical form. An analysis is also carried out to evaluate the dynamic forces on the moving element of a flapper valve resulting from the motion of the fluid. Equivalent spring force and damping force are detected, as well as some unstabilizing influences of negative damping and negative apparent mass. General descriptions of the origin of these forces are also given.

2.5, 3.2, 4.2

Aircraft, Hydraulic

\*2.2-5 PRESSURE FLOW CHARACTERISTICS OF PNEUMATIC VALVES

Ezekiel, F. D. et al.

AMERICAN SOCIETY OF MECHANICAL ENGINEERS, TRANSACTIONS

79:1577-90, October 1957

The pertinent subject headings in this article are: (1) Flow Through a Single Orifice, (2) Steady Flow Through Two Orifices in Series, (3) Steady-Flow Characteristics of Single Orifice Control, (4) Steady-State Three-Way Valve Characteristics, (5) Steady-State Four-Way Valve Characteristics, (6) Closed-Center Valve, (7) Open-Center Valve (Underlapped), and (8) A Method for Handling Reverse Flows.

1.4

Aircraft, Pneumatic, Servo Control Valves

\*2.2-6 STATIC-FLOW CHARACTERISTICS OF SINGLE AND TWO-STAGE SPRING-LOADED GAS PRESSURE REGULATORS

Iberall, A. S.

AMERICAN SOCIETY OF MECHANICAL ENGINEERS, TRANSACTIONS

pp 363-373, April 1954

see also paper 53-F-5

A theoretical investigation of greater completeness than is usually presented has been made of gas pressure regulators. Emphasis has been placed on the application to their design. The analysis is summarized in graphical form in which the

characteristics of the regulator may be obtained by ruler and compass constructions. Brief attention is given to the errors inherent in the simplifications made in the analysis.

2.4, 3.3

Aircraft, Pneumatic, Pressure Regulator, 2 Stage

2.2-7 RESISTANCE COEFFICIENTS FOR LAMINAR AND TURBULENT FLOW THROUGH ONE-HALF-INCH VALVES AND FITTINGS

Kittredge, C. P.

AMERICAN SOCIETY OF MECHANICAL ENGINEERS, TRANSACTIONS  
79:1759-63, November 1957

Apparatus and test procedures to determine resistance coefficients for laminar and turbulent flow through 1/2-in. I.P.S. valves, fittings, and fabricated bends are described. Resistance coefficients are given as functions of Reynolds number. Results of the investigation are discussed briefly.

Industrial, Hydraulic

2.2-8 APPLICATION LIMITS AND ACCURACIES OF CONTROL VALVE FLOW COEFFICIENT  $C_v$

Lin, D. J. et al.

AMERICAN SOCIETY OF MECHANICAL ENGINEERS

Paper 56-IRD-22 for meeting of September 17-21, 1956

Industrial

2.2-9 AN EXPERIMENTAL STUDY OF TWO DIMENSIONAL GAS FLOW THROUGH VALVE TYPE ORIFICES

Stenning, A. H.

AMERICAN SOCIETY OF MECHANICAL ENGINEERS

Paper 54-A-45. 1954

Aircraft, Pneumatic

2.2-10 HYDRAULIC LOSS AND FLUID DISCHARGE COEFFICIENTS THROUGH ORIFICES OF CYLINDRICAL SPOOL VALVE HYDRAULIC PERFORMANCE MECHANISM

Khokhlov, V. A.

AVTOMATIKA I TELEMEXHANIKA.

16:64-70, #1, 1955

1.4

Aircraft, Hydraulic, Servo Control Valve, Spool



2.2-11 FLOW CHARACTERISTICS OF PISTON TYPE VALVES

MacLellan, G. D.

INSTITUTION OF MECHANICAL ENGINEERS

Symposium on Recent Mechanical Engineering Developments in Automatic Control, London, January 5-7, 1960

Industrial

2.2-12 SOME MODEL EXPERIMENTS ON SPECIAL CONTROL VALVES

Firth, D. et al.

INSTITUTION OF MECHANICAL ENGINEERS, PROCEEDINGS

168:385-402, #13, 1954

A description is given of some model experiments undertaken to resolve problems occurring in the design of special control valves for use in the Hydraulic Machinery Laboratory of the Mechanical Engineering Research Laboratory.

Four types are dealt with: (1) a valve to control flows varying from 1 to 30 cu ft per sec in a flowmeter calibrating system; (2) a valve to control flows of up to 30 cu ft per sec in an open pump testing rig with a maximum input of 350 hp; and (4) a hydraulically balanced in-line valve to control flows varying from 1 to 15 cu ft per sec in a service supply.

2.5

Industrial, Hydraulic, Flow Control Valve

\*2.2-13 RESISTANCE CHARACTERISTICS OF CONTROL VALVE ORIFICES

Shearer, J. L.

INSTITUTION OF MECHANICAL ENGINEERS

Proceedings of Symposium on Recent Mechanical Engineering Developments in Automatic Control, 1960. pp 35-41

Orifices of the kind used in automatic control components are discussed from the point of view of their flow resistance characteristics and the factors which influence these characteristics. Real measured characteristics are evaluated in light of the theory for ideal orifices. The wide departure of real hydraulic orifice characteristics from ideal characteristics at low Reynolds numbers and for small valve openings as reported by various workers is discussed. Characteristics for both liquid and gas flows are discussed and compared. Recent work on pneumatic valves is described in which the jet stream exhibits bi-stable operation.

2.1, 2.4

Aircraft

2.2-14 A STUDY OF PRESSURE AND FLOW IN A POPPET VALVE MODEL

Tidor, O. M.

MASSACHUSETTS INSTITUTE OF TECHNOLOGY, DEPARTMENT OF  
MECHANICAL ENGINEERING

SB Thesis. 1954

The pressure and flow in a poppet valve was studied by means of a large-scale, two-dimensional, glass-sided model. Reynolds number was used to establish dynamic similitude between the valve and the model. Air injection into the oil stream was used to chart streamlines, which were observed through the glass faces.

Aircraft, Hydraulic, 2-Way Valve, Poppet

2.2-15 PRESSURE DROPS IN OXYGEN EQUIPMENT

Iberall, A. S.

NATIONAL BUREAU OF STANDARDS

Report No. 1115, 1951

Industrial

2.2-16 EXPERIMENTAL FORMULAE FOR DISCHARGE AND LIFTING FORCE OF FLAT SEATED VALVE (7TH REPORT)

Oki, I.

JAPAN SOCIETY OF MECHANICAL ENGINEERS, BULLETIN

4:87-93, #13, February 1961

In the 4th report we studied the relations between valve-lift, discharge, lifting-force and angle of issuing-jet for nine kinds of flat-seated valve, all of which discharge water freely in the air. From the experimental data thus obtained, non-dimensional discharge  $q_0$  and lifting-force  $p_0$  are computed and expressed as functions of opening-ratio  $l/d_0$  or diametral-ratio  $d/d_0$ , where  $l$  stands for valve-lift,  $d$  for valve-diameter and  $d_0$  for valve-port diameter. These experimental formulae give fundamental values for discharge and lifting force of disc valve and could be referred to as standard formulae in the research on disc valves of any kind.

3.2

Industrial, Water, Flow Control Valve, Flat Poppet

2.2-17 CHARACTERISTICS OF DISC VALVES IN ANGLE-VALVE-TYPE CHAMBERS (5TH REPORT)

Oki, I. et al.

JAPAN SOCIETY OF MECHANICAL ENGINEERS, BULLETIN.

2:644-50, November 1959

In an angle-valve-type valve box specially prepared, a series of experiments was carried out on disc valves with flat or conical seat under a head of about two meters. Thus, the relations among valve lift, discharge and lifting force were studied, whereby many factors in the characteristics of disc valves under these conditions were made clear.

### 3.2

Industrial, Water, Flow Control Valve, Poppet

#### 2.2-18 SOME CONSIDERATIONS ON THE CHARACTERISTICS OF DISC VALVES AS DISCLOSED BY OUR EXPERIMENTS (6TH REPORT)

Ok1, I.

JAPAN SOCIETY OF MECHANICAL ENGINEERS, BULLETIN.

2:651-6, November 1959

We have made an over-all study of our experimental researches on disc valves which were reported one after another since the year 1921. Many factors have been thereby brought into light as to the characteristics of disc valves with flat or conical seat, through which water was discharged in valve chambers of vertical-cylinder type or angle-valve type, or discharged freely into the air.

Industrial, Water Flow Control Valve, Poppet

#### 2.2-19 INVESTIGATION OF LOSSES IN BUTTERFLY VALVES

James, J. W.

UNIVERSITY OF TORONTO, DEPARTMENT OF MECHANICAL ENGINEERING

Thesis. April 15, 1951

Industrial, Butterfly Valves

#### 2.2 CROSS REFERENCES

1.3-1	1.4-2	2.1-2	2.4-9	2.5-2	3.2-3	4.2-3	7.0-2
-2	-4		-14	-4	-6		-3
-5	-5		-16		-7		-4
-6	-6		-17		-9		
-8	-7				-11		
-9					-12		
-13					-15		
-14					-16		
					-17		
					-19		

## Flow Through Composite Systems

### 2.3-1 USING FLOW COEFFICIENTS TO DESIGN PNEUMATIC SYSTEMS

Riske, G.  
HYDRAULICS AND PNEUMATICS  
pp 74-82, October 1960

Flow coefficients are useful tools for designing a pneumatic system at lowest cost. They eliminate the guesswork in avoiding large pressure drops in valves and plumbing.

2.4, 4.1

Aircraft, Pneumatic

### 2.3-2 PRESSURE LOSSES IN PNEUMATIC SYSTEMS

Riske, G.  
PRODUCT ENGINEERING  
30:50-4, October 26, 1959

The author shows how to simplify calculations for pressure drops of components in series. His nomograph method is an extension of the helpful National Bureau of Standards "Flow-factor" technique previously described for our readers.

2.4

Aircraft, Pneumatic

### 2.3-3 THEORY OF HYDRAULIC FLOW CONTROL

Sverdrup, N. M.  
PRODUCT ENGINEERING  
pp 161-176, April 1955

In the design of any hydraulic circuit, the rate of flow is determined by the resistance of the various components and by the pressure differential across the circuit. Because, in spite of its importance, there is a serious lack of published data on hydraulic resistance, equations are derived herein for the flow rate of any circuit--including both parallel and series types. This is followed by a flow analysis of such components as valves, venturis, orifices and other flow-limiting devices. Comprehensive examples illustrate the application of the analyses to practical design problems.

2.1, 2.4, 2.6

Aircraft, Hydraulic

2.3-4 FUNDAMENTAL CHARACTERISTICS OF HIGH PERFORMANCE HYDRAULIC  
SYSTEMS

Campbell, J. E.  
U. S. AIR MATERIAL COMMAND  
TR 5997. June 1950  
Contract W 33-0380ac-21859

Aircraft, Hydraulic

2.3 CROSS REFERENCES

1.2-5	2.1-7	2.4-2	2.5-2	6.2-7	7.0-4
		-16			-13
		-17			

## Valve Sizing Formulas

### 2.4-1 VALVE FLOW COEFFICIENT $C_v$ AND ITS CONTRIBUTION IN CONTROL VALVE SIZING

Rockwell, R. A.  
HEATING AND VENTILATING  
51:76-9, August 1954

Sizing of a flow control valve is premised on a full knowledge and weighed evaluation of flow data. Most sizing procedures make use of the valve flow coefficient,  $C_v$ , which materially simplifies the problem. The use of  $C_v$  provides a simple method applicable to a wide variety of valve constructions, valve sizes, and flow conditions.

Industrial

### 2.4-2 HOW TO SELECT CONTROL VALVE SIZE

Holzbock, W. G.  
CHEMICAL ENGINEERING  
66:171-6, #8, 1959

Valve and process characteristics, as well as pressure drops in pipeline and valve, plus specific gravity, viscosity and volume of flow are all factors you must consider.

2.3

Industrial

### 2.4-3 METHOD FOR PREDICTING PRESSURE DROPS IN PNEUMATIC COMPONENTS AND SYSTEMS

Slawsky, M. M. et al.  
CHEMICAL ENGINEERING  
60:170, September 1953  
See 2.4-16

Aircraft, Pneumatic

### 2.4-4 ACCURATE VALVE SIZING FOR FLASHING LIQUIDS

Hanssen, A. J.  
CONTROL ENGINEERING  
8:89-90, February 1961

Of the various methods proposed for sizing control valves for flashing liquids, the one based on the downstream density of the liquid-vapor mixture seems the most accurate. With the aid of specially constructed curves and known inlet conditions, the instrument engineer can size a valve with a few simple

calculations. Here the author explains the development and use of such curves, and presents usable charts covering six of the more common process fluids.

Industrial, Hydraulic

2.4-5 FLOW AREA EQUATIONS FOR RATING POPPET-TYPE VALVE CAPACITY

Lopera, D. J.

DESIGN NEWS

Reprint from Vol. 16, No. 3 February 1961

This article correlates the flow equations for the equivalent sharp-edge orifice diameter, NBS flow factor and the flow coefficient for the poppet-type valve. bib.

Aircraft, Hydraulic

2.4-6 VALVE SIZING ACCURACY

Rockwell, R. A.

INSTRUMENTATION, 6, Fourth Quarter 1952

The determination of the control valve size for a given application is not an exact science. While it is always premised on a full knowledge of the actual flow conditions, one or more of the conditions are frequently by necessity approximations. It is the evaluation of these flow data, therefore, that really determines the final valve size. Common sense, combined with experience, are the prime requisites.

(This paper continues to discuss the whys and wherefores of the flow coefficient,  $C_v$ .) bib.

Industrial

2.4-7 VALVE CAPACITY AND  $C_v$

Beard, C. S.

INSTRUMENTS AND AUTOMATION

29-282-4, February 1956

The  $C_v$  technique for valve sizing is becoming standard, yet formulas for flow capacity of a valve are presented in too many different ways at present. This clear resume of the various formulas for liquid, gas, and steam flow through valves should do much to clarify perspective and establish a more nearly standard--or at least better accepted--type of formulation.

Industrial

2.4-8 VALVE SIZING

Beard, C. S.

INSTRUMENTS AND AUTOMATION

29:2220-3, 1956

Basic factors in valve sizing include (1) maximum and minimum flows to be controlled, (2) maximum and minimum pressure-differentials across valve, (3) specific gravity, (4) temperature, (5) viscosity, (6) flashing, and (7) rangeability. Here are the basic procedures, with emphasis on the orders of magnitude of the various considerations.

Industrial

2.4-9 VALVE SIZING METHODS

Brockett, G. F.

INSTRUMENTS

p 752-800, June 1952

This comparison of three common methods of valve sizing is an important step leading to a standard acceptable to everyone. A society program for developing such a standard is needed.

2.2, 2.6

Industrial

2.4-10 CORRELATION OF VALVE SIZING METHODS

Brockett, G. F.

ISA CONFERENCE, New Jersey, April 1952

Industrial

2.4-11 SIZING AND SELECTION OF CONTROL VALVES

Kneisel, O.

SYMPOSIUM, ISA, New Jersey, 1953

Industrial

2.4-12 VALVE SIZING EQUATIONS FOR COMPUTERS

Lovett, O. P., Jr.

ISA JOURNAL, November 1959

DuPont's use of a digital computer to size control valves required an evaluation of valve-sizing techniques. Given are the resulting equations for liquid, gas, steam and Dowtherm, which also can be solved with a slide rule.

Industrial



2.4-13 COMPARING GAS FLOW FORMULAS FOR CONTROL VALVE SIZING

Turnquist, R. O.

ISA JOURNAL. 8:43-5, June 1961

Industrial, Pneumatic

2.4-14 PRACTICAL DETERMINATION OF CONTROL VALVE  $C_v$

Wing, P. Jr.

ISA JOURNAL. 7:90-4, September 1960

Many instrument men tend to assume that flow through control valves should be as accurately determinable as is flow through sharp-edged orifices. This article tells why valve sizing will remain more art than science for some time to come.

2.2, 2.5

Industrial

2.4-15 UPDATING K-FACTOR FORMULA FOR PRESSURE DROPS IN AIR VALVES

Dahle, B.

PRODUCT ENGINEERING

29:74-8, April 14, 1958

This consistent technique estimates pressure losses in a pneumatic system, component by component. Author's charts give K-factors for actual valves and fittings; nomogram provides fast pressure-drop answers.

2.1

Aircraft, Pneumatic

\*2.4-16 A METHOD FOR PREDICTING PRESSURE DROPS IN PNEUMATIC COMPONENTS AND SYSTEMS

Slawsky, M. M.

SOCIETY OF AUTOMATIVE ENGINEERS

Preprint No. 81 for Meeting April 20, 1953, See 2.4-3

A method for predicting the pressure drop in a pneumatic component or a combination of components for any specified flow and upstream pressure is described. Certain parameters are emphasized which enable the correlation between flow, pressure, and geometry to be represented by a single flow curve. This curve is independent of upstream pressure and is reasonably accurate for all flows ranging from zero to sonic. The relation between the geometry of the component and the flow characteristic is derived from considerations obtaining at sonic flow. A procedure for extending this method to the calculation of pressure drop in

a pneumatic system composed of several components is developed. A comparison between the calculated and measured values for several typical cases is given.

2.1, 2.2, 2.3

Aircraft, Pneumatic

2.4-17 CONTRIBUTIONS TO THE METHODS OF CALCULATION AND MEASUREMENT OF PRESSURE DROP IN PNEUMATIC COMPONENTS AND SYSTEMS

Slawsky, M. M. et al.

U. S. NATIONAL BUREAU OF STANDARDS

R-3683. October 1954

AD 65102

A method for predicting the pressure drop in a pneumatic component or a combination of components for any specified flow and upstream pressure is described. Certain parameters are emphasized which enable the correlation between flow, pressure, and geometry to be represented by a single flow curve. This curve is independent of upstream pressure and is reasonably accurate for all flows ranging from zero to sonic. The relation between the geometry of the component and the flow characteristic is derived from considerations obtaining at sonic flow. A procedure for extending this method to the calculation of pressure drop in a pneumatic system composed of several components is developed. A comparison between the calculated and measured values for several typical cases is given.

2.1, 2.2, 2.3, 2.5

Aircraft, Pneumatic

2.4 CROSS REFERENCES

1.4-2	2.1-7	2.2-1	2.3-1	2.5-4	7.0-2
		-6	-2		-3
		-13	-3		-4

## Internal Passage Design for Flow

### 2.5-1 DETERMINATION AND CORRELATION OF FLOW CAPACITIES OF PNEUMATIC COMPONENTS

Tsai, D. H., et al.  
COMPRESSED GAS ASSOCIATION, Supplement to Annual Report #45,  
January 1958, p 5-11  
Also see Compressed Air and Hydraulics 23:415-6, Sept. 1958  
See 2.5-4

### 2.5-2 FLOW FACTORS IN FLUID PASSAGE DESIGN

Riske, G.  
MACHINE DESIGN  
32:154-9, April 14, 1960

Predicting performance of hydraulic or pneumatic systems depends upon knowledge of flow efficiency. Analyzing losses is simplified by using flow factors in fluid passage design.

2.1, 2.2, 2.3

Aircraft, Pneumatic

### 2.5-3 EFFECT OF SIZE OF ENTRANCE AND EXIT MEASURING SECTIONS ON THE FLOW FACTOR AND THE CHARACTERISTIC CURVE

Thompson, R. C., et al.  
U. S. NATIONAL BUREAU OF STANDARDS  
Report No. 3367, June 22, 1954

Aircraft, Pneumatic

### \*2.5-4 DETERMINATION AND CORRELATION OF FLOW CAPACITIES OF PNEUMATIC COMPONENTS

Tsai, D. H., et al.  
U. S. NATIONAL BUREAU OF STANDARDS  
Circular 588, October 1957

Some of the problems of measurement and correlation of flow capacities of pneumatic components are discussed. A dimensionless "area factor," defined as the ratio of the "effective area" of the component to some reference area is introduced. The physical significance of the area factor and its experimental determination are discussed in some detail. Sample data are also included to show that this area factor provides a valid and convenient basis for comparing the flow capacities of components, regardless of their size and design, and over a wide range of test conditions.

2.1, 2.2, 2.4

Aircraft, Pneumatic

## 2.5 CROSS REFERENCES

1.2-18	1.3-1	1.4-7	2.1-7	2.2-1	2.4-14	4.2-3
	-2			-4	-17	
	-5			-12		
	-6					
	-13					

## Cavitation and Other Flow Phenomena

### 2.6-1 CAVITATION CHARACTERISTICS OF GATE VALVES AND GLOBE VALVES USED AS FLOW REGULATORS UNDER HEADS UP TO 125 FEET

Ball, I. W.

AMERICAN SOCIETY OF MECHANICAL ENGINEERS, TRANSACTIONS

79 1275-81, 1957

The series of tests discussed in this paper was made for the purpose of determining whether or not gate valves or globe valves could be used satisfactorily for regulating releases from irrigation distribution systems under heads up to about 125 feet. A pressure relationship or "cavitation index" was found to be a useful means of determining the limits of differential head and back pressure to either control the location of, minimize, or eliminate cavitation damage.

Industrial, Water Globe and Gate Valves

### 2.6-2 CAVITATING VENTURI FOR FLOW CONTROL

Wright, B. S. et al.

CHEMICAL ENGINEERING

63 221-2, #11, 1956

Flow through a venturi designed to cavitate remains constant independent of downstream pressure variations.

2.1

Aircraft

### 2.6-3 CAVITATION IN CONTROL VALVES

Stiles, G. F.

INSTRUMENTS & CONTROL SYSTEMS

34 2086-93, November 1961

No known material can withstand cavitation erosion, which starts at critical pressure differential. Here is how to design out the risk of cavitation.

Industrial

### 2.6-4 THE TEAPOT EFFECT - A PROBLEM

Reinder, M.

PHYSICS TODAY

Volume 9, #9, 1956

A discussion of the phenomena associated with the apparent uphill flow of fluids around corners. bib.

Aircraft

## 2.6 CROSS REFERENCES

2.2-1    2.3-3    2.4-9    3.2-6    5.4-1

### 3.0 STEADY-STATE FORCES

This section contains those articles and reports concerned primarily with the steady-state forces acting on the valve closure. As before, articles involving both forces (Section 3.0) and transients (Section 4.6) have been placed under transients. Since the analysis of most valves consists only of a static force analysis, subsection 3.3, Detailed Static Force Analyses, was included even though no material was found directly applicable to this heading. Cross references to pertinent data could thus be noted. The section is subdivided as follows:

3.1 Lateral Forces - Friction and Hydraulic Lock

3.2 Flow Forces

3.3 Detailed Static Force Analyses

## Lateral Forces- Friction and Hydraulic Lock

- 3.1-1 CONTRIBUTIONS TO HYDRAULIC CONTROL -5. LATERAL FORCES ON  
HYDRAULIC PISTONS  
Blackburn, J. F.  
AMERICAN SOCIETY OF MECHANICAL ENGINEERS, TRANSACTIONS  
75 1175-80, 1953

Sticking or excessive friction of pistons or valves in their bores has always caused trouble to designers and users of hydraulic equipment. The phenomena involved are complex and incompletely understood. This paper shows that large lateral forces may be caused by hydrodynamic phenomena alone, without the complicating effects of dirt in the oil. It presents expressions describing the lateral force for certain cases of simple geometry, with experimental verification, and discusses other cases qualitatively. Finally, it summarizes briefly present ideas concerning the frictional phenomena involved and lists several questions to which the answers must be obtained by further investigation.

1.4

Aircraft, Hydraulic, Spool Valve

- 3.1-2 THE REDUCTION OF FRICTION IN PISTON TYPE HYDRAULIC SERVO VALVES  
Earl, A. G.  
GREAT BRITAIN, ROYAL AIRCRAFT ESTABLISHMENT  
Technical Note GW 312. May 1954. CONFIDENTIAL  
AD 35006

1.4, 5.4

Aircraft, Hydraulic, Spool Valve

- \*3.1-3 AN INVESTIGATION OF HYDRAULIC LOCK  
Sweeney, D. C., et al.  
PRESENTED TO THE INSTITUTE OF MECHANICAL ENGINEERS  
May 13, 1955

Hydraulic lock is a phenomenon encountered in piston-type control valves governing the supply of high-pressure oil to mechanical equipment. It is liable to occur when conditions are such as to produce an axial pressure gradient in the fluid contained in the clearance space surrounding the piston lands and its effect is to cause sticking or locking of the piston in its enclosing cylinder.

A preliminary investigation carried out in the Mechanical Engineering Department of Birmingham University indicated that true hydraulic lock is essentially a hydrodynamic effect, resulting from asymmetric pressure distribution in the clearance space between piston and cylinder. Thus if, owing to machining imperfections in the piston lands or cylinder bore, the flow of fluid in the clearance space is either diverging or converging, an asymmetric distribution of pressure will, in general, result and will be accompanied by a transverse thrust on the piston. If the clearance is divergent in the direction of flow, the piston will be forced against the cylinder wall; if convergent, the action of any thrust arising will be to exert a centralizing effect.

The present paper deals with an extension of the investigation referred to above, the object being to examine, both theoretically and experimentally, the effect on hydraulic lock of the employment of tapered piston lands. For this purpose, a mathematical analysis was made of the pressure distribution in the clearance space between piston lands and cylinder bore and of the accompanying side forces on the piston for a range of selected conditions. To establish the validity of the analysis, experiments were carried out on a cylinder of uniform bore in conjunction with dumbbell-shaped pistons having lands of such form as to give various taper-clearance ratios. In general, the procedure was as follows: high-pressure oil was supplied through the cylinder wall to the annular space between the two lands of the piston, the oil then flowing outward in both directions through the clearance space. Pressure tapings at a number of points in the cylinder wall allowed the pressure distribution in the clearance space to be determined, and suitable provision was made for the measurement of any locking force acting on the piston.

1.4

Aircraft, Hydraulic, Spool Valve

### 3.1-4 A STUDY OF SEAL FRICTION IN HYDRAULIC SERVOMECHANISMS

Feldman, M. S.

MASSACHUSETTS INSTITUTE OF TECHNOLOGY, INSTRUMENTATION  
LABORATORY

Master's Thesis. Report T-62. May 1954

Contract AF 33(616)2039

AD 33887

The friction forces encountered in a high performance hydraulic servomechanism may drastically affect the servo characteristics. The main sources of friction are the hydraulic seals used in the servo actuating cylinder.



In this thesis, the frictional characteristics of the two kinds of hydraulic actuator seals (i.e., piston and rod) were studied separately. Seals made of rubber, cast iron, and Teflon were tested. The static and kinetic friction force levels were investigated. The relative effects of the various seals on the dynamic response of the servo were also examined. Some of the other topics included are as follows: a summary of friction theory, a description of the test equipment and procedures, and a discussion of the methods used to evaluate the test data.

Of the seals tested, two-element Teflon rings, used in conjunction with an "O"-ring backup, had the lowest friction levels. The dynamic response tests showed that all of the test seals affected the servo characteristics to approximately the same degree. However, a high seal friction level will actually deteriorate the response time of the servo; and thus may seriously affect its dynamic characteristics.

1.4, 5.2

Aircraft, Hydraulic

3.1-5 INVESTIGATION OF EFFECT OF REDUCTION OF VALVE FRICTION IN A POWER CONTROL SYSTEM BY USE OF A VIBRATOR

Phillips, W. H.

NATIONAL ADVISORY COMMITTEE ON AERONAUTICS

RM 155E18a. CONFIDENTIAL. No Date

AD 67025

1.4

Aircraft, Hydraulic

3.1 CROSS REFERENCES

1.2-2      5.4-4      7.0-4

-8

## Flow Forces

### 3.2-1 COMPENSATION OF STEADY-STATE FLOW FORCES IN SPOOL-TYPE HYDRAULIC VALVES

Clark, R. N.

AMERICAN SOCIETY OF MECHANICAL ENGINEERS, TRANSACTIONS

79:1784-8, November 1957

Three heretofore unreported schemes for reducing the steady-state flow forces in spool-type hydraulic valves are described. Experimental data are presented which compare the steady-state flow-force characteristics of valves using each of these schemes to the characteristics of uncompensated valves.

1.4

Aircraft, Hydraulic, Spool Valve

### 3.2-2 STEADY-STATE AXIAL-FLOW FORCES ON PNEUMATIC SPOOL-TYPE CONTROL VALVES

Feng, T. Y.

AMERICAN SOCIETY OF MECHANICAL ENGINEERS

Paper 57-A-129 for meeting December 1-6, 1957

See 3.2-18

The momentum theory is used to determine the steady-state axial-flow on a pneumatic control-valve spool, caused by the compressible fluid passing through the sharp-edged orifice. The experimental results compare favorably with the theoretical calculations for valve displacements of 0.005 in. and less at supply pressures not exceeding 500 psig. Pneumatic flow forces as compared with hydraulic flow forces on the same valve spool are higher in the unchoked flow regime ( $P_{\text{down}}/P_{\text{up}} > 0.528$ ) but lower in the choked-flow regime ( $P_{\text{down}}/P_{\text{up}} \leq 0.528$ ).

1.4

Aircraft, Pneumatic, Spool Valve

### 3.2-3 STATIC AND DYNAMIC CONTROL CHARACTERISTICS OF FLAPPER NOZZLE VALVES

Feng, T. Y.

AMERICAN SOCIETY OF MECHANICAL ENGINEERS, TRANSACTIONS, SERIES D.

81:275-84, September 1959

A basic study was conducted on a flapper-nozzle hydraulic control valve to explore in detail its static and dynamic control characteristics. These static and dynamic control characteristics are presented and both the theoretical and experimental

results compared. Correlation between the theoretical and experimental results were found to be quite good.

1.4, 2.2, 4.2

Aircraft, Hydraulic, Servo Control, Flapper-Nozzle Valve

**3.2-4 DYNAMIC FORCE REACTIONS IN DOUBLE-PORTED CONTROL VALVES**

King, C. F. et al.

AMERICAN SOCIETY OF MECHANICAL ENGINEERS, TRANSACTIONS

73:1101-7, November 1951

Torsional force reactions on V-port inner valves, and vertical force reactions on plug-type inner valves in double-ported control-valve bodies are of sufficient magnitude to cause concern if pressure drop is high. These forces are proportional to the mass velocity of the flowing fluid. It is possible to design inner valves so that these forces will be reduced to a point where they are not objectionable.

Industrial, Flow Control Valve

**3.2-5 CONTRIBUTIONS TO HYDRAULIC CONTROL--1. STEADY-STATE AXIAL FORCES ON CONTROL VALVE PISTONS**

Lee, S. Y., et al.

AMERICAN SOCIETY OF MECHANICAL ENGINEERS, TRANSACTIONS

74:1005-1011, 1952

A theory is given of the origin of the steady-state force exerted upon a piston by fluid flowing past its corner. Brief reference is made to a considerable body of experimental evidence in support of that theory, and a practical valve construction is described which very nearly eliminates that force.

1.4

Aircraft, Hydraulic, Spool Valve

**3.2-6 TORQUE AND CAVITATION CHARACTERISTICS OF BUTTERFLY VALVES**

Sarpkaya, T.

AMERICAN SOCIETY OF MECHANICAL ENGINEERS, TRANSACTIONS, SERIES E.

28:511-8, December 1961

The present study deals with torque and cavitation characteristics of idealized two-dimensional and axially symmetrical butterfly valves. Theoretical results obtained for the two-dimensional case are compared with the ones obtained experimentally and by a relaxation technique. Based on the results of the

two-dimensional case, an approximate solution is presented for the more general and practical case of three-dimensional butterfly valves. The results are in good agreement with the actual flow tests.

2.2, 2.6

Aircraft, Liquid, Butterfly Valve

3.2-7 DISCHARGE COEFFICIENTS AND STEADY-STATE FLOW FORCES FOR HYDRAULIC POPPET VALVES

Stone, J. A.

AMERICAN SOCIETY OF MECHANICAL ENGINEERS, TRANSACTIONS, SERIES D, JOURNAL OF BASIC ENGINEERING. 82:144-54, March 1962

See also paper 59-HYD-18

See 3.2-16

Experiments were run on a poppet valve operating in hydraulic oil. The experimental values of the flow forces and discharge coefficients were about 25 percent below the predicted theoretical values. Although there was some scatter in the values of discharge coefficients, there was good correlation for the flow forces.

Flow forces are strongly influenced by the downstream configuration. The smaller the diameter of the downstream chamber, the higher the forces.

2.2

Aircraft, Hydraulic, Poppet Valve

3.2-8 CONCERNING THE POSSIBILITY OF DETERMINING AN AXIAL HYDRODYNAMIC FORCE IN A VALVE

Krassov, I. M.

AUTOMATION AND REMOTE CONTROL

19:210-3, March 1958

The paper deals with an axial hydrodynamic force that appears in valve hydraulic amplifier when the working liquid flows through it. The amplifier described may be a meter of the force. The experimental results are presented.

1.4

Aircraft, Hydraulic, Spool Valve

3.2-9 TORQUE AND FLOW CHARACTERISTICS OF A BUTTERFLY VALVE OPERATING AT PRESSURE RATIOS ABOVE THE CRITICAL

Robinson, A.H.

GREAT BRITAIN, NATIONAL GAS TURBINE ESTABLISHMENT

NGTE Memo 304. July 1957

JSRP Control No. 57134

AD 146316

A lenticular butterfly valve of 0.125 thickness/diameter ratio has been tested at pressure ratios up to 4/1. Nondimensional torque and flow characteristics are presented for the valve installed in a straight pipe and in a bulkhead across a large duct. It is shown that the flow characteristics are of the form formally associated with the discharge of air through any orifice, and are only affected by the valve installation insofar as this affects the entry conditions and effective flow area. The torque characteristics, however, are affected by the valve installation to a much greater extent but their general form can be explained by a simplified two-dimensional consideration of the flow conditions.

2.2

Aircraft, Pneumatic, Butterfly Valve

### 3.2-10 NULL POSITION FLOW FORCES IN 3-WAY SERVOVALVES

Harrison, H. L.

HYDRAULICS AND PNEUMATICS

14:81-6, July 1961

Stability of a 3-way hydraulic valve depends on the balance of flow forces in the valve's null position. This article analyzes a theoretical valve. In a future article, these principles will be applied to an actual valve design.

1.4, 4.2

Aircraft, Hydraulic, Servo Control, Spool Valve

### 3.2-11 PERFORMANCE ANALYSIS OF BUTTERFLY VALVES

Cohn, S. D.

INSTRUMENTS

24:880-4, August 1951

Data on butterfly valves obtained by different experimenters are correlated in terms of coefficients of flow ( $C_q$ ), thrust ( $C_s$ ), and torque ( $C_t$ ). The coefficients are derived in terms of both static pressure differential and total pressure differential, including velocity head. Two classes of operation are considered: (1) where delivery is limited by a downstream pressure greater than atmosphere, and (2) where downstream pressure is atmospheric or less and where, therefore, delivery depends only on the opening of the valve. All in all, this is the most informative single article on butterfly valves published in the last decade.

2.2

Industrial, Liquid, Butterfly Valve

3.2-12 BUTTERFLY CONTROL VALVES

Dally, C. A.  
INSTRUMENTS

25.1717-9. 1761-2. 1764, December 1952

Operation of butterfly valves is clearly understood from examination of the unbalanced and static torques. Selection and sizing involves consideration of the torques, the system characteristics, valve operators, and valve flow characteristics.

2.2

Industrial, Butterfly Valve

3.2-13 A STUDY OF AXIAL FORCES ON RECIPROCATING PRESSURE REGULATOR VALVES FOR THE MODEL FM 12 FUEL CONTROL ADVANCED COMPONENT DEVELOPMENT PROGRAM

Long, H. A. et al.  
MARQUARDT AIRCRAFT COMPANY  
Report 5393. CONFIDENTIAL. 25 April 1954  
Contract AF33(616)38  
AD 43108

Aircraft

3.2-14 A PNEUMATIC FLAPPER VALVE STUDY

Norwood, R. E.  
MASSACHUSETTS INSTITUTE OF TECHNOLOGY, DEPARTMENT OF  
MECHANICAL ENGINEERING  
SM Thesis. 1959

Aircraft, Flapper Valve

3.2-15 A CONTINUED STUDY OF FLAPPER VALVES

Pawlak, R. J.  
MASSACHUSETTS INSTITUTE OF TECHNOLOGY, DEPARTMENT OF  
MECHANICAL ENGINEERING  
SM Thesis. August 1959

One of the important phases of the proper design of a hot gas flapper-type servovalve for use in flight control systems is the thorough understanding of the characteristics of the variable downstream orifice of the valve. Norwood initiated this work with a recent Master's thesis. Using sharp-edge nozzles, he discovered and studied a hysteresis-type jumping effect of the fluid flow pattern. This thesis, a continuation of Norwood's work, shows that a small flat on a nozzle's metering edge eliminates the jumping effect and makes the pressure-flapper force characteristics linear and much more desirable from the design standpoint. The slope of these pressure-flapper force characteristics is influenced by different size

nozzles, different amounts of flat on the nozzle tips, and different nozzle-flapper spacings. Each of these influences is described in this thesis. Theoretical analyses for both sharp-edge nozzles and nozzles with flats are presented as an aid in predicting the slope of these characteristics. The theory and experiments are compared to explain what is happening in the actual situation.

This thesis is also an extension of the work reported by Hohorst in a Master's thesis on the dynamic stability of a flapper valve-chamber system. Work was continued because of the lack of agreement between Hohorst's theoretical analysis and experimental work. It is shown that with improved experimental technique, with the necessary modifications of the theory in view of the newly found pressure-flapper force characteristics, and with careful consideration for describing the physical system in terms of the analytical parameters, the stability criteria initiated by Hohorst over the limited range considered in this thesis, do accurately predict the point of marginal stability and can now be used confidently as a useful tool in the future design of pneumatic and hot gas servovalves.

1.4, 2.2, 4.2

Aircraft, Hot Gas, Servo Control, Flapper-Nozzle Valve

3.2-16 INVESTIGATION OF DISCHARGE COEFFICIENTS AND STEADY-STATE FLOW FORCES FOR POPPET-TYPE VALVES

Stone, J. A.

MASSACHUSETTS INSTITUTE OF TECHNOLOGY, DEPARTMENT OF MECHANICAL ENGINEERING

SM Thesis. January 1957

See 3.2-7

2.2

Aircraft, Hydraulic, Poppet Valve

3.2-17 DESIGN AND DEVELOPMENT OF AN APPARATUS TO STUDY THE FLOW-INDUCED FORCES IN A POPPET-TYPE VALVE

Stone, J. A.

MASSACHUSETTS INSTITUTE OF TECHNOLOGY, DEPARTMENT OF MECHANICAL ENGINEERING

SB Thesis. 1955

Apparatus was designed to study the steady-state flow forces acting on a poppet-type flow valve. An analytical study was made of the apparatus and experiments were run.

The apparatus is easy to use but in its present form does not give usable data. There is a large hysteresis in the force readings and the sensitivity is very low. The apparatus gives good results in reading valve openings. The analytical method was difficult to use but gave a simple answer.

It is recommended that further work be done on the apparatus to reduce the hysteresis and increase the sensitivity. Different valve configurations should be made and tests run. With a few modifications, the apparatus can be used for dynamic studies.

2.2

Aircraft, Hydraulic, Poppet Valve

### 3.2-18 STEADY STATE AXIAL FLOW FORCES ON PNEUMATIC SPOOL-TYPE CONTROL VALVES

Feng, T. Y  
PRODUCT ENGINEERING  
29 19-11 Mid-September 1958  
See 3.2-2

### 3.2-19 CONTRIBUTION TO THE STUDY OF BUTTERFLY VALVES

Gaden, D  
WATER POWER Part 1, pp. 456-74 December 1951  
Part 2, pp. 16-22, January 1952

A description and discussion of reduced-scale model tests made by Ateliers des Charmilles S. A., Geneva. bib.

2.2

Industrial, Water, Butterfly Valve

## 3.2 CROSS REFERENCES

1.2-2	1.3-5	1.4-2	2.2-4	4.2-3	5.3-1	7.0-4
-8		-4	-16			
-14		-6	-17			

### Detailed Static Force Analyses

## 3.3 CROSS REFERENCES

1.2-23	1.3-1	2.2-6	4.2-3	7.0-4
	-5			
	-6			
	-8			
	-13			
	-14			



#### 4.0 TRANSIENT FACTORS

In many cases of valve design, only a simple approximation of response time is required to either select configuration or confirm acceptability. Subsection 4.1 is intended to contain such material. The transient analysis of valves and establishment of stability criteria is covered by subsection 4.2. This material could be considered simply more detailed and rigorous than 4.1. Analyses and test data on the basic aspects of unsteady flow are contained under 4.3. The subsection headings are listed below:

- 4.1 Simple Response Time
- 4.2 Transient Analysis and Stability
- 4.3 Unsteady Flow, Blowdown and Charging

## Simple Response Time

### 4.1-1 DESIGN OF A HIGH SPEED VALVE

Heitland, H. H.

CALIFORNIA INSTITUTE OF TECHNOLOGY, GUGGENHEIM JET  
PROPULSION CENTER

Technical Report 34. AROD Report 834:47. June 1961

Contract DA 04-495-ORD-1634

AD 262899

See 4.1-6

### 4.1-2 DETERMINING CLOSURE TIME IN MISSILE CONTROL VALVES

Kissner, R. L.

ELECTRONICS

33:88-9, October 14, 1960

Waveshape of the energizing current to the solenoid is differentiated and shaped to trigger circuits timing the interval between circuit closure and final solenoid position.

Aircraft, Solenoid Valve

### 4.1-3 HOW TO DETERMINE PNEUMATIC VALVE RESPONSE

Grover, D. P.

APPLIED HYDRAULICS AND PNEUMATICS

12:91-4, October 1959

More and more, designers must actuate mechanisms with rapid-fire signals from a programming control. Using this procedure developed at Armour Research, you can determine how long to energize a solenoid valve for best operation of a fast-cycling air cylinder.

Aircraft, Pneumatic, Solenoid Valve

### 4.1-4 DYNAMICS OF GAS-OPERATED MECHANISMS

Hirsch, R. A.

MACHINE DESIGN DATA SHEET

Reprint July 20, 1961

Nondimensional graphs simplify calculation of velocity, distance and time.

Aircraft, Pneumatic

4.1-5 CALCULATING TIME LAG OF HYDRAULIC AND PNEUMATIC VALVES

Dodge, L.  
PRODUCT ENGINEERING  
27:158-60, June 1956

Formulas and curves for calculating the operating time required by springs and solenoids to open or close valves; method for determining frictional resistance of valve spools; design suggestions for increasing the speed of operation.

4.2

Aircraft, Spool Valves

4.1-6 DESIGN OF A HIGH SPEED VALVE

Heitland, H.H.  
REVIEW OF SCIENTIFIC INSTRUMENTS  
32:1203-4, November 1961  
See 4.1-1

A high-speed valve has been designed for opening a deLaval nozzle in times less than  $10^{-3}$  seconds.

Aircraft, Pneumatic, Pressure-Actuated Valve, Poppet

4.1-7 FAST ACTING GAS VALVE

Wetstone, D. M.  
REVIEW OF SCIENTIFIC INSTRUMENTS  
32:1209-11, November 1961

The design and operation of an electro-dynamically drive valve, which is employed to deliver rapidly a gas pulse (0.6 cc STP) with a sharp front to the annulus of a coaxial plasmoid source of small aspect ratio (2-mm annulus at 2-cm radius) is described. The spring-loaded piston holds the plenum closed against pressures up to 2 atm. The piston is driven open by eddy currents induced by discharging a capacitor through a coil surrounding the plenum. A piston velocity of 5 cm/msec is achieved in less than 20  $\mu$ sec and is maintained for 7 mm of travel. The arrival of a gas front (air) at the annulus was detected in 100  $\mu$ sec after firing, employing hot-wire anemometry. The subsequent axial position and velocity of this front in the source annulus were determined as functions of time and position, respectively. It was found that the initial axial velocity of the front exceeded the stagnation sound speed (though not the vacuum escape speed) and remained constant until the displacement thickness from wall friction reached the half-annulus spacing.

Aircraft, Pneumatic, Capacitive Discharge Coil Valve

#### 4.1 CROSS REFERENCES

1.3-1	2.3-1	7.0-14
-2		
-5		
-6		
-8		
-9		
-14		

## Transient Analysis and Stability

### 4.2-1 EFFECT OF OIL COLUMN ACOUSTIC RESONANCE ON HYDRAULIC VALVE SQUEAL

Ainsworth, F. W.

AMERICAN SOCIETY OF MECHANICAL ENGINEERS, TRANSACTIONS  
78:773-8, May 1956.

See also paper 55-SA-14

An outline is presented of a theory that oil-column resonance is one likely cause of control-valve oscillation. It is shown analytically and experimentally that acoustic resonance of the oil in the lines which are attached to the valve can cause an otherwise stable valve to squeal. Methods of eliminating the oscillation are given.

1.4

Aircraft, Hydraulic, Spool Valve

### 4.2-2 CONTRIBUTIONS TO HYDRAULIC CONTROL--2. TRANSIENT FLOW FORCES AND VALVE INSTABILITY

Lee, S. Y.

AMERICAN SOCIETY OF MECHANICAL ENGINEERS, TRANSACTIONS  
74:1013+, August 1952

An outline is presented of a theory of a transient force which is one likely cause of oscillation of control valves, with supporting experimental evidence and methods of eliminating it.

1.4

Aircraft, Hydraulic, Spool Valve

### \*4.2-3 DYNAMIC BEHAVIOR OF A SIMPLE PNEUMATIC PRESSURE REDUCER

Tsai, D. H., et al.

AMERICAN SOCIETY OF MECHANICAL ENGINEERING, TRANSACTIONS

Paper No. 60-WA-186 for November 27, 1960, Also see 4.2-11

This paper presents an analysis of the dynamic behavior of a simple pneumatic pressure reducer. Both the nonlinear and the linearized problems were studied. Some experimental results also were obtained on a working reducer model to check the validity of the analysis. The agreement between the nonlinear solutions and the experimental results was satisfactory. The nonlinear and the linearized solutions were compared in detail so as to bring out the essential features of the dynamic behavior in both cases. The stability problem was studied also, and a set of stability criteria for the linearized case was

formulated in terms of the design and operating parameters of the reducer. In the few sample cases studied, these criteria gave correct qualitative predictions of the stability of the reducer in both the linearized case and the nonlinear case. The flow forces on three typical flowmetering valves were determined by experimental measurements (Appendix 2). These results were used in the analytical part of the paper.

2.2, 2.5, 3.2, 3.3

Aircraft, Pneumatic, Pressure Reducer, Poppet

4.2-4

#### HOW TO CALCULATE CONTROL VALVE INSTABILITY

Turnbull, D. E.

AUTOMATION PROGRESS

4:156-8, 172, May 1959

Most hydraulic control systems depend for their performance on the behavior of a spool- or piston-type control valve. There are several factors which may cause instability of such valves: some have been known and analyzed for some time and, after outlining the, the author describes recent work, including his own, in deriving expressions for the effects of other factors, such as load on the system. The calculated results are shown to agree well with experimental work and should enable designers to eliminate instability.

1.4

Aircraft, Hydraulic, Spool Valve

4.2-5

#### TRANSIENTS IN MECHANICAL SYSTEMS

Muller, J. T.

BELL SYSTEM TECHNICAL JOURNAL

Excerpt from opening paragraphs: "A study of the response of an electrical network or system to the input of transients in the form of short-duration pulses is an accepted method of analysis of the network. By comparing the input and the output, conclusions may be drawn as to the respective merit of the various components.

Until recently, similar procedures were only of academic interest with mechanical systems. However, the tests for mechanical ruggedness, which are required of electronic gear in order to pass specifications for the armed forces, are an example of the application of transients to a mechanical system. These tests are known as High Impact Shock Tests.

A basic part of an electrical system is a damped resonant network consisting of an inductance, a capacitance and a resistance. A mass, a spring and a friction device is the equivalent mechanical network called a simple mechanical system and a combination of such networks is a general mechanical system. It is, of course, advantageous to keep the mechanical system as simple as possible without detracting from the general usefulness of the results obtained."

Aircraft

4.2-6 THE DESCRIBING FUNCTIONS RELATING THE INERTIAL REACTION FORCE AND THE FLOW RATE TO THE SPOOL DISPLACEMENT OF A HYDRAULIC PISTON-TYPE CONTROL VALVE

Noton, G. J.  
ENGLISH ELECTRIC COMPANY, LIMITED  
Report No. L.C.t. 029. 7 February 1956  
JSRP Control #560665  
AD 108656

This report contains the derivation of the describing functions relating the reaction force and flowrate to the displacement of a hydraulic, piston-type control valve. It also contains a brief analysis of the mechanics of the self-sustained oscillations of this valve when controlling the position of an inertial load. The source of the energy sustaining these oscillations is discussed in detail in L.C.t. 028 (Noton and Turnbull, 1956).

The describing functions enable the approximate resonant frequency of a hydraulic servomechanism incorporating such a valve to be deduced provided the transfer functions of the other components of the system are known.

A few methods which might eliminate or reduce the oscillations are briefly reviewed.

1.4

Aircraft, Hydraulic, Spool Valve

4.2-7 SOME FACTORS INFLUENCING THE STABILITY OF PISTON-TYPE CONTROL VALVES

Noton, G. J. et al.  
INSTITUTION OF MECHANICAL ENGINEERS, PROCEEDINGS  
172:1065-81, #40, 1958

The reaction force on an open, spool-type control valve acts in such a direction as to close the valve. For this reason, a 4-way valve, having its closed position at the center of its stroke, can overshoot if the reaction force imparts sufficient

energy to it during closure. If there is insufficient damping on the spool, a continuous oscillation may arise and the present work investigates the dynamic behavior of a common type of hydraulic position-control system in which such an oscillation has been found to occur.

Good agreement is obtained between the predicted and experimental minimum amplitudes and frequencies of oscillation and also between the theoretical and measured pressure fluctuations in the system. A graphical solution of the equation of motion of the system is included in the results and with the aid of "Describing Functions" the approximate dynamic behavior of the system considered may be derived.

#### 1.4

Aircraft, Hydraulic, Spool Valve

4.2-8

#### PNEUMATIC OPERATORS FOR THROTTLING CONTROL

Eckman, D. P.

INSTRUMENTS, December 1951

Analysis of the response and characteristics of spring-diaphragm, springless diaphragm, and springless piston valve operators shows the advantages of a new positioner which uses a pneumatic rotary motor.

#### 3.3

Industrial

4.2-9

#### CONTROL VALVE DYNAMICS

Lovett, O. P., Jr.

INSTRUMENT SOCIETY OF AMERICA

Presented at Fall Instrument Automation Conference  
and Exhibit, Los Angeles, California

Preprint No. 9-LA-61. September 1961

Industrial Valve

4.2-10

#### REGULATOR ANALYSIS

Lefkowitz, I., et al.

ISA JOURNAL

2:361 1955

Industrial Regulator



\*4.2-11      DYNAMIC BEHAVIOR OF A SIMPLE PNEUMATIC PRESSURE REDUCER  
                  Tsai, D. H. et al.  
                  U. S. NATIONAL BUREAU OF STANDARDS, PNEUMATICS LAB-  
                  ORATORY  
                  NBS Report 6600. December 1959  
                  Contract NAer-01826, NAer-01880, NAer-01881  
                  Bureau of Naval Weapons Report RAAE-32-1  
                  AD 232176

See 4.2-3

#### 4.2 CROSS REFERENCES

1.2-15	1.3-2	1.4-2	2.2-4	3.2-3	4.1-5	7.0-4
-16	-5	-4		-10		
-17	-12	-6		-15		
	-13	-7				

## Unsteady Flow, Blowdown and Charging

4.3-1

### NONLINEAR PROPERTIES OF CIRCULAR ORIFICES

Thurston, G. B. et al.  
ACOUSTICAL SOCIETY OF AMERICA, JOURNAL  
29:992-1001, September 1957  
Also see 4.3-7

The results of an experimental study of the nonlinear fluid flow properties of thin, square-edged, circular orifices are described. Liquids were used at low frequencies. The flow conditions considered are a sinusoidal oscillation of the fluid in the orifice and a sinusoidal oscillation with a steady flow component added. For the sinusoidal flow condition the pressure differential developed across the orifice contains higher odd harmonics. The addition of a steady flow component adds second harmonic to the pressure, as well as influences the magnitude of the odd harmonics. Further, in this case, the steady pressure component is a function of the magnitude of both the sinusoidal and steady flow components. An equation descriptive of the pressure-flow relation is presented. In this equation the orifice properties are specified by three constants, two of which are the acoustic resistance and acoustic inertance as normally measured at low amplitudes of excitation. The relations derived from this equation are compared with experimental measurements.

Aircraft, Hydraulic

4.3-2

### ON THE DECOMPRESSION OF A PUNCTURED PRESSURIZED CABIN IN VACUUM FLIGHT

Demetriades, S. T.  
AMERICAN ROCKET SOCIETY JOURNAL  
pp. 35, 36 January-February 1954

This article derives the fundamental equation for sonic blowdown through an isentropic nozzle. bib.

Aircraft, Pneumatic

4.3-3

### NONSTEADY DISCHARGE OF SUBCRITICAL FLOW

Rudinger, G.  
AMERICAN SOCIETY OF MECHANICAL ENGINEERS  
Paper 60-WA-152 for Meeting November 1960

The calculation of a nonsteady flow discharging into the atmosphere, or into a large reservoir, is generally based on the assumption that the effective exit pressure is the same as if the flow were steady. In reality, however, the steady-flow boundary conditions are asymptotically approached after a disturbance produced by an incident wave, and

recently published investigations provide a better approximation to these transient boundary conditions. Utilizing these results, one can compute the rate of discharge and compare it with the rate obtained in the conventional manner. The difference between the results of the two calculations is used to define a lag error in the conventional calculations. Examples for discharges through an open end and through a sharp-edged orifice indicate that the actual transient flow rate may deviate considerably from that computed on the basis of steady-flow boundary conditions.

Aircraft, Pneumatic

- 4.3-4 SYMPOSIUM ON MEASUREMENT IN UNSTEADY FLOW  
ASME Hydraulic Division Conference, Worcester, Mass.  
May 21-23, 1962

Aircraft

- 4.3-5 TIME OF DISCHARGE OF HIGH PRESSURE GASES  
Geyer, E. W.  
ENGINEER  
168:30-63, 1938

Aircraft, Pneumatic

- 4.3-6 BLOWDOWN, CHARGING AND PUMPING PROCESSES USING PRESSURIZED GAS  
CALIFORNIA INSTITUTE OF TECHNOLOGY, JET PROPULSION LABORATORY  
Literature Search 135. CONFIDENTIAL

Aircraft

- 4.3-7 NONLINEAR PROPERTIES OF CIRCULAR ORIFICES  
Thurston, G. B.  
OKLAHOMA A & M COLLEGE, RESEARCH FOUNDATION  
Technical Report No. 2. May 1957  
Contract DA23-072-ORD-583. Project TB2-0001(1336)

See 4.3-1

- 4.3-8 SOME GEOMETRICAL EFFECTS ON THE NONLINEAR PROPERTIES OF ORIFICES  
Thurston, G. B. et al.  
OKLAHOMA A & M COLLEGE, RESEARCH FOUNDATION  
Technical Report #3. May 1957  
Contract DA 23-072-ORD-583. Project TB2-0001(1336)  
AD 134911

The results of a study of the effect of some geometrical conditions on the nonlinear properties of fluid flow through orifices is presented. The geometrical conditions considered are interaction between circular orifices; circular, rectangular, and square shape; square, round, and bevel-edged conditions; nonsymmetric bevel-edged orifice. These samples are studied for sinusoidal fluid motion in the orifice. It is found that for all symmetric samples, the basic form of the odd harmonic pressure components developed is unchanged by geometry. For the nonsymmetric sample, the pressure contains both odd and even harmonics as well as a steady component.

Aircraft, Hydraulic

43-9

#### ON THE FLOW IN A HIGH PRESSURE VALVE

Goldsworthy, F. A.

ROYAL SOCIETY, PROCEEDINGS, SERIES A.

218:69-87, June 1953

This paper develops an approximate theory which seeks to determine the flow in a valve. The dependence of the flow upon such parameters as the initial pressure ratio across the valve, the speed of opening and design of the valve is indicated. An idealized type of valve is selected--two cones initially joined at their apices and having equal solid angles, are "telescoped" together with constant velocity. This valve allows a transformation of the equations of motion (considered here to be unsteady and one dimensional) to a form identical with those governing unsteady spherical motion. A similarity solution of these equations is then found. The strengths of the shock and contact discontinuity, which move into the low-pressure side on opening the valve, are obtained for various values of the initial pressure ratio and the Mach number of the valve (the ratio of the velocity of "telescoping" to the initial velocity of sound). A "critical" relationship is established between the initial pressure ratio and the Mach number of the valve such that the flow velocity at the throat is just sonic; i.e., the valve has "choked;" elsewhere the flow velocity is subsonic. Above this "critical" pressure ratio the theory indicates that "choking" persists and the supersonic flow is established ahead of the throat and is bounded by a second shock, which follows the contact surface and the first shock already mentioned. The flow exhibits the principal features of steady flow in a nozzle; typical quantitative differences are exhibited in several practical examples worked out on the basis of the theory.

Aircraft, Pneumatic, Poppet Valve

4.3.10 ANALYTICAL INVESTIGATION OF BLOWDOWN AND CHARGING PROCESSES  
IN SINGLE GAS RECEIVER INCLUDING EFFECTS OF HEAT TRANSFER.  
PARTS 1 & 2

Reynolds, W. C.

STANFORD UNIVERSITY, DEPARTMENT OF MECHANICAL ENGINEERING  
Technical Report Nos. T-1, T-2, October 1955 and December  
1956

Contract N 6 ONR-251, Task Order 6

Technical Report T-2. In this report, experimental data for the blowdown process in a single air receiver is presented and discussed in detail. The data indicate that the analyses presented in an earlier report are useful for design purposes and give reasonable performance predictions for blowdown systems where heat transfer from and through the receiver walls is important. The data and analyses indicate that heat transfer may be neglected only for extremely rapid blowdown processes, and must definitely be considered in the design of most technical systems involving blowdown.

Aircraft, Pneumatic

4.3-11 PRESSURE HISTORY OF A GAS TANK BLED BY A VENT VALVE

Baer, H. W.

THOMPSON RAMC WOOLDRIDGE INCORPORATED

Report GM TM 44, EM #7-2, WDD Document No. 7 2074, No date

Contract AF18(600)1, 90

AD 210922

The pressure history is evolved for a mixture of ideal gases which expand adiabatically through a loss-less valve of known characteristics.

The cross-sectional area of the valve is computed for a stipulated weight flow at given temperature and pressure. Furthermore an expression for the molecular weight of a mixture of two gases is derived as a function of the state of the two gases and the weight of one of them.

The history of the pressure ratio is computed and shown in graphical form for a case with known initial properties of the expanding gas.

Aircraft, Pneumatic

4.3 CROSS REFERENCES

1.3-1

2

-12

## 5.0 VALVE SEALING

The primary objective of most valves is to shut off flow. In rocket and spacecraft applications, the leakage requirements often exceed the state of the art. Emphasis has been placed herein on valve sealing as being both fundamental and yet analytically neglected. Data have been collected on the subject matter under the subsections listed below in an attempt to shed some light on this most important phase of valve design. Cross-references will contain such material as was considered pertinent to each subsection. The divisions of the section are as follows:

### 5.1 Leakage and Analogous Flows

### 5.2 Seals, Leak-Detection Methods and Measurements

### 5.3 Seating

### 5.4 Contamination

### 5.5 Friction and Wear

Investigation of the references cited under 5.1 will show that most of the material is "analogous flows." Subsection 5.2 covers the subject material indicated. Subsection 5.3 is meant to contain only information contributing directly to the understanding and analysis of valve seating; i.e., information on the relationship of stress, surface finish, geometry, wear, etc., on leakage. The prosaic article on seat hardness was included more because of title applicability than content. The co-article on microtopology sets the theme of the subsection. Valve contamination references are contained under 5.4. The subject matter under 5.5 has been included primarily for data on the basic wear process. Accompanying information on friction should not be confused with the friction data of 3.1 which deals specifically with valves.

## Leakage and Analogous Flows

### 5.1-1 FLOW OF COMPRESSIBLE FLUID IN THIN PASSAGES

Grinnell, S. K.

AMERICAN SOCIETY OF MECHANICAL ENGINEERS, TRANSACTIONS

78:765-71, May 1956. See also paper 55-SA-13

Pressure distribution and weight-flow rate can be predicted for laminar compressible-fluid flow in a thin passage by use of the methods presented in this paper. A simplified method can be used readily when the fluid forces due to viscous action predominate over those due to acceleration of the fluid. A more complicated trial-and-error method seems to be required for larger passages where, though the flow may be laminar, the momentum effects due to acceleration of the compressible fluid are appreciable. An experimental apparatus was used to examine the validity of the analytical work. Experimental pressure distributions agree within a maximum deviation of 50 percent with predictions of the simplified theory. Dimensionless plots of pressure distribution are presented with experimental curves of flowrate vs pressure ratio for various ratios of passage length,  $L$ , to passage height,  $h$ . These plots, together with simple equations, have been prepared for direct use by the designer.

2.1

Aircraft, Pneumatic

### 5.1-2 GENERAL METHOD FOR CORRELATING LABYRINTH SEAL LEAK RATE DATA

Heffner, F. E.

AMERICAN SOCIETY OF MECHANICAL ENGINEERS, TRANSACTIONS  
SERIES D

82:265-75, June 1960

The proper selection of an optimum labyrinth seal for a given application depends upon an accurate estimate of the seal leak rate. Suitable accuracy, particularly for straight labyrinth seals, can only be obtained from actual seal tests. Testing a complete series of seals is time consuming and expensive. A method for correlating test data is presented which allows calculation of the leak rates for an entire family of labyrinth seals on the basis of tests of only two characteristic seals. Leak rates predicted by the method are within 3 percent of the basic test data.

2.1

Aircraft, Pneumatic

5.1-3 PRESSURE DROP AND FLOW CHARACTERISTICS OF SHORT CAPILLARY TUBES  
AT LOW REYNOLDS NUMBERS

Kreith, F. et al.

AMERICAN SOCIETY OF MECHANICAL ENGINEERS, TRANSACTIONS

79:1070-8, July 1957

The pressure drop and flow characteristics of short capillary tubes have been investigated experimentally for length-to-diameter ratios varying from 0.45 to 18 at diameter Reynolds numbers ranging from 8 to 1500....The results of this study have application to: (a) Simulating flow through screens, doors, cracks, and fissures in small-scale model testing of buildings in atmospheric wind tunnels. (b) Automatic control devices where capillary tubes are used as hydraulic resistances in a larger line and in nozzle-flapper combinations. (c) Heat pumps and air conditioning equipment where short capillary tubes are used as two-way control valves. (d) Flow through compact heat exchangers and porous materials.

2.1

Aircraft, Hydraulic

5.1-4 THROUGH FLOW IN CONCENTRIC AND ECCENTRIC ANNULI OF FINE CLEARANCE  
WITH AND WITHOUT RELATIVE MOTION OF BOUNDARIES

Tao, L. N. et al.

AMERICAN SOCIETY OF MECHANICAL ENGINEERS, TRANSACTIONS

77:1291-301, November 1955. See also paper 54-A-175

The problem of the through-flow across annuli of fine clearance has been investigated both theoretically and experimentally. The study includes the effects due to the relative motion of the walls and to varying degrees of eccentricity of the bounding surface. The experimental work was carried up to a Reynolds number, based on the diametral clearance, of 30,000. The theoretical results are presented both graphically and in the form of equations. Nomographs are included for rapid solution of certain engineering problems.

2.1

Aircraft, Hydraulic

5.1-5 FLUID MECHANICS APPROACH TO LABYRINTH SEAL LEAKAGE PROBLEM

Vermes, G.

AMERICAN SOCIETY OF MECHANICAL ENGINEERS, TRANSACTIONS,  
SERIES A

JOURNAL OF ENGINEERING FOR POWER

83:161-9, April 1961



The paper describes investigations of labyrinth seals carried out recently; derives new theoretical and semitheoretical formulas for computation of the leakage which agree within 5 percent with the tests for three different types of seals; off-design performance of the seals is treated theoretically and experimentally.

2.1

Aircraft, Hydraulic

5.1-6 LABYRINTH SEAL LEAKAGE ANALYSIS

Zabriskie, W. et al.

AMERICAN SOCIETY OF MECHANICAL ENGINEERS, TRANSACTIONS,  
SERIES D

JOURNAL OF BASIC ENGINEERING.

81:332-6, September 1959

The leakage flow through labyrinth seals in turbomachinery has been the subject of increasing concern as refinements and advances in design are made. Accurate knowledge of seal leakage is necessary in at least three areas of design: (a) estimating the effect of seal leakage on performance; (b) regulating the leakage flow required for cooling purposes; (c) determining the thrust-bearing load which is a function of the pressure drop through the seal. This paper is concerned primarily with the fluid-flow aspect of gas leakage through labyrinth seals of the types commonly used in gas and steam turbines. This includes staggered and unstaggered seals of the axial type, which are most commonly used in turbomachinery. The attention to fluid flow considerations does not imply that material compatibility and operating problems of expansion, deformation, and rub-in are unimportant. In fact, these mechanical considerations may overrule the fluid flow considerations. For the foregoing reasons, it is desirable to be able to predict seal leakage flows, and thus this aspect of seal design has been singled out for consideration here.

2.1

Aircraft, Pneumatic

5.1-7 THE PERMEABILITY OF FABRICS TO AIR WITH PARTICULAR REFERENCE TO PARACHUTE MATERIALS. PART III. A STUDY OF AIR FLOW THROUGH SINGLE APERTURES OF SMALL SIZE

Goodings, A. C. et al.

CANADA, ONTARIO RESEARCH FOUNDATION

No report number. December 1961

AD 272525

A study of air flow was carried out on single apertures of small size extending downward to areas comparable with the interstitial areas in parachute fabrics. While the flow behavior, even in the case of the smallest holes examined, can be described as approximating the nonfrictional conditions of the Bernoulli equation, the discharge coefficients calculated on this basis show a considerable range in magnitude. Factors influencing this spread are considered in the light of the experimental results.

2.1

Aircraft, Pneumatic

- 5.1-8      GAS FLOW THROUGH SMALL ORIFICES  
            Osburn, J. O. et al.  
            CHEMICAL ENGINEERING PROGRESS  
            50:198-9, April 1954

Measurements were made of the rate of flow of air and helium through small circular holes in thin plastic film. The results are shown as a graph of orifice coefficient vs Reynolds number. The findings are similar to those previously reported for a square-edged orifice, and extend the range of orifice coefficient measurements to lower Reynolds numbers.

2.1

Aircraft, Pneumatic

- 5.1-9      LOW PRESSURE GAS FLOW IN A CONSOLIDATED POROUS MEDIA. I. FLOW THROUGH A POROUS CERAMIC  
            Ash, R.  
            FARADAY SOCIETY, TRANSACTIONS  
            56:1357-71, 1960

Experiments have been carried out near room temperature on low-pressure gas flow through a porous porcelain ceramic made in the form of a cylindrical rod about 0.3 cm in dia. and nearly 50 cm in length, the flow occurring along the axial direction only. The gases used were the inert gases; hydrogen, nitrogen, oxygen, ethane, carbon dioxide, and sulphur dioxide.

2.1

Aircraft, Pneumatic

- 5.1-10     FLOW THROUGH AND BLOCKAGE OF CAPILLARY LEAKS  
            Burrows, G.  
            INSTITUTION OF CHEMICAL ENGINEERS, TRANSACTIONS  
            39:55-63, #1, 1961

To help in understanding the behavior of small leaks in vacuum equipment, the various types of gas flow that can occur through small-bore capillaries are considered, and some formulae are derived that represent flowrates under different conditions. The factors that control the flow of liquids through capillaries are reviewed, together with the behavior to be expected when a volatile liquid evaporates from a capillary into a vacuum. The limitations imposed by porosities are examined, taking into account the special features of adsorbed flow. Some causes of capillary blockage are investigated, including surface tension and surface adhesion effects, and the conditions under which the influence of viscosity exerts a significant restriction. The removal of such blockage by a pressure difference and by evaporation is discussed.

2.1

Aircraft, Pneumatic and Hydraulic

5.1-11 FLOW OF AIR THROUGH RADIAL LABYRINTH GLANDS

Kearton, W. J.

INSTITUTION OF MECHANICAL ENGINEERS, PROCEEDINGS

169:539-52, #30, 1955

A theory for the flow of air through a radial gland has been worked out for both outward and inward flow. Expressions are derived for the pressure distribution in each kind of flow, and it is shown that the critical pressure ratio can be reached only in the final constriction. Experiments were made on a gland having a single ring and also on a 20-ring gland of the staggered type. The discharge coefficients in the latter gland were lower than those in the single-ring gland, possibly due to the different approach conditions. The observed pressure distribution in the multiring gland agreed well with the theoretical value. Finally, some experiments were made with unstaggered radial glands under various conditions. Discharge coefficients greater than unity were measured.

2.1

Aircraft, Pneumatic

5.1-12 ALMOST FREE MOLECULE FLOW THROUGH AN ORIFICE

Liu, V. C. et al.

JOURNAL OF THE AEROSPACE SCIENCES

27:875-6, November 1960

2.1

Aircraft, Pneumatic

5.1-13 FLUID FLOW THROUGH POROUS METALS  
Green, L. Jr., et al.  
JOURNAL OF APPLIED MECHANICS  
18:39-45, March 1951

A method is outlined for correlating experimental data obtained in studies of the flow of gases and liquids through porous metals. The correlation is based upon the suggestion of Forcheimer that the pressure gradient attending the flow of a liquid through a porous medium can be expressed as a function of flowrate by a simple quadratic equation. An equation of this type defines two length parameters necessary for characterization of a porous structure and permits a general definition of the Reynolds number for a structure of arbitrary complexity.

2.1

Aircraft, Pneumatic and Hydraulic

5.1-14 PHYSICAL THEORY FOR CAPILLARY FLOW PHENOMENA  
Miller, E. E. et al.  
JOURNAL OF APPLIED PHYSICS  
27:324-32, 1956

From the assumption that the microscopic behavior of the liquid in an unsaturated porous medium is controlled by the physical laws of surface tension and viscous flow, differential equations governing the macroscopic flow in such a medium are deduced. No special pore-shape assumptions are required, but one topological approximation is needed; i.e., that neither isolated drops nor isolated bubbles occur. Several nonessential simplifying assumptions are used; i.e., that the macroscopic properties of the medium, the character of the liquid, and the pressure of the gas are independent of position, time, and direction. The macroscopic equations are obtained in a fully reduced form, permitting comparison between two media--or between two flow systems--that differ only by scaling factors.

A novel feature of this calculation is its prediction that the liquid-transmission and liquid-capacity properties of an unsaturated medium will exhibit hysteresis in their dependences upon the liquid-gas pressure differential,  $p$ . The properties of the medium depend upon the pressure history but are invariant to monotonic time-scale distortions of that history. Such time-invariant functionals have been termed by the authors "hysteresis functions," symbolized by the subscript,  $H$ ; e.g.,  $F_H(p)$ . Although methods for measuring and describing the characteristics of specific "hysteresis functions" have not yet been developed, the general validity of this analysis can be studied experimentally by testing predictions that are contained in the reduced variables.

2.1

Aircraft, Hydraulic

5.1-15 FLOW OF GASES IN POROUS MEDIA

Wilson, L. H. et al.

JOURNAL OF APPLIED PHYSICS

22:1027-30, August 1951

This paper presents a brief theoretical review of the viscous and free molecular flow phenomena. The equations which describe these two types of flow are applied to flow through porous media and are combined to yield a semiempirical equation which may be used not only for the viscous and free molecular flow, but also for the transition region between these. Experimentally determined limiting values of the ratio of molecular mean free path to pore diameter are reported. These ratios may be used to indicate the nature of flow in a porous media provided the pore size is known, or they may be used to determine pore size experimentally.

2.1

Aircraft, Pneumatic

5.1-16 A NOTE ON THE FLOW OF GASES THROUGH VERY FINE TUBES

Sears, G. W.

JOURNAL OF CHEMICAL PHYSICS

22:1252-3, July 1954

It is shown that Knudsen's laws of flow for rarefied gases must be modified for very fine tubes. Gas flow occurs by diffusion of molecules in the adsorbed layer on the tube walls as well as in the gas phase. When the tube dimension is comparable to the mean free path in the gas film, the two flow mechanisms become comparable in effectiveness.

2.1

Aircraft, Pneumatic

5.1-17 FLUID FRICTION IN ANNULI OF SMALL CLEARANCE

Nootbaar, R. F. et al.

PROCEEDINGS OF 2nd MIDWESTERN CONFERENCE ON FLUID MECHANICS

Ohio State University Engineering

Experiment Station Bulletin #149

PP 185-99, 1952

2.1

Aircraft

5.1-18 CONSTRUCTION OF SMALL FIXED LEAKS OF PREDICTABLE THROUGHPUT

Gordon, S. A.

REVIEW OF SCIENTIFIC INSTRUMENTS

29:501-4, June 1958

A method is described by which glass capillary leaks with extremely small flow rates can be easily and rapidly produced. The predictability of these leak rates is determined by the resolution of the optical system used in measurement of bore diameter. Data are given which will allow construction of such leaks. A manifold of leaks is described which will introduce gas into a high-vacuum system at several different fixed leak rates. It contains no moving parts or high vapor pressure material on the high-vacuum side, yet the leak rates can be manipulated over a wide range. The characteristic features of these leaks are shown to be reasonable in light of well-established theory.

2.1

Aircraft, Pneumatic

5.1-19 CONTROLLED CAPILLARY GAS LEAK

Smither, R. K.

REVIEW OF SCIENTIFIC INSTRUMENTS

27:964-5, November 1956

A relatively simple adjustable capillary leak is described in which the gas flow is controlled by regulating the temperature of the gas in the capillary. This capillary leak contains no moving parts and can be controlled from a distance. The actual controlled flow is compared with the theoretical predictions, and a calibration curve is shown.

2.1

Aircraft, Pneumatic

5.1-20 LOW FLOW VARIABLE LEAK

Milican, R.

UNION CARBIDE NUCLEAR COMPANY

Research and Development Report, KY-166. February 1956

Contract W 7405-eng-26

AD 92901

2.1

Aircraft

**5.1-21 THERMALLY OPERATED GLASS VALVE TO PROVIDE VERY SMALL CONTROLLED  
GAS FLOW RATES**

**Forman, R.**

**U. S. NATIONAL BUREAU OF STANDARDS**

**NBS Report 1762. June 27, 1952**

**ATI 168762**

**2.1**

**Aircraft, Pneumatic**

**5.1 CROSS REFERENCES**

**5.2-15    5.4-1    7.0-4**

## Seals, Leak-Detection Methods and Measurements

### 5.2-1 TESTING OF METAL BOSS SEALS

Kupiec, H. P.  
AIRCRAFT EQUIPMENT TESTING COMPANY  
W TR 55-163. April 1955  
Contract AF33(600)26548  
AD 74322

The metal boss seal was conceived by Wright Air Development Center to meet the requirements of hydraulic and pneumatic systems with operating pressures up to 5000 psi, and temperatures as low as -100°F, and as high as 600°F. Basic development on the seal was accomplished by Wright Air Development Center. Further development work and testing of the seal were performed by the Aircraft Equipment Testing Company. The application of the metal boss seal involves the use of deformable metal ring in conjunction with standard AN hydraulic fittings with AND10056 or AND10057 fitting ends in standard AND10050 bosses. It is concluded that the metal boss seal possesses the desirable characteristics for a boss seal as indicated by tests conducted on size -5, -8, and -12. The metal boss seal is considered relatively simple and reliable. With proper choice of material, it is possible that this seal design may be suitable for operating temperatures above 600°F. This seal is being considered as a replacement for the current standard AN6290 synthetic rubber gasket.

Aircraft

### 5.2-2 COMPOSITE SEAL MATERIALS FOR EXTREME ENVIRONMENTS

Headrick, R. E.  
ARMOUR RESEARCH FOUNDATION  
FINAL REPORT, ASD TR 62-286. March 1962  
Contract AF33(616)7310, Project 7340  
AD 274082

Aircraft

### 5.2-3 COMPOSITE INORGANIC RESILIENT SEAL MATERIAL

Smith, L. L.  
ARMOUR RESEARCH FOUNDATION  
WADC TR 59-338, part 4. March-November 1961  
Contract AF33(616)7310, Project 7340  
AD 275606

The principal objective of this research program is for research on and the evaluation of composite materials suitable for use as static and dynamic seals at temperatures ranging from cryogenic to 1500°F and pressures up to 5000 psi.



The principal areas covered by the report are as follows:

1. Materials Research. Composites made of stainless steel or molybdenum skeletons impregnated with babbitt for cryogenic temperatures and copper for elevated temperatures were obtained using carbon molds for casting.
2. Static Seals. Included are studies of low- and high-pressure seals for space vehicles. In testing six-inch-diameter molybdenum-silver seals, spring-types such as C-rings were found to require less clamping force than solid types such as O-rings. Babbitt and indium fillers for cryogenic seals were successfully employed with molybdenum and stainless steel skeletons at -319°F to retain 2000-psi helium pressure.
3. Dynamic Seals. The sealing of rotating and reciprocating shafts with metallic composite seals is discussed, as well as dynamic test fixtures developed on the project.

Using a stainless steel-silver seal with a rotating shaft flame-sprayed with chromium carbide, successful sealing was obtained at 84°F and 757°F, 5000 rpm, and pressures of up to 4000 psi.

6.1, 6.2

Aircraft

- 5.2-4 SEALS COMPATIBLE WITH LIQUID ROCKET PROPELLANTS, INCLUDING  
IRFNA (BIBLIOGRAPHY)  
ARMED SERVICES TECHNICAL INFORMATION AGENCY  
ARB 133

Aircraft

- 5.2-5 SEALS FOR SPACECRAFT (BIBLIOGRAPHY)  
ARMED SERVICES TECHNICAL INFORMATION AGENCY  
ARB 085

Aircraft

- 5.2-6 DETERMINATION OF LEAKAGE VALUE OF SEALS  
Meyer, E. A. et al.  
BJORKSTEN RESEARCH LABORATORIES, INCORPORATED  
WADC TR 54-16. November 1953  
Contract AF33(038)15981  
AD 41362

Aircraft

- 5.2-7 EVALUATION OF HIGH TEMPERATURE HYDRAULIC SEALS  
Webster, E. A.  
DOUGLAS AIRCRAFT COMPANY, INCORPORATED  
Report DEV 1792. WADC TR 55-120. January 1955  
Contract AF33(616)235  
AD 70011

Aircraft

- 5.2-8 MECHANICAL SEALING AS IT STANDS TODAY  
Lymer, A.  
ENGINEERING  
191:572-3, April 21, 1961

As mechanical seals are required to perform new and more arduous duties, it becomes increasingly important to understand the basic mechanism of the sealing process.

Industrial

- 5.2-9 ALL METAL REED SEAL EVALUATION FOR 0-3000 PSIG PRESSURE  
HYDRAULIC SERVICE  
Hatfield, J. N.  
FULTON-SYLPHON COMPANY  
WADC TR 55-302. June 1955  
Contract AF33(606)28968  
AD 97637

Evaluation tests of all-metal reed seals were conducted by the Engineering Department of Fulton Sylphon Division, Robertshaw Fulton Controls Co., Knoxville, Tennessee. The tests were performed during the first quarter of the year 1955. Leakage rates and total leakages were accurately measured while the test shaft cycled through the reed seals. Physical wear on the seals was determined by measuring with a machinist's microscope before and after testing. At temperatures of 30°F and 70°F, test results indicate the feasibility of using an all-metal reed seal in aircraft hydraulic systems at normal operating pressures up to 3000 psig.

5.5

Aircraft, Hydraulic

- 5.2-10 BUBBLE LEAK DETECTION  
Biram, J. G. S.  
GREAT BRITAIN, ATOMIC ENERGY RESEARCH ESTABLISHMENT  
AERE Report No. CE/R 2066; HX 2797. March 1957  
AD 154814

Aircraft

5.2-11 A RESEARCH PROGRAM ON THE INVESTIGATION OF SEAL MATERIALS FOR HIGH TEMPERATURE APPLICATION

Baskey, R. H.

HORIZONS INCORPORATED

WADC TR 58-181. June 1957-March 1958

Contract AF33(616)3891

AD 155689

Novel rotating seal materials for potential aircraft applications at high speed and high temperatures were developed and tested under conditions of no external lubrication. These materials were arrived at after a systematic study of the wear behavior of:

1. Pure refractory hard metals.
2. Binary alloys of pure refractory hard metals, bonded with nickel.
3. Ternary alloys of pure refractory hard metals, bonded with nickel and infiltrated with silver.

Tests were conducted to determine the benefit derived from additions of nickel or silver to the refractory hard metals. The nickel acts as a tough, oxidation-resistant matrix. The silver was added to act as a lubricant as it softens at high temperatures. This aids the shearing action between mating surfaces and lowers the surface friction.

Ternary alloys prepared by powder metallurgy techniques consisting of high percentages by weight of a refractory hard metal, with nickel and silver additions, show superior wear qualities when run against either tool steel or Inconel. Tests were made at sliding speeds of 30,000 fpm and ambient temperatures up to 1350°F. The best alloys contained either tungsten boride (WB) or chromium nitride (CrN) as the hard refractory metal.

The WB alloy exhibited a constant wear rate at all temperatures against tool steel. The wear rate of the CrN alloy decreased at the higher temperatures.

All ternary alloys run against Inconel displayed a decrease in wear rate at ambient temperatures over 600°F. The wear decreased as a function of temperature for several ternary alloys against tool steel.

An impregnated graphite seal coated with an oxidation resistant layer of zirconium carbide showed improved wear properties over a regular graphite impregnated seal at an ambient temperature of 1050°F and sliding speeds of 14,000 fpm against stainless steel type 303.

The finest wear performance was attained when Kentanium K162B ran against Kentanium K162B at sliding speeds of 14,000 fpm in an ambient temperature of 1100°F.

It is hypothesized that the wear process is drastically influenced by the oxidation occurring on the rubbing surfaces and that with proper choice of materials, stable, complex oxides are formed which provide the correct solid lubricating film on each component and markedly lower the wear rate as the temperature is increased.

5.5, 6.1

Aircraft

5.2-12 INVESTIGATION OF HYDRAULIC LOW FRICTION TEFLON CAP SEALS

Bruno, J. O.  
HYDRA-POWER CORPORATION  
WADC TR 57-163. December 1957  
Contract AF33(600)28637  
AD 118213

A low friction rod seal was required for hydraulic actuators which would increase "O" ring life and minimize rod seal leakage. A test actuator, rod seals and corresponding hydraulic impulse and driving circuits were designed and built. Both static and cycling tests were conducted on various size seals with varying cross sectional "O" ring squeeze. Final design criteria are shown. Recommendations are made for additional tests of similar and related nature.

Aircraft, Hydraulic

5.2-13 STATIC SEAL STUDIES

Heywood, W. A.  
U.S. ATOMIC ENERGY COMMISSION, KNOLLS ATOMIC POWER LABORATORY  
KAPL 974. June 1953  
Contract W 31-109-eng-52  
AD 23076

Aircraft

5.2-14 CONTROL ROD GAS SEALS

Heywood, W. A.  
U. S. ATOMIC ENERGY COMMISSION, KNOLIS ATOMIC POWER LABORATORY  
KAPL 1161. January 1955  
Contract W 31-109-eng 52  
AD 56428

Aircraft

5.2-15 LEAKAGE AND WEAR IN MECHANICAL SEALS

Mayer, E.

MACHINE DESIGN

32:106-13, March 3, 1960

What are the major factors causing leakage and wear in mechanical seals?

Can leakage be calculated accurately?

What can be done to reduce leakage and wear?

Tests on unbalanced seals for 20,000 hours, with five face material combinations and three different fluids, have given some answers:

No fluid pressure exists between seal faces, in contrast to previous theories. Leakage, wear, and friction are determined by boundary lubrication. Surface width has no influence on leakage. Physical results confirm a new theory of fluid-exchange flow.

Leakage varies with the square of the distance between touching faces, and inversely with the square of the face pressure. No influence of viscosity has been noticed. Leakage is the same for all fluids, but nearly 100 times greater for external than for internal rotating seals.

Results reported are not limited to mechanical seals and may also be used for oil seals, piston rings and clutches.

5.1, 5.5

Aircraft

5.2-16 PARKER O-RING HANDBOOK

PARKER SEAL COMPANY

Catalogue 5700, Revised October 1959

Aircraft

5.2-17 SEALS FOR PRESSURES UP TO 10,000 ATMOSPHERES

Daniels, W. B. et al.

REVIEW OF SCIENTIFIC INSTRUMENTS

28:1058-9, December 1957

This note discusses the use of "armored" O-ring seals for the pressure range to 10,000 atmospheres. In addition, a simple high-pressure pump piston seal and a proprietary surface treatment to reduce liability of galling of steel parts are described.

Aircraft, Hydraulic

5.2-18      DEVELOPMENT OF ROTARY AND TRANSLATORY SEALS  
             SYRACUSE UNIVERSITY, RESEARCH INSTITUTE  
             Final Report. July 1952-August 1954  
             Contract DA 30-115-ORD-363. Project TR 5-5059T  
             AD 48377

Aircraft

## 5.2 CROSS REFERENCES

1.3-12	5.5-4	6.1-1	6.2-7	7.0-5
-13	-11			

## Seating

### 5.3-1 SEAT HARDNESS OF FLOW CONTROL VALVES

Fallows, D. H.

ENGINEER

197:934, June 25, 1954

The Canadian market is of growing importance to a number of engineering firms in this country. The author here draws attention to the circumstances, differing from those in the United Kingdom, under which valves are used in Canada. He recommends in particular, the fitting of hard valve seats, not less than 500 Brinell, and has certain other pertinent remarks to make about the design of valves, from his experience as an engineering executive.

### 5.4

Industrial, Flow Control, Plug Valve

### \*5.3-2 SURFACE MICROTOPOGRAPHY

Tolansky, S.

INTERNATIONAL SCIENCE AND TECHNOLOGY

9:32-9, September 1962

Knowing the true character of the surface of materials, even down to microstructures of molecular dimensions, is becoming increasingly important. Such information can tell how surfaces are formed, how they are distorted under various influences, how they are destroyed. Multiple-beam interferometry is one of the most powerful tools for examining the microtopography of a surface. As presently practiced, it can magnify the vertical dimension of surface irregularities up to 500,000 times. This sensitivity means that vertical displacements as small as 5 angstroms can be detected by the interference of many light beams reflected from the surface under study with those reflected from a reference optical flat above it. Viewed in this manner, tiny areas of a surface are characterized by a pattern of fringes--an optical contour map quite similar to the geologist's topographic contours. The microstructures thus revealed are providing clues to puzzles in a whole host of disciplines--from crystal physics to metallurgy.

### 5.5

Aircraft

### 5.2 CROSS REFERENCES

1.3-1	1.3-8	5.4-1	6.2-2
-2	-9		
-5	-13		
-6			

## Contamination

\*5.4-1

### INVESTIGATION OF DIRT SENSITIVITY OF TURBO ENGINE CONTROL COMPONENTS

Ash, J. E. et al.

ARMOUR RESEARCH FOUNDATION

WADC TR 54-479. PB 122476. October 1954

Contract AF33(616)421

AD 76873

Main objective of this program was: (1) to analyze the effect of basic geometric parameters of the valve assembly on the friction force caused by dirt particles, (2) to establish the criteria for deposition of the dirt particles in the flow channels of various geometry, (3) to develop a method for computation of the leakage flow through a smooth and a grooved clearance space.

The effect of the contaminant in the fuel on the friction force was studied on two types of valves: sleeve valve and double-poppet valve. It was found that the friction caused by dirt particles generally increased with the spool diameter, the rate of flow and the pressure differential across the valve assembly. The friction also increased with the time intervals between two consecutive movements of the valve spool, and tended to level off after one hour. The effect of the bearing length on the friction was less pronounced. The optimum surface finish was found to be 5 to 10 microinches RMS, and the surface hardness about 60 RC (for Arizona Road Dust). Surfaces smoother than 5 microinch RMS and harder than 60 RC brought no further reduction in friction. It was also found that a constant rotary motion applied to either sleeve or spool of a valve assembly almost eliminated the friction entirely.

The phenomenon of deposition of the dirt particles was studied theoretically, as well as by experiments conducted on transparent models of an actual sleeve valve, pipe bends, channels with restriction in flow, for different fluid velocities and sizes of dirt particles. Specific recommendations were presented to avoid undesirable dirt deposition.

A fundamental study was made of the leakage flow through annular clearance spaces for concentric, offset, and cocked positions of a cylindrical and tapered spool inside a sleeve. The experimental data obtained with spools of different clearances were found to be in close agreement with theory. In addition, the effect of the circumferential grooves inside the annular clearances were found to be in close agreement with theory. In addition, the effect of the circumferential grooves inside the annular clearance space upon the leakage flow was investigated. This led to the establishment of criteria for the design of optimum groove shapes and spacing. It was found that the grooves under certain conditions may give more leakage flow than the smooth spool.



The essential findings of this investigation were summarized and presented in a condensed form with an intention to serve as a guide for the problems concerning dirt sensitivity of valves.

1.4, 2.1, 2.6, 3.1, 3.2, 5.1, 5.3, 5.5

Aircraft, Hydraulic, Spool and Poppet Valves

**5.4-2 ESTABLISHMENT OF DESIGN CRITERIA FOR THE DEVELOPMENT OF DIRT INSENSITIVE FLUID PRESSURE CONTROL ELEMENTS**

Lee, J. C. et al.

ARMOUR RESEARCH FOUNDATION

AAF TR 6442. PB 118492. March 1952

Contract AF33(038)6494

Aircraft, Hydraulic

**5.4-3 EFFECTS ON SERVOVALVES (CONTAMINATION REPORT)**

Meagher, G. F.

HYDRAULICS AND PNEUMATICS

15:49-51, February 1962

If fluid power is to march confidently into the promised land of servo systems, the big obstacle it will have to overcome is contamination. Component designers and system designers recognize this and are working on the problem in two ways. First, they are making components less susceptible to dirt. Second, they are making systems cleaner by using better filtration. The following six articles, prepared by experts in contamination control, point out servovalve design features, methods of evaluating and classifying contamination, and filter cleaning techniques.

1.4, 3.1

Aircraft, Hydraulic, Servo Control, Spool Valve

**5.4-4 SERVOVALVE HYSTERESIS**

Osgood, R. E.

HYDRAULICS AND PNEUMATICS

15:51-3, February 1962

Servovalve hysteresis may be caused by slide sticking in the valve. This report presents design factors for optimum slide design to reduce sensitivity to contamination.

1.4, 3.1

Aircraft, Hydraulic, Servo Control, Spool Valve

5.4-5 PARTICLE EVALUATION (CONTAMINATION REPORT)

Rebert, C. J.

HYDRAULICS AND PNEUMATICS

15:58-64, February 1962

A single number which indicates total particle volume is a simpler way to indicate contamination than particle count by size.

1.4

Aircraft, Hydraulic

5.4-6 SERVOVALVE DESIGN (CONTAMINATION REPORT)

Wheeler, H. L. Jr.

HYDRAULICS AND PNEUMATICS

15:54-6, February 1962

Servo valve reliability and performance depend on many factors, including valve design, its filtering, and the contaminants the filters must intercept. Part 1 of this series discusses servo valve design and major trouble spots. Two more articles will deal with filter design and contamination testing.

1.4

Aircraft, Hydraulic, Servo Control, Spool Valve

5.4-7 CONTAMINATION AND SERVOVALVES. PART 3 - CONTAMINANTS

Wheeler, H. L. Jr. et al.

HYDRAULICS AND PNEUMATICS

15:93-95 July 1962

Articles in the February and April issues of Hydraulics and Pneumatics pointed out where contamination collects in servo valves and how it is filtered. This article analyzes the contaminants.

1.4

Aircraft, Hydraulic, Servo Control, Spool Valve

5.4 CROSS REFERENCES

1.2-16    1.4-2    3.1-4    5.3-1    7.0-4

## Friction and Wear

### 5.5-1 FRICTION AND WEAR OF METALS IN GASES UP TO 600 C

Cornelius, D. F. et al.

AMERICAN SOCIETY OF LUBRICATION ENGINEERS, TRANSACTIONS  
(ASLE)

4:20-32, April 1961

Apparatus is described for measuring friction and wear in controlled atmospheres. A comparison is made of the room temperature behavior of copper, mild steel and brass, rubbed against a hardened tool steel, in four environments--vacuum ( $10^{-3}$  mm Hg), dry helium, dry carbon dioxide, and dry air. The effect of varying the water vapor content in air is also discussed.

The initial selection of rubbing pairs for service at elevated temperatures in gaseous environments under unlubricated conditions, is based on their long-term resistance to corrosion and their ability to give low wear rates. In general, therefore, the materials must be hard. Several alloys having chromium contents of between 1% and 30%, and hardness values in the range 200 to 1000 vpn have been investigated. These included two low-chromium nitrided steels, a tungsten-chromium tool steel, and a series of four Co-Cr-W alloys. Specific wear rates and friction coefficients varied markedly with temperature, and values in the ranges  $10^{-13}$ - $10^{-8}$  cm<sup>3</sup>/cm kg and 0.1-0.8, respectively, were obtained in both dry carbon dioxide and dry helium. Lowest wear rates were observed with the nitrided steels. The diverse characteristics observed are discussed on the basis of current theories of adhesive wear.

## 6.2

### Aircraft

### 5.5-2 STUDY OF EFFECT OF WEAR PARTICLES AND ADHESIVE WEAR AT HIGH CONTACT PRESSURES

Sciulli, E. B. et al.

AMERICAN SOCIETY OF LUBRICATION ENGINEERS, TRANSACTIONS(ASLE)

1:312-8, #2, 1958

The wear rate and friction characteristics were determined for certain combinations of cobalt base alloys and stainless steels when rubbed together at unit pressures up to 300,000 psi in an environment of demineralized water at room temperature. Wear rate and friction data were collected both in the presence and absence of wear particles. A study was also made on the effect of sliding-surface geometry in trapping wear particles.

The results suggest that an exponential relationship exists between wear rate and stress for the materials of test and this relationship is influenced by material combinations and sliding velocity. Entrapped wear particles also affect the wear rate.

Because the wear rate appears to increase sharply at some nominal contact stress when the data are plotted on Cartesian coordinates, the authors define an "Apparent Critical Stress," using this term and a wear factor term to aid in the evaluation and discussion of results.

#### 5.5-3 METAL WEAR BY SCORING

Olson, J. H. et al.

AMERICAN SOCIETY OF METALS

Preprint 204 for meeting October 17-21, 1960

Score loads have been determined for a variety of ferrous-ferrous and ferrous-nonferrous combinations by progressively loading lubricated reciprocating samples until scoring occurs. For two hardened steel surfaces, the score resistance increases hyperbolically as the average finish improves from 60 to 3 microinches. It is shown that score temperatures are constant and that smoothly finished samples do not score until high loads are attained because they remain comparatively cool. Furthermore, higher score loads can be attained and score damage minimized by utilizing an aluminum base, rather than steel, under hard plated surfaces to enhance the thermal conductivity and prevent loss of the oil film. Data reported agree well with the mechanism of scoring proposed by Crook and Shotter.

Aircraft

#### 5.5-4 CHARACTERISTICS GOVERNING THE FRICTION AND WEAR BEHAVIOR OF REFRACTORY MATERIALS FOR HIGH TEMPERATURE SEALS AND BEARINGS

Sibley, L. B. et al.

BATTELLE MEMORIAL INSTITUTE

WADD TR 60-54. May 1958-May 1959

Contract AF33(616)3995. Project 7350

AD 243897

An investigation of the basic factors involved in the wear and friction of ceramics, cermets, and high-temperature alloys sliding at speeds of 100 to 200 fps and temperatures from 500 to 1000 C (1000 F to 1800 F) has been made. Bearing pressures covered a range of 5 to 50 psi. Statistical correlation of measured wear rates with friction and material properties indicates that, at these temperatures, the wear rate of ceramics and cermets may be approximately described by the following relationship:

$$\text{Wear rate} \propto \frac{\mu}{R^{1.25} D^{0.75}}$$

where  $\mu$  is the coefficient of friction, R is the thermal-stress-resistance factor, and D is the thermal diffusivity of the mated material on which wear predominates, which is usually the material with the lowest thermal-stress resistance.

A mechanism of wear has been evolved based on the above correlation and on the experimental study of friction and wear surface-temperature fluctuations using special transducers and color motion picture photography. The predominant wear mechanism in the high-speed sliding of ceramic and cermet materials appears to involve formation of hot spots at asperity contacts and subsequent fracture of the material near these hot spots as a result of thermal stresses. In this situation, the wear rate is influenced both by the configuration of the rubbing parts and by the thermal-stress-resistance properties of the materials. When one of the mating surfaces is interrupted, the total wear is greater. Wear tends to predominate on parts with interrupted wear surfaces, such as slider bearings, in comparison with their continuous mating surfaces or ring surfaces, such as in face seals, and on ceramic and cermet materials with low thermal-stress-resistance factor and low thermal diffusivity.

Promising commercial materials for high-temperature dry sliding bearings, gas bearings, and seals include  $\text{Al}_2\text{O}_3$ -Cr-Mo cermets, SiC ceramics, and TiC-Ni-Mo cermets. One experiment with a SiC-Si<sub>3</sub>N<sub>4</sub> ring stator mated against a TiC-Ni-Mo-NbC rotor, as in a face seal, was operated for a total of 20 hours up to 1000 C (about 1800 F), 200-fps sliding speed, and 20-psi unit load with only slight surface damage and a total wear of 6.7 mils, most of which occurred on the rotor.

5.2, 6.1, 6.2

Aircraft

#### \*5.5-5 WEAR OF MATERIALS: IMPACT ON DESIGN FAILURE

Barkan, H. E.

ELECTRO-TECHNOLOGY

68:95-102, July 1961

It is the purpose of this article to present, among other phases of the subject, an exposition of all the types of mechanisms of wear, the relevant hypotheses, the service factors that affect the nature and extent of wear, the various techniques and materials used to inhibit or minimize wear, and finally, methods for calculating predictability of wear. A bibliography is provided for further study of the subject. The author's approach throughout is to present the theoretical core of the subject of wear in practical terms applicable to the needs and problems of the design engineer. The title of the article--"Wear of Materials-Impact on Design Failure"--is, in fact, a terse summary of its purpose.

Aircraft

#### 5.5-6 SINGLE CONTACTS AND MULTIPLE ENCOUNTERS

Archard, J. F.

JOURNAL OF APPLIED PHYSICS

32:1420-5, August 1961

The analysis of wear experiments suggests that most of the events which occur in rubbing are contacts between protuberances which are deformed elastically and which separate without damage; an asperity encounter with damage is a relatively rare event. Apparatus for the study of isolated single contacts is described. A single contact which is deformed elastically does not obey Amontons' law, but an assembly of such contacts (multiple contact conditions) should do so. It is shown that under multiple contact conditions, the load which can be borne by elastic deformation of the protuberances may be as much as a million times larger than that which can be borne by each individual asperity contact. Reflection electron microscopy shows that many irregularities on worn surfaces must bear their share of the load without plastic flow. Recent experiments suggest that, although a worn particle is produced very infrequently, it is nevertheless the direct consequence of the many preceding encounters which occurred without apparent damage.

Aircraft

#### 5.5-7 INFLUENCE OF SURFACE ENERGY ON FRICTION AND WEAR PHENOMENA

Rabinowicz, E.

JOURNAL OF APPLIED PHYSICS

32:1440-4, August 1961

A number of friction and wear phenomena are explicable in terms of the surface energy of adhesion of the contacting materials. In the friction field, it is found qualitatively that high friction coefficients are found for sliding materials with high surface energy/hardness ratios and conversely. Unfortunately, it is not easy to test this relationship quantitatively because the derived expression contains parameters which cannot be independently controlled. However, in the wear field, it has been found possible to derive an expression for the size of loose wear particles that is proportional to the surface energy/hardness ratio, the nondimensional constant of proportionality being 60,000. Experiments with 15 different materials show the validity of this expression. Another phenomenon, adhesion, which also seems to be governed by surface energy considerations, is discussed in qualitative terms.

Aircraft

#### 5.5-8 MASS AND ENERGY BALANCE FOR WEAR PROCESS

Chenea, P. F. et al.

LUBRICATION ENGINEERING

12:123-5, March-April 1956

5

A mathematical treatment is given of one phase of the wear processes which is defined as "fatigue wear." This wear is envisioned as a sink for energy after a disturbed surface has become saturated with internal energy; that is, has become work hardened to the limit, and the additional energy is used to increase the surface area (produces abraded particles). A mass and energy balance is presented to describe the process.

Aircraft

5.5-9 HOW WEAR IS INFLUENCED BY SURFACE FINISH

Sonntag, A.

METAL PROGRESS

77:140-2, April 1960

Digest of "The Significance of Surface Finish on Friction Wear and Lubrication," by A. Sonntag. Paper presented at Seminar on Friction, Lubrication and Wear, Lucerne, Switzerland, Sept. 1959.

5.5-10 THEORY OF ABRASION OF SOLIDS SUCH AS METALS

Goddard, J. et al.

NATURE (LONDON)

184:333-5, August 1, 1959

Aircraft

5.5-11 FRICTION AND WEAR IN WATER LUBRICATED SEALS

Cornell, R. L. et al.

PRODUCT ENGINEERING

32:48-41, July 24, 1961

Comprehensive investigation of seal wear under boundary lubrication shows that graphite against chrome-plated steel gives the best combination of low wear rate and low friction.

5.2

Aircraft

5.5-12 MORE SURFACE POLISHING--LESS GALLING

Moore, W. H.

PRODUCT ENGINEERING

29:63-5, November 24, 1958

Of many factors that inhibit galling of metals, the most important is a preconditioned surface. Here are test results showing why components should be "worn-in" before they take loads, and why cast irons are less likely to gall than the steels or brasses.

Aircraft.

5.5-13 NEW COEFFICIENTS PREDICT WEAR OF METAL PARTS

Rabinowicz, E.  
PRODUCT ENGINEERING  
29:71-3, June 23, 1958

What are the effects of galling...poor oil...dust...surface cracks? These coefficients give answers that can lengthen life of a sliding system. With equations and other data are included examples of applications to design problems.

Aircraft

5.5-14 EXPERIMENTAL STUDY OF FRICTION AND WEAR DURING ABRASION OF METALS

Avient, B. W. E. et al.  
ROYAL SOCIETY, PROCEEDINGS, SERIES A  
258:159-80, October 18, 1960

Aircraft

5.5-15 A LITERATURE SURVEY OF BEARINGS, FRICTION, WEAR AND LUBRICATION PERTINENT TO CRYOGENIC APPLICATIONS

Barrick, P. L. et al.  
U. S. NATIONAL BUREAU OF STANDARDS  
NBS Report 6018. October 1958

6.1, 6.2

Aircraft

5.5-16 CONTACT STRESS AND LOAD AS PARAMETERS IN METALLIC WEAR

Dorinson, A. et al.  
WEAR-USURE-VERSCHLEISS  
4:93-110, March-April 1961

The course of metallic wear in the presence of oil was investigated over a range of applied loads at two stress levels: 10,898 kg/cm<sup>2</sup> and 4922 kg/cm<sup>2</sup>. The wear process was found to be multistage in nature, showing first a more or less abrupt rise, then a leveling-off and finally transition to accelerated wear. At equivalent stages in the wear process, the depth rate of wear was found to depend on the nominal contact stress rather than on the load. This can be explained by a model in which the deformation of asperities is related to their depth distribution, which governs the average depth to which the contacting specimens are abraded. The volume wear data of Archard are shown to be consistent with this model when the geometry of the specimen pieces is taken into account.

Aircraft

5.5 CROSS REFERENCES

1.2-15    1.4-2    5.2-9    5.3-2    5.4-1    7.0-8  
                             -11  
                             -15



## 6.0 VALVE DESIGN DATA

Support data used by valve designers of an especially up-to-date or comprehensive nature (i.e., handbooks) have been included in this section. The subsections are far from complete but have been included simply to round out the survey subject of "Valve Design." Some question has been raised by preliminary reviewers of the contents relative to the lack of a subsection on manufacturing practices specific to valves. Very little of such information is available in the field and oft times is not even known by the designer. What data are available will be found primarily in section 1.0. The section is subdivided as follows:

- 6.1 Materials and Fluids
- 6.2 Environmental Criteria and Reliability
- 6.3 Miscellaneous Reports and Data

Preceding Page Blank

## Materials and Fluids

### 6.1-1 HYDROGEN HANDBOOK, A COMPILATION OF PROPERTIES, HANDLING AND TESTING PROCEDURES, COMPATIBILITY WITH MATERIALS AND BEHAVIOR AT LOW TEMPERATURES

ARTHUR D. LITTLE, INC.

Under Contract with PARKER AIRCRAFT CO.

AFFTC TR 60-19. April 1960

Contract AF33(616)6710

AD 242285

This report summarizes (1) our experience with and the available technical information on the development of two prototype valves, one for a cryogenic gas service and the other for a cryogenic liquid service (these valves are under development by Parker Aircraft Co. for Government agency); (2) bibliographical information on the physical and mechanical properties of specific construction materials for temperature range of  $-420^{\circ}\text{F}$  to  $+200^{\circ}\text{F}$  (these materials include some austenitic stainless steels and Teflon plastics); (3) the thermodynamic properties of helium, hydrogen, and nitrogen fluids with which the valves may be used or tested; (4) the hazards associated with the transportation and storage of hydrogen and with its use for testing the prototype valves for leakage across the seats; and (5) the sources and availability of hydrogen, and the Los Angeles regulations that apply to its transportation and use.

5.2, 6.2

Aircraft

### 6.1-2 TITAN II STORABLE PROPELLANT HANDBOOK

Liberto, R. R.

BELL AEROSYSTEMS COMPANY

AFBSD-TR-62-2

Contract AF04(694)72

Summarized are the physical properties, materials compatibility, handling techniques, flammability and explosivity hazards, and procedures for storing, cleaning, and flushing of the Titan II propellants,  $\text{N}_2\text{O}_4$  as the oxidizer and a nominal 50/50 blend of UDMH and  $\text{N}_2\text{H}_4$  as the fuel. The data presented were derived both from a literature survey and from a test program conducted at Bell Aerosystems Company and at the U.S. Bureau of Mines.

Aircraft

### 6.1-3 CHARACTERISTICS OF KEL-F

CALIFORNIA INSTITUTE OF TECHNOLOGY, JET PROPULSION LABORATORY

Literature Search 369

October 1961

Aircraft

6.1-4 CHARACTERISTICS OF TEFLON  
CALIFORNIA INSTITUTE OF TECHNOLOGY, JET PROPULSION LABORATORY  
Literature Search 370. October 1961

Aircraft

6.1-5 MATERIALS SELECTOR ISSUE  
MATERIALS IN DESIGN ENGINEERING  
October 1961

This issue of Materials in Design Engineering features a summary of the latest available data on engineering materials, forms, finishes, and joining and fastening methods. The issue consists of two major sections: a Data Section and a Directory Section.

The Data Section consists of nine subsections and contains: (1) extensive data on physical, mechanical, chemical, electrical, thermal, and fabricating properties of virtually all important engineering materials, including finishes and coatings; (2) an indication of test conditions; (3) listings of available forms and typical uses; (4) descriptions of forming methods and the types of parts that can be produced; and (5) information on methods by which materials can be joined. Most information is given in tabular form for easy comparison.

The Directory Section contains the names and addresses of leading suppliers of engineering materials, finishes, forms and shapes. A full explanation of the organization and use of the Directory Section is given.

Industrial

6.-1-6 CRYOGENIC MATERIALS DATA HANDBOOK  
Durham, T. F., et al.  
U.S. NATIONAL BUREAU OF STANDARDS, CRYOGENIC ENGINEERING  
LABORATORY  
Contract No. AF04(647)59-3

This handbook of data on solid materials at low temperatures was prepared under the sponsorship of the Air Force Ballistic Missile Division by personnel of the Properties of Materials Section, Cryogenic Engineering Laboratory, National Bureau of Standards, Boulder, Colorado. It contains certain mechanical and physical properties of selected metals and nonmetals over the temperature range -454°F to +500°F.

The materials and properties selected are listed in the Index. The materials are mostly ones in current use for missile applications at cryogenic temperatures, but a few have been included because of their potential for such uses. The properties are those which are most generally useful to the designer. The

compilation is believed to include all reliable data which have appeared in the literature from 1950 through 1959 and recent data which have appeared in the literature from 1950 through 1959, and recent data from test laboratories. In some cases, the data reported have not yet been published. Information from a few papers published prior to 1940 has also been included.

A summary of the testing procedures used at the Cryogenic Engineering Laboratory and the proper identification of the materials tested are included in the Monograph section. The results of these tests appear in the Handbook and are designated by reference number 137. The Handbook also includes the results of fatigue tests and a review of the literature for fatigue data on sixteen alloys by Battelle Memorial Institute. The test results are reported using reference number 805, and the test procedures are included in the Monograph Section.

Aircraft

6.1-7 TABLES OF THERMAL PROPERTIES OF GASES  
U. S. NATIONAL BUREAU OF STANDARDS  
Circular 564, November 1955

Aircraft

6.1-8 THE PHYSICAL AND THERMODYNAMIC PROPERTIES OF HELIUM  
WHITTAKER CONTROLS, Los Angeles, Calif.  
September 1960

This report briefly summarizes currently available information on the physical and thermodynamic properties of gaseous helium. The information is presented in both tabular and diagrammatic form to facilitate its use by design and test engineers who work with pressurized helium.

The reported property values for helium cover the pressure range of 14.7 to 6000 psia, and the temperature range of -440°F to 600°F, with minor exceptions where data were limited or unavailable.

Aircraft

6.1 CROSS REFERENCES

2.1-7	5.2-3	5.5-4	6.2-1	7.0-4
	-11	-15	-6	-14
			-7	

Environmental Criteria and Reliability

\*6.2-1 ROCKETS IN SPACE ENVIRONMENT

Gray, P. D. et al.  
AEROJET-GENERAL CORPORATION  
Project 3058-03, 6753-01  
Contract AF04(611)7441

PHASE I--PARAMETER STUDY, Report No. 2112--Environmental factors constituting the space environment between 300 and 22,000 n.mi. altitude were defined. The propulsion system materials and components most likely to be exposed to this environment were established, and available data regarding the behavior of these materials in the space environment were surveyed. Deficiencies in these data were determined, and appropriate tests were planned for obtaining data now lacking.

PHASE II--INDIVIDUAL COMPONENT INVESTIGATION, Report No. 2263--Components and materials having use or potential for use in space propulsion system were tested according to plans formulated during Phase I. Test data indicated that, in many cases, materials and components now used in liquid propellant propulsion systems would be suitable for space applications.

1.2, 6.1

Aircraft, Pneumatic, Solenoid Valve, Poppet

6.2-2 A THEORETICAL TECHNIQUE FOR PREDICTING THE RELIABILITY OF SOLENOID VALVES

Eisenlohr, G. M. et al.  
ARINC RESEARCH CORPORATION, WASHINGTON, D.C.  
Special Technical Report. Publication No. 173-4-278.  
January 1962  
Contract SD-77  
AD 272194

A technique is presented for determining the reliability of solenoid valves. It is believed this effort was a step toward the prediction of the reliability of mechanical and electro-mechanical devices. However, a detailed empirical analysis should be performed in the near future either to refute or substantiate the theoretical modes of failure analysis as well as the theoretical prediction technique presented. The present effort did not include this highly desirable aspect because of time limitations. It is pointed out that an empirical analysis should include considerations such as the effects of vacuum conditions, temperature, wear compatibility between unlike materials, and stress concentration between seat and poppet.

1.2, 5.3

Aircraft, Pneumatic, Solenoid Valve, Poppet, Metal to Metal

- 6.2-3 EFFECT OF HARD VACUUM AND LOW G CONDITIONS ON HYDRAULIC FLUIDS  
AND SYSTEMS (BIBLIOGRAPHY)  
ARMED SERVICES TECHNICAL INFORMATION AGENCY  
ARB 10656

Aircraft, Hydraulic

- \*6.2-4 BEHAVIOR OF MATERIALS IN SPACE ENVIRONMENTS  
Jaffe, L. D., et al.  
AMERICAN ROCKET SOCIETY JOURNAL  
March 1962  
pp. 320 to 346

Special problems relating to the behavior of materials in outer space arise from both the absence and the presence of surrounding matter; i.e., from vacuum and from particles in space. Although in the last few years much information on the nature of these particles and the effect that they have on materials has been gained, the gaps in our knowledge remain great. However, in order to design and build equipment to operate in space, engineering judgments must be formed on the basis of available information. This paper attempts to synthesize the best of the current information while discarding that which is no longer applicable.

Aircraft

- 6.2-5 ENVIRONMENTAL FACTORS INFLUENCING METALS APPLICATIONS IN SPACE  
VEHICLES  
Allen, J. M.  
RATTELLE MEMORIAL INSTITUTE, DEFENSE METALS INFORMATION  
CENTER  
OTS PB 151101; DMIC Report No. 142  
Contract AF18(600)1375

Metals will be used extensively both in the vehicle structure and in the supporting and auxiliary equipment that is used for space flight. This report describes the specialized environments which are imposed on metals and the possible consequences of these environments. In general, the specialized environments are identified with (1) the natural environment of space, (2) the entry into an atmosphere, or (3) the power-conversion system utilized by the vehicle.

Aircraft

- 6.2-6 HOW TEMPERATURE AFFECTS INSTRUMENT ACCURACY  
Gitlin, R.  
CONTROL ENGINEERING  
pp. 70-78, April 1955

Temperature changes can affect the spring constant of a resilient member, the resistance of an electrical conductor, or the magnetic properties of a permanent magnet. And since all precision instrument and control components use these elements, the accuracy of a component depends partly on the ability of a designer to compensate for these changes in ambient temperature. He does this by using materials that are insensitive to temperature change, by combining elements that vary in an opposite manner under the same change, or by keeping the component at a constant temperature regardless of ambient variation.

As the first of a series, this article discusses the effect of temperature change on various mechanical and electrical elements. Succeeding issues of Control Engineering will suggest practical methods of compensating for these temperature effects and will discuss the compensating techniques used in a variety of commercially available components.

## 6.1

### Aircraft

#### \*6.2-7 STUDY OF CRITERIA FOR HYDRAULIC AND PNEUMATIC SYSTEMS FOR SPACE VEHICLES

Cannon, C. H.  
 LOCKHEED AIRCRAFT CORP., Georgia Division  
 WADC TR 59-217 Part 1, April 1959  
 Contract AF33(616)5797  
 AD 230623

The object of this program is to determine the role of hydraulics and pneumatics in space vehicles and to establish the design criteria for such systems. In determining the role of hydraulic and pneumatic systems, their characteristics are compared to those of other type systems.

The initial effort encompassed a study of the natural and induced environments to which hydraulic and pneumatic equipment would be exposed in all phases of space flight. From this point the study proceeded to the determination of the criteria which provide the basis for the design of hydraulic and pneumatic systems and equipment. Certain hypothetical vehicles were then devised, one or more of which would encounter the environmental conditions noted above. The study was completed with an examination of typical hydraulic and pneumatic systems for space vehicles.

2.1, 2.3, 5.2, 6.1

### Aircraft

#### 6.2 CROSS REFERENCES

1.2-16	1.3-1	1.3-6	1.42	5.2-3	5.5-1	6.1-1
	-2	-8			-4	
	-5	-13			-15	
		-14				

## Miscellaneous Reports and Data

### 6.3-1 BIBLIOGRAPHY ON DIAPHRAGMS AND ANEROIDS

Van Der Pyl, L. M.

AMERICAN SOCIETY OF MECHANICAL ENGINEERS

Paper No. 60-WA-122 for Meeting November 27, 1960

This report abstracts 171 papers on the subject. bib.

### 6.3-2 PNEUMATIC MANUAL

NORTH AMERICAN AVIATION, INC.

Report No. AL-2435

March 1956

### 6.3-3 SPRINGS

CALIFORNIA INSTITUTE OF TECHNOLOGY, J. E. P. W.  
LABORATORY

Literature Search 347. May 1961

## 6.3 CROSS REFERENCES

7.0-9

-11

-12

-14

-15



## 7.0 BOOKS

The following section includes books containing information on practically all the various subsections. Those noticeably absent are 1.3, Analysis, Design, and Test of Specific Valves; 2.5, Internal Passage Design for Flow; 2.6, Cavitation and Other Flow Phenomena; 4.3, Unsteady Flow, Blowdown and Charging; 5.4, Seating; and 6.2, Environmental Criteria and Reliability. It is believed that there are no texts which deal in depth, either descriptively or analytically, with the headings underlined.

## Books

- 7.0-1 **FLUID METERS, THEIR THEORY AND APPLICATION**  
ASME Research Committee on Fluid Meters, Fifth Edition, 1959  
New York, American Society of Mechanical Engineers
- 2.1
- Industrial
- 7.0-2 **REGULATORS AND RELIEF VALVES**  
Beard, C. S.  
Pittsburgh, Pennsylvania, Instruments Publishing Co., 1959
- 1.1, 2.2, 2.4
- Industrial
- 7.0-3 **CONTROL VALVES (Revised Edition)**  
Beard, C. S.  
Pittsburgh, Pennsylvania, Instruments Publishing Co., 1960
- 1.1, 2.2, 2.4
- Industrial
- \*7.0-4 **FLUID POWER CONTROL**  
Blackburn, J. F. et al.  
New York, Technology Press--John Wiley & Sons, 1960
- 1.1, 1.2, 1.4, 2.1, 2.2, 2.3, 2.4, 3.1, 3.2, 3.3, 4.2, 5.1, 5.4, 6.1
- Aircraft, Hydraulic, Servo Control Valves
- 7.0-5 **INTERNATIONAL CONFERENCE ON FLUID SEALING**  
British Hydromechanics Research Association, April 1961
- 5.2
- Industrial
- 7.0-6 **FLOW OF FLUIDS THROUGH POROUS MATERIALS**  
Collins, R. E.  
New York, Reinhold Publishing Corporation, 1961
- 2.1
- Industrial

7.0-7 FLUID PRESSURE MECHANISMS

Conway, H. G.

New York, Pitman Publishing Corporation, 1958

1.1, 1.4

Industrial

7.0-8 FRICTION AND WEAR

Davies, R.

New York, Elsevier Publishing Company, 1959

5.5

Industrial

7.0-9 FLUID POWER HANDBOOK AND DIRECTORY, 1962,'63

Hydraulics and Pneumatics, ed.

Cleveland, Ohio, Industrial Publishing Corporation

1.1, 6.3

Industrial

7.0-10 PROCEEDINGS OF THE CONFERENCE ON LUBRICATION AND WEAR

Institution of Mechanical Engineers

London, October 1-3, 1957

5.5

Industrial

7.0-11 GAS TABLES

J. H. Keenan and J. Kaye

New York, John Wiley and Sons, Inc.

6.3

Aircraft

7.0-12 HANDBOOK OF ASTRONAUTICAL ENGINEERING

H. H. Koelle, Ed.

New York, McGraw-Hill Book Company, 1961

Sections 20.55 through 20.553 present a brief resume of liquid propellant propulsion systems, hydraulic and pneumatic components. Included are descriptions of pressure regulators, relief valves, solenoid valves, filters, check valves, pressure switches and miscellaneous other control elements.

1.1, 6.3

Aircraft

**7.0-13 FLUID POWER CONTROLS**

Pippenger, J. J. et al.  
New York, McGraw-Hill, 1959

1.1, 2.3

Industrial, Hydraulic

**7.0-14 ELECTROMAGNETIC DEVICES**

Roters, H. C.  
New York, John Wiley and Sons, Inc., 1941

4.1, 6.1, 6.3

Industrial

**7.0-15 DYNAMICS AND THERMODYNAMICS OF COMPRESSIBLE FLUID FLOW**

Shapiro, A. H.  
New York, Ronald Press Company

2.1, 6.3

Aircraft, Pneumatic

**7.0-16 A SYMPOSIUM ON INTERNAL COMBUSTION ENGINE VALVES**

Reprints of Technical Papers  
Published by Valve Division, Thompson Products, Inc.  
Cleveland, Ohio, 1956

1.2

Industrial

# AUTHOR INDEX

Allen, J. M.	6.2-5	Cohn, S. D.	3.2-11
Ainsworth, F. W.	4.2-1	Collins, R. E.	7.0-6
Archard, J. F.	5.5-6	Conison, J.	1.2-5
Ash, J. E.	5.4-1	Conway, H. G.	7.0-7
Ash, R.	5.1-9	Cornelius, D. F.	5.5-1
Avient, B. W. E.	5.5-14	Cornell, R. L.	5.5-11
Bacha, C. P.	1.3-6	Dahle, B.	1.2-14
	1.3-7		2.4-15
Baer, H. W.	4.3-11	Dally, C. A.	3.2-12
Ball, J. W.	2.6-1	Daniels, W. B.	5.2-17
Barkan, H. E.	5.5-5	Davies, R.	7.0-8
Barrick, P. L.	5.5-15	Demetriades, S. T.	4.3-2
Baskey, R. H.	5.2-11	Dobbins, R. A.	2.1-16
Beard, C. S.	1.1-1	Dodge, L.	1.2-8
	1.1-6		4.1-5
	1.1-14	Dorinson, A.	5.5-16
	1.1-15	Downey, R. R.	1.2-15
	2.4-7	Durham, T. F.	6.1-6
	2.4-8		
	7.0-2	Earl, A. G.	3.1-2
	7.0-3	Eckman, D. P.	4.2-8
Bell, K. J.	2.1-1	Edwards, T. W.	1.1-19
Bigham, J. E.	1.2-4	Ehrich, F. F.	2.2-4
Biram, J. G. S.	5.2-10	Eisenlohr, G. M.	6.2-2
Blackburn, J. F.	2.2-3	Ezekiel, F. D.	2.2-5
	3.1-1		
	7.0-4	Fallows, D. H.	5.3-1
Borchert, W. O.	1.3-10	Feldman, M. S.	3.1-4
Brockett, G. F.	1.1-16	Feng, T. Y.	3.2-2
	2.4-9		3.2-3
	2.4-10		3.2-18
Brown, N. P.	1.2-23	Firth, D.	2.2-12
Bruno, J. O.	5.2-12	Forman, R.	5.1-21
Burrows, G.	5.1-10		
		Gaden, D.	3.2-19
Callagan, E. E.	2.1-13	Gaines, W. L.	1.2-7
Campbell, J. E.	2.3-4	Geyer, E. W.	4.3-5
Cannon, C. H.	6.2-7	Gitlin, R.	6.2-6
Chamberlain, R. E.	1.3-11	Goddard, J.	5.5-10
Chelomey, V. N.	1.4-8	Gold, H.	1.3-4
Chenea, P. F.	5.5-8	Goldsworthy, F. A.	4.3-9
Clark, R. N.	3.2-1	Goodings, A. C.	5.1-7

Gordon, S. A.	5.1-18	Iapera, D. J.	2.4-5
Grace, H. P.	2.1-2	Lee, J. C.	5.4-2
Gray, P. D.	6.2-1	Lee, S. Y.	1.1-2
Graziano, E. E.	1.4-3		3.2-5
Green, L. Jr.	5.1-13		4.2-2
Gresham, W. A. Jr.	2.1-8	Lefkowitz, I.	4.2-10
Grinnel, S. K.	5.1-1	Leibleich, N.	1.1-21
Grover, D. P.	4.1-3	Lemp, J. F. Jr.	1.2-22
		Liberto, R. R.	6.1-2
Hanssen, A. J.	2.4-4	Lin, D. J.	2.2-8
Harrison, H. L.	3.2-10	Liu, V. C.	5.1-12
Hatfield, J. N.	5.2-9	Lohrentz, J.	2.1-10
Hearrick, R. E.	5.2-2	Long, H. A.	3.2-13
Heffner, F. E.	5.1-2	Lovett, O. P. Jr.	2.4-12
Heitland, H. H.	4.1-1		4.2-9
	4.1-6	Love, R. E.	1.1-17
Henke, R. W.	1.1-10	Lymer, A.	5.2-8
Heywood, W. A.	5.2-13		
	5.2-14	MacLellan, G. D.	2.2-11
Hirsch, R. A.	4.1-4	Madigan, M. F.	1.2-20
Hockenhull, I.	1.3-15	Mann, J. R.	1.4-6
Holzbock, W. G.	1.1-2	Mann, R. W.	1.2-16
	1.1-3	Martin, M. W.	1.2-6
	2.4-2	Marton, F. D.	1.2-9
Horacek, H. P.	1.3-1	Mayer, E.	5.2-15
Howe, W. H.	1.2-10	McLean, H. J.	1.1-5
Hughes, P. R.	1.3-9	McPherson, M. B.	2.2-1
		Meagher, G. F.	5.4-3
Iberall, A. S.	2.2-6	Meyer, E. A.	5.2-6
		Milican, R.	5.1-20
Jaffe, L. D.	6.2-4	Miller, E. E.	5.1-14
James, J. W.	2.2-19	Mills, R. I.	1.2-21
Jobson, D. A.	2.1-9	Moore, W. H.	5.5-12
		Morris, A. E.	1.1-11
Kearton, W. J.	5.1-10	Murihead, J. C.	1.2-3
	5.1-11	Muller, J. T.	4.2-5
Keenan, J. H.	7.0-11	Murdock, J. W.	2.1-19
Khokhlov, V. A.	2.2-10		
King, C. F.	3.2-4	Neal, A. E.	1.3-8
Kissner, R. L.	4.1-2	Nootbaar, R. F.	5.1-17
Kittredge, C. P.	2.2-7	Norwood, R. E.	3.2-14
Kneisel, O.	2.4-11	Noton, G. J.	4.2-6
Kowalski, S.	1.2-17		
Krassov, I. M.	3.2-8		
Kreith, F.	5.1-3	Oki, I	2.2-16
Kupiec, H. P.	5.2-1		2.2-17
			2.2-18

Olson, J. H.	5.5-3	Smither, R. K.	5.1-19
Osburn, J. O.	5.1-8	Sonntag, A.	5.5-9
Osgood, R. E.	5.4-4	Stemming, A. H.	2.2-9
		Stiles, G. F.	2.6-3
Pawlak, R. J.	3.2-15	Stone, J. A.	3.2-7
Perry, A. J. Jr.	2.1-3		3.2-16
Phillips, W. H.	3.1-5		3.2-17
Pippenger, J. J.	1.1-12	Sverdrup, N. M.	2.1-14
	1.1-20		2.3-3
	7.0-13	Sweeney, D. C.	3.1-3
Polentz, L. M.	2.1-5		
	2.1-6	Tao, L. N.	5.1-4
		Thomas, C. W.	2.2-2
Rabinowicz, E.	5.5-7	Thompson, R. C.	2.5-3
	5.5-13	Thurston, G. B.	4.3-1
Read, F. W.	1.3-3		4.3-7
Rebert, C. J.	5.4-5		4.3-8
Reid, K. N. Jr.	1.4-7	Tidor, O. M.	2.2-14
Reiner, M.	2.6-4	Tolansky, S.	5.3-2
Reynolds, W. C.	4.3-10	Tomlinson, L. E.	1.3-14
Riske, G.	2.3-1	Tsai, D. H.	2.5-1
	2.3-2		2.5-4
	2.5-2		4.2-3
Robinson, A. H.	3.2-9		2-11
Robinson, C. S. L.	2.1-11	Tuffias, R. H.	2.1-12
Robinson, D. W.	1.2-13	Turnbull, D. E.	4.2-4
Roby, M. A.	1.2-11	Turnquist, R. O.	2.4-13
Rockwell, R. A.	2.4-1		
	2.4-6	Ulrich, R. D.	2.1-4
Roters, H. C.	7.0-14		
Roth, G. L.	1.1-4	Van Der Pyl, J. M.	6.3-1
Rudinger, G.	4.3-3	VanDerrlin, E.	1.2-1
Russell, J. G.	2.1-17	Vermes, G.	5.1-5
Sarpkaya, T.	3.2-6	Washburn, W. D.	1.1-18
Sciulli, E. B.	5.5-2	Webster, E. A.	5.2-7
Sears, G. W.	5.1-16	Wetstone, D. M.	4.1-7
Shapiro, A. H.	7.0-15	Wheeler, H. L. Jr.	5.4-6
Shearer, J. L.	2.2-13		5.4-7
Shearer, L. L.	1.4-5	Wildhack, W. A.	2.1-15
Sibley, L. B.	5.5-4	Wilson, L. H.	5.1-15
Slawsky, M. M.	2.4-3	Wing, P. Jr.	2.4-14
	2.4-16	Wright, B. S.	2.6-2
	2.4-17		
Smith, L. K.	1.3-2	Zabriskie, W.	5.1-6
Smith, L. L.	5.2-3		
Smith, R. E.	2.1-18		

## LATE ENTRIES

1. AERO-SPACE APPLIED THERMODYNAMICS MANUAL SOCIETY OF  
AUTOMOTIVE ENGINEERS, INC., COMMITTEE A-9  
AERO-SPACE ENVIRONMENTAL CONTROL SYSTEMS, 1960
2. OIL HYDRAULIC POWER AND ITS INDUSTRIAL APPLICATION  
Earnst, Walter; New York, McGraw-Hill, 1960
3. CONTROL SYSTEMS COMPONENTS  
Gibson and Tuteur; New York, McGraw-Hill, 1958
4. FINAL REPORT, OXIDIZER SHUTOFF VALVE, 6-1/2 INCH INLET,  
PART NO. 1316-588263  
Burton, S.D.  
PARKER AIRCRAFT CO.  
Report 1316-R1420, AFFTC-TR-60-49. November 1960  
Contract AF33(616)-5891. Project 6753
5. DESIGN OF HYDRAULIC CONTROL SYSTEMS  
Lewis and Stern; New York, McGraw-Hill, 1962



# BIBLIOGRAPHY SUBJECTS INDEX

SUBJECT	PAGE
1.0 VALVE SELECTION AND EVALUATION	A-7
1.1 General Description of Valves and Applications	A-8
1.2 Description of Specific Valve Designs and Applications	A-14
1.3 Analysis, Design and Test of Specific Valves	A-21
1.4 Selected References on Servo Valves	A-28
2.0 STEADY FLOW CHARACTERISTICS	A-35
2.1 Flow Through Single Elements	A-36
2.2 Flow Through Valves	A-43
2.3 Flow Through Composite Systems	A-49
2.4 Valve Sizing Formulas	A-51
2.5 Internal Passage Design for Flow	A-56
2.6 Cavitation and Other Flow Phenomena	A-58
3.0 STEADY STATE FORCES	A-59
3.1 Lateral Forces - Friction and Hydraulic Lock	A-60
3.2 Flow Forces	A-63
3.3 Detailed Static Force Analyses	A-69
4.0 TRANSIENT FACTORS	A-71
4.1 Simple Response Time	A-72
4.2 Transient Analysis and Stability	A-75
4.3 Unsteady Flow, Blowdown and Charging	A-80
5.0 VALVE SEALING	A-85
5.1 Leakage and Analogous Flows	A-86
5.2 Seals, Leak Detection and Measurements	A-95
5.3 Seating	A-102
5.4 Contamination	A-103
5.5 Friction and Wear	A-106
6.0 VALVE DESIGN DATA	A-113
6.1 Materials and Fluids	A-114
6.2 Environmental Criteria and Reliability	A-117
6.3 Miscellaneous Reports and Data	A-120
7.0 BOOKS	A-121

Preceding Page Blank

## APPENDIX B

### INDUSTRY SURVEY

The purpose of the survey was to establish poppet and seat design approaches, fabrication and analysis as is presently represented within the industry. Industry was approached through a form letter and personal interviews in which design information on proven valves was requested for handbook presentation.

The information received from numerous manufacturers has been sifted and reduced to portray the pertinent features of the poppet and seat or "closure mechanism."

The object of the presentation technique has been to indicate the more salient features of seat construction and show the interrelationship between seat and closure with a semi-schematic representation of the valve assembly. The relative proportions and geometry of the seat have been maintained; however, as with any artistic rendering, the interpretation of the minute detail must be viewed with practical judgment, particularly in the "soft" seat constructions.

KEY PARAMETERS noted with each design are, in most cases, based upon a specific application and it is assumed that the information received from industry is correct. Because few valves undergo complete qualification testing, the degree of adherence to all performance claims, or combinations thereof, is unknown.

Capacity-size relationships have been indicated by orifice diameter, physical dimensions and tube size, as applicable. The orifice size is based upon flow data and a discharge coefficient of 0.65, except when an efficient flow passage necessitated the use of a higher value to reflect a reasonable size.

A brief discussion of each design presents available information on applications, construction, fabrication, advantages and disadvantages. This information primarily reflects the opinions of individual manufacturers, editorial comments being held to a minimum.

The following 37 designs have been grouped into the 6 categories noted in the contents on the basis of the poppet or closure configuration.

Patent rights have been noted within this report as received from their respective sources, and no representations are made (by Rocketdyne) with respect to the patent or proprietary rights of any of the 37 designs described herein.

## FACTORS IN VALVE DESIGN

Many valve failures result from simple design oversights which could have been avoided had the interrelationships of environment, materials, stress, and dynamics been considered. To aid in evaluating the following designs a brief outline of the factors to be considered in valve design is listed below. While most of the forces and their effects cannot be explicitly calculated, a qualitative evaluation could save many laboratory hours during development.

- I. Specification: Requirements are established by system and component analysis.
  - A. Operating, proof and burst pressures
  - B. Fluid media and contaminants
  - C. Flow capacity
  - D. Leakage
  - E. Actuation and response data
  - F. Environmental criteria
    - 1. Temperature
    - 2. Vibration, acceleration, and shock
    - 3. Altitude, radiation, humidity, salt spray, sand and dust, etc.
    - 4. Life, operational, and storage
  - G. Reliability
  - H. Configurational restrictions

1. Size and weight
  2. Mounting and port size
  3. Fail safe conditions
  4. Instrumentation output, etc.
- II. Configuration Analysis: Approach is determined in part by each of the following:
- A. Preliminary design
  - B. Past experience
  - C. Specification (requirements)
  - D. Time and costs
- III. Functional Analysis: This part of the design determines by analysis what the sizes of various functional parts should be. In addition, some critical performance characteristics are predicted. The following items are considered:
- A. Operating characteristics
    1. Flow capacity
    2. Response times
    3. Actuation pressures
    4. Power requirements
    5. Leakage
    6. Control accuracy
    7. Fluid media compatibility
  - B. Materials
  - C. Effect of single and combined environment on operating characteristics and materials
  - D. Reliability
- IV. Design Analysis: This part of the design consists of packaging (via layout) the various functional features and analyzing the design as required. Portions of the functional analysis are repeated and extended as necessary. Items considered are:
- A. Materials; properties, and compatibility
  - B. Flow capacity
    1. Passage geometry; dictated in large by configuration analysis
    2. Areas and proportions
  - C. Static force study
    1. Fluid pressures
    2. Steady flow
    3. Seating
    4. Actuation
    5. Friction
    6. Temperature change
    7. Acceleration
    8. Spring
    9. Assembly and mounting
    10. Storage

- D. Dynamic force study
    - 1. Transient pressures
    - 2. Transient flow
    - 3. Inertia
    - 4. Actuation
    - 5. Friction
    - 6. Impact
    - 7. Transient temperature
    - 8. Vibration and shock
  - E. Stress and deformation study: This portion of the design analysis utilizes the applicable parts of previous studies to define limits of acceptability.
  - F. Dimensional analysis: This includes preparation of detail drawings and analysis thereof to ensure compatibility with functional and design considerations.
- IV. Design Review, Fabrication, Development, Qualification, and Production.

## CLASSIFICATION OF VALVES

Early in the survey it was noted that industry acceptance of a standardized classification for valves was almost nonexistent. A classification of valves has been prepared, and included in the report, that will aid in defining nomenclature and assist future efforts at standardizations. This list will also facilitate selection of appropriate names and help in locating published material.

### I. General Classification Categories

#### A. Industry

- 1. Aircraft (missile, rockets and/or space craft)
- 2. Industrial

#### B. Service Categories

- 1. General effluents controlled
  - a. Hydraulic (liquid)
  - b. Pneumatic (gas)
  - c. Cryogenic
  - d. Corrosive fluid
  - e. Propellant
    - (1) Oxidizer
    - (2) Fuel
  - f. Hot gas

2. Operating conditions
  - a. High (low) pressure
  - b. High (low) temperature
  - c. Vacuum
3. Specific names\*
  - a. Gas generator
  - b. Ignition monitor
  - c. Priority valve, et al.

C. General mode of control

1. Directional control
2. Flow control
3. Pressure control
4. Servo control

## II. Descriptors Specific to Valves

A. Control (line) function

1. Relief (safety)
2. Check (nonreturn)
3. Pressure regulator (reducer)
4. Flow regulator
5. Vent (dump)
6. Sequence
7. Throttle
8. Flow limit
9. Selector (2 way, 3 way, 4 way, anyway)
10. Shuttle

B. Valve closure mechanism and seating

1. Ball
2. Butterfly
3. Poppet
  - a. Spherical
  - b. Conical
  - c. Flat
4. Gate (blade)
5. Plug (cock)
6. Needle
7. Slide or plate (shear seal)
8. Diaphragm (Saunders type)
9. Spool
  - a. Packed (dynamic seals)
  - b. Lapped (close fit)

C. Seating and sliding valvular actions

1. Reciprocating
2. Rotary

---

\*This category has been noted only because of popular usage--its continuance is not recommended.

3. Pivoted, hinged or swing (flapper)
4. Iris
5. Contractable or expansible sleeve
6. Flexing disc (plate or annular member)

D. Actuation means (independent of line conditions)

1. Manual
2. Electric Motor
3. Solenoid
4. Capacitive discharge (eddy currents)
5. Fluid pressure actuated
  - a. Piston or bellows
  - b. Diaphragm
  - c. Motor
6. Explosive discharge

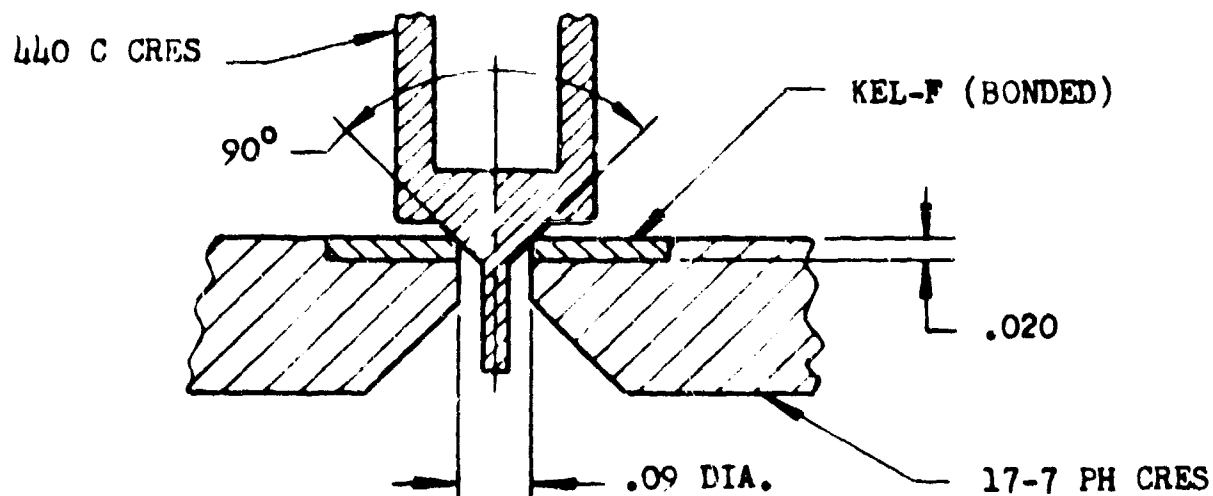
E. Construction and functional arrangement

1. Globe
2. Angle
3. Venturi
4. Double seated
5. Balanced
6. Pilot operated
7. Pilot

## **CONICAL POPPET SEAT DESIGNS**



### CONICAL POPPET SEAT DESIGN



### KEY PARAMETERS

VALVE TYPE: DOME LOADED PRESSURE  
REGULATOR  
FLOW MEDIA: NITROGEN  
INLET PRESSURE: 390 TO 500 PSIG  
REGULATED PRESSURE:  $280 \pm 5$  PSIG  
OPERATING TEMPERATURE:  $-30$  TO  $+120$  F  
LEAKAGE: 3 SCC/HR MAX  $\text{ON}_2$   
CAPACITY: .05 INCH ORIFICE (MAIN VALVE)  
LIFE: 5000 CYCLES  
VIBRATION:  $0.1 \text{ G}^2/\text{CPS}$  RANDOM  
TUBE SIZE:  $1/4$  IN,  $3/8$  OUT

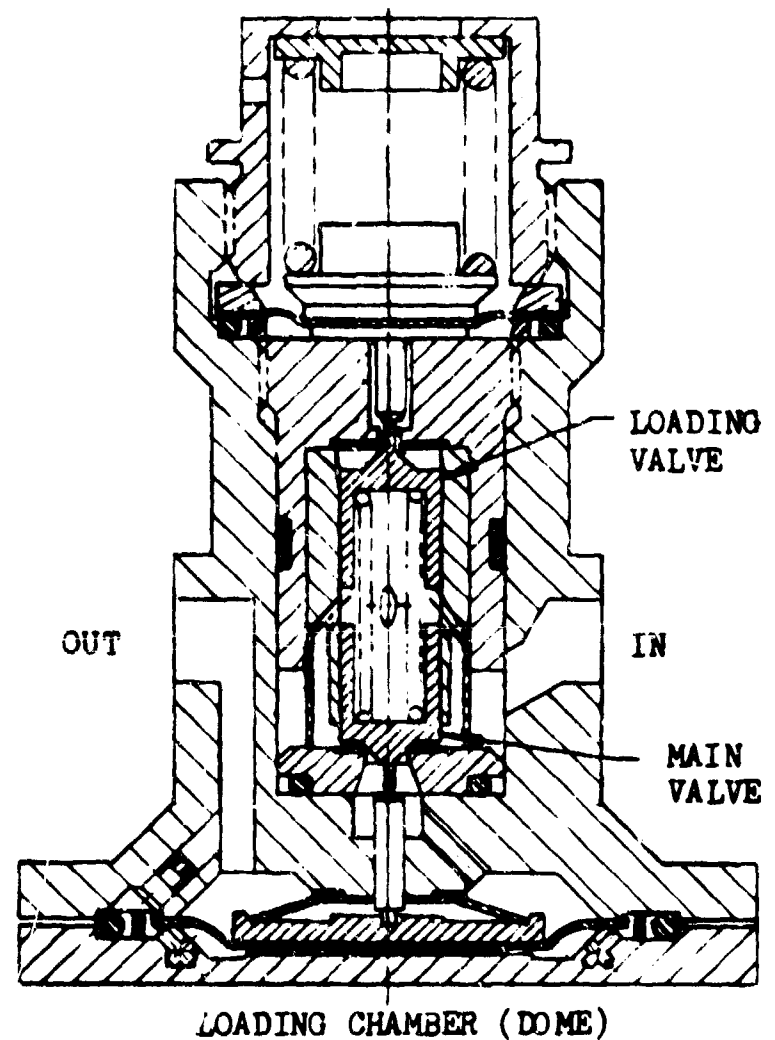


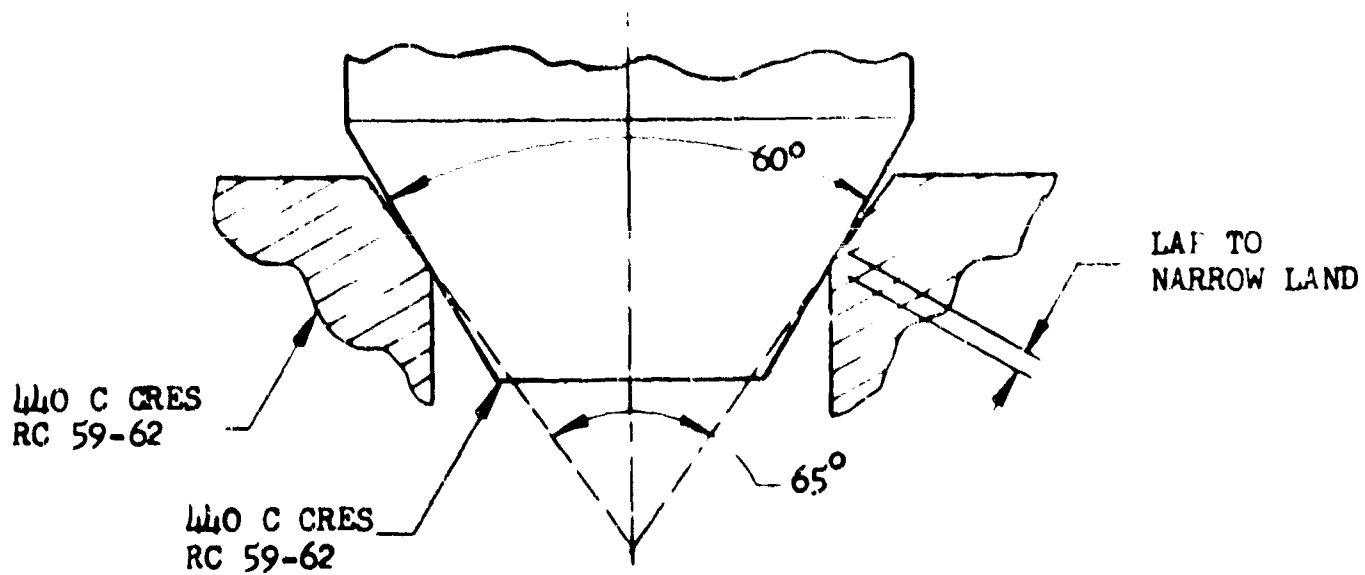
Figure B-1. Space Engine Regulator—Rocketdyne, A Division of North American Aviation, Inc.

## SPACE ENGINE REGULATOR

This pressure regulator was designed to control propellant tank pressurization in a small rocket engine system. The design features constant pressure regulation over a wide range of inlet pressures and a small leakage rate with low seating forces.

A 90-degree included angle poppet is seated on a 0.020-inch thick Kel-F ring that is epoxy bonded into the counterbore in the seat prior to drilling the bore of the seat. To maintain an adequate bond, the bonding surface of the seat counterbore must be roughened by wet blasting and the bonding surface of the Kel-F etched prior to bonding. The sealing surface on the seat is formed by forcing the poppet onto the seat when 7720-psig proof pressure is applied to the inlet port of the regulator. The corner of the Kel-F bore yields to form a slight chamfer that matches the 8-microinch finish on the poppet cone to provide the seal.

## CONICAL POPPET SEAT DESIGN



### KEY PARAMETERS

VALVE TYPE: PILOT OPERATED PRESSURE  
RELIEF VALVE  
FLOW MEDIA: HYDRAULIC OIL (MIL-O-5606)  
OPERATING PRESSURE: ADJUSTABLE  
300 TO 500 PSI  
OPERATING TEMPERATURE: -65 TO +160 F  
LEAKAGE: 2 CCM HYDRAULIC OIL  
LIFE: 50,000 CYCLES  
VIBRATION: 10 G TO 2000 CPS  
TUBE SIZE: 3/4 INCH

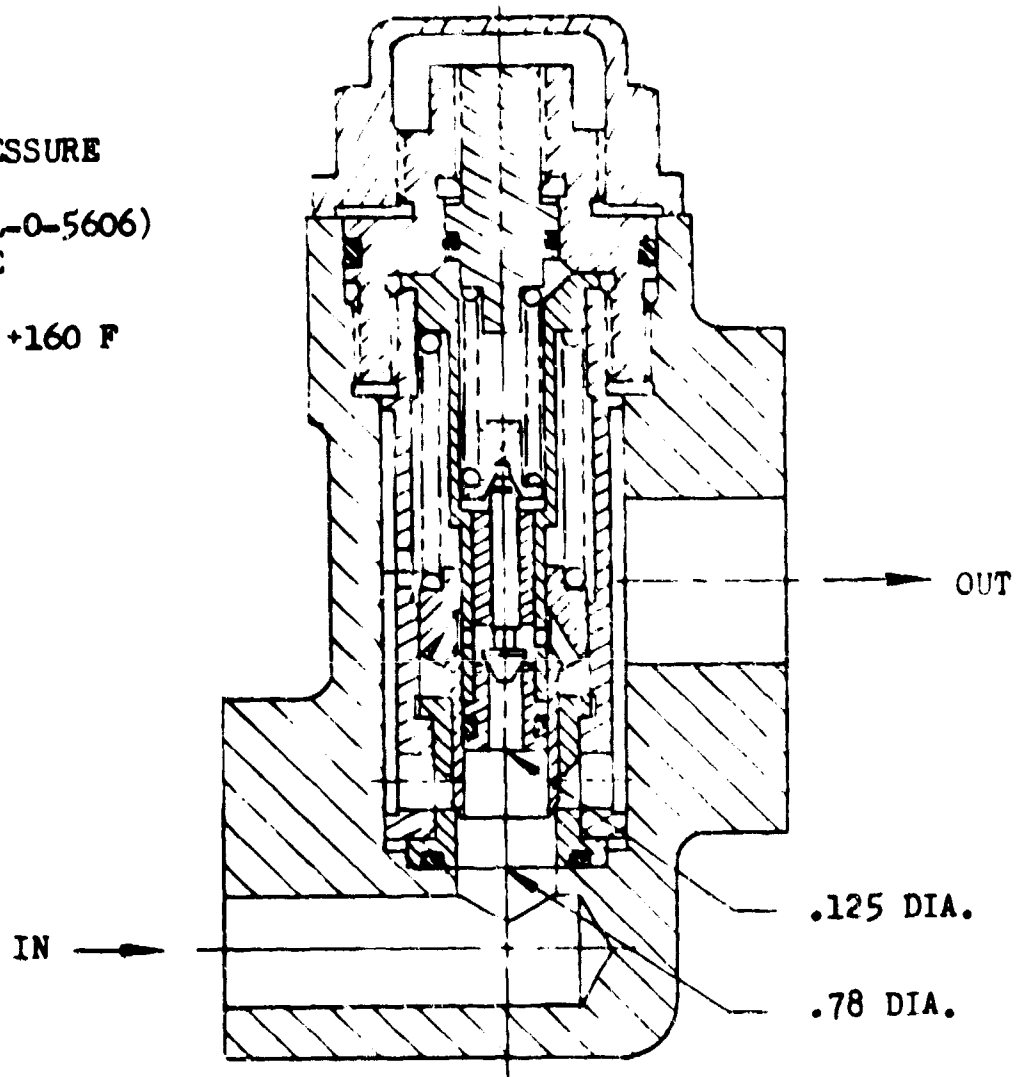


Figure B-2.

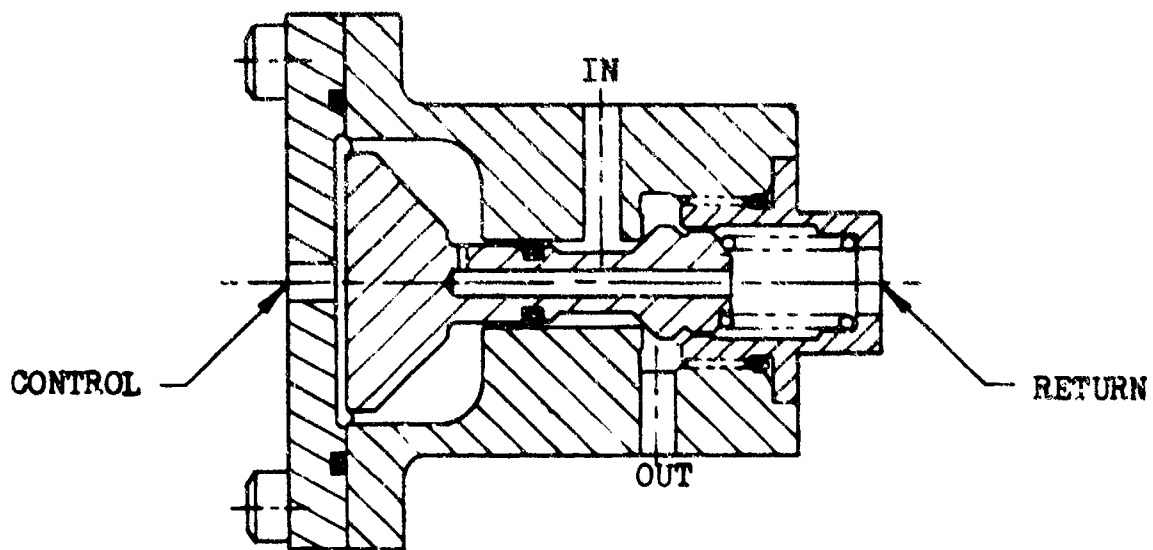
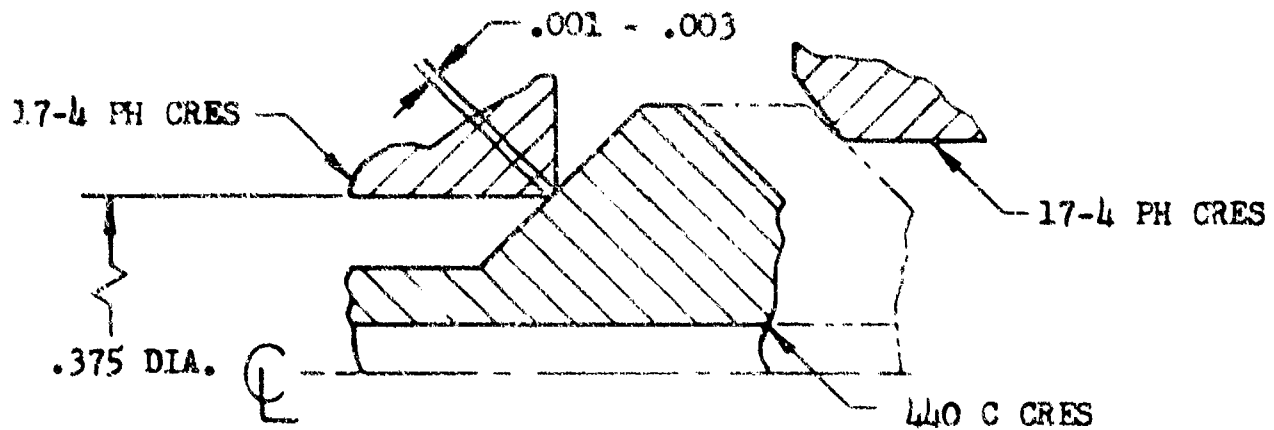
Hydraulic Relief Valve--Benbow  
Manufacturing Corporation

## HYDRAULIC RELIEF VALVE

This pilot-operated hydraulic relief valve utilizes differential angle conical poppets and seats (for both the pilot and main valve) as a simple approach to obtaining a relatively narrow seat land. The basic machining of a cone is generally less difficult than a spherical surface, however, the conical poppet has more stringent concentricity and normality requirements.

Match lapping of the seats is required to maintain leakage within acceptable limits. To hold the narrow seat land, close lap control is necessary as changes in land width affect the relief setting while excessive width can cause instability.

### CONICAL POPPET SEAT DESIGN



### KEY PARAMETERS

VALVE TYPE: 3-WAY PRESSURE ACTUATED  
VALVE  
FLOW MEDIA: RP-1; INERT GAS ACTUATED  
OPERATING PRESSURE: 1000 PSIG  
ACTUATION PRESSURE: 30 PSIG  
OPERATING TEMPERATURE: -30 TO 200 F  
LEAKAGE: 10 CCM MAX RP-1  
CAPACITY: 0.14-INCH ORIFICE  
LIFE: 10,000 CYCLES  
VIBRATION: 25 G TO 2000 CPS  
TUBE SIZE: 1/4 INCH

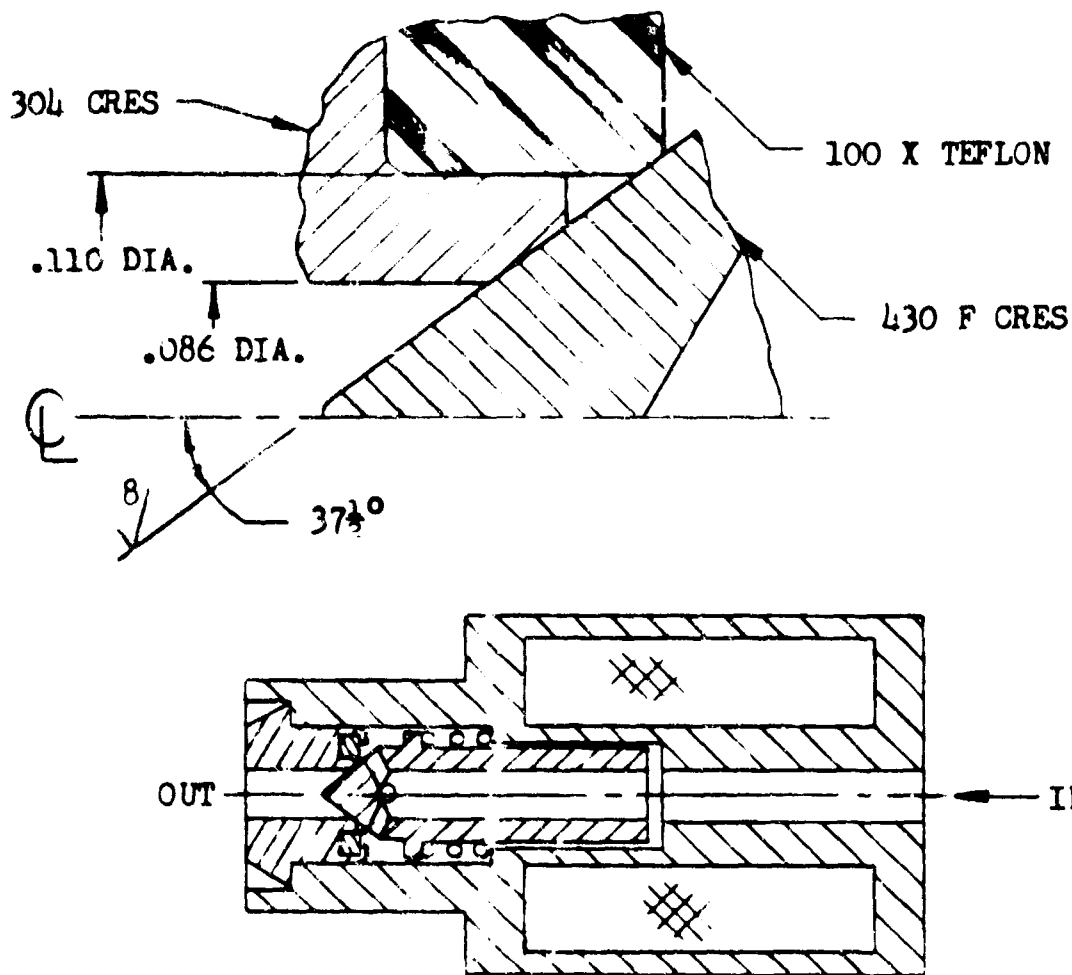
Figure B-3. Ignition Monitor Valve--Rocketdyne, A Division of North American Aviation, Inc.

## IGNITION MONITOR VALVE

A metal conical poppet seating on a lapped metal seat is utilized in this design to obtain a very close balance of inlet pressure. The narrow seat land width allows a large variation in inlet pressure with minor affect on the actuating pressure. A high speed of actuation is accomplished by allowing rising outlet pressure (during stroking) to act over a restricted poppet return seat area. The action obtained is similar to a Belleville spring operating in the negative rate region.

While the one dynamic seal in the valve allows a simple pressure balance, the attendant hysteresis problems necessitated the use of a special Teflon "cap" seal to minimize friction force changes.

## CONICAL POPPET SEAT DESIGN



### KEY PARAMETERS

VALVE TYPE: 2-WAY DIRECT OPERATED SOLENOID VALVE, 28 VDC  
FLOW MEDIA: NITROGEN TETROXIDE, UDMH, HYDRAZINE  
OPERATING PRESSURE: 325 PSIG  
OPERATING TEMPERATURE: -65 TO +160 F  
LEAKAGE: 0.02 SCCM MAX  $\text{GN}_2$   
CAPACITY: 0.06 INCH ORIFICE  
RESPONSE: 90 CPS AT 24 VDC  
LIFE: 10,000 CYCLES  
TUBE SIZE: 1/4 INCH

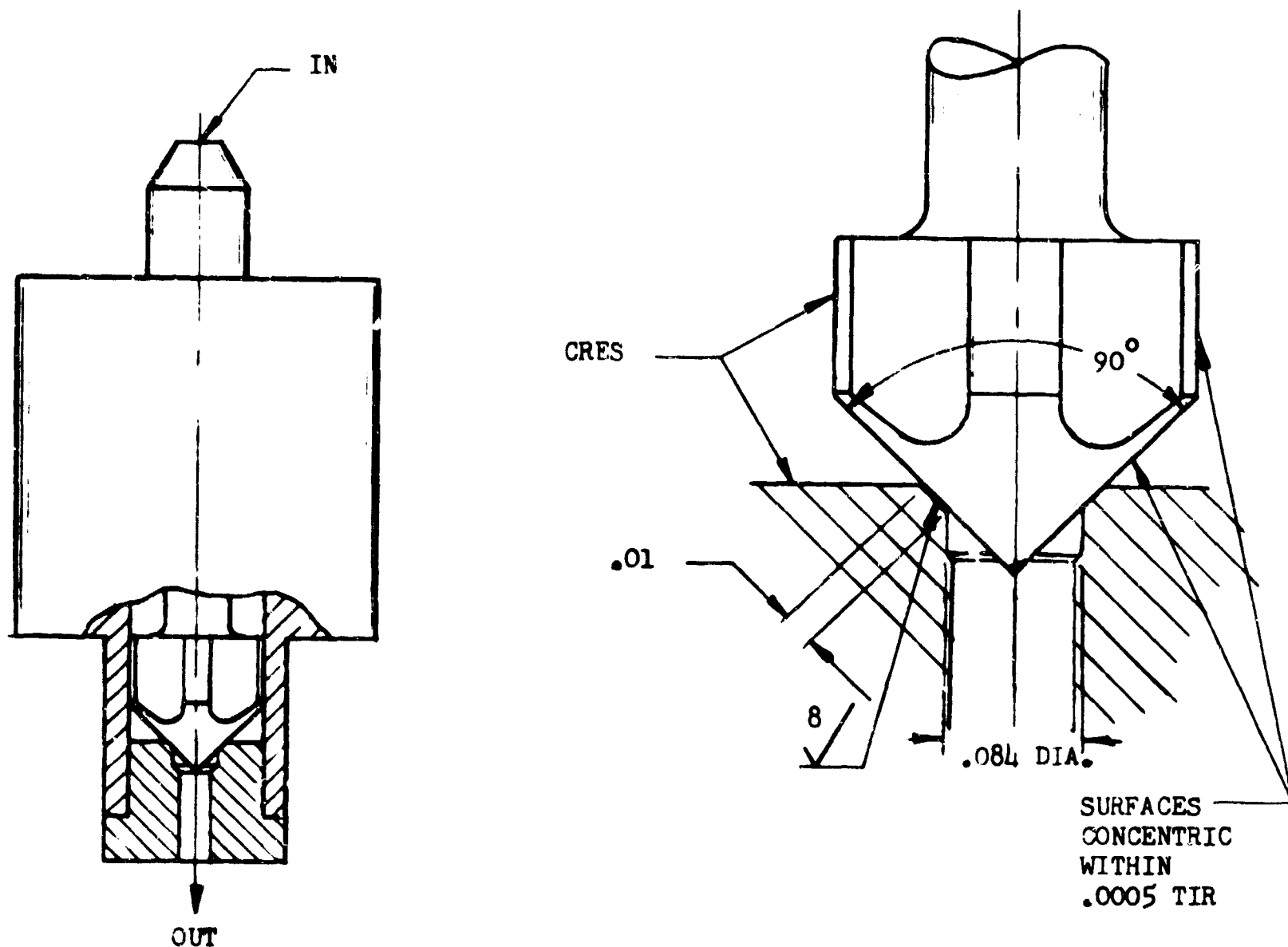
Figure B-4. Propellant Control Solenoid Valve I—  
Rocketdyne, A Division of North  
American Aviation, Inc.

### PROPELLANT CONTROL SOLENOID VALVE I

This valve must maintain an effective seal of chemically active rocket engine propellants. A controlled stress "soft" seat is obtained by utilizing a plastic seal in combination with a centering metal stop. While enhancing the probability of a tight seal, the seat design necessitates a larger solenoid due to additional unbalanced pressure area between the sealing surface and the metal to metal stop. The major problem encountered with the design is the tendency of the plastic seal to take a permanent set (cold flow) while operating near maximum material operating temperatures.



## CONICAL POPPET SEAT DESIGN



### KEY PARAMETERS

VALVE TYPE: 2-WAY DIRECT OPERATED  
SOLENOID VALVE, 28 VDC  
FLOW MEDIA: NITROGEN TETROXIDE, UDMH,  
HYDRAZINE  
OPERATING PRESSURE: 300 PSIA  
OPERATING TEMPERATURE: -65 TO +165 F  
LEAKAGE: 1.0 SCC/HR MAX NITROGEN AT 200 PSIG  
CAPACITY: 0.07 INCH ORIFICE  
LIFE: 80,000 CYCLES WATER AT 70 F & 200 PSI

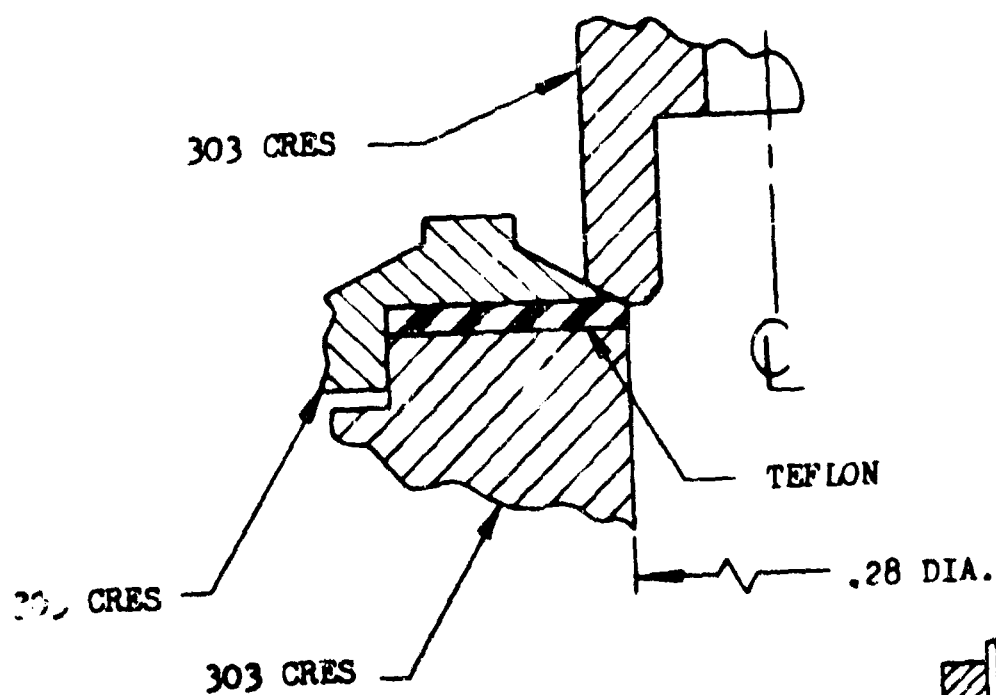
Figure B-5. Propellant Control Solenoid Valve II--  
Minneapolis-Honeywell Regulator  
Company, Aeronautical Division

## PROPELLANT CONTROL SOLENOID VALVE II

The conical closure shown illustrates a simple approach to design an economical, fast-response, hypergolic propellant valve. While this design does not match the performance capabilities of the spherically seated valve, careful attention to finish concentricity and normality result in an endurance life and leakage level suitable to many applications.

The primary disadvantages of this design are the close match lapping and poppet to seat alignment necessary to obtain suitable leakage-life characteristics. Additionally, fine (10 micron) filtration of fluid contaminants is necessary.

# CONICAL POPPET SEAT DESIGN



## KEY PARAMETERS

VALVE TYPE: PNEUMATIC RELIEF VALVE  
 FLOW MEDIA: AIR, NITROGEN, HELIUM  
 CRACKING PRESSURE: 240 TO 310 PSIG ADJUSTMENT  
 RESEAT PRESSURE: 10 PSIG MAX BELOW CRACKING PRESSURE  
 OPERATING TEMPERATURE: +30 TO +200 F  
 LEAKAGE: 0.2 SCC/HR MAX AIR AT RESEAT PRESSURE  
 CAPACITY: 0.25 INCH ORIFICE  
 VIBRATION: 14 G<sup>2</sup>/CPS RANDOM  
 TUBE SIZE: 3/8 INCH

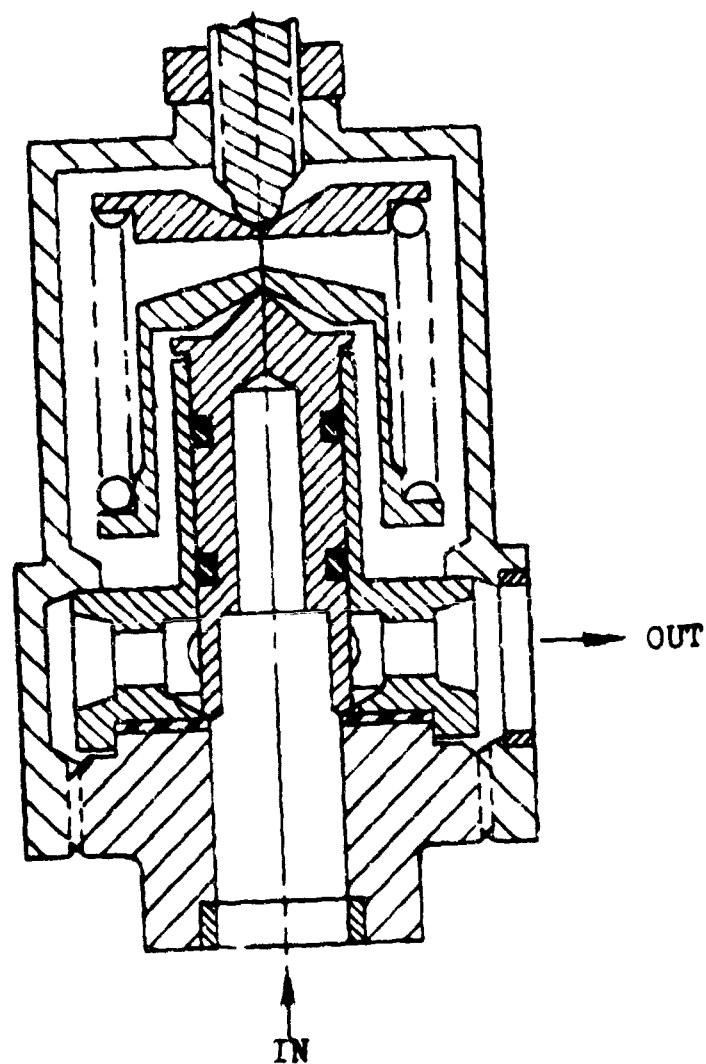


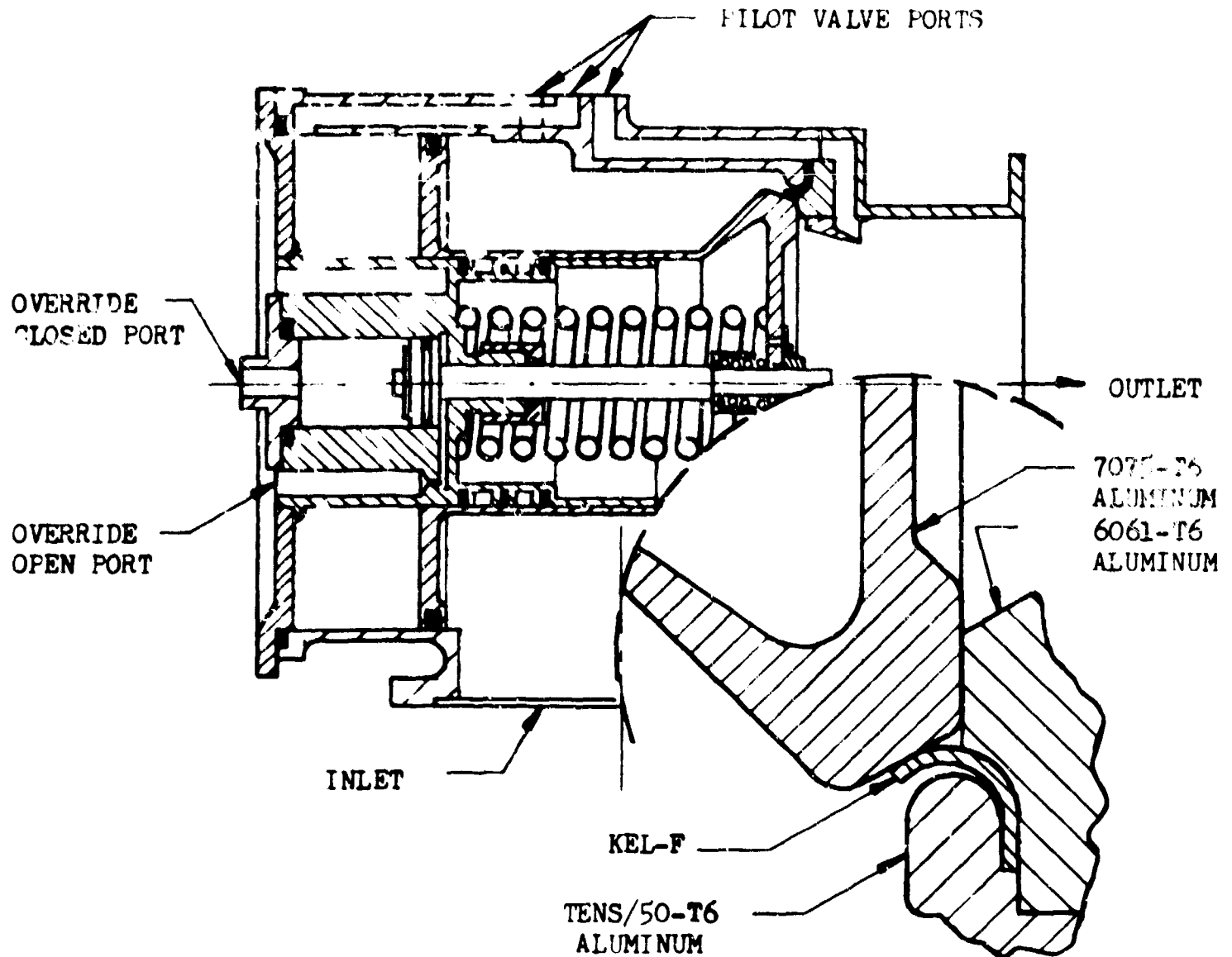
Figure B-6. Pneumatic Relief Valve—  
 Clary Dynamics  
 Corporation

## PNEUMATIC RELIEF VALVE

A notable feature of this flight-weight relief valve is the poppet guide and spring arrangement resulting in minimum space and axisymmetric loading. While this design utilizes a metal lip to provide controlled seat loading, a previous design did not and was subsequently destroyed during vibration testing.

This seat is particularly susceptible to cold flow of the Teflon ring. Attendant problems are increased leakage and maintenance of repeatable crack and reseal pressures.

## CONICAL POPPET SEAT DESIGN



### KEY PARAMETERS

VALVE TYPE: MAIN VALVE, PILOT OPERATED VENT  
AND PRESSURE RELIEF VALVE  
FLOW MEDIA: AIR, NITROGEN, HELIUM, LIQUID OXYGEN  
OPERATING PRESSURE: ADJUSTABLE 30 TO 60 PSIG  
OPERATING TEMPERATURE: -300 TO +160 F  
LEAKAGE: 200 SCIM MAX HELIUM AT -290 F  
SIZE: 4-INCH LINE  
LIFE: 5000 CYCLES AT 68 PSIG and -250 F  
VIBRATION: 10 G TO 500 CPS

Figure B-7. Tank Vent Valve—Rocketdyne, A Division  
of North American Aviation, Inc.

## TANK VENT VALVE

This design illustrates the pressure-loaded plastic lip seal used in the main valve of a pilot actuated vent and relief valve.

Development of this poppet seal took place during a state-of-the-art improvement program\* for extreme environment components. No major problems were encountered.

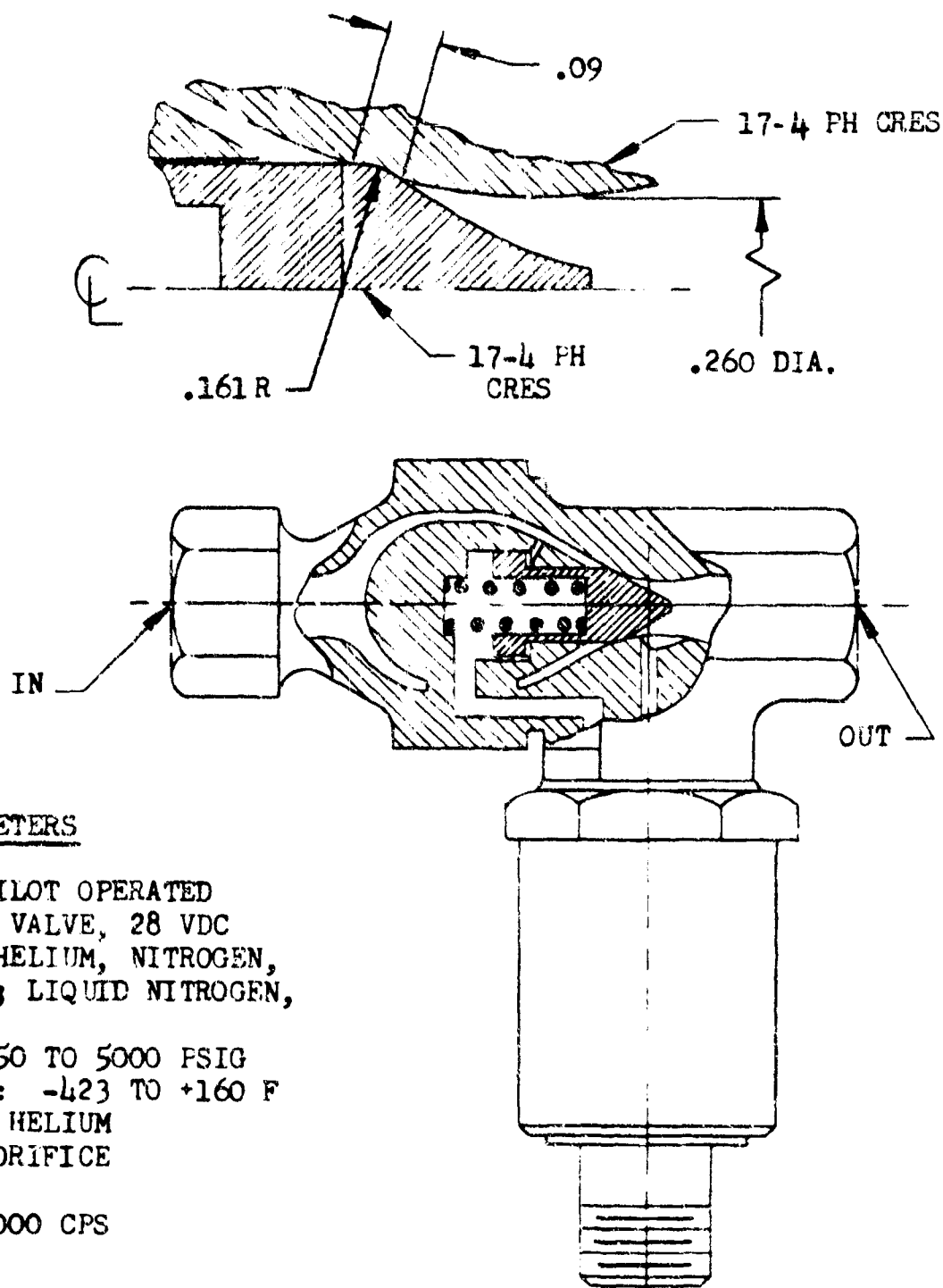
The success of this seal is directly attributable to its flexibility and deformation control provided by the positive stop design. However, seal fabrication does require the use of hot forming techniques and special dies. Close control of the poppet and seal surface finish is required.

---

\*AFBMD-TR-60-55, Design, Development, and Testing of Advanced Liquid Oxygen Tank Vent and Relief Valve, Part No. 551430, North American Aviation, Inc., March 1960.

## **SPHERICAL POPPET SEAT DESIGNS**

SPHERICAL POPPET SEAT DESIGN



KEY PARAMETERS

VALVE TYPE: 2-WAY, PILOT OPERATED  
SOLENOID VALVE, 28 VDC  
FLOW MEDIA: GASEOUS HELIUM, NITROGEN,  
HYDROGEN; LIQUID NITROGEN,  
HYDROGEN  
OPERATING PRESSURE: 50 TO 5000 PSIG  
OPERATING TEMPERATURE: -423 TO +160 F  
LEAKAGE: 10 SCIM MAX HELIUM  
CAPACITY: 0.25 INCH ORIFICE  
LIFE: 10,000 CYCLES  
VIBRATION: 30 G TO 2000 CPS  
TUBE SIZE: 3/8 INCH

Figure B-8. Piloted Solenoid Valve--  
North American Aviation,  
Inc.



## PILGATED SOLENOID VALVE

The spherical seat and poppet utilized in this valve underwent extensive development under a 2-year state-of-the-art valve improvement program.\* Some of the numerous designs tried were poppets with copper, Kel-F, or Teflon inserts--laminates of corrosion resistant steel and Teflon, and all metal configurations.

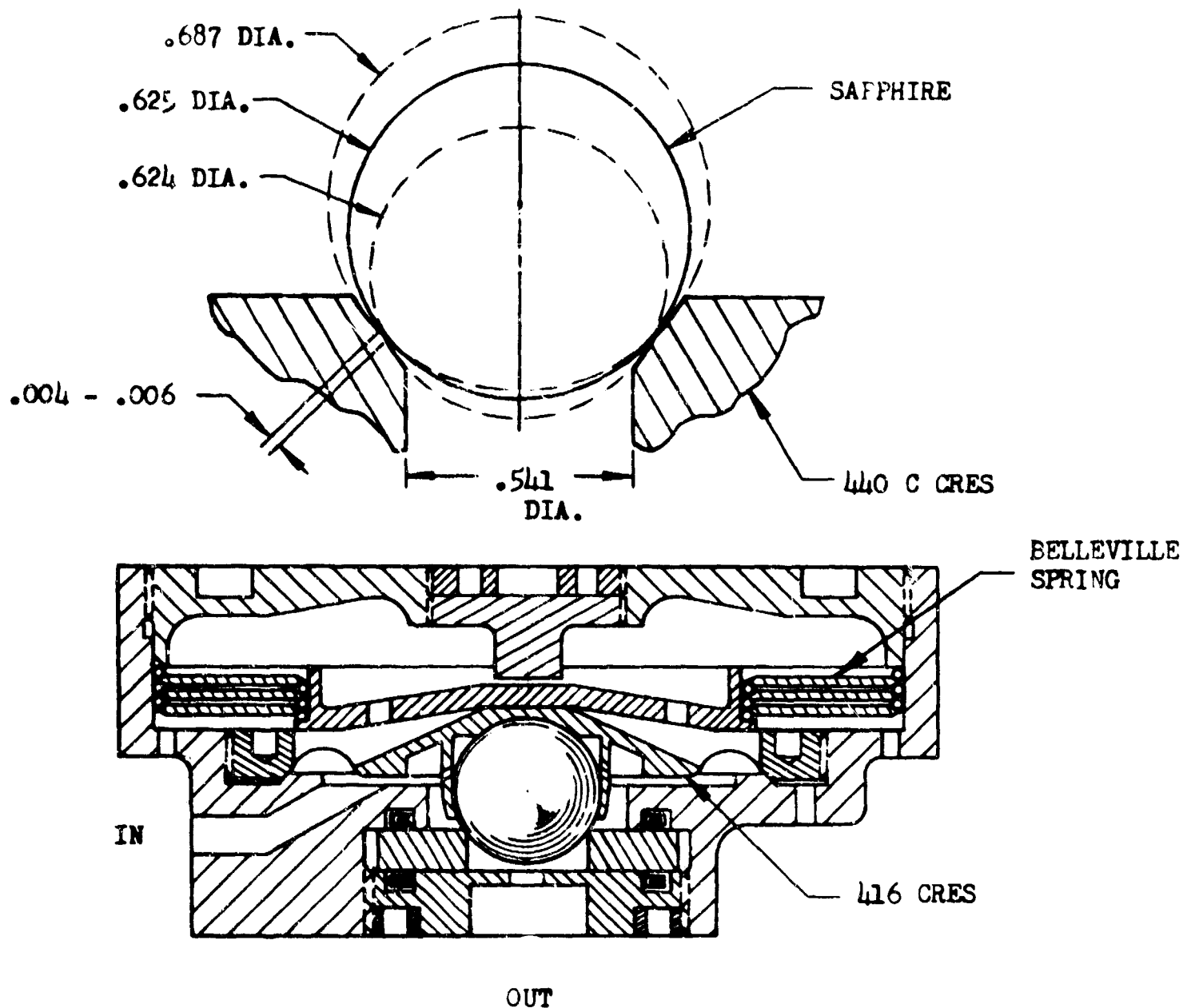
Most of the soft seats exhibited low leakage at ambient conditions and excessive leakage at cryogenic temperatures. In addition, the poor impact resistance displayed by Kel-F and Teflon during high-pressure valve operation resulted in the adoption and successful employment of the corrosion resistant steel, spherically lapped configuration shown.

Final match lapping of the poppet and seat is accomplished with special fixtures. A "mirror bright finish," when inspected at 20 to 40 power magnification, is specified for both seating surfaces.

---

\*AFBMD-TR-58-18, Design, Development, and Testing of Advanced Pneumatic Solenoid Valve, North American Aviation, Inc., November 1959.

### SPHERICAL POPPET SEAT DESIGN



### KEY PARAMETERS

VALVE TYPE: PRESSURE RELIEF VALVE  
FLOW MEDIA: AIR, NITROGEN, HELIUM  
CRACKING PRESSURE: 50 TO 100 PSIG  
FULL FLOW PRESSURE: WITHIN + 2.5% CRACKING PRESSURE  
RESEAT PRESSURE: NOT LESS THAN 94% OF CRACKING PRESSURE  
OPERATING TEMPERATURE: -450 TO +300 F  
LEAKAGE: 5 SCCM MAX HELIUM  
CAPACITY: 0.12 ORIFICE  
RESPONSE: 5 MILLISECONDS  
LIFE: 50,000 CYCLES  
VIBRATION: 65 G TO 2000 CPS

Figure B-9. Snap Action Relief Valve--  
Frebank Company

## SNAP ACTION RELIEF VALVE

This snap action pressure relief valve employs a pressure sensing diaphragm and the inherent instability of a Belleville spring to actuate the poppet at a set cracking pressure. The design was the subject of considerable development effort under a state-of-the-art improvement program.\* A sapphire-to-metal poppet and seat was selected to provide positive stroke control for operation of the Belleville springs in the negative rate region, maintain material compatibility with storable propellants, and improve the vibration characteristics by decreasing the weight of the poppet. The spherical ball seats on a narrow land width seat to provide a low leakage rate with relatively low seat loads and to closely control the effective diameter of the seating surface.

The horizontal deflection of the metal diaphragm is unpredictable when the poppet and diaphragm are assembled in the body, with the resultant inconsistent concentricity of the poppet to the seat for each assembly.

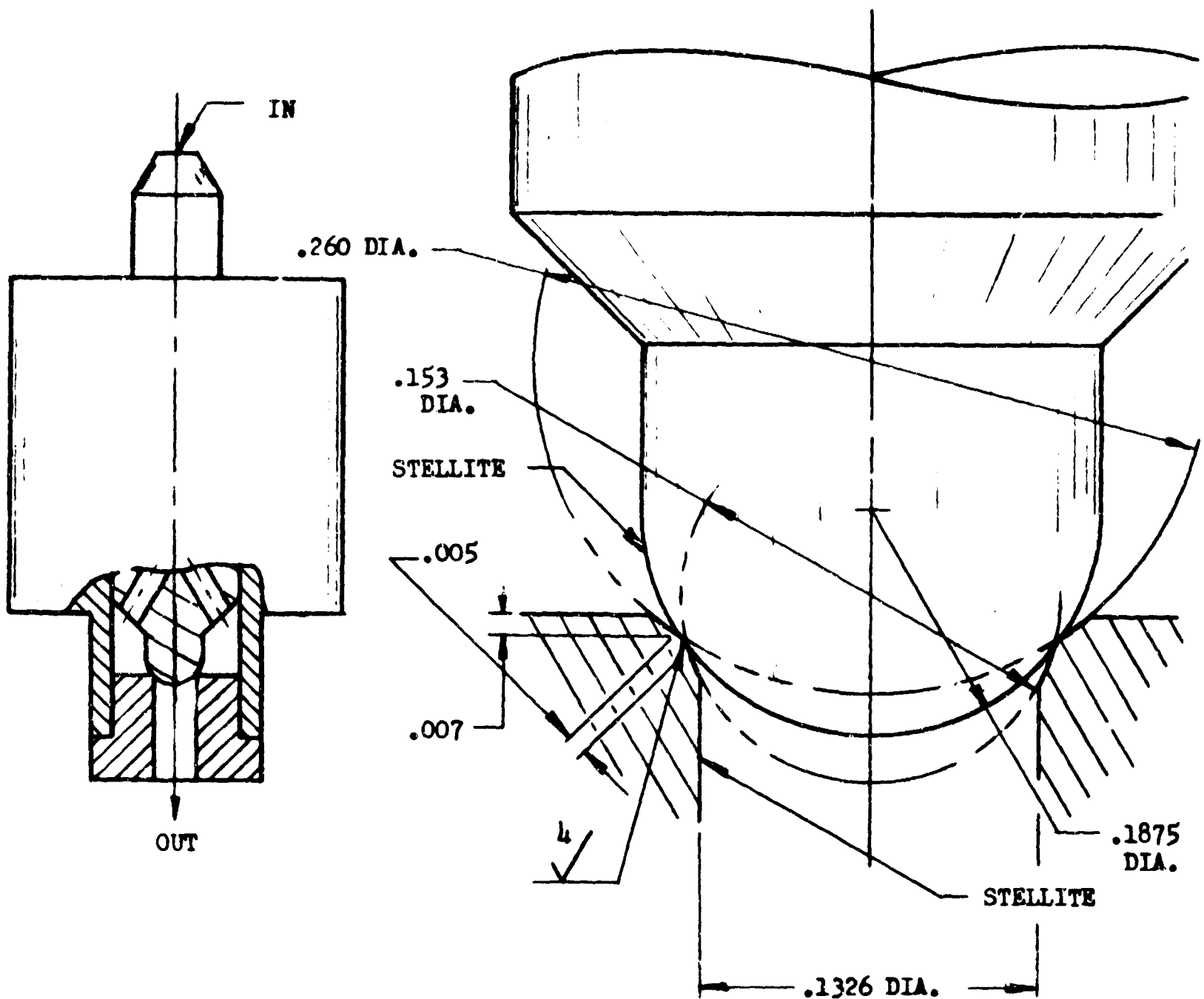
Notable in the development of the valve was the attempt to eliminate the problem by guiding the poppet onto the seat. The perpendicular spring force of the installed diaphragm was sufficient to cause galling of the guide. The addition of dry film lubricants did not eliminate the problem.

Due to the above problem the valve must be repetitiously assembled and tested to obtain an assembly that meets the delineated requirements.

---

\*AFBSD-TR-61-71, Design Development and Testing of Non-Modulating Pressure Control Valves, Frebank Company, December 1961.

# SPHERICAL POPPET SEAT DESIGN



## KEY PARAMETERS

VALVE TYPE: 2-WAY, DIRECT OPERATED SOLENOID VALVE, 28 VDC  
 FLOW MEDIA: NITROGEN TETROXIDE, UDMH, HYDRAZINE  
 TEST MEDIA: NITROGEN  
 OPERATING PRESSURE: 300 PSIA  
 OPERATING TEMPERATURE: -65 TO +165 F  
 LEAKAGE: 1.0 SCC/HR MAX NITROGEN AT 100 PSIG  
 CAPACITY: 0.07 INCH ORIFICE  
 LIFE: 500,000 CYCLES (DESIGN OBJECTIVE; 100,000 PROVEN)

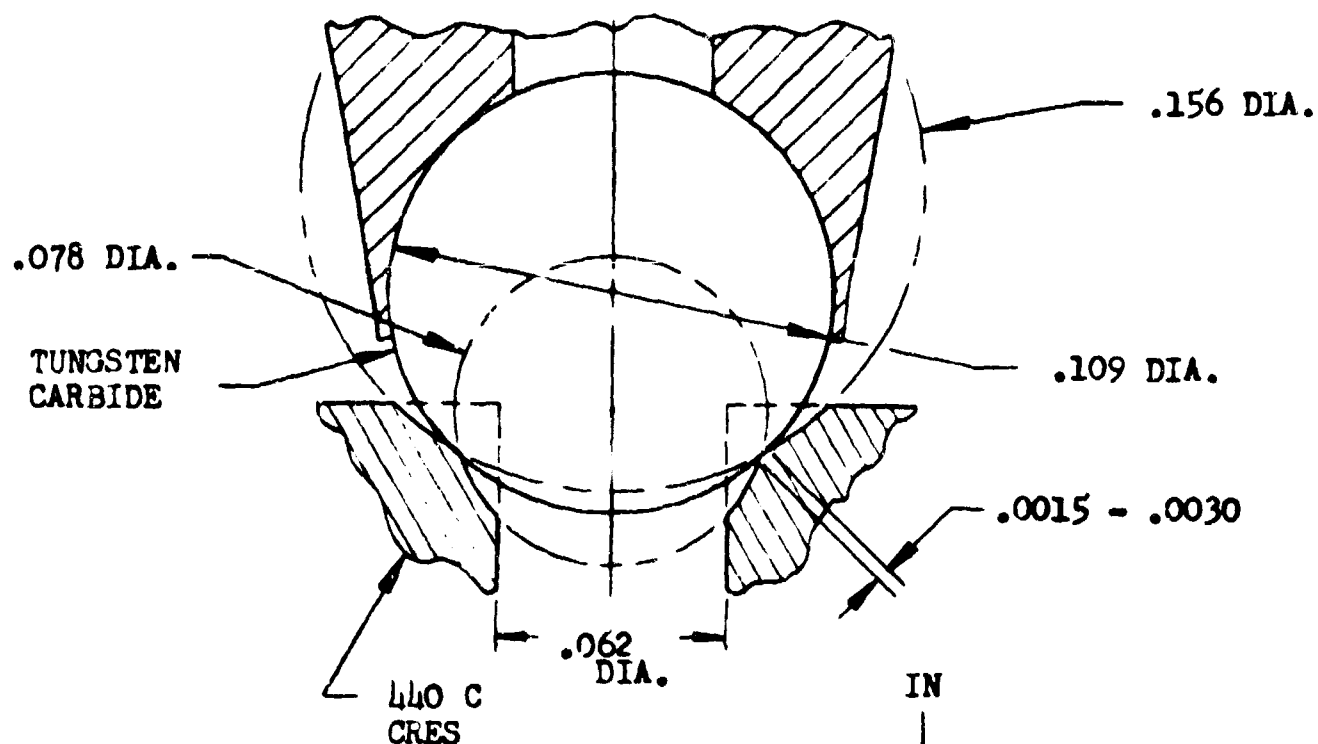
Figure B-10. Propellant Control Solenoid Valve III--  
 Minneapolis-Honeywell Regulator  
 Company, Aeronautical Division

### PROPELLANT CONTROL SOLENOID VALVE III

The spherically lapped seat design shown is utilized in a storable propellant control valve where extreme endurance life is required. As the spherical seat allows some angular misalignment, an endurance life greater than a similar conical design is expected. Additional advantages of the design are compatibility with extreme space environments (temperature, hard vacuum, and radiation), a shorter stroke than required for the conical design and excellent centering and sealing characteristics.

On the negative side, performance characteristics are obtained only through extreme control of poppet sphericity and fluid contaminants. (Valves currently under test employ integral 10-micron filters.)

# SPHERICAL POPPET SEAT DESIGN



## KEY PARAMETERS

VALVE TYPE: 2-WAY, DIRECT OPERATED  
SOLENOID VALVE, 28 VDC  
FLOW MEDIA: NITROGEN TETROXIDE, UDMH,  
HYDRAZINE  
TEST MEDIA: HELIUM, NITROGEN, WATER  
OPERATING PRESSURE: 280 PSIG  
OPERATING TEMPERATURE: -20 TO +160 F  
LEAKAGE: 0.5 SCCM MAX HELIUM  
CAPACITY: .060 INCH ORIFICE  
RESPONSE: .006 + .0005 SEC  
LIFE: 50,000 CYCLES  
VIBRATION: 20 G TO 2000 CPS  
TUBE SIZE: 1/4 INCH

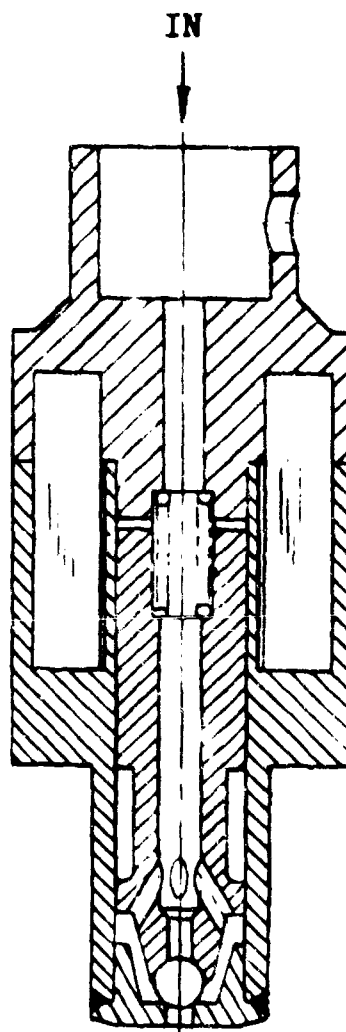


Figure B-11. Propellant Control Solenoid Valve IV--  
Rocketdyne, A Division of North  
American Aviation, Inc.

## PROPELLANT CONTROL SOLENOID VALVE IV

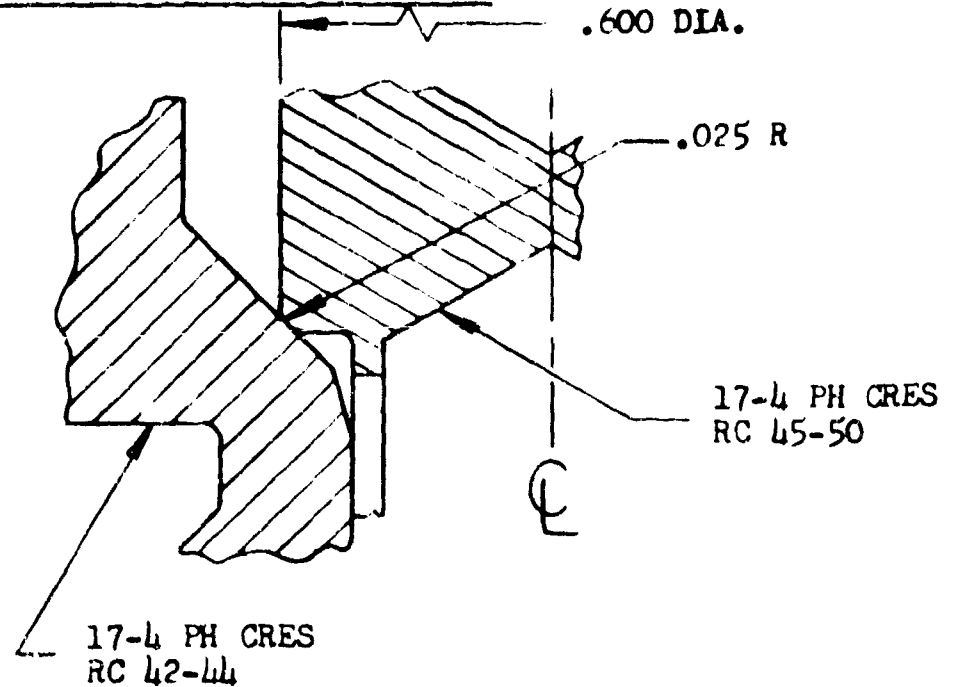
This valve was designed to control fuel or oxidizer fluids for storable propellant rocket engines. The design employs a poppet with a trapped metal ball and a lapped, narrow metal seat.

The narrow seat with uniform width that is essential for good leakage performance is obtained by lapping the seating surface with three sizes of balls as shown. The seat must be generated from a round smooth bore and a flat smooth face which is normal to the bore and the line of poppet travel. In addition, the concentricity of the bore with the poppet must be closely controlled. This design utilizes a loose fit between the seat guide and body that allows the seat to center itself on the poppet ball prior to welding the seat in place. The poppet ball is maintained spherical within 25 millionths.

A hardened, high-strength material is used for the seat to provide a low seat stress relative to the yield stress of the material for an increased endurance life, while preserving the narrow seat width.

The major problems with the design have been the maintenance of concentricity of the seat with the poppet upon assembly and the requirement of skilled, trained personnel for precision lapping to meet the leakage requirements.

CONICAL POPPET SEAT DESIGN



KEY PARAMETERS

VALVE TYPE: CHECK VALVE  
FLOW MEDIA: HYDRAULIC OIL, AIR,  
NITROGEN, HELIUM,  
CRYOGENIC FLUIDS  
TEST MEDIA: AIR OR NITROGEN  
OPERATING PRESSURE: 3000 PSIG  
CRACKING PRESSURE: 2 TO 10 PSIG  
OPERATING TEMPERATURE: -300 TO +450 F  
LEAKAGE: ZERO BUBBLE GN<sub>2</sub> FOR 5 MINUTES  
UNDER WATER  
CAPACITY: .15 INCH ORIFICE  
LIFE: 10,000 CYCLES GN<sub>2</sub> AT 3000 PSIG  
AND 70 F  
TUBE SIZE: 1/4 INCH

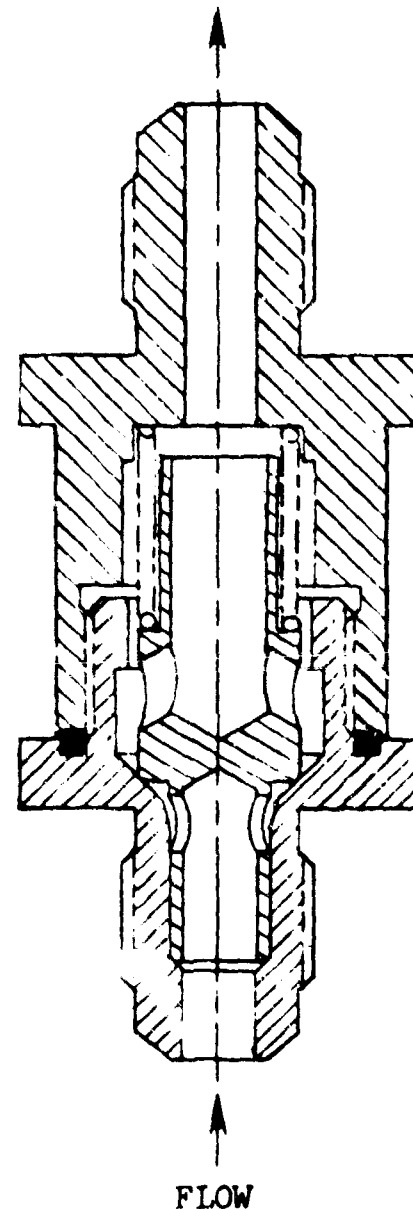


Figure B-12. All-Metal Check Valve—Randall Engineering Corporation (Patent Pending)



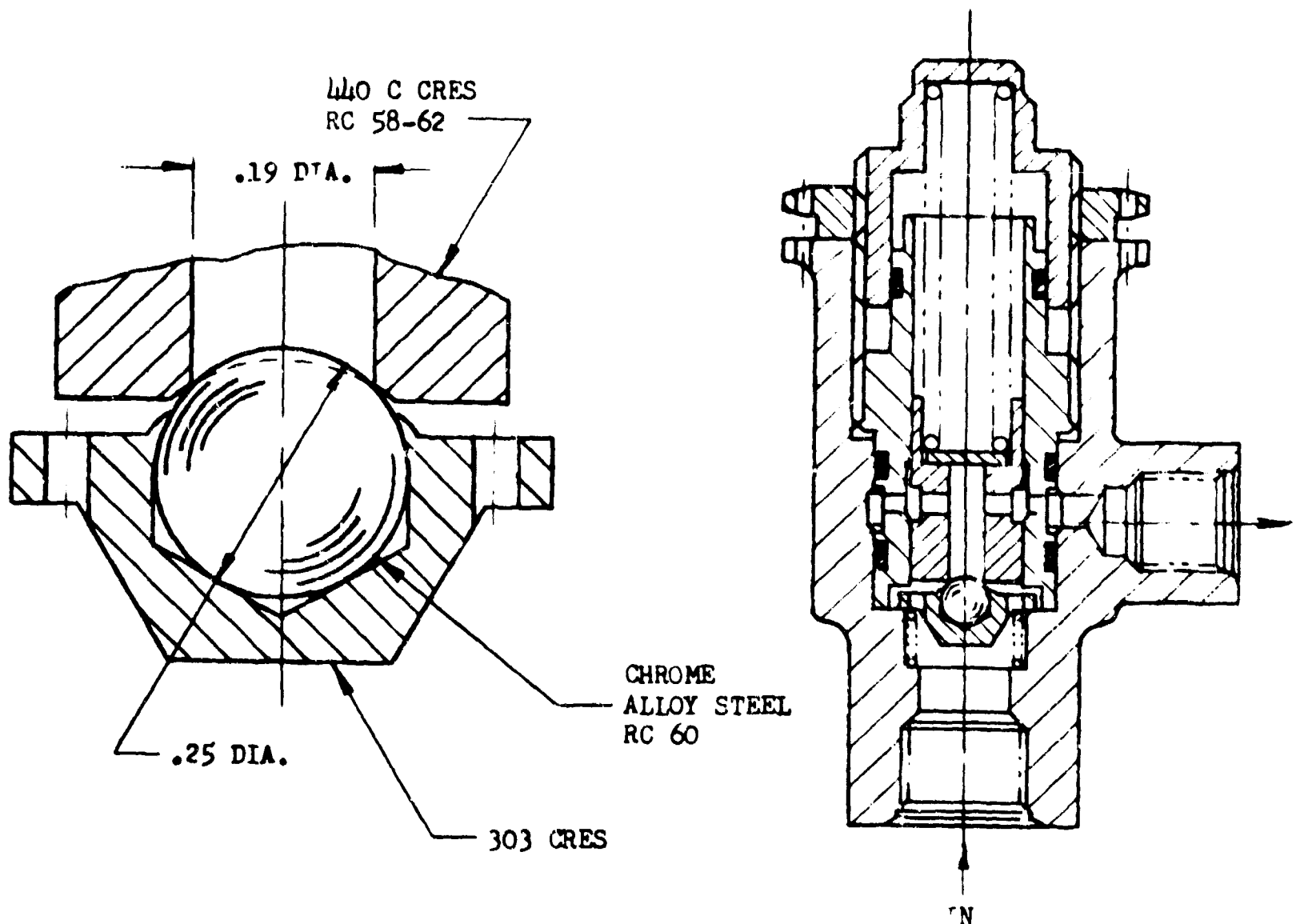
## ALL METAL CHECK VALVE

This all metal check valve is designed for high endurance and low leakage rates with multiple fluids, over a wide temperature range. The metal-to-metal closure seal is provided by seating a radiused corner of the poppet on a conical seat. A 16-microinch finish is ground on the poppet and seat preliminary to match lapping.

Utilization of the inlet port to guide the poppet reduces the size and weight of the unit, but provides a broken flow pattern with the associated additional pressure drop.

Modifications of the design shown have utilized stellite on the seating surfaces for ultra-high endurance (100,000 cycles) and a Teflon-coated (0.002-inch) poppet for cryogenic service.

# SPHERICAL POPPET SEAT DESIGN



## KEY PARAMETERS

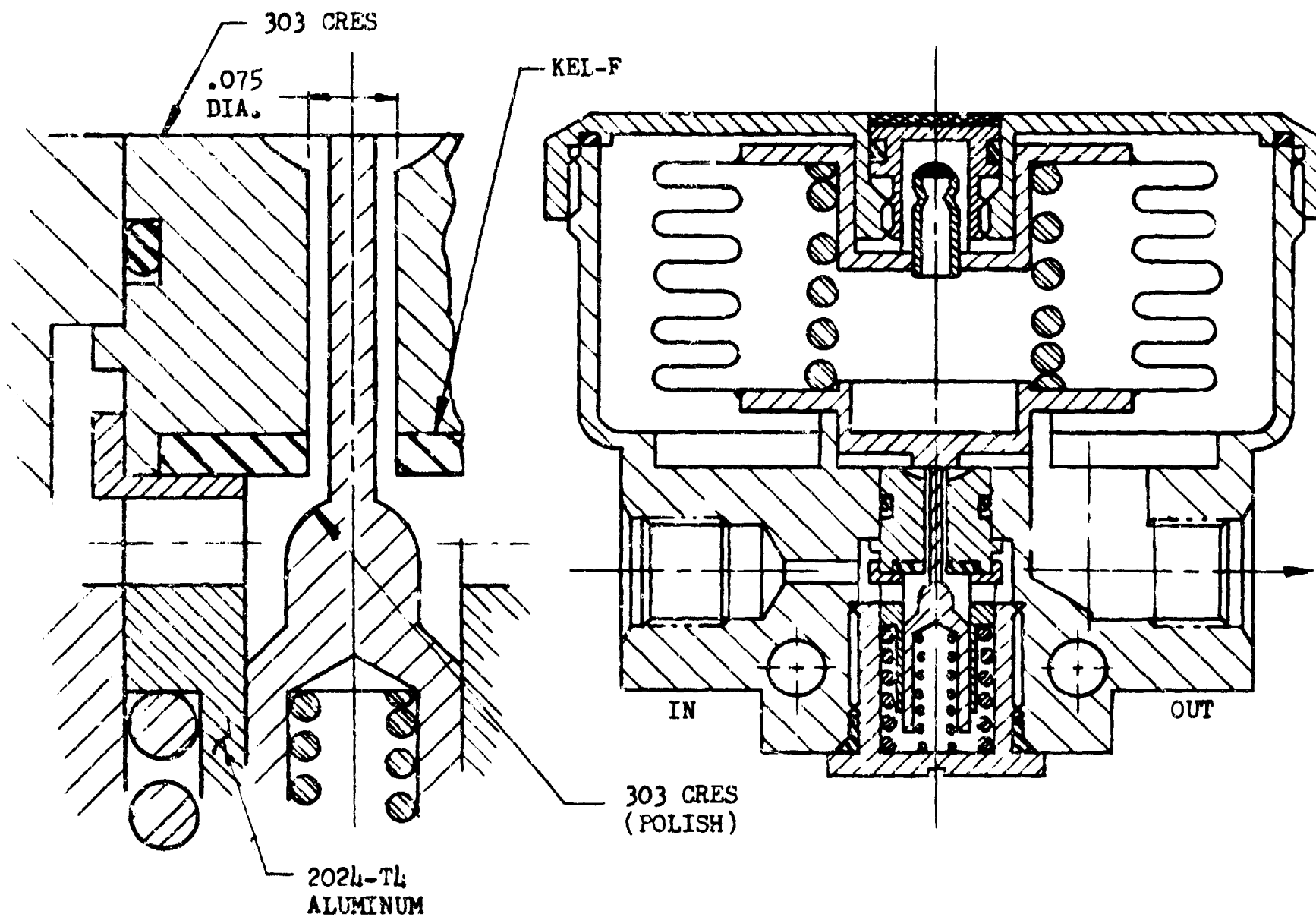
VALVE TYPE: INVERTED PRESSURE RELIEF VALVE  
FLOW MEDIA: HYDRAULIC OIL  
OPERATING PRESSURE: 100 TO 2300 PSI  
OPERATING TEMPERATURE: -65 TO +160 F  
LEAKAGE: 2 CCM HYDRAULIC OIL  
CAPACITY: 0.15 INCH ORIFICE  
LIFE: 50,000 CYCLES  
TUBE SIZE: 1/4 INCH

Figure B-13. Inverted Relief Valve—Denbow Manufacturing Corporation (U.S. Patent No. 2,239,078)

## INVERTED RELIEF VALVE

The inherent seat loading characteristics of this inverted design and the narrow seat width results in low leakage. The seat is fabricated by cylindrically lapping the bore, flat lapping the face and then spherically lapping the face with an oversize tungsten carbide ball. The resulting seat geometry leaves a sharp corner free from burrs that the poppet coins into a narrow land during valve assembly. No attempt is made to match lap the seat and poppet for hydraulic service. Pneumatic service, however, dictates match lapping to satisfy the more stringent leakage requirements.

## SPHERICAL POPPET SEAT DESIGN



### KEY PARAMETERS

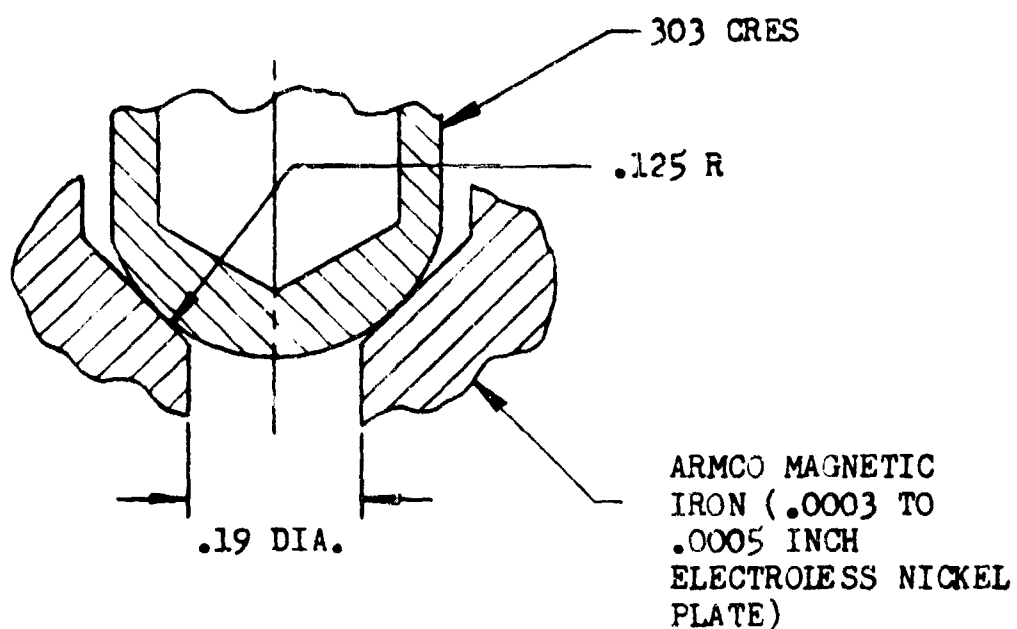
VALVE TYPE: PRESSURE REGULATOR  
FLOW MEDIA: AIR, NITROGEN  
INLET PRESSURE: 25 TO 750 PSIG  
REGULATED PRESSURE:  $31 \pm 0.5$  PSIA  
OPERATING TEMPERATURE:  $-65$  TO  $+160$  F  
LEAKAGE: 1.0 SCIM MAX  
CAPACITY: 0.022 INCH ORIFICE  
VIBRATION: 2 G TO 100 CPS  
10 G, 100 TO 500 CPS  
TUBE SIZE: 1/4 INCH

Figure B-14. Absolute Pressure Regulator--  
Clary Dynamics Corporation

### ABSOLUTE PRESSURE REGULATOR

This pressure regulator handles engine bleed air on a current fighter aircraft. The spherical poppet segment engaging the Kel-F seat is highly polished to meet the leakage requirement. The design originally utilized a conical poppet; however, with the light seating loads available, the spherical poppet was found necessary to meet regulation and lockup requirements.

## SPHERICAL POPPET SEAT DESIGN



### KEY PARAMETERS

VALVE TYPE: 2-WAY, DIRECT-OPERATED  
SOLENOID VALVE, 28 VDC  
FLOW MEDIA: FC-75 SILICONE FLUID  
TEST MEDIA: WATER  
OPERATING PRESSURE: 200 PSIG  
OPERATING TEMPERATURE: -65 TO +160 F  
LEAKAGE: 10.0 CCM MAX  
CAPACITY: 0.14 INCH ORIFICE  
LIFE: 2,000,000 CYCLES  
TUBE SIZE: 1/4 INCH

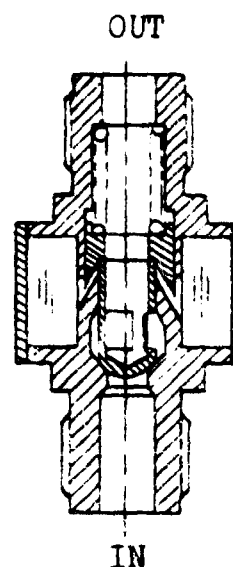


Figure B-15. Hydraulic Control Solenoid Valve—  
Clary Dynamics Corporation

## HYDRAULIC CONTROL SOLENOID VALVE

This design, employing a spherical poppet and conical seat to control the flow of a hydraulic fluid, utilizes a minimum number of parts to effect a simple design of relatively low cost capable of over 2,000,000 cycles. However, low seat stress inherent in the design necessitates a high leakage allowance.

# SPHERICAL POPPET SEAT DESIGN

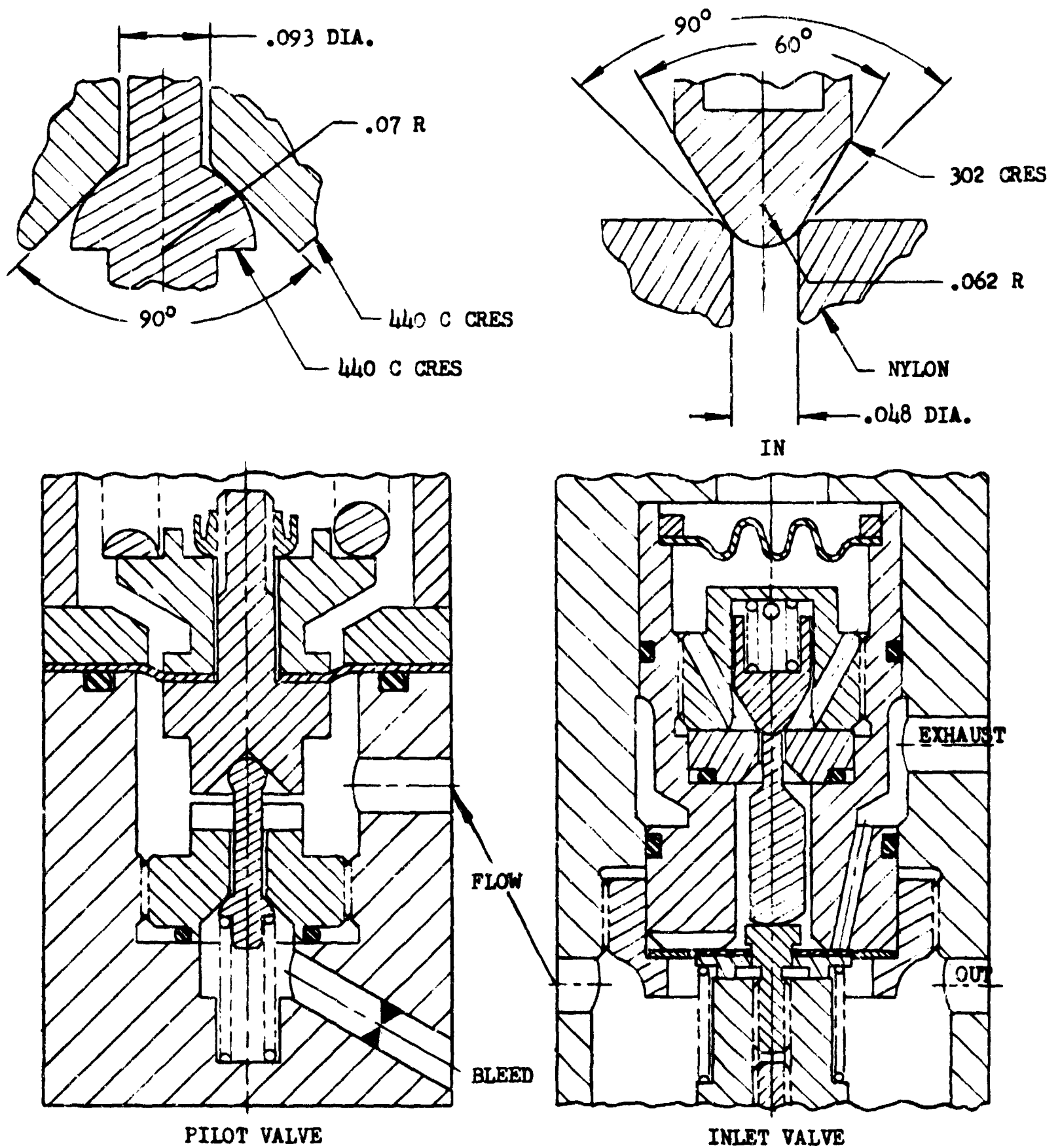


Figure B-16. Precision Loader—Rocketdyne, A Division of North American Aviation, Inc.



## PRECISION LOADER

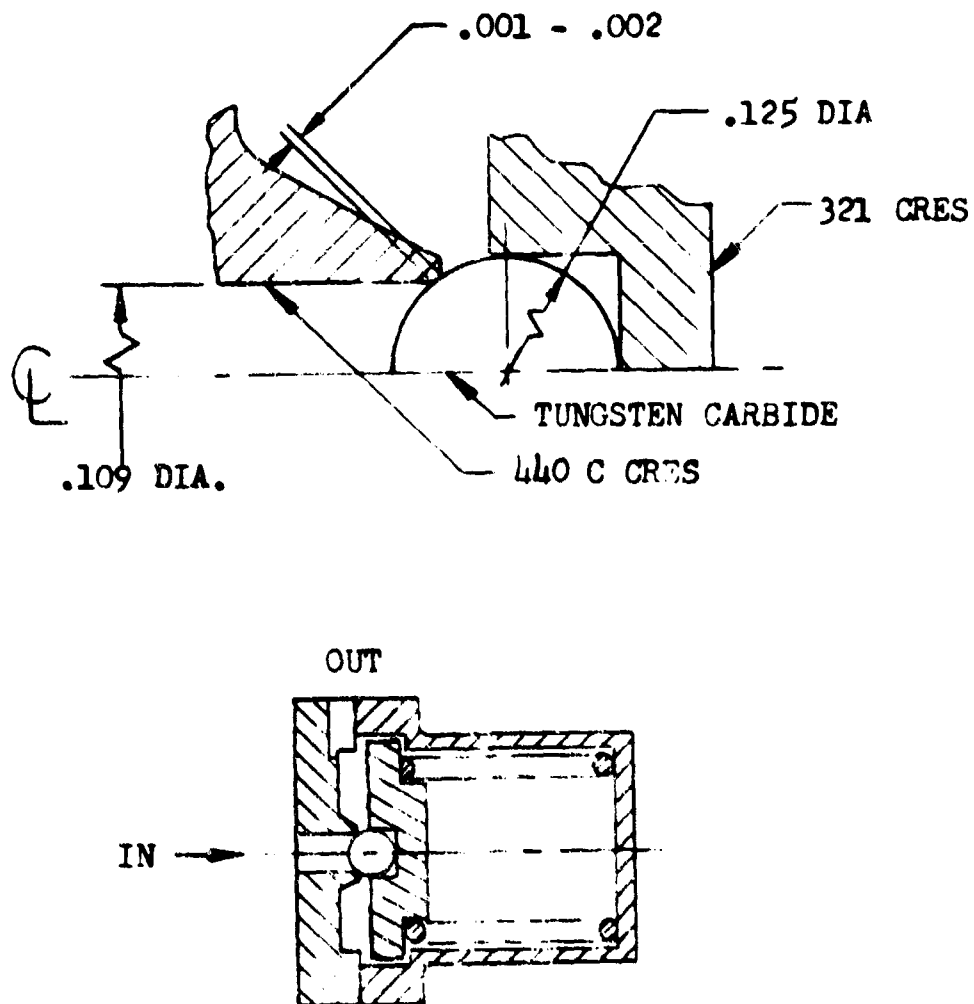
### KEY PARAMETERS

VALVE TYPE:	PRESSURE LOADING REGULATOR	
FLOW MEDIA:	AIR, NITROGEN, HELIUM	
REGULATED PRESSURE:	150 to 900 psig	
INLET PRESSURE:	50-psig ABOVE REGULATED PRESSURE TO 3000 psig	
OPERATING TEMPERATURE:	-30 to +165 F	
LEAKAGE:	INLET VALVE:	5-scim MAXIMUM AIR
	PILOT VALVE:	10-scim MAXIMUM AIR
CAPACITY:	INLET VALVE:	0.029-INCH ORIFICE
	PILOT VALVE:	0.004-INCH ORIFICE
TUBE SIZE:	1/4 INCH	

The illustrated designs are the inlet and pilot valves for a low volume, high-pressure regulator. This regulator is normally capable of  $\pm 1.5\%$  steady-state accuracy; however, because neither valve is damped, the regulator is vibration sensitive.

Leakage is not critical because the regulator continuously bleeds a fixed amount of gas overboard, eliminating the requirement for tight lockup.

# SPHERICAL POPPET SEAT DESIGN



## KEY PARAMETERS

VALVE TYPE: PRESSURE RELIEF VALVE  
 FLOW MEDIA: HELIUM  
 FULL OPEN PRESSURE: 4000 PSIG  
 RESEAT PRESSURE: 3500 PSIG  
 OPERATING TEMPERATURE: -320 TO 140 F  
 LEAKAGE: 10 SCIM MAX HELIUM  
 CAPACITY: 0.015 INCH ORIFICE  
 LIFE: 1000 CYCLES  
 VIBRATION: 25 G TO 2000 CPS

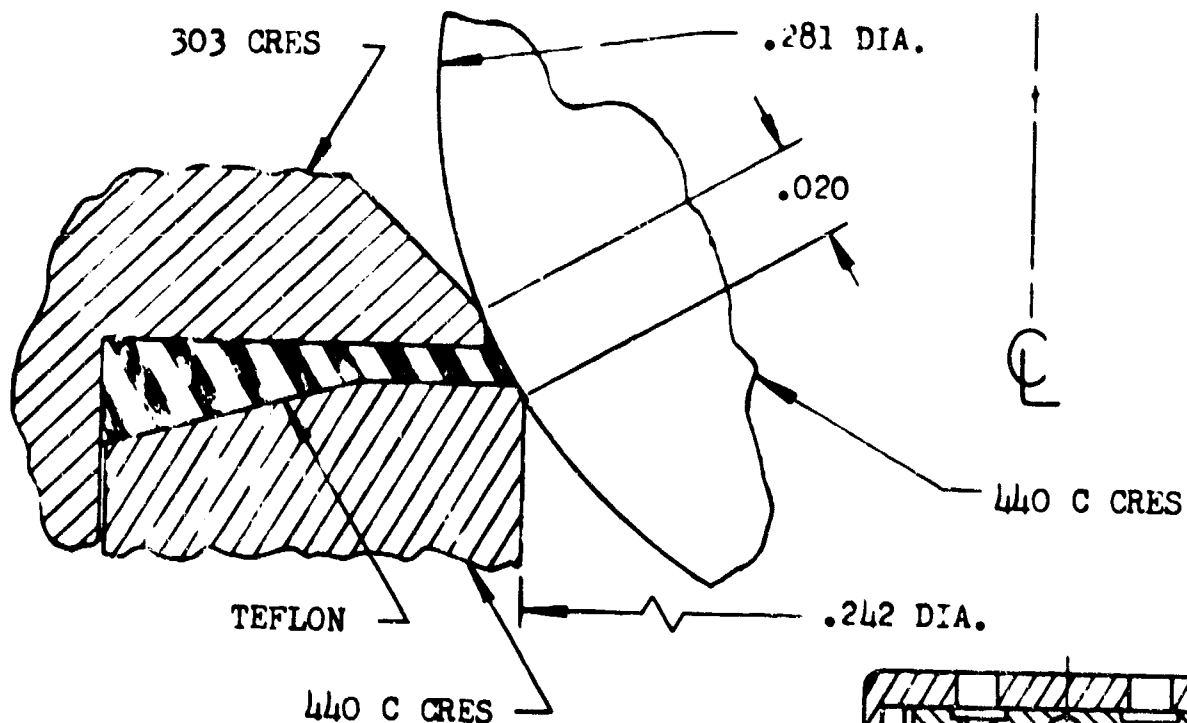
Figure B-17. High-Pressure Relief Valve—Rocketdyne, A Division of North American Aviation, Inc.

## HIGH-PRESSURE RELIEF VALVE

This high-pressure relief valve employs a tungsten carbide ball seating on a lapped metal seat. The ball is allowed to float freely between liftoff from the seat and the upper-limit stop. The stop is provided to minimize instability caused by the rapid back-and-forth transfer of effective poppet area during stroking. An extremely narrow seat land width is maintained to obtain repeatable crack and reseal pressures. This controlled narrow seat also guarantees the high seat stress required for low leakage. The leakage is further reduced by precision lapping the seat to obtain a 2-microinch finish and maintaining the sphericity of the ball within 25 millionths.

Precise manufacturing procedures and extreme control of contamination are required to obtain satisfactory operation.

## SPHERICAL POPPET SEAT DESIGN



### KEY PARAMETERS

VALVE TYPE: PRESSURE RELIEF VALVE  
FLOW MEDIA: HELIUM  
OPERATING PRESSURE: 4500 TO 4650 PSIG (DISC  
RUPTURE, CRACK, FULL FLOW,  
AND RESEAT)  
OPERATING TEMPERATURE: +30 TO +160 F  
LEAKAGE: ZERO BEFORE DISC RUPTURE  
20 SCIM MAX HELIUM, AFTER FIRST  
ACTUATION  
CAPACITY: 0.0021 INCH ORIFICE  
LIFE: 1000 CYCLES  
TUBE SIZE: 1/4 INCH

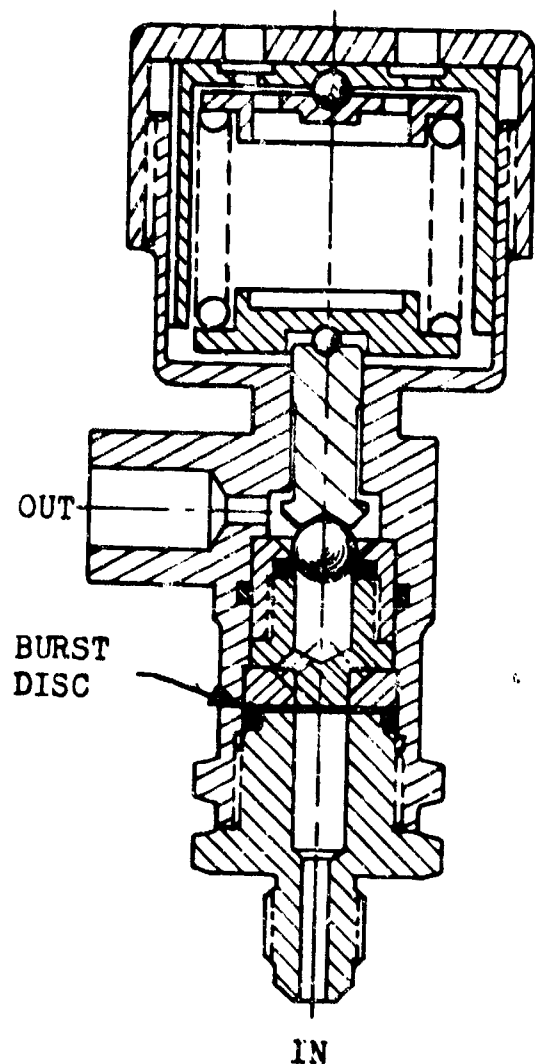


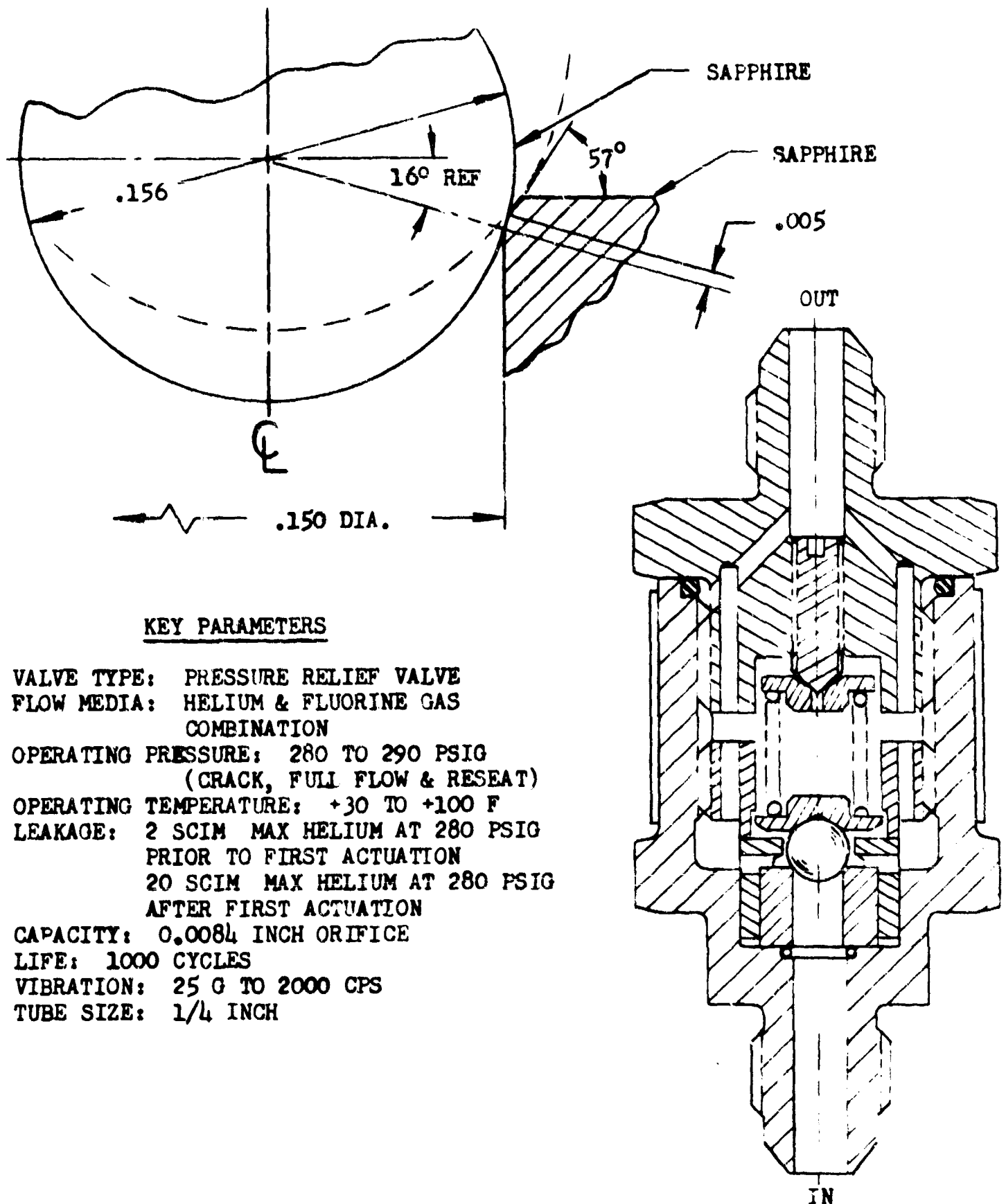
Figure B-18. High-Pressure Relief Valve—Aqualite Corporation  
(U.S. Patent No. 2,960,096)

## HIGH-PRESSURE RELIEF VALVE

This valve was designed and developed to operate as a thermal relief valve for the main helium supply tank of a space vehicle. The use of a Teflon burst disc guarantees extremely low leakage prior to the initial activation. (Burst and flow are both accomplished in the piston annulus.) Disc rupture, cracking, full flow and reseal to 20-scim helium leakage is maintained within 3.3%. Unique in the design is the combination Teflon-metal seat which affords low leakage. Accuracy is maintained by almost complete freedom from friction and bind through the use of ball joints.

While this component has proved its capability as a relief valve, the burst disc function has not been thoroughly demonstrated. Annular width, Teflon thickness, edge radius, installation and temperature change all cause variation in burst pressure. A statistical test program is required to ensure design feasibility.

### SPHERICAL POPPET SEAT DESIGN



#### KEY PARAMETERS

VALVE TYPE: PRESSURE RELIEF VALVE  
FLOW MEDIA: HELIUM & FLUORINE GAS  
COMBINATION  
OPERATING PRESSURE: 280 TO 290 PSIG  
(CRACK, FULL FLOW & RESEAT)  
OPERATING TEMPERATURE: +30 TO +100 F  
LEAKAGE: 2 SCIM MAX HELIUM AT 280 PSIG  
PRIOR TO FIRST ACTUATION  
20 SCIM MAX HELIUM AT 280 PSIG  
AFTER FIRST ACTUATION  
CAPACITY: 0.0084 INCH ORIFICE  
LIFE: 1000 CYCLES  
VIBRATION: 25 G TO 2000 CPS  
TUBE SIZE: 1/4 INCH

Figure B-19. Fluorine Tank Relief Valve—Whittaker Controls  
Division of Telecomputing Corporation

## FLUORINE TANK RELIEF VALVE

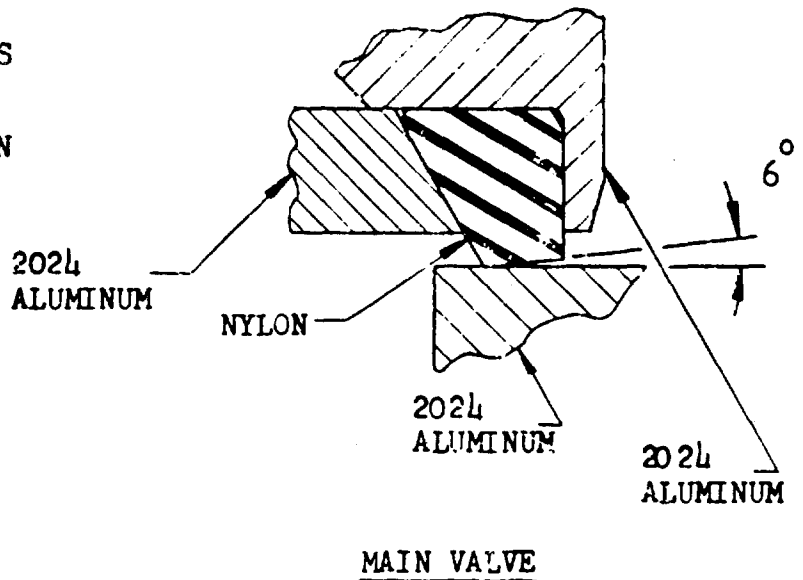
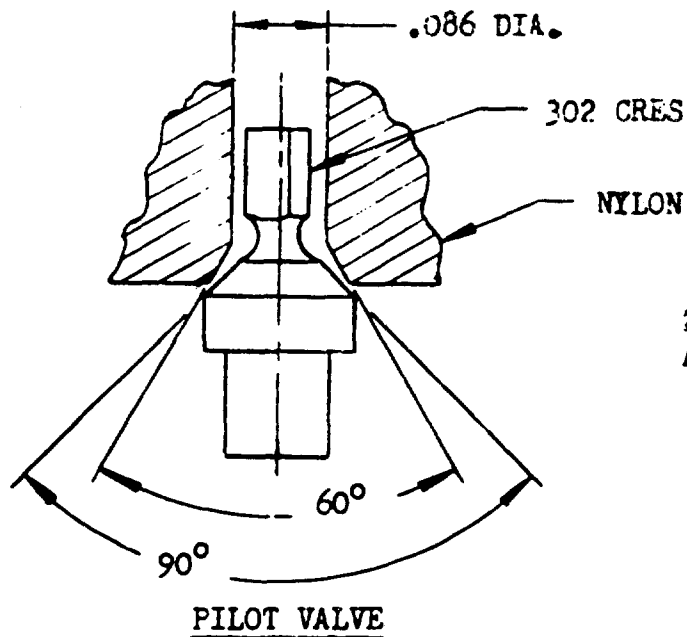
This valve was designed for use as a thermal relief in a fluorine tank pressurization system. Compatibility of materials is achieved by the use of stainless steel and sapphire ball and seat. The 3.3% crack, full-open to reseal accuracy, results through the combination of a narrow seat land, freedom from friction and bind and a narrow operation temperature range.

The ability of this valve to function during 25-g vibration has been thoroughly demonstrated, the final design evolving after a series of minor redesigns. Unstable buzzing during initial cracking generally occurs but does not affect the accuracy or leakage. Extreme contamination sensitivity requires careful cleaning and filtration procedures.

**FLAT POPPET SEAT DESIGNS**



# CONICAL AND FLAT POPPET SEAT DESIGNS



## KEY PARAMETERS

VALVE TYPE: PILOT OPERATED PRESSURE  
RELIEF VALVE  
 FLOW MEDIA: AIR, NITROGEN, HELIUM  
 CRACKING PRESSURE: ADJUSTABLE FROM  
300 TO 1000 PSIG  
 RESEAT PRESSURE: NOT MORE THAN 10%  
BELOW CRACKING PRESSURE  
 OPERATING TEMPERATURE: -30 TO +150 F  
 LEAKAGE: 2 SCIM MAX AIR AT 200 PSI  
BELOW CRACKING PRESSURE  
FROM EACH SEAT  
 CAPACITY: 0.7 INCH ORIFICE  
 LIFE: 1000 CYCLES  
 VIBRATION: 25 G TO 2000 CPS  
 TUBE SIZE: 1 INCH

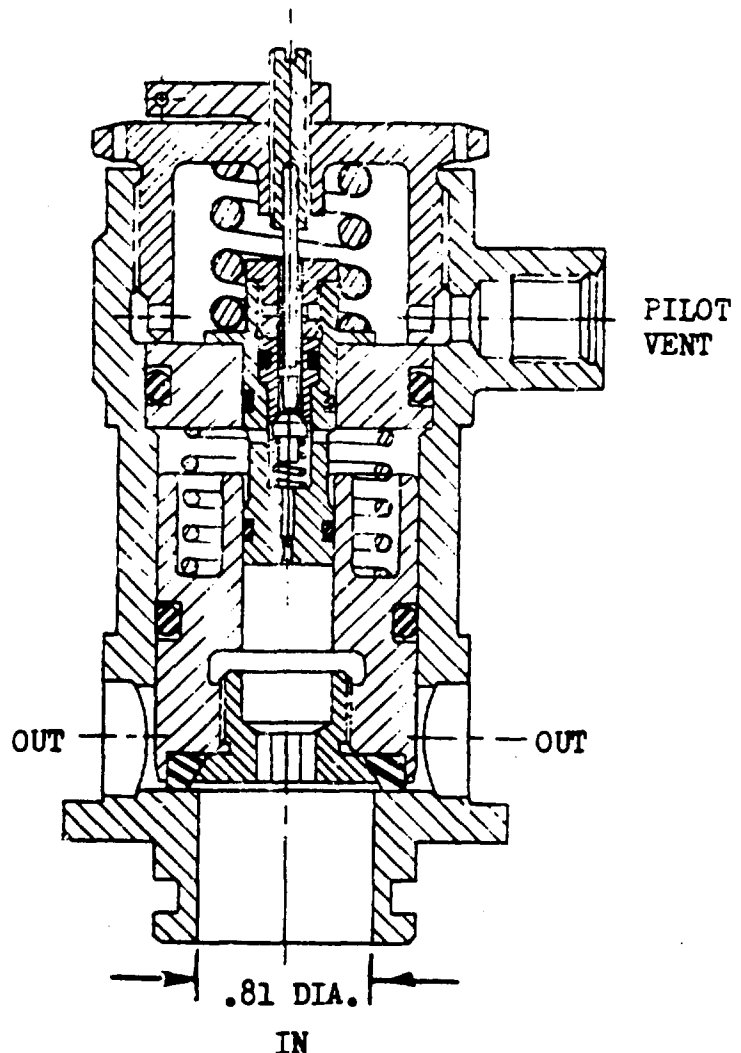


Figure B-20. High-Capacity Relief Valve—Rocketdyne, A Division of North American Aviation, Inc.

## HIGH CAPACITY RELIEF VALVE

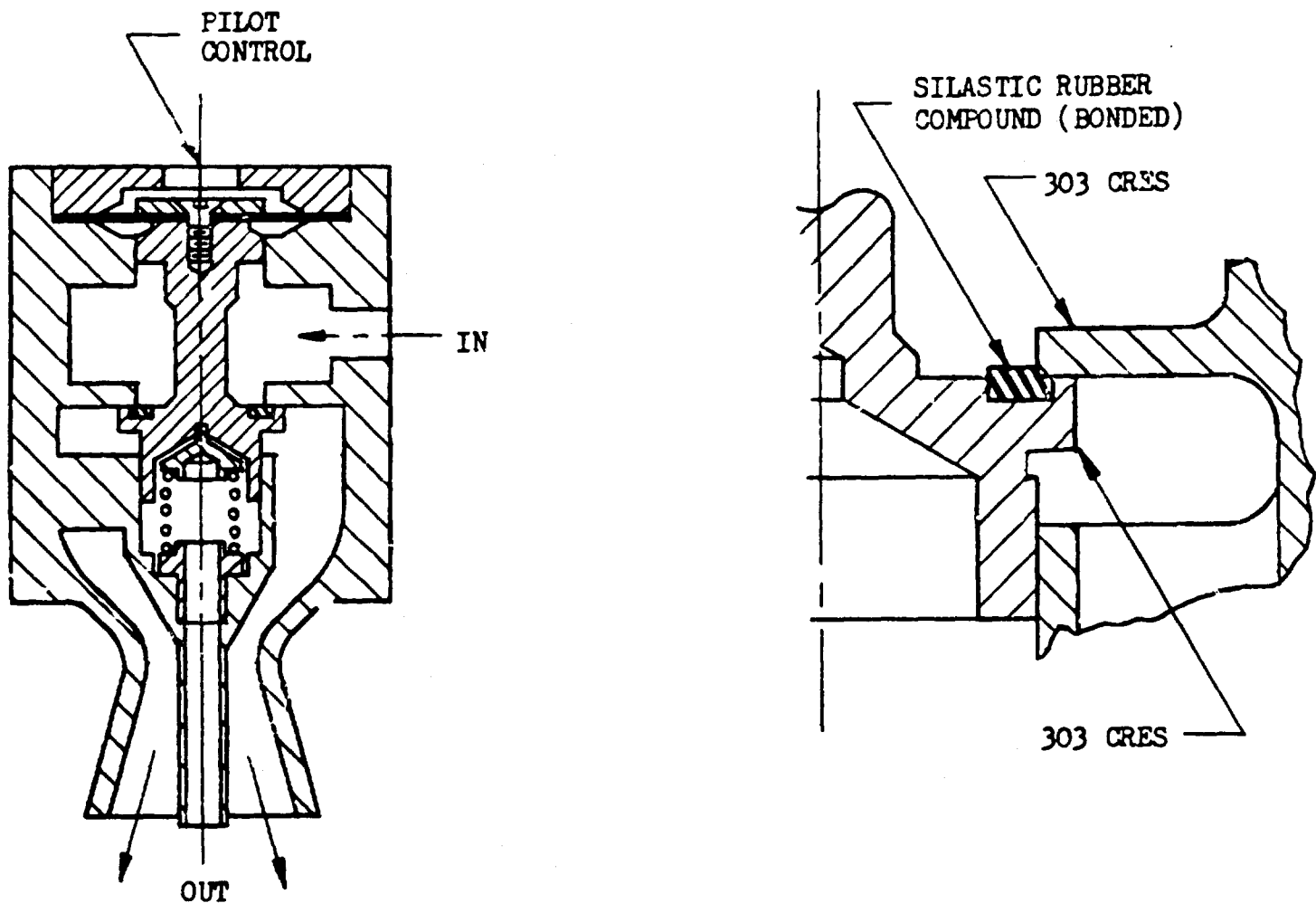
This pilot-operated relief valve is designed to protect pneumatic systems and tanks from over pressurization. Pilot operation allows the use of a relatively small reference spring which results in high capacity to weight ratio. In addition, full-open capacity is achieved rapidly when the cracking pressure is reached.

The pilot valve employs a conical metal poppet and nylon seat. A relatively large differential angle ensures a narrow land contact for close control of the relief setting. Yielding of the nylon balances out the seat load to provide a tight seal.

The main valve utilizes a flat nylon poppet and flat metal seat. This configuration, yielding under high load, forms a resilient seat capable of successfully withstanding the impact stresses concomitant with piloted operation.

Problem areas associated with this design are: (1) The nylon pilot seat changes dimensions which result in variations in actuation pressure, (2) small misalignments of the poppet members and O-ring stiction can cause large changes in actuation pressure.

## FLAT POPPET SEAT DESIGN



### KEY PARAMETERS

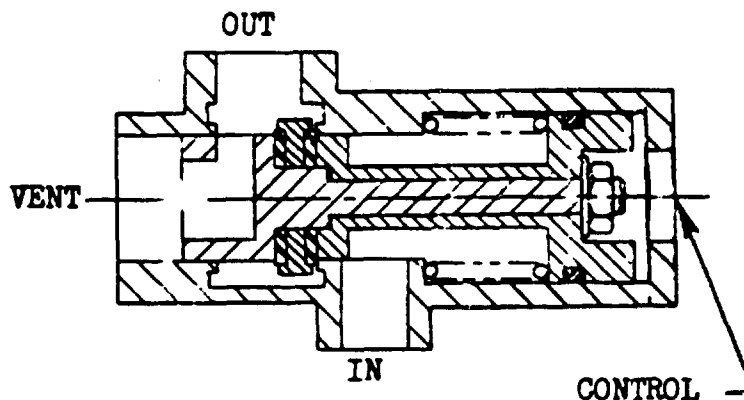
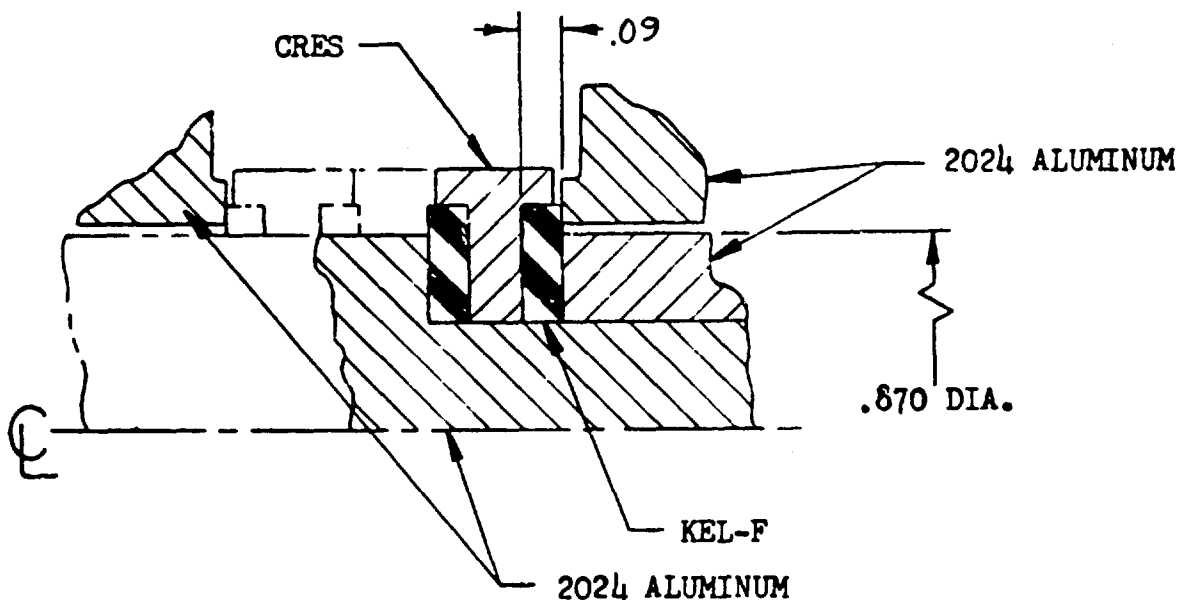
VALVE TYPE: MODULATING FLOW CONTROL AND SHUTOFF VALVE  
FLOW MEDIA: NITROGEN  
OPERATING PRESSURE: 180 TO 225 PSIG  
OPERATING TEMPERATURE: +30 TO +160 F  
LEAKAGE: .08 SCCM GN<sub>2</sub> AT 170 PSIG AND AMBIENT TEMPERATURE  
LIFE: 1,000,000 CYCLES AT 170 PSIG AND AMBIENT TEMPERATURE (LEAKAGE MAINTAINED AFTER CYCLING)  
VIBRATION: 3 G TO 1200 CPS

Figure B-21. Electro-Pneumatic Thrust Controller—The Bendix Corporation, Bendix Pacific Division

## ELECTRO-PNEUMATIC THRUST CONTROLLER

This design delineates the main valve of a pilot actuated space capsule thrust controller. The significant features of the valve are the extremely low leakage rate and the long life. The flat poppet has a silastic rubber compound bonded to the poppet face that seals on a flat seat. The seat member provides a metal-to-metal stop for the poppet with the resilience of the rubber providing the seal. The seal is protected from high vacuum by the parent metal of the poppet to prevent sublimation.

# FLAT POPPET SEAT DESIGN



## KEY PARAMETERS

VALVE TYPE: 3-WAY, PRESSURE ACTUATED  
FLOW MEDIA: HELIUM, NITROGEN, RP-1  
OPERATING PRESSURE: 750 PSIG  
ACTUATION PRESSURE: 750 PSIG  
OPERATING TEMPERATURE: -65 TO 160 F  
LEAKAGE: 1.0 SCIM MAX GN<sub>2</sub>  
CAPACITY: 0.50 INCH ORIFICE  
LIFE: 10,000 CYCLES  
VIBRATION: 25 G TO 2000 CPS  
TUBE SIZE: 3/4 INCH

Figure B-22. Tank Pressurization Valve—Rocketdyne, A Division of North American Aviation, Inc.

## TANK PRESSURIZATION VALVE

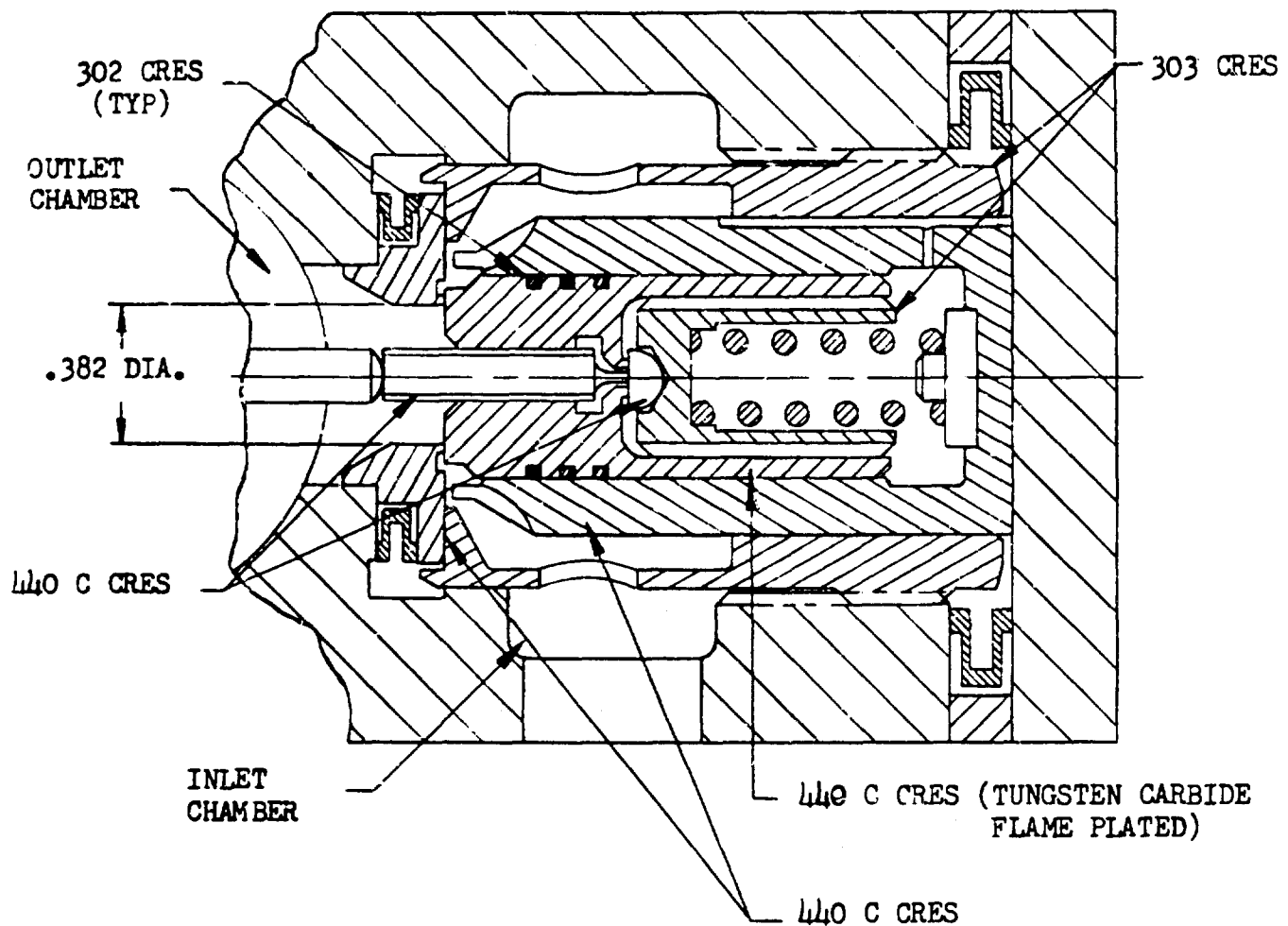
Notable in this three-way, noninterflow valve design is the simplicity of construction. The sandwich seat of plastic, assembled into the valve through the outlet port and clamped by a two-piece poppet, allows a one-piece body of geometric simplicity. The seat and poppet construction is basically a high-load design, capable of withstanding the impacts caused by rapid actuation. Relatively long bolted members considerably reduce impact stress and compensate for differential thermal expansion of materials.

Due to the high capacity and long stroke of this valve, side loads during actuation presented a severe bearing galling problem and necessitated the addition of a dry film lubricant to the bearings and a filtered pneumatic system.

The unbalanced poppet configuration employed in this design allows high seat loads but renders the valve susceptible to dynamic instability if the actuation pressure is obtained from a common inlet line with insufficient capacity.

During the development of the valve it was found that reduction of the seat stress from 4500 to 1200 psi would allow maintenance of the leakage while increasing life cycle reliability.

# FLAT POPPET SEAT DESIGN



## KEY PARAMETERS

VALVE TYPE: PILOTED INLET VALVE  
APPLICATION: MODULATING PRESSURE REGULATOR  
FLOW MEDIA: AIR, NITROGEN, HELIUM  
OPERATING PRESSURE: 230 TO 5000 PSIG  
OPERATING TEMPERATURE: -320 TO 500 F  
LEAKAGE: 25 SCIM MAX HELIUM  
CAPACITY: 0.31 INCH ORIFICE  
LIFE: 10,000 CYCLES  
VIBRATION: 25 G AT 5 TO 2000 CPS

Figure B-23. Regulator Inlet Valve—Rocketdyne, A Division of North American Aviation, Inc.

## REGULATOR INLET VALVE

This design reduces the forces required to operate the main poppet but retains the full unbalance when seated to maintain high seat stress and minimum leakage. The illustration details construction of both the main poppet and the pilot fully seated. A force applied to the pilot push rod acts to open the pilot seat. The open pilot allows the pressure in the pilot chamber (initially equal to supply pressure) to decay sufficiently to permit the pressure forces to open the main poppet. In the modulating regulator application, regulator actuator forces operate the pilot to position the main poppet in accordance with the flow demand imposed upon the regulator. The unbalanced forces consist of only the pilot chamber pressure acting over the pilot seat and the pilot spring force.

This design was used successfully in a modulating regulator designed and developed as part of a 2-year state-of-the-art improvement program\* for the Air Force Ballistic Missile Division. The digital computer simulation of the regulator actuator and inlet valve predicted constant limit cycling of the inlet valve, but no observable cycling of regulated pressure. In practice, however, the effect of the oscillating inlet valve was destructive instability. This necessitated the incorporation of coulomb friction damping between the main poppet and sleeve to stabilize the system.

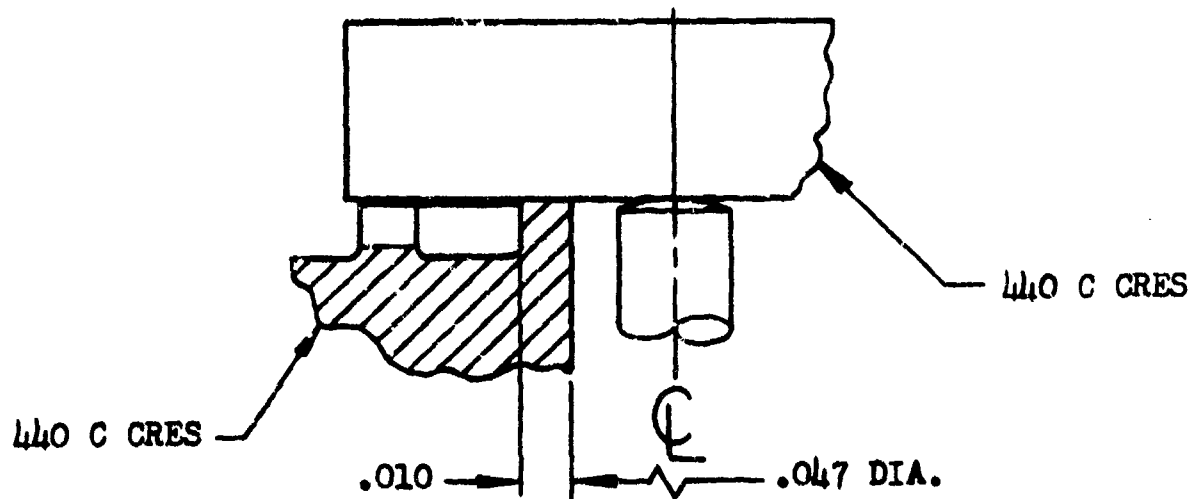
Leakage across the flat-lapped seats under minimum pressure conditions (230-psig in and 30-psig out) was maintained below the specified value at seat stresses as low as 2650 psi on the main seat and 475 psi on the pilot seat. At maximum supply pressure, maximum main seat stress was 66,000 psi. Seat flatness was better than 1/2 a helium light band.

---

\*AFBMD-TR-60-74, Design, Development, and Testing of Advanced Helium Pressure Regulator, North American Aviation, Inc July 1960



### FLAT POPPET SEAT DESIGN



### KEY PARAMETERS

VALVE TYPE: 3-WAY DIRECT OPERATED  
SOLENOID VALVE, 28 VDC  
FLOW MEDIA: AIR, NITROGEN, HELIUM  
OPERATING PRESSURE: 750 PSIG  
OPERATING TEMPERATURE: -320 TO  
+160 F  
LEAKAGE: 5 SCIM MAX HELIUM  
AT -320 F  
CAPACITY: .030 INCH ORIFICE  
RESPONSE: 10 MILLISECONDS  
LIFE: 10,000 CYCLES  
VIBRATION: 25 G TO 2000 CPS

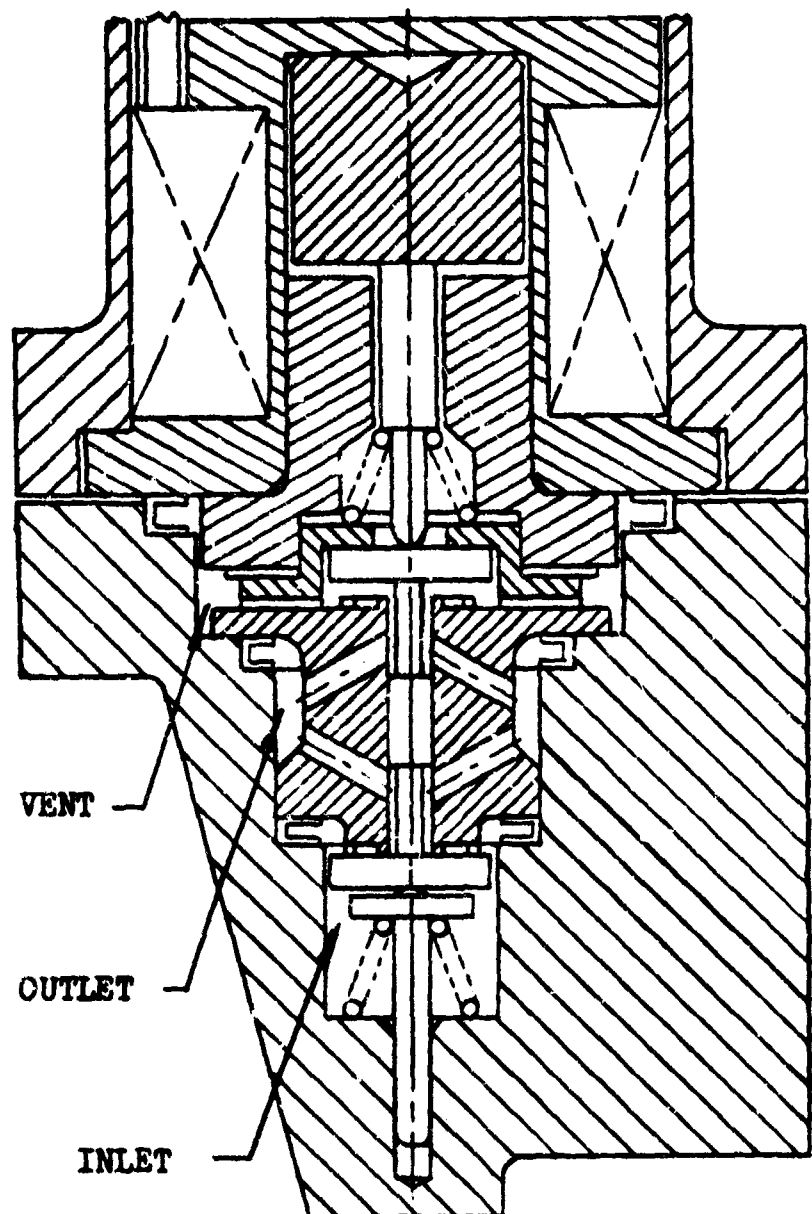


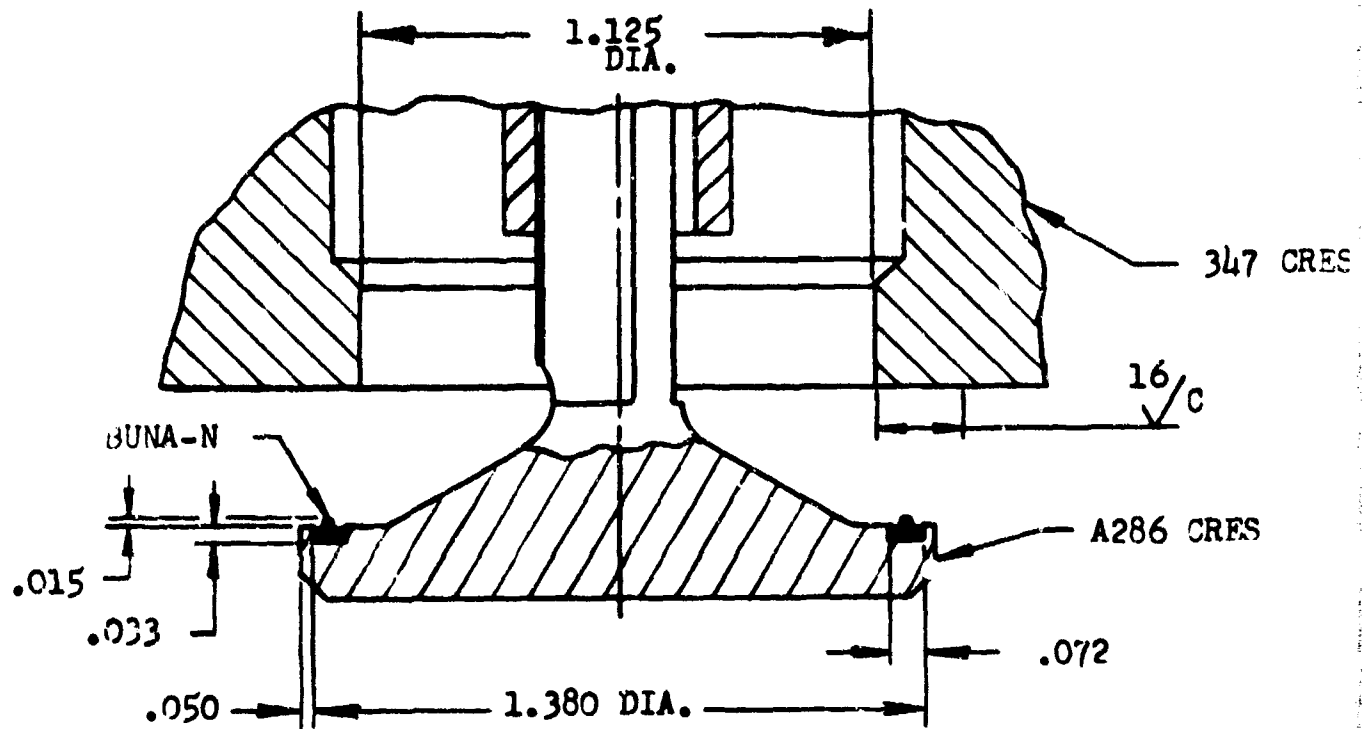
Figure B-24. Pilot Control Solenoid Valve—  
Weston Hydraulics, Ltd.

## PILOT CONTROL SOLENOID VALVE

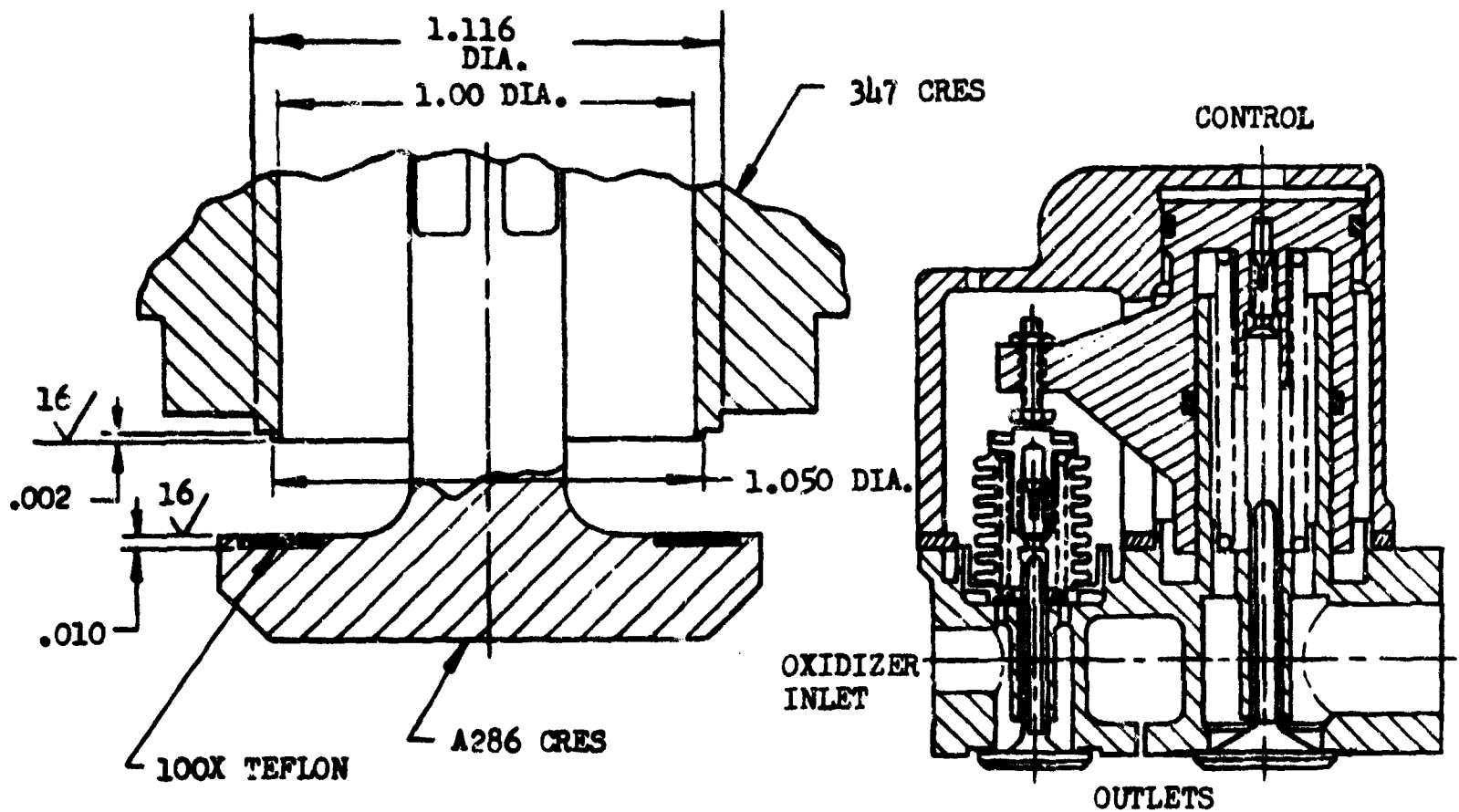
Metal-to-metal flat poppets and seats are used in this design to obtain low leakage over a wide range of temperatures. The combination of size and operating pressure economically allows an unbalance design which eliminates the need for dynamic seals and external bleed.

The poppet discs and seats are lapped extremely flat (less than 1 light band) to obtain bubble-tight leakage of helium at room temperature. The proved cycle life is due to the extreme hardness of the seat materials in addition to the outer seat land used to facilitate lapping and ensure uniform application of seating load (or stress).

### FLAT POPPET SEAT DESIGN



### FUEL VALVE



### OXIDIZER VALVE

Figure B-25. Gas Generator Control Valves—Rocketdyne, A Division of North American Aviation, Inc.

## GAS GENERATOR CONTROL VALVES

### KEY PARAMETERS

VALVE TYPE:	2-WAY, PRESSURE ACTUATED, DUAL POPPET VALVE	
FLOW MEDIA:	LIQUID NITROGEN, OXYGEN, RP-1 FUEL	
OPERATING PRESSURE:	800 psig	
ACTUATING PRESSURE:	300 psig	
OPERATING TEMPERATURE:	OXIDIZER VALVE:	-320 to +160 F
	FUEL VALVE:	-40 to +160 F
LEAKAGE:	OXIDIZER PORT:	5-scim MAXIMUM GASEOUS NITROGEN AT -320 F
	FUEL PORT:	1.0-scim MAXIMUM GASEOUS NITROGEN AT 70 F
CAPACITY:	OXIDIZER PORT:	0.61-INCH ORIFICE
	FUEL PORT:	0.94-INCH ORIFICE
LIFE:	2500 CYCLES	
VIBRATION:	20 g to 2000 cps	

This dual poppet configuration controls the flow of fuel and cryogenic fluid to a missile gas generator. The design approach has proved both advantageous and reliable in meeting stringent leakage requirements while positively ensuring a controlled opening of both valves.

100X Teflon molded seal is bonded to the oxidizer poppet face under heat and pressure. Critical temperature, pressure and cleanliness controls are mandatory if adequate adhesion is to be obtained. A final machining after bonding provides the finished seat surface. The step configuration precludes the necessity of maintaining close normality and flatness, and provides the high loading required for cryogenic sealing with Teflon.

A major design consideration is the stressing of the Teflon seal. The seat stress must not exceed 5000 psi or extrusion will occur. Under ideal conditions, stresses below 150 psi have provided bubble-tight sealing at 800 psig and cryogenic temperatures.

Disadvantages of the design are the rigorous manufacturing and functional test controls required to preclude separation of the Teflon seal from the poppet face.

The fuel poppet employs a Buna-N rubber seal that is chemically bonded into a machined undercut in the poppet face. The special cross-section profile of the rubber seal has a protrusion in the center and voids on both sides. When the poppet is seated, the protrusion is compressed to fill the void until the steel face of the poppet bottoms on the body seat. The major problems associated with the design are temperature limitations inherent with the use of rubber seals and the specialized manufacturing processes required.

# FLAT POPPET SEAT DESIGN

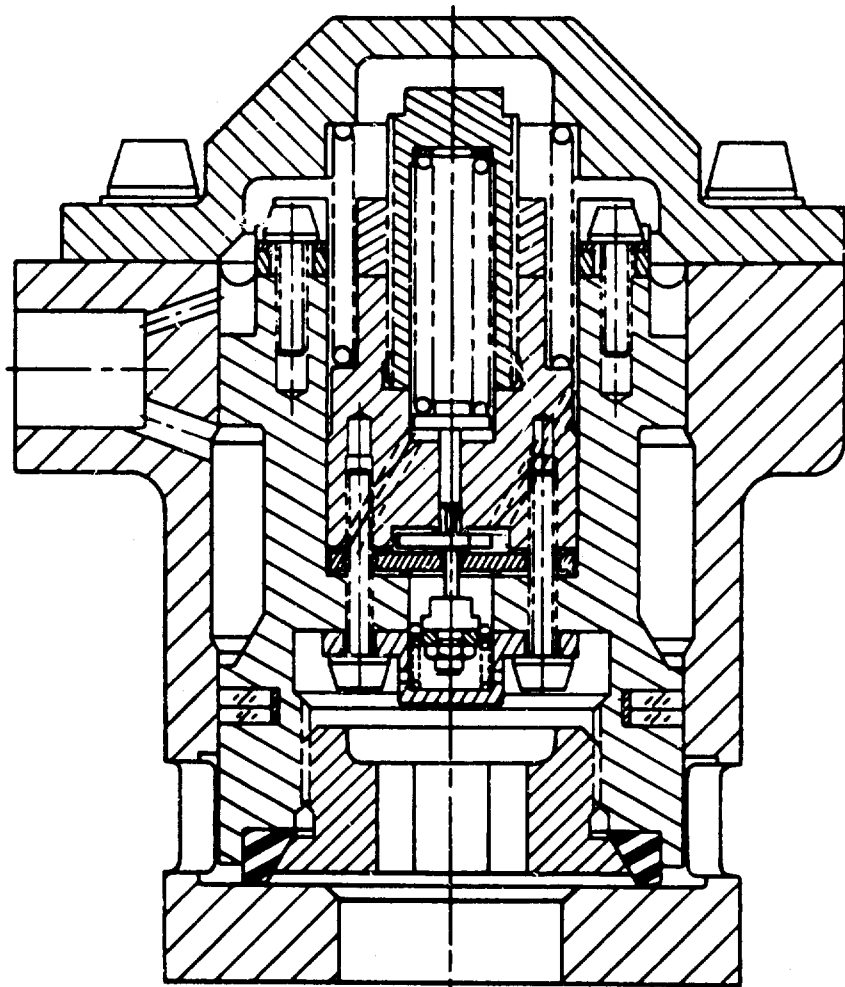
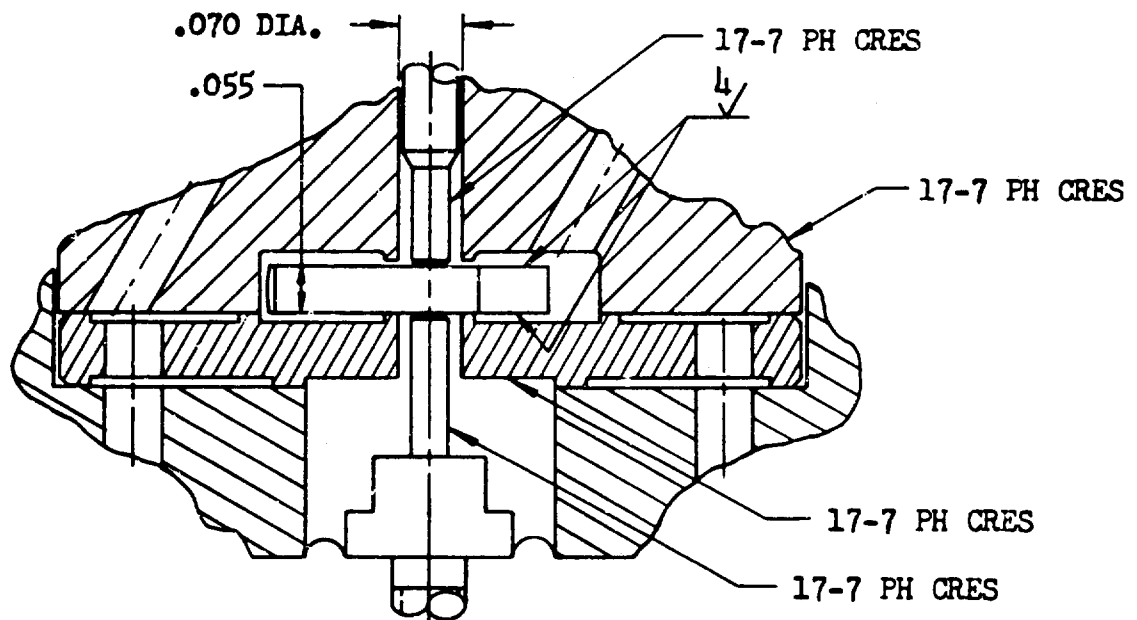


Figure B-26. Low Temperature Relief Valve—Rocketdyne, A Division of North American Aviation, Inc.

## LOW-TEMPERATURE RELIEF VALVE

### KEY PARAMETERS

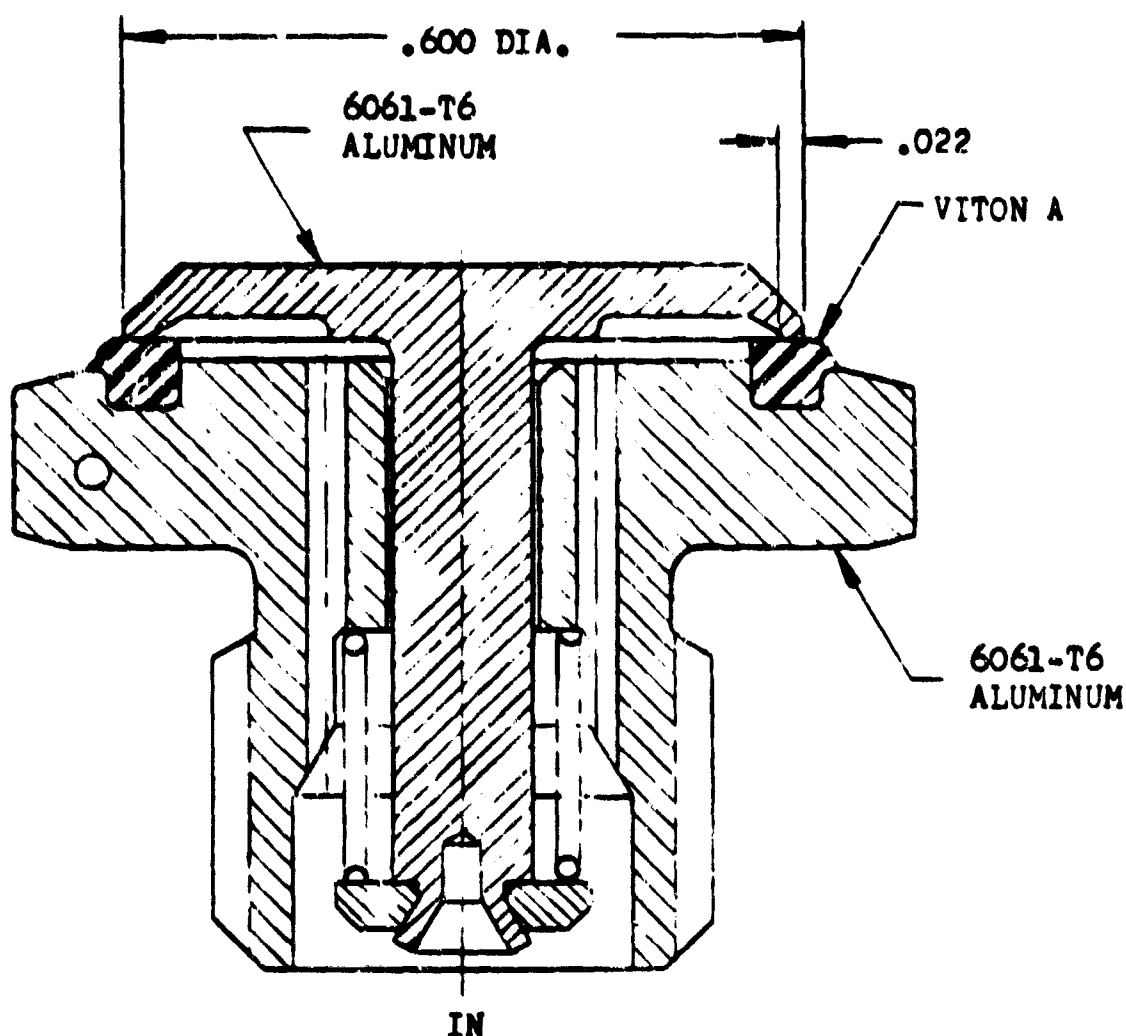
VALVE TYPE:	PILOT-OPERATED RELIEF VALVE
FLOW MEDIA:	AIR, NITROGEN OR HELIUM
CRACKING PRESSURE:	300 to 540 psig
OPERATING TEMPERATURE:	-250 to +140 F
LEAKAGE:	10-ccm HELIUM AT 10% BELOW CRACKING PRESSURE
CAPACITY:	0.023-INCH ORIFICE-PILOT VALVE; 0.5-INCH ORIFICE-MAIN VALVE
VIBRATION:	25 g AT 5 TO 2000 cps

This three-way pilot valve design is entirely contained within the main poppet of the pilot-operated pressure relief valve shown. A flat lapped metal-to-metal poppet and seat construction provides low leakage and accurate control from room to cryogenic temperatures. Because of the high loads available, a soft nylon seal is used on the larger main valve, with resultant low leakage and relative ease of manufacture.

The major problem experienced with the design has been the inclination of the poppet to "rock" off the seat upon actuation, resulting in poor reseal characteristics. Factors contributing to this problem are:

1. Inadequate guiding of the actuation pins.
2. Failure to provide a full radius on the contact end of the actuation pin.
3. Failure to adequately center the actuation pins on the poppet.

### FLAT POPPET SEAT DESIGN



### KEY PARAMETERS

VALVE TYPE: CHECK VALVE  
FLOW MEDIA: AIR, NITROGEN, HELIUM, OXYGEN  
OR RP-1 FUEL VAPORS  
OPERATING PRESSURE: 0 TO 1000 PSIG  
CRACKING PRESSURE: 3 TO 5 PSIG  
FULL OPEN PRESSURE: 10 PSIG  
OPERATING TEMPERATURE: -320 TO +160 F  
LEAKAGE: MEASURED IN FREE FLOW DIRECTION  
AT 0.5 PSIG  
-320 F: 10 SCIM MAX HELIUM  
-65 TO +160 F: ZERO BUBBLE LEAKAGE  
FOR 3 MINUTES  
CAPACITY: .06 INCH ORIFICE  
LIFE: 10,000 CYCLES  
VIBRATION: 25 G TO 2000 CPS  
TUBE SIZE: 1/4 INCH

Figure B-27. Vent Port Check Valve—Rocketdyne, A Division of North American Aviation, Inc.



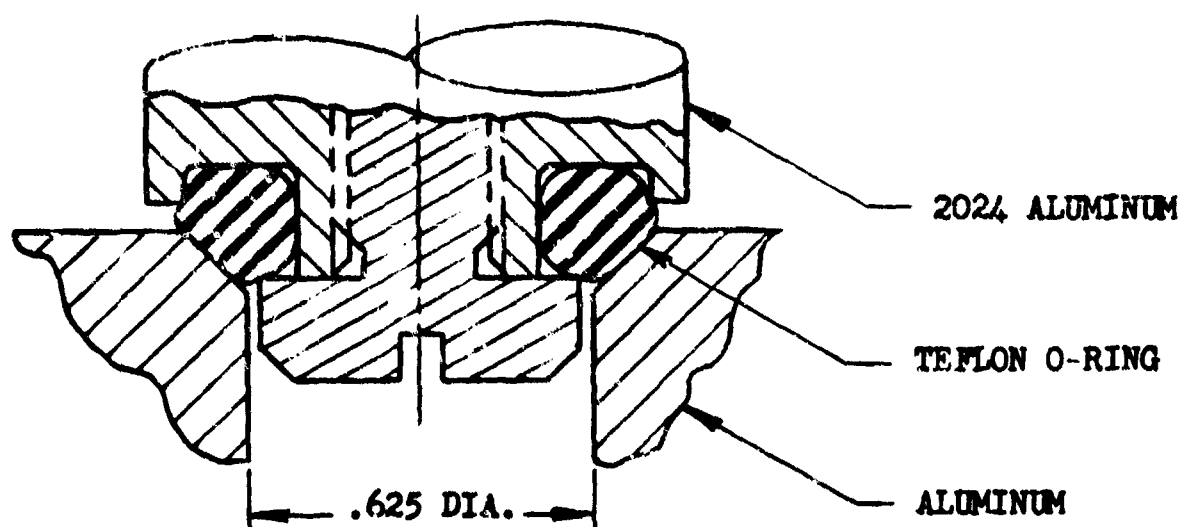
## VENT PORT CHECK VALVE

This component represents a series of valves designed to protect the internal portion of components (which require a vent to atmosphere) against the entrance of moisture or contaminants. The large external seat configuration ensures the maintenance of a low cracking pressure in the event of ice formation over the valve. The flat-lapped molded Viton A rubber seat construction results in an excellent seal throughout a wide range of temperatures and conditions.

After considerable service experience it was found that following several days storage the Viton rubber would cling to the poppet causing a substantial increase in cracking pressure. This problem was solved by the application of a nonremovable dry film lubricant to the rubber.

## **SPECIAL POPPET SEAT DESIGNS**

### G-RING DESIGN



### KEY PARAMETERS

VALVE TYPE: PRESSURE ACTUATED  
SHUT-OFF VALVE  
FLOW MEDIA: RP-1 OR MIL-O-5606  
OPERATING PRESSURE: 0 TO 1500 PSIG  
ACTUATING PRESSURE: 750 PSIG  
OPERATING TEMPERATURE: -65 TO +165 F  
LEAKAGE: 1 SCIM MAX GN<sub>2</sub>  
CAPACITY: 0.52 INCH ORIFICE  
LIFE: 2500 CYCLES AT 1000 PSIG  
VIBRATION: 25 G TO 2000 CPS  
TUBE SIZE: 3/4 INCH

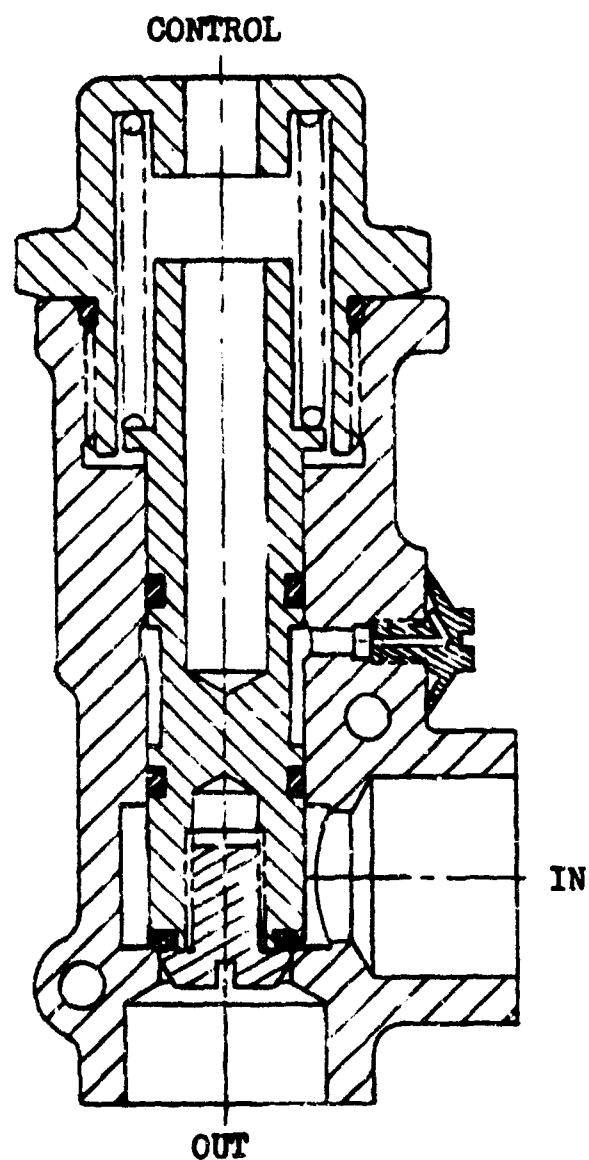


Figure B-28. Fuel Igniter Shutoff Valve—Rocketdyne, A Division of North American Aviation, Inc.

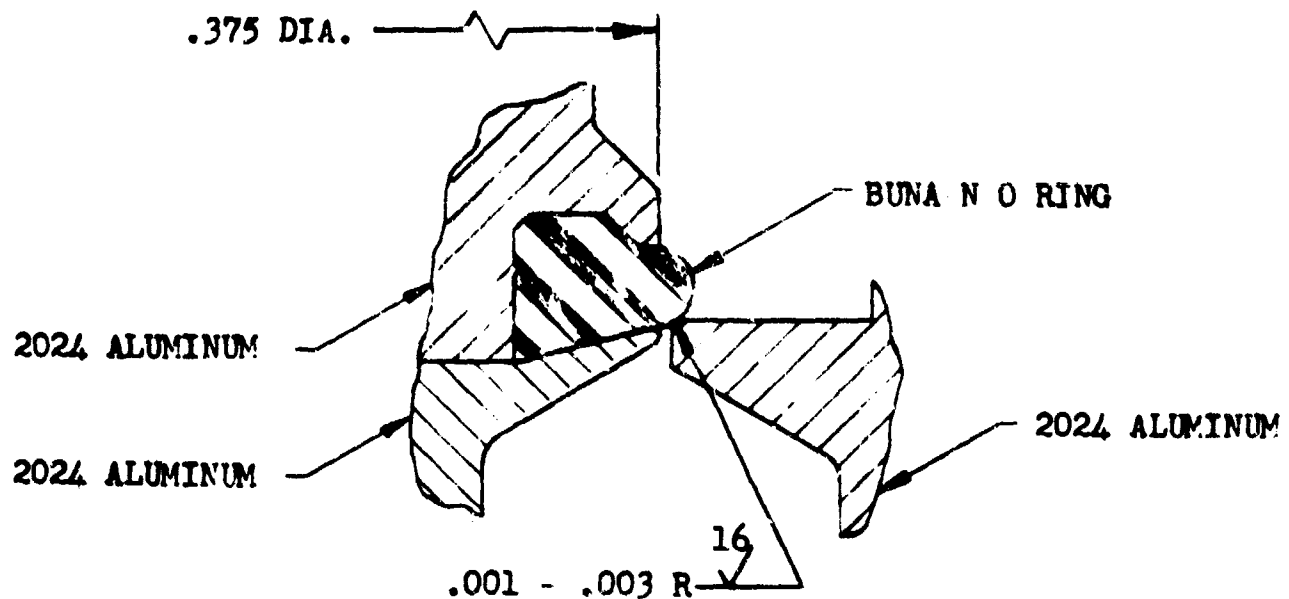
## FUEL IGNITER SHUTOFF VALVE

This design represents one of many ways to achieve a plastic-to-metal poppet and seat. The use of plastic results in low leakage with relatively little effort in manufacturing as compared with metal-to-metal designs. The Teflon allows a wide range of compatibility.

Since the critical sealing element utilized in this design is plastic, careful attention must be given to loads and deflections, with due consideration to high-temperature effects. Leakage performance improves as unit loading on the seat increases; therefore, for best leakage performance, a unit stress equal to the yield stress is used. There has been no attempt to control the maximum seat load dimensionally. The material is allowed to deflect until the acceptable unit load is achieved or metal-to-metal contact occurs.

The major problems with the design are those associated with the plastic seal, i.e. (1) material compatibility with extreme temperatures, (2) feasibility of retention of the plastic for small size valves, and (3) inaccurate prediction of the effective seat area due to wide seat land.

### EXTRUDED O-RING SEAT DESIGN



### KEY PARAMETERS

VALVE TYPE: 28 VDC, 2 WAY, DIRECT  
OPERATED SOLENOID VALVE  
FLOW MEDIA: AIR, NITROGEN, HELIUM  
OPERATING TEMPERATURE: 65 TO 160 F  
OPERATING PRESSURE: 1000 PSIG  
LEAKAGE: 1.0 SCIM MAX GN<sub>2</sub>  
CAPACITY: 0.25 INCH ORIFICE  
RESPONSE: 0.03 SECONDS  
LIFE: 10,000 CYCLES  
VIBRATION: 25 G TO 2000 CPS  
TUBE SIZE: 3/8 INCH

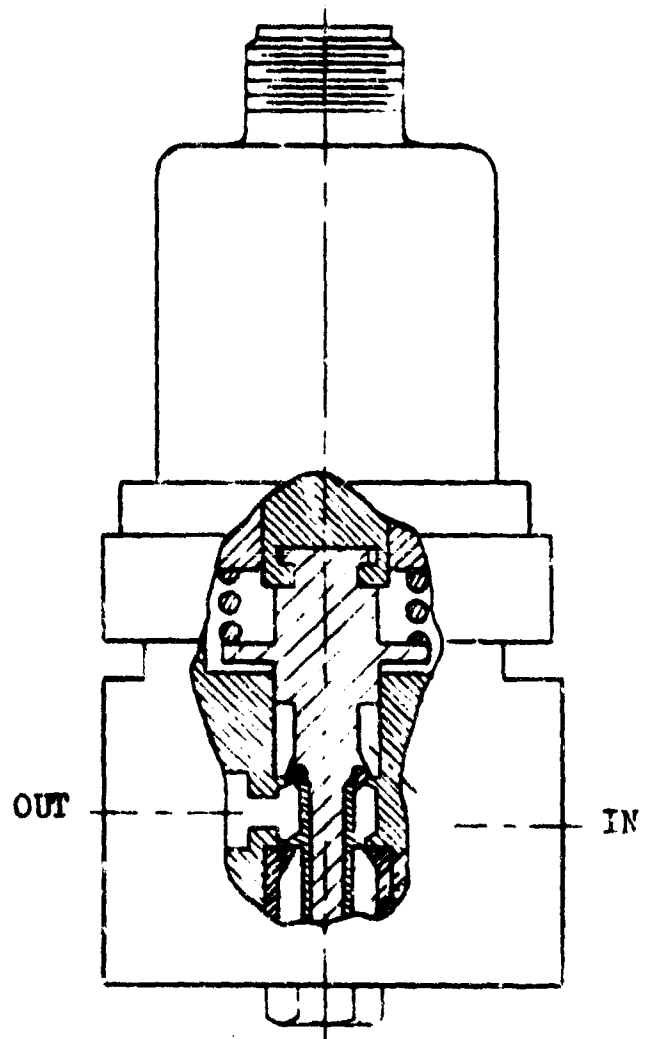


Figure B-29. Two-Way Solenoid Valve—Rocketdyne, A Division of North American Aviation, Inc. (Futurecraft Patent No. 2,971,090 Licensed to NAA)

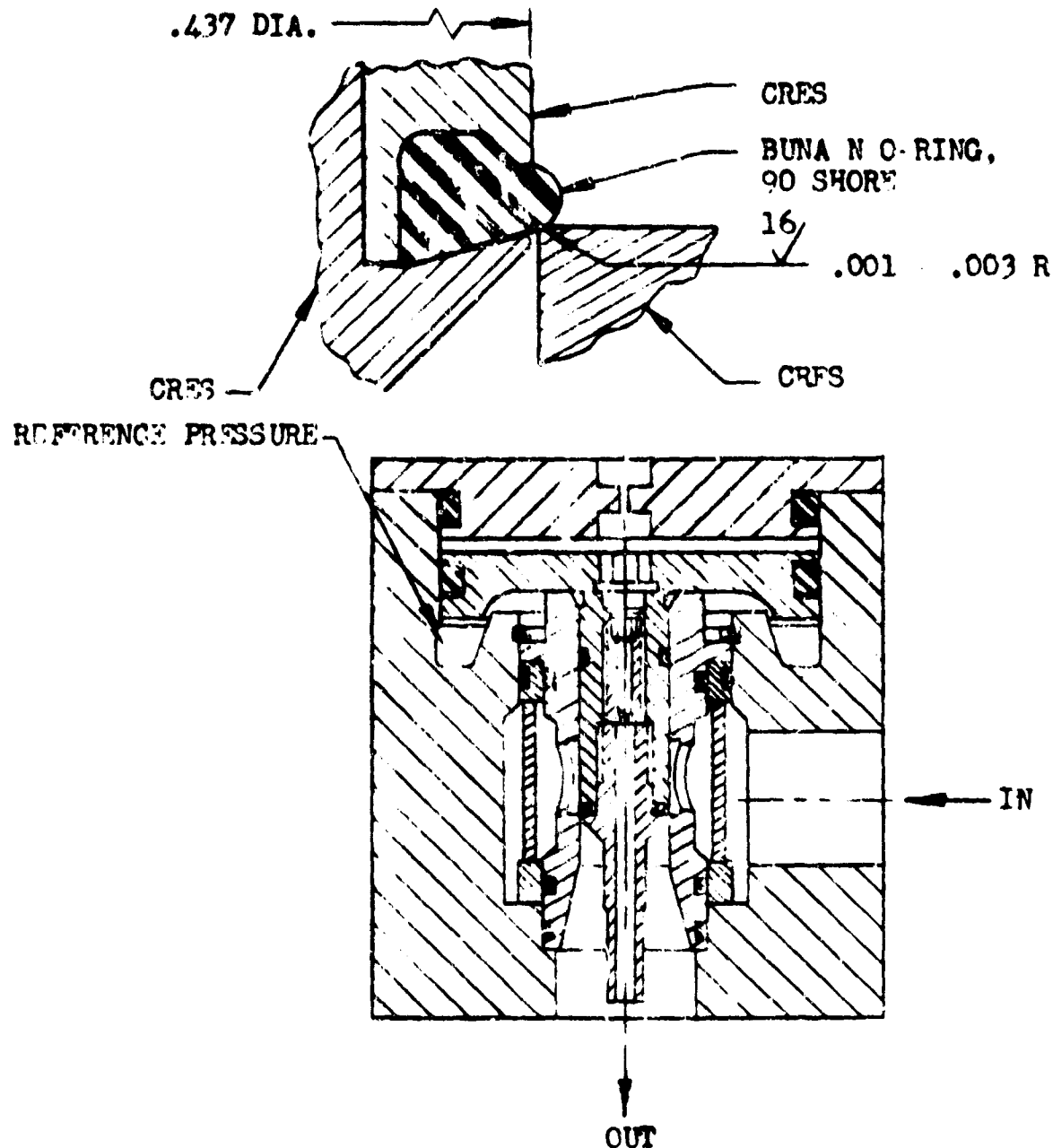
## TWO-WAY SOLENOID VALVE

This valve incorporates a seat design proved by long use to be extremely reliable. The flexible rubber seal is utilized to obtain low leakage and to pressure balance the poppet by double seating, thus eliminating dynamic seals. By surrounding the poppet with inlet pressure, all external bleed holes are eliminated. Although the valve shown is a two-way solenoid valve and rated for 1000 psig, the seat design has been used for three-way or four-way, normally open or normally closed applications up to 3000 psig.

Leakage, which is normally near zero, is easily increased by imperfections in the rubber finish, which may or may not be manifested in the functional test. In addition, the rubber seat has a limited temperature range and fluid media application, and renders prediction of the amount of imbalance across the seats a difficult task.

Versatility of the valve is limited by inability to withstand reverse flow. High pressure drop in the reverse direction can cause blowout of the seals. Not usually recognized is the fact that the sudden shutdown or venting of a system often causes reverse flow and valves of this type can be damaged.

EXTRUDED O-RING SEAT DESIGN



KEY PARAMETERS

VALVE TYPE: PRESSURE REGULATOR  
FLOW MEDIA: AIR, HELIUM, NITROGEN  
INLET PRESSURE: 50 PSIG ABOVE REGULATED  
PRESSURE TO 3000 PSIG  
REGULATED PRESSURE: 100 TO 800 PSIG  
ADJUSTABLE  
OPERATING TEMPERATURE: -65 TO +160 F  
LEAKAGE: 1 SCIN MAX HELIUM  
CAPACITY: 0.29 INCH ORIFICE  
LIFE: 10,000 CYCLES  
VIBRATION: 25 G TO 2000 CPS

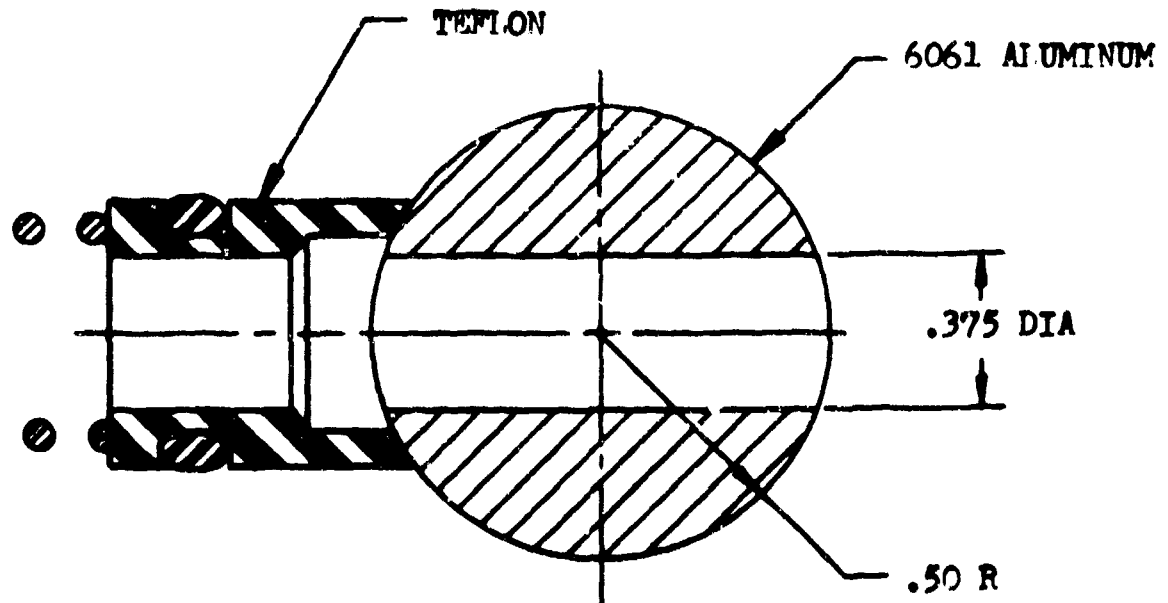
Figure B-30. Balanced Pressure Regulator—Rocketdyne, A Division of North American Aviation, Inc. (Futurecraft Patent No. 2,971,090 Licensed to North American Aviation, Inc.)

## BALANCED PRESSURE REGULATOR

This compact pneumatic pressure regulator utilizes a balanced poppet to maintain a constant regulated pressure without regard to variations in supply pressure or rapidly fluctuating flow demands. The design is a typical application of flexible rubber on the poppet sealing against a metal seat. The advantage of the design lies in the tight shutoff with near balanced seating that can be achieved with the soft poppet. The flexibility of the poppet seal permits some tolerance stackup and imperfections in the seat surface. The application of the design is limited by: (1) the temperature limitations of the seal material, (2) pressure seeping behind the O-ring will blow out the seal upon sudden venting, and (3) inadvertent reverse flow will also blow out the seal.



## ROTATING CYLINDER DESIGN



### KEY PARAMETERS

VALVE TYPE: CYLINDRICAL VALVE  
FLOW MEDIA: AIR, NITROGEN, HELIUM  
OPERATING PRESSURE: 0 TO 600 PSIG  
OPERATING TEMPERATURE: -65 TO +165 F  
LEAKAGE: 15 SCCM MAX ON<sub>2</sub>  
SIZE: 0.375 INCH HOLE  
LIFE: 1000 CYCLES AT AMBIENT TEMPERATURE

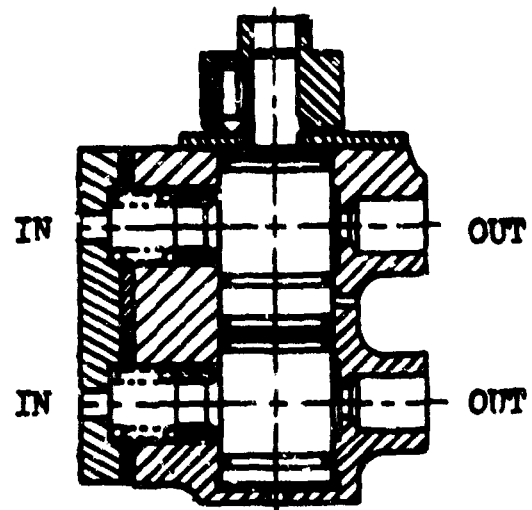


Figure B-31. Cylindrical Valve—Rocketdyne, A Division of North American Aviation, Inc.

## CYLINDRICAL VALVE

This cylindrical design is easier to fabricate than a comparable ball valve, yet provides the same pressure drop and overtravel characteristics. The design is limited to those applications where accurate definition of the effective seat area is not critical and a nonmetallic seal is acceptable.

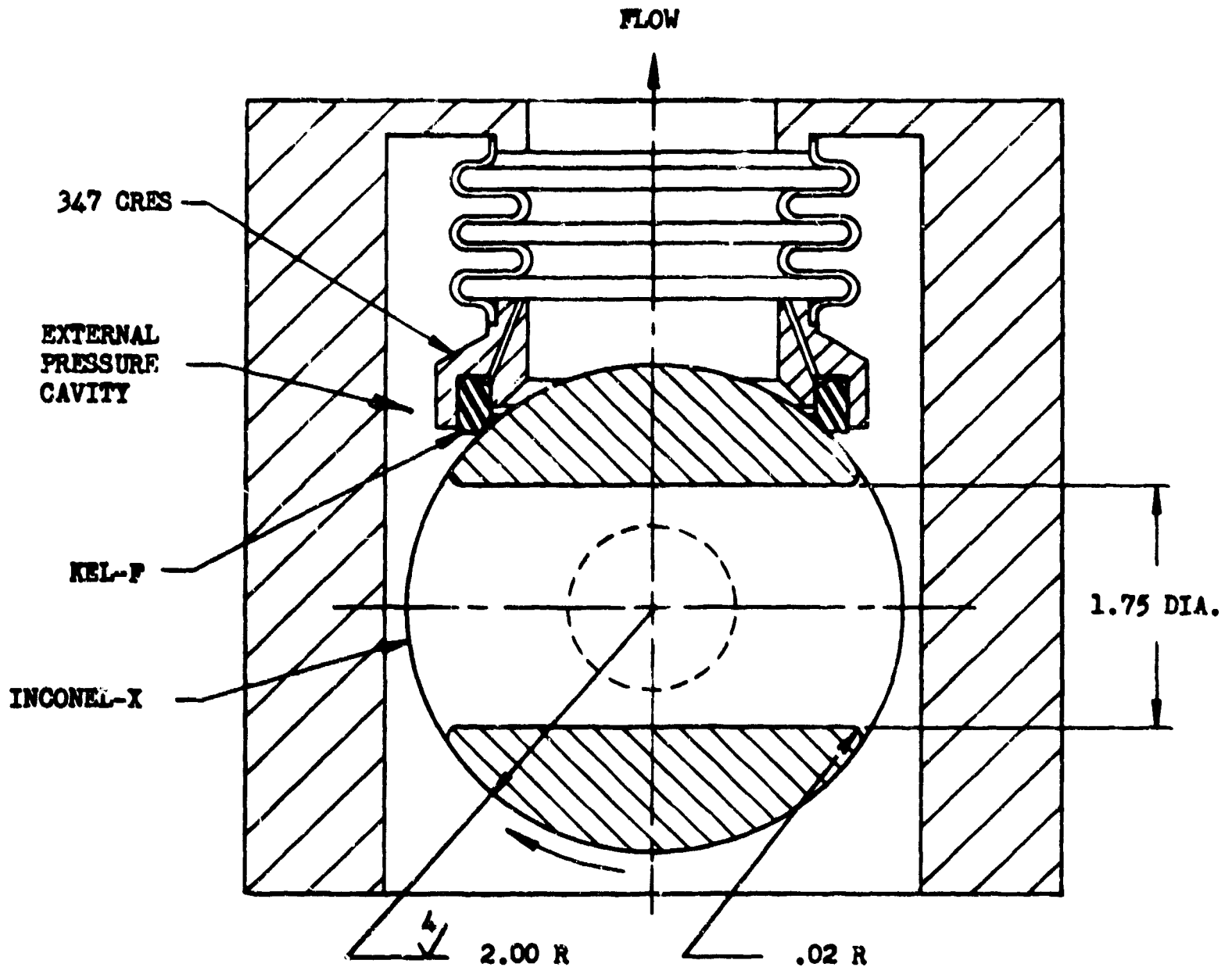
The design involves no fabrication problems, although reasonable care must be exercised to ensure the required finishes and dimensional controls. The seat surface is easily generated by conventional cylindrical grinding methods.

The nonuniform type of seat loading and the variable width and difference in radius between the seal and the cylinder make the unit load limits and the effective area difficult to define. The seal distortion, resulting from fluid pressure loading, is a complex function of seal material properties and geometry, specifically the wrap-around angle.

The wiping action of the seal limits the choice of material to those with minimum galling tendency. Previous experience has shown nonmetallic seals (usually carbon or plastic) to have nongalling characteristics superior to metals, although some combinations of metals may be used with minimum risk.

## ROTATING BALL DESIGNS

## ROTATING BALL DESIGN



### KEY PARAMETERS

VALVE TYPE: BALL VALVE  
FLOW MEDIA: LIQUID OXYGEN  
TEST MEDIA: LIQUID NITROGEN  
OPERATING PRESSURE: 1800 PSIG  
OPERATING TEMPERATURE: -320 TO 160 F  
LEAKAGE: 20 SCIM MAX GN<sub>2</sub>  
SIZE: 1.75 INCH HOLE  
LIFE: 1000 CYCLES  
VIBRATION: 25 G TO 2000 CPS

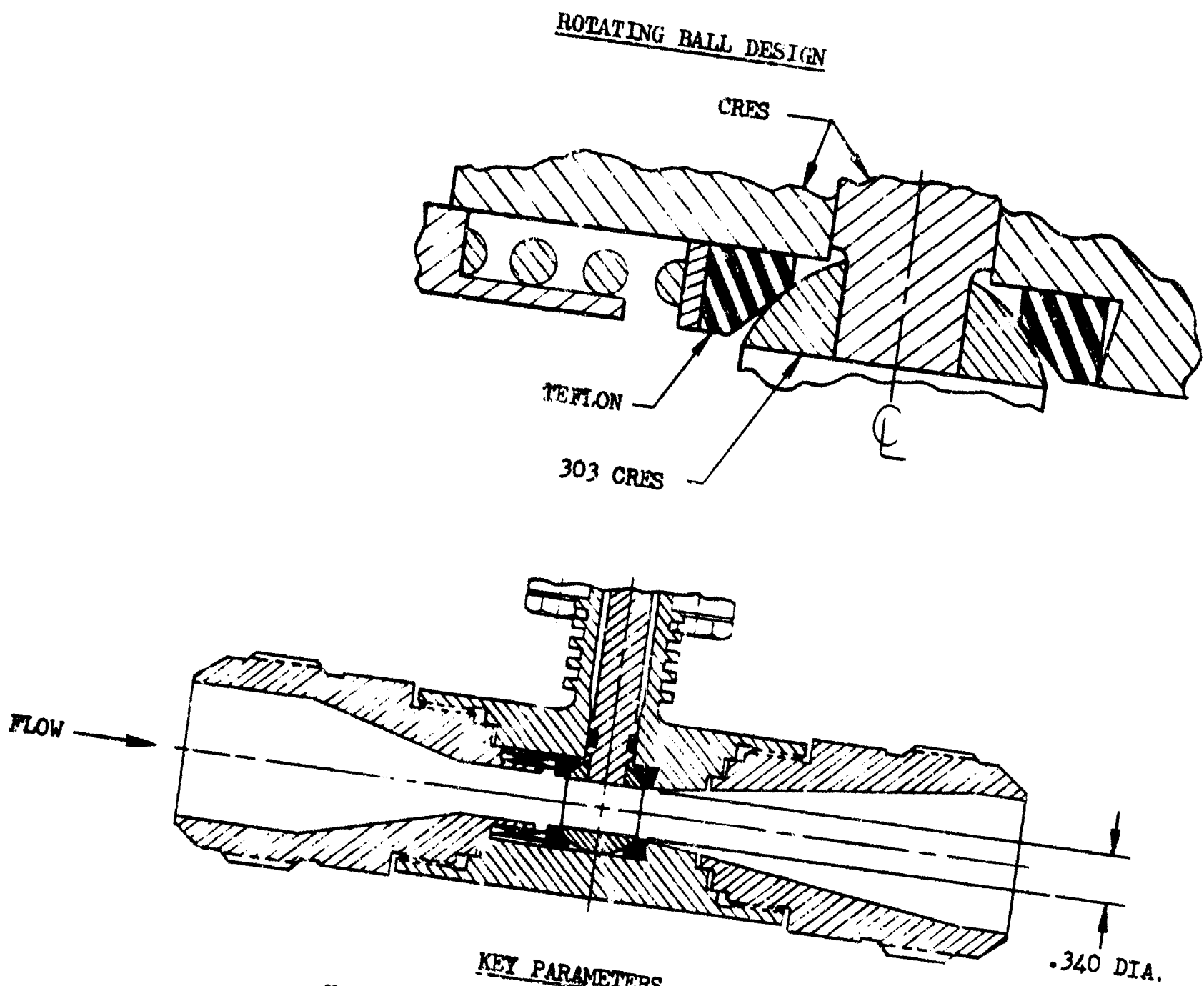
Figure B-32. Propellant Ball Valve—Rocketdyne, A Division of North American Aviation, Inc.

## PROPELLANT BALL VALVE

This valve features the low pressure drop and overtravel characteristics for which ball valves are noted. Requirements arise where pressure drops of less than 5 psi are required in a high-velocity line, or an overtravel requirement exists, such as the simultaneous operation of two valves. An exceedingly large, or streamlined poppet-type valve would be necessary to meet the equivalent pressure drop requirement.

The seal in this configuration is a machined Kel-F ring inserted into a machined groove, with an initial line contact with the ball. The pressure and spring force against the seal cause the plastic to yield, increasing the contact area until the stress balances out at the yield stress or less. The illustrated valve utilizes a balanced bellows. The ball seal contact diameter is only slightly larger than the effective pressure diameter of the bellows to ensure positive contact between the seal and ball. The bellows spring force aids in sealing at low pressure. The seal line of the plastic at the bottom of the retainer groove is designed to seek its yield stress area in the same manner as the ball seal. The effective diameter of this seal line should be equal to or greater than the seal-to-ball line to prevent external pressure from tending to separate the bellows from the ball.

Good manufacturing practices are necessary to meet the noted leakage. A 4-microinch finish and 0.0005 sphericity is maintained on the ball to match a 16-microinch surface on the contact face of the seal. The seal and retainer are held concentric within 0.005 TIR, with a 16-microinch finish on the seal and bottom surface of the groove.



KEY PARAMETERS

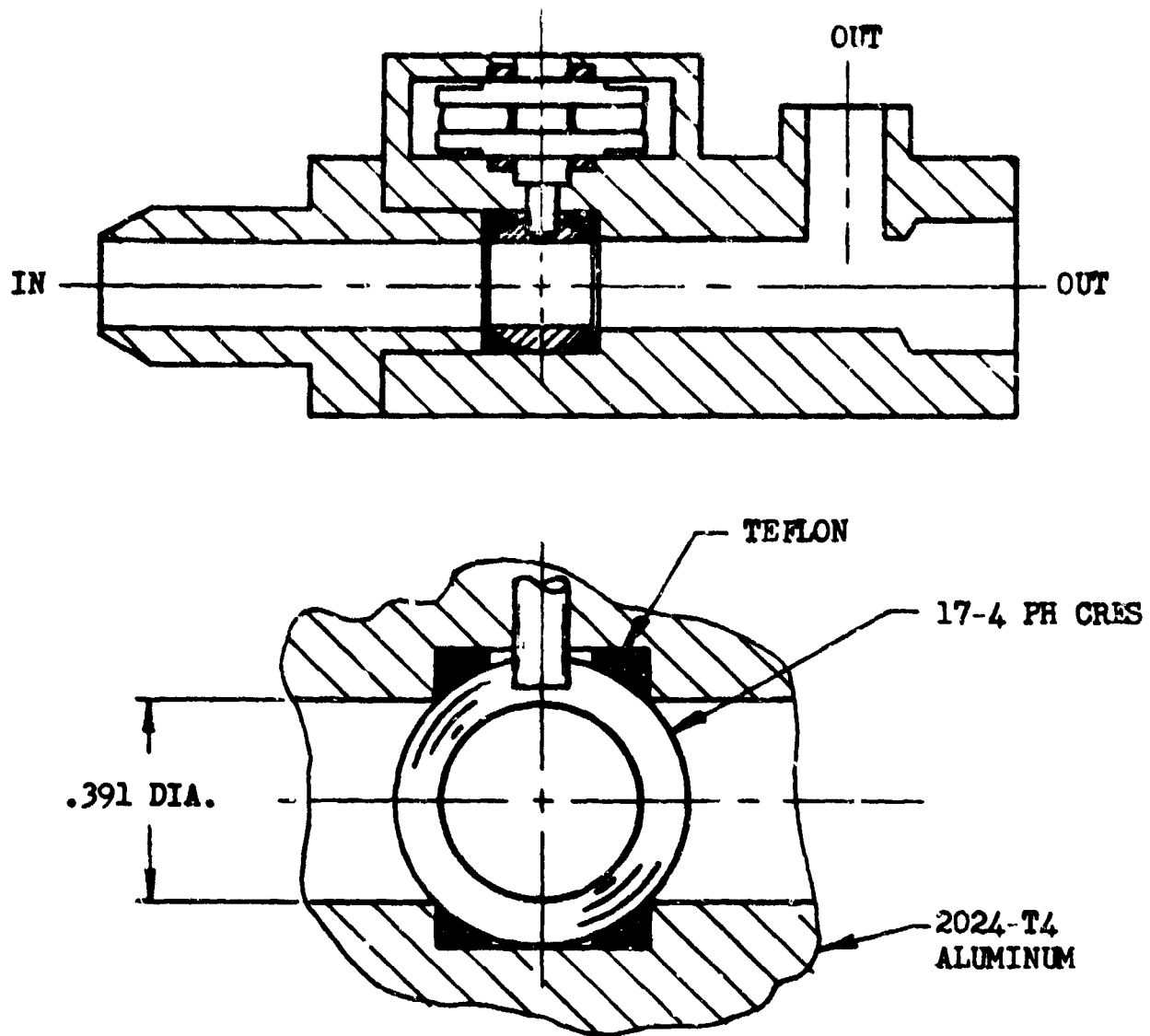
VALVE TYPE: BALL VALVE  
 FLOW MEDIA: LIQUID HYDROGEN OR  
 LIQUID OXYGEN  
 TEST MEDIA: LIQUID NITROGEN  
 OPERATING PRESSURE: 50 PSIG  
 OPERATING TEMPERATURE: -423 TO 160 F  
 LEAKAGE: 1.1 SCIM MAX GN<sub>2</sub>  
 SIZE: 0.340 INCH HOLE  
 LIFE: 100 CYCLES  
 VIBRATION: 20 G TO 2000 CPS  
 TUBE SIZE: 1 INCH

Figure B-33. Cryogenic Ball Valve—Clary Dynamics Corporation

## CRYOGENIC BALL VALVE

This ball valve is designed for low pressure cryogenic service in a spacecraft propulsion system. The outstanding features of the design are the spring-loaded ball seals and the use of a small ball in a larger line to meet the flow requirements. The spring-loaded seals minimize the problems of seal fitting during assembly and allow for substantial tolerance buildup of mating parts and wear. The inherent low pressure drop characteristic of a ball valve coupled with the venturi sections in the flow passage allows use of the smaller ball to decrease the sealing area and reduce the weight of the valve and actuator. However, the venturi sections tend to increase the installation length.

### ROTATING BALL DESIGN



### KEY PARAMETERS

VALVE TYPE: BALL VALVE  
FLOW MEDIA: IRFNA OR UDMH  
TEST MEDIA: HELIUM  
OPERATING PRESSURE: 70 PSIG  
OPERATING TEMPERATURE: -65 F TO +160 F  
LEAKAGE: 10 SCC/HR MAX HELIUM  
SIZE: .391 INCH HOLE  
LIFE: 50 CYCLES

Figure B-34. Propellant Control Ball Valve--  
Clary Dynamics Corporation



## PROPELLANT CONTROL BALL VALVE

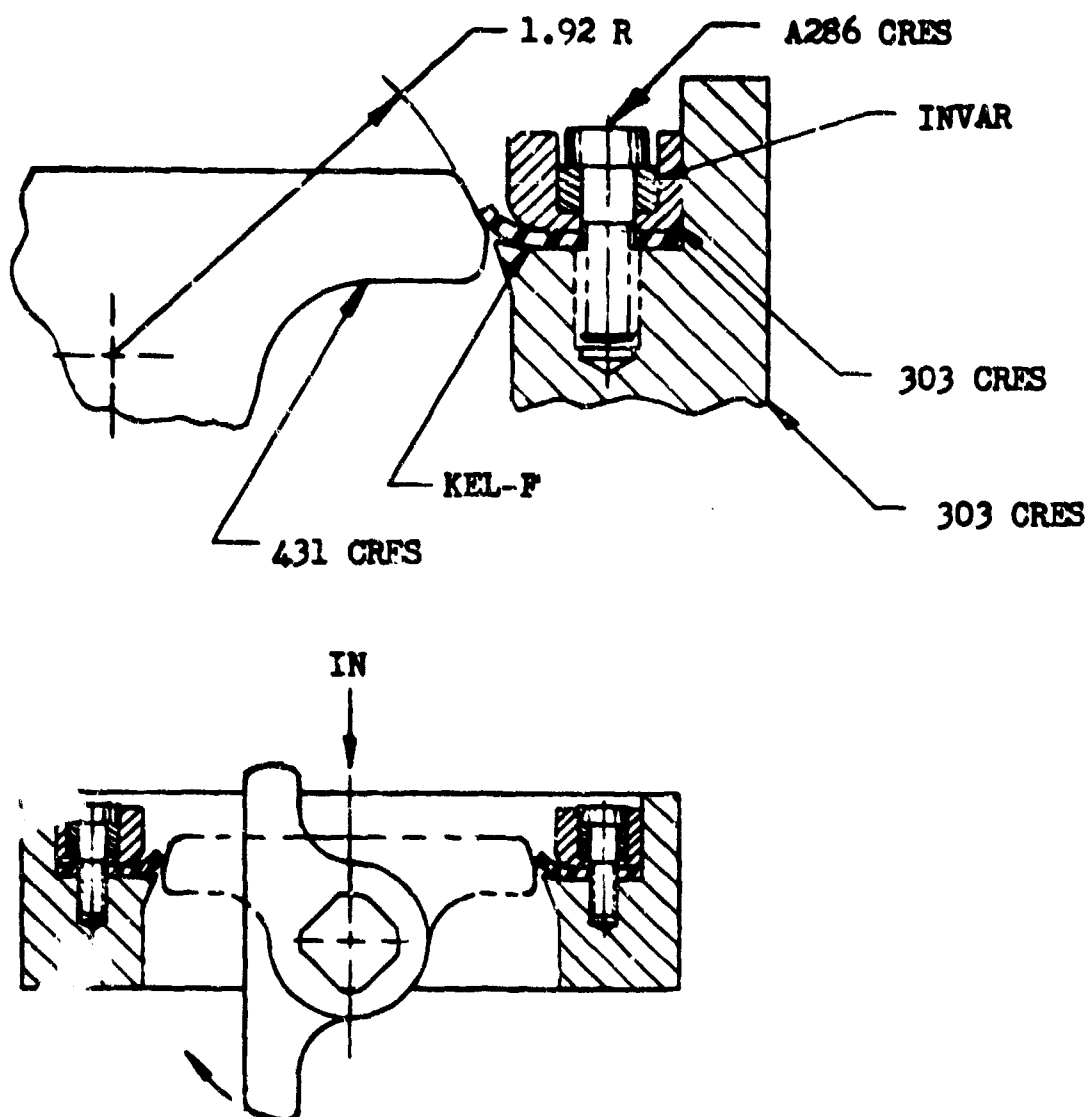
This ball valve was originally designed for helium service, and has subsequently been used with storable hypergolic propellants in a satellite rocket engine system. The ball is retained between Teflon seals, without provision for spring preloading. The seal loading is accomplished by bringing the inlet fitting into direct contact with the seal, after individually fitting the seals to the valve.

The simplicity of the design concept is the basis for several disadvantages that must be considered:

1. The design is not suitable for long life or field repair.
2. Individual seal fitting is critical and tedious.
3. The design is particularly susceptible to finish imperfections on the rotating ball.

**BUTTERFLY DESIGNS**

### BUTTERFLY DESIGN



### KEY PARAMETERS

VALVE TYPE: BUTTERFLY VALVE  
FLOW MEDIA: LIQUID OXYGEN  
OPERATING PRESSURE: 1000 PSIG  
OPERATING TEMPERATURE: -423 TO 160 F  
LEAKAGE: 5 SCIM GASEOUS NITROGEN AMBIENT;  
300 SCIM CRYOGENIC  
SIZE: 3 INCH LINE  
LIFE: 2000 CYCLES  
VIBRATION: 25 G TO 2000 CPS

Figure B-35. Propellant Butterfly Valve—Rocketdyne, A Division of North American Aviation, Inc. (U.S. Patent No. 2,893,582)

## PROPELLANT BUTTERFLY VALVE

This design is a high-pressure butterfly valve for control of liquid propellants or cryogenic fluids. The valve utilizes a section of a steel sphere as the gate and a Kel-F plastic lip seal. The lip seal is bolted to the valve body with a serrated retaining ring and closely spaced, multiple bolts. The 0.015 to 0.020 high serration prevents unwanted shifting of the seal on the body and provides the high loading necessary for preventing leakage between the flange and the seal. Invar spacers are used in the retainer for cryogenic service to ensure that the thermal contraction of the combined lip seal retainer, and Invar spacer is equal to that of the bolt. This arrangement does not permit a decrease in bolt torque with decreasing temperatures. The seal back-up is shown integrally machined with the body, but has been shown to be unnecessary for cryogenic service since the seal is raised off the back lip and supported by the gate when the valve is closed.

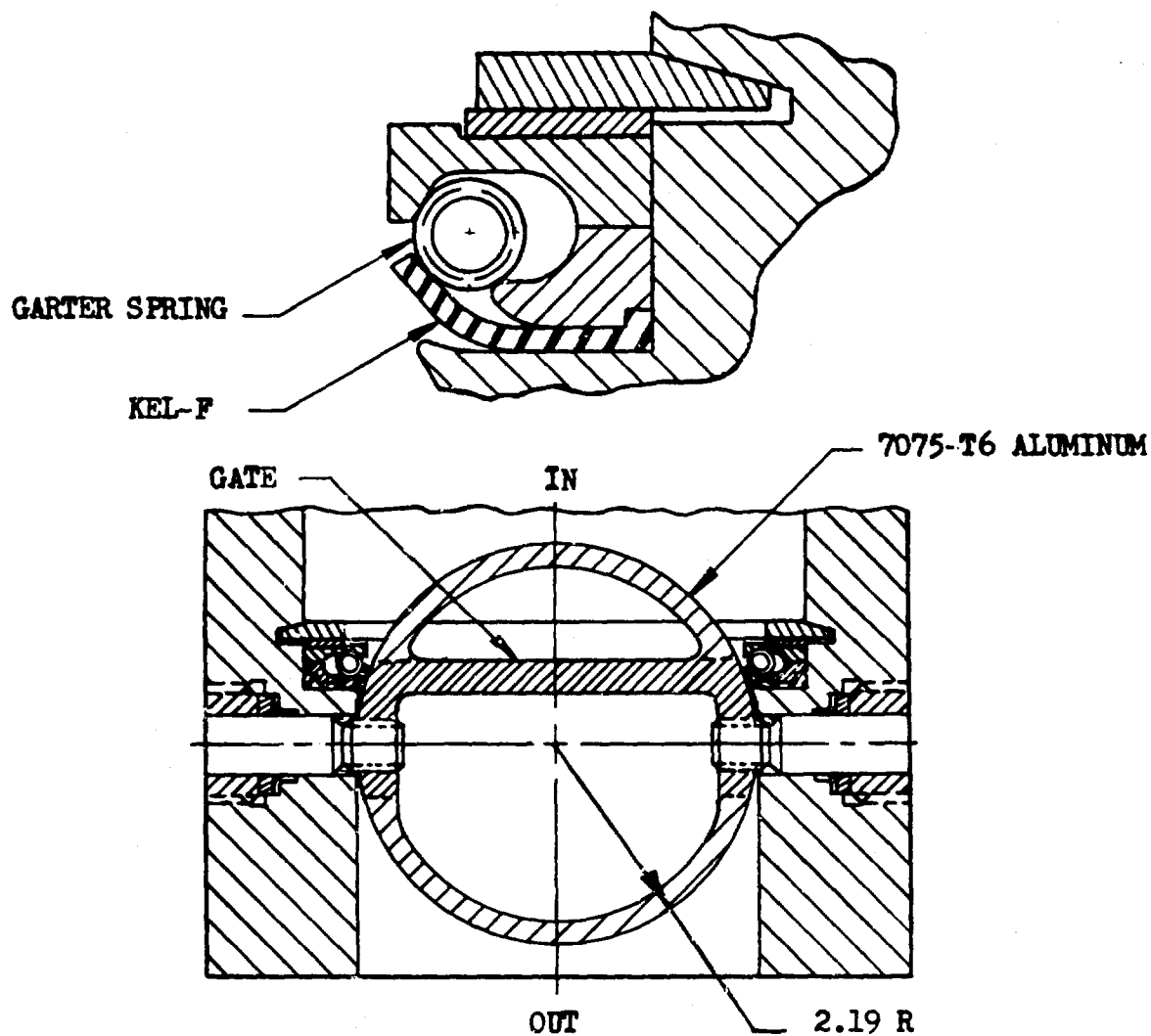
The dynamic seal is obtained by forming the seat at approximately a 10-degree angle from the tangent to the gate to allow the seal to bear on the gate at the radiused corner (0.005 to 0.010 inch). Flexing of the Kel-F lip at installation and under pressure causes more of the lip to bear on the gate maintaining the seating stress below the yield stress of the material. The radial interference between the gate and seal is designed to be approximately 0.01 in./in. of the inside diameter of the seal, when an 0.075-inch-thick seal is used. Thinner seals will provide greater and thicker seals, less interference.

The two major problems with the design have been: (1) maintaining an effective seal during and after chilldown to cryogenic temperatures, and (2) limiting the seal deflection during valve closure so as to prevent the seal from being damaged by deflecting down into the path of the gate while closing.

Advantages of the design are: (1) unique combinations of low weight, low pressure drop, low actuation energy requirements, and short installation length, and (2) Kel-F seal is capable of: resisting cold flow, flexibility at cryogenic temperatures, maintaining a seal by conformance to imperfections in gate and housing, and compatibility with most propellants.

Disadvantages of the seal design are: (1) complex retention design, (2) seal fabrication is limited to forming from sheet material of essentially the same thickness as required for the seal, and (3) the seals must receive thermal treatment to control crystallinity for maximum strength and flexibility.

MODIFIED BUTTERFLY DESIGN



KEY PARAMETERS

VALVE TYPE: BUTTERFLY VALVE  
FLOW MEDIA: LIQUID OXYGEN  
TEST MEDIA: LIQUID NITROGEN  
OPERATING PRESSURE: 40 PSIG  
OPERATING TEMPERATURE: -320 TO +160 F  
LEAKAGE: 30 SCIM MAX @ 80 PSIG  
(12 SCIM MAX @ 6 PSIG)  
SIZE: 4½ INCH LINE  
LIFE: 1000 CYCLES  
VIBRATION: 20 G TO 2000 CPS

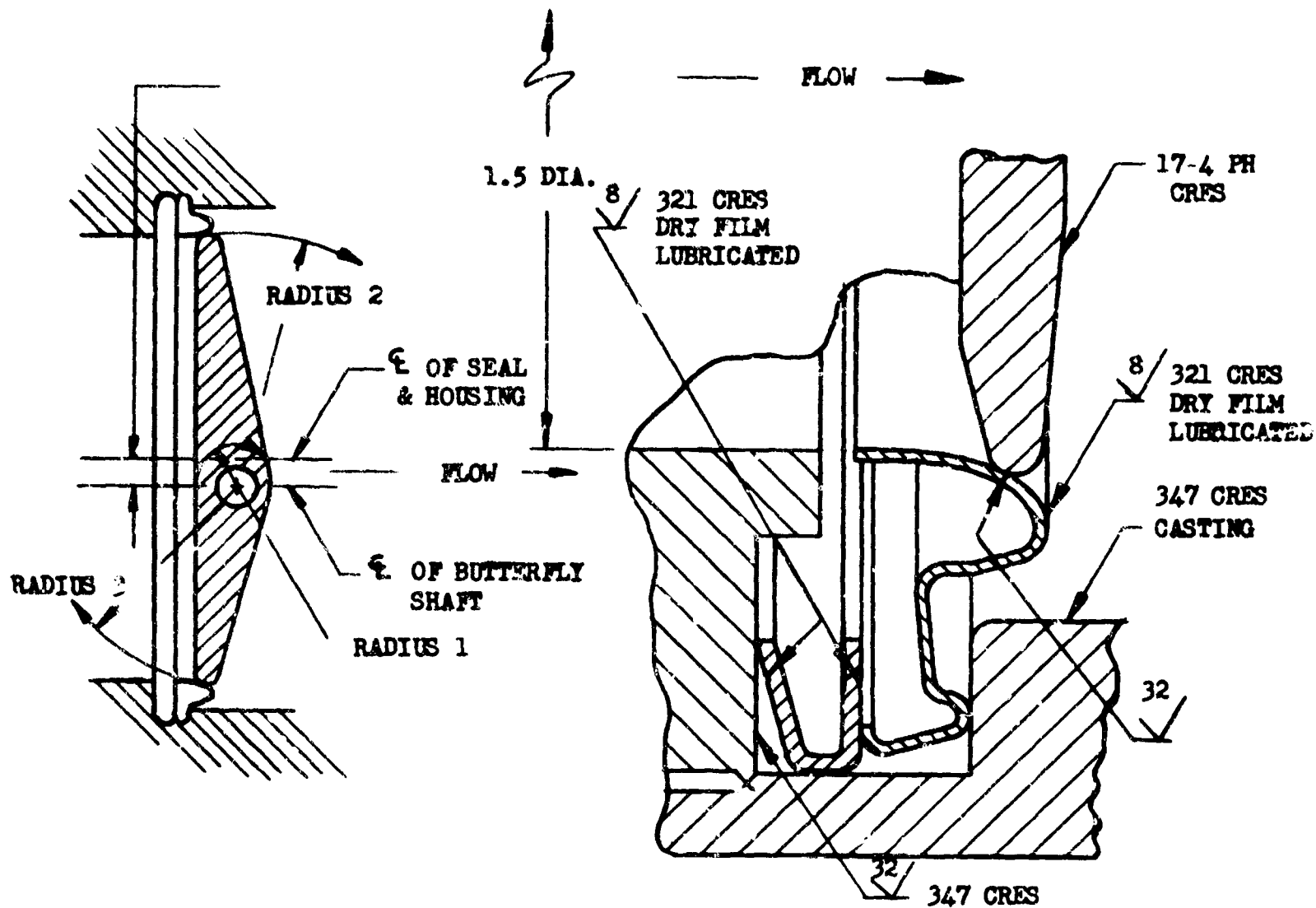
Figure B-36. Modified Butterfly Valve—Clary Dynamics Corporation (U.S. Patent No. 2,988,320)

## MODIFIED BUTTERFLY VALVE

This modified butterfly valve possesses the unique feature of supporting and protecting the seal from flow forces and icing when the valve is open, thereby ensuring a uniform sealing surface free from cold flow effects. Since the seal is unsupported during a portion of its rotation, the edge of the gate is generously radiused where it initially contacts the seal. When the valve is closed, sealing is augmented by forcing the plastic lip seal against the gate with both differential pressure and spring force.

The major problem associated with the design is the prevention of seal destruction through its deflection into the gate path during closure. The cost of fabrication of this design is relatively high.

## BUTTERFLY DESIGN



### KEY PARAMETERS

VALVE TYPE: BUTTERFLY VALVE  
FLOW MEDIA: AIR  
OPERATING PRESSURE: 7 TO 205 PSIG  
OPERATING TEMPERATURE: -75 TO +250 F  
FLUID TEMPERATURE: -75 TO +750 F  
LEAKAGE: 350 SCIM MAX AIR AT 650 F  
SIZE: 1½ INCH LINE  
LIFE: 100,000 CYCLES AT 50 PSIG & 70 F

Figure B-37. Metal Seal Butterfly Valve—Aero-Corry Division of Aeroflow Dynamics, Inc. (Patent Pending)



## METAL-SEAL BUTTERFLY VALVE

This butterfly valve was designed for use in an airborne system to control the delivery of engine bleed air. The most significant design feature is the incorporation of a two-piece floating seal that provides relatively low leakage characteristics and long life under large variations of temperature.

The two-piece convoluted seal is restrained axially within the valve body, but is allowed to float within the valve housing. By this means, the effect of differential expansion between the gate and the valve housing due to variation of temperature, pressure, etc., is negligible.

Binding between the gate and seal is minimized by forming the under lips of the seal to an involute profile, so that contact with the radiused edge of the gate is always in a direction normal to the seal surface. All free edges of the seal members are within the housing to provide protection from flow forces.

The gate has an off-center shaft to form a plugging action as it goes into the seal and to give an unbalanced open moment to aid in the opening of the valve. Radius No. 1 shows the path of the maximum diameter of the butterfly as it pulls away from the seal to decrease interference of the gate and seal. Radii No. 2 and 3 delineate the paths taken at the maximum diameter radius of the seal edges to relieve the interference fit of the seal. This action pulls the gate away from the seal on the first movement and allows no contact after the first 5 degrees of rotation to increase the life of the seal.

The disadvantages of the design lie in the relatively low pressure limitations, the expensive tooling, and the excessive machinery setup time required for manufacture.